

Introduction to Hadronic Final State Reconstruction in Collider Experiments (Part I)

Peter Loch

University of Arizona

Tucson, Arizona

USA



The material presented in this lecture series, which has been designed for ATLAS graduate students at the University of Arizona, is mostly used to explain complex signal features of calorimeters and other detectors we are using to analyze the final states in hadron collider experiments. Its intent is to be educational only, and it most certainly does not represent present evaluations of the actual performance of any of the experiments mentioned. Matter of fact, in some cases older low performance features, long since understood and corrected, are enhanced in the discussion for educational purposes, just to highlight the motivations and tools for the solutions applied. Also, there is a clear bias towards the methodology used by the ATLAS experiment, because I have been involved in this experiment for now 15 years. A serious attempt was made to show only common knowledge or otherwise approved specific material, of course – and to provide citations when available and appropriate.

The more than 200 slides comprising this lecture series would not have been possible to collect without the direct or indirect input from the HERA, Tevatron, and LHC experiment communities, and from colleagues from theory and phenomenology. It is a bit unfortunate that not all the knowledge available today, reflecting the result of hard work of so many people, could be included here. Nevertheless, I like to acknowledge everybody who helped getting us where we are today with the understanding of the detectors and the physics of hadron collisions, in particular with respect to jet reconstruction. I like to recognize and thank the colleagues who, in the last few years, spent nearly endless hours with me discussing topics related to these lectures, and without whom I am sure my own understanding of these subjects would not be as far advanced as it is today. Please find the names on the next slide.

For those of you who are reading these slides, and would like to use them for the purposes they have been put together for, please feel free to do so. Please let me know of any even smallest error or inconsistency, or any improvement concerning the wording and displayed material – thank you for that! I also appreciate suggestions for extension or change of focus, of course. The best way to contact me is by e-mail loch AT physics.arizona.edu.

Tucson, April 29, 2010

Peter Loch
Department of Physics, University of Arizona
Tucson, Arizona 85721
USA



The following people significantly contributed with their work and ideas to the material of this lecture series – in some case probably without their personal knowledge (yes, I was listening). Also, these are the people who pushed my understanding of the jets in the hadron collider environment in sometimes more or less controversial discussions, which I deeply enjoyed, by issuing relevant comments, or by raising interesting questions. Last but not least I am grateful to the colleagues who invited me to report on jet physics related topics at workshops, conferences, and seminars, either in form of lectures, or as introductory or status talks. Thank you all for this – it helped me a lot to understand the often complex signal features we see in hadron collisions.

Argonne National Laboratory (USA)

Esteban Fullana Torregrosa, Tom LeCompte, Jimmy Proudfoot, Belen Salvachua, Zach Sullivan

Brookhaven National Laboratory (USA)

Ketevi Assamagan, Hong Ma, Frank Paige, Srinu Rajagopalan

Carleton University (Canada)

Gerald Oakham, Manuella Vincter

CERN (Switzerland)

David Berge, Tancredi Carli, Daniel Froidevaux, Fabiola Gianotti, Peter Skands, Guillaume Unal

CalTech/Columbia (USA)

David Lopez, K.Perez, Zach Taylor

DESY Hamburg (Germany)

Kerstin Borras, Jörg Gayler, Hannes Jung

Fermi National Laboratory (USA)

W.Giele

Florida State University (USA)

Rick Field

IFAE Barcelona (Spain)

Martine Bosman

INFN Milan (Italy)

Leonardo Carminati, Donatella Cavalli, Silvia Resconi

INFN Pavia (Italy)

Giacomo Polesello

INFN Pisa (Italy)

Paolo Francavilla, Vincent Giangiobbe, Chiara Roda

Lawrence Berkeley National Laboratory/UC Berkeley (USA)

Christian Bauer, Beate Heinemann, Marjorie Shapiro, Jesse Thaler

LPSC Grenoble (France)

Pierre-Antoine Delsart

LPNHE /UPMC Universite de Paris 6 (France)

Bernard Andrieu

LPTHE/UPMC Universite de Paris 6 (France)

Matteo Cacciari, Gavin Salam

Michigan State University (USA)

Joey Huston

Max Planck Institut für Physik München (Germany)

Paola Giovaninni, Andreas Jantzs, Sven Menke, Horst Oberlack, Guennadi Pospelov, Vladimir Shekelyan, Peter Schacht, Rolf Seuster

Rutherford Appleton Laboratory Didcot (UK)

Monika WIELERS



Simon Fraser University (Canada)

D.O'Neil , D.Schouten, T.Spreitzer

SLAC (USA)

David Miller, Michael Peskin, Ariel Schwartzman

Universidad de Sonora, Hermosillo (Mexico)

Maria Elena Tejeda-Yeomans

Universität Freiburg (Germany)

Kristin Lohwasser, Iacopo Vivarelli

Universität Heidelberg (Germany)

Victor Lendermann, Pavel Weber

Universität Mainz (Germany)

Sebastian Eckweiler, Stefan Tapprogge

Universität Wuppertal (Germany)

Christian Zeitnitz

University College London (UK)

Jon Butterworth, Mario Campanelli, Adam Davison, S.Dean,
N.Kostantinidis, P.Sherwood

University of Arizona (USA)

Ken Johns, Venkat Kaushik, Caleb Lampen, Xiaowen Lei, Prolay
Mal, Chiara Paleari, Frederik Rühr, John Rutherford, Alexander
Savine, Shufang Shu, Michael Shupe

UC Davis (USA)

John Conway

University of Chicago (USA)

Georgios Choudalakis, Frank Merritt

University of Glasgow (UK)

Craig Buttar , Arthur Moraes

University of Oregon (USA)

D.Soper, E. Torrence

University of Oxford (UK)

C.Doglioni, Cigdem Issever

University of Sheffield (UK)

Dan Tovey

University of Toronto (Canada)

Peter Krieger, Richard Teuscher

University of Victoria (Canada)

Frank Berghaus, Michel Lefebvre, Jean-Rafael Lessard, Rob
McPherson

University of Washington (USA)

Steve Ellis, Chris Vermillion, Jon Walsh

Not working in HEP anymore...

Levan Babukhadia, Ambreesh Gupta, Kai Voss

*... and all the other colleagues whom I may have forgotten and,
so I hope, will forgive me for that!*



Introduction

Sources of jets and missing transverse energy at LHC

Hadron collision environment

Principles of calorimetry in High Energy Physics

Interaction of particles and matter

Calorimeter design principles

Characteristic features of operating calorimeters in hadron collider experiments

Hadronic final state in high energy hadron collisions

Characteristic signatures at highest energies

Experimentalist's view on partons and particles

What are jets?

Theoretical guidelines for finding jets

Jet finding algorithms and jet definition

Reconstructing jets in the experiment

Calibrating jets

Jet substructure reconstruction

Focus on the experimental aspects

Unfolding hadron collider physics from detector signals

Triggering, acceptance, calibration, resolution

Mostly discussed using the LHC collision experiments (“ATLAS bias”)

Accumulation of experiences from previous experiments

Occasional highlights from SPS, HERA, Tevatron,...

Lecture style

Informal

Please ask questions – we should have sufficient time!

Student talks

Possibility to present selected aspects (end of semester)

Material

Some material is private to the ATLAS experiment

Mostly used to explain signal features

Use only material with publication reference for public talks

Slides on the web

Look for link on <http://atlas.physics.arizona.edu/~loch>

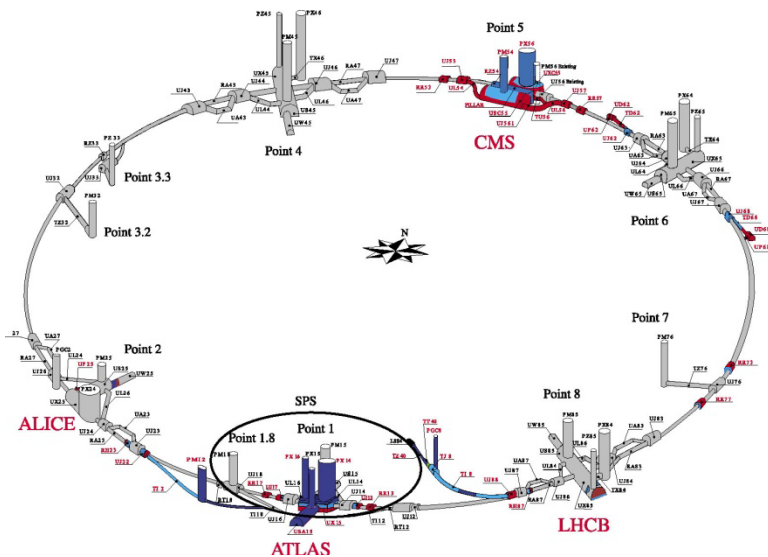
Will try to upload as soon as possible after each session

Literature

Embedded in slides

Will extract and put on the web soon!





Machine

Occupies old LEP tunnel at CERN, Geneva, Switzerland & France

About 27 km long

50-100m underground

1232 bending magnets

392 focusing magnets

All superconducting

~96 tons of He for ~1600 magnets

Beams (design)

pp collider

7 TeV on 7 TeV (14 TeV collision energy)

Luminosity $10^{34} \text{ cm}^{-2}\text{s}^{-1}$

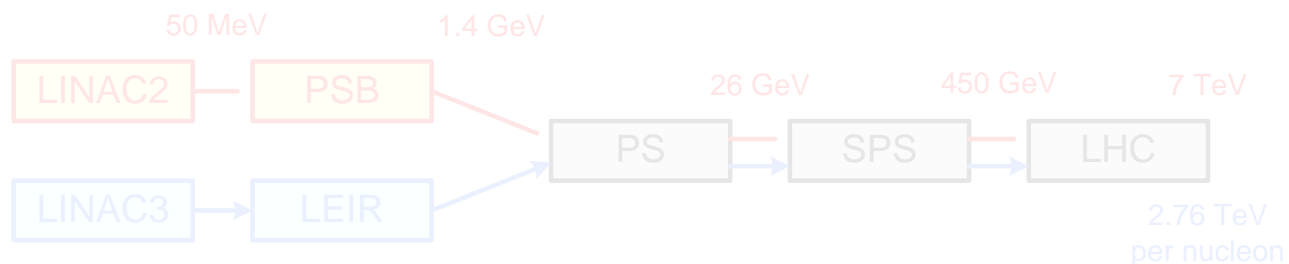
2808 x 2808 bunches

Bunch crossing time 25 ns (40 MHz)

~20 pp collisions/bunch crossing

Heavy ion collider (Pb)

Collision energy 1150 TeV (2.76 TeV/nucleon)



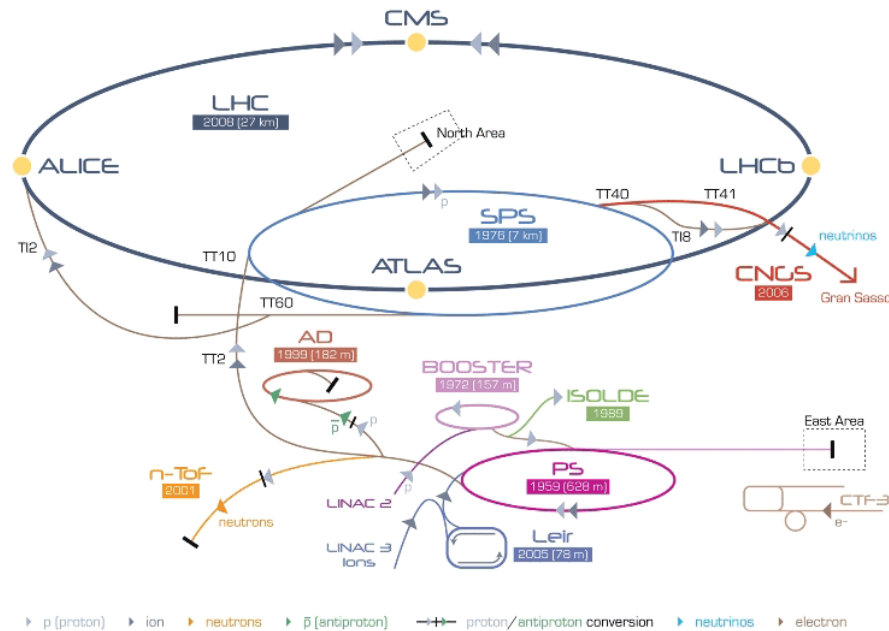
Proton acceleration chain:

LINAC→Proton Synchrotron Booster (PSB)→Proton Synchrotron (PS)→Super Proton Synchrotron (SPS)→LHC

Pb ion acceleration chain:

LINAC→Low Energy Ion Injector Ring (LEIR)→Proton Synchrotron (PS)→Super Proton Synchrotron (SPS)→LHC





LHC Large Hadron Collider SPS Super Proton Synchrotron PS Proton Synchrotron

AD Antiproton Decelerator CTF-3 Clic Test Facility CNCS Cern Neutrinos to Gran Sasso ISOLDE Isotope Separator OnLine DEvice
LEIR Low Energy Ion Ring LINAC LInear ACcelerator n-ToF Neutrons Time Of Flight

Machine

Occupies old LEP tunnel at CERN, Geneva, Switzerland & France
About 27 km long
50-100m underground
1232 bending magnets
392 focusing magnets
All superconducting
~96 tons of He for ~1600 magnets

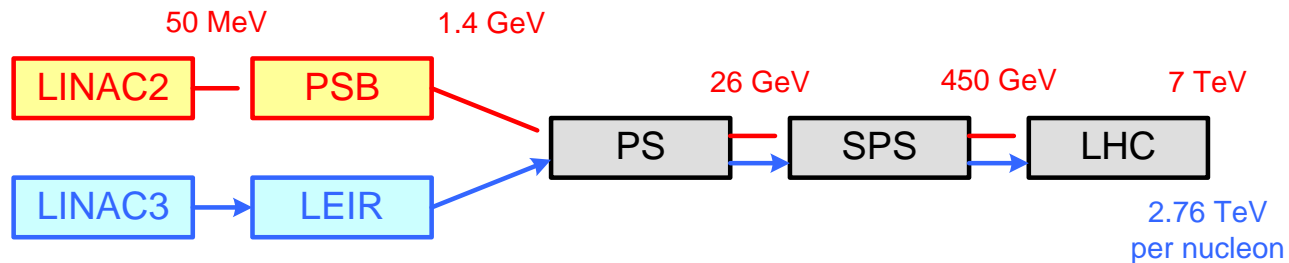
Beams (design)

pp collider

7 TeV on 7 TeV (14 TeV collision energy)
Luminosity $10^{34} \text{ cm}^{-2}\text{s}^{-1}$
2808 x 2808 bunches
Bunch crossing time 25 ns (40 MHz)
~20 pp collisions/bunch crossing

Heavy ion collider (Pb)

Collision energy 1150 TeV (2.76 TeV/nucleon)



Proton acceleration chain:

LINAC→Proton Synchrotron Booster (PSB)→Proton Synchrotron (PS)→Super Proton Synchrotron (SPS)→LHC

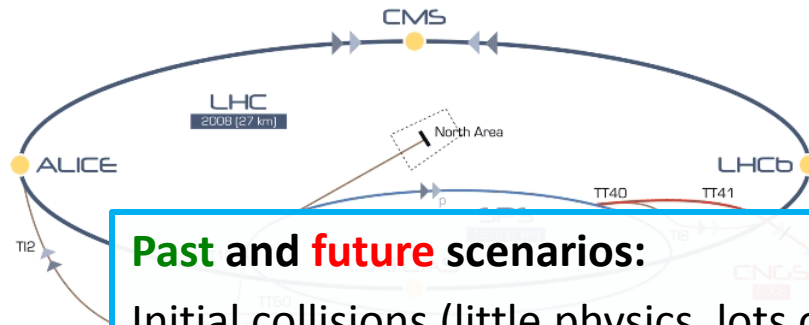
Pb ion acceleration chain:

LINAC→Low Energy Ion Injector Ring (LEIR)→Proton Synchrotron (PS)→Super Proton Synchrotron (SPS)→LHC



Machine

Occupies old LEP tunnel at CERN, Geneva, Switzerland & France
About 27 km long
50-100m underground
1232 bending magnets
392 focusing magnets
All superconducting



Past and future scenarios:

Initial collisions (little physics, lots of detector commissioning)

2009 900 GeV center of mass energy

2.38 TeV center of mass (world record)

Collisions for physics (restart mid-February 2010)

2010 7 TeV center of mass energy, 10^{29} - 10^{32} $\text{cm}^{-2}\text{s}^{-1}$, up to 1 fb^{-1}

-2011

2012 Shutdown to prepare for **14 TeV** center of mass energy

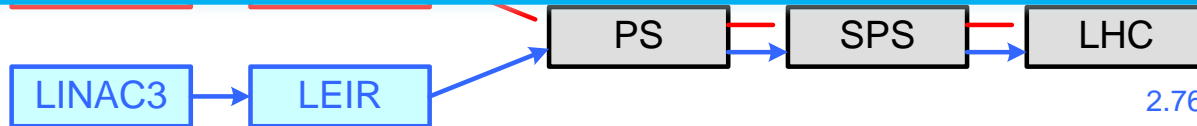
Latest status and plans at

50 MeV

LINAC2

<http://lhc-commissioning.web.cern.ch/lhc-commissioning/>

7 TeV



Proton acceleration chain:

LINAC→Proton Synchrotron Booster (PSB)→Proton Synchrotron (PS)→Super Proton Synchrotron (SPS)→LHC

Pb ion acceleration chain:

LINAC→Low Energy Ion Injector Ring (LEIR)→Proton Synchrotron (PS)→Super Proton Synchrotron (SPS)→LHC



Enormous reach in (x, Q^2)

Low x at relatively high Q^2
 Mostly uncovered so far

No experimental data for parton densities

Validation of proton structure part of LHC physics program

Must rely on evolution of HERA structure functions

QCD probes whole region

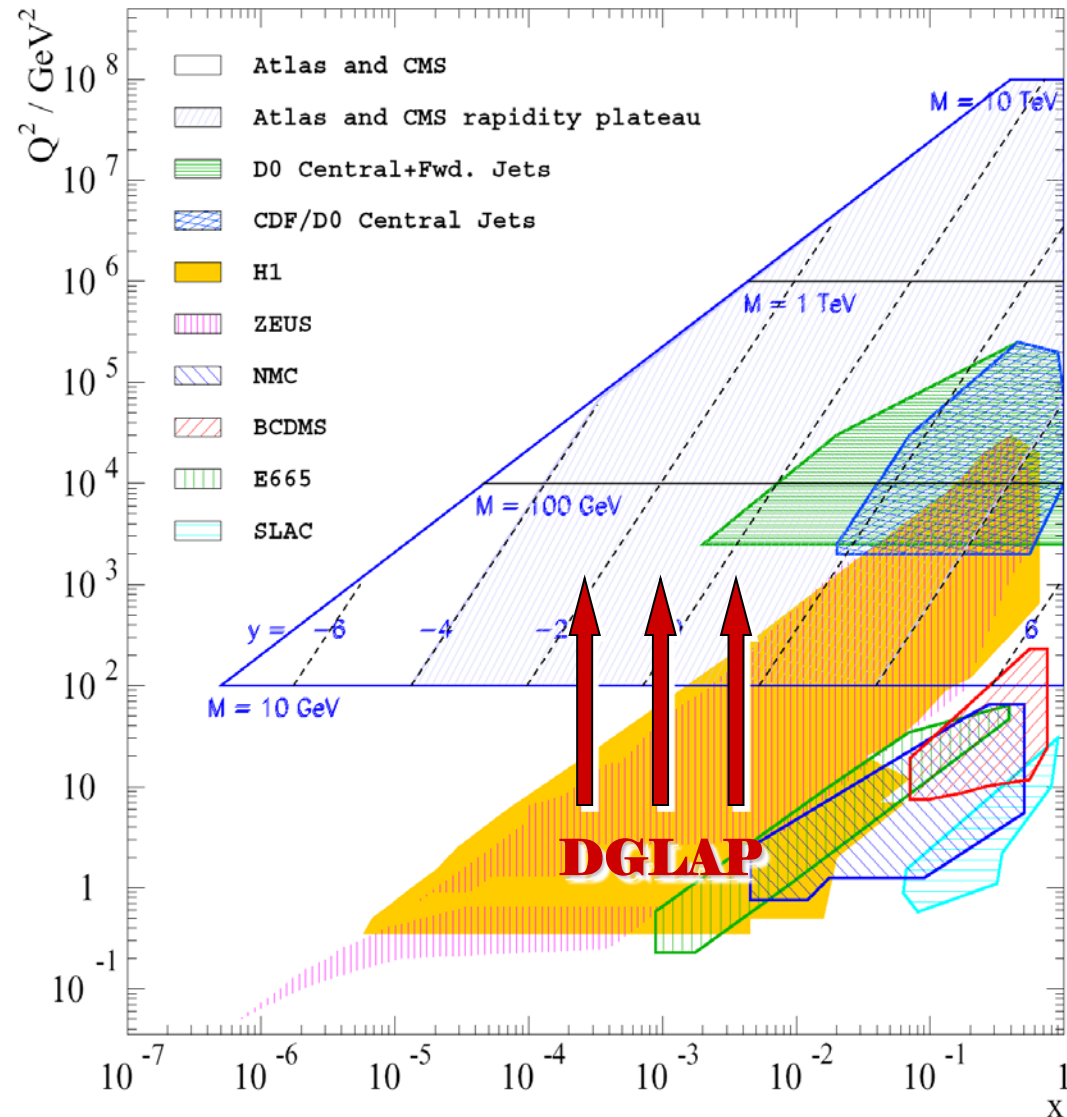
Di-jet production

b/c-quark jets

Prompt photons

$$x_{1,2} = \frac{E_T}{\sqrt{s}} \left(e^{\pm\eta_1} + e^{\mp\eta_2} \right)$$

$$Q^2 \approx 2E_T^2 \cosh^2 \eta^* (1 - \tanh \eta^*)$$



Fragmentation of gluons and (light) quarks in QCD scattering

Most often observed interaction at LHC

Decay of heavy Standard Model (SM) particles

Prominent example:

$$t \Rightarrow bW \Rightarrow jjjj$$

$$t \Rightarrow bW \Rightarrow lvjj$$

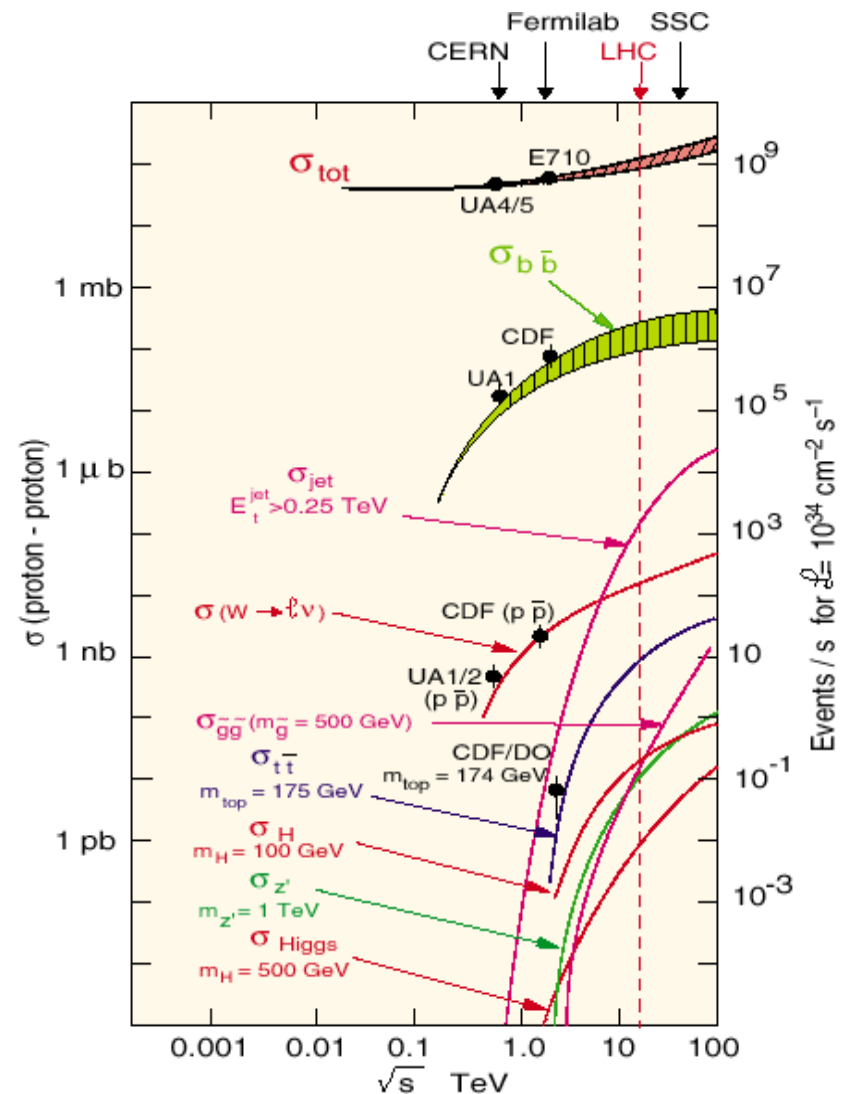
Associated with particle production in Vector Boson Fusion (VBF)

E.g., Higgs

$$q\tilde{q} \Rightarrow q'\tilde{q}'WW \Rightarrow Hjjj$$

Decay of Beyond Standard Model (BSM) particles

E.g., SUSY



Fragmentation of gluons and (light) quarks in QCD scattering

Most often observed interaction at LHC

Decay of heavy Standard Model (SM) particles

Prominent example:

$$t \Rightarrow bW \Rightarrow jjjj$$

$$t \Rightarrow bW \Rightarrow lvjjj$$

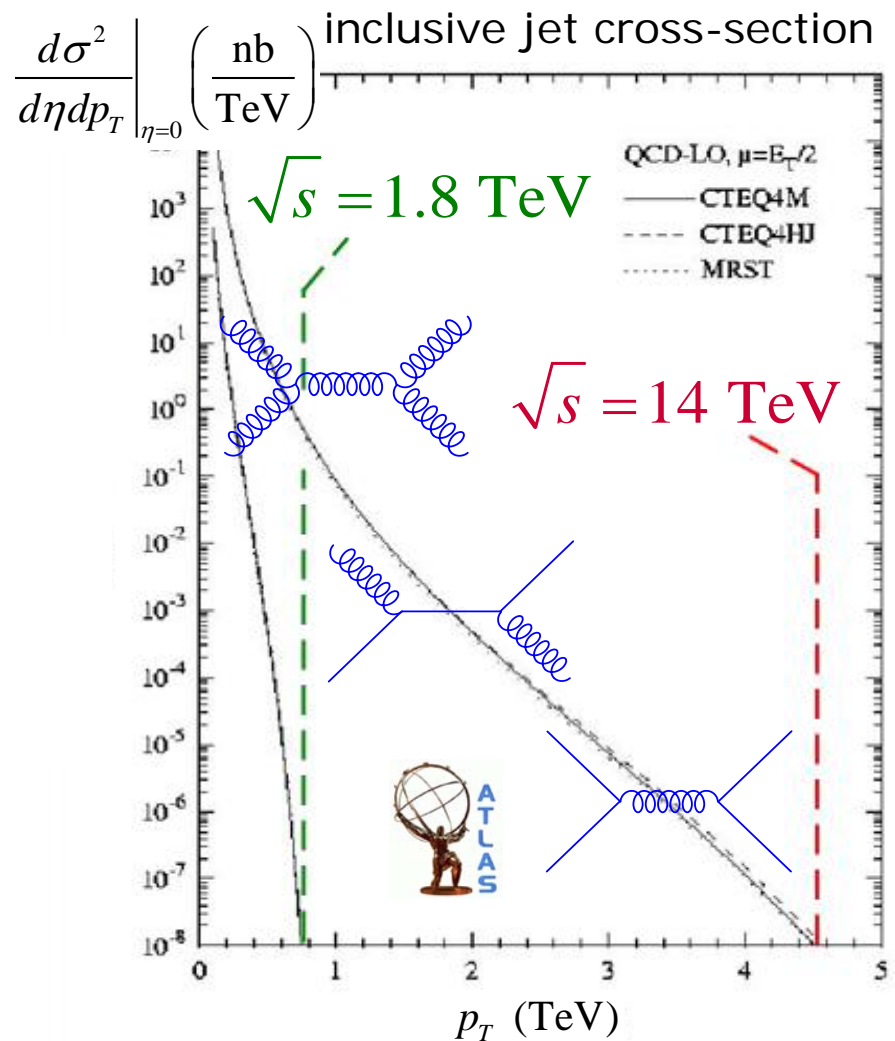
Associated with particle production in Vector Boson Fusion (VBF)

E.g., Higgs

$$q\tilde{q} \Rightarrow q'\tilde{q}'WW \Rightarrow Hjjj$$

Decay of Beyond Standard Model (BSM) particles

E.g., SUSY



Fragmentation of gluons and (light) quarks in QCD scattering

Most often observed interaction at LHC

Decay of heavy Standard Model (SM) particles

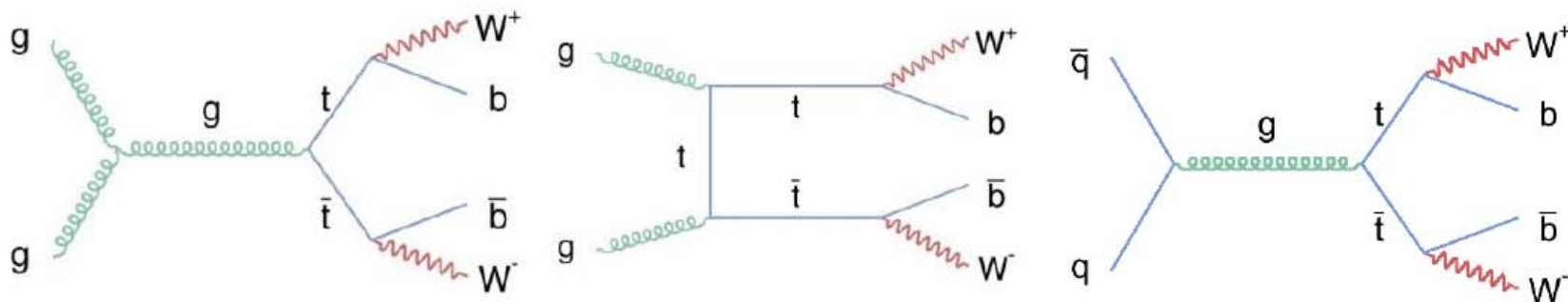
Prominent example:

$$t \rightarrow bW \rightarrow jjj$$

$$t \rightarrow bW \rightarrow l\nu jj$$

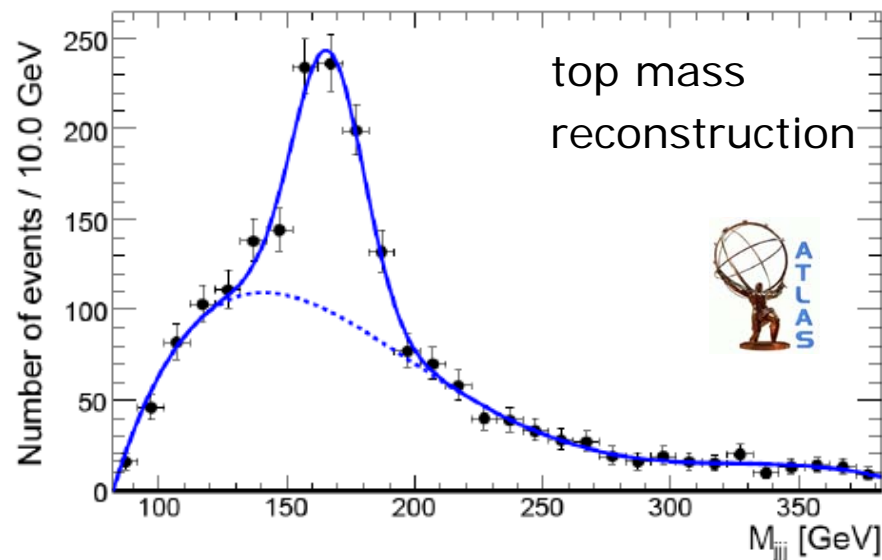
Associated with particle production in Vector Boson Fusion (VBF)

E.g., Higgs



$gg \rightarrow tt$ 85%

$qq \rightarrow tt$ 15%



Fragmentation of gluons and (light) quarks in QCD scattering

Most often observed interaction at LHC

Decay of heavy Standard Model (SM) particles

Prominent example:

$$t \Rightarrow bW \Rightarrow jjjj$$

$$t \Rightarrow bW \Rightarrow l\nu jjj$$

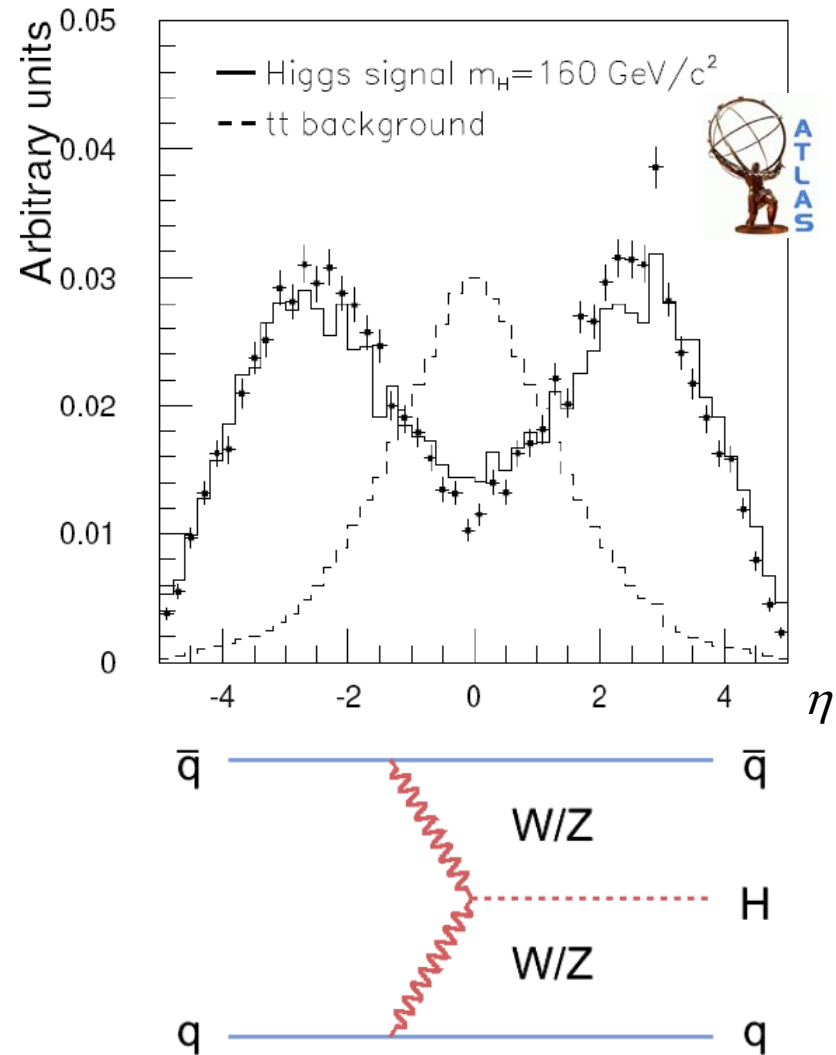
Associated with particle production in Vector Boson Fusion (VBF)

E.g., Higgs

$$q\bar{q} \rightarrow q'\bar{q}'WW \rightarrow Hjj$$

Decay of Beyond Standard Model (BSM) particles

E.g., SUSY



Fragmentation of gluons and (light) quarks in QCD scattering

Most often observed interaction at LHC

Decay of heavy Standard Model (SM) particles

Prominent example:

$$t \Rightarrow bW \Rightarrow jjjj$$

$$t \Rightarrow bW \Rightarrow lvjj$$

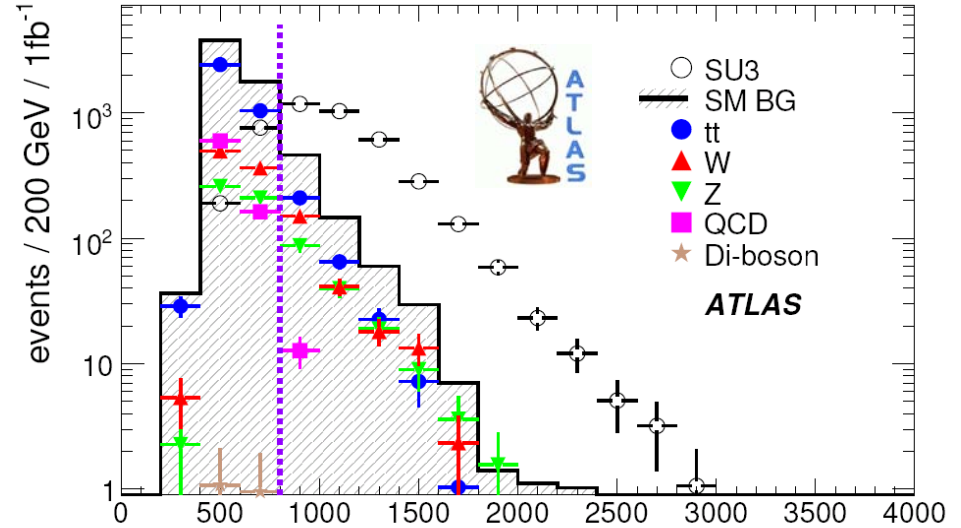
Associated with particle production in Vector Boson Fusion (VBF)

E.g., Higgs

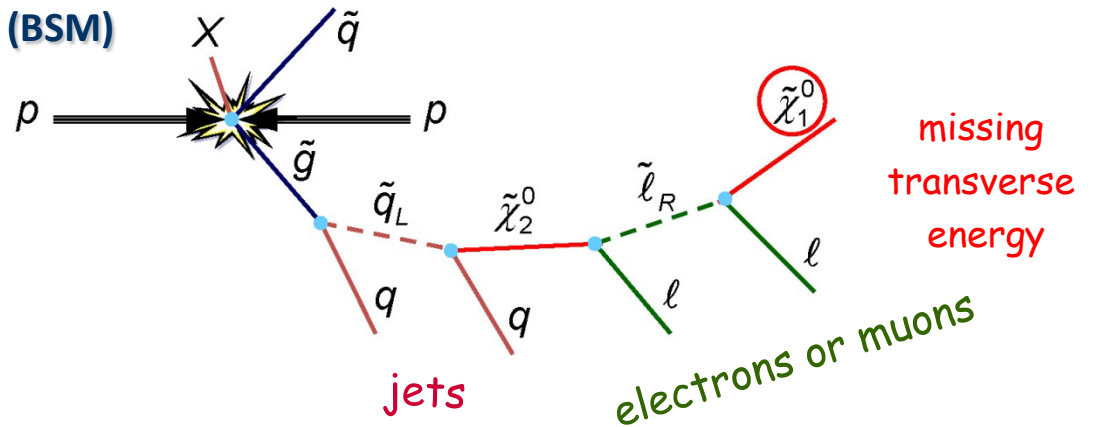
$$q\tilde{q} \Rightarrow q'\tilde{q}'WW \Rightarrow Hjjj$$

Decay of Beyond Standard Model (BSM) particles

E.g., SUSY



$$M_{eff} = \sum_{jets} |p_{T,j}| + \sum_{leptons} |p_{T,\ell}| + \cancel{p}_T$$



Collisions of other partons in the protons generating the signal interaction

Unavoidable in hadron-hadron collisions

Independent soft to hard multi-parton interactions

No real first principle calculations

Contains low p_T (non-perturbative) QCD

Tuning rather than calculations

Activity shows some correlation with hard scattering (radiation)

p_{Tmin} , p_{Tmax} differences

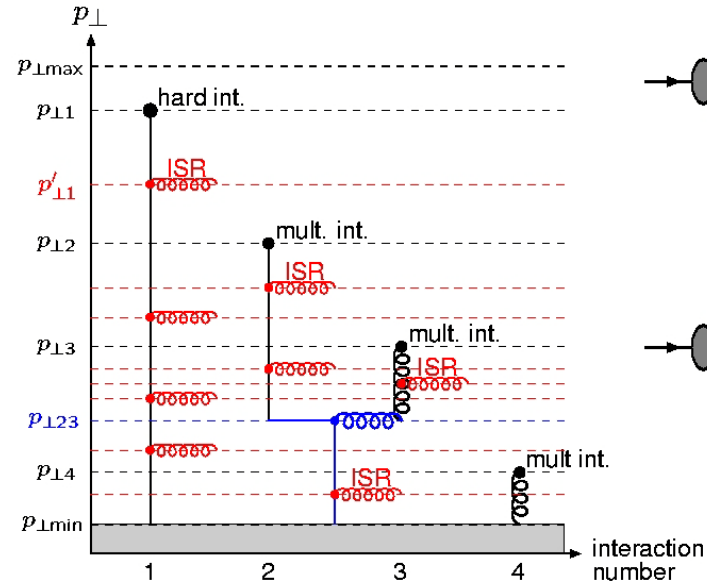
Typically tuned from data in physics generators

Carefully measured at Tevatron

Phase space factor applied to LHC tune in absence of data

One of the first things to be measured at LHC

Interleaved Multiple Interactions



Collisions of other partons in the protons generating the signal interaction

Unavoidable in hadron-hadron collisions

Independent soft to hard multi-parton interactions

No real first principle calculations

Contains low p_T (non-perturbative) QCD

Tuning rather than calculations

Activity shows some correlation with hard scattering (radiation)

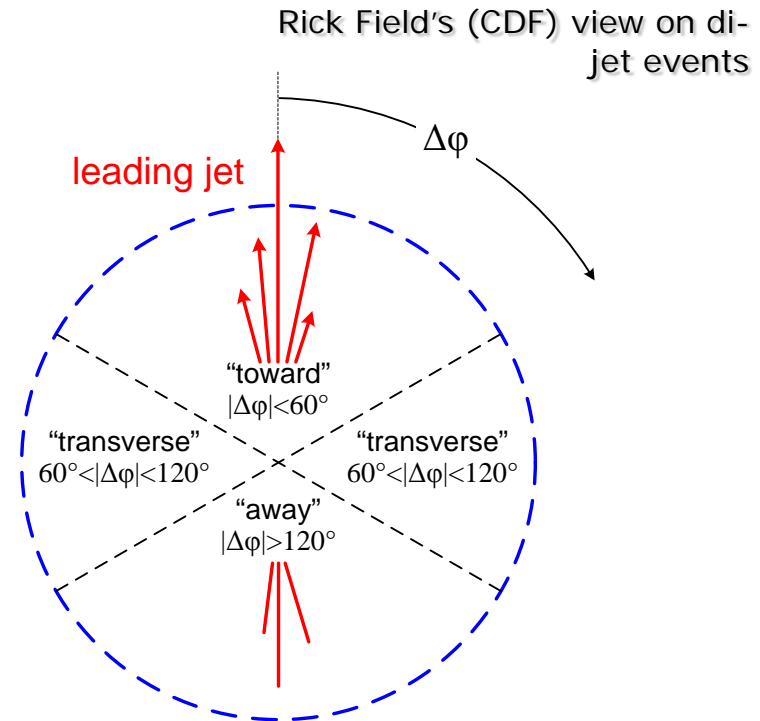
p_{Tmin} , p_{Tmax} differences

Typically tuned from data in physics generators

Carefully measured at Tevatron

Phase space factor applied to LHC tune in absence of data

One of the first things to be measured at LHC



Look at activity (p_T , # charged tracks) as function of leading jet p_T in transverse region



Collisions of other partons in the protons generating the signal interaction

Unavoidable in hadron-hadron collisions

Independent soft to hard multi-parton interactions

No real first principle calculations

Contains low p_T (non-perturbative) QCD

Tuning rather than calculations

Activity shows some correlation with hard scattering (radiation)

p_{Tmin} , p_{Tmax} differences

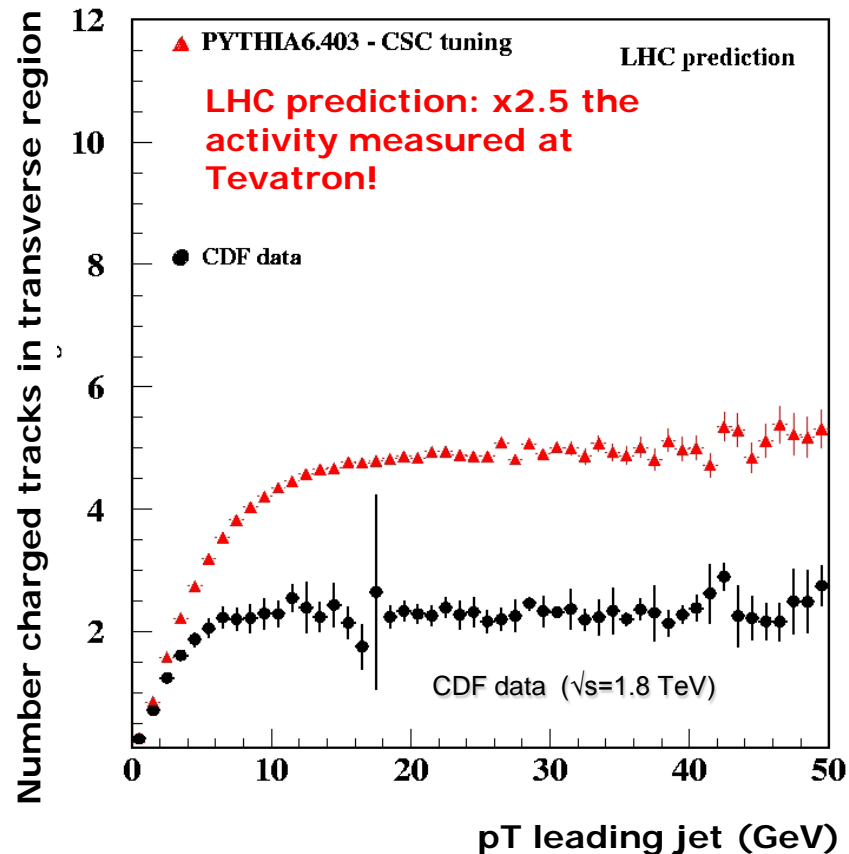
Typically tuned from data in physics generators

Carefully measured at Tevatron

Phase space factor applied to LHC tune in absence of data

One of the first things to be measured at LHC

CDF data: Phys.Rev, D, **65** (2002)



Model depending extrapolation to LHC:

$$\sim \ln^2 \sqrt{s} \quad \text{for PYTHIA}$$

$$\sim \ln \sqrt{s} \quad \text{for PHOJET}$$

but both agree Tevatron/Sp \bar{p} S data!



Multiple interactions between partons in other protons in the same bunch crossing

Consequence of high rate (luminosity) and high proton-proton total cross-section (~ 75 mb)

Statistically independent of hard scattering

Similar models used for soft physics as in underlying event

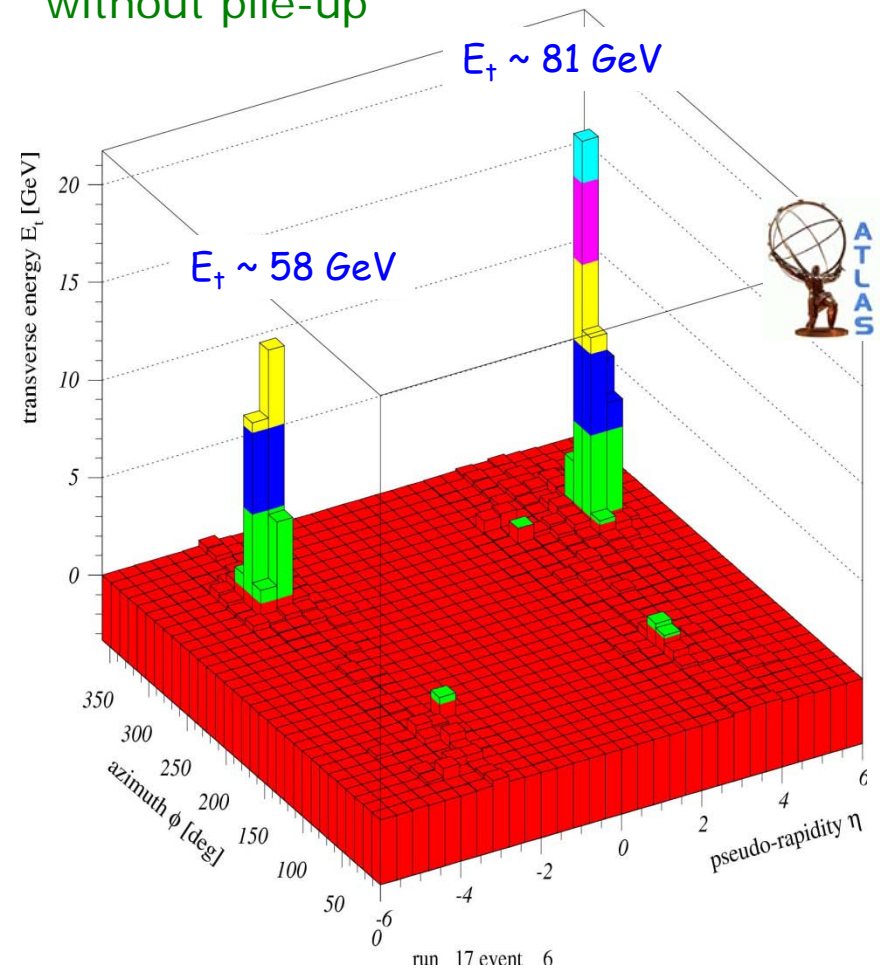
Signal history in calorimeter increases noise

Signal 10-20 times slower (ATLAS) than bunch crossing rate (25 ns)

Noise has coherent character

Cell signals linked through past shower developments

without pile-up



Prog.Part.Nucl.Phys.
60: 484-551, 2008



Multiple interactions between partons in other protons in the same bunch crossing

Consequence of high rate (luminosity) and high proton-proton total cross-section (~ 75 mb)

Statistically independent of hard scattering

Similar models used for soft physics as in underlying event

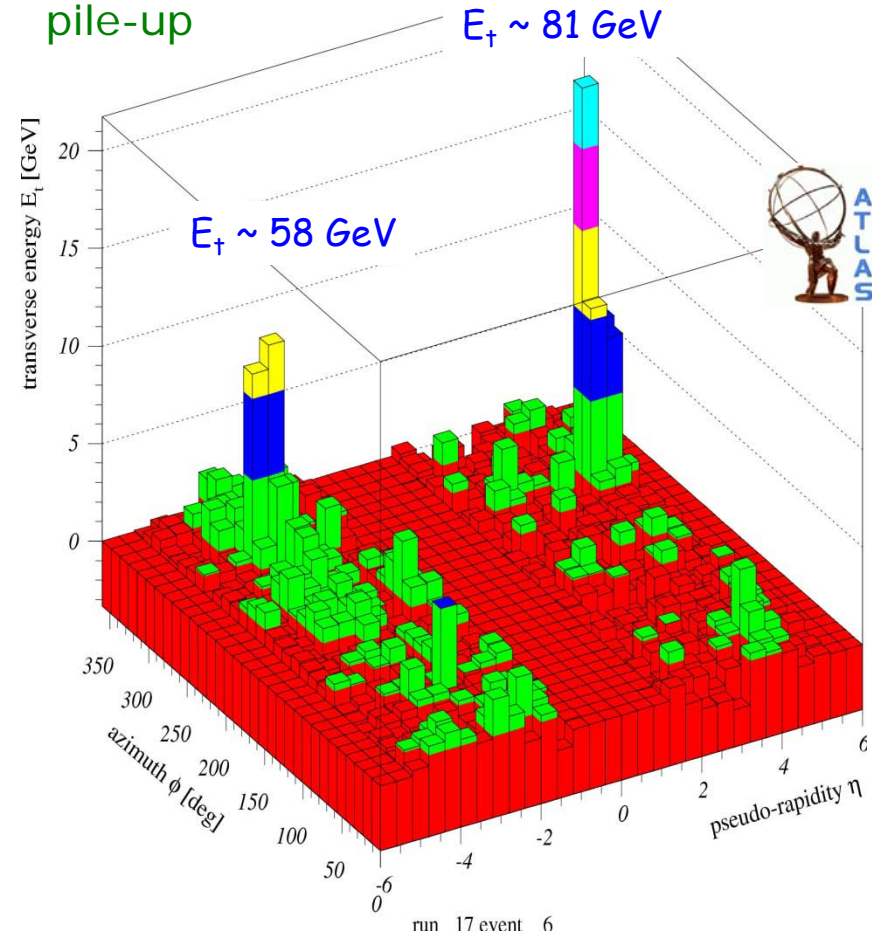
Signal history in calorimeter increases noise

Signal 10-20 times slower (ATLAS) than bunch crossing rate (25 ns)

Noise has coherent character

Cell signals linked through past shower developments

with design luminosity
pile-up



Multiple interactions between partons in other protons in the same bunch crossing

Consequence of high rate (luminosity) and high proton-proton total cross-section (~ 75 mb)

Statistically independent of hard scattering

Similar models used for soft physics as in underlying event

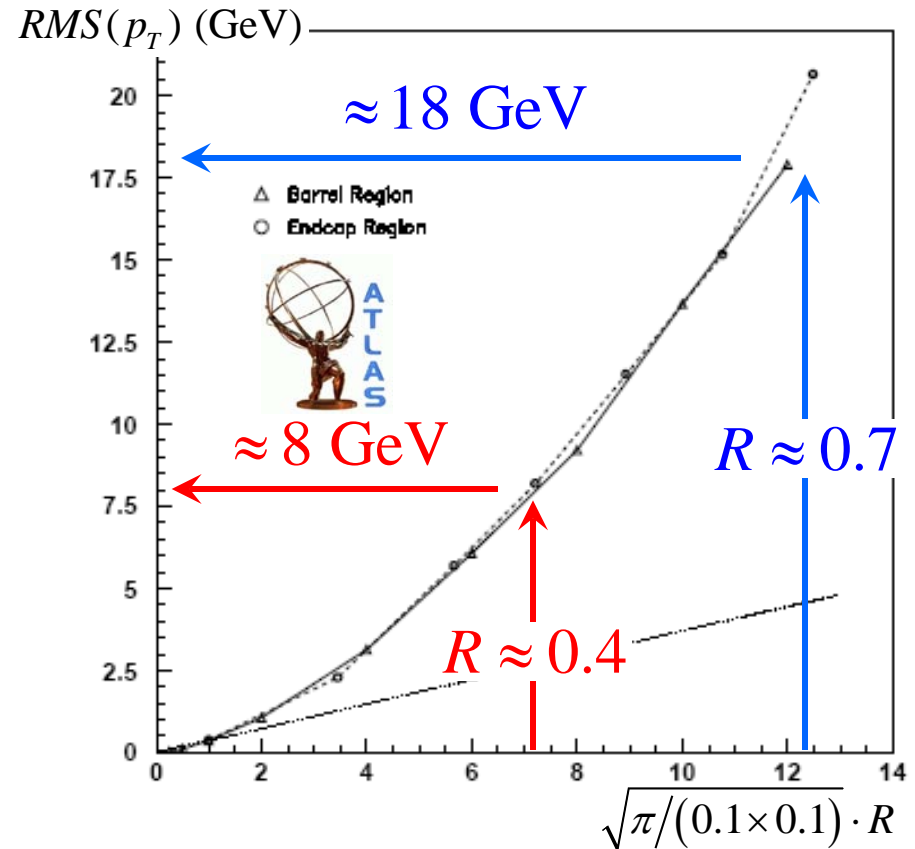
Signal history in calorimeter increases noise

Signal 10-20 times slower (ATLAS) than bunch crossing rate (25 ns)

Noise has coherent character

Cell signals linked through past shower developments

$$L = 10^{34} \text{ cm}^{-2} \text{ s}^{-1}$$



Prog.Part.Nucl.Phys.
60: 484-551, 2008



Jet calibration requirements very stringent

Systematic jet energy scale
uncertainties to be extremely
well controlled

Top mass reconstruction

Jet cross-sections

Relative jet energy resolution
requirement

Inclusive jet cross-section

Di-quark mass spectra cut-off in SUSY

$$\Delta m_{top} < 1 \text{ GeV} \Rightarrow \frac{\Delta E_{jet}}{E_{jet}} < 1\%$$

$$\frac{\sigma}{E} = \begin{cases} \frac{50\%}{\sqrt{E(\text{GeV})}} \oplus 3\% & |\eta| < 3 \\ \frac{100\%}{\sqrt{E(\text{GeV})}} \oplus 5\% & |\eta| > 3 \end{cases}$$

Event topology plays a role at 1% level of precision

Extra particle production due to event color flow

Color singlet (e.g., W) vs color octet (e.g., gluon/quark) jet source

Small and large angle gluon radiation

Quark/gluon jet differences



Introduction to Hadronic Final State Reconstruction in Collider Experiments (Part II)

Peter Loch

University of Arizona

Tucson, Arizona

USA



Detector needs for multi-purpose collider experiments

Tracking for charged particle momentum measurement

Calorimeters for charged and neutral particle energy measurement

Muon spectrometers (tracking) for muon momentum measurements

Underlying physics for calorimetry: particle interaction with matter

Electromagnetic cascades

Hadronic cascades

Muon energy loss

Calorimetric principles in particle detection

Conversion of deposited energy into an extractable signal in homogeneous and sampling calorimeters

Minimum ionizing particles and muons

General signal features of electromagnetic and hadronic showers

Calorimeter characteristics in sampling calorimeters

Sampling fraction

Signal linearity and relative resolution

Non-compensation

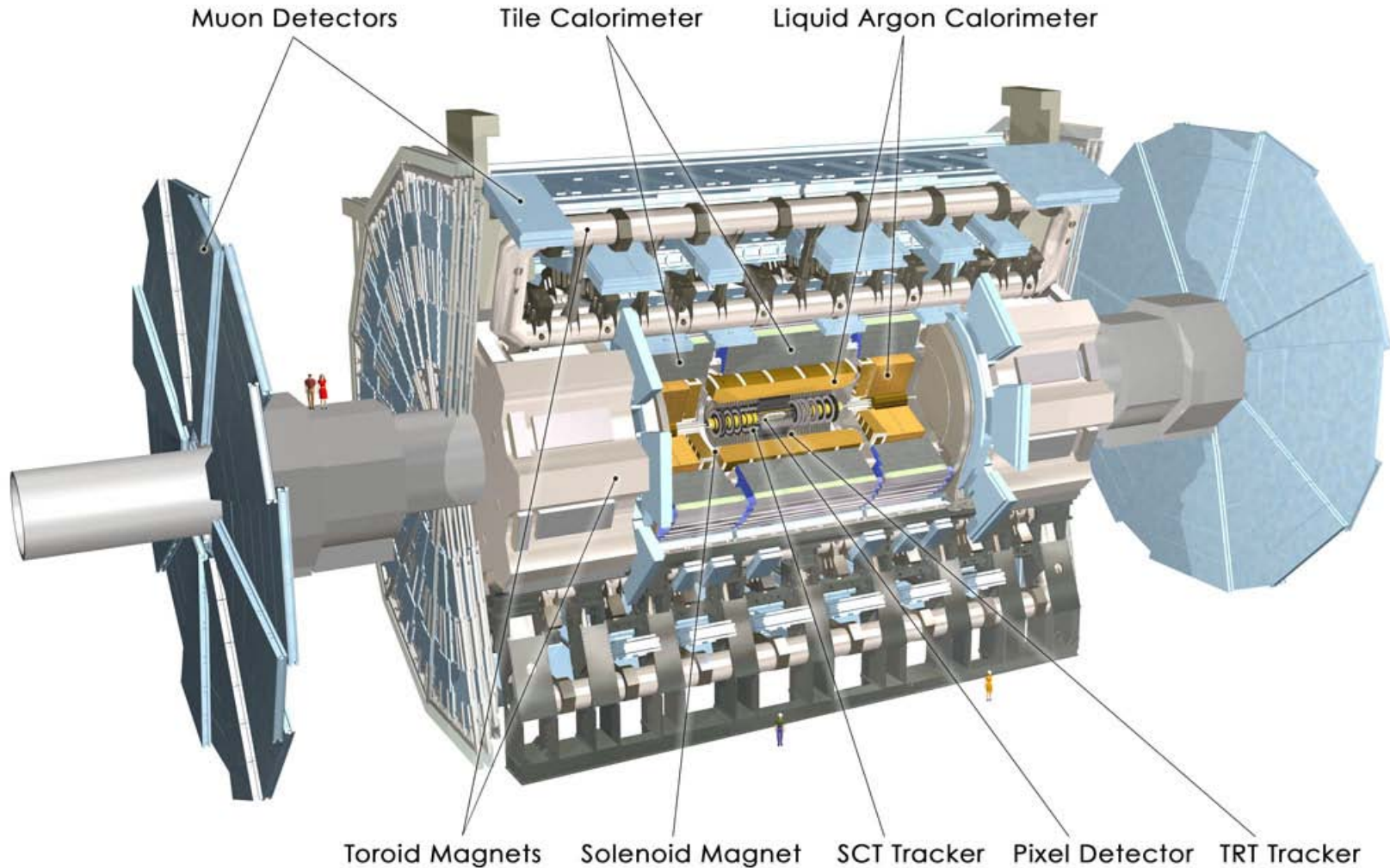
Signal extraction

Charge collection

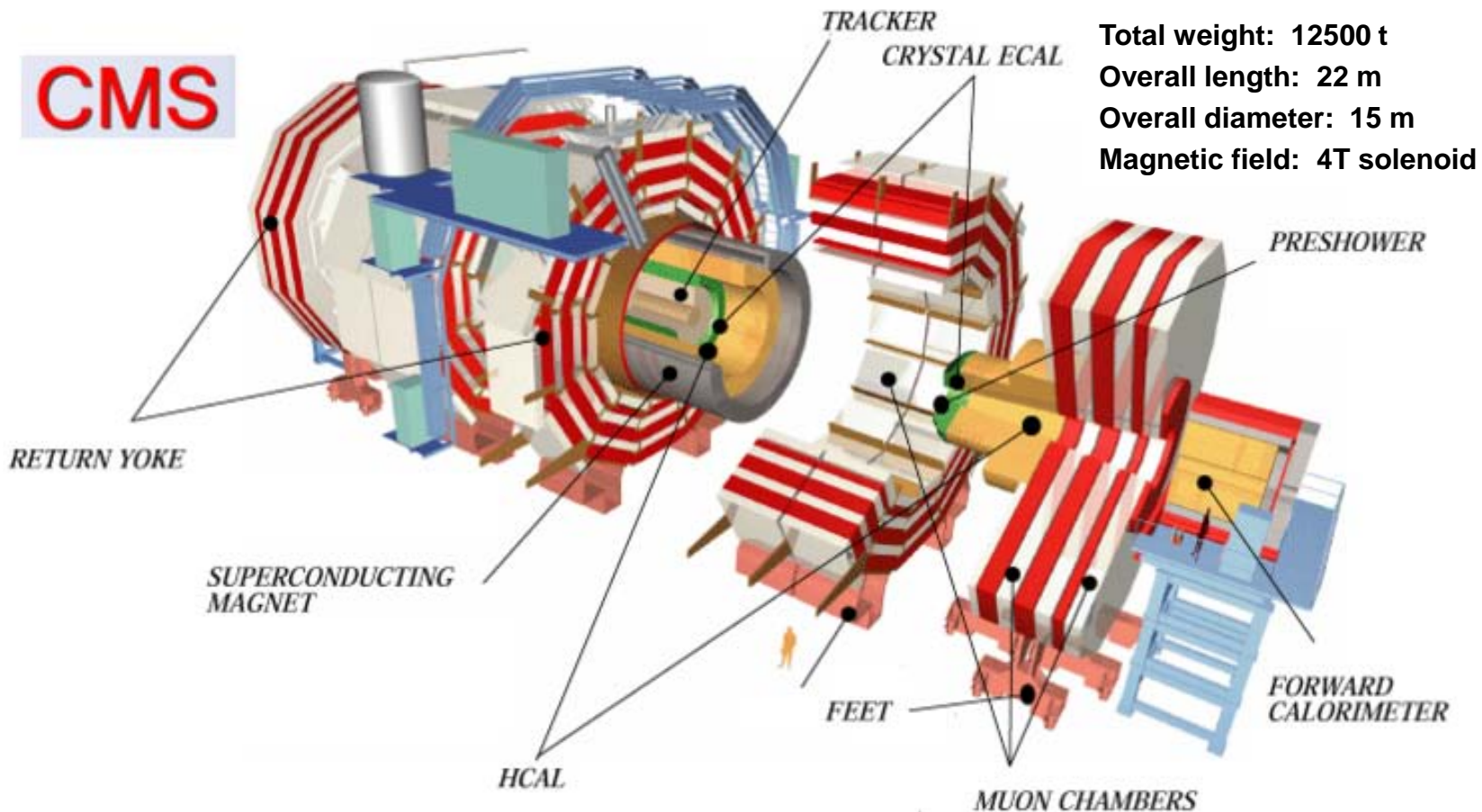
Current measurement

Pulse shapes





Total weight : 7000 t
Overall length: 46 m
Overall diameter: 23 m
Magnetic field: 2T solenoid
+ toroid



Tracking (inner detector)

Closest to the interaction vertex

Reconstructs charged particle tracks in magnetic field

Charged particles generate current Silicon pixel elements → fit tracks to (x,y,z) space points defined by hit sensor location

Collect secondary charges from gas ionizations by passing charged particles on wires in electric fields → fit tracks to space point in (x,y) plane and z from pulse timing

Solenoid field allows very precise p_T reconstruction and less precise p reconstruction

Reconstructs interaction vertices

Vertex reconstructed from track fits

More than one vertex possible

B-decays

Multiple proton interaction (pile-up)

Primary vertex defined by $\sum_{\text{tracks}} p_T = \max$ or $\sum_{\text{tracks}} p_T^2 = \max$

Advantages and limitations

Very precise for low p_T measurements $\frac{\Delta p_T}{p_T} \sim p_T$

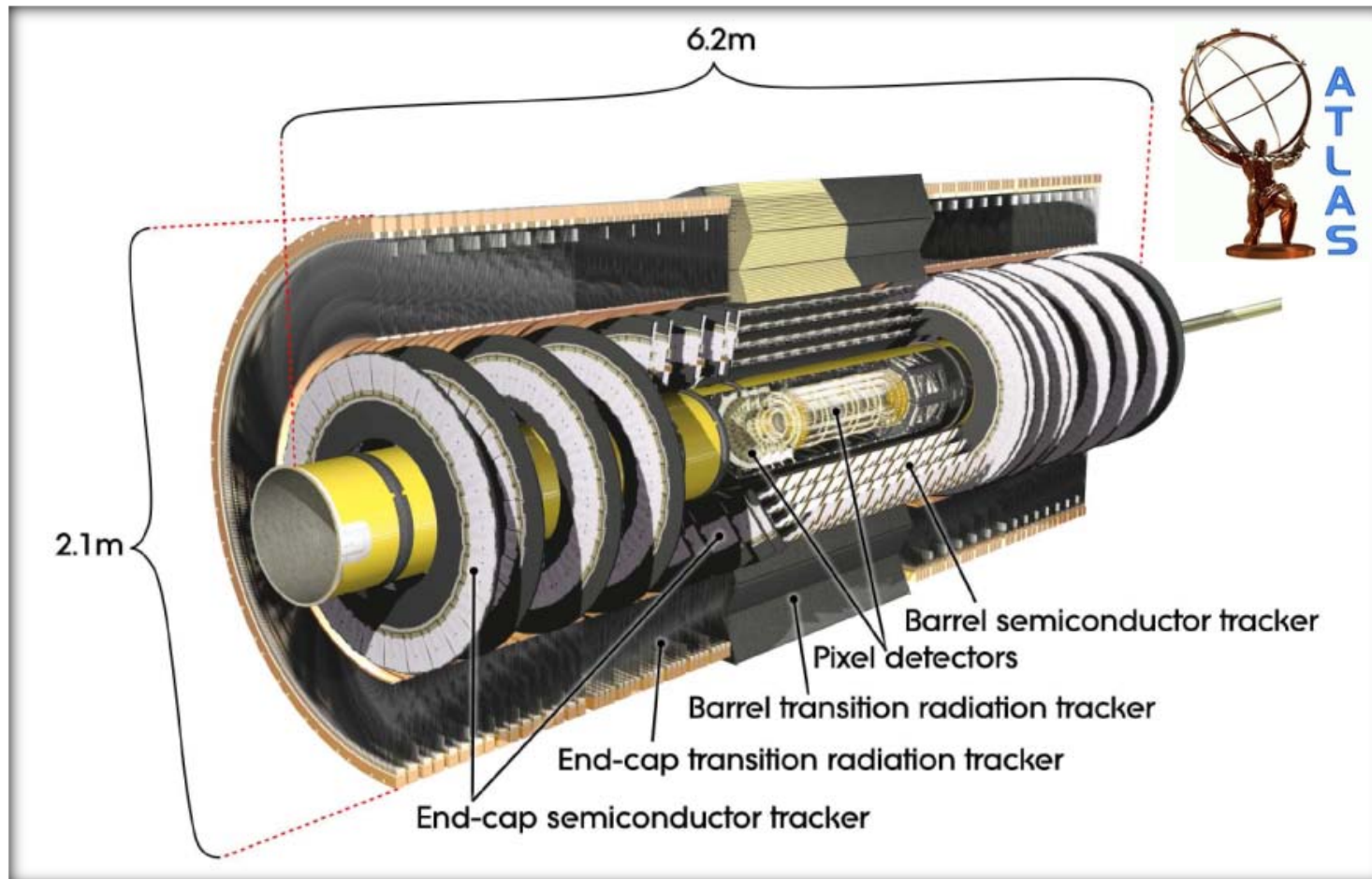
Only sensitive to charged particles

Limited polar angle coverage

Forward region in experiment excluded



Tracking (inner detector)



very precise for low p_T measurements $\frac{1}{p_T} \sim p_T$

Only sensitive to charged particles

Limited polar angle coverage

Forward region in experiment excluded

(x,y,z)
sensitive to
pulse



Calorimeters

Usually wrapped around inner detector

Measures the energy of charged and neutral particles

Uses the energy deposited by particles to generate signal

Collects light or electric charges/current from this energy deposit in relatively small volumes

Only works if particle energy can be fully absorbed

Signals are space points with energy

Reconstructs direction and energy from known position of energy deposit

Needs assumption for “mass” to convert signal to full four momentum

ATLAS: $m = 0$

Advantages and limitations

Gets more precise with increasing particle energy

Gives good energy measure for all particles except muons and neutrinos

Muons not fully absorbed!

Large coverage around interaction region

“ 4π ” detector – except for holes for beam pipes

Relation of incoming (deposited) energy and signal is particle type dependent

Also need to absorb all energy – large detector system

Does not work well for low energies

Particles have to reach calorimeter

Noise in readout

Slow signal formation in LHC environment



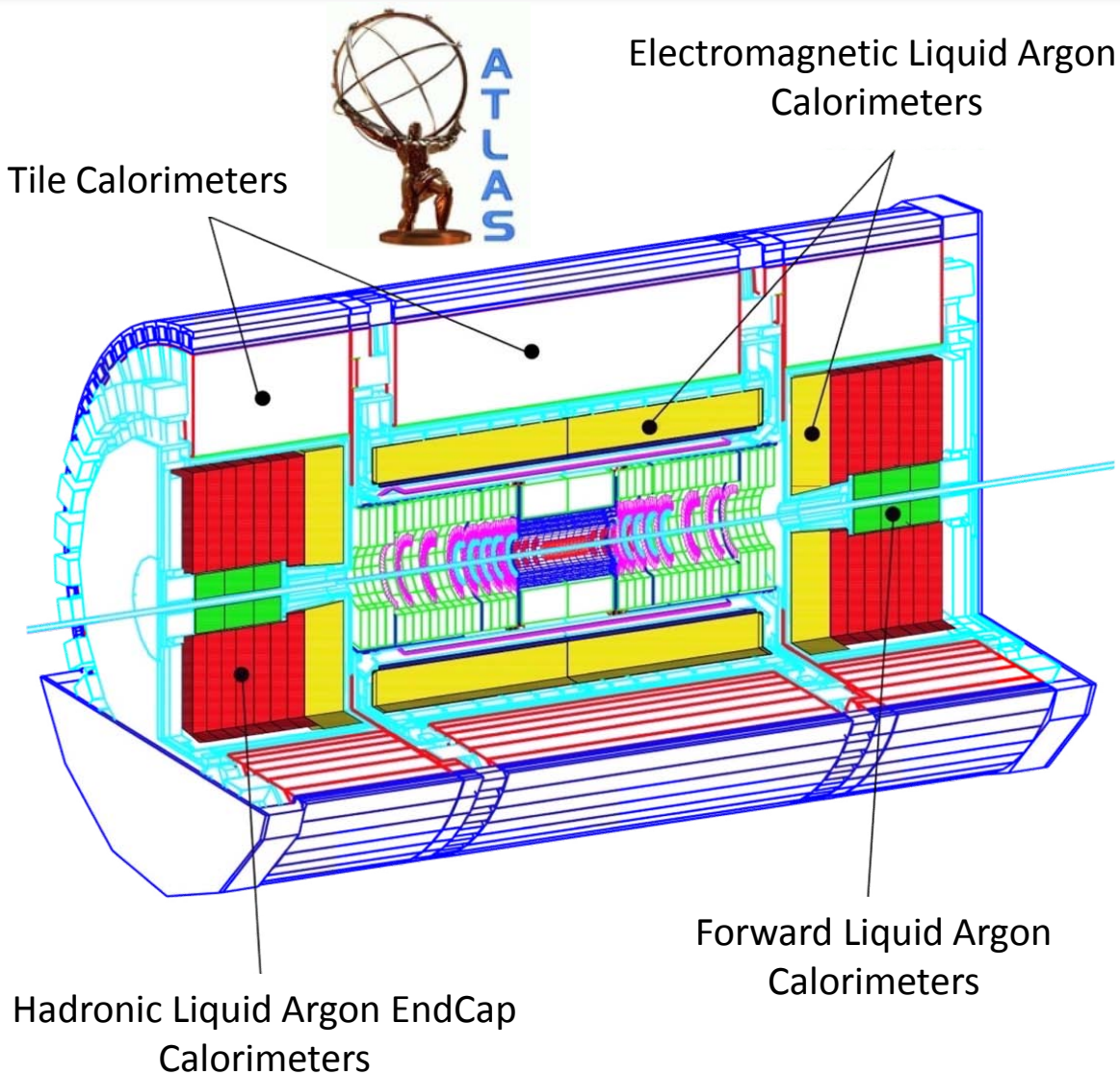
Calorim

Us

M

Si

Ac



all volumes



Cascades or showers

Most particles entering matter start a shower of secondary particles

Exception: muons and neutrinos

The character of these cascades depends on the nature of the particle

Electrons, photons: cascades are formed by QED processes

Hadrons: cascades are dominantly formed by QCD processes

Extensions/size of these showers

Again depends on particle type

Electromagnetic showers typically small and compact

Hadronic showers much larger

Common feature: shower depths scales approximately as $\log(E)$

Higher energies do not require much deeper detectors!

Shower development and age

Shower maximum

Depth at which energy of shower particles is too small to continue production of secondaries

Age of shower

Depth of shower

Shower width

Extend of shower perpendicular to direction of flight of incoming particle



QED drives cascade development

High energetic electrons entering material emit photons in the electric field of the nuclei

Bremsstrahlung

High energetic photons produce e+e- pairs in the electric field of the nuclei

Pair production

Rossi's shower model (1952!)

Simple model of interplay of electron energy loss and photon pair production

Uses critical energy as cutoff for shower development

Electron energy loss through bremsstrahlung after 1 radiation length (X_0) in matter: $E_0/2$

Assume this energy is taken by 1 photon, meaning the energy of each shower particle after $t X_0$ is: $E(t) = E_0/2^{N(t)}$, with $N(t) = 2^t$

The shower develops until $E(t) = E_c$ (critical energy - ionization loss becomes large and suppresses further radiation) at

the shower maximum $t_{\max} = \frac{\ln(E_0/E_c)}{\ln 2}$



QED drives cascade development

High energetic electrons entering material emit photons in the electric field of the nuclei

Bremsstrahlung

High energetic photons produce e⁺e⁻ pairs in the electric field of the nuclei

Pair production

Rossi's shower model (1952!)

Simple model of interplay of electron energy loss and photon pair production

Uses critical energy as cutoff for shower development

Electron energy loss through bremsstrahlung after 1 radiation length (X_0) in matter: $E_0/2$

Assume this energy is taken by 1 photon, meaning the energy of each shower particle after $t X_0$ is: $E(t) = E_0/2^{N(t)}$, with $N(t) = 2^t$

The shower develops until $E(t) = E_c$ (critical energy - ionization loss becomes large and suppresses further radiation) at

the shower maximum $t_{\max} = \frac{\ln(E_0/E_c)}{\ln 2}$



QED drives cascade development

High energetic electrons entering material emit photons in the electric field of the nuclei

Bremsstrahlung

High energetic photons produce e+e- pairs in the electric field of the nuclei

Pair production

Rossi's shower model (1952!)

Simple model of interplay of electron energy loss and photon pair production

Uses critical energy as cutoff for shower development

Electron energy loss through bremsstrahlung after 1 radiation length (X_0) in matter: $E_0/2$

Assume this energy is taken by 1 photon, meaning the energy of each shower particle after $t X_0$ is: $E(t) = E_0/2^{N(t)}$, with $N(t) = 2^t$

The shower develops until $E(t) = E_c$ (critical energy - ionization loss becomes large and suppresses further radiation) at

the shower maximum $t_{\max} = \frac{\ln(E_0/E_c)}{\ln 2}$



QED drives cascade development

High energetic electrons entering material emit photons in the electric field of the nuclei

Bremsstrahlung

High energetic photons produce e⁺e⁻ pairs in the electric field of the nuclei

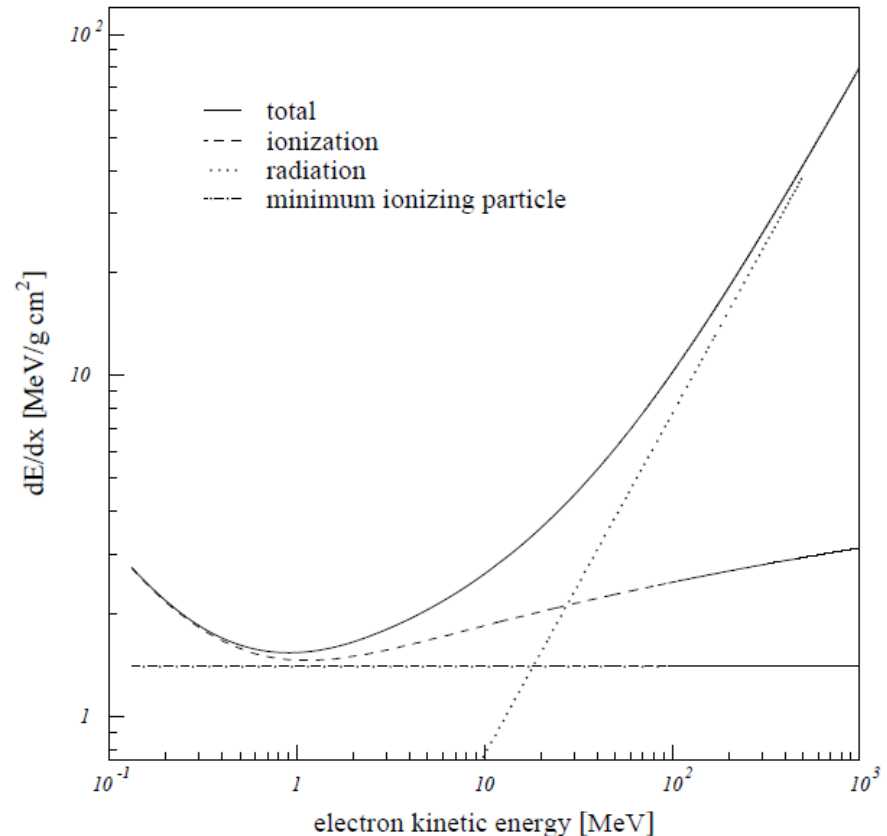
Pair production

Rossi's shower model (1952!)

Simple model of interplay of electron energy loss and photon pair production

Uses critical energy as cutoff for shower development

Electron energy loss through bremsstrahlung after 1 radiation length (X_0) in matter: $E_0/2$
Assume this energy is taken by 1 photon, meaning the energy of each shower particle after $t X_0$ is: $E(t) = E_0/2^{N(t)}$, with $N(t) = 2^t$



QED drives cascade development

High energetic electrons entering material emit photons in the electric field of the nuclei

Bremsstrahlung

High energetic photons produce e^+e^- pairs in the electric field of the nuclei

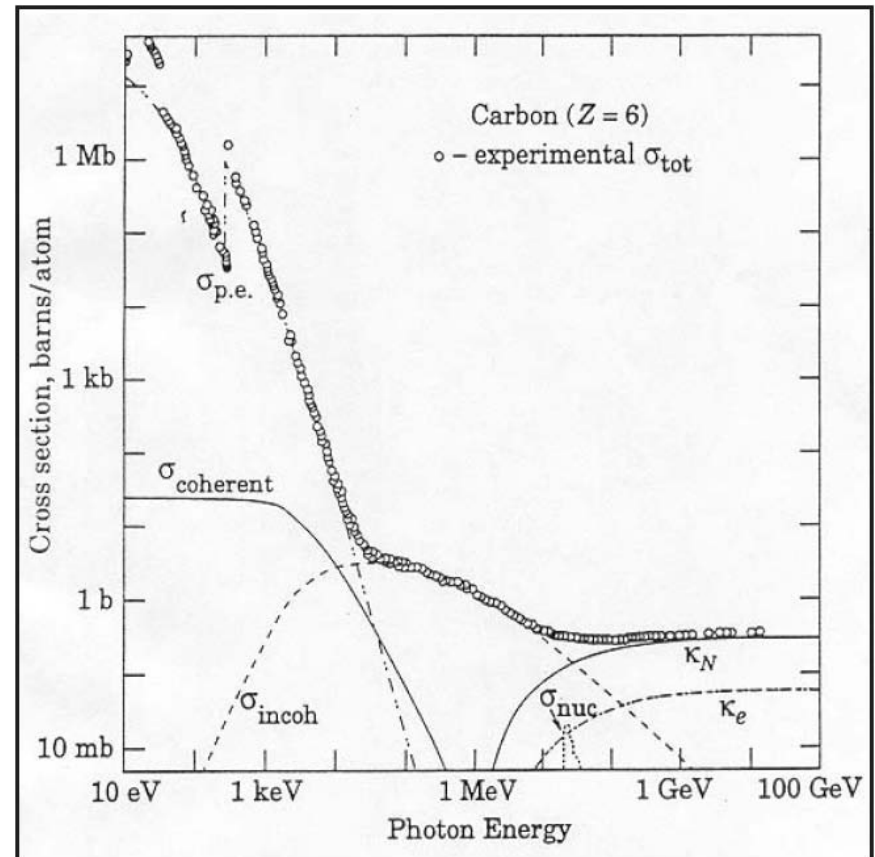
Pair production

Rossi's shower model (1952!)

Simple model of interplay of electron energy loss and photon pair production

Uses critical energy as cutoff for shower development

Electron energy loss through bremsstrahlung after 1 radiation length (X_0) in matter: $E_0/2$
Assume this energy is taken by 1 photon, meaning the energy of each shower particle after $t X_0$ is: $E(t) = E_0/2^{N(t)}$, with $N(t) = 2^t$



QCD drives fast shower development

Hadron interacts with nucleon in nuclei

Like a fixed target collision

Develops intra-nuclear cascade (fast)

Hadron production

Secondary hadrons escape nucleus

Neutral pions decay immediately into 2 photons → electromagnetic cascade

Other hadrons can hit other nucleons → internuclear cascade

Slow de-excitation of nuclei

Remaining nucleus in excited state

Evaporates energy to reach stable (ground) state

Fission and spallation possible

Binding energy and low energetic photons

Large process fluctuations

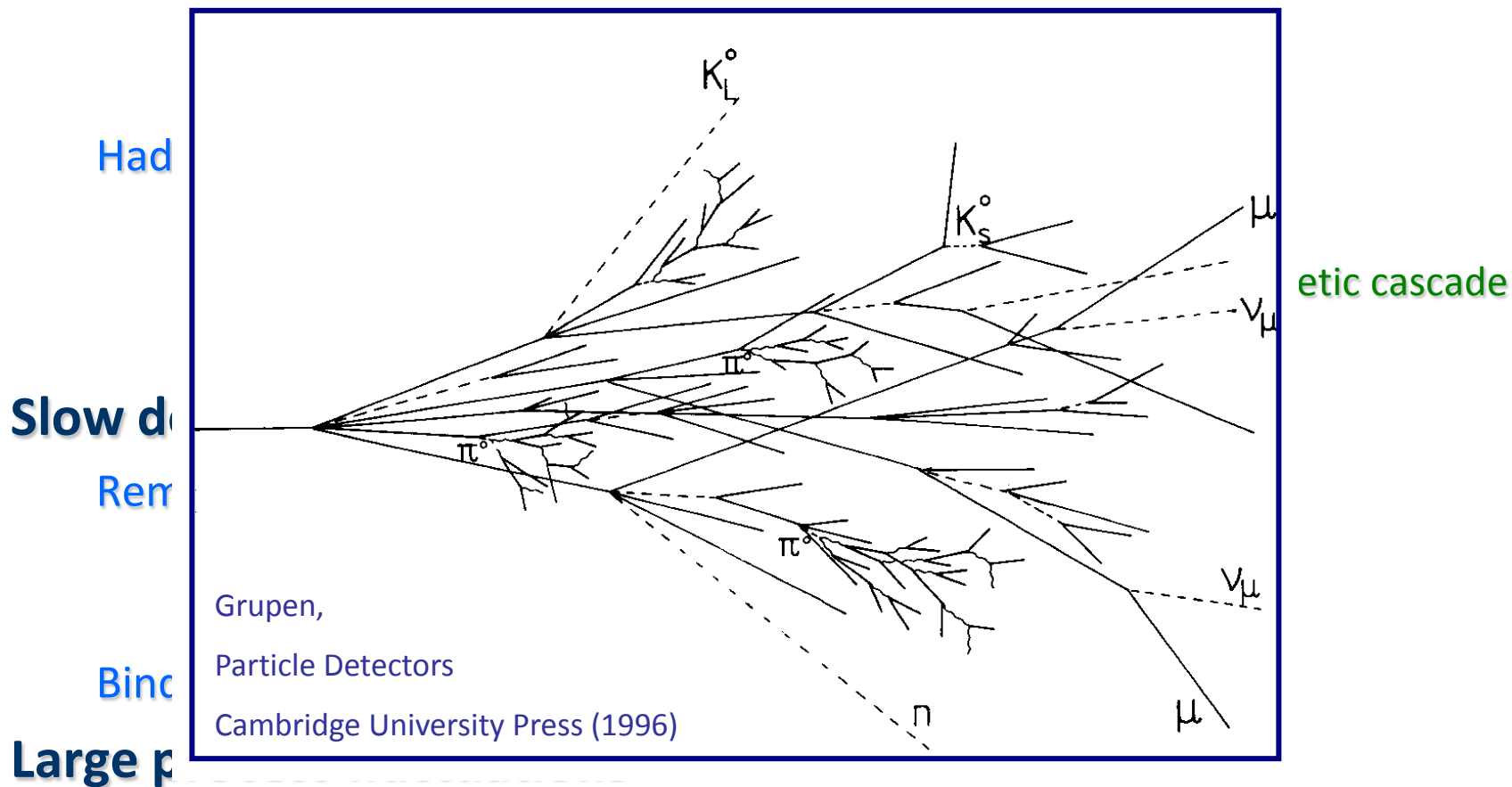
~200 different interactions

Probability for any one of those < 1%!



QCD drives fast shower development

Hadron interacts with nucleon in nuclei



~200 different interactions

Probability for any one of those < 1%!

Introduction to Hadronic Final State Reconstruction in Collider Experiments (Part III)

Peter Loch
University of Arizona
Tucson, Arizona
USA

Full absorption detector

Idea is to convert incoming particle energy into detectable signals

Light or electric current

Should work for charged and neutral particles

Exploits the fact that particles entering matter deposit their energy in particle cascades

Electrons/photons in electromagnetic showers

Charged pions, protons, neutrons in hadronic showers

Muons do not shower at all in general

Principal design challenges

Need dense matter to absorb particles within a small detector volume

Lead for electrons and photons, copper or iron for hadrons

Need “light” material to collect signals with least losses

Scintillator plastic, noble gases and liquids

Solution I: combination of both features

Crystal calorimetry, BGO

Solution II: sampling calorimetry



Sampling calorimeters

Use dense material for absorption power...

No direct signal

...in combination with highly efficient active material

Generates signal

Consequence: only a certain fraction of the incoming energy is directly converted into a signal

Typically 1-10%

Signal is therefore subjected to sampling statistics

The same energy loss by a given particle type may generate different signals

Limit of precision in measurements

Need to understand particle response

Electromagnetic and hadronic showers



Electromagnetic showers

Particle cascade generated by electrons/positrons and photons in matter

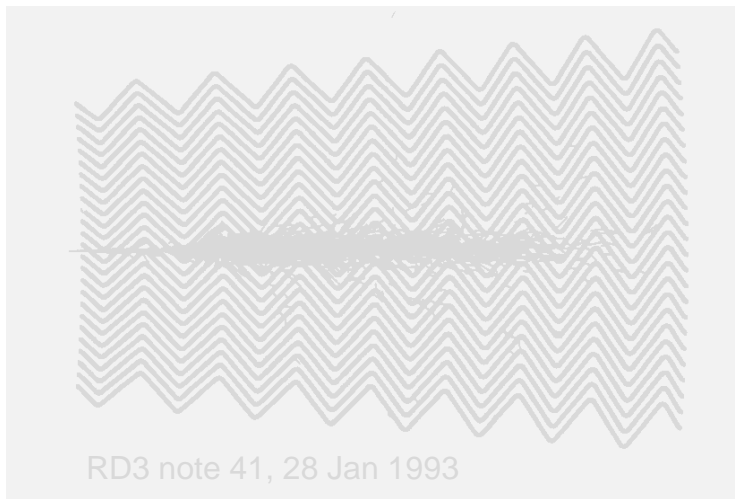
Developed by bremsstrahlung & pair-production

Compact signal expected

Regular shower shapes

Small shower-to-shower fluctuations

Strong correlation between longitudinal and lateral shower spread



Shower depth scales in **radiation length** X_0 :

$$X_0 \approx \frac{716.4 \cdot A}{Z(Z+1) \ln \frac{278}{\sqrt{Z}}} \text{ g} \cdot \text{cm}^{-2}$$

Approximation good within $\pm 2\%$ for all materials except **Helium (5% low)**

Shower width scales in **Moliere Radii** R_M :

$$R_M \approx \frac{E_s}{E_c} X_0 \approx \frac{21 \text{ MeV} \cdot (Z+1.2)}{800 \text{ MeV}} X_0$$

$$= 0.0265 \cdot X_0 (Z+1.2)$$

(90% energy containment radius)

$$\text{with } \begin{cases} E_s \approx 21 \text{ MeV} \\ E_c \approx \frac{800 \text{ MeV}}{Z+1.2} \end{cases}$$

[C. Amsler et al.](#) (Particle Data Group), Physics Letters **B667**, 1 (2008) and 2009 partial update for the 2010 edition



Electromagnetic showers

Particle cascade generated by electrons/positrons and photons in matter

Developed by bremsstrahlung & pair-production

Compact signal expected

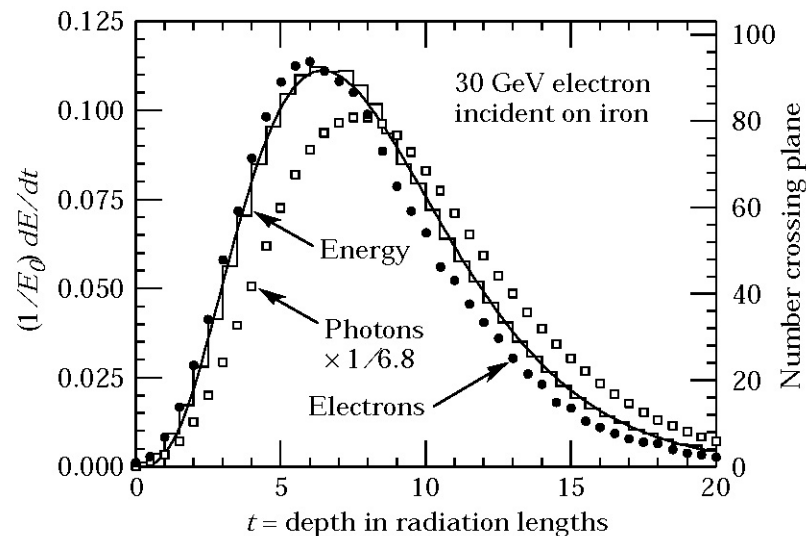
Regular shower shapes

Small shower-to-shower fluctuations

Strong correlation between longitudinal and lateral shower spread



RD3 note 41, 28 Jan 1993



$$\frac{dE}{dt} = E_0 b \frac{(bt)^{a-1} e^{-bt}}{\Gamma(a)}, \text{ with } t = x/X_0$$

$$t_{\max} = (a-1)/b = 1.0 \times (\ln y + C_j),$$

with $y = E/E_c$ and

$$C_j = \begin{cases} -0.5 & \text{for } e^\pm \\ +0.5 & \text{for } \gamma \end{cases}$$

[C. Amisler et al.](#) (Particle Data Group), Physics Letters **B667**, 1 (2008) and 2009 partial update for the 2010 edition

Electromagnetic showers

Particle cascade generated by electrons/positrons and photons in matter

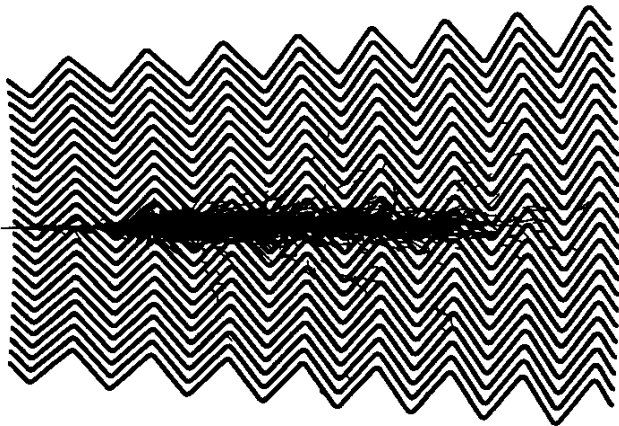
Developed by bremsstrahlung & pair-production

Compact signal expected

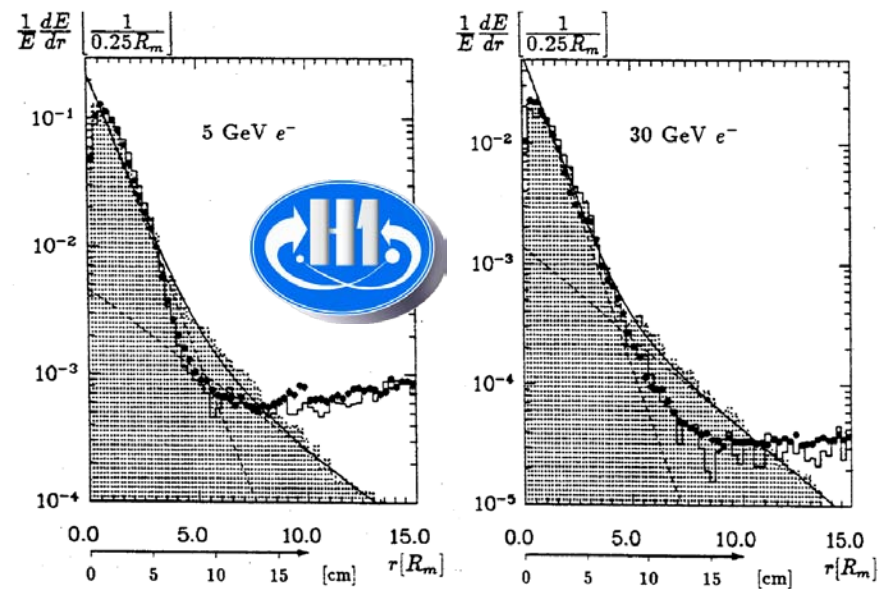
Regular shower shapes

Small shower-to-shower fluctuations

Strong correlation between longitudinal and lateral shower spread



RD3 note 41, 28 Jan 1993



P. Loch (Diss.), University of Hamburg 1992

$$\frac{1}{E} \frac{dE}{dr} = a(E) \cdot e^{-\alpha(E)r} + b(E) \cdot e^{-\beta(E)r}$$

[G.A. Akopdzhanov et al.](#) (Particle Data Group), Physics Letters **B667**, 1 (2008) and 2009 partial update for the 2010 edition

Hadronic signals

Much larger showers

Need deeper development

Wider shower spread

Large energy losses without signal generation in hadronic shower component

Binding energy losses

Escaping energy/slow particles (neutrinos/neutrons)

Signal depends on size of electromagnetic component

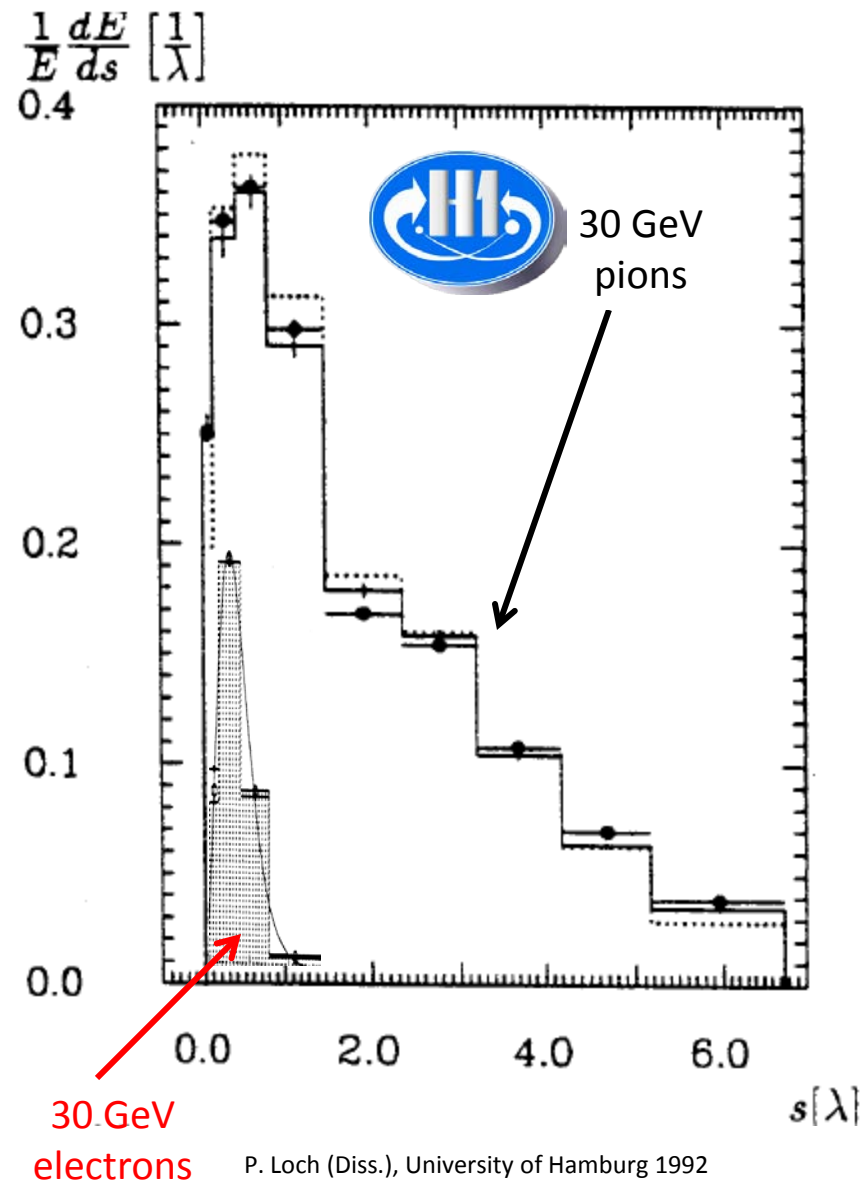
Energy invested in neutral pions lost for further hadronic shower development

Fluctuating significantly shower-by-shower

Weakly depending on incoming hadron energy

Consequence: non-compensation

Hadrons generate less signal than electrons depositing the same energy



Electromagnetic

Compact

Growths in depth $\sim \log(E)$

Longitudinal extension scale is radiation length X_0

Distance in matter in which $\sim 50\%$ of electron energy is radiated off

Photons $9/7 X_0$

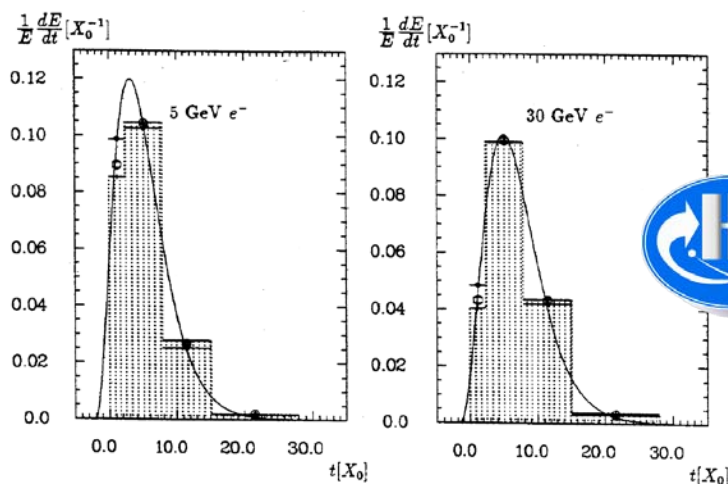
Strong correlation between lateral and longitudinal shower development

Small shower-to-shower fluctuations

Very regular development

Can be simulated with high precision

1% or better, depending on features



Hadronic

Scattered, significantly bigger

Growths in depth $\sim \log(E)$

Longitudinal extension scale is interaction length $\lambda \gg X_0$

Average distance between two inelastic interactions in matter

Varies significantly for pions, protons, neutrons

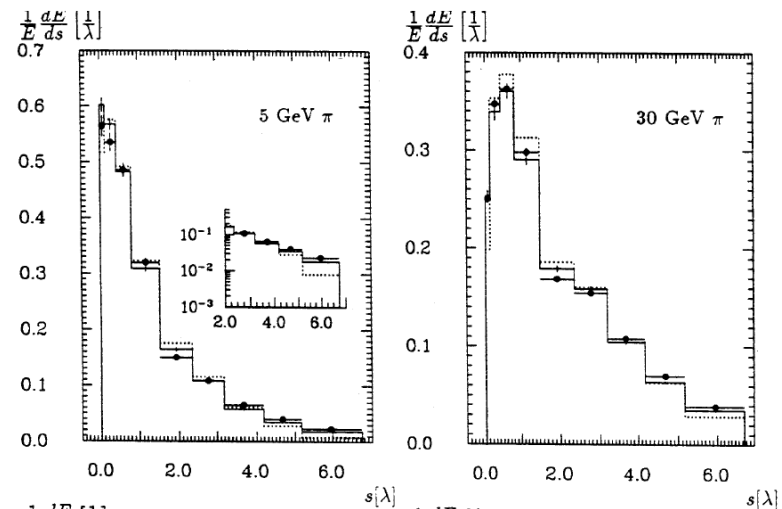
Weak correlation between longitudinal and lateral shower development

Large shower-to-shower fluctuations

Very irregular development

Can be simulated with reasonable precision

$\sim 2-5\%$ depending on feature



Signal features in sampling calorimeters

Collected from ionizations in active material

Not all energy deposit converted to signal

Proportional to incoming electron/photon

C.f. Rossi's shower model,
Approximation B

Only charged tracks contribute to signal

Only pair-production for photons

Energy loss is constant

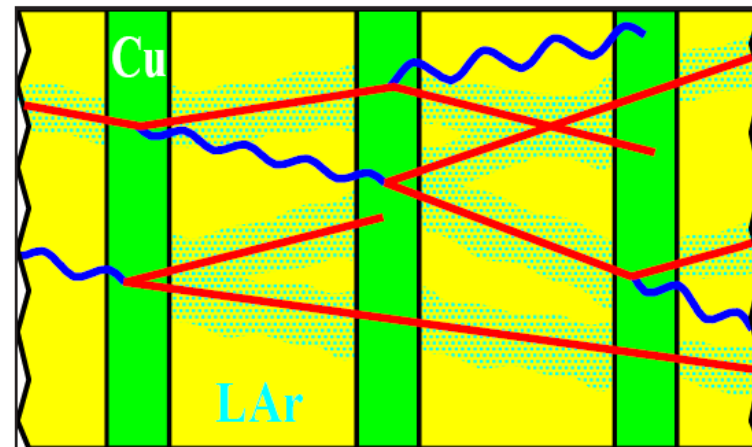
Signal proportional to integrated shower particle path

Stochastic fluctuations

Sampling character

Sampling fraction

Describes average fraction of deposited energy generating the signal



Integrated shower particle track length:

$$T = \int_0^{t_{\max}} N(t) dt \Rightarrow T_c = \frac{2}{3} T = \frac{2}{3 \ln 2} \frac{E_0}{E_c}$$

(only charged tracks ionize!)

Number of crossings of active material:

$$N_x = \frac{T_c}{d_{\text{active}}} \propto E_0$$

Deposited energy contributing to the signal:

$$E_{\text{vis}} = N_x \int_0^{d_{\text{active}}} \frac{dE}{dx} dx = N_x \Delta E \propto E_0$$

Stochastic nature of sampling:

$$\sigma(N_x) = \sqrt{N_x} \Rightarrow \sigma(E_{\text{vis}}) \propto \sqrt{N_x \Delta E} \propto \sqrt{E_0}$$



Characterizes sampling calorimeters

Ratio of energy deposited in active material and total energy deposit

Assumes constant energy loss per unit depth in material

Ionization only

Can be adjusted when designing the calorimeter

Material choices

Readout geometry

Multiple scattering

Changes sampling fraction

Effective extension of particle path in matter

Different for absorber and active material

Showering

Cannot be included in sampling fraction analytically

Need measurements and/or simulations

$$S = \frac{E_{\text{vis}}}{E_{\text{dep}}} = \frac{dE/dx|_{\text{active}} \cdot d_{\text{active}}}{dE/dx|_{\text{active}} \cdot d_{\text{active}} + dE/dx|_{\text{absorber}} \cdot d_{\text{absorber}}}$$

$$= \frac{dE/dx|_{\text{active}}}{dE/dx|_{\text{active}} + dE/dx|_{\text{absorber}} \cdot d_{\text{absorber}}/d_{\text{active}}}$$

(with Rossi's assumption $dE/dx|_{\text{active}} = \text{const}$

and $dE/dx|_{\text{absorber}} = \text{const}$)



Characterizes sampling calorimeters

Ratio of energy deposited in active material and total energy deposit

Assumes constant energy loss per unit depth in material

Ionization only

Can be adjusted when designing the calorimeter

Material choices

Readout geometry

Multiple scattering

Changes sampling fraction

Effective extension of particle path in matter

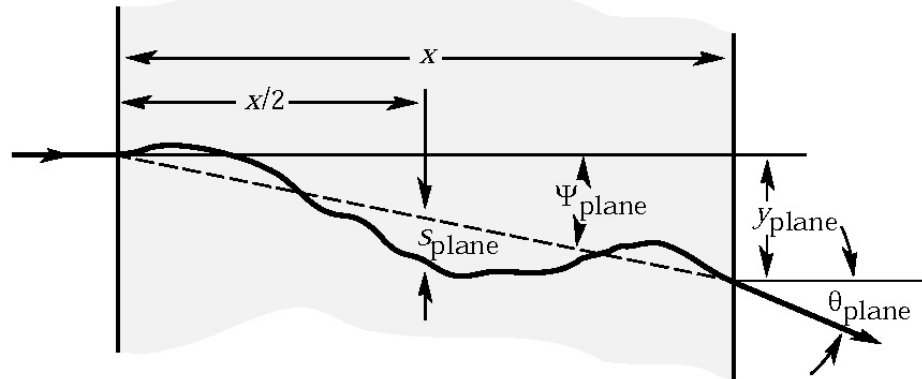
Different for absorber and active material

Showering

Cannot be included in sampling fraction analytically

Need measurements and/or simulations

C. Amsler *et al.* (Particle Data Group), Physics Letters **B667**, 1 (2008) and 2009 partial update for the 2010 edition



$$S = \frac{E_{\text{vis}}}{E_{\text{dep}}} = \frac{dE/dx|_{\text{active}}}{dE/dx|_{\text{active}} + dE/dx|_{\text{absorber}} \cdot d_{\text{absorber}}/d_{\text{active}} \cdot \cos\theta_{\text{active}}/\cos\theta_{\text{absorber}}}$$

Approximation:

$$\theta = \frac{13.6 \text{ MeV}}{\beta c p} z \sqrt{x/X_0} \left[1 + 0.038 \cdot \ln \frac{x}{X_0} \right]$$

with

$$\begin{cases} \beta c & \text{particle velocity} \\ p & \text{particle momentum} \\ z & \text{particle charge number} \\ x/X_0 & \text{material thickness in radiation length} \end{cases}$$

(good to 11% for singly charged particles with $\beta = 1$ for all matter and within $10^{-1} < x/X_0 < 100$)



Characterizes sampling calorimeters

Ratio of energy deposited in active material and total energy deposit

Assumes constant energy loss per unit depth in material

Ionization only

Can be adjusted when designing the calorimeter

Material choices

Readout geometry

Multiple scattering

Changes sampling fraction

Effective extension of particle path in matter

Different for absorber and active material

Showering

Cannot be included in sampling fraction analytically

Need measurements and/or simulations

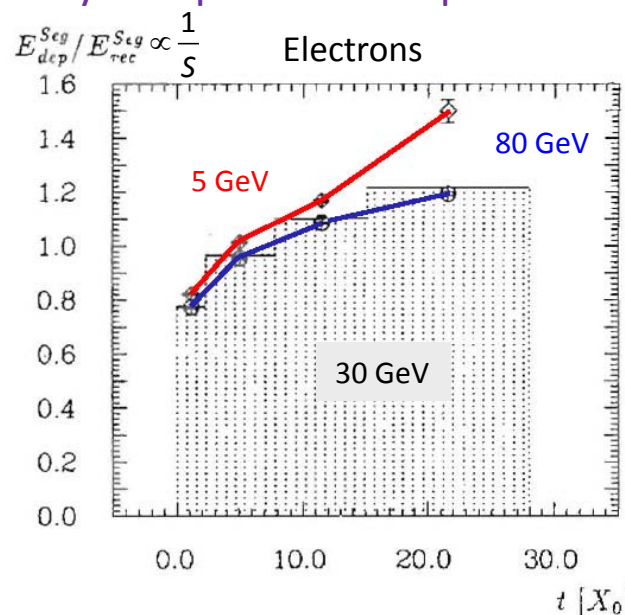
$$S = \frac{E_{\text{vis}}}{E_{\text{dep}}} \propto \frac{A(E_0)}{E_0}$$

$A(E_0)$ is the calorimeter signal from test beams or simulation, converted to energy units.

Showering changes the electron sampling fraction mostly due to the strong dependence of photon capture (photo-effect) on the material (cross-section $\sim Z^5$) leading to a non-proportional absorption of energy carried by soft photons deeper in the shower!



P. Loch (Diss.),
University of
Hamburg 1992



Example: charge collection in noble liquids

Charged particles ionizing active medium when traversing it

Fast passage compared to electron drift velocity in medium

Electrons from these ionizations are collected in external electric field

Similar to collection of 1-dim "line of charges" with constant charge density

Resulting (electron) current is base of signal

Positive ions much slower

Can collect charges or measure current

Characteristic features

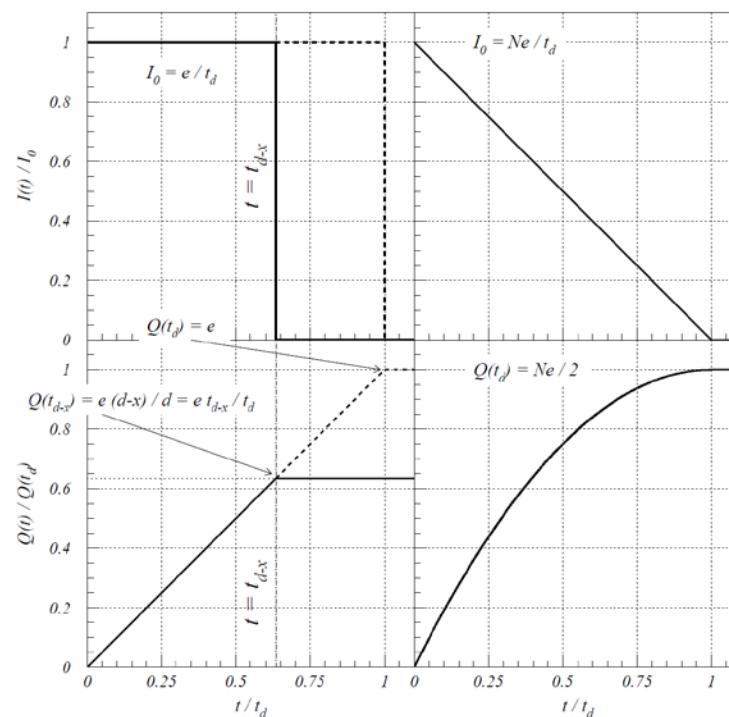
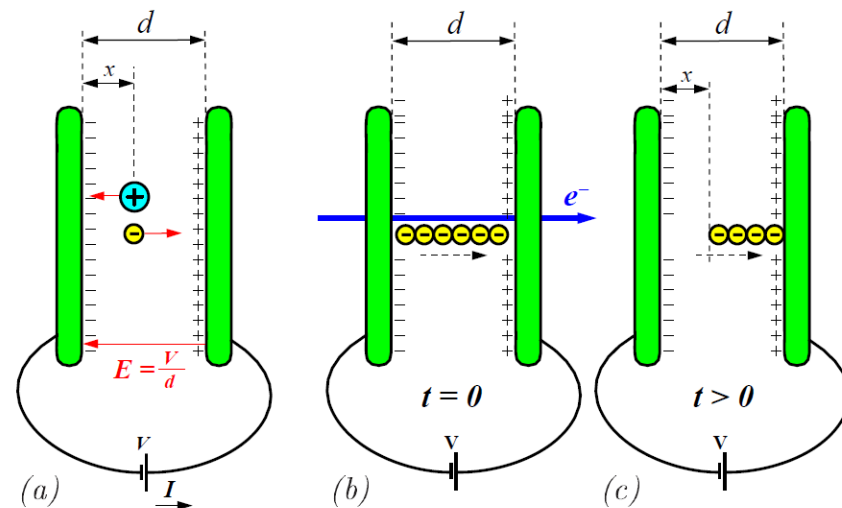
Collected charge and current are proportional to energy deposited in active medium

$$Q(t = t_d) = \frac{N_e e}{2}; \quad I(t = t_0) = \frac{N_e e}{t_d}; \quad N_e = \frac{E_{\text{vis}}}{E_{\text{ion}}}$$

Drift time for electrons in active medium

Determines charge collection time

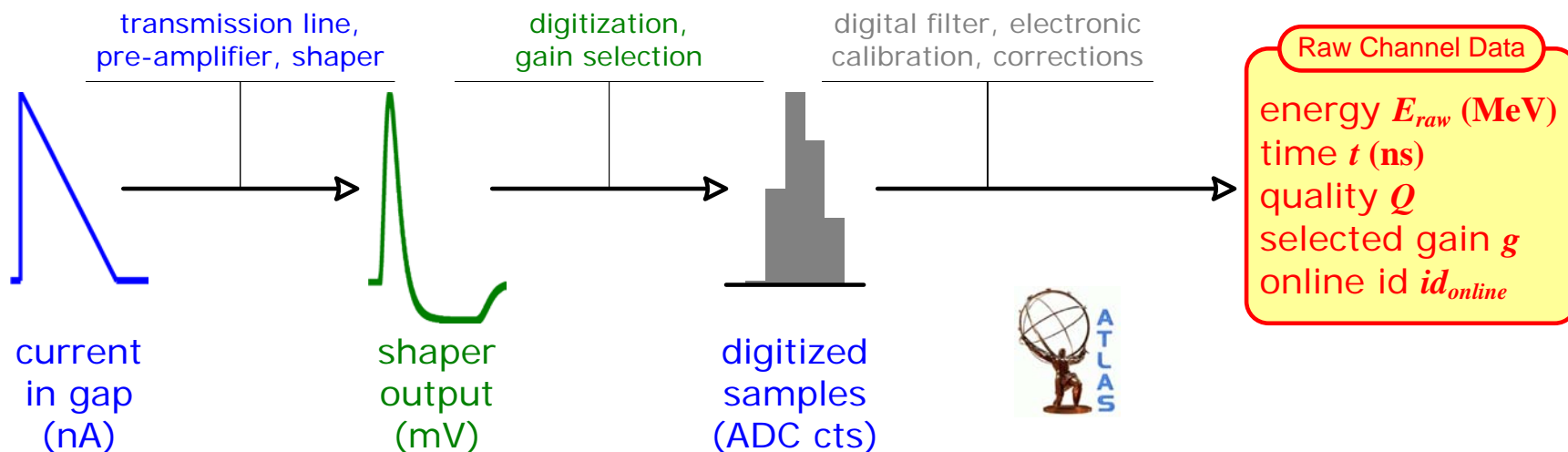
Can be adjusted to optimize calorimeter performance



Introduction to Hadronic Final State Reconstruction in Collider Experiments (Part IV)

Peter Loch
University of Arizona
Tucson, Arizona
USA





What is response?

Reconstructed calorimeter signal

Based on the direct measurement – the raw signal
 May include noise suppression

Has the concept of **signal (or energy) scale**

Mostly understood as the basic signal before final calibrations

Does not explicitly include particle or jet hypothesis

Uses only calorimeter signal amplitudes, spatial distributions, etc.

$$E_{raw} = A_{peak} \times \underbrace{[\text{ADC} \rightarrow \text{nA}]}_{\text{current calibration}}$$

$$\times \underbrace{([\text{HV}] \times [\text{cross-talk}] \times [\text{purity}])}_{\text{electronic and efficiency corrections}}$$

$$\times \underbrace{[\text{nA} \rightarrow \text{MeV}]}_{\text{energy calibration}}$$



Slow signal collection in liquid argon calorimeters

~450 ns @ 1 kV/mm drift time versus 40 MHz/25 ns bunch crossing time

Measure only $I_0 = I(t_0)$
(integrate <25 ns)

Applying a fast bi-polar signal shaping

Shaping time ~15 ns

With well known shape

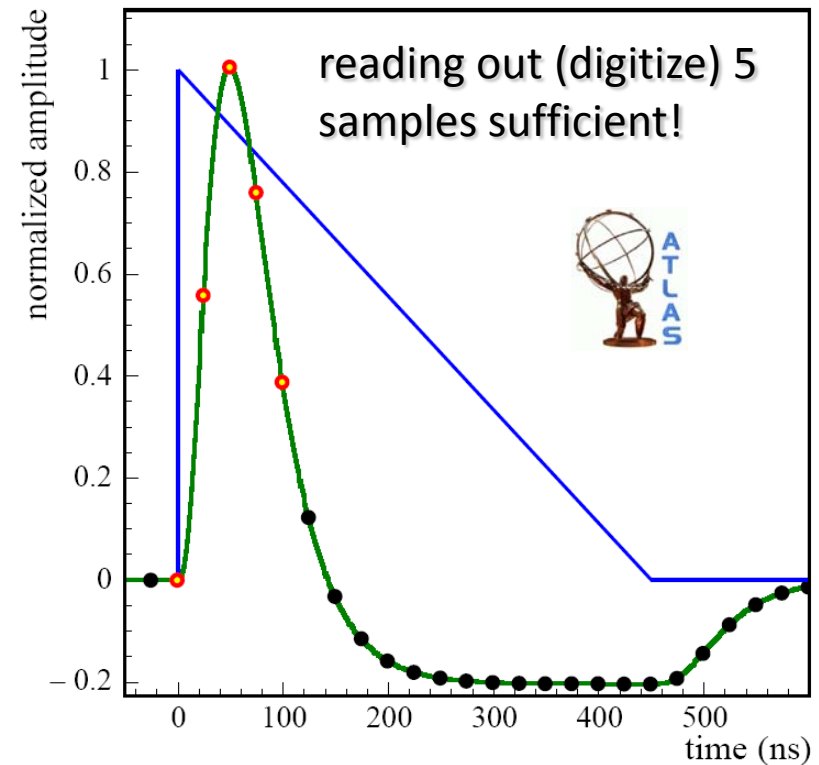
Shaped pulse integral = 0

Net average signal contribution from pile-up = 0

Need to **measure the pulse shape** (time sampled readout)

Total integration ~25 bunch crossings

23 before signal, 1 signal, 1 after signal



What is digital filtering

Unfolds the expected (theoretical) pulse shape from a measured pulse shape

Determines signal amplitude and timing

Minimizes noise contributions

Noise reduced by ~1.4 compared to single reading

Note: noise depends on the luminosity

Requires explicit knowledge of pulse shape

Folds triangular pulse with transmission line characteristics and active electronic signal shaping

Characterized by signal transfer functions depending on R , L , C of readout electronics, transmission lines

Filter coefficients from calibration system

Pulse “ramps” for response

Inject known currents into electronic chain

Use output signal to constrain coefficients

Noise for auto-correlation

Signal history couples fluctuations in time sampled readings

Signal amplitude A_{peak} (energy):

$$A_{\text{peak}} = \sum_{i=1}^{N_s} a_i (s_i - p), \text{ with } \begin{cases} a_i & \text{digital filter coefficient} \\ s_i & \text{reading in time sample} \\ p & \text{pedestal reading} \end{cases}$$

Signal peak time t_{peak} :

$$A_{\text{peak}} t_{\text{peak}} = \sum_{i=1}^{N_s} b_i (s_i - p)$$

W.E. Cleland and E.G. Stern, Nucl. Inst. Meth. **A338 (1994) 467**.



What is digital filtering

Unfolds the expected (theoretical) pulse shape from a measured pulse shape

Determines signal amplitude and timing

Minimizes noise contributions

Noise reduced by ~ 1.4 compared to single reading

Note: noise depends on the luminosity

Requires explicit knowledge of pulse shape

Folds triangular pulse with transmission line characteristics and active electronic signal shaping

Characterized by signal transfer functions depending on R , L , C of readout electronics, transmission lines

Filter coefficients from calibration system

Pulse “ramps” for response

Inject known currents into electronic chain

Use output signal to constrain coefficients

Noise for auto-correlation

Signal history couples fluctuations in time sampled readings

Signal amplitude A_{peak} (energy):

$$A_{\text{peak}} = \sum_{i=1}^{N_s} a_i (s_i - p), \text{ with } \begin{cases} a_i & \text{digital filter coefficient} \\ s_i & \text{reading in time sample} \\ p & \text{pedestal reading} \end{cases}$$

Signal peak time t_{peak} :

$$A_{\text{peak}} t_{\text{peak}} = \sum_{i=1}^{N_s} b_i (s_i - p)$$

W.E. Cleland and E.G. Stern, Nucl. Inst. Meth. **A338 (1994) 467**.



Constraints for digital filter coefficients a_i :

$$\sum_{i=1}^{N_s} a_i g_i = 1, \text{ with } g_i \text{ being the}$$

normalized physics pulse shape

$$\sum_{i=1}^{N_s} a_i \frac{\partial g_i}{\partial t} = 0$$





S_i signal amplitude in sample i
 P analog-to-digital converter pedestal
 N_s number of digital samples (def. 5)
 a_i digital filter coefficient
 R_{ij} noise auto-correlation
 g_i normalized physics pulse shape:

Filter Coefficients

Determined by:

- Known pulse shape
- Minimizing noise

to 1st order
independent
of time jitter!

$$\sum_{i=1}^{N_s} a_i g_i = 1$$

$$\sum_{i=1}^{N_s} a_i \frac{\partial g_i}{\partial t} = \sum_{i=1}^{N_s} a_i g'_i = 0$$

$$\sum_{i=1}^{N_s} \sum_{j=1}^{N_s} a_i a_j \sigma_i \sigma_j R_{ij} \rightarrow \min$$

$$a_i = \sum_{j=1}^{N_s} R_{ij}^{-1} (\lambda g_j - \mu g'_j) \left\{ \begin{array}{l} \lambda = \frac{1}{\Delta} \sum_{i=1}^{N_s} \sum_{j=1}^{N_s} R_{ij}^{-1} g'_i g'_j \\ \mu = \frac{1}{\Delta} \sum_{i=1}^{N_s} \sum_{j=1}^{N_s} R_{ij}^{-1} g_i g'_j \\ \Delta = \left(\sum_{i=1}^{N_s} \sum_{j=1}^{N_s} R_{ij}^{-1} g'_i g'_j \right) \cdot \left(\sum_{i=1}^{N_s} \sum_{j=1}^{N_s} R_{ij}^{-1} g_i g_j \right) - \left(\sum_{i=1}^{N_s} \sum_{j=1}^{N_s} R_{ij}^{-1} g_i g'_j \right)^2 \end{array} \right.$$

Lagrange Multipliers



What does signal or energy scale mean?

Indicates a certain level of signal reconstruction

Standard reconstruction often stops with a **basic signal scale**

Electromagnetic energy scale is a good reference

Uses direct signal proportionality to electron/photon energy

Accessible in test beam experiments

Can be validated with isolated particles in collision environment

Provides good platform for data and simulation comparisons

Does not necessarily convert the electron signal to the true photon/electron energy!

Hadronic signals can also be calculated on this scale

Good platform for comparisons to simulations

But does not return a good estimate for the deposited energy in non-compensating calorimeters – see later discussion!

Is not a fundamental concept of physics!

Is a calorimeter feature

Definition varies from experiment to experiment

Recall electrons/photons in sampling calorimeters:

$$E_{\text{vis}} = N_x \int_0^{d_{\text{active}}} \frac{dE}{dx} dx = N_x \Delta E \propto E_0$$

Electron sampling fraction S_e relates signal and deposited energy:

$$S_e = \frac{E_{\text{vis}}}{E_{\text{dep}}} \approx \frac{E_{\text{vis}}}{E_0} \rightarrow E_{\text{rec}}^{\text{em}} = \frac{1}{S_e} E_{\text{vis}} = c_e A \equiv E_{\text{dep}} \approx E_0$$

with c_e being the electron calibration constant.

(S_e is a unitless fraction, c_e converts a signal unit into an energy unit, e.g. nA \rightarrow MeV)

Response often denoted $e = e(E_{\text{dep}}) = E_{\text{rec}}^{\text{em}}(c_e, A)$



Single hadron response:

$$\pi(E_0) = f_{em}(E_0) \cdot e + (1 - f_{em}(E_0)) \cdot h$$

with $\left\{ \begin{array}{l} f_{em}(E_0) \text{ intrinsic em fraction} \\ h \text{ response of pure} \\ \text{hadronic shower branch} \end{array} \right.$

Non-compensation measure:

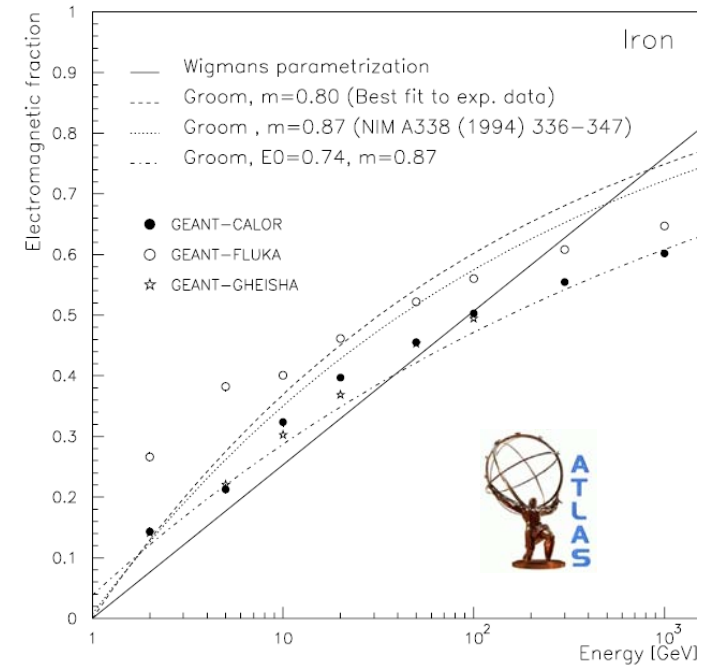
$$\frac{e}{\pi} = \frac{1}{f_{em}(E_0) + (1 - f_{em}(E_0)) \cdot h/e}$$

Popular parametrization by Groom et al.:

$$f_{em}(E_0) = 1 - (E_0/E_{base})^{m-1}$$

$$m = 0.80 - 0.85, E_{base} = \begin{cases} 1.0 \text{ GeV} & \text{for } \pi^\pm \\ 2.6 \text{ GeV} & \text{for } p \end{cases}$$

D.Groom et al., NIM A338, 336-347 (1994)



Observable

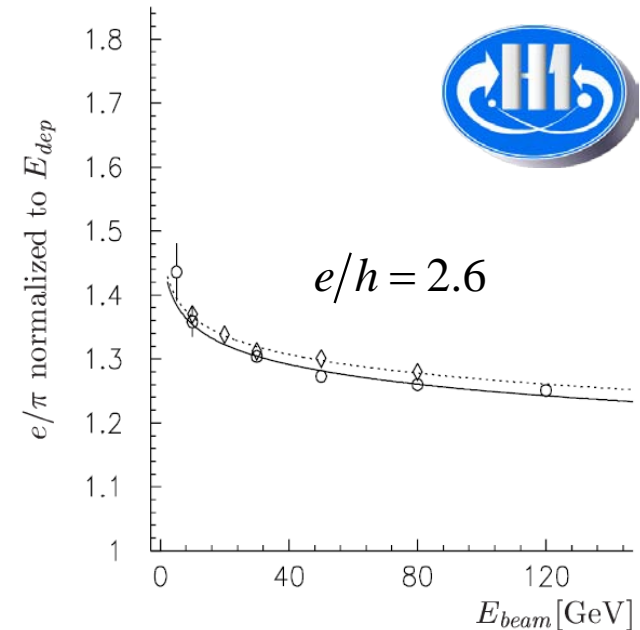
$$\frac{e}{\pi} = \frac{e}{\left(E_0/E_{\text{base}}\right)^{m-1} h + \left(1 - \left(E_0/E_{\text{base}}\right)^{m-1}\right) e}$$

$$= \frac{1}{1 - \left(1 - h/e\right) \left(E_0/E_{\text{base}}\right)^{m-1}}$$

provides experimental access to characteristic calorimeter variables in pion test beams by fitting h/e , E_{base} and m from the energy dependence of the pion signal on electromagnetic energy scale:

$$\frac{e}{\pi} = \frac{E_0}{E_{\text{rec}}^{\text{em}}(\pi)} \approx \frac{E_{\text{dep}}}{E_{\text{rec}}^{\text{em}}(\pi)}$$

Note that e/h is often constant, for example: in both H1 and ATLAS about 50% of the energy in the hadronic branch generates a signal independent of the energy itself



Complex mixture of hadrons and photons

Not a single particle response
 Carries initial electromagnetic energy

Mainly photons

Very simple response model

Assume the hadronic jet content is represented by 1 particle only

Not realistic, but helpful to understand basic response features

More evolved model

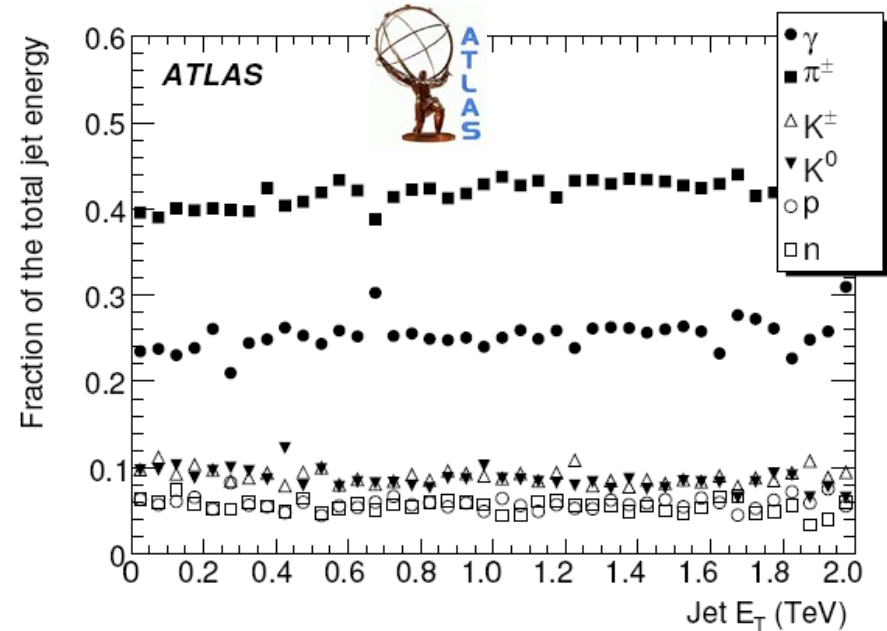
Use fragmentation function in jet response

This has some practical considerations

E.g. jet calibration in CDF

Gets non-compensation effect

Does not address acceptance effect due to shower overlaps



Complex mixture of hadrons and photons

Not a single particle response
Carries initial electromagnetic energy

Mainly photons

Very simple response model

Assume the hadronic jet content is represented by 1 particle only

Not realistic, but helpful to understand basic response features

More evolved model

Use fragmentation function in jet response

This has some practical considerations

E.g. jet calibration in CDF

Gets non-compensation effect

Does not address acceptance effect due to shower overlaps

$$\frac{j(E_{\text{jet}})}{e} = f_{\gamma}^{\text{jet}} + (1 - f_{\gamma}^{\text{jet}}) \cdot \left(f_{\text{em}} + (1 - f_{\text{em}}) \frac{h}{e} \right)$$

$$f_{\text{em}} = f_{\text{em}}(E_{\text{jet}}^{\text{had}}), \quad E_{\text{jet}}^{\text{had}} = (1 - f_{\gamma}^{\text{jet}}) E_{\text{jet}}$$

[single particle approximation]

$$f_{\text{em}} = 1 - \left(\frac{E_{\text{jet}}^{\text{had}}}{E_{\text{base}}} \right)^{1-m}$$

[Groom's parameterization]



Complex mixture of hadrons and photons

Not a single particle response
 Carries initial electromagnetic energy

Mainly photons

Very simple response model

Assume the hadronic jet content is represented by 1 particle only

Not realistic, but helpful to understand basic response features

More evolved model

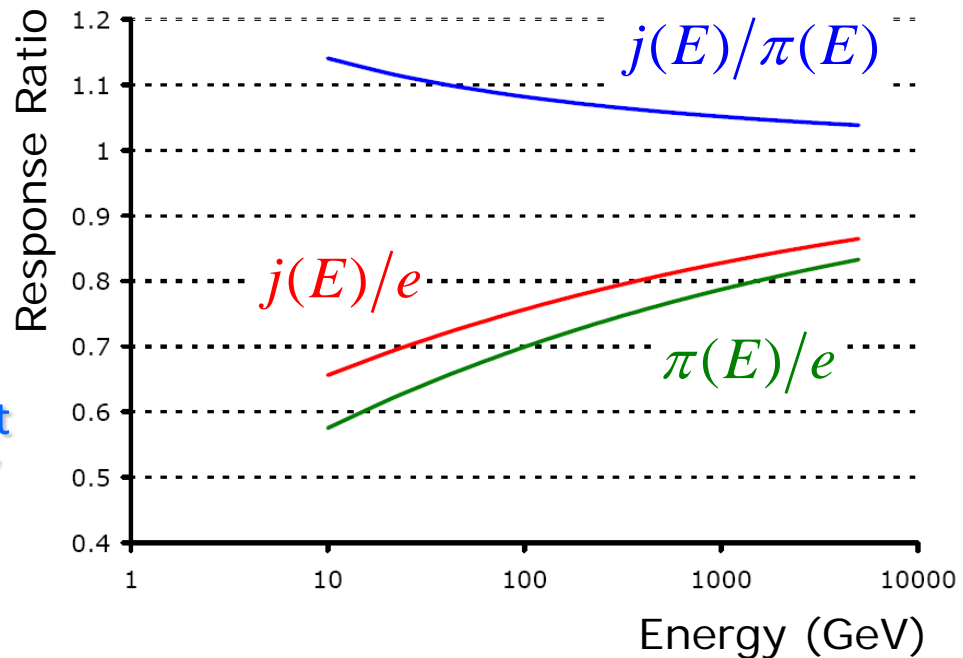
Use fragmentation function in jet response

This has some practical considerations

E.g. jet calibration in CDF

Gets non-compensation effect

Does not address acceptance effect due to shower overlaps



Complex mixture of hadrons and photons

Not a single particle response
Carries initial electromagnetic energy

Mainly photons

Very simple response model

Assume the hadronic jet content is represented by 1 particle only

Not realistic, but helpful to understand basic response features

More evolved model

Use fragmentation function in jet response

This has some practical considerations

E.g. jet calibration in CDF

Gets non-compensation effect

Does not address acceptance effect due to shower overlaps

$$\begin{aligned}
 & \frac{j(E_{\text{jet}})}{e} \\
 &= f_{\gamma}^{\text{jet}} \\
 &+ \underbrace{\left(1 - f_{\gamma}^{\text{jet}}\right) \int_{\text{hadrons}} \left[f_{\text{em}}(E_{\text{had}}) + (1 - f_{\text{em}}(E_{\text{had}})) \frac{h}{e} \right] dE_{\text{had}}}_{\text{composition of hadronic component given by jet fragmentation function}} \\
 &= f_{\gamma}^{\text{jet}} \\
 &+ \left(1 - f_{\gamma}^{\text{jet}}\right) \sum_{\text{hadrons}} \left[1 - \left(\frac{E_{\text{had}}}{E_{\text{base}}}\right)^{m-1} + \left(\frac{E_{\text{had}}}{E_{\text{base}}}\right)^{m-1} \frac{h}{e} \right] \\
 &= f_{\gamma}^{\text{jet}} + \left(1 - f_{\gamma}^{\text{jet}}\right) \sum_{\text{hadrons}} \left(1 + \left(E_{\text{had}}/E_{\text{base}}\right)^{m-1} (h/e - 1) \right)
 \end{aligned}$$



Noise

Fluctuations of the “zero” or “empty” signal reading

Pedestal fluctuations

Independent of the signal from particles

At least to first order

Mostly incoherent

No noise correlations between readout channels

Noise in each channel is independent oscillator

Gaussian in nature

Pedestal fluctuations ideally follow normal distribution around 0

Width of distribution (1σ) is noise value

Signal significance

Noise can fake particle signals

Only signals exceeding noise can be reliably measured

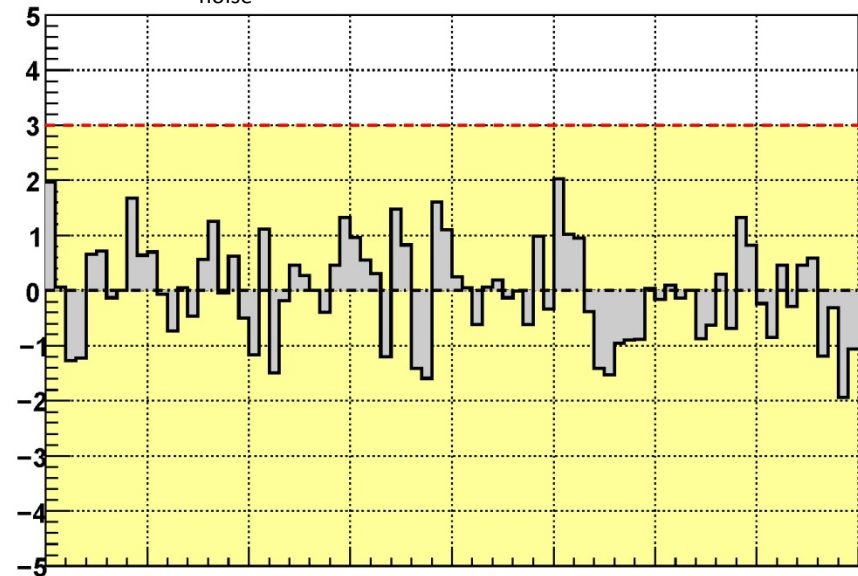
Signals larger than $3 \times$ noise are very likely from particles

Gaussian interpretation of pedestal fluctuations

Calorimeter signal reconstruction aims to suppress noise

Average contribution = 0, but adds to fluctuations!

Reading (σ_{noise})



Spatial Coordinate/Calorimeter Cell

Small signal:

Noise only

Signal on top of noise

Sum of noise and signal

Signal after noise suppression



Noise

Fluctuations of the “zero” or “empty” signal reading

Pedestal fluctuations

Independent of the signal from particles

At least to first order

Mostly incoherent

No noise correlations between readout channels

Noise in each channel is independent oscillator

Gaussian in nature

Pedestal fluctuations ideally follow normal distribution around 0

Width of distribution (1σ) is noise value

Signal significance

Noise can fake particle signals

Only signals exceeding noise can be reliably measured

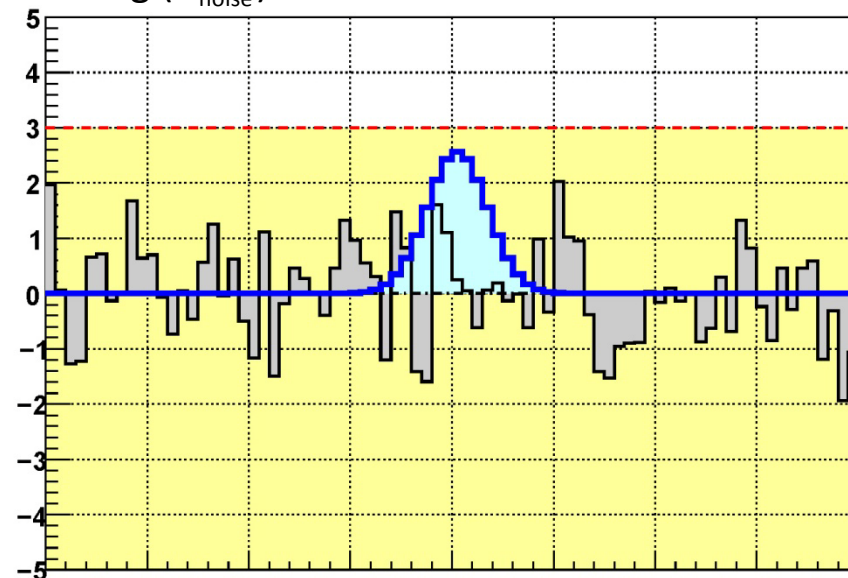
Signals larger than $3 \times$ noise are very likely from particles

Gaussian interpretation of pedestal fluctuations

Calorimeter signal reconstruction aims to suppress noise

Average contribution = 0, but adds to fluctuations!

Reading (σ_{noise})



Spatial Coordinate/Calorimeter Cell

Small signal:

Noise only

Signal on top of noise

Sum of noise and signal

Signal after noise suppression



Noise

Fluctuations of the “zero” or “empty” signal reading

Pedestal fluctuations

Independent of the signal from particles

At least to first order

Mostly incoherent

No noise correlations between readout channels

Noise in each channel is independent oscillator

Gaussian in nature

Pedestal fluctuations ideally follow normal distribution around 0

Width of distribution (1σ) is noise value

Signal significance

Noise can fake particle signals

Only signals exceeding noise can be reliably measured

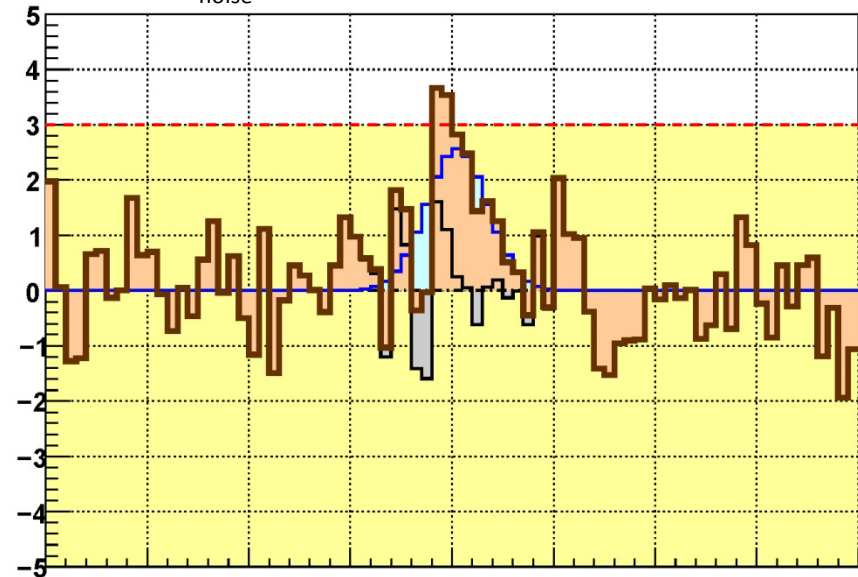
Signals larger than $3 \times$ noise are very likely from particles

Gaussian interpretation of pedestal fluctuations

Calorimeter signal reconstruction aims to suppress noise

Average contribution = 0, but adds to fluctuations!

Reading (σ_{noise})



Spatial Coordinate/Calorimeter Cell

Small signal:

Noise only

Signal on top of noise

Sum of noise and signal

Signal after noise suppression



Noise

Fluctuations of the “zero” or “empty” signal reading

Pedestal fluctuations

Independent of the signal from particles

At least to first order

Mostly incoherent

No noise correlations between readout channels

Noise in each channel is independent oscillator

Gaussian in nature

Pedestal fluctuations ideally follow normal distribution around 0

Width of distribution (1σ) is noise value

Signal significance

Noise can fake particle signals

Only signals exceeding noise can be reliably measured

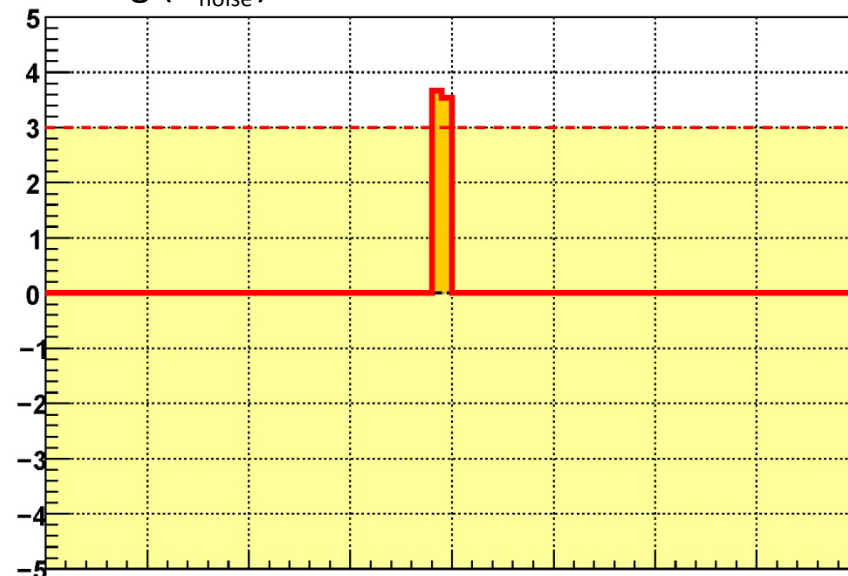
Signals larger than $3 \times$ noise are very likely from particles

Gaussian interpretation of pedestal fluctuations

Calorimeter signal reconstruction aims to suppress noise

Average contribution = 0, but adds to fluctuations!

Reading (σ_{noise})



Spatial Coordinate/Calorimeter Cell

Small signal:

Noise only

Signal on top of noise

Sum of noise and signal

Signal after noise suppression



Noise

Fluctuations of the “zero” or “empty” signal reading

Pedestal fluctuations

Independent of the signal from particles

At least to first order

Mostly incoherent

No noise correlations between readout channels

Noise in each channel is independent oscillator

Gaussian in nature

Pedestal fluctuations ideally follow normal distribution around 0

Width of distribution (1σ) is noise value

Signal significance

Noise can fake particle signals

Only signals exceeding noise can be reliably measured

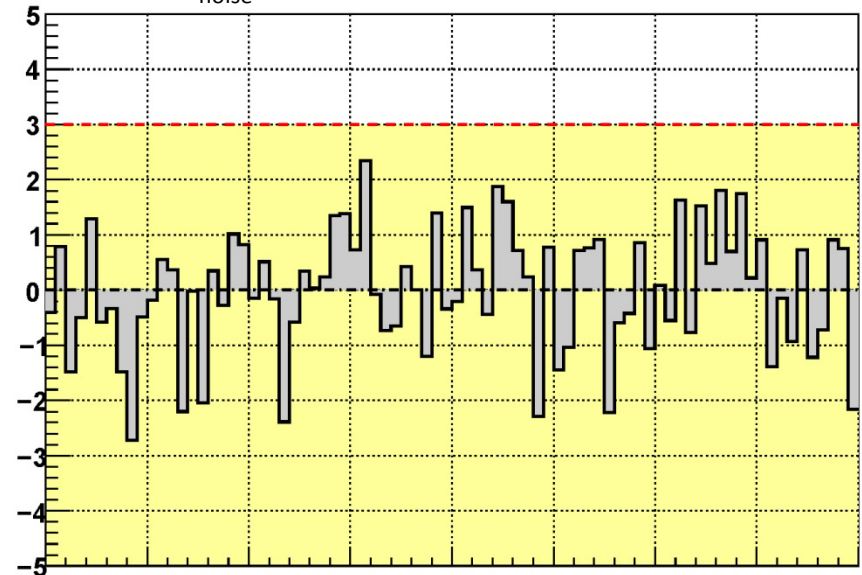
Signals larger than $3 \times$ noise are very likely from particles

Gaussian interpretation of pedestal fluctuations

Calorimeter signal reconstruction aims to suppress noise

Average contribution = 0, but adds to fluctuations!

Reading (σ_{noise})



Spatial Coordinate/Calorimeter Cell

Large signal:

Noise only

Signal on top of noise

Sum of noise and signal

Signal after noise suppression



Noise

Fluctuations of the “zero” or “empty” signal reading

Pedestal fluctuations

Independent of the signal from particles

At least to first order

Mostly incoherent

No noise correlations between readout channels

Noise in each channel is independent oscillator

Gaussian in nature

Pedestal fluctuations ideally follow normal distribution around 0

Width of distribution (1σ) is noise value

Signal significance

Noise can fake particle signals

Only signals exceeding noise can be reliably measured

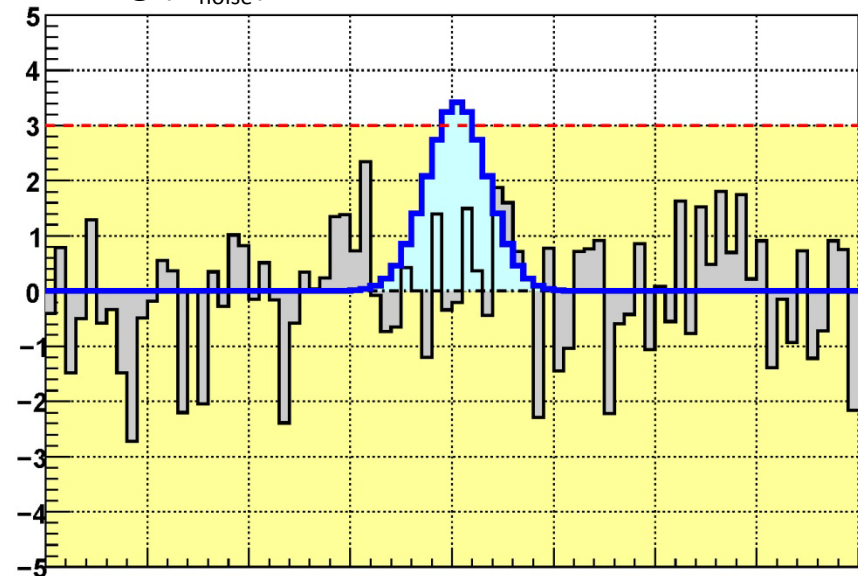
Signals larger than $3 \times$ noise are very likely from particles

Gaussian interpretation of pedestal fluctuations

Calorimeter signal reconstruction aims to suppress noise

Average contribution = 0, but adds to fluctuations!

Reading (σ_{noise})



Spatial Coordinate/Calorimeter Cell

Large signal:

Noise only

Signal on top of noise

Sum of noise and signal

Signal after noise suppression



Noise

Fluctuations of the “zero” or “empty” signal reading

Pedestal fluctuations

Independent of the signal from particles

At least to first order

Mostly incoherent

No noise correlations between readout channels

Noise in each channel is independent oscillator

Gaussian in nature

Pedestal fluctuations ideally follow normal distribution around 0

Width of distribution (1σ) is noise value

Signal significance

Noise can fake particle signals

Only signals exceeding noise can be reliably measured

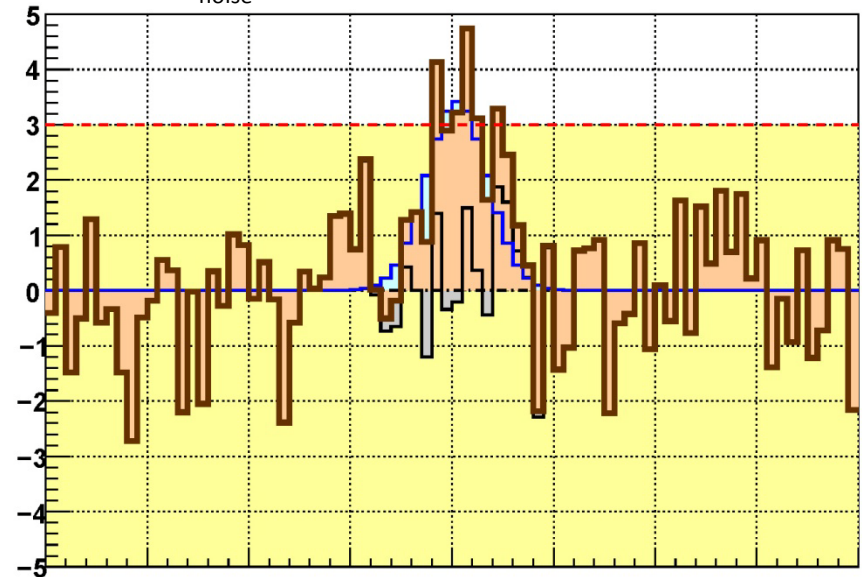
Signals larger than $3 \times$ noise are very likely from particles

Gaussian interpretation of pedestal fluctuations

Calorimeter signal reconstruction aims to suppress noise

Average contribution = 0, but adds to fluctuations!

Reading (σ_{noise})



Spatial Coordinate/Calorimeter Cell

Large signal:

Noise only

Signal on top of noise

Sum of noise and signal

Signal after noise suppression



Noise

Fluctuations of the “zero” or “empty” signal reading

Pedestal fluctuations

Independent of the signal from particles

At least to first order

Mostly incoherent

No noise correlations between readout channels

Noise in each channel is independent oscillator

Gaussian in nature

Pedestal fluctuations ideally follow normal distribution around 0

Width of distribution (1σ) is noise value

Signal significance

Noise can fake particle signals

Only signals exceeding noise can be reliably measured

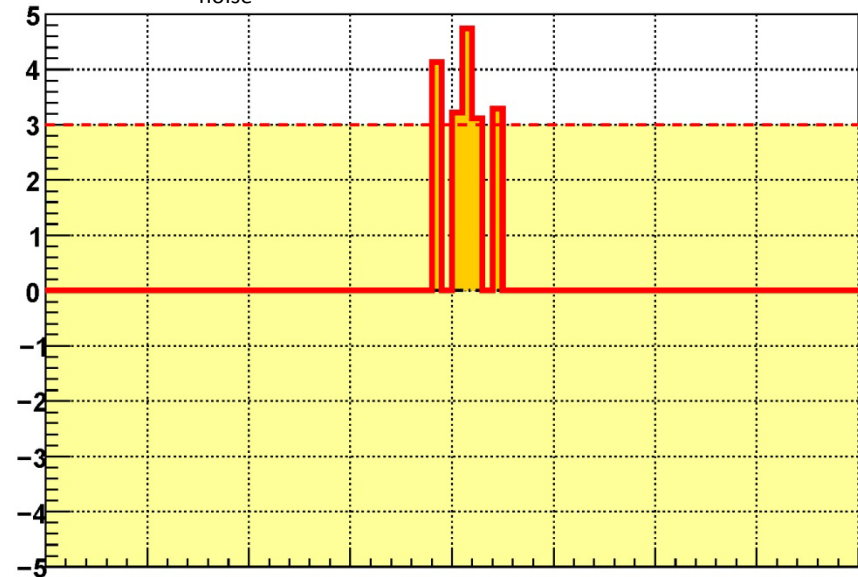
Signals larger than $3 \times$ noise are very likely from particles

Gaussian interpretation of pedestal fluctuations

Calorimeter signal reconstruction aims to suppress noise

Average contribution = 0, but adds to fluctuations!

Reading (σ_{noise})



Spatial Coordinate/Calorimeter Cell

Large signal:

Noise only

Signal on top of noise

Sum of noise and signal

Signal after noise suppression



Noise

Fluctuations of the “zero” or “empty” signal reading

Pedestal fluctuations

Independent of the signal from particles

At least to first order

Mostly incoherent

No noise correlations between readout channels

Noise in each channel is independent oscillator

Gaussian in nature

Pedestal fluctuations ideally follow normal distribution around 0

Width of distribution (1σ) is noise value

Signal significance

Noise can fake particle signals

Only signals exceeding noise can be reliably measured

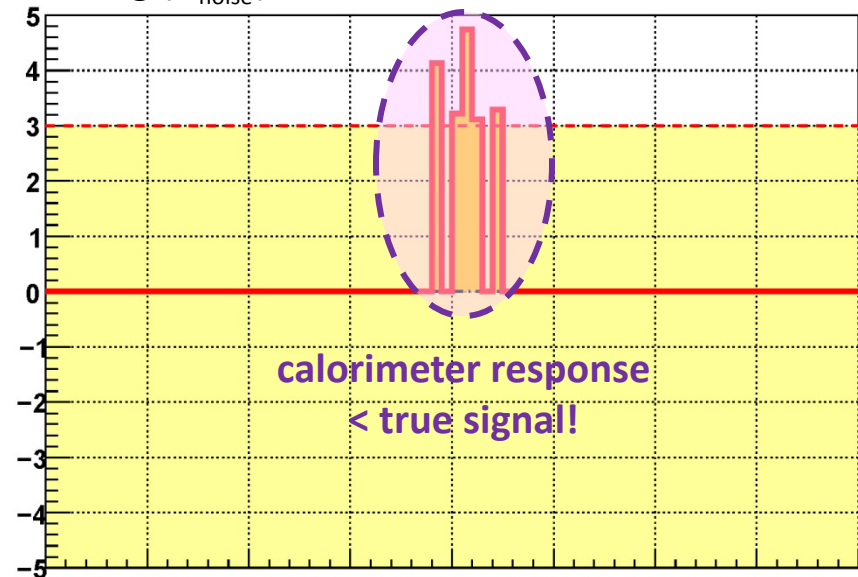
Signals larger than $3 \times$ noise are very likely from particles

Gaussian interpretation of pedestal fluctuations

Calorimeter signal reconstruction aims to suppress noise

Average contribution = 0, but adds to fluctuations!

Reading (σ_{noise})



Spatial Coordinate/Calorimeter Cell

Large signal:

Noise only

Signal on top of noise

Sum of noise and signal

Signal after noise suppression



Noise

Fluctuations of the “zero” or “empty” signal reading

Pedestal fluctuations

Independent of the signal from particles

At least to first order

Mostly incoherent

No noise correlations between readout channels

Noise in each channel is independent oscillator

Gaussian in nature

Pedestal fluctuations ideally follow normal distribution around 0

Width of distribution (1σ) is noise value

Signal significance

Noise can fake particle signals

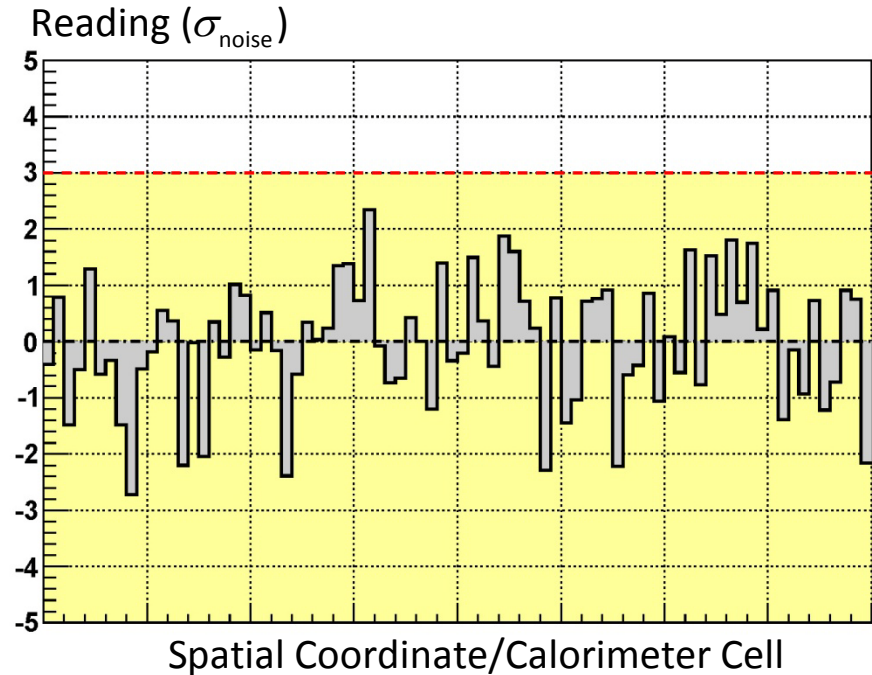
Only signals exceeding noise can be reliably measured

Signals larger than $3 \times$ noise are very likely from particles

Gaussian interpretation of pedestal fluctuations

Calorimeter signal reconstruction aims to suppress noise

Average contribution = 0, but adds to fluctuations!



Small signal, two particles:

Noise only

Signal on top of noise

Sum of noise and signal

Signal after noise suppression



Noise

Fluctuations of the “zero” or “empty” signal reading

Pedestal fluctuations

Independent of the signal from particles

At least to first order

Mostly incoherent

No noise correlations between readout channels

Noise in each channel is independent oscillator

Gaussian in nature

Pedestal fluctuations ideally follow normal distribution around 0

Width of distribution (1σ) is noise value

Signal significance

Noise can fake particle signals

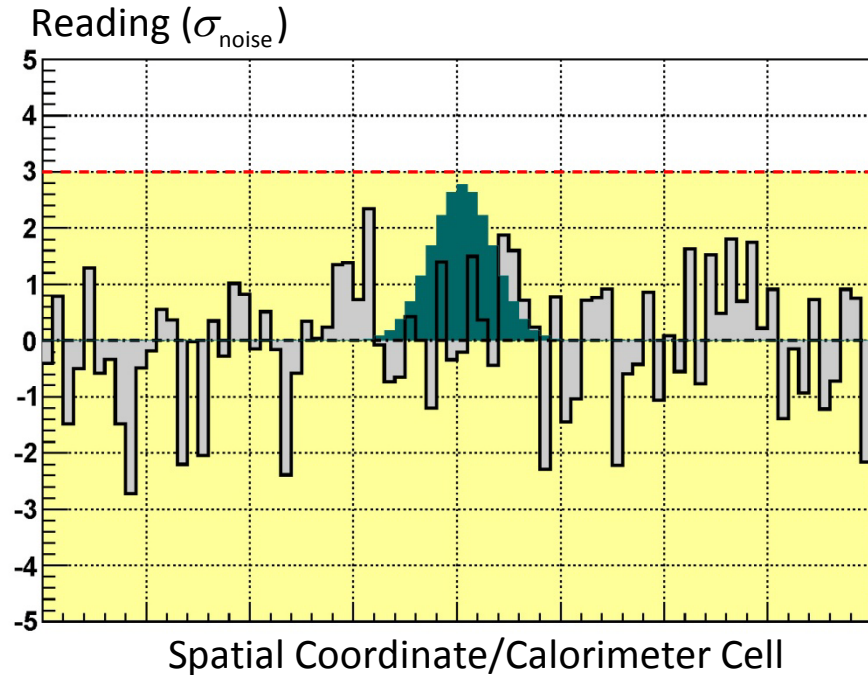
Only signals exceeding noise can be reliably measured

Signals larger than $3 \times$ noise are very likely from particles

Gaussian interpretation of pedestal fluctuations

Calorimeter signal reconstruction aims to suppress noise

Average contribution = 0, but adds to fluctuations!



Small signal, first particle:

Noise only

Signal on top of noise

Sum of noise and signal

Signal after noise suppression



Noise

Fluctuations of the “zero” or “empty” signal reading

Pedestal fluctuations

Independent of the signal from particles

At least to first order

Mostly incoherent

No noise correlations between readout channels

Noise in each channel is independent oscillator

Gaussian in nature

Pedestal fluctuations ideally follow normal distribution around 0

Width of distribution (1σ) is noise value

Signal significance

Noise can fake particle signals

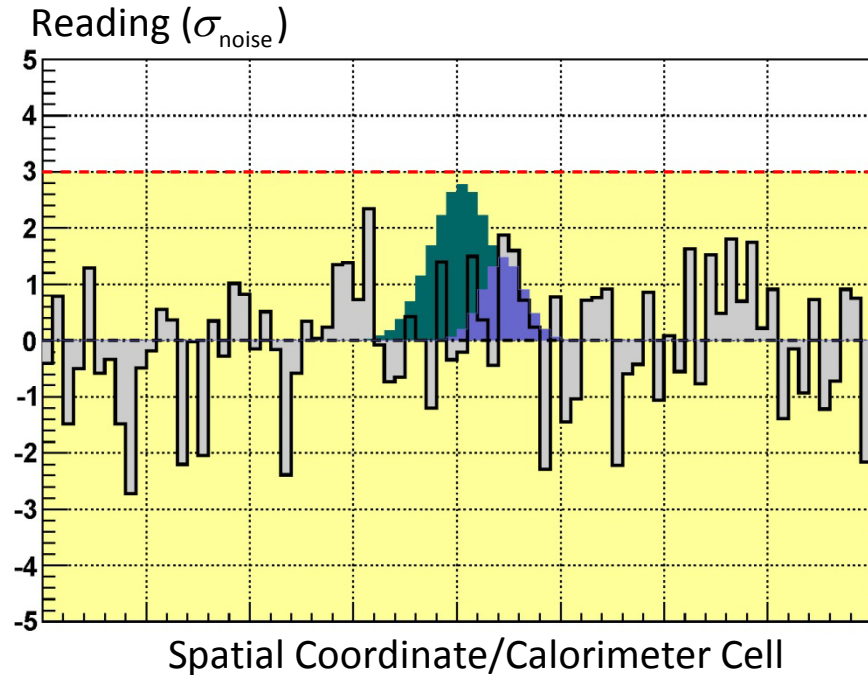
Only signals exceeding noise can be reliably measured

Signals larger than $3 \times$ noise are very likely from particles

Gaussian interpretation of pedestal fluctuations

Calorimeter signal reconstruction aims to suppress noise

Average contribution = 0, but adds to fluctuations!



Small signal, first and second particle:

Noise only

Signal on top of noise

Sum of noise and signal

Signal after noise suppression



Noise

Fluctuations of the “zero” or “empty” signal reading

Pedestal fluctuations

Independent of the signal from particles

At least to first order

Mostly incoherent

No noise correlations between readout channels

Noise in each channel is independent oscillator

Gaussian in nature

Pedestal fluctuations ideally follow normal distribution around 0

Width of distribution (1σ) is noise value

Signal significance

Noise can fake particle signals

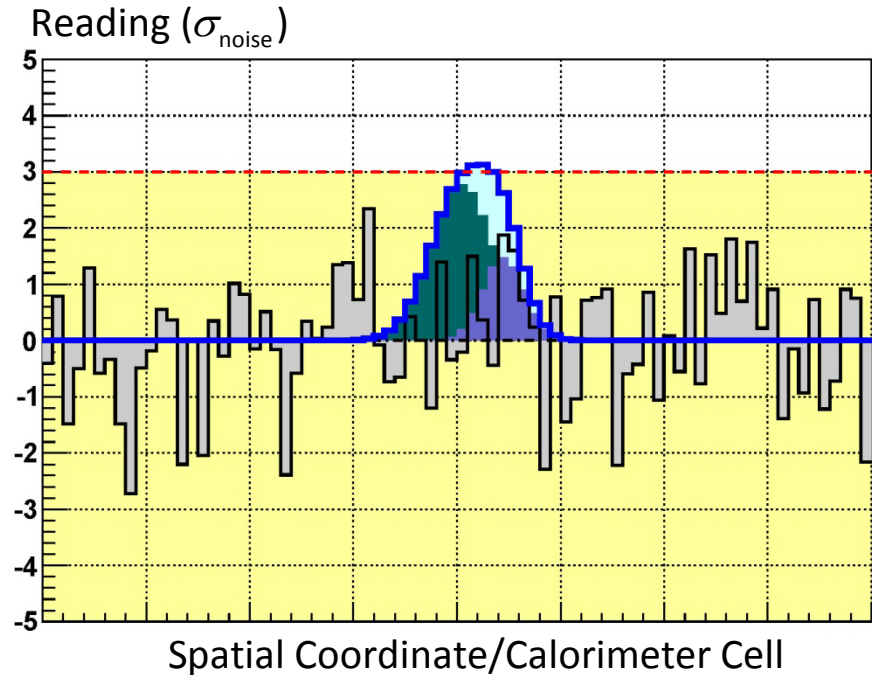
Only signals exceeding noise can be reliably measured

Signals larger than $3 \times$ noise are very likely from particles

Gaussian interpretation of pedestal fluctuations

Calorimeter signal reconstruction aims to suppress noise

Average contribution = 0, but adds to fluctuations!



Small signal, two particle, sum:

Noise only

Signal on top of noise

Sum of noise and signal

Signal after noise suppression



Noise

Fluctuations of the “zero” or “empty” signal reading

Pedestal fluctuations

Independent of the signal from particles

At least to first order

Mostly incoherent

No noise correlations between readout channels

Noise in each channel is independent oscillator

Gaussian in nature

Pedestal fluctuations ideally follow normal distribution around 0

Width of distribution (1σ) is noise value

Signal significance

Noise can fake particle signals

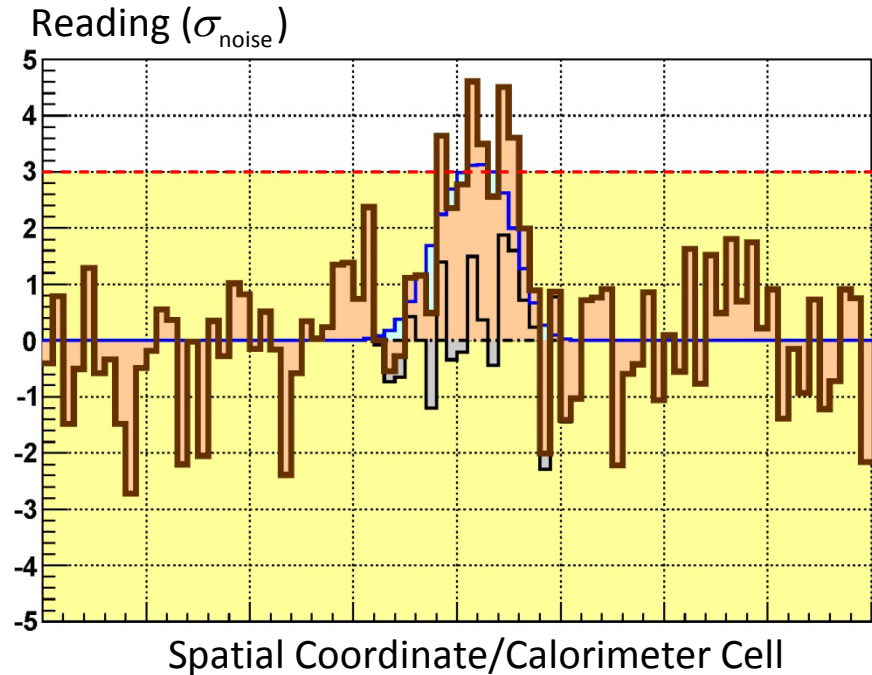
Only signals exceeding noise can be reliably measured

Signals larger than $3 \times$ noise are very likely from particles

Gaussian interpretation of pedestal fluctuations

Calorimeter signal reconstruction aims to suppress noise

Average contribution = 0, but adds to fluctuations!



Small signal, two particles:

Noise only

Signal on top of noise

Sum of noise and signal

Signal after noise suppression



Noise

Fluctuations of the “zero” or “empty” signal reading

Pedestal fluctuations

Independent of the signal from particles

At least to first order

Mostly incoherent

No noise correlations between readout channels

Noise in each channel is independent oscillator

Gaussian in nature

Pedestal fluctuations ideally follow normal distribution around 0

Width of distribution (1σ) is noise value

Signal significance

Noise can fake particle signals

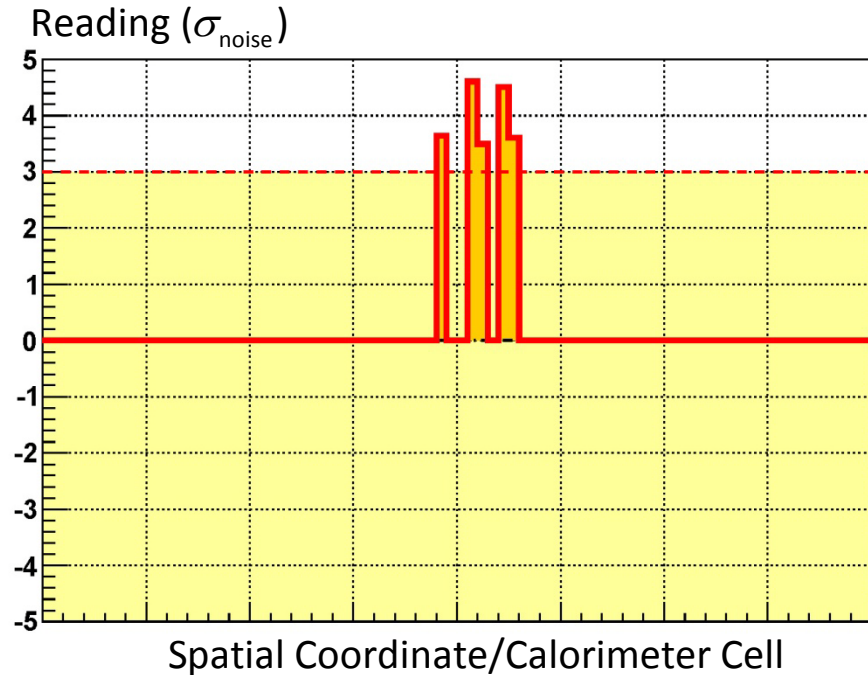
Only signals exceeding noise can be reliably measured

Signals larger than $3 \times$ noise are very likely from particles

Gaussian interpretation of pedestal fluctuations

Calorimeter signal reconstruction aims to suppress noise

Average contribution = 0, but adds to fluctuations!



Small signal, two particles:

Noise only

Signal on top of noise

Sum of noise and signal

Signal after noise suppression



Noise

Fluctuations of the “zero” or “empty” signal reading

Pedestal fluctuations

Independent of the signal from particles

At least to first order

Mostly incoherent

No noise correlations between readout channels

Noise in each channel is independent oscillator

Gaussian in nature

Pedestal fluctuations ideally follow normal distribution around 0

Width of distribution (1σ) is noise value

Signal significance

Noise can fake particle signals

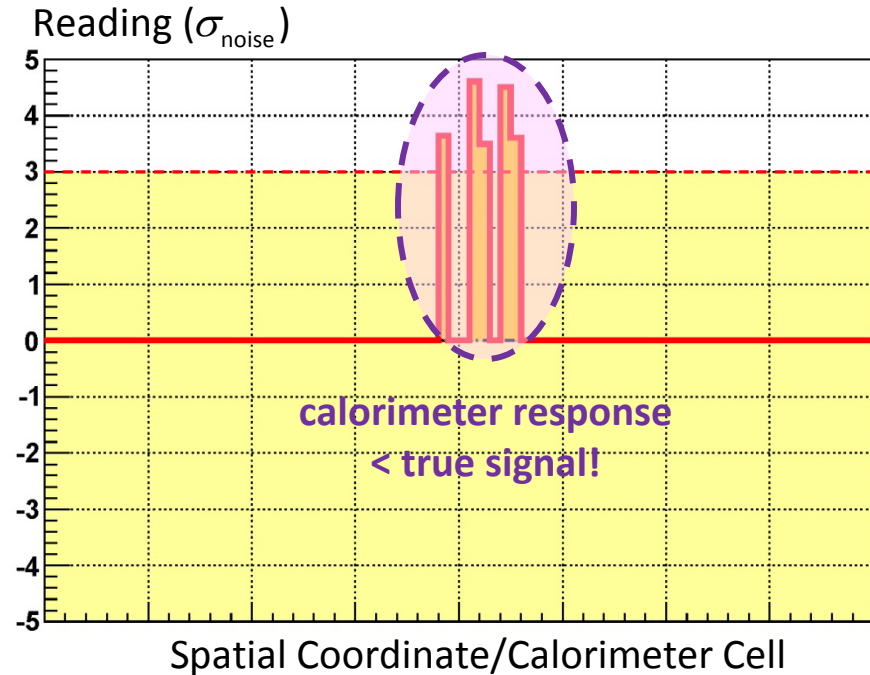
Only signals exceeding noise can be reliably measured

Signals larger than $3 \times$ noise are very likely from particles

Gaussian interpretation of pedestal fluctuations

Calorimeter signal reconstruction aims to suppress noise

Average contribution = 0, but adds to fluctuations!



Small signal, two particles:

Noise only

Signal on top of noise

Sum of noise and signal

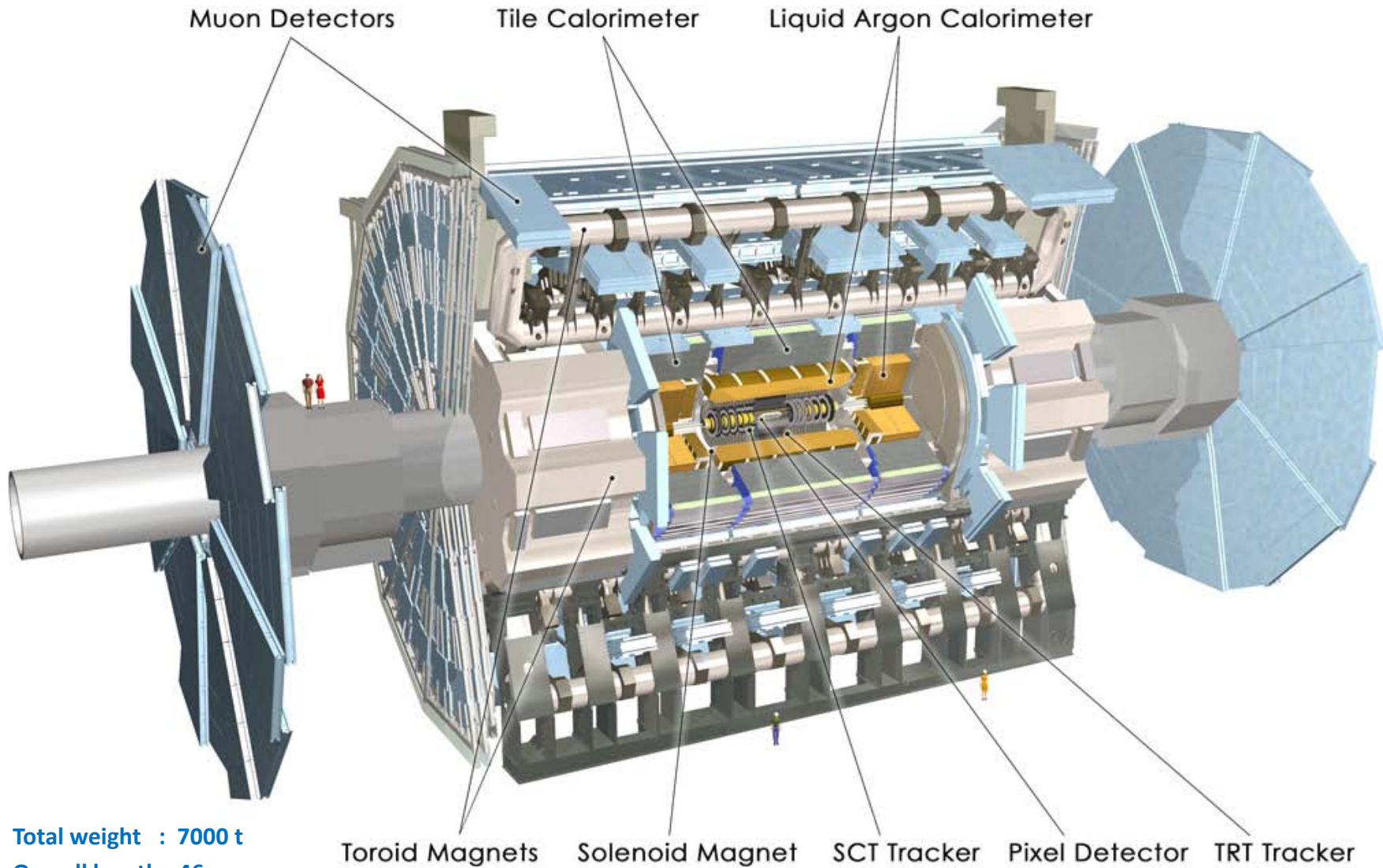
Signal after noise suppression



Introduction to Hadronic Final State Reconstruction in Collider Experiments (Supplement to Part IV: The ATLAS Calorimeter System)

Peter Loch
University of Arizona
Tucson, Arizona
USA



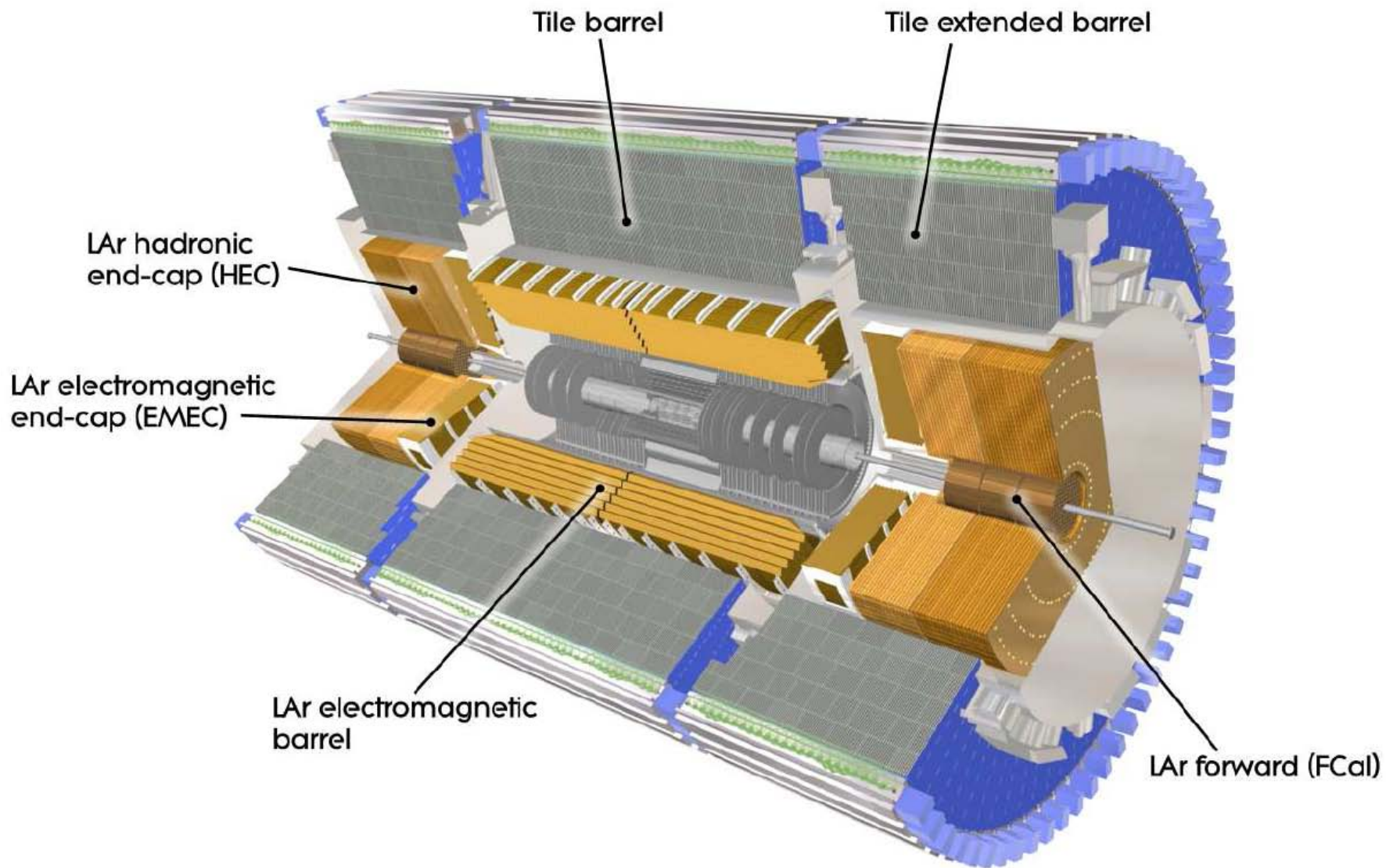


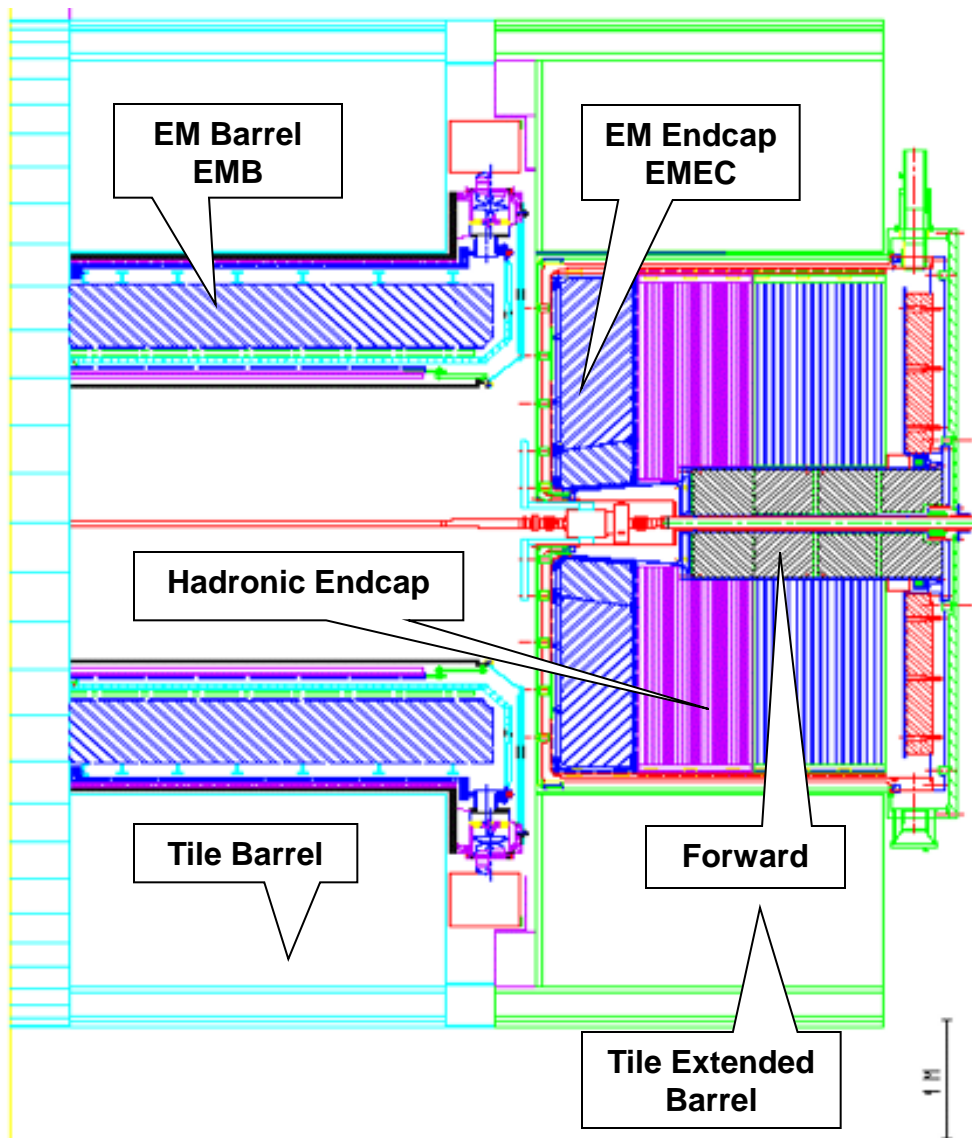
Total weight : 7000 t

Overall length: 46 m

Overall diameter: 23 m

Magnetic field: 2T solenoid + (varying) toroid field





Electromagnetic Barrel

$$|\eta| < 1.4$$

Liquid argon/lead

Electromagnetic EndCap

$$1.375 < |\eta| < 3.2$$

Liquid argon/lead

Hadronic Tile

$$|\eta| < 1.7$$

Scintillator/iron

Hadronic EndCap

$$1.5 < |\eta| < 3.2$$

Liquid argon/copper

Forward Calorimeter

$$3.2 < |\eta| < 4.9$$

Liquid argon/copper and liquid argon/tungsten

Varying (high) granularity

Mostly projective or pseudo-projective readout geometries

Nearly 200,000 readout channels in total

Overlaps and transitions

Some complex detector geometries in crack regions



Highly segmented lead/liquid argon accordion calorimeter

Projective readout geometry in pseudo-rapidity and azimuth

More than 170,000 independent readout channels

No azimuthal discontinuities (cracks)

Total depth $> 24 X_0$ (increases with pseudo-rapidity)

Three depth segments

+ pre-sampler (limited coverage, only $\eta < 1.8$)

Strip cells in 1st layer

Thin layer for precision direction and e/π and e/γ separation

Total depth $\approx 6 X_0$ (constant)

Very high granularity in pseudo-rapidity

$\Delta\eta \times \Delta\phi \approx 0.003 \times 0.1$

Deep 2nd layer

Captures electromagnetic shower maximum

Total depth $\approx 16-18 X_0$

High granularity in both directions

$\Delta\eta \times \Delta\phi \approx 0.025 \times 0.025$

Shallow cells in 3rd layer

Catches electromagnetic shower tails

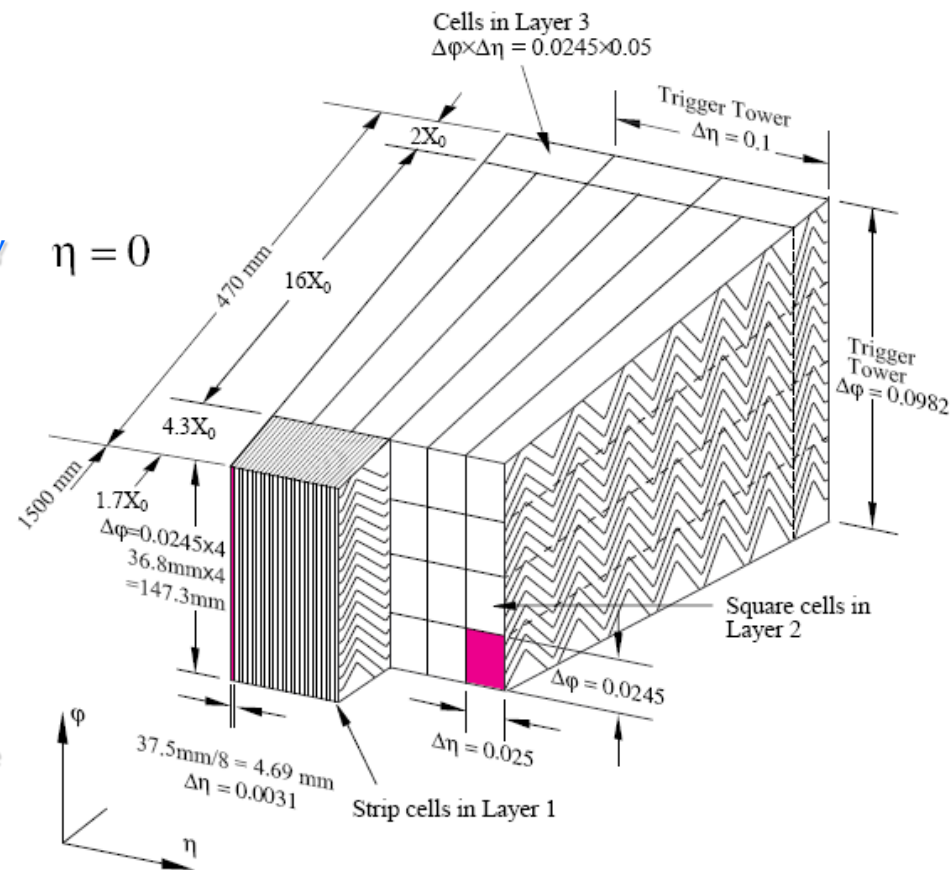
Electron and photon identification

Total depth $\approx 2-12 X_0$ (from center to outer edge in pseudo-rapidity)

Relaxed granularity

$\Delta\eta \times \Delta\phi \approx 0.05 \times 0.025$

Electromagnetic Barrel



Central and Extended Tile calorimeter

Iron/scintillator with tiled readout structure

Three depth segments

Quasi-projective readout cells

Granularity first two layers

$$\Delta\eta \times \Delta\phi \approx 0.1 \times 0.1$$

Third layer

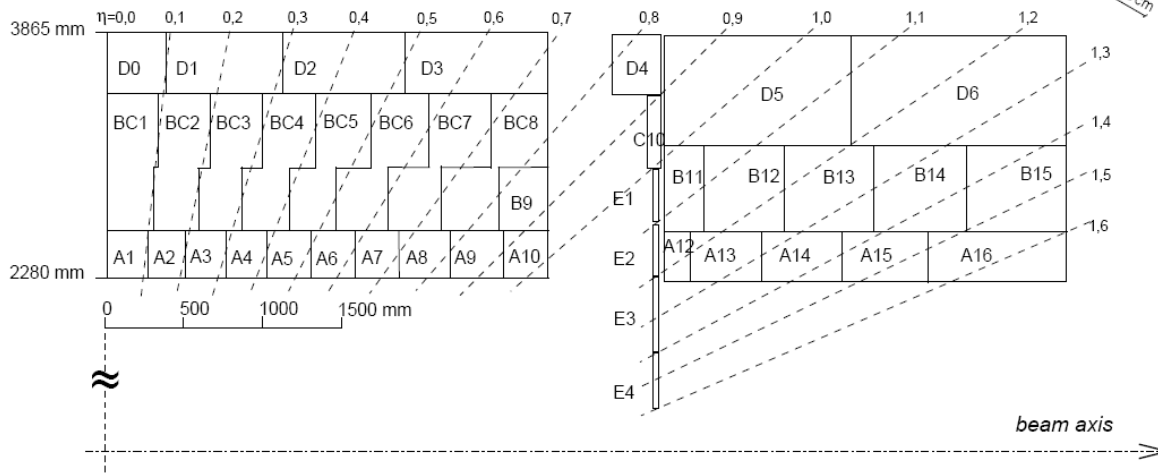
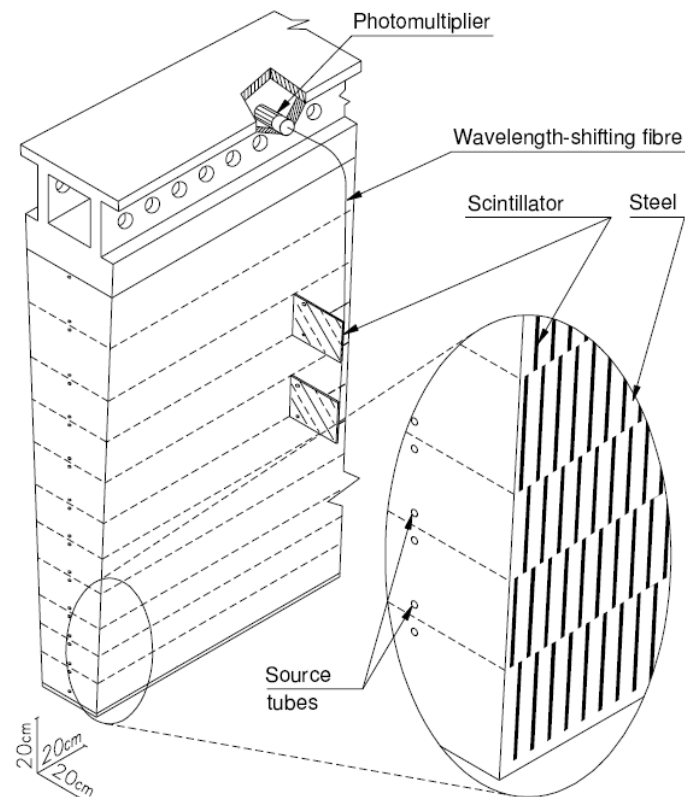
$$\Delta\eta \times \Delta\phi \approx 0.2 \times 0.1$$

Very fast light collection

~50 ns reduces effect of pile-up to ~3 bunch crossings

Dual fiber readout for each channel

Two signals from each cell



Electromagnetic “Spanish Fan” accordion

Highly segmented with up to three longitudinal segments

Complex accordion design of lead absorbers and electrodes

Looks like an unfolded spanish fan

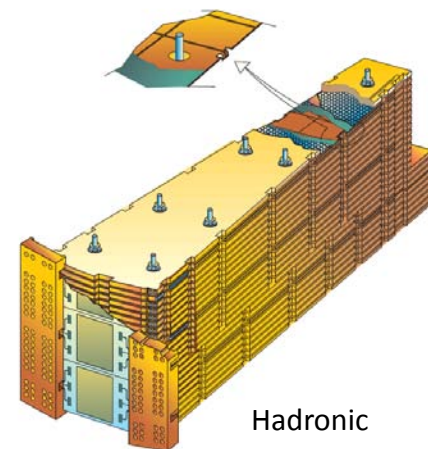
Hadronic liquid argon/copper calorimeter

Parallel plate design

Four longitudinal segments

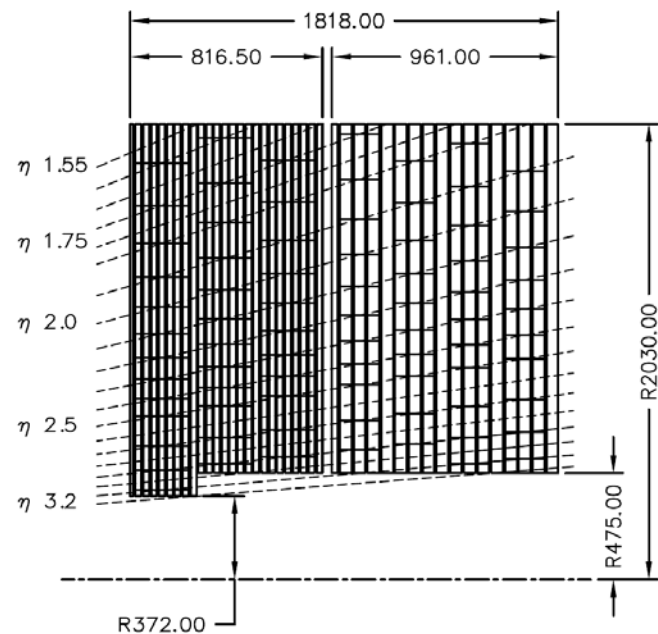
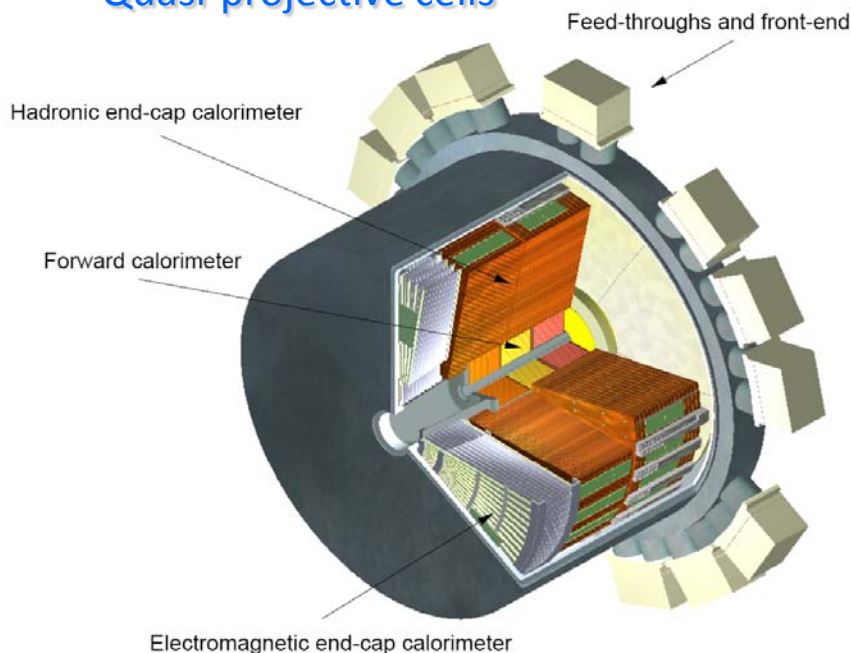
Quasi-projective cells

$$\Delta\eta \times \Delta\phi \approx \begin{cases} 0.025 \times 0.025 & |\eta| < 2.5, \text{ middle layer} \\ 0.1 \times 0.1 & 2.5 < |\eta| < 3.2 \end{cases}$$



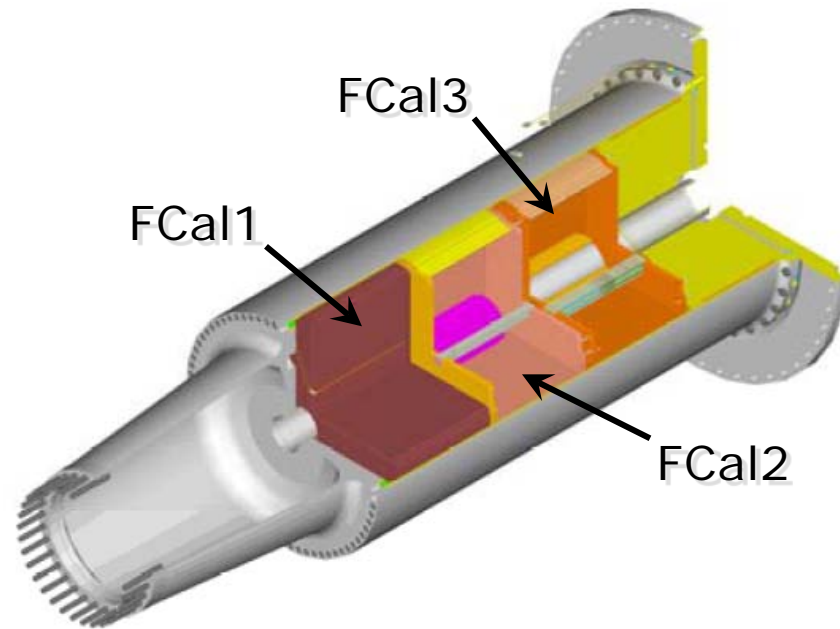
Hadronic
EndCap
wedge

$$\Delta\eta \times \Delta\phi \approx \begin{cases} 0.1 \times 0.1 & |\eta| < 2.5 \\ 0.2 \times 0.2 & 2.5 < |\eta| < 3.2 \end{cases}$$



Design features

- Compact absorbers
 - Small showers
- Tubular thin gap electrodes
 - Suppress positive charge build-up (Ar^+) in high ionization rate environment
 - Stable calibration
- Rectangular non-projective readout cells



Electromagnetic FCal1

- Liquid argon/copper
- Gap $\sim 260 \mu\text{m}$

Hadronic FCal2

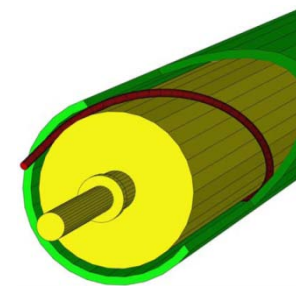
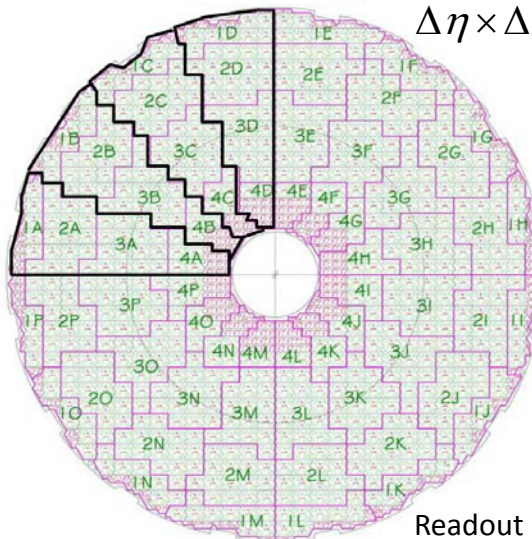
- Liquid argon/tungsten
- Gap $\sim 375 \mu\text{m}$

Hadronic FCal3

- Liquid argon/tungsten
- Gap $\sim 500 \mu\text{m}$



$$\Delta\eta \times \Delta\phi \approx 0.2 \times 0.2$$



Forward calorimeter electrode



Non-compensating calorimeters

Electrons generate larger signal than pions depositing the same energy

Typically $e/\pi \approx 1.3$

High particle stopping

power over whole

detector acceptance $|\eta| < 4.9$

$\sim 26\text{-}35 X_0$ electromagnetic
calorimetry

$\sim 10 \lambda$ total for hadrons

Hermetic coverage

No significant cracks in
azimuth

Non-pointing transition between barrel, endcap and forward

Small performance penalty for hadrons/jets

High granularity

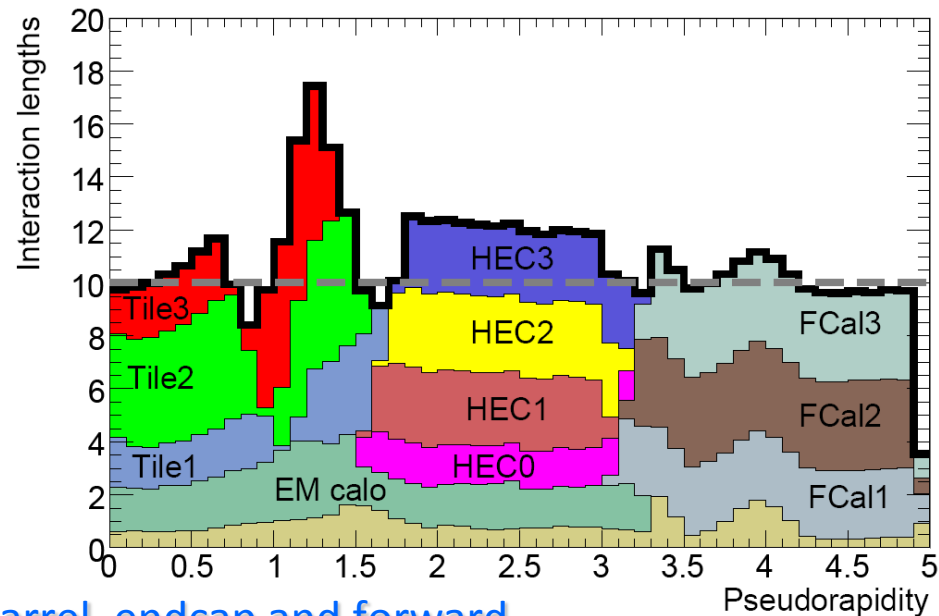
Nearly 200,000 readout channels

Highly efficient particle identification

Jet substructure resolution capabilities

Local hadronic calibration using signal shapes

...



Introduction to Hadronic Final State Reconstruction in Collider Experiments (Part V)

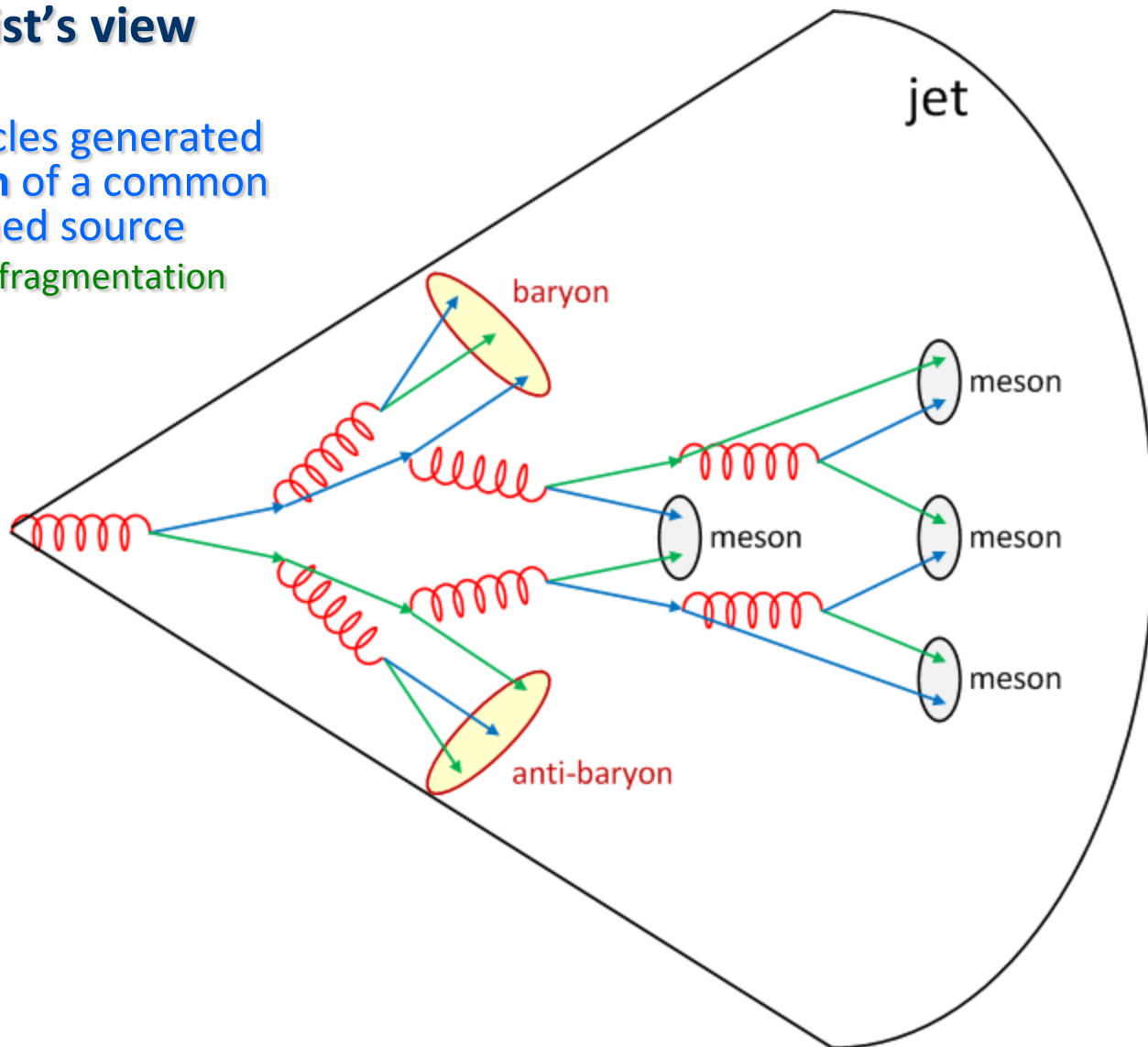
Peter Loch
University of Arizona
Tucson, Arizona
USA



The experimentalist's view (...my view)

A bunch of particles generated
by **hadronization** of a common
otherwise confined source

Quark-, gluon fragmentation



The experimentalist's view (...my view)

A bunch of particles generated
by **hadronization** of a common
otherwise confined source

Quark-, gluon fragmentation

Consequence of **common source**

Correlated kinematic properties

Jet reflects the source by sum
rules and conservation

Interacting particles in jet
generate observable signal in
detector

Protons, neutrons, pions, kaons,
photons, electrons, muons, and
others with laboratory lifetimes $>$
10 ps (incl. corresponding anti-
particles)

Non-interacting particles in jet
do not contribute to directly
observable signal

Neutrinos, mostly

$$(E_{\text{jet}}, \vec{p}_{\text{jet}}) = \sum_{\text{all particles}} (E_{\text{particle}}, \vec{p}_{\text{particle}})$$

$$= (E_{\text{parton}}, \vec{p}_{\text{parton}})$$

$$q_{\text{jet}} = \sum_{\text{all particles}} q_{\text{particle}} = q_{\text{parton}}$$

$$m_{\text{jet}} = \sqrt{E_{\text{jet}}^2 - |\vec{p}_{\text{jet}}|^2}$$

$$= \sqrt{\left[\sum_{\text{all particles}} E_{\text{particle}} \right]^2 - \left| \sum_{\text{all particles}} \vec{p}_{\text{particle}} \right|^2}$$

$$= \sqrt{E_{\text{parton}}^2 - |\vec{p}_{\text{parton}}|^2} = m_{\text{parton}}$$



The experimentalist's view (...my view)

A bunch of particles generated by **hadronization** of a common otherwise confined source

Quark-, gluon fragmentation

Consequence of **common source**

Correlated kinematic properties

Jet reflects the source by sum rules and conservation

Interacting particles in jet generate observable signal in detector

Protons, neutrons, pions, kaons, photons, electrons, muons, and others with laboratory lifetimes > 10 ps (incl. corresponding anti-particles)

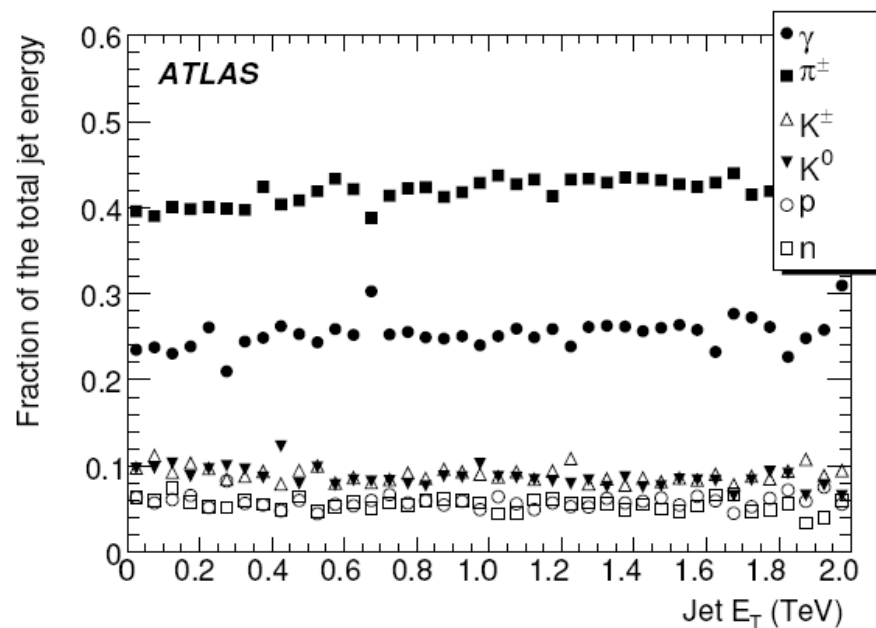
Non-interacting particles in jet so not contribute to directly observable signal

Neutrinos, mostly

$$(E_{\text{jet}}, \vec{p}_{\text{jet}})^{\text{obs}} = \sum_{\text{interacting particles}} (E_{\text{particle}}, \vec{p}_{\text{particle}}) \neq (E_{\text{parton}}, \vec{p}_{\text{parton}})$$

$$q_{\text{jet}}^{\text{obs}} \neq q_{\text{parton}}$$

$$m_{\text{jet}}^{\text{obs}} \neq m_{\text{parton}}$$



Particle jet composition generated by PYTHIA



What is fragmentation?

Hadronization of partons into particles

Confinement in QCD: gluon pair production

Gluon radiation

How can fragmentation be measured in an experiment?

Reconstruct charged tracks in a given jet

Momentum fraction carried by these tracks reflects charged (hadron) production in hadronization

High track reconstruction efficiency and low momentum acceptance needed!

Final state in e^+e^- collisions at LEP ideal – very clean collision environment without underlying event, at center-of-mass energies from 90 to 209 GeV

Fragmentation functions are derived from LEP data (1989-2000)

Can we measure the fragmentation of a given jet in hadron colliders?

Basically impossible, as collision environment is too “messy”

Accidental inclusion of charged tracks not from jet (underlying event, pile-up)

Loss of relevant tracks hard to detect

Need to rely on models fully describing collision event

Compare composition of detector jets with particle jets from simulations (generators) like PYTHIA, which implement the LEP fragmentation functions!



Parton jets – what is this?

Basically a representation of an individual final state parton before hadronization

Still called a jet because a jet finding algorithm is applied to the simulated partonic final state

Jet finders explicitly or implicitly apply spatial and kinematic resolution parameters and (kinematic) thresholds to the interactions

Two or more close-by partons can be combined to one jet

A parton may not make it into a jet because it is below threshold

Parton jets are “biased” with respect to the jet finding algorithm and its configuration

Two different jet finders may generate two different views on the partonic event

Particle jets

These are jets from final state particles with lifetime > 10 ps

E.g., after hadronization of partons

Sometimes non-observable particles like neutrinos or particles with very specific signal characteristics (muons) may not be included

E.g., the muon generated in semi-leptonic b-decays may not be considered part of the b-jet

Here a jet finder is mandatory to produce these jets

Needs to recombine the bundle of particles coming from the same source (parton)

Subjects particles to the same resolution parameters and thresholds as used for parton jets

Attempt to match parton and particle jets may allow to understand effect of fragmentation on jet finding efficiencies, mis-clustering (wrong particles combined), and bias on kinematic reconstruction

Particle jets are a good “truth” reference for detector jets

After all, particles generate the detector signal



Parton “jets”

Theoretical concept converting matrix element calculations in to jet picture

Depends on the order of the calculation

Useful tool to link experimental results to calculations in di-quark resonance reconstruction

E.g., hadronic decays of the W boson and heavier new particles like Z'

Much less meaningful concept in QCD analysis like inclusive jet cross-section

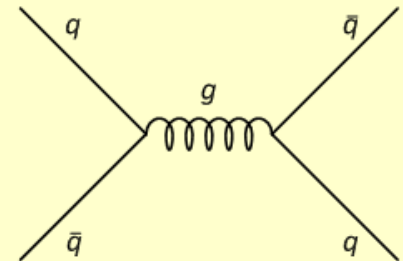
Jet counting as function of p_T

Number of parton jets not strictly linked to number of particle jets

Boundary between matrix element, radiation, parton showering, and underlying event washed out at particle level

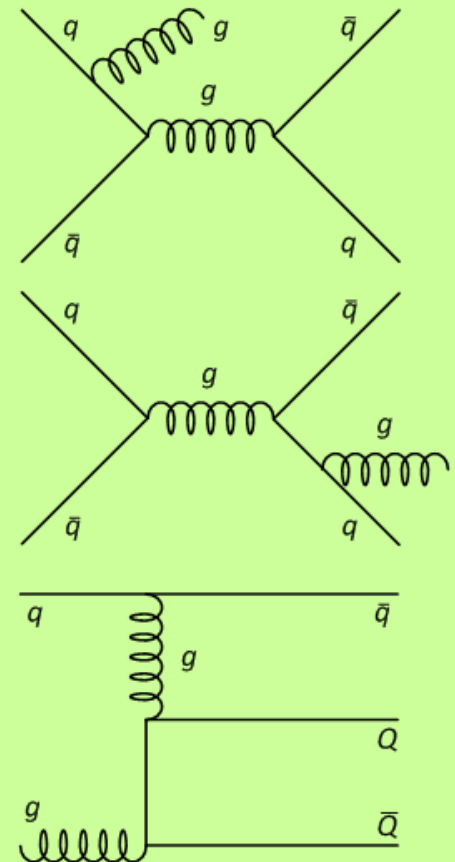
QCD LO:

$$N_{\text{jets}} = 2$$



QCD NLO:

$$N_{\text{jets}} = 3$$



Parton “jets”

Theoretical concept converting matrix element calculations in to jet picture

Depends on the order of the calculation

Useful tool to link experimental results to calculations in di-quark resonance reconstruction

E.g., hadronic decays of the W boson and heavier new particles like Z' at LO

Much less meaningful concept in QCD analysis like inclusive jet cross-section

Jet counting as function of p_T

Number of parton jets not strictly linked to number of particle jets

Boundary between matrix element, radiation, parton showering, and underlying event washed out at particle level

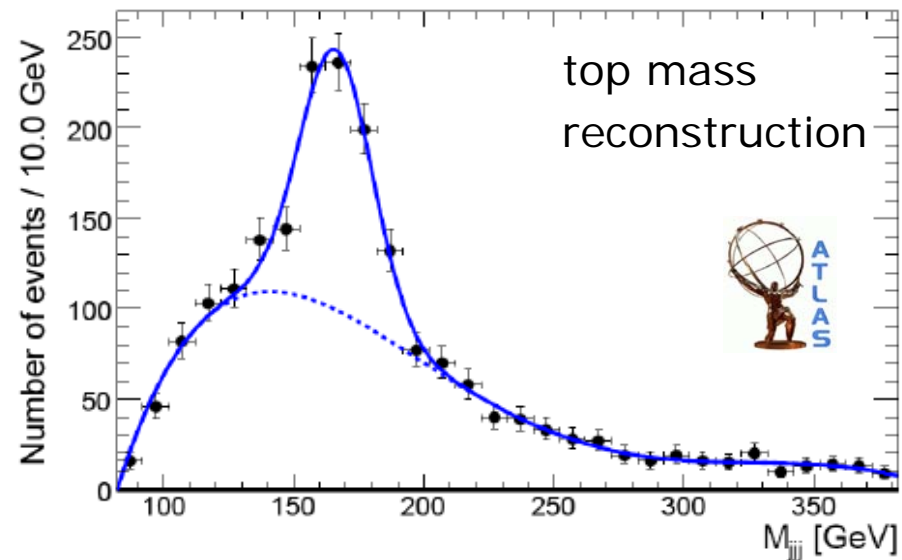
LO decays are easy to tag:

$$W \rightarrow q\bar{q}' \quad (2\text{-prong decay})$$

$$Z' \rightarrow q\bar{q}' \quad (2\text{-prong decay})$$

$$t \rightarrow Wb \rightarrow q\bar{q}'b \quad (3\text{-prong decay})$$

→ expectations for number of jets from decayed particle hypothesis at given order + mass of jet system pointing to certain source!



Parton “jets”

Theoretical concept converting matrix element calculations in to jet picture

Depends on the order of the calculation

Useful tool to link experimental results to calculations in di-quark resonance reconstruction

E.g., hadronic decays of the W boson and heavier new particles like Z'

Much less meaningful concept in QCD analysis like inclusive jet cross-section

Jet counting as function of p_T

Number of parton jets not strictly linked to number of particle jets

Boundary between matrix element, radiation, parton showering, and underlying event washed out at particle level

Basic QCD $2 \rightarrow 2$ processes at LO:

$$gg \rightarrow gg, gq \rightarrow gq, q\bar{q} \rightarrow q'\bar{q}'$$

but often observe more than 2 jets in final state due to higher order

contributions, initial and final state radiation, and additional interactions from the underlying event

→ no obvious additional constraint on the appropriate parton level model from the observable final state, like in case of heavy particle decays!

→ experimental final state "includes" all orders of calculations and collision environment!!



Collection of particles from common source

Several sources in each collision

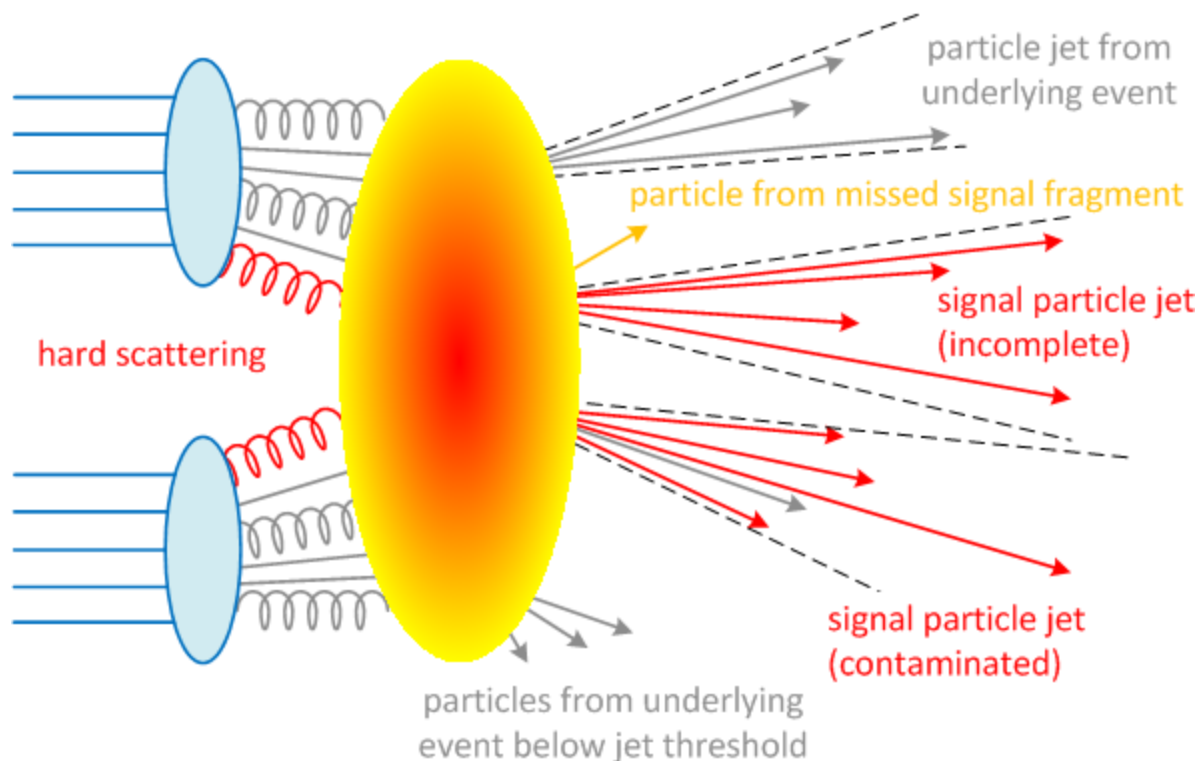
Hard scattering, multiple parton interactions in the underlying event, initial and final state radiation

Describe the simulated collision viewed with a microscope (idealized)

Microscope **technology** – jet finding algorithm

Resolution – ability of a jet finder to (spatially) resolve jet structures of collision, typically a configuration parameter of the jet finder

Sensitivity – kinematic threshold for particle bundle to be called a jet, another configuration parameter of the jet finder



Good reconstruction reference for detector jets

Provide a truth reference for the reconstructed jet energy and momentum

E.g., can be used in simulations together with fully simulated detector jets to calibrate those (we will follow up on this point later!)

Extract particle jets from measurement by calibration and unfolding signal characteristics from detector jets

Understand effect of experimental spatial resolution and signal thresholds at particle level

Remember: electromagnetic and hadronic showers have lateral extension → diffusion of spatial particle flow by distributing the particle energy laterally!

Remember: noise in calorimeter imply a “useful” signal threshold → may introduce acceptance limitations for particle jets!

Good reference for physics

Goal of all selection and unfolding strategies in physics analysis

Reproduce particle level event from measurement as much as possible!

Require correct simulations of all aspects of particle spectrum of collision right

Matrix element, parton showers, underlying event (non-perturbative soft QCD!), parton density functions,...

Parton shower matching to higher order matrix calculation in complex pp collision environment is a hot topic among theorists/phenomenologists today!

Allow to compare results from different experiments

Specific detector limitations basically removed

Also provides platform for communication with theorists (LO and some NLO)

Important limitations to be kept in mind

NLO particle level generators not available for all processes (more and more coming)

NNLO etc. not in sight



Basic idea

Attempt to collect all particles coming from the same source in a given collision

Re-establishing the original correlations between these particles to reconstruct the kinematics and possibly even the nature of the source

Is an algorithmic challenge

Many algorithms on the market, with different limitations

No universal algorithm or algorithm configuration for all final state analysis

More later, but good to know right away!

Requires theoretical and experimental guidelines

Theory – physical features of particle jets addressed by sum (recombination) rules, stability of algorithm, validity for higher order calculations,...

Experiment – requirements for features of measured jets to allow most precise unfolding of particle jet, drives detector designs!

Guidelines often not very appreciated by older analysis/experiments

Often focus on extracting signal structures from experiment without worrying too much about theoretical requirements

LO analysis: apply any jet algorithm to measured signals and corresponding simulations with expectations to get the same physics

LHC kinematic reach and phase space need considerations of higher order calculations – need jet finders valid to (arbitrary!) order!



Very important at LHC

Often LO (or even NLO) not sufficient to understand final states

Potentially significant K-factors can only be applied to jet driven spectra if jet finding follows theoretical rules

E.g., jet cross-section shapes

Need to be able to compare experiments and theory

Comparison at the level of distributions

ATLAS and CMS will unfold experimental effects and limitations independently – different detector systems

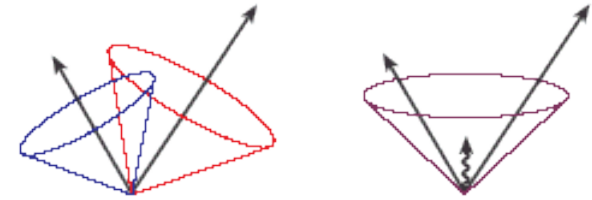
Theoretical guidelines

Infrared safety

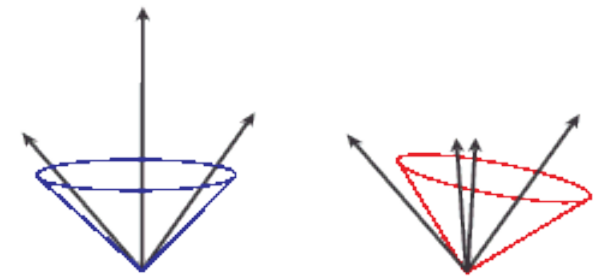
Adding or removing soft particles should not change the result of jet clustering

Collinear safety

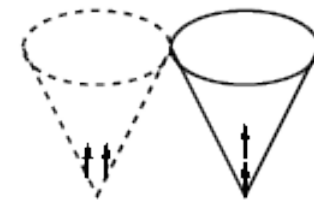
Splitting of large p_T particle into two collinear particles should not affect the jet finding



infrared sensitivity
(soft gluon radiation merges jets)



collinear sensitivity (1)
(sensitive to E_+ ordering of seeds)



collinear sensitivity (2)
(signal split into two towers below threshold)

Introduction to Hadronic Final State Reconstruction in Collider Experiments (Part VI)

Peter Loch
University of Arizona
Tucson, Arizona
USA

Very important at LHC

Often LO (or even NLO) not sufficient to understand final states

Potentially significant K-factors can only be applied to jet driven spectra if jet finding follows theoretical rules

E.g., jet cross-section shapes

Need to be able to compare experiments and theory

Comparison at the level of distributions

ATLAS and CMS will unfold experimental effects and limitations independently – different detector systems

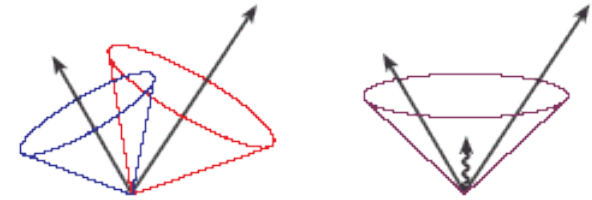
Theoretical guidelines

Infrared safety

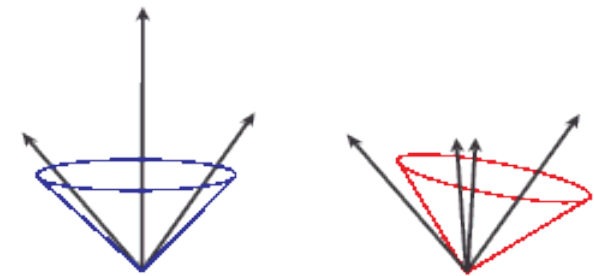
Adding or removing soft particles should not change the result of jet clustering

Collinear safety

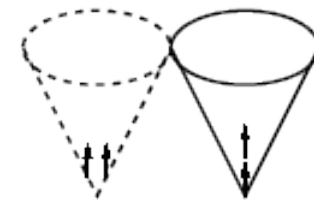
Splitting of large p_T particle into two collinear particles should not affect the jet finding



infrared sensitivity
(soft gluon radiation merges jets)



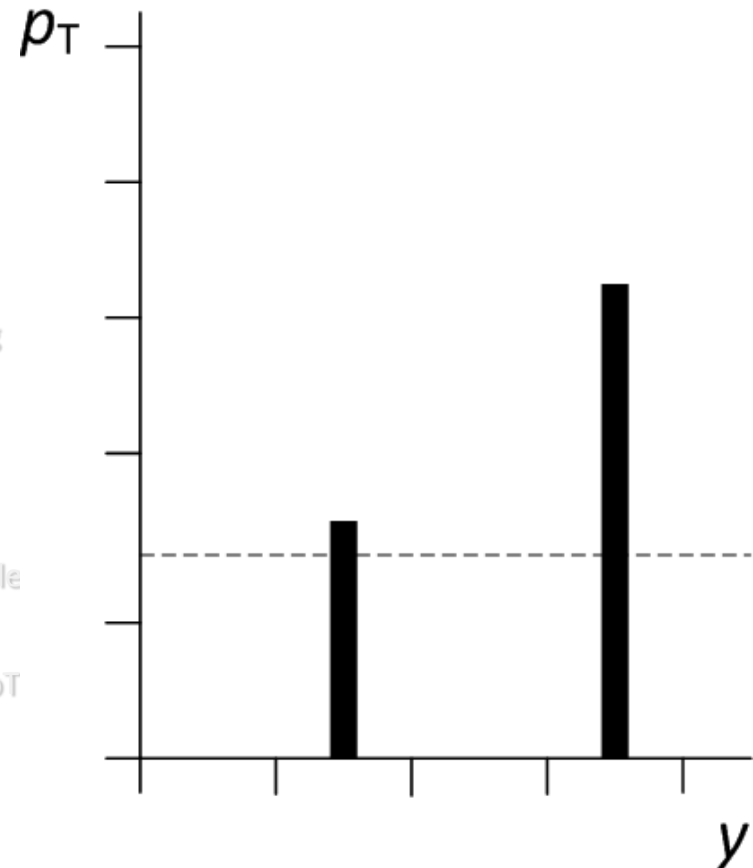
collinear sensitivity (1)
(sensitive to E_+ ordering of seeds)



collinear sensitivity (2)
(signal split into two towers below threshold)

Use following jet finder rules:

- Find particle with largest p_T above a seed threshold
 - Create an ordered list of particles descending in p_T and pick first particle
- Draw a cone of fixed size around this particle
 - Resolution parameter of algorithm
- Collect all other particles in cone and re-calculate cone directions from those
 - Use four-momentum re-summation
- Collect particles in new cone of same size and find new direction as above
 - Repeat until direction does not change \rightarrow cone becomes stable
- Take next particle from list if above p_T seed threshold
- Repeat procedure and find next proto-jet
 - Note that this is done with all particles, including the ones found in previous cones
- Continue until no more proto-jets above threshold can be constructed
 - The same particle can be used by 2 or more jets
- Check for overlap between proto-jets
 - Add lower p_T jet to higher p_T jet if sum of particle p_T in overlap is above a certain fraction of the lower p_T jet (merge)
 - Else remove overlapping particles from higher p_T jet and add to lower p_T jet (split)
- All surviving proto-jets are the final jets



Use following jet finder rules:

Find particle with largest p_T above a seed threshold

Create an ordered list of particles descending in p_T and pick first particle

Draw a cone of fixed size around this particle

Resolution parameter of algorithm

Collect all other particles in cone and re-calculate cone directions from those

Use four-momentum re-summation

Collect particles in new cone of same size and find new direction as above

Repeat until direction does not change \rightarrow cone becomes stable

Take next particle from list if above p_T seed threshold

Repeat procedure and find next proto-jet

Note that this is done with all particles, including the ones found in previous cones

Continue until no more proto-jets above threshold can be constructed

The same particle can be used by 2 or more jets

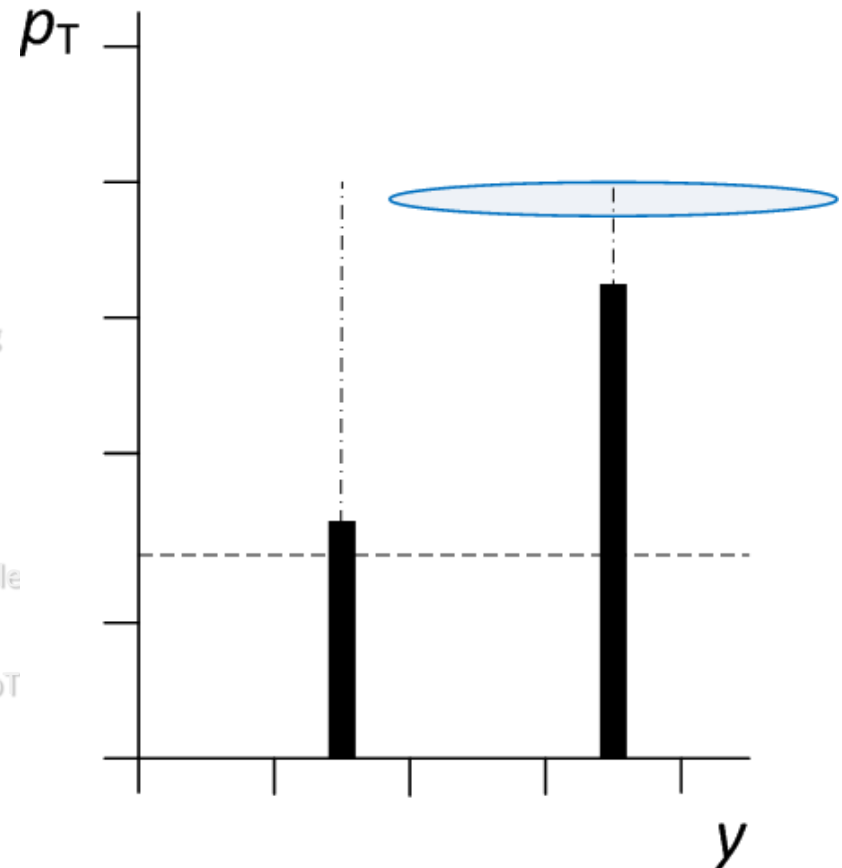
Check for overlap between proto-jets

Add lower p_T jet to higher p_T jet if sum of particle p_T in overlap is above a certain fraction of the lower p_T jet (merge)

Else remove overlapping particles from higher p_T jet and add to lower p_T jet (split)

All surviving proto-jets are the final jets

$$\Delta R = \sqrt{\Delta\eta^2 + \Delta\phi^2} < R_{\text{cone}}$$



Use following jet finder rules:

Find particle with largest pT above a seed threshold

Create an ordered list of particles descending in pT and pick first particle

Draw a cone of fixed size around this particle

Resolution parameter of algorithm

Collect all other particles in cone and re-calculate cone directions from those

Use four-momentum re-summation

Collect particles in new cone of same size and find new direction as above

Repeat until direction does not change → cone becomes stable

Take next particle from list if above pT seed threshold

Repeat procedure and find next proto-jet

Note that this is done with all particles, including the ones found in previous cones

Continue until no more proto-jets above threshold can be constructed

The same particle can be used by 2 or more jets

Check for overlap between proto-jets

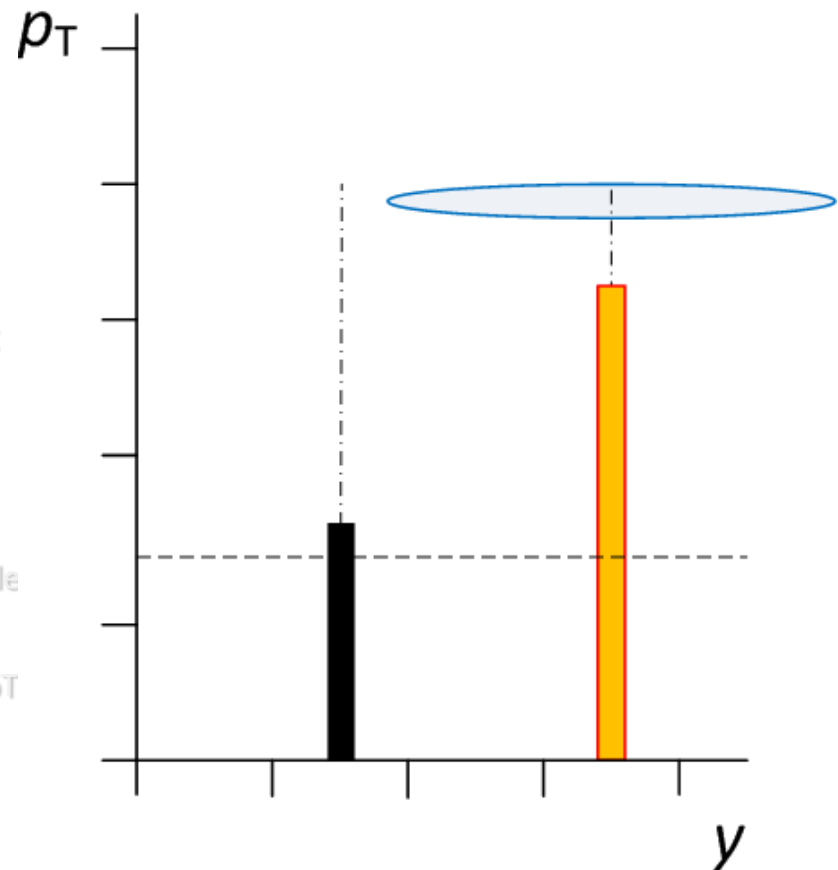
Add lower pT jet to higher pT jet if sum of particle pT in overlap is above a certain fraction of the lower pT jet (merge)

Else remove overlapping particles from higher pT jet and add to lower pT jet (split)

All surviving proto-jets are the final jets

$$\Delta R = \sqrt{\Delta\eta^2 + \Delta\phi^2} < R_{\text{cone}}$$

(first protojet)



Use following jet finder rules:

Find particle with largest p_T above a seed threshold

Create an ordered list of particles descending in p_T and pick first particle

Draw a cone of fixed size around this particle

Resolution parameter of algorithm

Collect all other particles in cone and re-calculate cone directions from those

Use four-momentum re-summation

Collect particles in new cone of same size and find new direction as above

Repeat until direction does not change \rightarrow cone becomes stable

Take next particle from list if above p_T seed threshold

Repeat procedure and find next proto-jet

Note that this is done with all particles, including the ones found in previous cones

Continue until no more proto-jets above threshold can be constructed

The same particle can be used by 2 or more jets

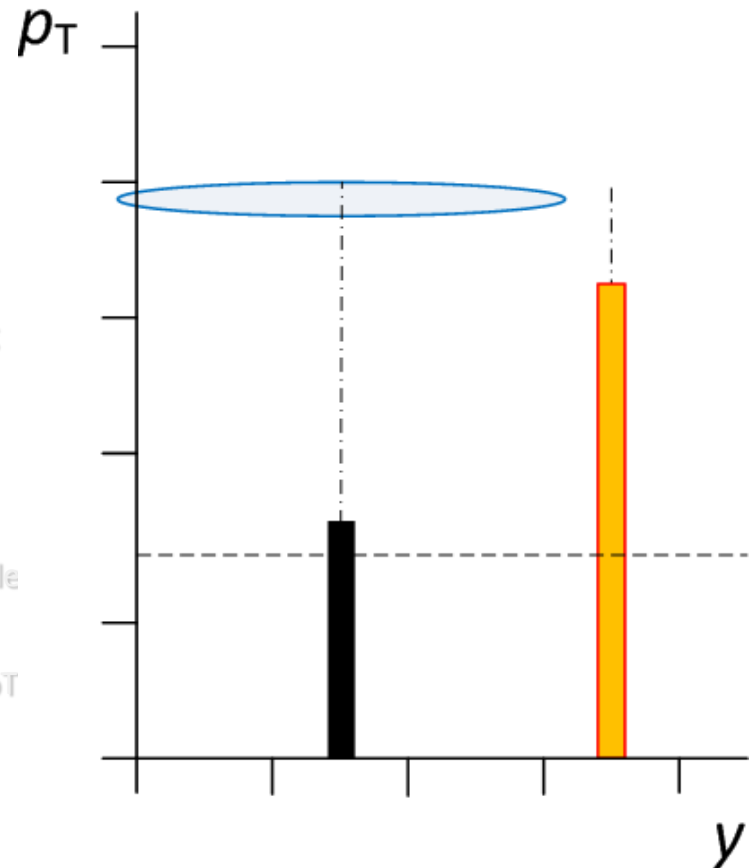
Check for overlap between proto-jets

Add lower p_T jet to higher p_T jet if sum of particle p_T in overlap is above a certain fraction of the lower p_T jet (merge)

Else remove overlapping particles from higher p_T jet and add to lower p_T jet (split)

All surviving proto-jets are the final jets

$$\Delta R = \sqrt{\Delta\eta^2 + \Delta\phi^2} < R_{\text{cone}}$$



Use following jet finder rules:

Find particle with largest p_T above a seed threshold

Create an ordered list of particles descending in p_T and pick first particle

Draw a cone of fixed size around this particle

Resolution parameter of algorithm

Collect all other particles in cone and re-calculate cone directions from those

Use four-momentum re-summation

Collect particles in new cone of same size and find new direction as above

Repeat until direction does not change \rightarrow cone becomes stable

Take next particle from list if above p_T seed threshold

Repeat procedure and find next proto-jet

Note that this is done with all particles, including the ones found in previous cones

Continue until no more proto-jets above threshold can be constructed

The same particle can be used by 2 or more jets

Check for overlap between proto-jets

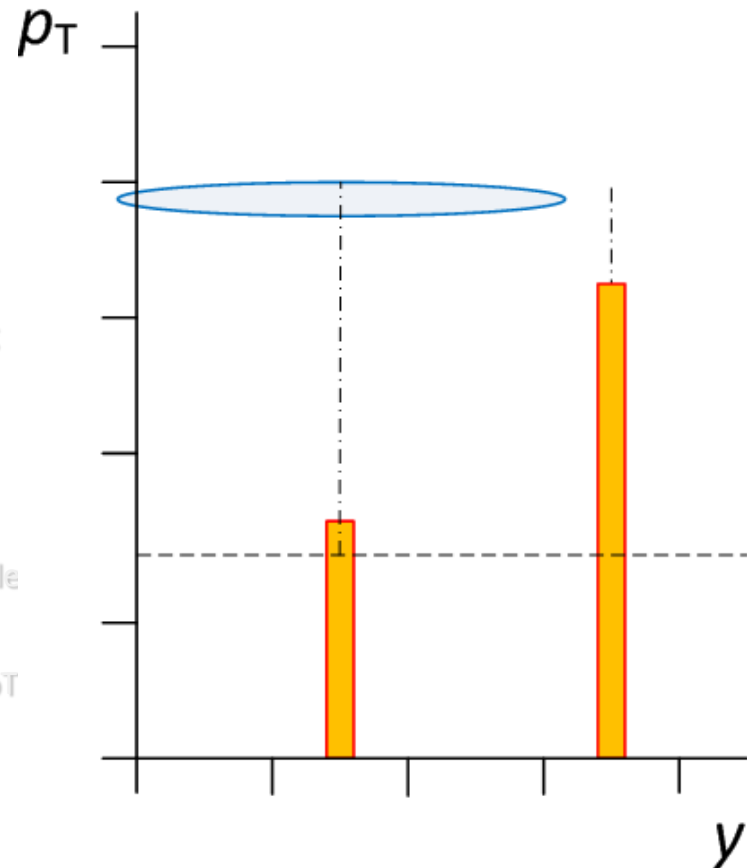
Add lower p_T jet to higher p_T jet if sum of particle p_T in overlap is above a certain fraction of the lower p_T jet (merge)

Else remove overlapping particles from higher p_T jet and add to lower p_T jet (split)

All surviving proto-jets are the final jets

$$\Delta R = \sqrt{\Delta\eta^2 + \Delta\phi^2} < R_{\text{cone}}$$

(second protojet)

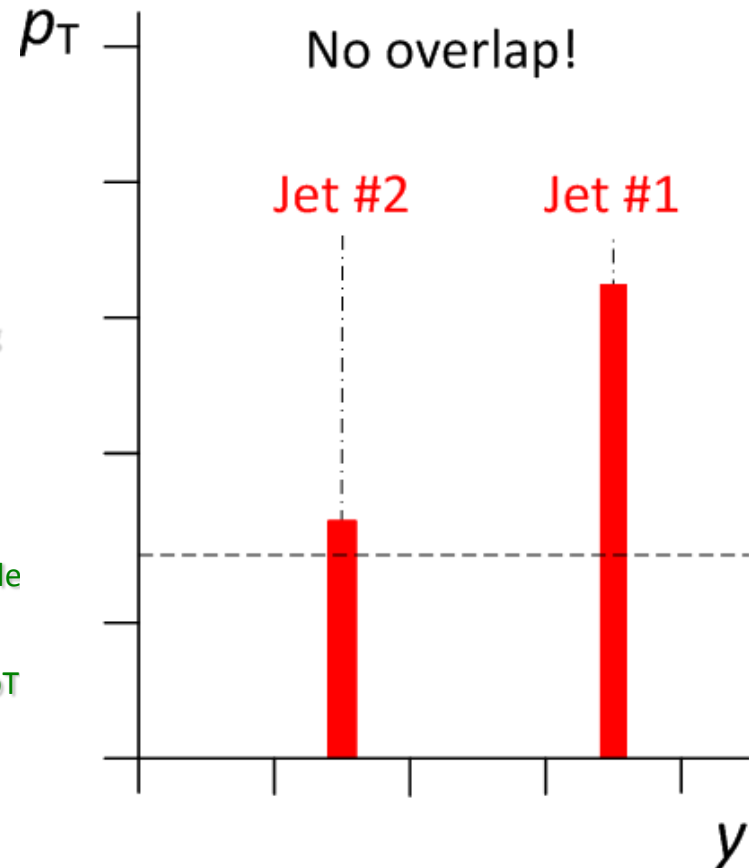


Use following jet finder rules:

- Find particle with largest p_T above a seed threshold
 - Create an ordered list of particles descending in p_T and pick first particle
- Draw a cone of fixed size around this particle
 - Resolution parameter of algorithm
- Collect all other particles in cone and re-calculate cone directions from those
 - Use four-momentum re-summation
- Collect particles in new cone of same size and find new direction as above
 - Repeat until direction does not change \rightarrow cone becomes stable
- Take next particle from list if above p_T seed threshold
- Repeat procedure and find next proto-jet
 - Note that this is done with all particles, including the ones found in previous cones
- Continue until no more proto-jets above threshold can be constructed
 - The same particle can be used by 2 or more jets
- Check for overlap between proto-jets
 - Add lower p_T jet to higher p_T jet if sum of particle p_T in overlap is above a certain fraction of the lower p_T jet (**merge**)
 - Else remove overlapping particles from higher p_T jet and add to lower p_T jet (**split**)
- All surviving proto-jets are the final jets

$$\Delta R = \sqrt{\Delta\eta^2 + \Delta\phi^2} < R_{\text{cone}}$$

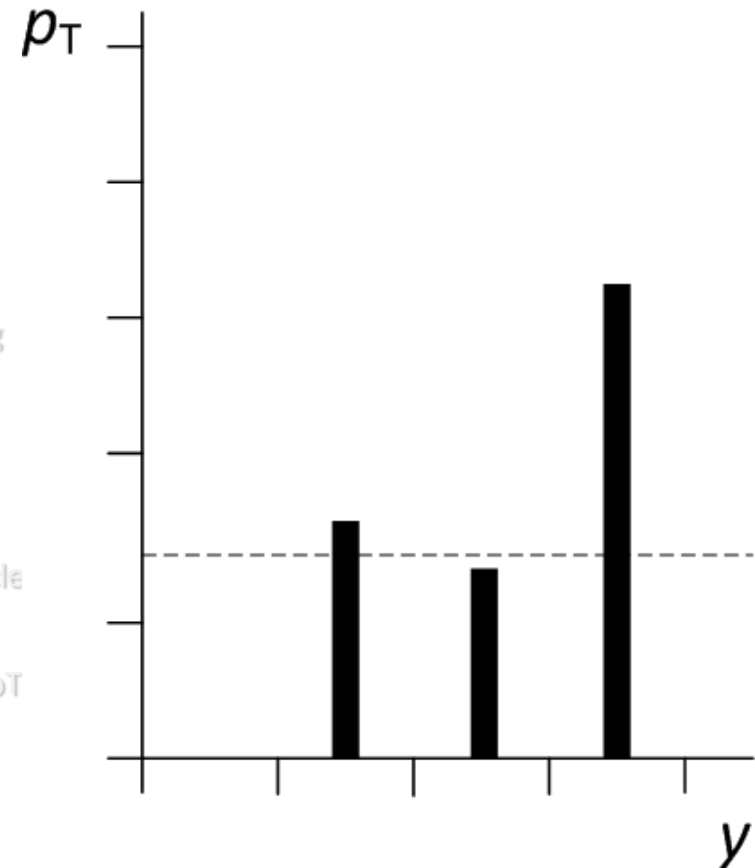
(two jets)



Use following jet finder rules:

- Find particle with largest pT above a seed threshold
 - Create an ordered list of particles descending in pT and pick first particle
- Draw a cone of fixed size around this particle
 - Resolution parameter of algorithm
- Collect all other particles in cone and re-calculate cone directions from those
 - Use four-momentum re-summation
- Collect particles in new cone of same size and find new direction as above
 - Repeat until direction does not change → cone becomes stable
- Take next particle from list if above pT seed threshold
- Repeat procedure and find next proto-jet
 - Note that this is done with all particles, including the ones found in previous cones
- Continue until no more proto-jets above threshold can be constructed
 - The same particle can be used by 2 or more jets
- Check for overlap between proto-jets
 - Add lower pT jet to higher pT jet if sum of particle pT in overlap is above a certain fraction of the lower pT jet (merge)
 - Else remove overlapping particles from higher pT jet and add to lower pT jet (split)
- All surviving proto-jets are the final jets

$$\Delta R = \sqrt{\Delta\eta^2 + \Delta\phi^2} < R_{\text{cone}}$$



Use following jet finder rules:

Find particle with largest p_T above a seed threshold

Create an ordered list of particles descending in p_T and pick first particle

Draw a cone of fixed size around this particle

Resolution parameter of algorithm

Collect all other particles in cone and re-calculate cone directions from those

Use four-momentum re-summation

Collect particles in new cone of same size and find new direction as above

Repeat until direction does not change \rightarrow cone becomes stable

Take next particle from list if above p_T seed threshold

Repeat procedure and find next proto-jet

Note that this is done with all particles, including the ones found in previous cones

Continue until no more proto-jets above threshold can be constructed

The same particle can be used by 2 or more jets

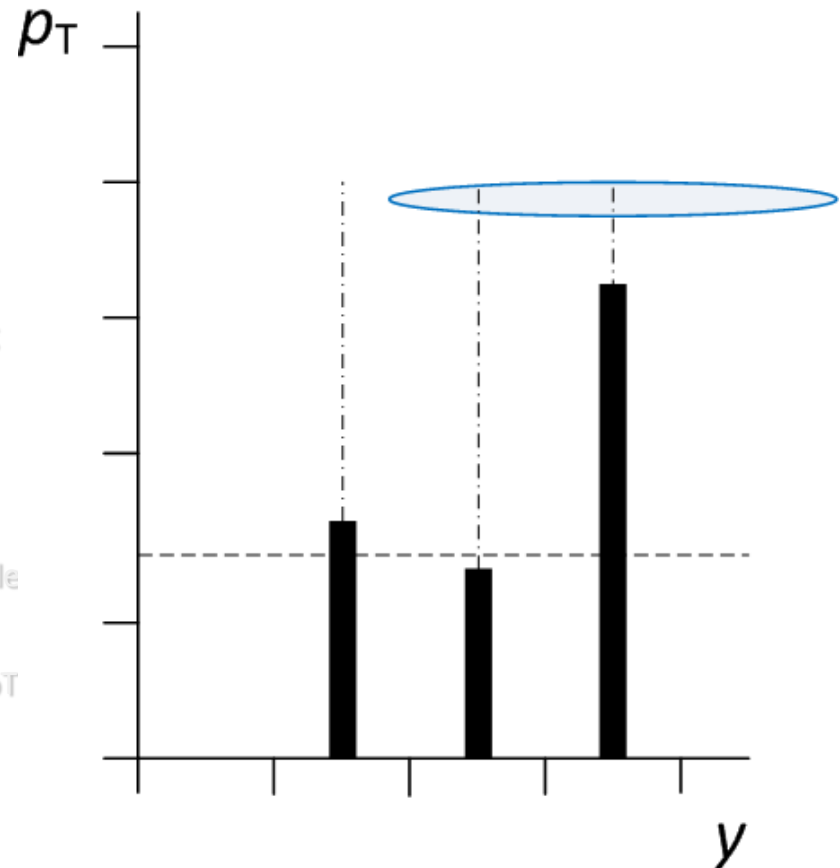
Check for overlap between proto-jets

Add lower p_T jet to higher p_T jet if sum of particle p_T in overlap is above a certain fraction of the lower p_T jet (merge)

Else remove overlapping particles from higher p_T jet and add to lower p_T jet (split)

All surviving proto-jets are the final jets

$$\Delta R = \sqrt{\Delta\eta^2 + \Delta\phi^2} < R_{\text{cone}}$$



Use following jet finder rules:

Find particle with largest p_T above a seed threshold

Create an ordered list of particles descending in p_T and pick first particle

Draw a cone of fixed size around this particle

Resolution parameter of algorithm

Collect all other particles in cone and re-calculate cone directions from those

Use four-momentum re-summation

Collect particles in new cone of same size and find new direction as above

Repeat until direction does not change \rightarrow cone becomes stable

Take next particle from list if above p_T seed threshold

Repeat procedure and find next proto-jet

Note that this is done with all particles, including the ones found in previous cones

Continue until no more proto-jets above threshold can be constructed

The same particle can be used by 2 or more jets

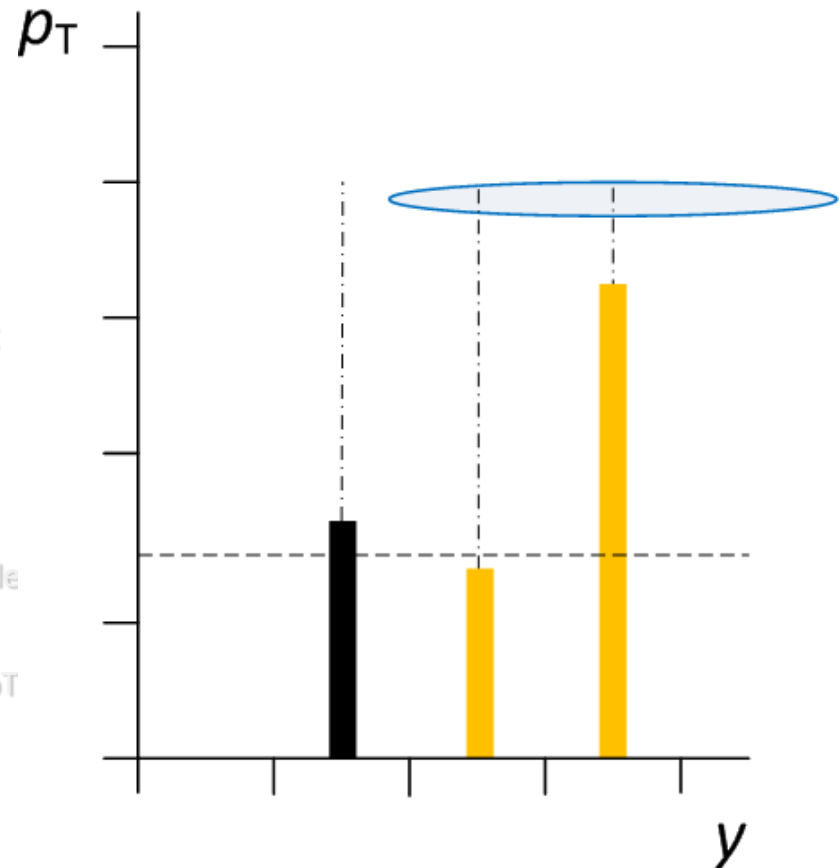
Check for overlap between proto-jets

Add lower p_T jet to higher p_T jet if sum of particle p_T in overlap is above a certain fraction of the lower p_T jet (merge)

Else remove overlapping particles from higher p_T jet and add to lower p_T jet (split)

All surviving proto-jets are the final jets

$$\Delta R = \sqrt{\Delta\eta^2 + \Delta\phi^2} < R_{\text{cone}}$$



Use following jet finder rules:

- Find particle with largest pT above a seed threshold
 - Create an ordered list of particles descending in pT and pick first particle
- Draw a cone of fixed size around this particle
 - Resolution parameter of algorithm
- Collect all other particles in cone and re-calculate cone directions from those
 - Use four-momentum re-summation
- Collect particles in new cone of same size and find new direction as above
 - Repeat until direction does not change → cone becomes stable

Take next particle from list if above pT seed threshold

Repeat procedure and find next proto-jet

Note that this is done with all particles, including the ones found in previous cones

Continue until no more proto-jets above threshold can be constructed

The same particle can be used by 2 or more jets

Check for overlap between proto-jets

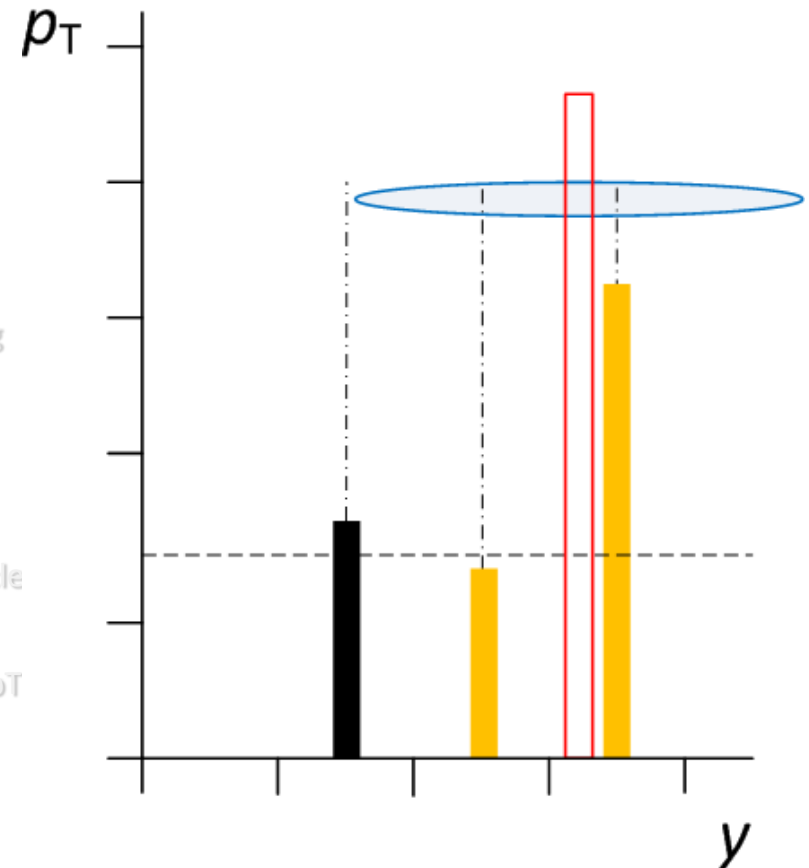
Add lower pT jet to higher pT jet if sum of particle pT in overlap is above a certain fraction of the lower pT jet (merge)

Else remove overlapping particles from higher pT jet and add to lower pT jet (split)

All surviving proto-jets are the final jets

$$\Delta R = \sqrt{\Delta\eta^2 + \Delta\phi^2} < R_{\text{cone}}$$

(first protojet)



Use following jet finder rules:

Find particle with largest p_T above a seed threshold

Create an ordered list of particles descending in p_T and pick first particle

Draw a cone of fixed size around this particle

Resolution parameter of algorithm

Collect all other particles in cone and re-calculate cone directions from those

Use four-momentum re-summation

Collect particles in new cone of same size and find new direction as above

Repeat until direction does not change \rightarrow cone becomes stable

Take next particle from list if above p_T seed threshold

Repeat procedure and find next proto-jet

Note that this is done with all particles, including the ones found in previous cones

Continue until no more proto-jets above threshold can be constructed

The same particle can be used by 2 or more jets

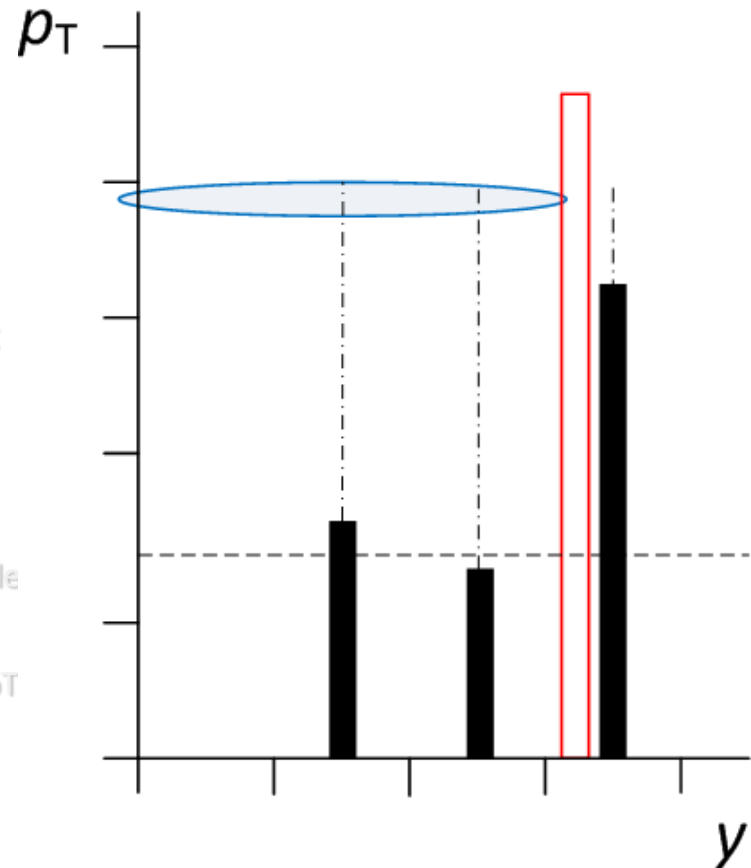
Check for overlap between proto-jets

Add lower p_T jet to higher p_T jet if sum of particle p_T in overlap is above a certain fraction of the lower p_T jet (merge)

Else remove overlapping particles from higher p_T jet and add to lower p_T jet (split)

All surviving proto-jets are the final jets

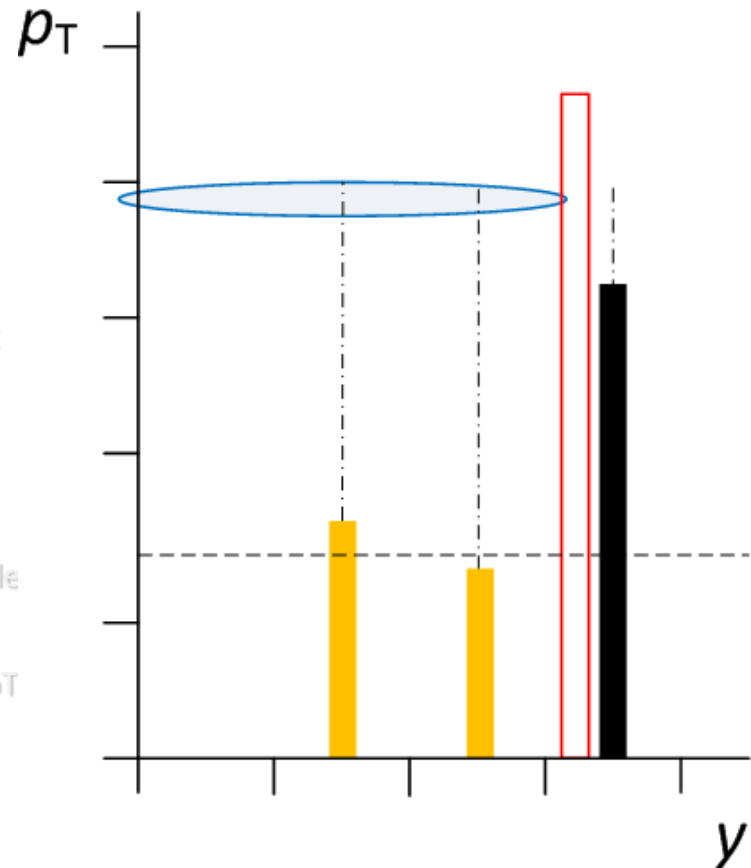
$$\Delta R = \sqrt{\Delta \eta^2 + \Delta \phi^2} < R_{\text{cone}}$$



Use following jet finder rules:

- Find particle with largest p_T above a seed threshold
 - Create an ordered list of particles descending in p_T and pick first particle
- Draw a cone of fixed size around this particle
 - Resolution parameter of algorithm
- Collect all other particles in cone and re-calculate cone directions from those
 - Use four-momentum re-summation
- Collect particles in new cone of same size and find new direction as above
 - Repeat until direction does not change \rightarrow cone becomes stable
- Take next particle from list if above p_T seed threshold
- Repeat procedure and find next proto-jet
 - Note that this is done with all particles, including the ones found in previous cones
- Continue until no more proto-jets above threshold can be constructed
 - The same particle can be used by 2 or more jets
- Check for overlap between proto-jets
 - Add lower p_T jet to higher p_T jet if sum of particle p_T in overlap is above a certain fraction of the lower p_T jet (merge)
 - Else remove overlapping particles from higher p_T jet and add to lower p_T jet (split)
- All surviving proto-jets are the final jets

$$\Delta R = \sqrt{\Delta\eta^2 + \Delta\phi^2} < R_{\text{cone}}$$



Use following jet finder rules:

Find particle with largest p_T above a seed threshold

Create an ordered list of particles descending in p_T and pick first particle

Draw a cone of fixed size around this particle

Resolution parameter of algorithm

Collect all other particles in cone and re-calculate cone directions from those

Use four-momentum re-summation

Collect particles in new cone of same size and find new direction as above

Repeat until direction does not change \rightarrow cone becomes stable

Take next particle from list if above p_T seed threshold

Repeat procedure and find next proto-jet

Note that this is done with all particles, including the ones found in previous cones

Continue until no more proto-jets above threshold can be constructed

The same particle can be used by 2 or more jets

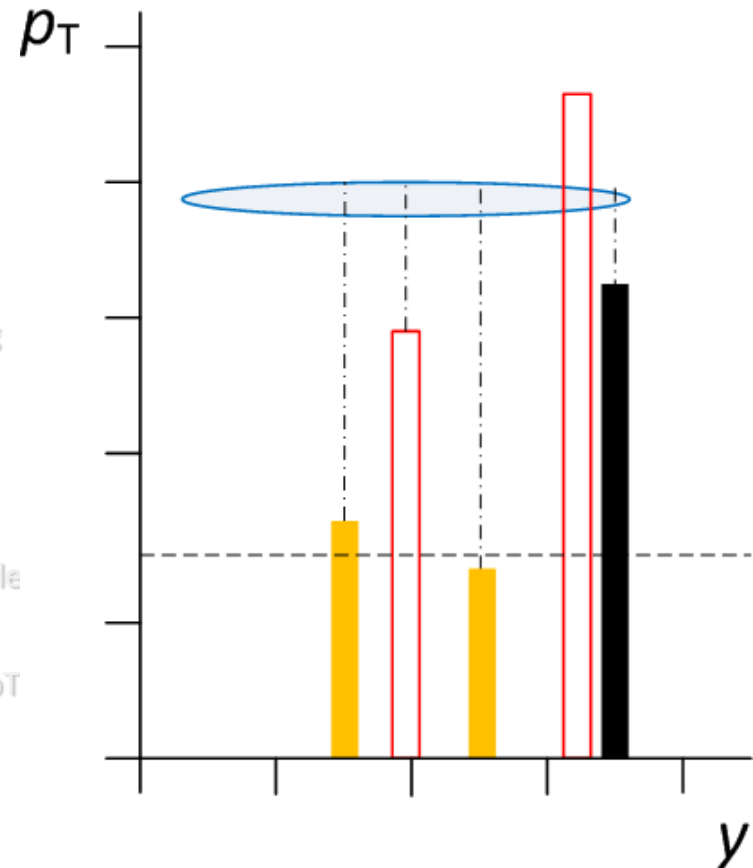
Check for overlap between proto-jets

Add lower p_T jet to higher p_T jet if sum of particle p_T in overlap is above a certain fraction of the lower p_T jet (merge)

Else remove overlapping particles from higher p_T jet and add to lower p_T jet (split)

All surviving proto-jets are the final jets

$$\Delta R = \sqrt{\Delta\eta^2 + \Delta\phi^2} < R_{\text{cone}}$$



Use following jet finder rules:

Find particle with largest p_T above a seed threshold

Create an ordered list of particles descending in p_T and pick first particle

Draw a cone of fixed size around this particle

Resolution parameter of algorithm

Collect all other particles in cone and re-calculate cone directions from those

Use four-momentum re-summation

Collect particles in new cone of same size and find new direction as above

Repeat until direction does not change \rightarrow cone becomes stable

Take next particle from list if above p_T seed threshold

Repeat procedure and find next proto-jet

Note that this is done with all particles, including the ones found in previous cones

Continue until no more proto-jets above threshold can be constructed

The same particle can be used by 2 or more jets

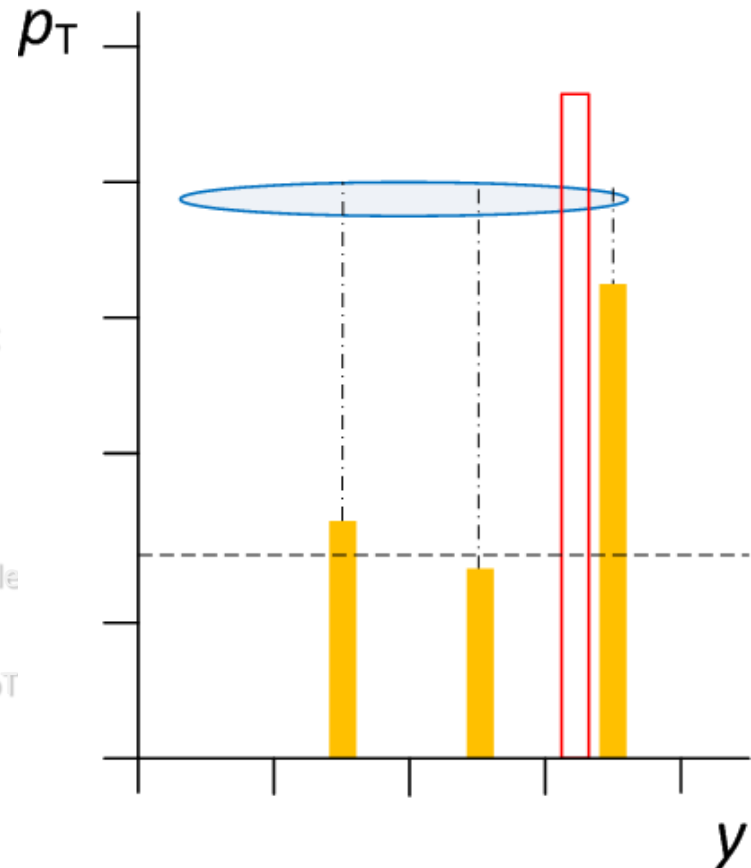
Check for overlap between proto-jets

Add lower p_T jet to higher p_T jet if sum of particle p_T in overlap is above a certain fraction of the lower p_T jet (merge)

Else remove overlapping particles from higher p_T jet and add to lower p_T jet (split)

All surviving proto-jets are the final jets

$$\Delta R = \sqrt{\Delta\eta^2 + \Delta\phi^2} < R_{\text{cone}}$$



Use following jet finder rules:

Find particle with largest p_T above a seed threshold

Create an ordered list of particles descending in p_T and pick first particle

Draw a cone of fixed size around this particle

Resolution parameter of algorithm

Collect all other particles in cone and re-calculate cone directions from those

Use four-momentum re-summation

Collect particles in new cone of same size and find new direction as above

Repeat until direction does not change \rightarrow cone becomes stable

Take next particle from list if above p_T seed threshold

Repeat procedure and find next proto-jet

Note that this is done with all particles, including the ones found in previous cones

Continue until no more proto-jets above threshold can be constructed

The same particle can be used by 2 or more jets

Check for overlap between proto-jets

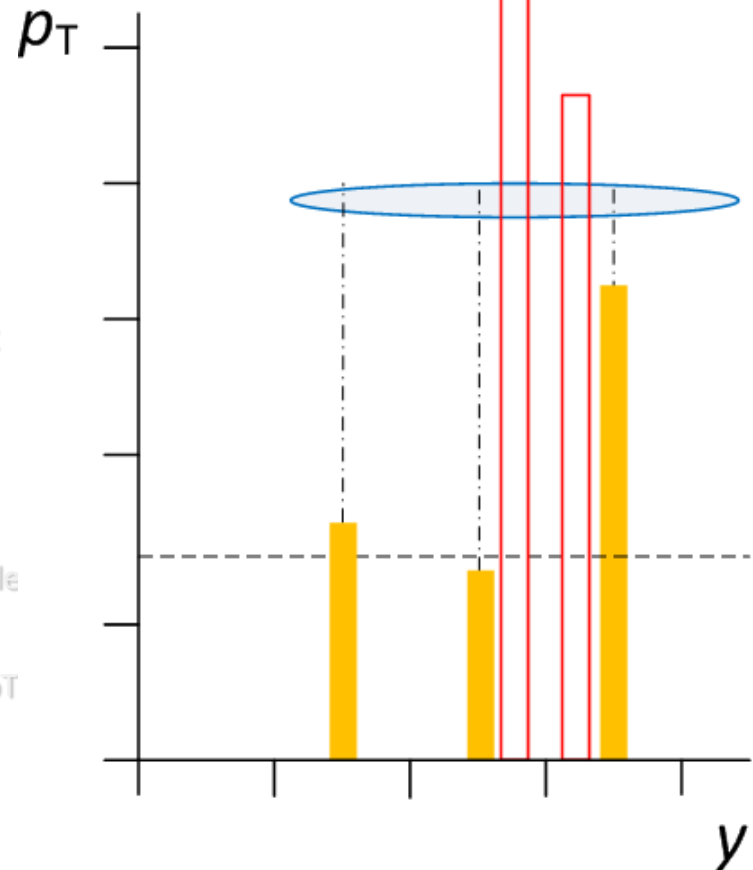
Add lower p_T jet to higher p_T jet if sum of particle p_T in overlap is above a certain fraction of the lower p_T jet (merge)

Else remove overlapping particles from higher p_T jet and add to lower p_T jet (split)

All surviving proto-jets are the final jets

$$\Delta R = \sqrt{\Delta\eta^2 + \Delta\phi^2} < R_{\text{cone}}$$

(second protojet)



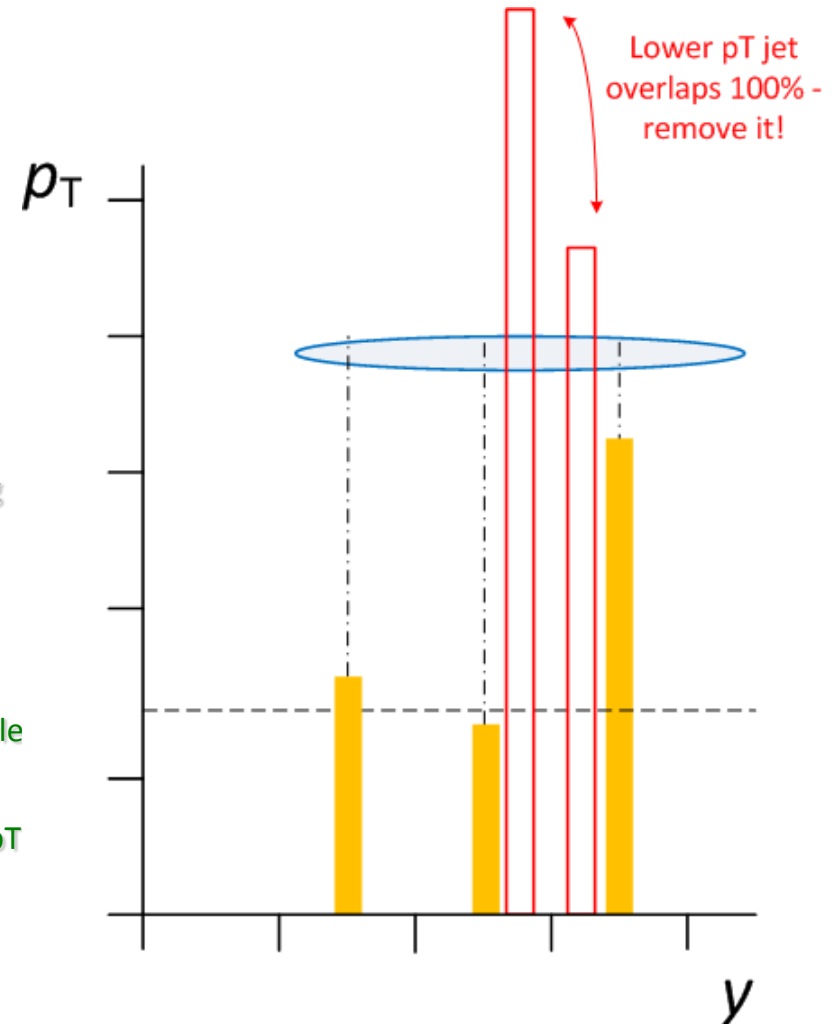
Use following jet finder rules:

- Find particle with largest p_T above a seed threshold
 - Create an ordered list of particles descending in p_T and pick first particle
- Draw a cone of fixed size around this particle
 - Resolution parameter of algorithm
- Collect all other particles in cone and re-calculate cone directions from those
 - Use four-momentum re-summation
- Collect particles in new cone of same size and find new direction as above
 - Repeat until direction does not change → cone becomes stable
- Take next particle from list if above p_T seed threshold
- Repeat procedure and find next proto-jet
 - Note that this is done with all particles, including the ones found in previous cones
- Continue until no more proto-jets above threshold can be constructed
 - The same particle can be used by 2 or more jets
- Check for overlap between proto-jets
 - Add lower p_T jet to higher p_T jet if sum of particle p_T in overlap is above a certain fraction of the lower p_T jet (**merge**)
 - Else remove overlapping particles from higher p_T jet and add to lower p_T jet (**split**)

All surviving proto-jets are the final jets

$$\Delta R = \sqrt{\Delta \eta^2 + \Delta \phi^2} < R_{\text{cone}}$$

(second protojet)

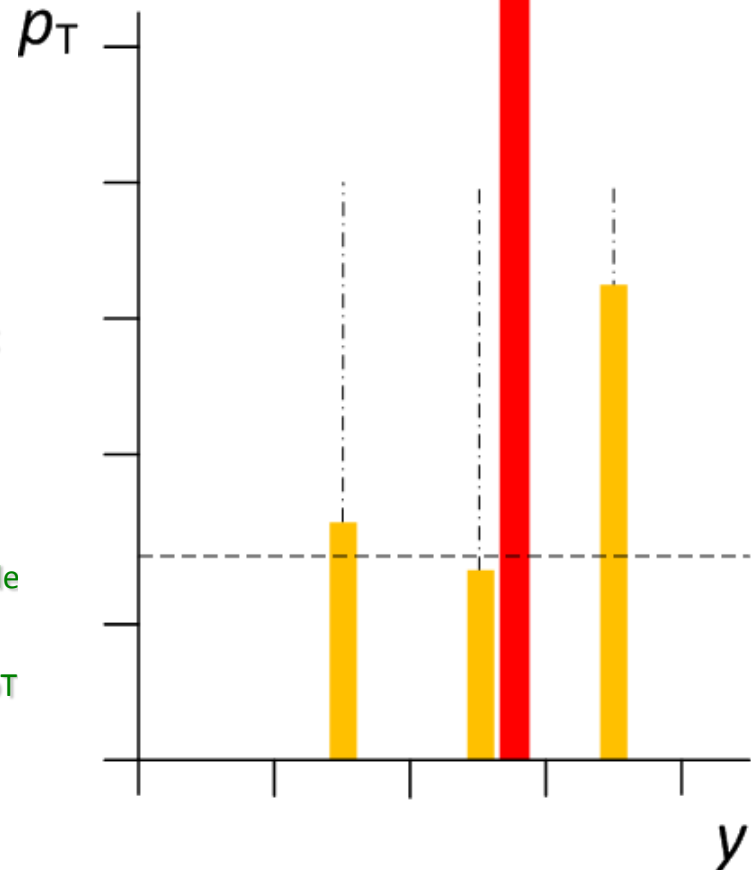


Use following jet finder rules:

- Find particle with largest pT above a seed threshold
 - Create an ordered list of particles descending in pT and pick first particle
- Draw a cone of fixed size around this particle
 - Resolution parameter of algorithm
- Collect all other particles in cone and re-calculate cone directions from those
 - Use four-momentum re-summation
- Collect particles in new cone of same size and find new direction as above
 - Repeat until direction does not change → cone becomes stable
- Take next particle from list if above pT seed threshold
- Repeat procedure and find next proto-jet
 - Note that this is done with all particles, including the ones found in previous cones
- Continue until no more proto-jets above threshold can be constructed
 - The same particle can be used by 2 or more jets
- Check for overlap between proto-jets
 - Add lower pT jet to higher pT jet if sum of particle pT in overlap is above a certain fraction of the lower pT jet (**merge**)
 - Else remove overlapping particles from higher pT jet and add to lower pT jet (**split**)
- All surviving proto-jets are the final jets

$$\Delta R = \sqrt{\Delta\eta^2 + \Delta\phi^2} < R_{\text{cone}}$$

(one jet)



Use following jet finder rules:

Find particle with largest p_T above a seed threshold

Create an ordered list of particles descending in p_T
and pick first particle

Draw a cone of fixed size around this particle

Resolution parameter of algorithm

Collect all other particles in cone and re-calculate
cone directions from those

Use four-momentum summation

Collect particles in new cone of same size and find
new direction as above

Repeat until direction does not change → cone
becomes stable

Take next particle from list if above p_T seed
threshold

Repeat procedure and find next proto-jet

Note that this is done with all particles, including
the ones found in previous cones

Continue until no more proto-jets above threshold
can be constructed

The same particle can be used by 2 or more jets

Check for overlap between proto-jets

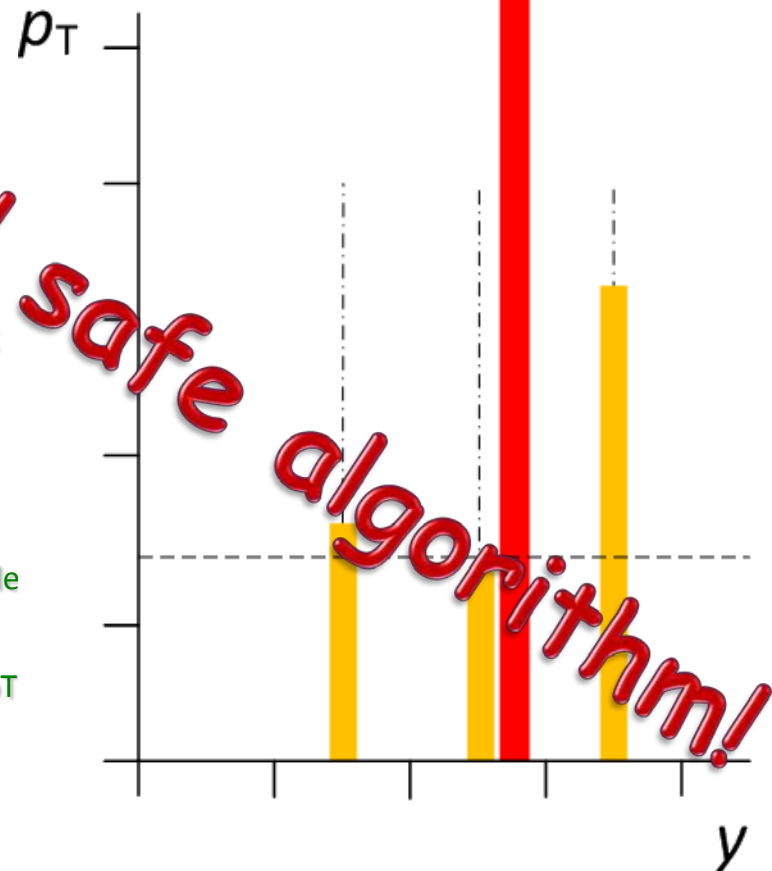
Add lower p_T jet to higher p_T jet if sum of particle
p_T in overlap is above a certain fraction of the
lower p_T jet (**merge**)

Else remove overlapping particles from higher p_T
jet and add to lower p_T jet (**split**)

All surviving proto-jets are the final jets

$$\Delta R = \sqrt{\Delta\eta^2 + \Delta\phi^2} < R_{\text{cone}}$$

(one jet)



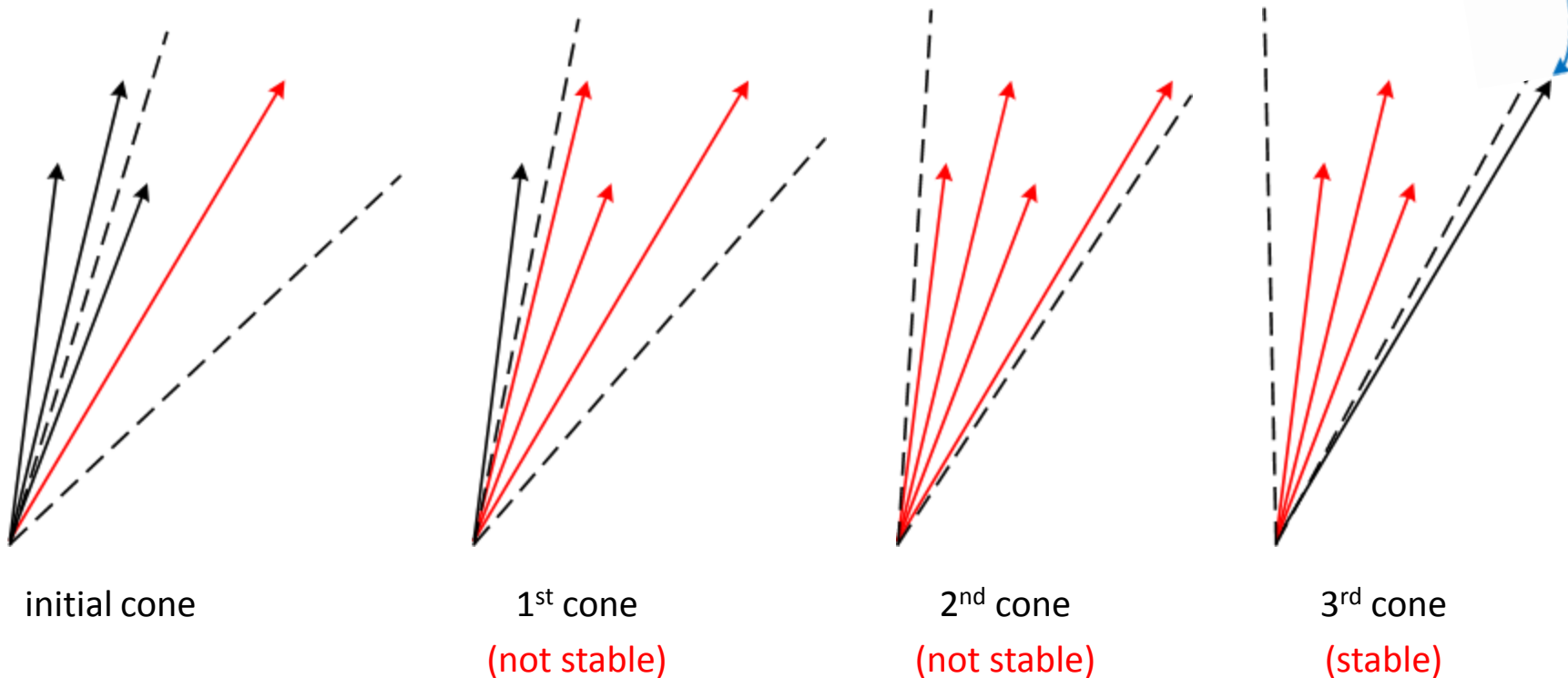
Other problems with iterative cone finders:

“Dark” tower problem

Original seed moves out of cone

Significant energy lost for jets

original seed lost for jets!

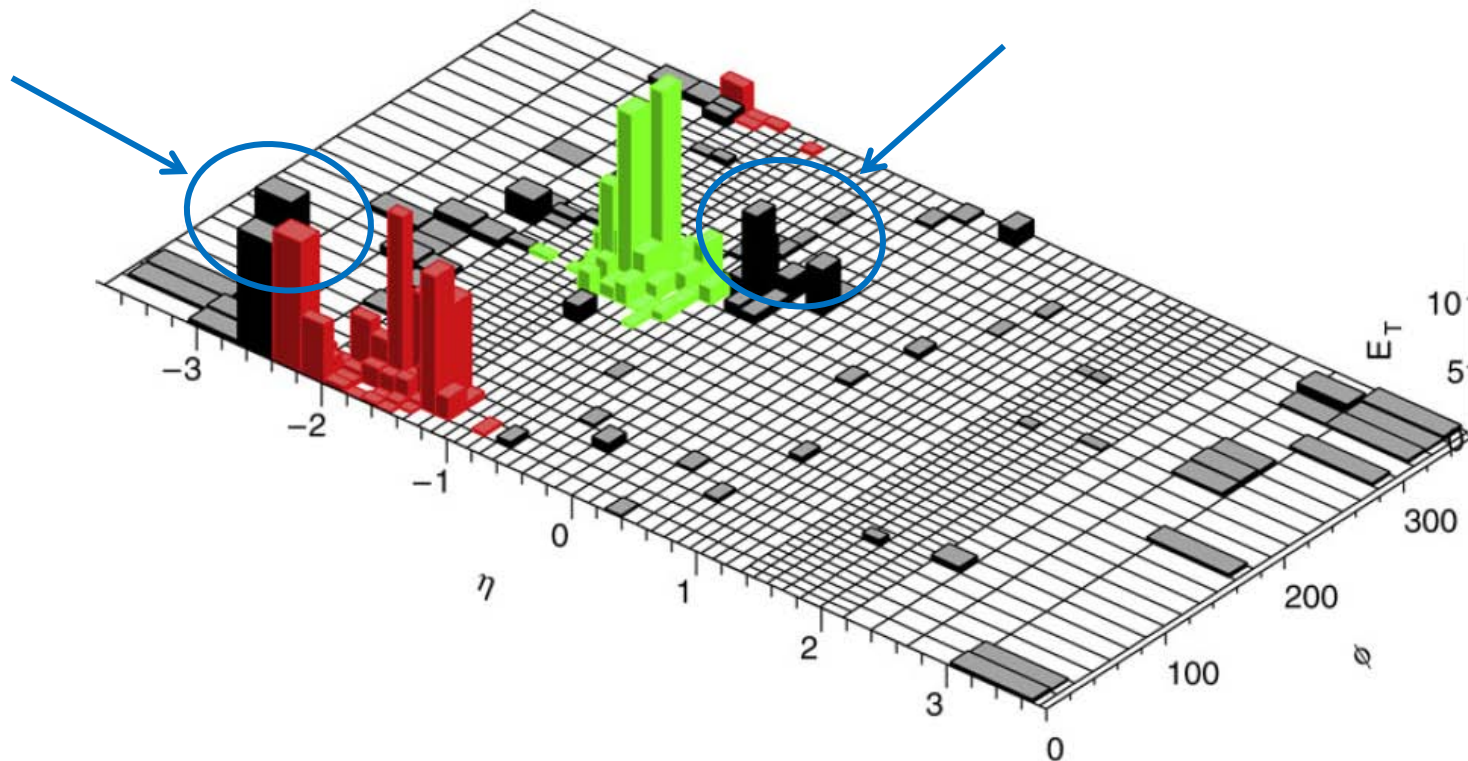


Other problems with iterative cone finders:

“Dark” tower problem

Original seed moves out of cone

Significant energy lost for jets



Advantages

Simple geometry based algorithm

Easy to implement

Fast algorithm

Ideal for online application in experiment

Disadvantages

Not infrared safe

Can partially be recovered by splitting & merging

Introduces split/merge p_T fraction f (typically 0.50 - 0.75)

Kills “trace” of perturbative infinities in experiment

Hard to confirm higher order calculations in “real life” without infinities!

Not collinear safe

Used p_T seeds (thresholds)

Jets not cone shaped

Splitting and merging potentially makes jets bigger than original cone size and changes jet boundaries



Motivated by gluon splitting function

QCD branching happens all the time

Attempt to undo parton fragmentation

Pair with strongest divergence likely belongs together

kT/Durham, first used in e^+e^-
Catani, Dokshitzer, Olsson,
Turnock & Webber 1991

Longitudinal invariant version for hadron colliders

Transverse momentum instead of energy

Catani, Dokshitzer, Seymour & Webber 1993

S.D. Ellis & D. Soper 1993

Valid at all orders!

$$\left[dk_j \right] \left| M_{g \rightarrow g, g_j}^2(k_j) \right| \simeq \frac{2\alpha_s C_A}{\pi} \frac{dE_j}{\min(E_i, E_j)} \frac{d\Theta_{ij}}{\Theta_{ij}}$$

$$(E_j \ll E_i, \Theta_{ij} \ll 1)$$

Distance between all particles i and j

$$y_{ij} = \frac{2\min(E_i^2, E_j^2)(1 - \cos \Theta_{ij})}{Q^2}$$

$y_{ij} < y_{\text{cut}} \rightarrow$ combine i and j , else stop

Drop normalization to Q^2 (not fixed in pp)

$$y_{ij} \rightarrow d_{ij} = \min(d_i, d_j) \Delta R_{ij}^2, \quad d_{i,j} = p_{Ti,j}^2$$

$$\Delta R_{ij}^2 = (y_i - y_j)^2 + (\varphi_i - \varphi_j)^2$$

$d_{ij} < d_{\text{cut}} \rightarrow$ combine i and j , else stop

(exclusive kT)

Inclusive longitudinal invariant clustering

$$d_{ij} = \min(d_i, d_j) \Delta R_{ij}^2 / R^2$$



Motivated by gluon splitting function

QCD branching happens all the time

Attempt to undo parton fragmentation

Pair with strongest divergence likely belongs together

kT/Durham, first used in e^+e^-
Catani, Dokshitzer, Olsson,
Turnock & Webber 1991

Longitudinal invariant version for hadron colliders

Transverse momentum instead of energy

Catani, Dokshitzer, Seymour & Webber 1993

S.D. Ellis & D. Soper 1993

Valid at all orders!

$$\left[dk_j \right] \left| M_{g \rightarrow g, g_j}^2(k_j) \right| \simeq \frac{2\alpha_s C_A}{\pi} \frac{dE_j}{\min(E_i, E_j)} \frac{d\Theta_{ij}}{\Theta_{ij}}$$

$$(E_j \ll E_i, \Theta_{ij} \ll 1)$$

Distance between all particles i and j

$$y_{ij} = \frac{2\min(E_i^2, E_j^2)(1 - \cos \Theta_{ij})}{Q^2}$$

$y_{ij} < y_{\text{cut}} \rightarrow$ combine i and j , else stop

Drop normalization to Q^2 (not fixed in pp)

$$y_{ij} \rightarrow d_{ij} = \min(d_i, d_j) \Delta R_{ij}^2, \quad d_{i,j} = p_{\text{Ti},j}^2$$

$$\Delta R_{ij}^2 = (y_i - y_j)^2 + (\varphi_i - \varphi_j)^2$$

$d_{ij} < d_{\text{cut}} \rightarrow$ combine i and j , else stop

(exclusive kT)

Inclusive longitudinal invariant clustering

$$d_{ij} = \min(d_i, d_j) \Delta R_{ij}^2 / R^2$$



Motivated by gluon splitting function

QCD branching happens all the time

Attempt to undo parton fragmentation

Pair with strongest divergence likely belongs together

kT/Durham, first used in e^+e^-
 Catani, Dokshitzer, Olsson,
 Turnock & Webber 1991

Longitudinal invariant version for hadron colliders

Transverse momentum instead of energy

Catani, Dokshitzer, Seymour & Webber 1993

S.D. Ellis & D. Soper 1993

Valid at all orders!

$$\left[dk_j \right] \left| M_{g \rightarrow g, g_j}^2(k_j) \right| \simeq \frac{2\alpha_s C_A}{\pi} \frac{dE_j}{\min(E_i, E_j)} \frac{d\Theta_{ij}}{\Theta_{ij}}$$

$$(E_j \ll E_i, \Theta_{ij} \ll 1)$$

Distance between all particles i and j

$$y_{ij} = \frac{2\min(E_i^2, E_j^2)(1 - \cos \Theta_{ij})}{Q^2}$$

$y_{ij} < y_{\text{cut}} \rightarrow$ combine i and j , else stop

Drop normalization to Q^2 (not fixed in pp)

$$y_{ij} \rightarrow d_{ij} = \min(d_i, d_j) \Delta R_{ij}^2, \quad d_{i,j} = p_{\text{T},i,j}^2$$

$$\Delta R_{ij}^2 = (y_i - y_j)^2 + (\varphi_i - \varphi_j)^2$$

$d_{ij} < d_{\text{cut}} \rightarrow$ combine i and j , else stop

(exclusive kT)

Inclusive longitudinal invariant clustering

$$d_{ij} = \min(d_i, d_j) \Delta R_{ij}^2 / R^2$$



Motivated by gluon splitting function

QCD branching happens all the time

Attempt to undo parton fragmentation

Pair with strongest divergence likely belongs together

kT/Durham, first used in e^+e^-
 Catani, Dokshitzer, Olsson,
 Turnock & Webber 1991

Longitudinal invariant version for hadron colliders

Transverse momentum instead of energy

Catani, Dokshitzer, Seymour & Webber 1993

S.D. Ellis & D. Soper 1993

Valid at all orders!

$$\left[dk_j \right] \left| M_{g \rightarrow g, g_j}^2(k_j) \right| \simeq \frac{2\alpha_s C_A}{\pi} \frac{dE_j}{\min(E_i, E_j)} \frac{d\Theta_{ij}}{\Theta_{ij}}$$

$$(E_j \ll E_i, \Theta_{ij} \ll 1)$$

Distance between all particles i and j

$$y_{ij} = \frac{2\min(E_i^2, E_j^2)(1 - \cos \Theta_{ij})}{Q^2}$$

$y_{ij} < y_{\text{cut}} \rightarrow$ combine i and j , else stop

Drop normalization to Q^2 (not fixed in pp)

$$y_{ij} \rightarrow d_{ij} = \min(d_i, d_j) \Delta R_{ij}^2, \quad d_{i,j} = p_{\text{T},i,j}^2$$

$$\Delta R_{ij}^2 = (y_i - y_j)^2 + (\varphi_i - \varphi_j)^2$$

$d_{ij} < d_{\text{cut}} \rightarrow$ combine i and j , else stop

(exclusive kT)

Inclusive longitudinal invariant clustering

$$d_{ij} = \min(d_i, d_j) \Delta R_{ij}^2 / R^2$$



Classic procedure

Calculate all distances d_{ji} for list of particles

Uses distance parameter

Calculate d_i for all particles

Uses pT

If minimum of both lists is a d_{ij} , combine i and j and add to list

Remove i and j , of course

If minimum is a d_i , call i a jet and remove from list

Recalculate all distances and continue all particles are removed or called a jet

Features

Clustering sequence is ordered in kT

Follows jet structure

Inclusive longitudinal invariant clustering

$$d_{ij} = \min(d_i, d_j) \Delta R_{ij}^2 / R^2$$

$$d_i = p_{Ti}^2$$

Alternatives

Cambridge/Aachen clustering

Uses angular distances only

Clustering sequence follows jet structure

Anti-kT clustering

No particular ordering, sequence not meaningful



Classic procedure

Calculate all distances d_{ji} for list of particles

Uses distance parameter

Calculate d_i for all particles

Uses pT

If minimum of both lists is a d_{ij} , combine i and j and add to list

Remove i and j , of course

If minimum is a d_i , call i a jet and remove from list

Recalculate all distances and continue all particles are removed or called a jet

Features

Clustering sequence is ordered in kT

Follows jet structure

Inclusive longitudinal invariant clustering

$$d_{ij} = \min(d_i, d_j) \Delta R_{ij}^2 / R^2$$

$$d_i = p_{Ti}^{2n}$$

Cambridge/Aachen ($n = 0$)

cluster smallest d_{ij} first until $d_{ij} > 1$

Alternatives

Cambridge/Aachen clustering

Uses angular distances only

Clustering sequence follows jet structure

Anti-kT clustering

No particular ordering, sequence not meaningful



Classic procedure

Calculate all distances d_{ji} for list of particles

Uses distance parameter

Calculate d_i for all particles

Uses pT

If minimum of both lists is a d_{ij} , combine i and j and add to list

Remove i and j , of course

If minimum is a d_i , call i a jet and remove from list

Recalculate all distances and continue all particles are removed or called a jet

Features

Clustering sequence is ordered in kT

Follows jet structure

Inclusive longitudinal invariant clustering

$$d_{ij} = \min(d_i, d_j) \Delta R_{ij}^2 / R^2$$

$$d_i = p_{Ti}^{2n}$$

Cambridge/Aachen ($n = 0$)

cluster smallest d_{ij} first until $d_{ij} > 1$

Anti-kT ($n = -1$)

follow classic algorithm

Alternatives

Cambridge/Aachen clustering

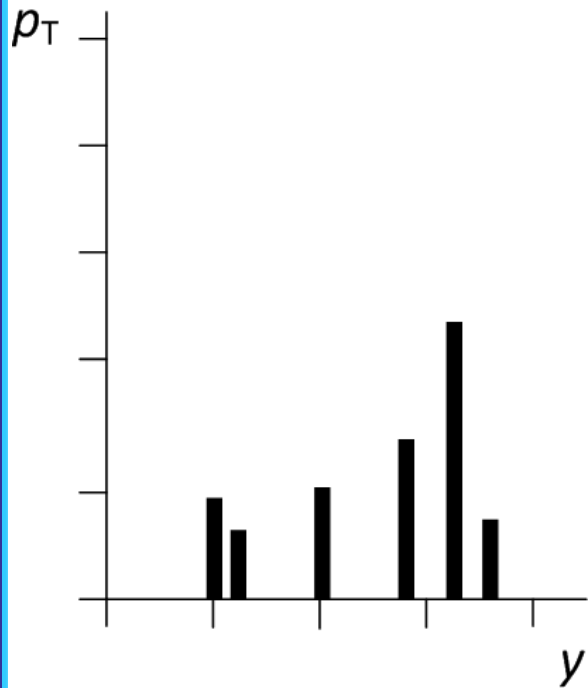
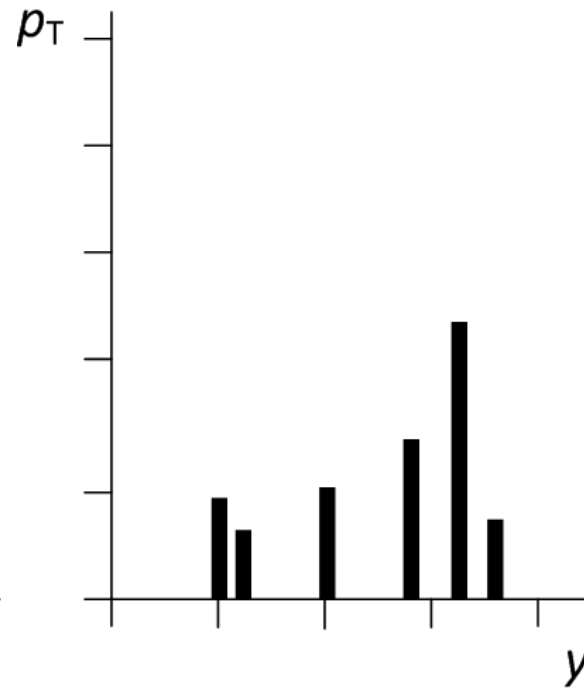
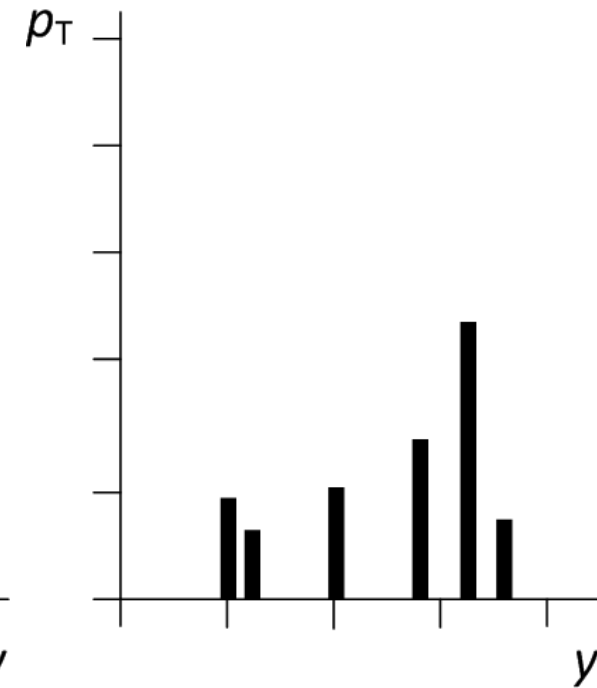
Uses angular distances only

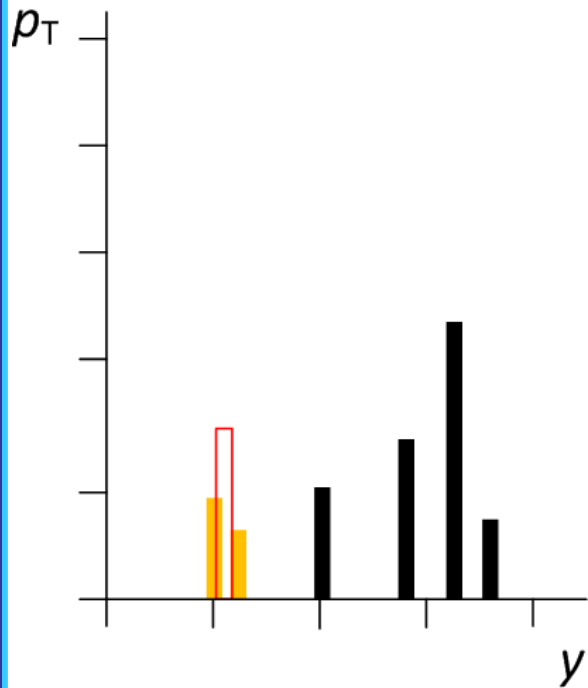
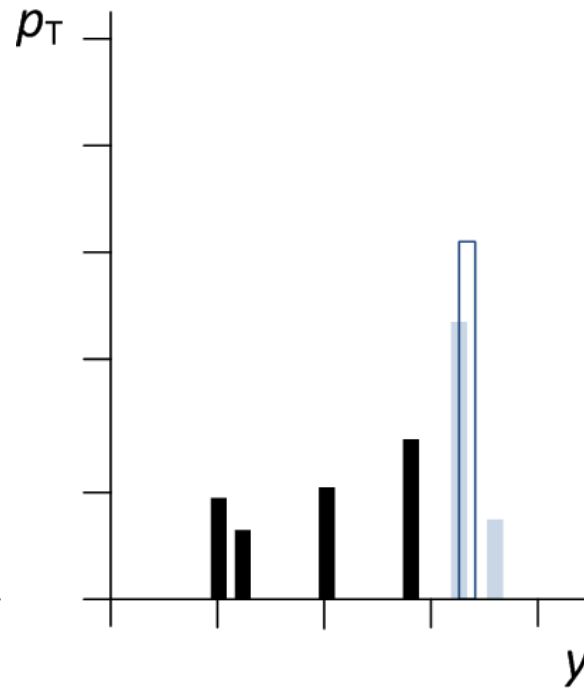
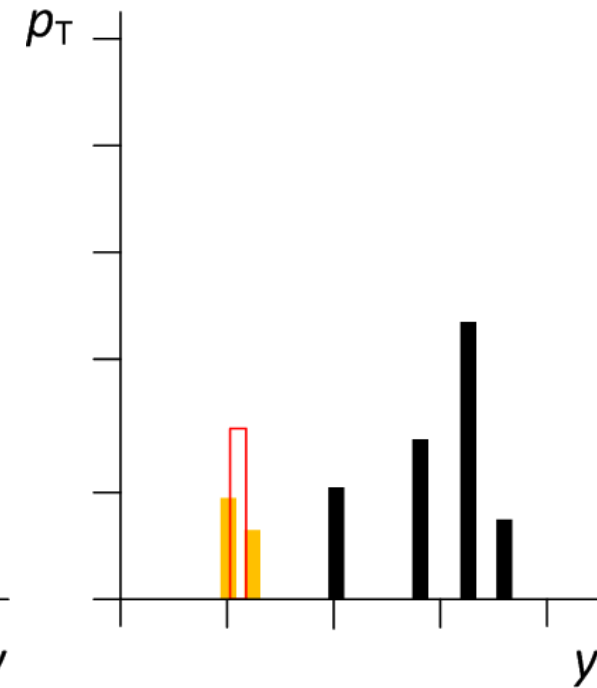
Clustering sequence follows jet structure

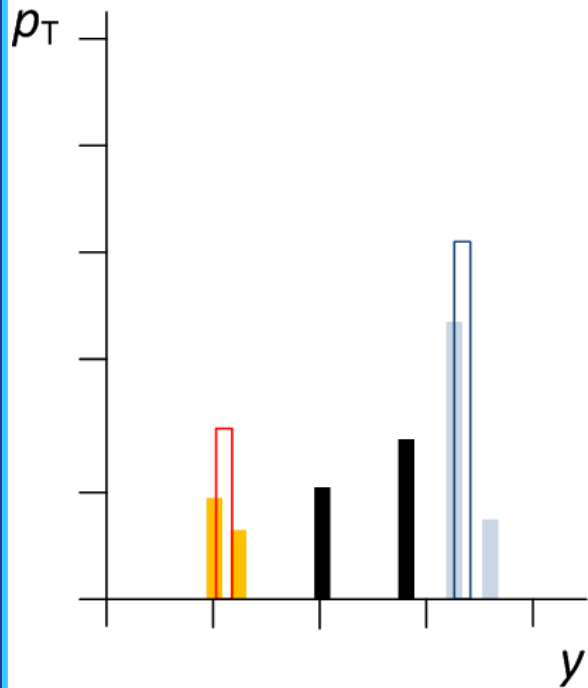
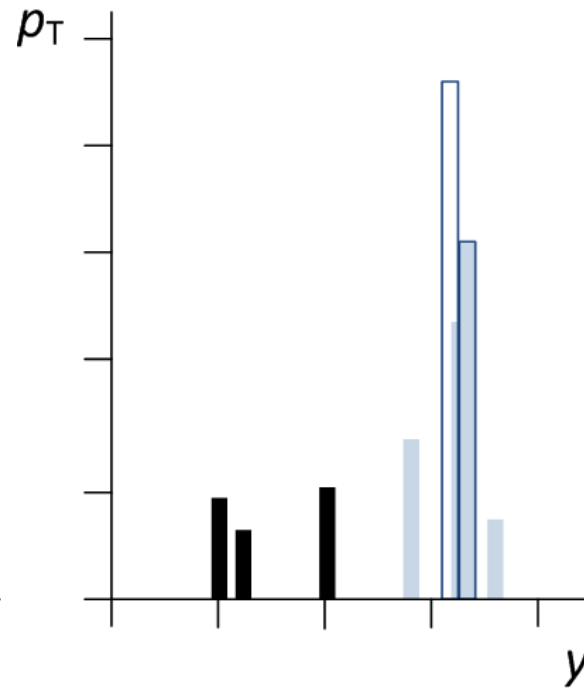
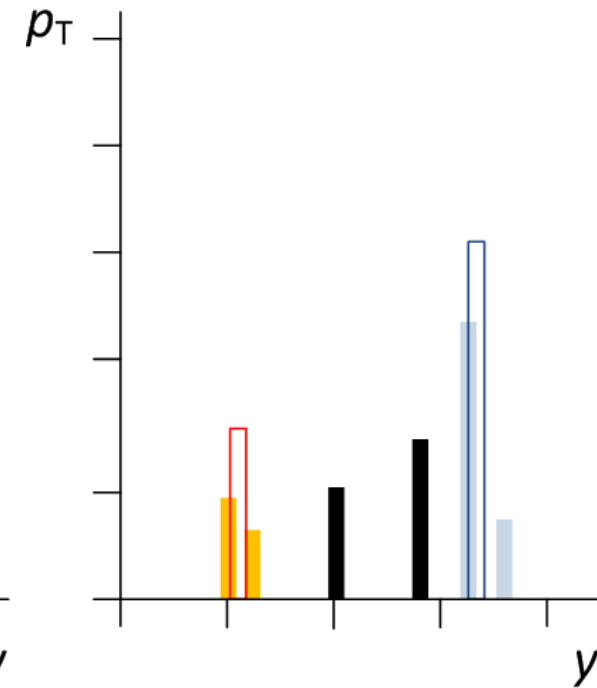
Anti-kT clustering

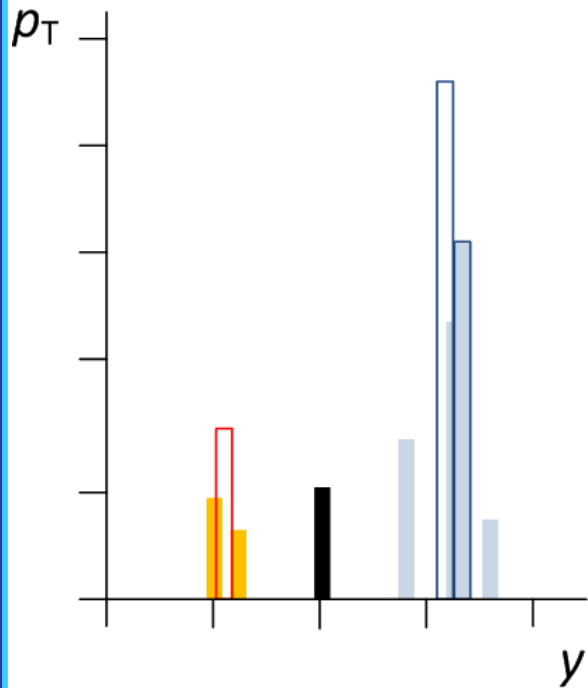
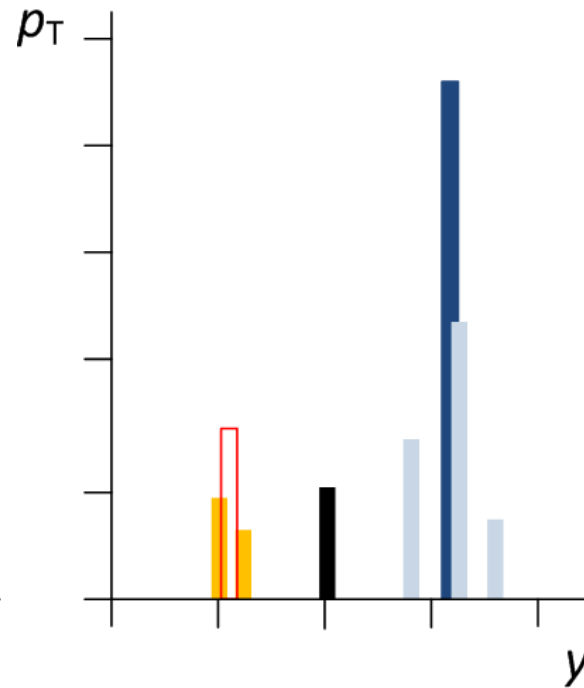
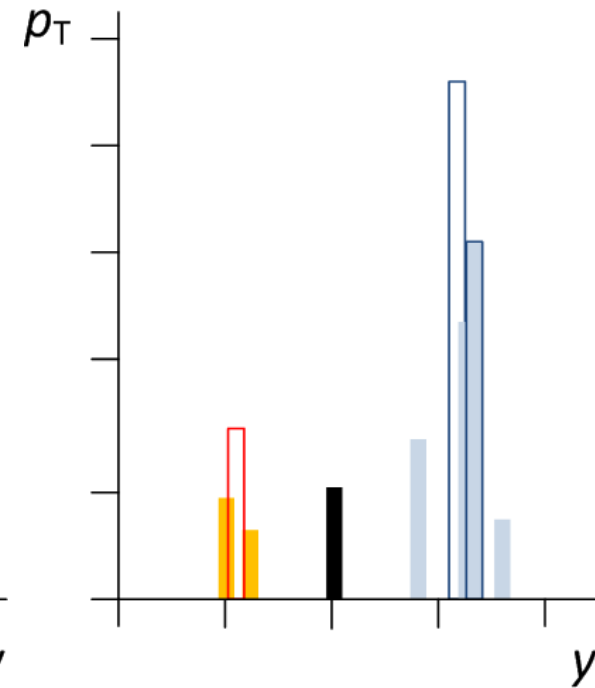
No particular ordering, sequence not meaningful

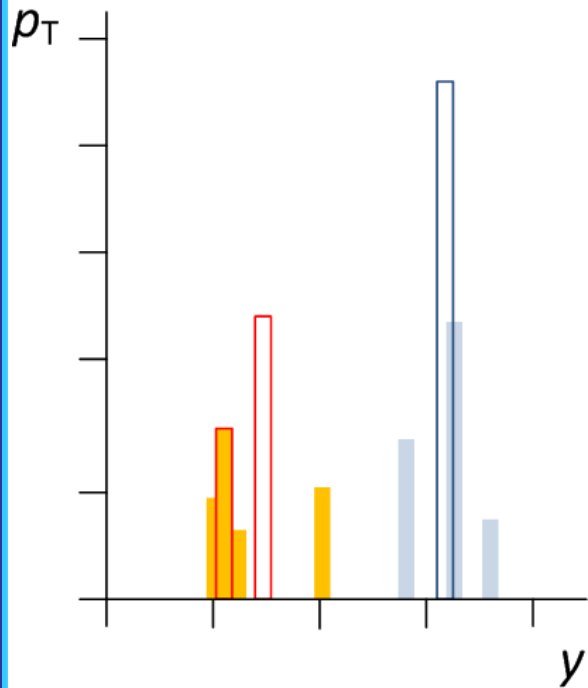
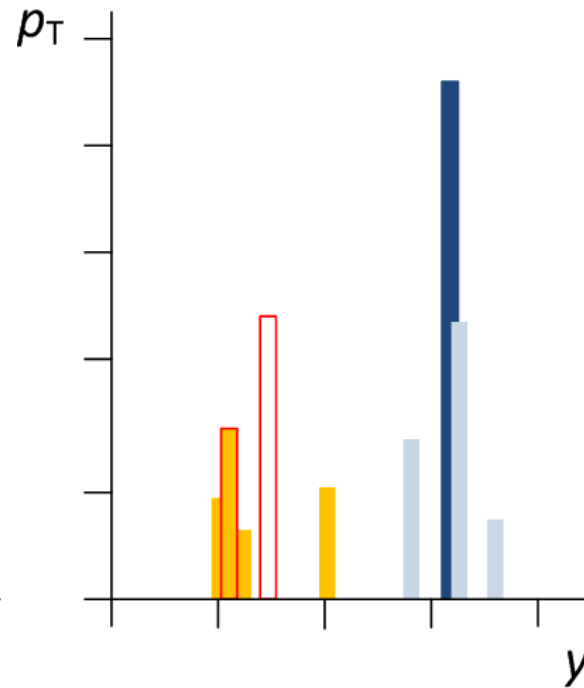
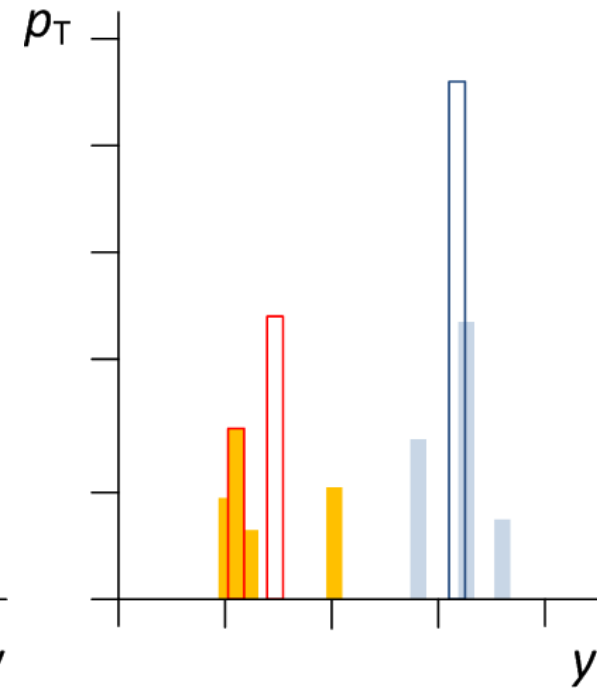


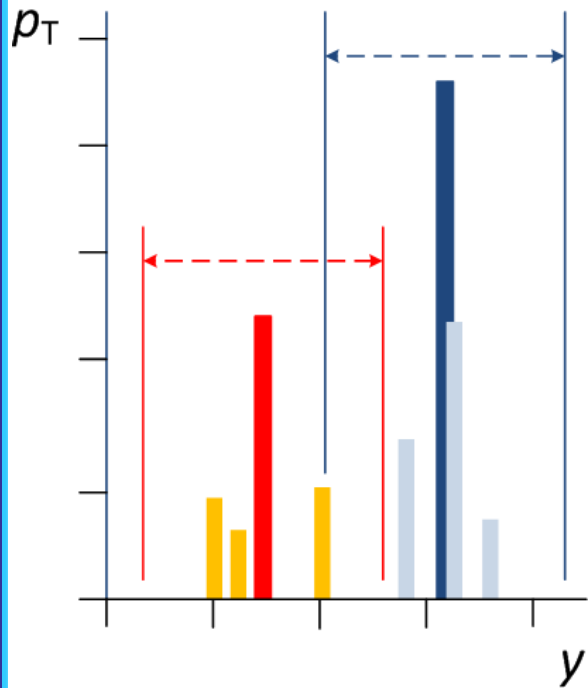
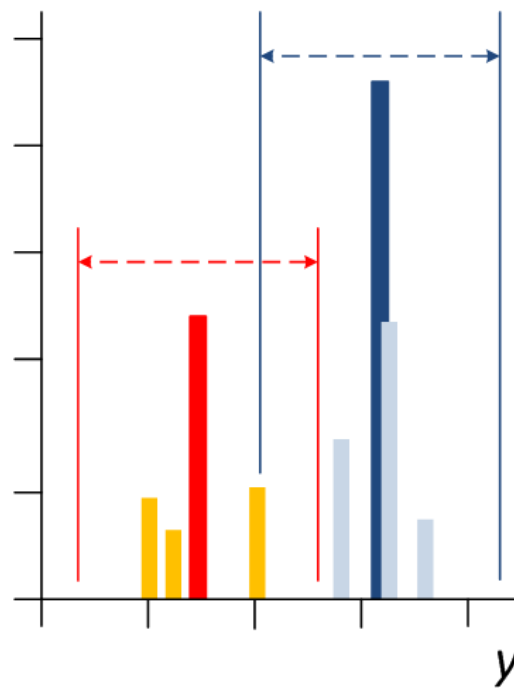
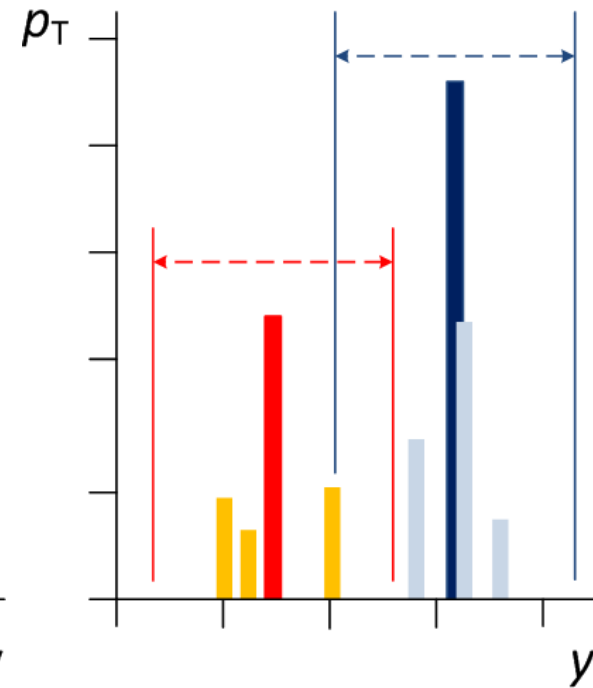
kT, $n=1$ Anti-kT, $n=-1$ Cambridge/Aachen, $n=0$ 

kT, $n=1$ Anti-kT, $n=-1$ Cambridge/Aachen, $n=0$ 

kT, $n=1$ Anti-kT, $n=-1$ Cambridge/Aachen, $n=0$ 

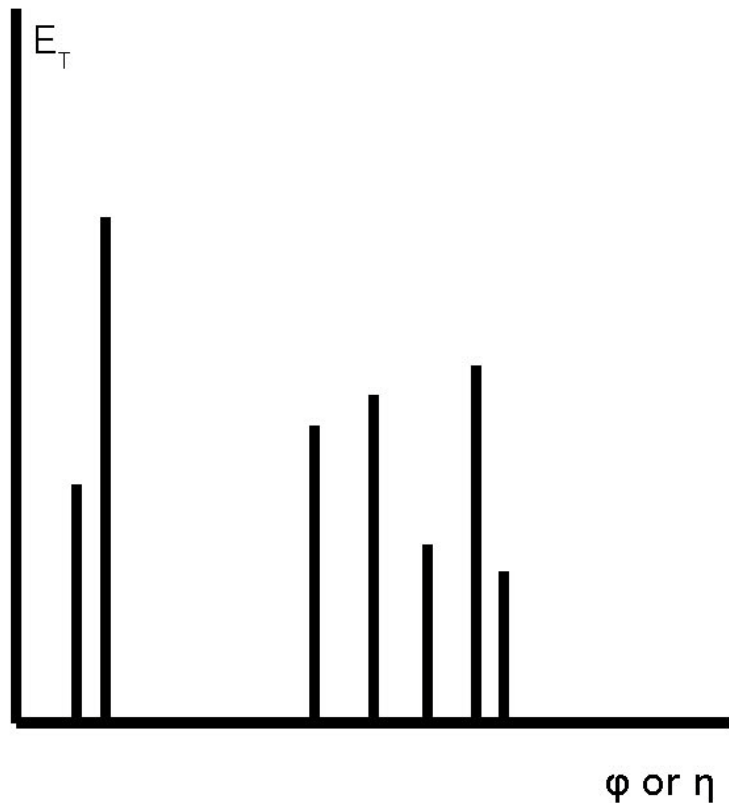
kT, $n=1$

 Anti-kT, $n=-1$

 Cambridge/Aachen, $n=0$


kT, $n=1$

 Anti-kT, $n=-1$

 Cambridge/Aachen, $n=0$


kT, $n=1$

 Anti-kT, $n=-1$

 Cambridge/Aachen, $n=0$


Clustering Algorithms

CTEQ-MCnet school 2008
Gavin Salam Lectures on Jets



Clustering Algorithms:

- Define a distance d_{ij} between two objects i, j :

$$\Delta R_{ij}^2 = (y_i - y_j)^2 + (\phi_i - \phi_j)^2$$

$$d_{ij} = \min(k_{ti}^2, k_{tj}^2) \Delta R_{ij}^2 / R^2$$

- and a distance d_{iB} between one object i and the beam direction B :

$$d_{iB} = k_{ti}^2$$

- Find the smallest of d_{ij}, d_{iB} .
 - If d_{ij} recombine i, j ;
 - If d_{iB} , i is a jet.

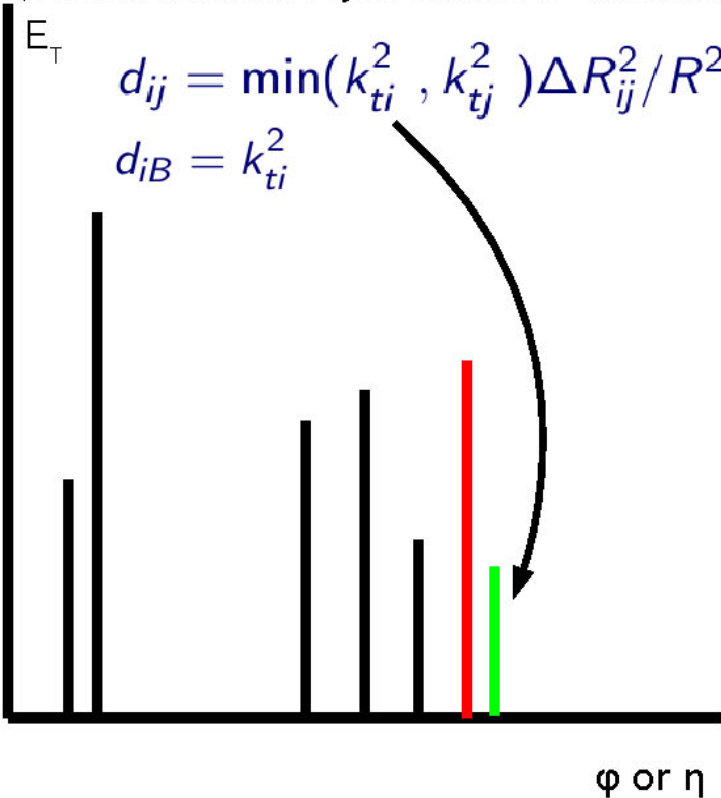
Clustering Algorithms

CTEQ-MCnet school 2008

Gavin Salam Lectures on Jets

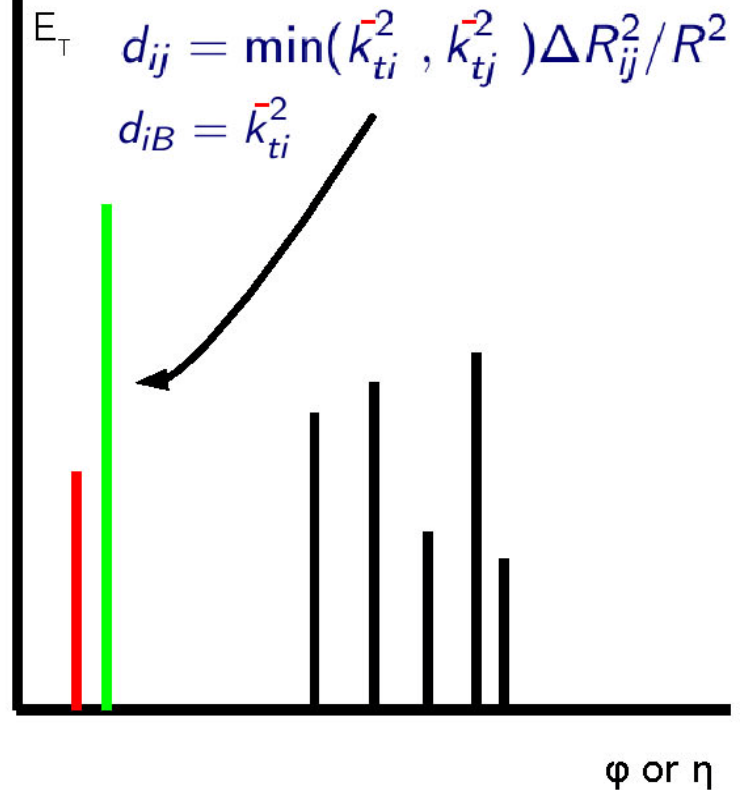
Kt

(Catani/Dokshitzer/Seymour/Webber - S.Ellis/Soper)



AntiKt

(Cacciari/Salam/Sovez)



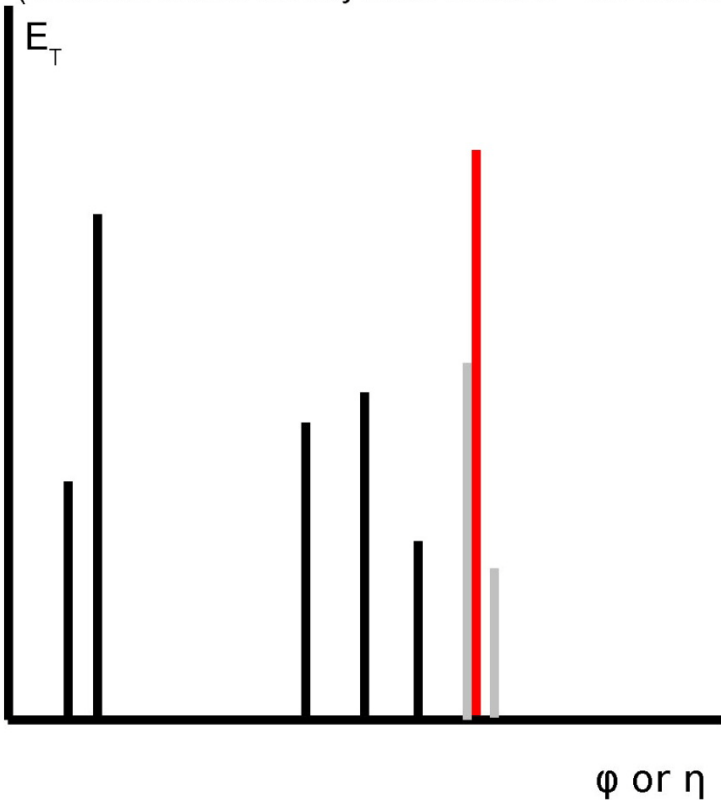
Clustering Algorithms

CTEQ-MCnet school 2008

Gavin Salam Lectures on Jets

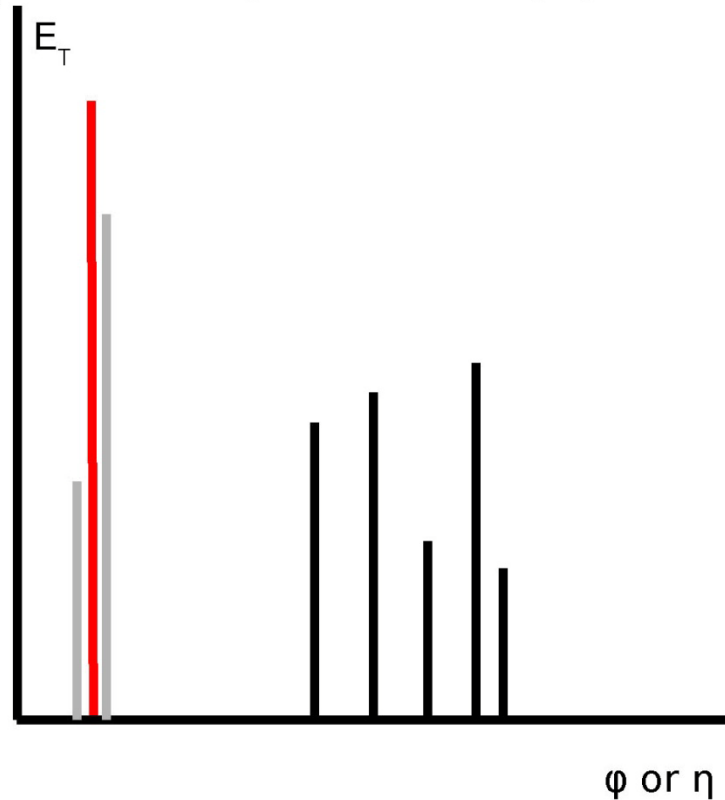
Kt

(Catani/Dokshitzer/Seymour/Webber - S.Ellis/Soper)



AntiKt

(Cacciari/Salam/Soyez)



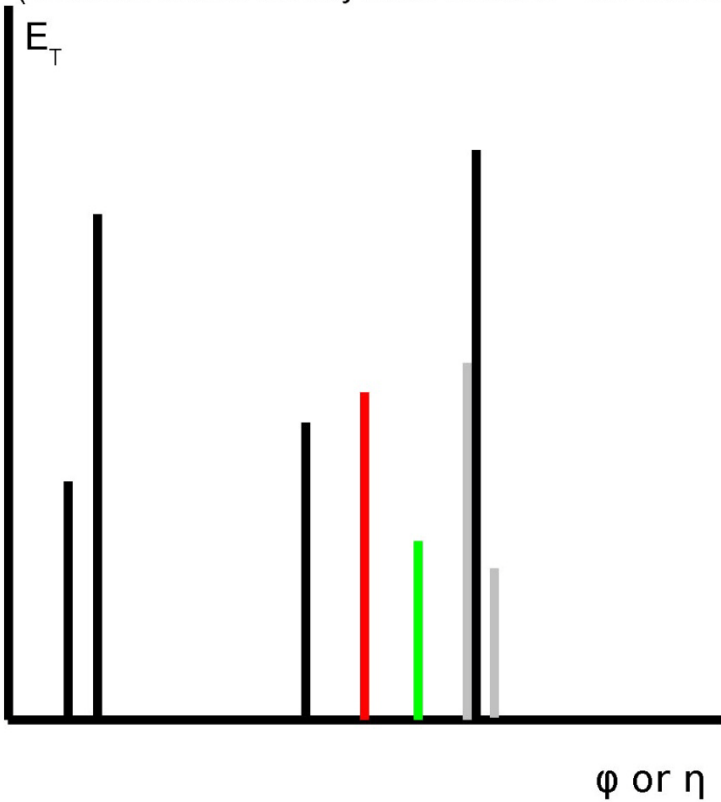
Clustering Algorithms

CTEQ-MCnet school 2008

Gavin Salam Lectures on Jets

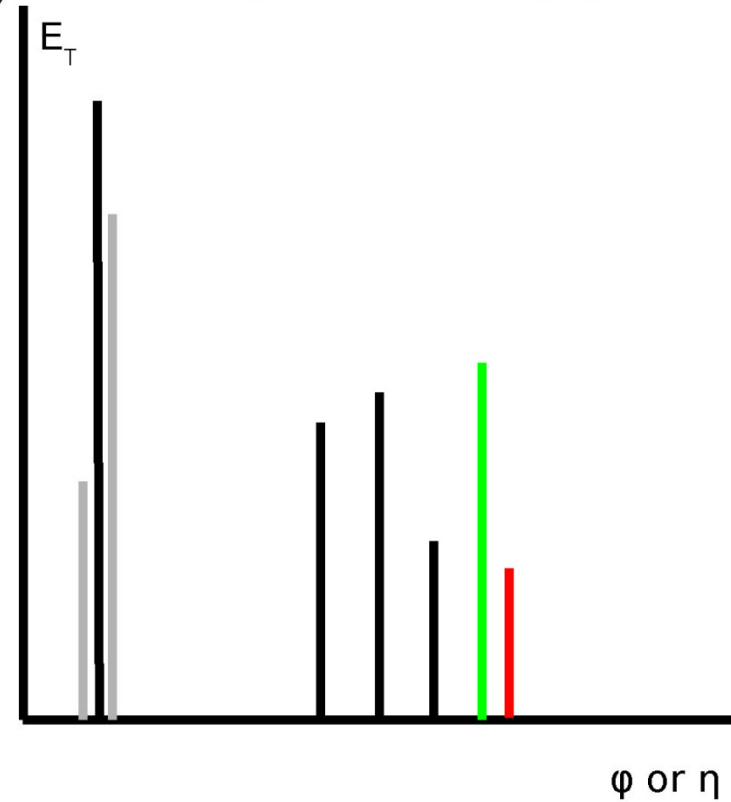
Kt

(Catani/Dokshitzer/Seymour/Webber - S.Ellis/Soper)



AntiKt

(Cacciari/Salam/Soyez)



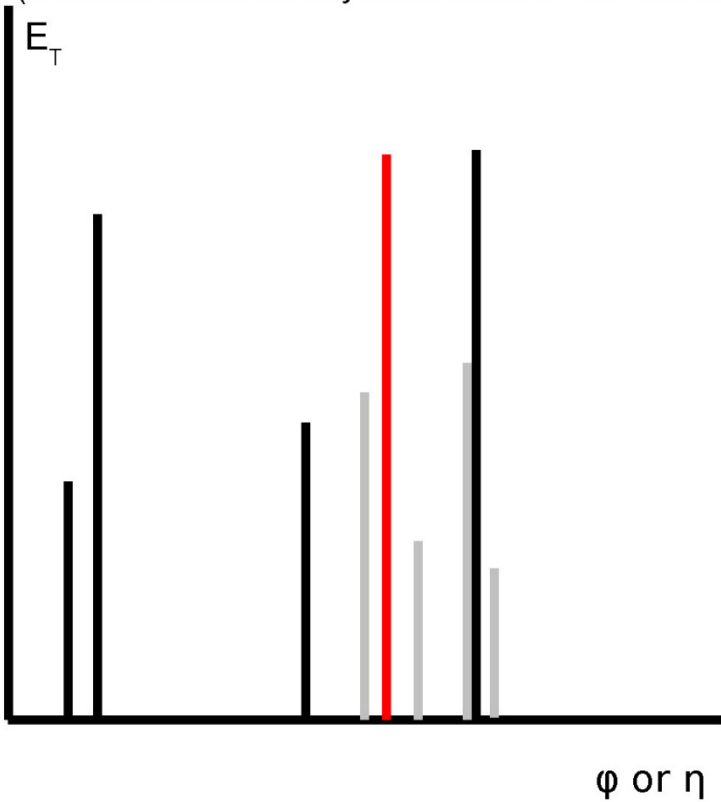
Clustering Algorithms

CTEQ-MCnet school 2008

Gavin Salam Lectures on Jets

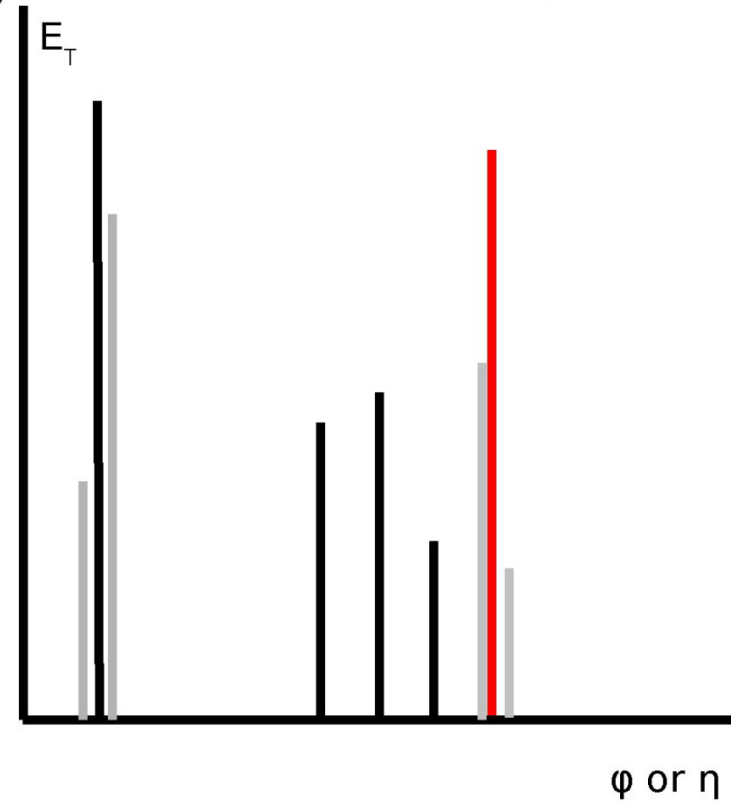
Kt

(Catani/Dokshitzer/Seymour/Webber - S.Ellis/Soper)



AntiKt

(Cacciari/Salam/Soyez)



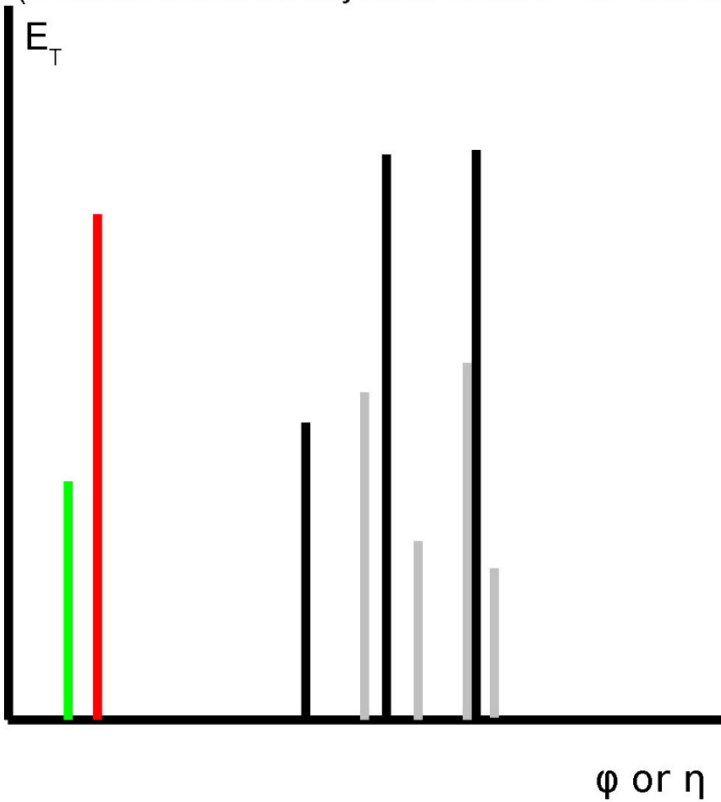
Clustering Algorithms

CTEQ-MCnet school 2008

Gavin Salam Lectures on Jets

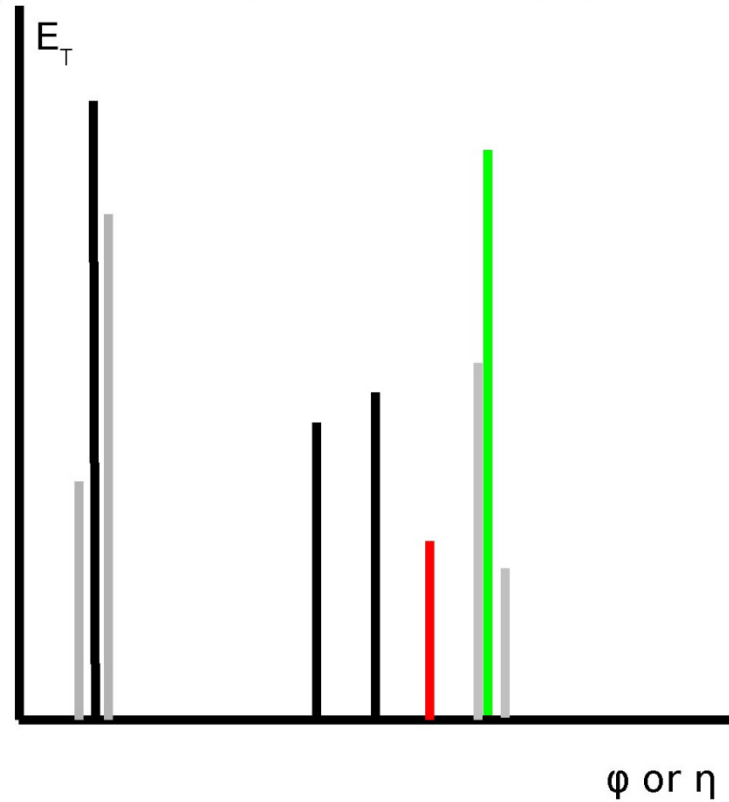
Kt

(Catani/Dokshitzer/Seymour/Webber - S.Ellis/Soper)



AntiKt

(Cacciari/Salam/Soyez)



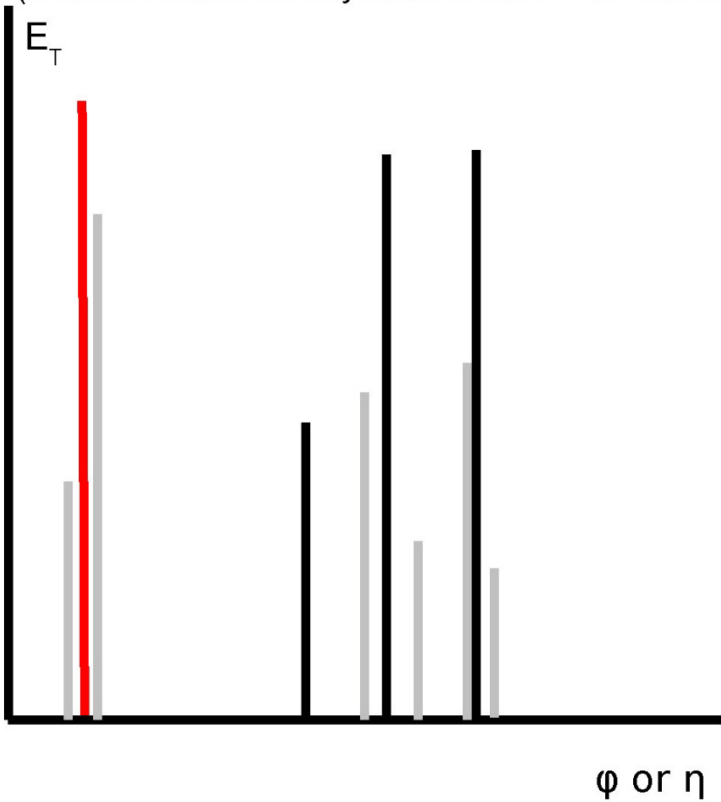
Clustering Algorithms

CTEQ-MCnet school 2008

Gavin Salam Lectures on Jets

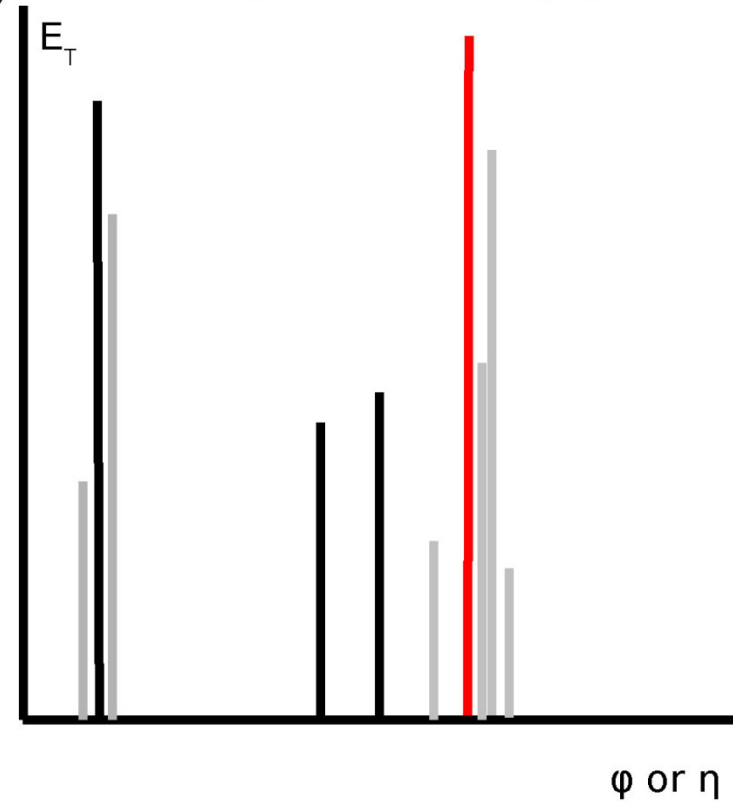
Kt

(Catani/Dokshitzer/Seymour/Webber - S.Ellis/Soper)



AntiKt

(Cacciari/Salam/Soyez)



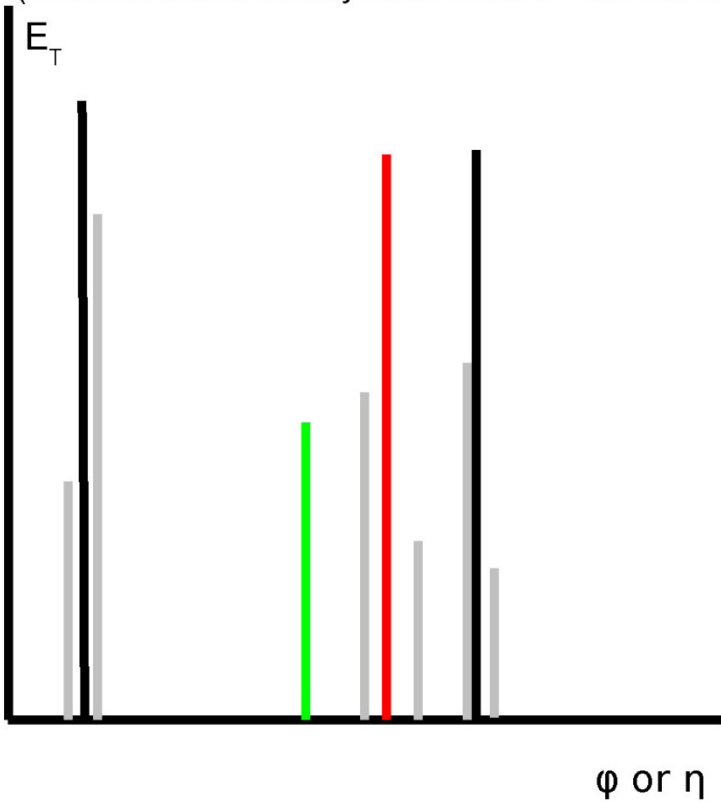
Clustering Algorithms

CTEQ-MCnet school 2008

Gavin Salam Lectures on Jets

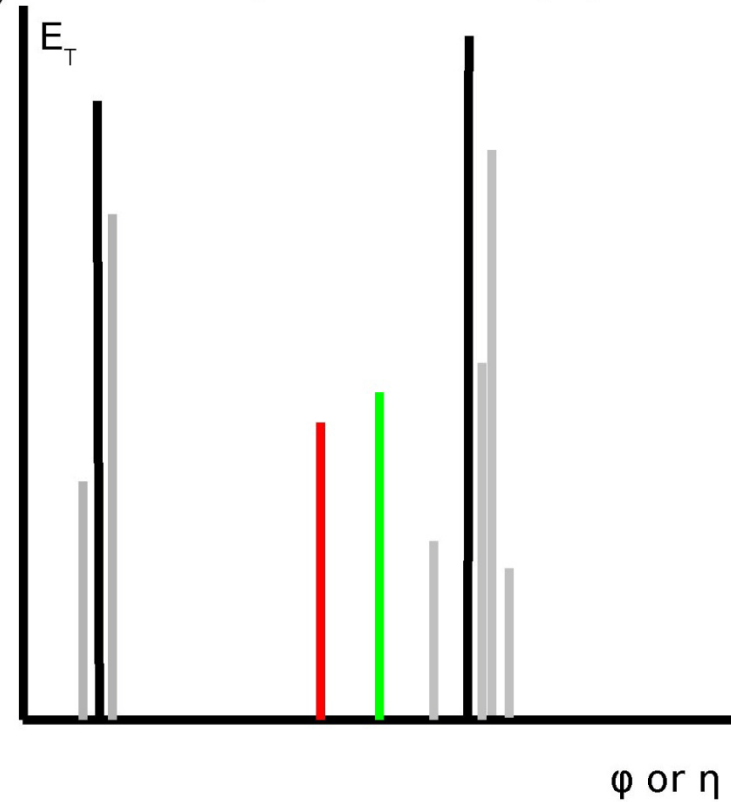
K_t

(Catani/Dokshitzer/Seymour/Webber - S.Ellis/Soper)



AntiK_t

(Cacciari/Salam/Soyez)



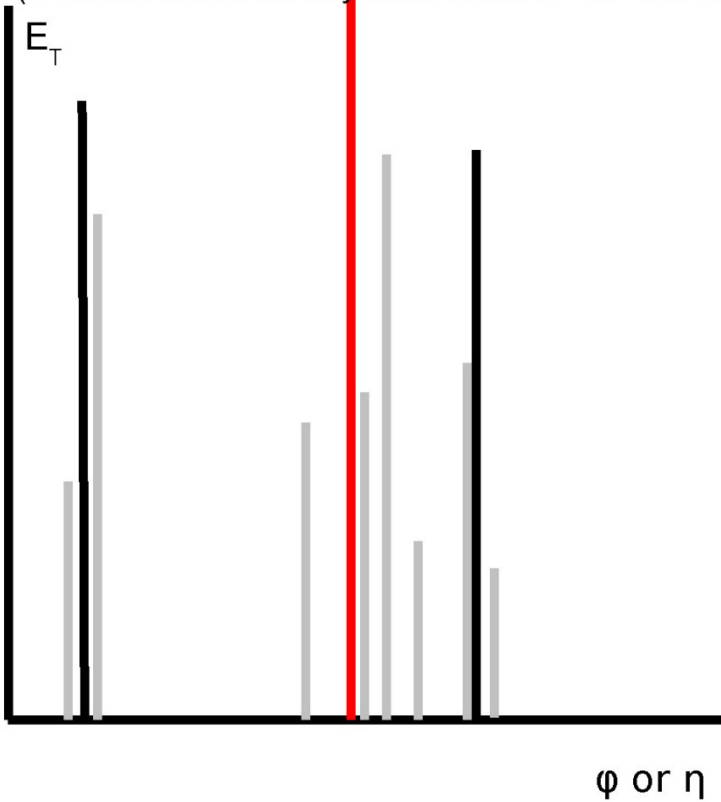
Clustering Algorithms

CTEQ-MCnet school 2008

Gavin Salam Lectures on Jets

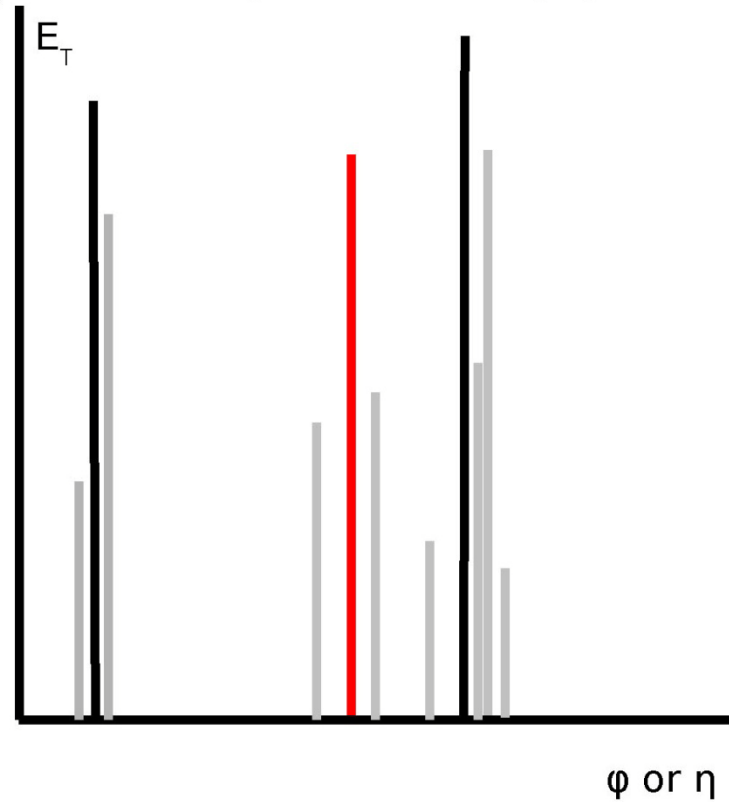
Kt

(Catani/Dokshitzer/Seymour/Webber - S.Ellis/Soper)



AntiKt

(Cacciari/Salam/Soyez)



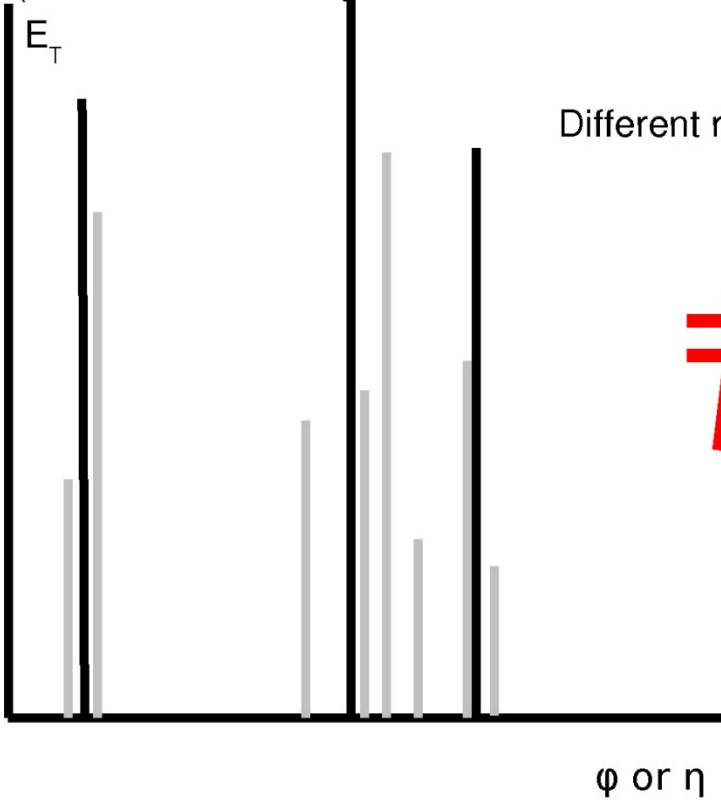
Clustering Algorithms

CTEQ-MCnet school 2008

Gavin Salam Lectures on Jets

K_t

(Catani/Dokshitzer/Seymour/Webber - S.Ellis/Soper)

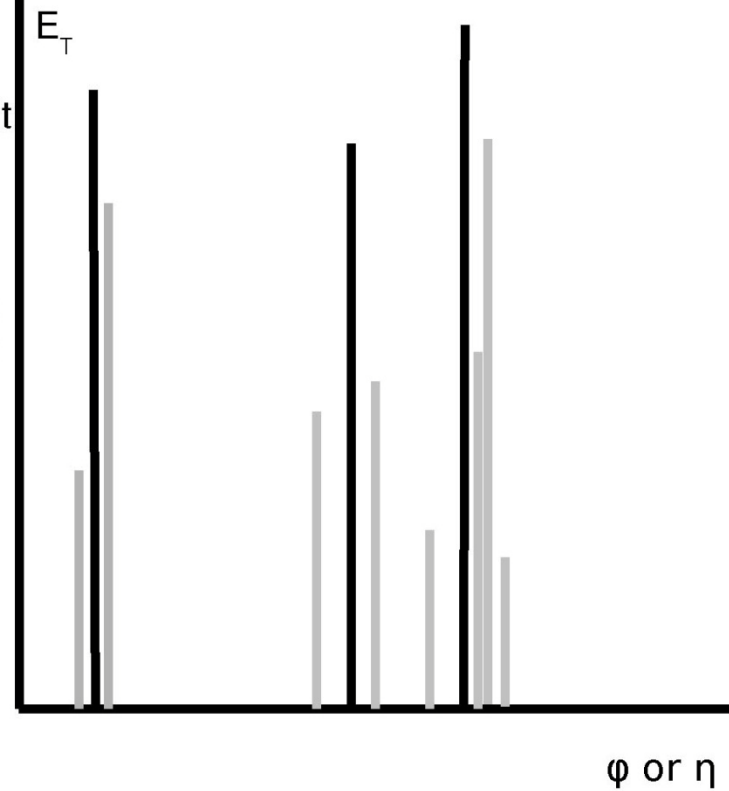


Different result

≠

AntiK_t

(Cacciari/Salam/Soyez)



Introduction to Hadronic Final State Reconstruction in Collider Experiments (Part VII & VIII)

Peter Loch
University of Arizona
Tucson, Arizona
USA



Need to be valid to any order of perturbative calculations

Experiment needs to keep sensitivity to perturbative infinities

Jet algorithms must be infrared safe!

Stable for multi-jet final states

Clearly a problem for classic (seeded) cone algorithms

Tevatron: modifications to algorithms and optimization of algorithm configurations

Mid-point seeded cone: put seed between two particles

Split & merge fraction: adjust between 0.5 – 0.75 for best “resolution”

LHC: need more stable approaches

Multi-jet context important for QCD measurements

Extractions of inclusive and exclusive cross-sections, PDFs

Signal-to-background enhancements in searches

Event selection/filtering based on topology

Other kinematic parameters relevant for discovery

Among consequences of IR unsafety:

	<i>Last meaningful order</i>			Known at
	JetClu, ATLAS cone [IC-SM]	MidPoint [IC _{mp} -SM]	CMS it. cone [IC-PR]	
Inclusive jets	LO	NLO	NLO	NLO (→ NNLO)
$W/Z + 1$ jet	LO	NLO	NLO	NLO
3 jets	none	LO	LO	NLO [nlojet++]
$W/Z + 2$ jets	none	LO	LO	NLO [MCFM]
m_{jet} in $2j + X$	none	none	none	LO

NB: \$30 – 50M investment in NLO



Need to be valid to any order of perturbative calculations

Experiment needs to keep sensitivity to perturbative infinities

Jet algorithms must be infrared safe!

Stable for multi-jet final states

Clearly a problem for classic (seeded) cone algorithms

Tevatron: modifications to algorithms and optimization of algorithm configurations

Mid-point seeded cone: put seed between two particles

Split & merge fraction: adjust between 0.5 – 0.75 for best “resolution”

LHC: need more stable approaches

Multi-jet context important for QCD measurements

Extractions of inclusive and exclusive cross-sections, PDFs

Signal-to-background enhancements in searches

Event selection/filtering based on topology

Other kinematic parameters relevant for discovery

**Starts to miss cones
at next order!**



Among consequences of IR unsafety:

	<i>Last meaningful order</i>			Known at
	JetClu, ATLAS cone [IC-SM]	MidPoint [IC _{mp} -SM]	CMS it. cone [IC-PR]	
Inclusive jets	LO	NLO	NLO	NLO (→ NNLO)
$W/Z + 1$ jet	LO	NLO	NLO	NLO
3 jets	none	LO	LO	NLO [nlojet++]
$W/Z + 2$ jets	none	LO	LO	NLO [MCFM]
m_{jet} in $2j + X$	none	none	none	LO

NB: \$30 – 50M investment in NLO



Attempt to increase infrared safety for seeded cone

Midpoint algorithm starts with seeded cone

Seed threshold may be 0 to increase collinear safety

Place new seeds between two close stable cones

Also center of three stable cones possible

Re-iterate using midpoint seeds

Isolated stable cones are unchanged

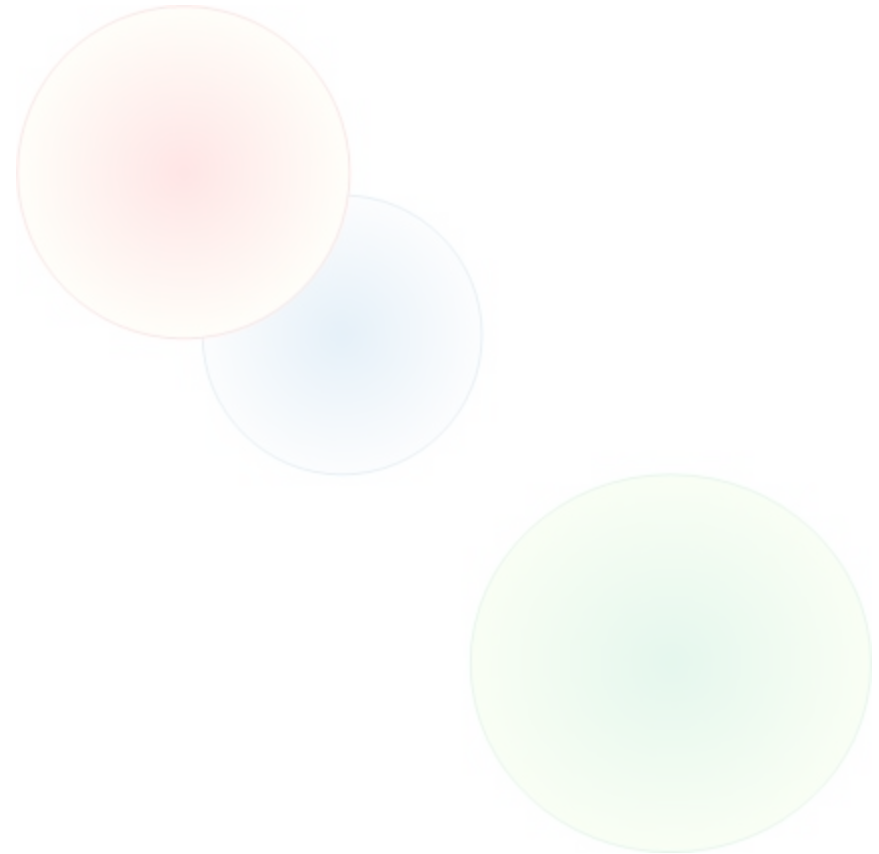
Still not completely safe!

Apply split & merge

Usually split/merge fraction 0.75

Find midpoints for stable cones within

$$\Delta R = \sqrt{\Delta y^2 + \Delta \phi^2} \leq 2R_{\text{cone}}$$



Attempt to increase infrared safety for seeded cone

Midpoint algorithm starts with seeded cone

Seed threshold may be 0 to increase collinear safety

Place new seeds between two close stable cones

Also center of three stable cones possible

Re-iterate using midpoint seeds

Isolated stable cones are unchanged

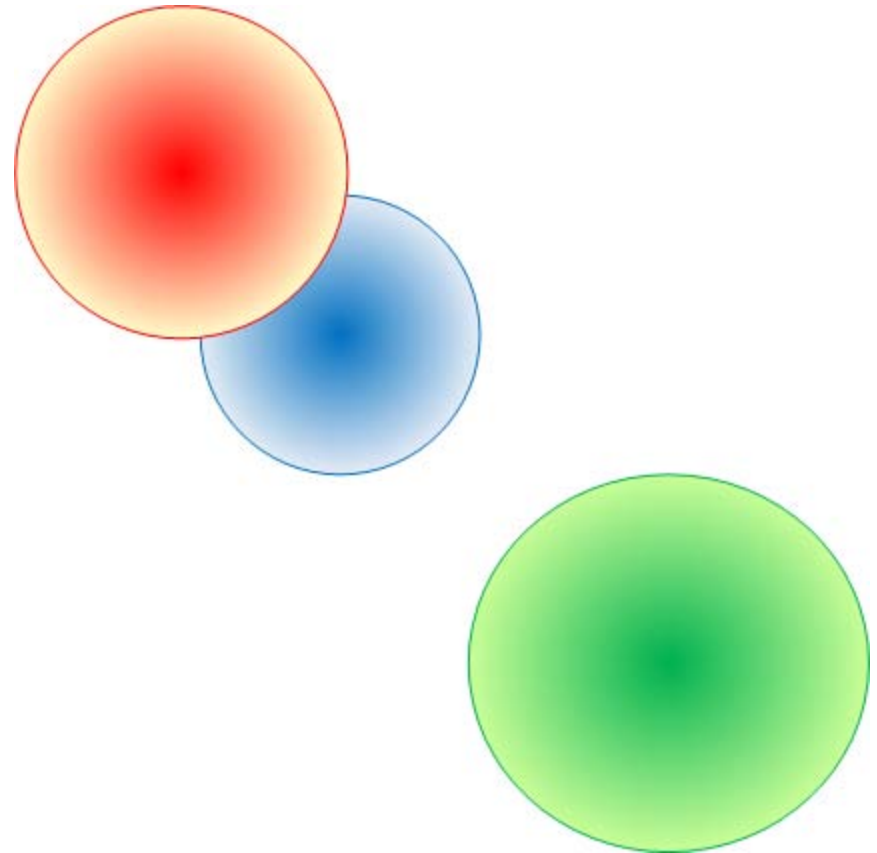
Still not completely safe!

Apply split & merge

Usually split/merge fraction 0.75

Find midpoints for stable cones within

$$\Delta R = \sqrt{\Delta y^2 + \Delta \phi^2} \leq 2R_{\text{cone}}$$



Attempt to increase infrared safety for seeded cone

Midpoint algorithm starts with seeded cone

Seed threshold may be 0 to increase collinear safety

Place new seeds between two close stable cones

Also center of three stable cones possible

Re-iterate using midpoint seeds

Isolated stable cones are unchanged

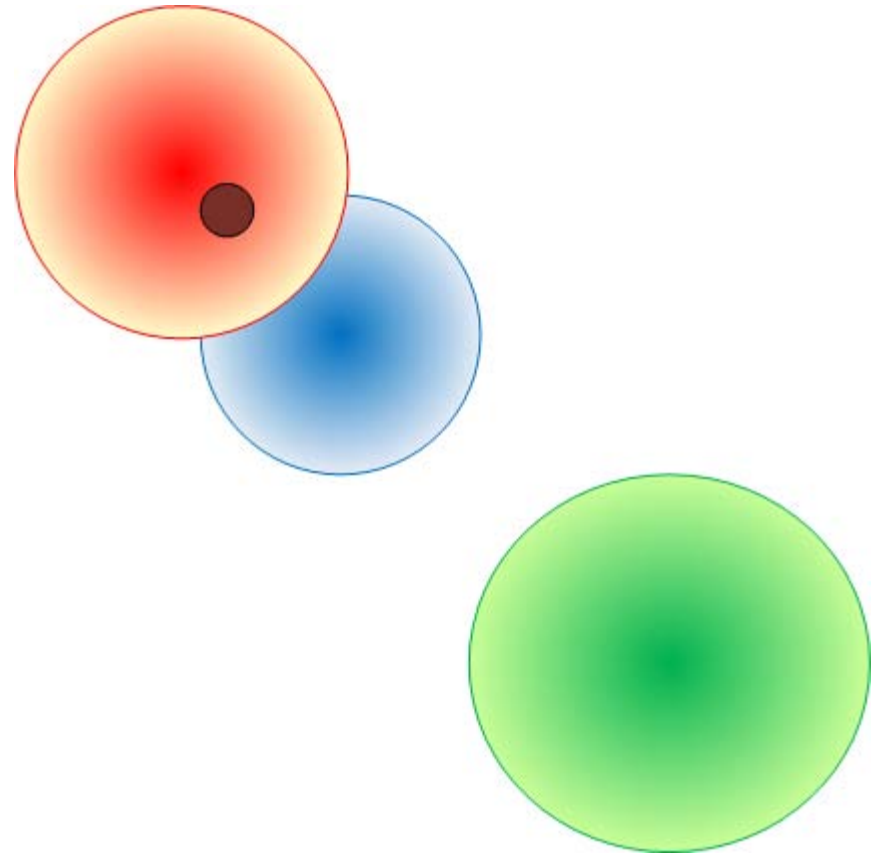
Still not completely safe!

Apply split & merge

Usually split/merge fraction 0.75

Find midpoints for stable cones within

$$\Delta R = \sqrt{\Delta y^2 + \Delta \phi^2} \leq 2R_{\text{cone}}$$



Attempt to increase infrared safety for seeded cone

Midpoint algorithm starts with seeded cone

Seed threshold may be 0 to increase collinear safety

Place new seeds between two close stable cones

Also center of three stable cones possible

Re-iterate using midpoint seeds

Isolated stable cones are unchanged

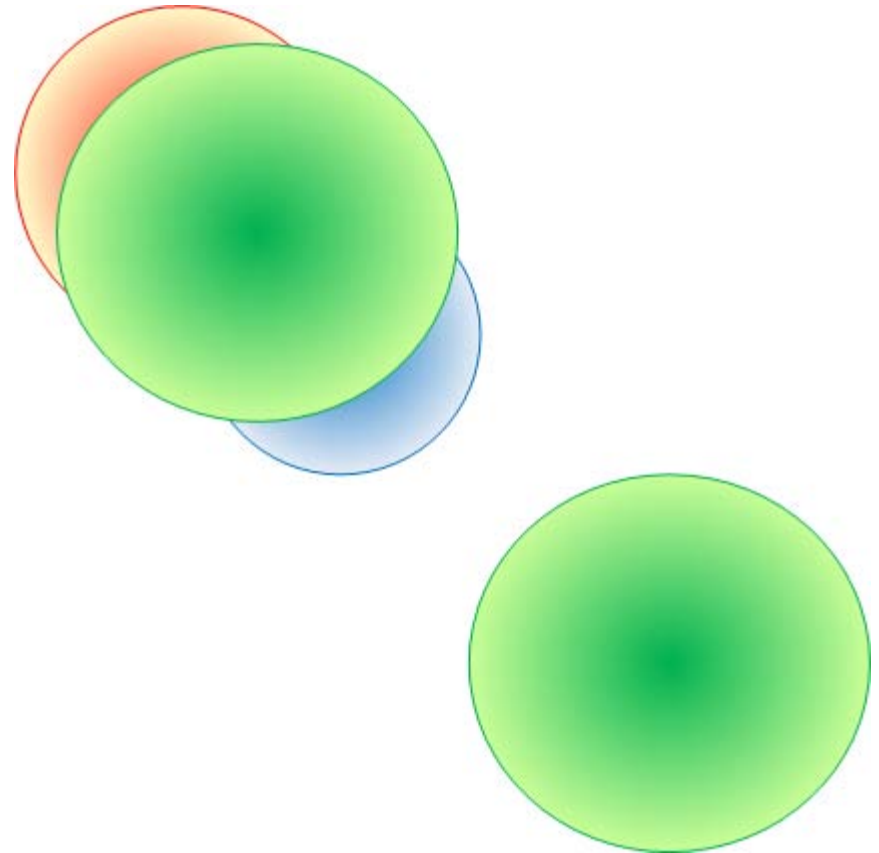
Still not completely safe!

Apply split & merge

Usually split/merge fraction
0.75

Find midpoints for stable cones within

$$\Delta R = \sqrt{\Delta y^2 + \Delta \phi^2} \leq 2R_{\text{cone}}$$



Attempt to increase infrared safety for seeded cone

Midpoint algorithm starts with seeded cone

Seed threshold may be 0 to increase collinear safety

Place new seeds between two close stable cones

Also center of three stable cones possible

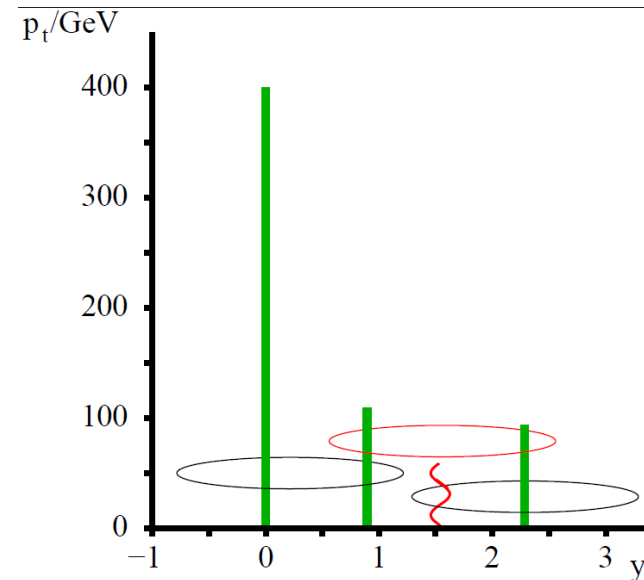
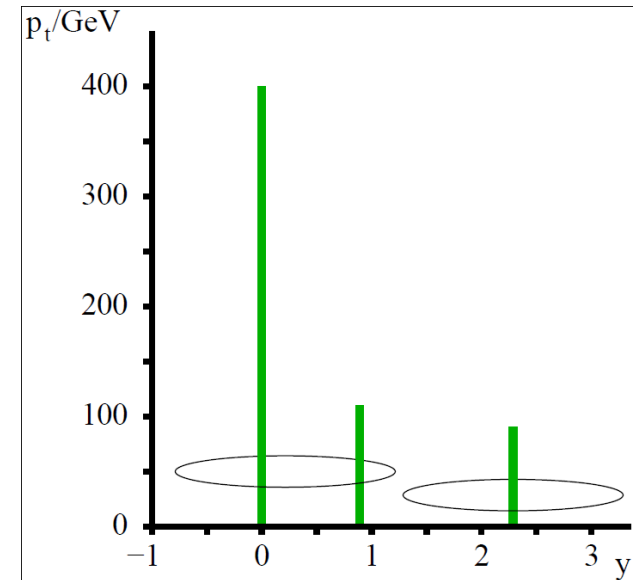
Re-iterate using midpoint seeds

Isolated stable cones are unchanged

Still not completely safe!

Apply split & merge

Usually split/merge fraction 0.75



(from G. Salam & G. Soyez, JHEP 0705:086,2007)



Improvements to cone algorithms: no seeds

All stable cones are considered

Avoid collinear unsafety in seeded cone algorithm

Avoid infrared safety issue

Adding infinitively soft particle does not lead to new (hard) cone

Exact seedless cone finder

Problematic for larger number of particles

Approximate implementation

Pre-clustering in coarse towers

Not necessarily appropriate for particles and even some calorimeter signals

Exact seedless cone for N particles:

$O(N \cdot 2^N)$ operations

N	# operations	remark
4	64	fixed order parton level
10	10240	very low multiplicity final state
100	$\sim 1.3 \cdot 10^{32}$	low multiplicity LHC final state
1,000	$\sim 1.6 \cdot 10^{153}$	typical LHC final state
10,000	∞	LHC high luminosity final state

Approximate seedless cone ($\Delta\eta \times \Delta\phi = 0.2 \times 0.2$):

N	# operations	remark
40	$\sim 4.4 \cdot 10^{13}$	surviving bins with two narrow jets
70	$\sim 8.3 \cdot 10^{22}$	surving bins with two wide jets



Improvements to cone algorithms: no seeds

All stable cones are considered

Avoid collinear unsafety in seeded cone algorithm

Avoid infrared safety issue

Adding infinitively soft particle does not lead to new (hard) cone

Exact seedless cone finder

Problematic for larger number of particles

Approximate implementation

Pre-clustering in coarse towers

Not necessarily appropriate for particles and even some calorimeter signals

Exact seedless cone for N particles:

$O(N \cdot 2^N)$ operations

N	# operations	remark
4	64	fixed order parton level
10	10240	very low multiplicity final state
100	$\sim 1.3 \cdot 10^{32}$	low multiplicity LHC final state
1,000	$\sim 1.6 \cdot 10^{153}$	typical LHC final state
10,000	∞	LHC high luminosity final state

Approximate seedless cone ($\Delta\eta \times \Delta\phi = 0.2 \times 0.2$):

N	# operations	remark
40	$\sim 4.4 \cdot 10^{13}$	surviving bins with two narrow jets
70	$\sim 8.3 \cdot 10^{22}$	surving bins with two wide jets



Improvements to cone algorithms: no seeds

All stable cones are considered

Avoid collinear unsafety in seeded cone algorithm

Avoid infrared safety issue

Adding infinitively soft particle does not lead to new (hard) cone

Exact seedless cone finder

Problematic for larger number of particles

Approximate implementation

Pre-clustering in coarse towers

Not necessarily appropriate for particles and even some calorimeter signals

Exact seedless cone for N particles:

$O(N \cdot 2^N)$ operations

N	# operations	remark
4	64	fixed order parton level
10	10240	very low multiplicity final state
100	$\sim 1.3 \cdot 10^{32}$	low multiplicity LHC final state
1,000	$\sim 1.6 \cdot 10^{153}$	typical LHC final state
10,000	∞	LHC high luminosity final state

Approximate seedless cone ($\Delta\eta \times \Delta\phi = 0.2 \times 0.2$):

N surviving bins with two narrow jets
 $40 \sim 4.4 \cdot 10^{15}$
 $70 \sim 1.2 \cdot 10^{22}$

Note: 100 particles need $\sim 10^{17}$ years to be clustered!



Improvements to cone algorithms: no seeds

All stable cones are considered

Avoid collinear unsafety in seeded cone algorithm

Avoid infrared safety issue

Adding infinitively soft particle does not lead to new (hard) cone

Exact seedless cone finder

Problematic for larger number of particles

Approximate implementation

Pre-clustering in coarse towers

Not necessarily appropriate for particles and even some calorimeter signals

Exact seedless cone for N particles:

$O(N \cdot 2^N)$ operations

N	# operations	remark
4	64	fixed order parton level
10	10240	very low multiplicity final state
100	$\sim 1.3 \cdot 10^{32}$	low multiplicity LHC final state
1,000	$\sim 1.6 \cdot 10^{153}$	typical LHC final state
10,000	∞	LHC high luminosity final state

Approximate seedless cone ($\Delta\eta \times \Delta\phi = 0.2 \times 0.2$):

N	# operations	remark
40	$\sim 4.4 \cdot 10^{13}$	surviving bins with two narrow jets
70	$\sim 8.3 \cdot 10^{22}$	surving bins with two wide jets



SISCone (Salam, Soyez 2007)

Exact seedless cone with geometrical (distance) ordering

Speeds up algorithm considerably!

Find all distinctive ways on how a segment can enclose a subset of the particles

Instead of finding all stable segments!

Re-calculate the centroid of each segment

E.g., pT weighted re-calculation of direction

“E-scheme” works as well

Segments (cones) are stable if particle content does not change

Retain only one solution for each segment

Still needs split & merge to remove overlap

Recommended split/merge fraction is 0.75

Typical times

$N^2 \ln N$ for particles in 2-dim plane

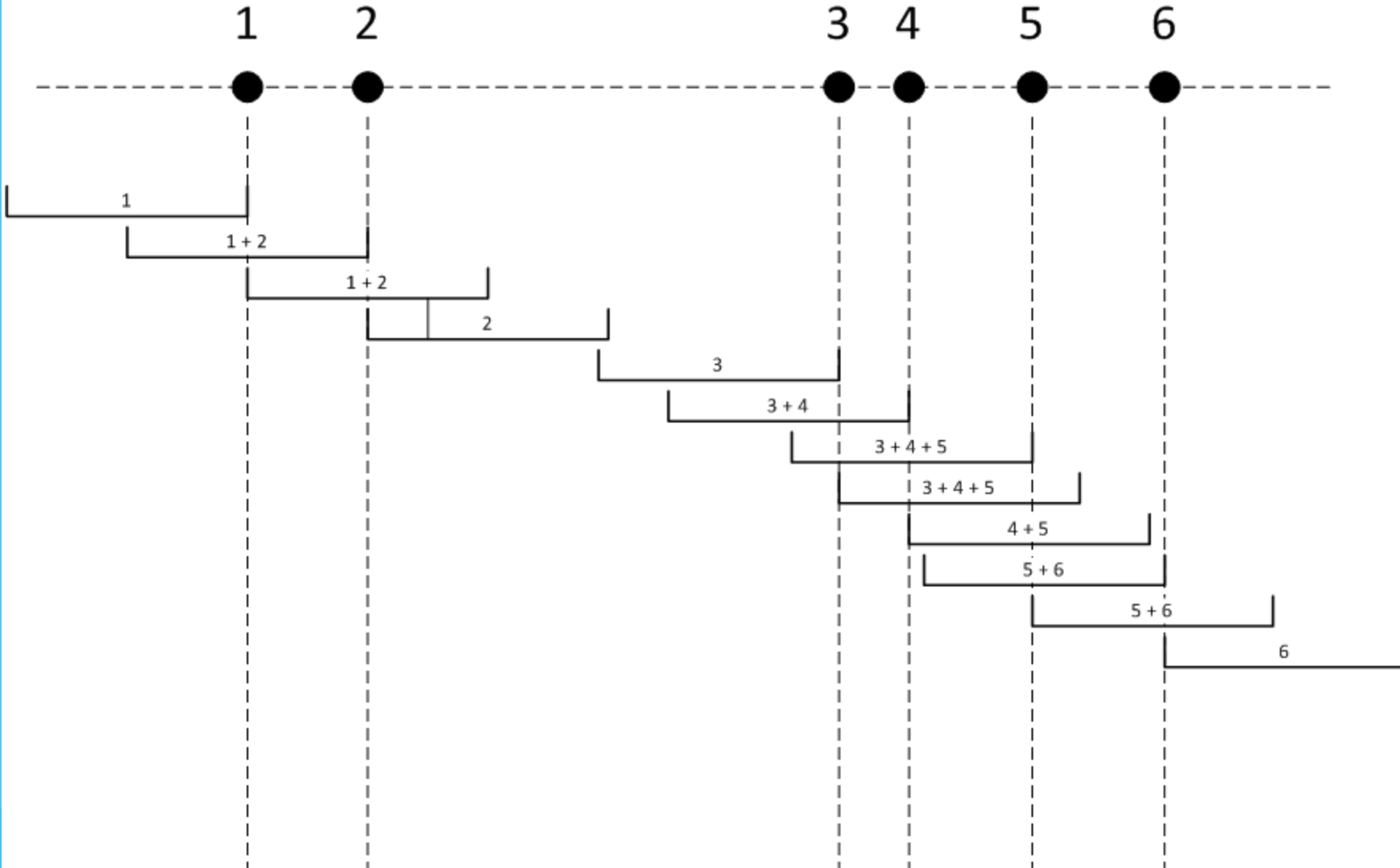
1-dim example:

See following slides!

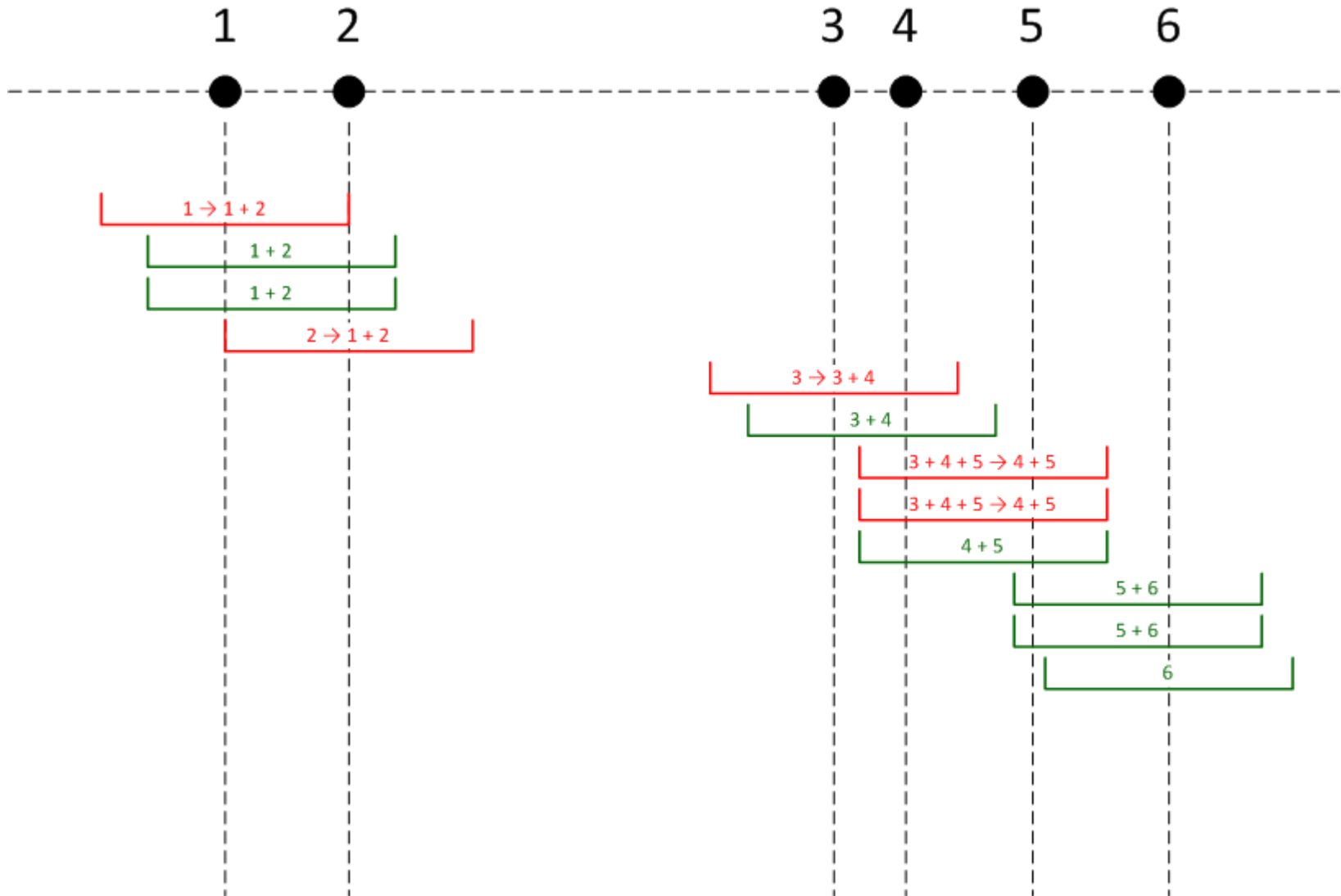
(inspired by G. Salam & G. Soyez, *JHEP* **0705:086,2007**)



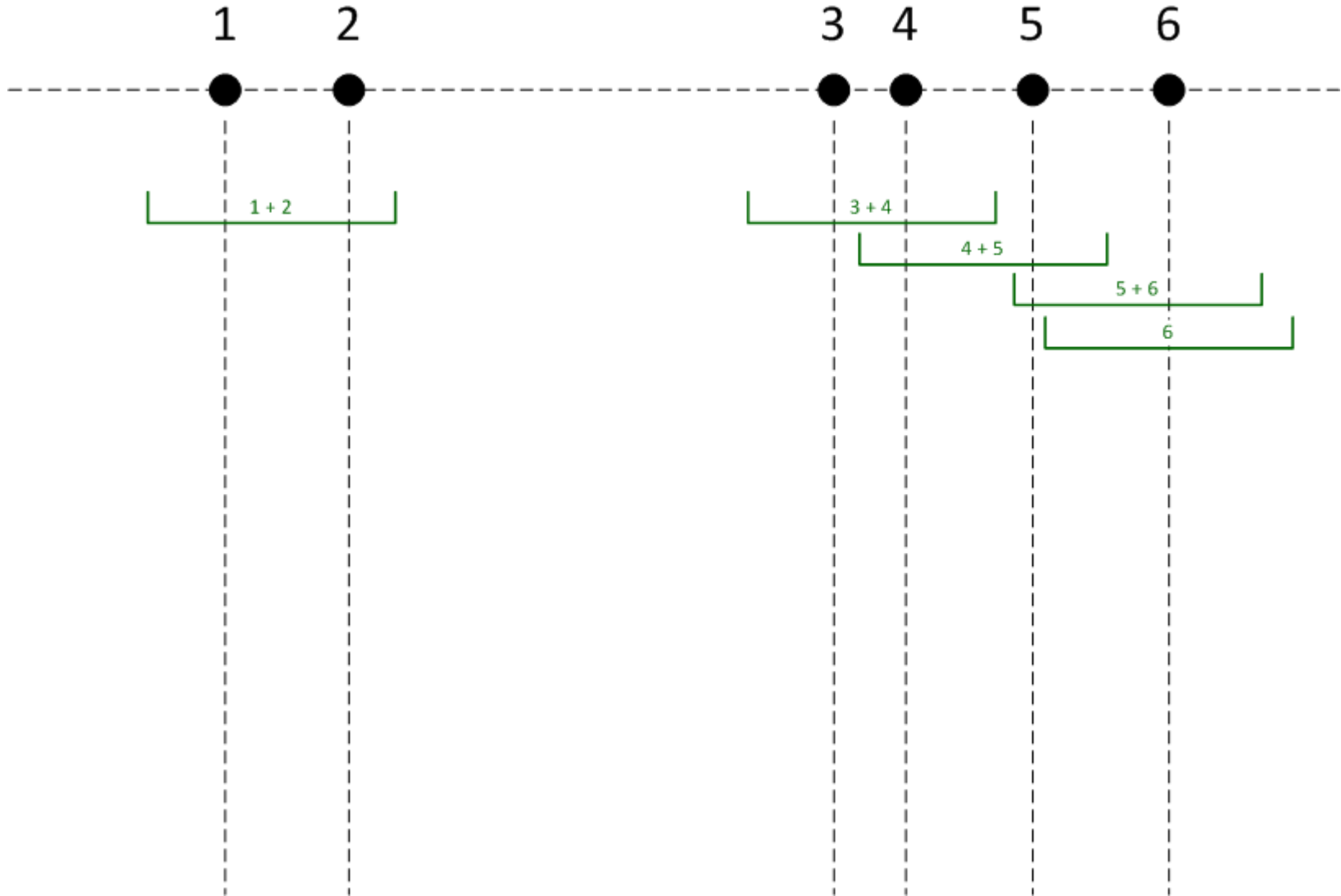
Find all distinctive segments of size $2R_{\text{cone}}$ ($O(N)$ operations in 1-dim)



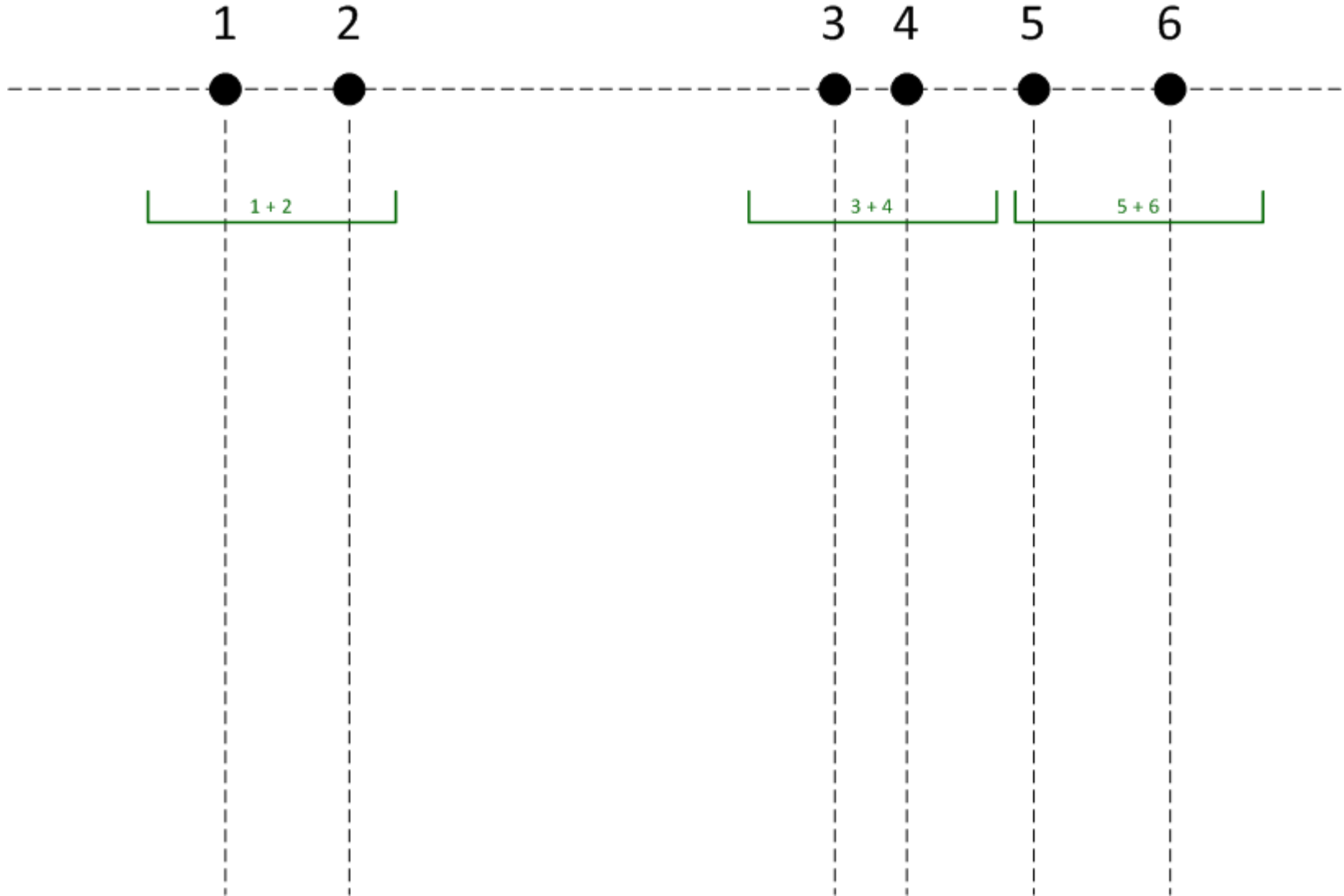
Reposition segments to centroids (green - unchanged, red - changed)



Retain only one stable solution for each segment



Apply split & merge



Similar ordering and combinations in 2-dim

Use circles instead of linear segments

(from G. Salam & G. Soyez, *JHEP* 0705:086,2007)

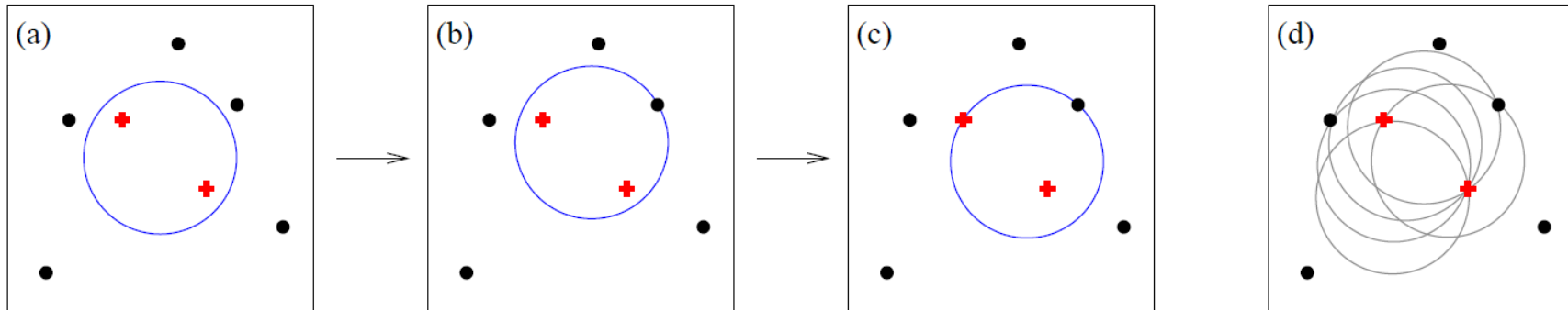


Figure 3: (a) Some initial circular enclosure; (b) moving the circle in a random direction until some enclosed or external point touches the edge of the circle; (c) pivoting the circle around the edge point until a second point touches the edge; (d) all circles defined by pairs of edge points leading to the same circular enclosure.

Still need split & merge

One additional parameter outside of jet/cone size

Not very satisfactory!

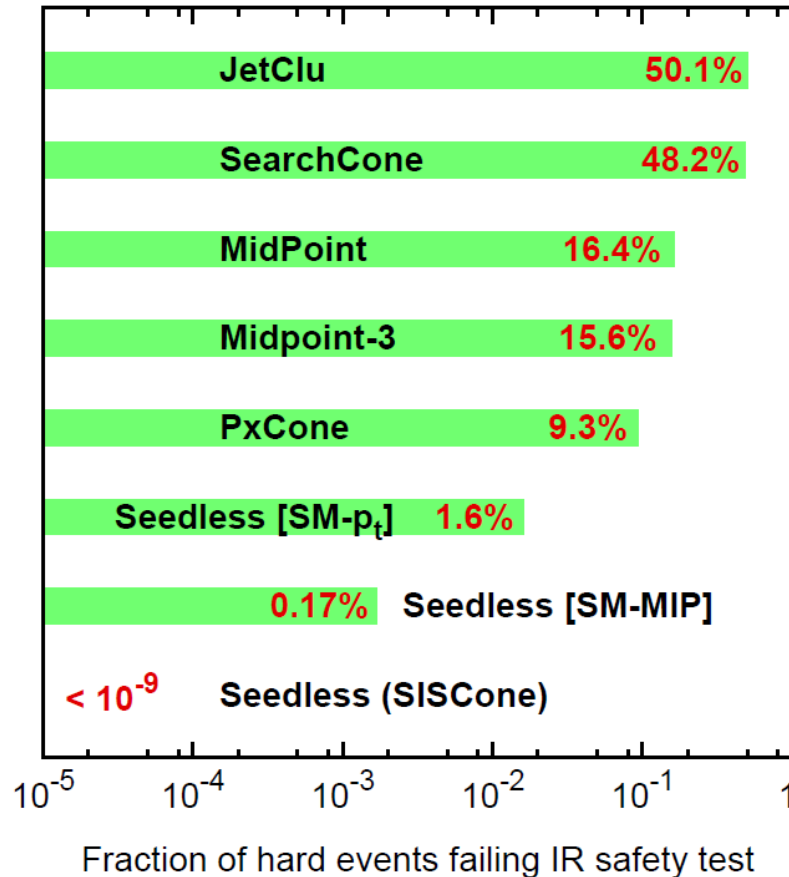
But at least a practical seedless cone algorithm

Very comparable performance to e.g. Midpoint!

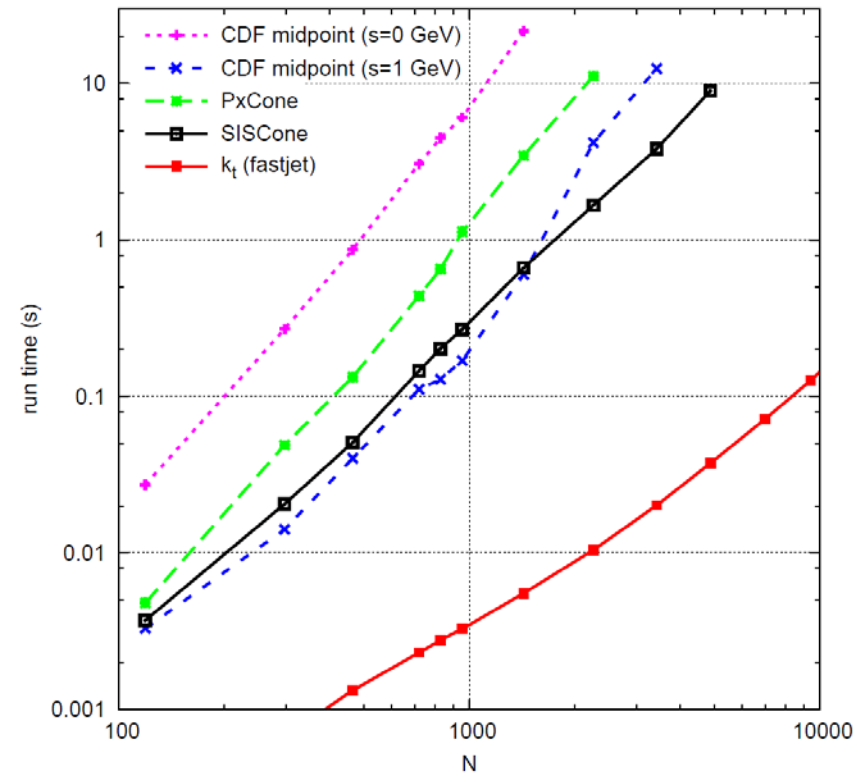


Infrared safety failure rates

(from G. Salam & G. Soyez, *JHEP* 0705:086,2007)



Computing performance



Computing performance an issue

Time for traditional kT is $\sim N^3$

Very slow for LHC

FastJet implementations

Use geometrical ordering to find out which pairs of particles have to be manipulated instead of recalculating them all!

Very acceptable performance in this case!

LHC events (pp collisions):

N	# operations	time [s]*
10	10^3	0.05
100	10^6	0.50
1,000	10^9	5.00

LHC events (heavy ion collisions):

N	# operations	time [s]*
10,000	10^{12}	$5 \cdot 10^3$
50,000	$1.25 \cdot 10^{14}$	$6.25 \cdot 10^5$

* on a modern computer (3 GHz clock)



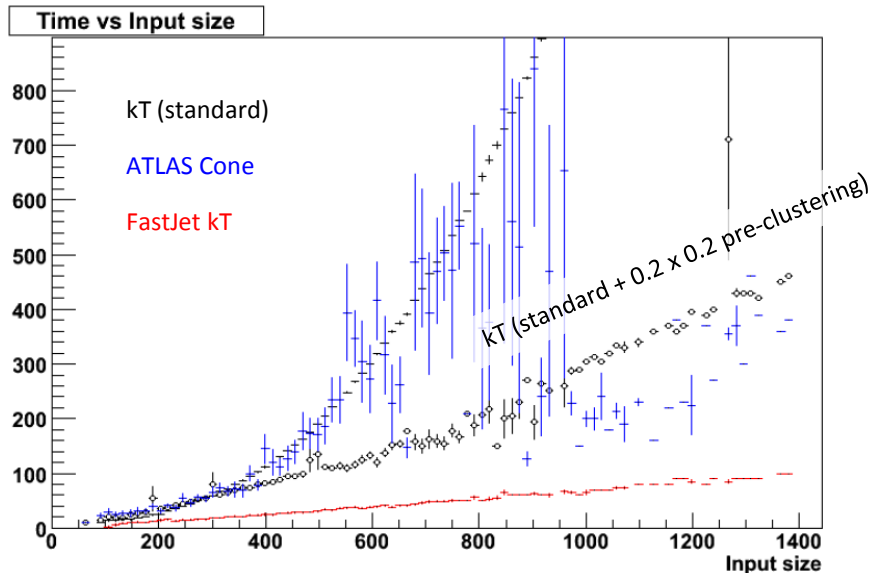
Computing performance an issue

Time for traditional kT is $\sim N^3$

Very slow for LHC

FastJet implementations

Use geometrical ordering to find out which pairs of particles have to be manipulated instead of recalculating them all!



FastJet implementations:

kT & Cambridge/Aachen $\sim N \ln N$

N	# operations	time [s]*
10	24	$0.1 \cdot 10^{-6}$
100	460	$2 \cdot 10^{-6}$
1,000	6,900	$35 \cdot 10^{-6}$
10,000	92,000	$0.5 \cdot 10^{-3}$
50,000	541,000	$3 \cdot 10^{-3}$

Anti-kT $\sim \sqrt{N^3}$

N	# operations	time [s]*
10	32	$0.2 \cdot 10^{-6}$
100	1,000	$5 \cdot 10^{-6}$
1,000	32,000	$0.2 \cdot 10^{-3}$
10,000	1,000,000	$5 \cdot 10^{-3}$
50,000	11,200,000	$56 \cdot 10^{-3}$



Address the search approach

Need to find minimum in
standard kT

Order N^3 operations

Consider geometrically nearest
neighbours in FastJet kT

Replace full search by search
over (jet, jet neighbours)

Need to find nearest neighbours
for each proto-jet fast

Several different approaches:
ATLAS (Delsart 2006) uses
simple geometrical model,
Salam & Cacciari (2006)
suggest Voronoi cells

Both based on same fact
relating d_{ij} and geometrical
distance in ΔR

Both use geometrically
ordered lists of proto-jets

Find minimum for N particles in standard kT:

$$\{d_{ij} = \min(d_i, d_j) \Delta R_{ij} / R, d_i = p_{T,i}^2\}, i, j = 1, \dots, N$$

$O(N^2)$ searches, repeated N times $\rightarrow O(N^3)$

FastJet kT uses nearest neighbours search:

$$d_{ij} = \min \wedge p_{T,i} < p_{T,j}$$

$$\Rightarrow R_{ij} < R_{ik} \quad \forall k \neq j, \text{ i.e. } (i, j) \text{ geometrical} \\ \text{nearest neighbours in } (y, \varphi) \text{ plane}$$

Proof:

Assume an additional particle k exists with
geometrical distance R_{ik} to particle i :

$$d_{ik} = \min(d_i, d_k) R_{ik} / R \leq d_i R_{ik} / R \\ > \min = d_{ij} = d_i R_{ij} / R$$

works only for $R_{ik} > R_{ij}$



Possible implementation

(P.A. Delsart, 2006)

Nearest neighbour search

Idea is to only limit recalculation of distances to nearest neighbours

Try to find all proto-jets having proto-jet k as nearest neighbour

Center pseudo-rapidity (or rapidity)/azimuth plane on k

Take first proto-jet j closest to k in pseudo-rapidity

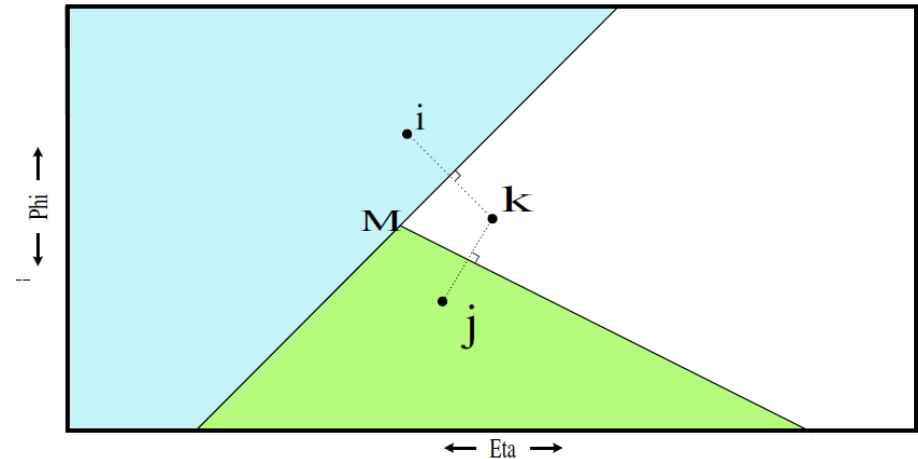
Compute middle line L_{jk} between k and j

All proto-jets below L_{jk} are closer to j than $k \rightarrow k$ is not nearest neighbour of those

Take next closest proto-jet i in pseudo-rapidity

Proceed as above with exclusion of all proto-jets above L_{ik}

Search stops when point below intersection of L_{jk} and L_{ik} is reached, no more points have k as nearest neighbour



Complexity estimate:

Assume N proto-jets are uniformly distributed in (η, φ) plane (rectangular with finite size, area A)

Average number of proto-jets in circle with radius R :

$$\bar{N} = N \frac{\pi R^2}{A}$$

If R is mean distance between two proto-jets:

$$\bar{N} \approx 1 \Rightarrow R \approx \sqrt{\frac{A}{\pi N}}$$

Computation of proto-jet k 's nearest neighbours is restricted to

$$\eta \approx [\eta_k - R, \eta_k + R] \mapsto \approx N \cdot 2R \propto \frac{N}{\sqrt{N}} = \sqrt{N} \text{ operations for } k$$

$\Rightarrow N\sqrt{N}$ total complexity (estimate)



Apply geometrical methods to nearest neighbour searches

Voronoi cell around proto-jet k
defines area of nearest
neighbours

No point inside area is closer
to any other protojet

Apply to protojets in pseudo-
rapidity/azimuth plane

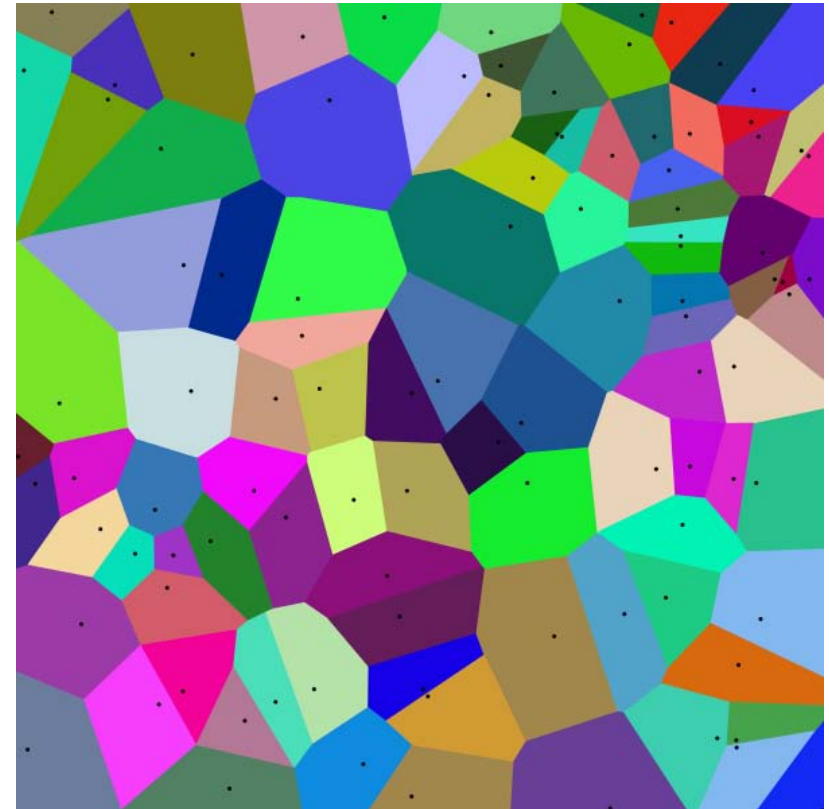
Useful tool to limit nearest
neighbour search

Determines region of re-
calculation of distances in kT

Allows quick updates without
manipulating too many long
lists

Complex algorithm!

Read [G. Salam & M. Cacciari,
Phys.Lett.B641:57-61 \(2006\)](#)



(source http://en.wikipedia.org/wiki/Voronoi_diagram)

Complexity estimate (Monte Carlo experiment):

$N \ln N$ total complexity



Various jet algorithms produce different jets from the same collision event

Clearly driven by the different sensitivities of the individual algorithms

Cannot expect completely identical picture of event from jets

Different topology/number of jets

Differences in kinematics and shape for jets found at the same direction

Choice of algorithm motivated by physics analysis goal

E.g., IR safe algorithms for jet counting in $W + n$ jets and others

Narrow jets for W mass spectroscopy

Small area jets to suppress pile-up contribution

Measure of jet algorithm performance depends on final state

Cone preferred for resonances

E.g., 2 – 3... n prong heavy particle decays like top, Z' , etc.

Boosted resonances may require jet substructure analysis – need kT algorithm!

Recursive recombination algorithms preferred for QCD cross-sections

High level of IR safety makes jet counting more stable

Pile-up suppression easiest for regularly shaped jets

E.g., Anti-kT most cone-like, can calculate jet area analytically even after split and merge

Measures of jet performance

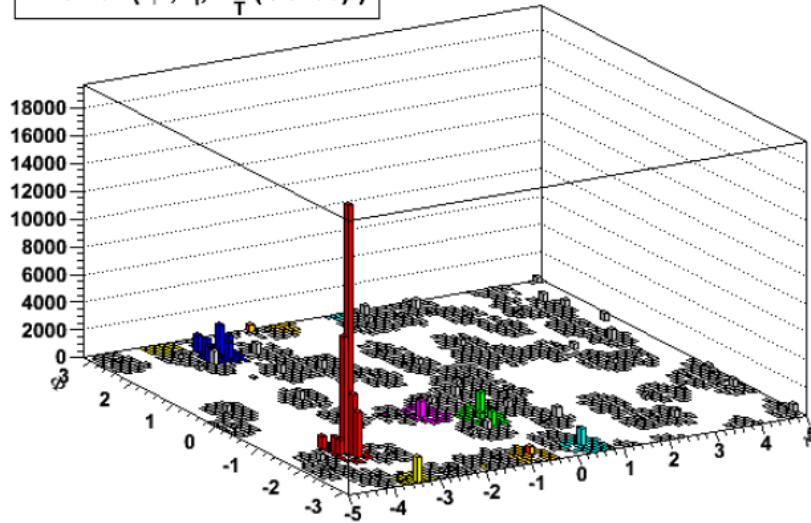
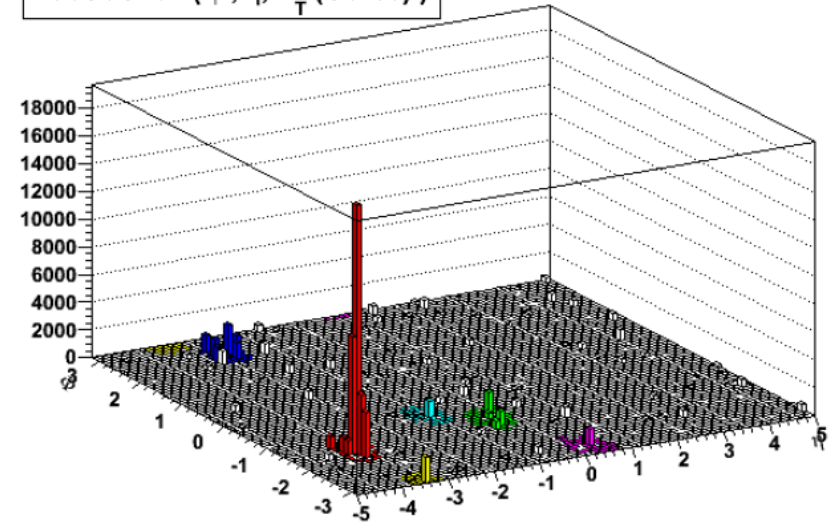
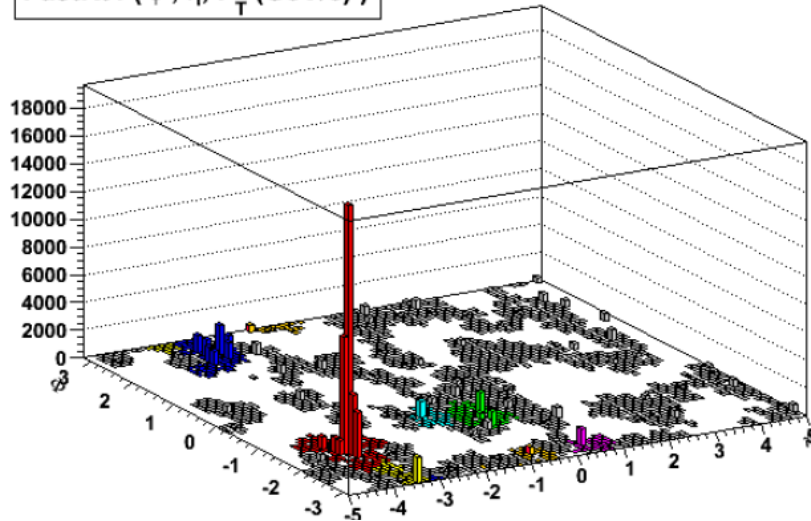
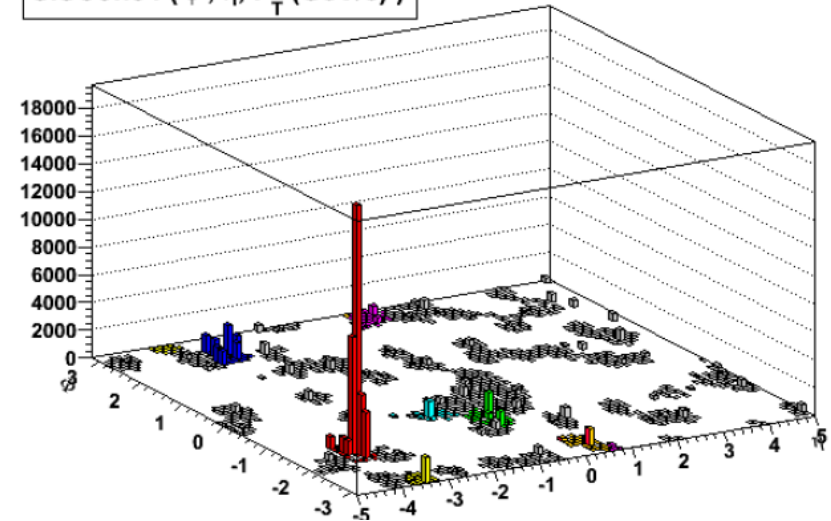
Particle level measures prefer observables from final state

Di-jet mass spectra etc.

Quality of spectrum important

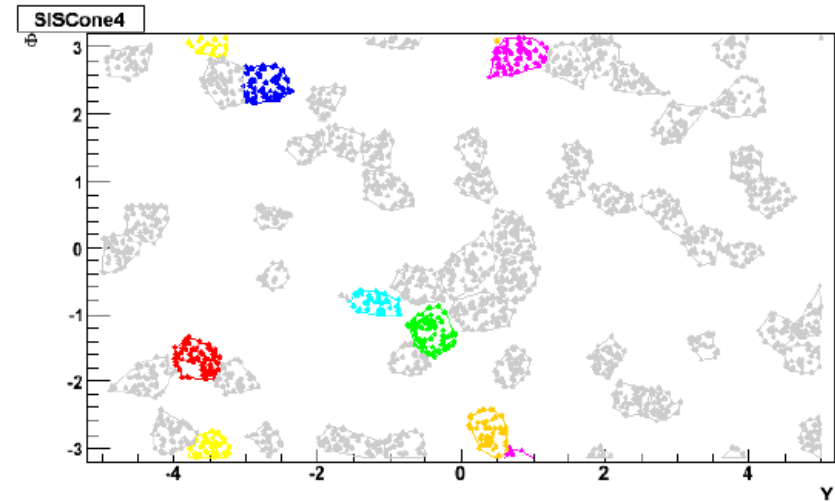
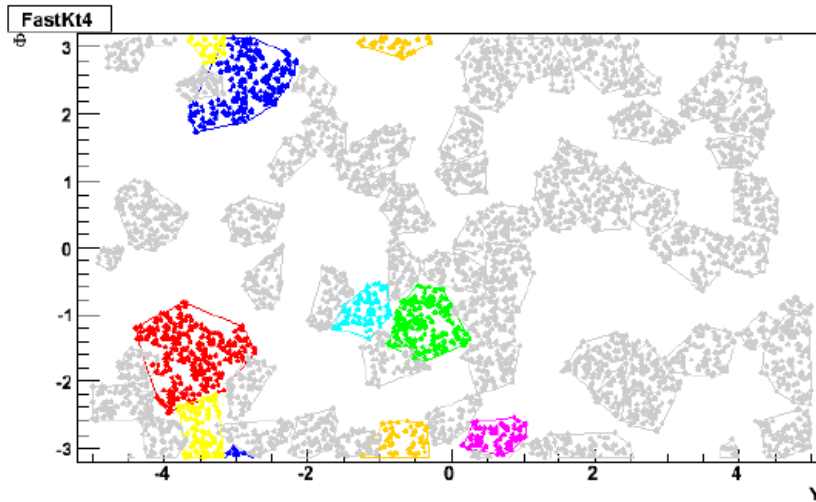
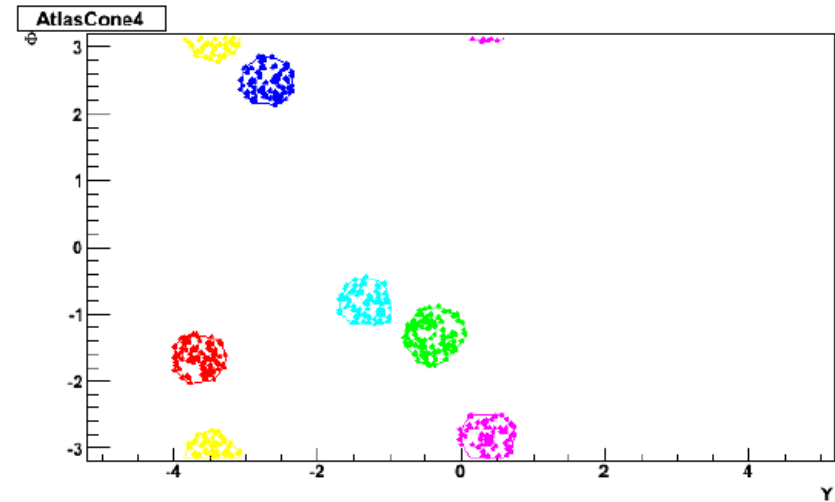
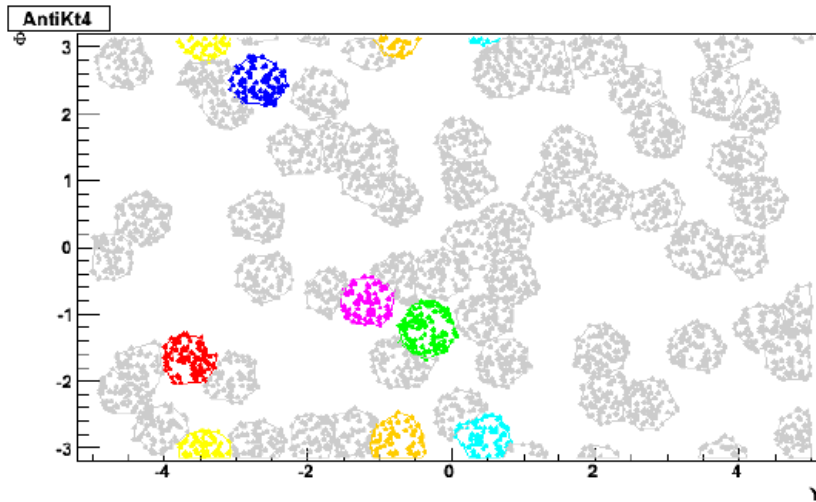
Deviation from Gaussian etc.



AntiKt4 (ϕ , η , P_T (GeV/c))

AtlasCone4 (ϕ , η , P_T (GeV/c))

FastKt4 (ϕ , η , P_T (GeV/c))

SISCone4 (ϕ , η , P_T (GeV/c))


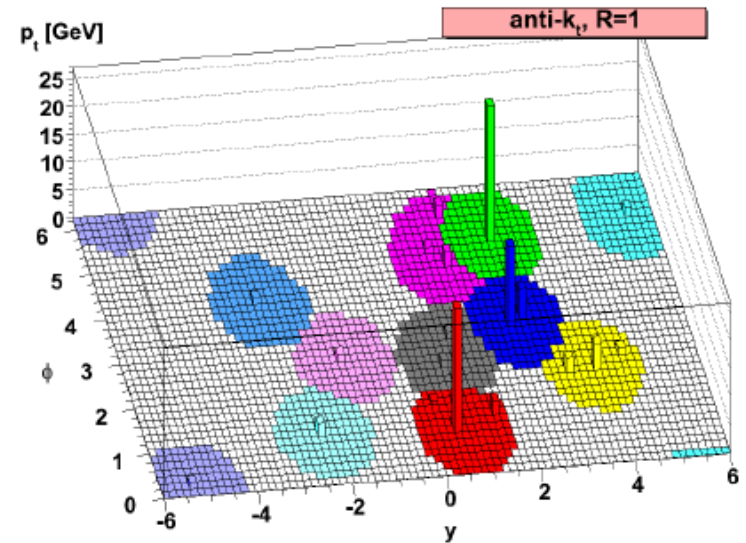
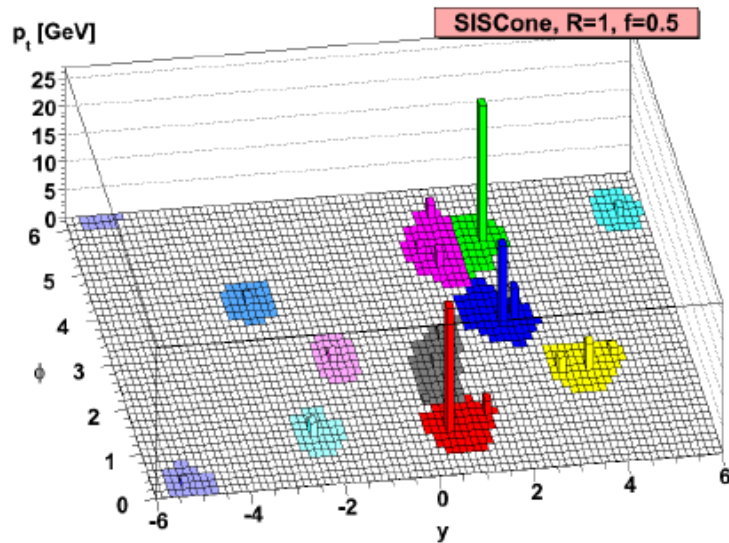
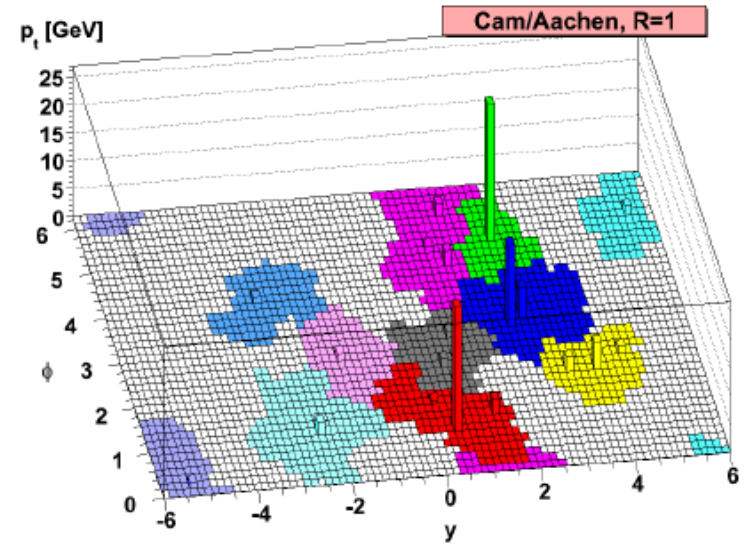
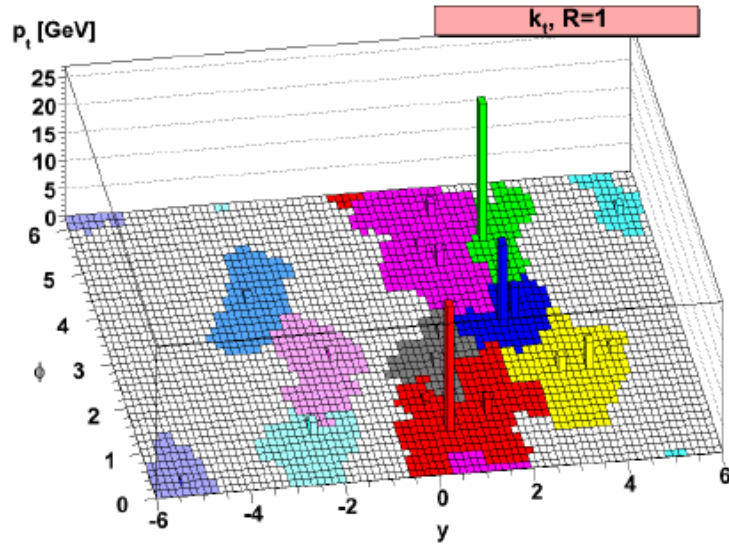
(from P.A. Delsart)





(from P.A. Delsart)





(from G. Salam's talk at the ATLAS Hadronic Calibration Workshop Tucson 2008)



Quality estimator for distributions

Best reconstruction: narrow Gaussian

We understand the error on the mean!

Observed distributions often deviate from Gaussian

Need estimators on size of deviations!

Should be least biased measures

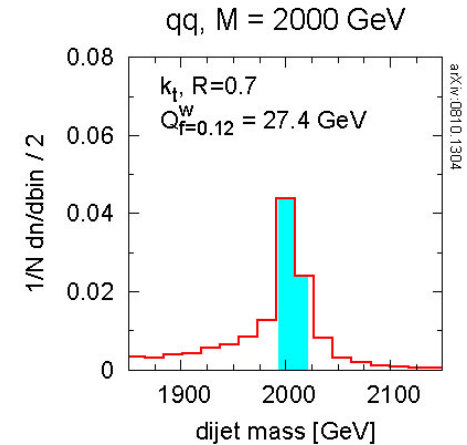
Best performance gives closest to Gaussian distributions

List of variables describing shape of distribution on next slide

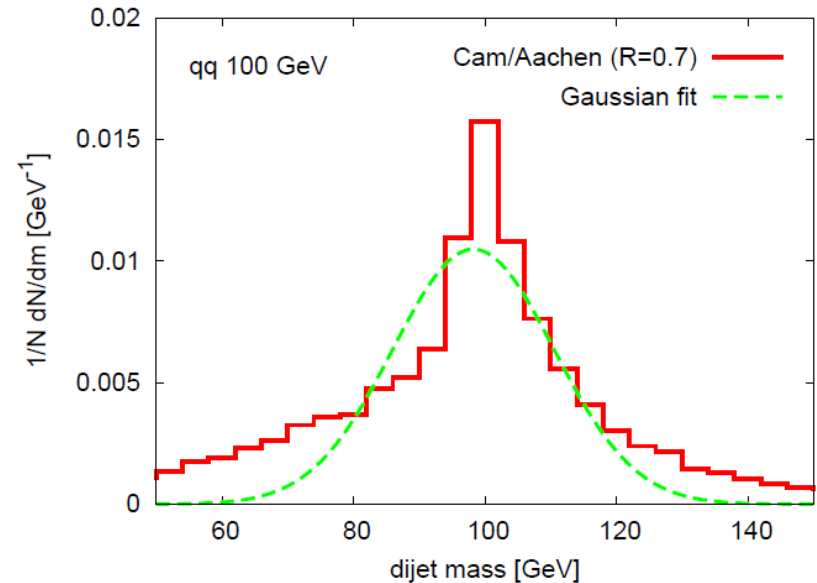
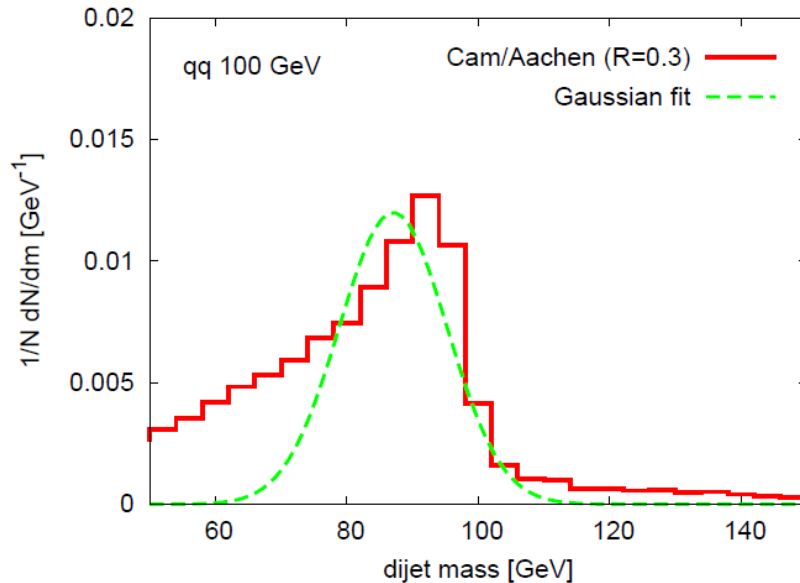
Focus on unbiased estimators

E.g., distribution quantile describes the narrowest range of values containing a requested fraction of all events

Kurtosis and skewness harder to understand, but clear message in case of Gaussian distribution!



(from Salam, Cacciari, Soyez,
<http://quality.fastjet.fr>)



Estimator

$$\langle R \rangle$$

$$R_{\text{median}}$$

$$R_{\text{mop}}$$

$$RMS = \sqrt{\langle R^2 \rangle - \langle R \rangle^2}$$

$$\gamma_3 = \frac{\sum_{i=1}^N (R_i - \langle R \rangle)^3}{N\sigma^3}$$

$$\gamma_4 = \frac{\sum_{i=1}^N (R_i - \langle R \rangle)^4}{N\sigma^4} - 3$$

$$Q_f^w$$

Quantity

statistical mean

median

most probable value

standard deviation

skewness/left-right asymmetry

kurtosis/"peakedness"

quantile

Expectation for Gaussian

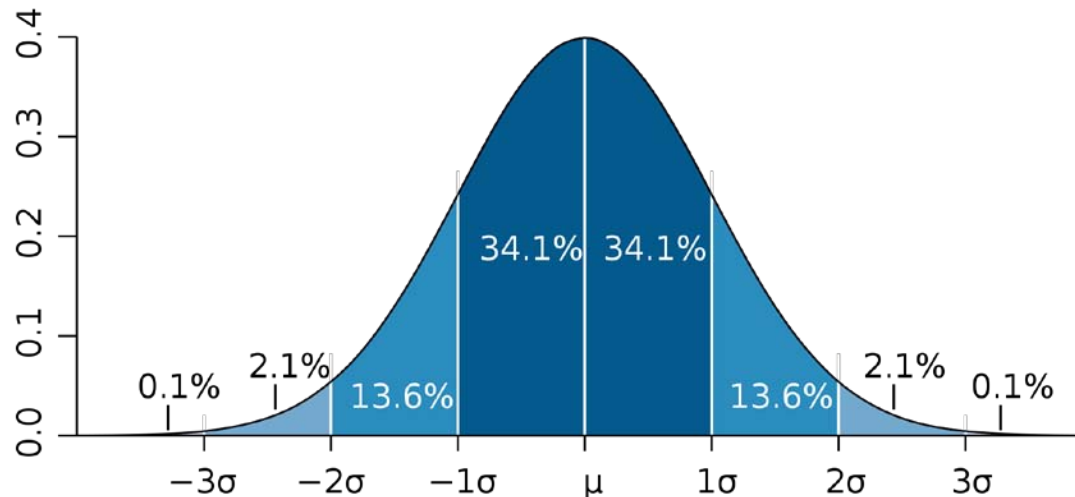
$$\mu = \langle R \rangle = R_{\text{mop}} = R_{\text{median}}$$

$$\sigma = RMS$$

0

0

$$Q_{f \approx 68\%}^w = 2\sigma$$



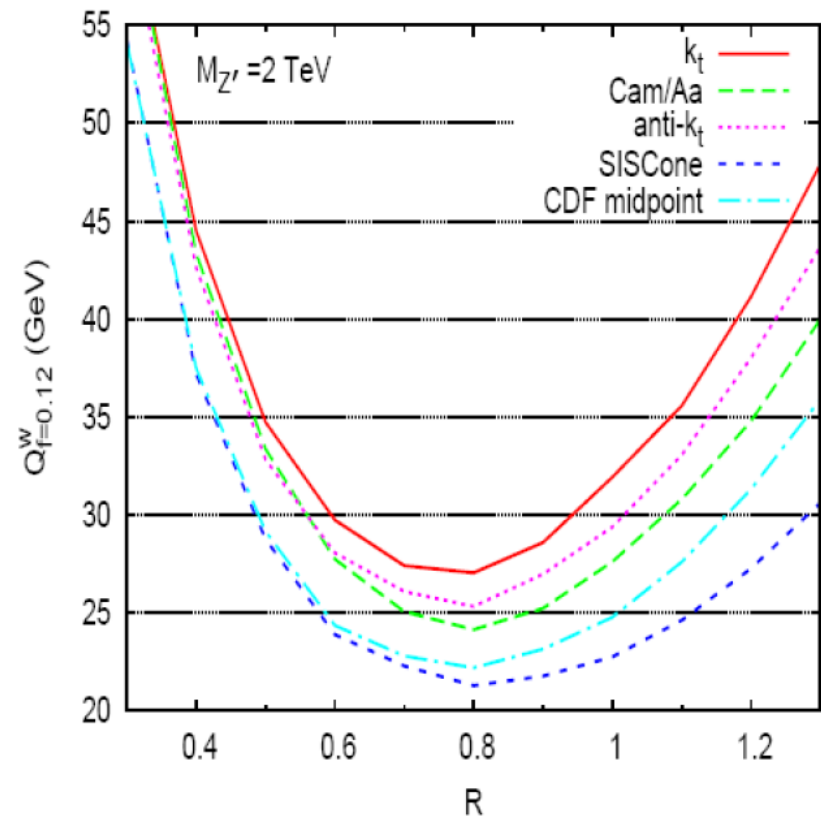
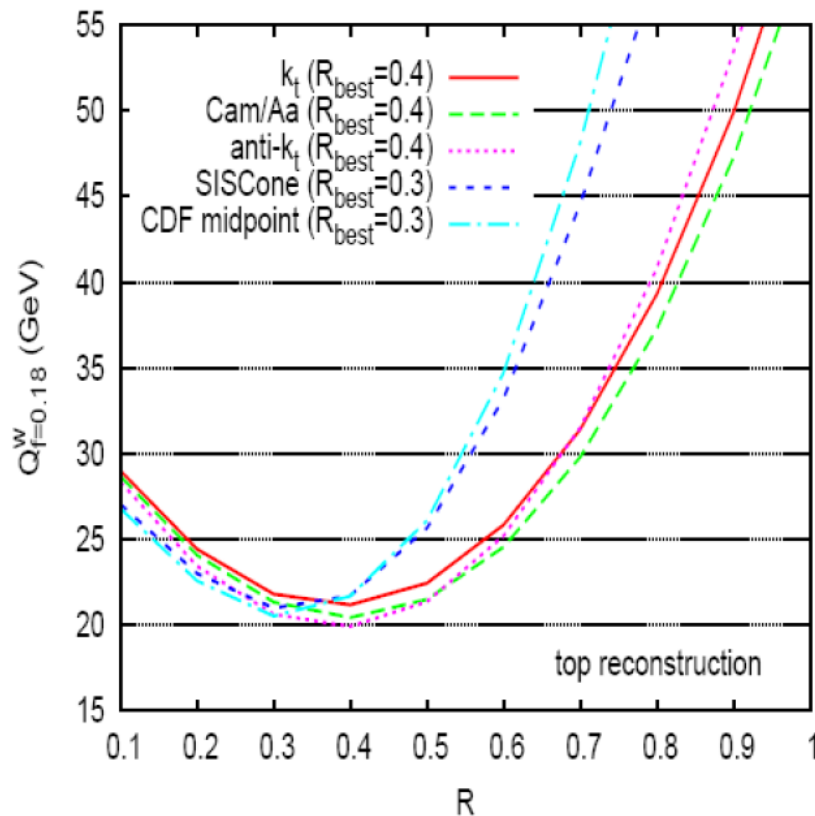
Quality of mass reconstruction for various jet finders and configurations

Standard model – top quark hadronic decay

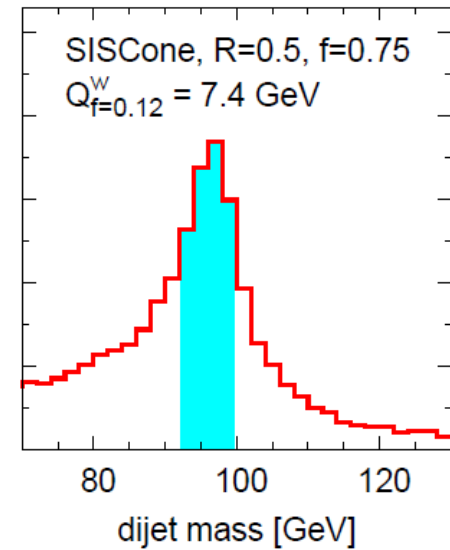
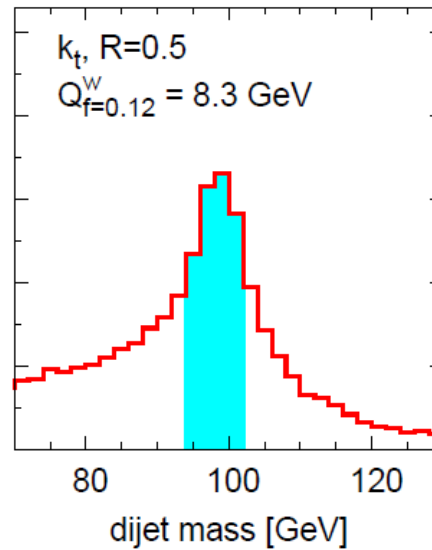
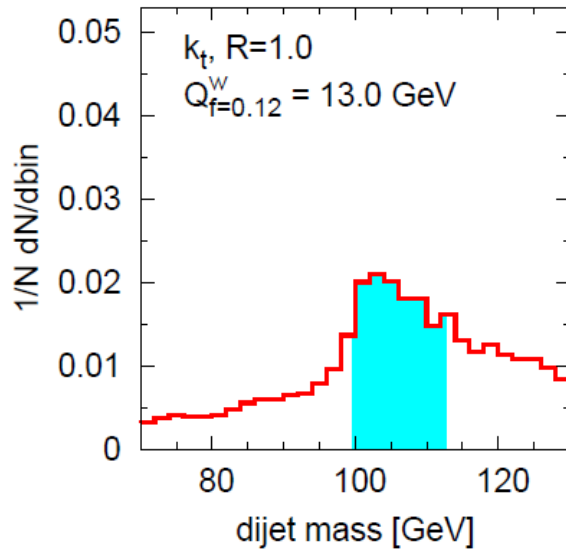
Left plot – various jet finders and distance parameters

BSM – Z' (2 TeV) hadronic decay

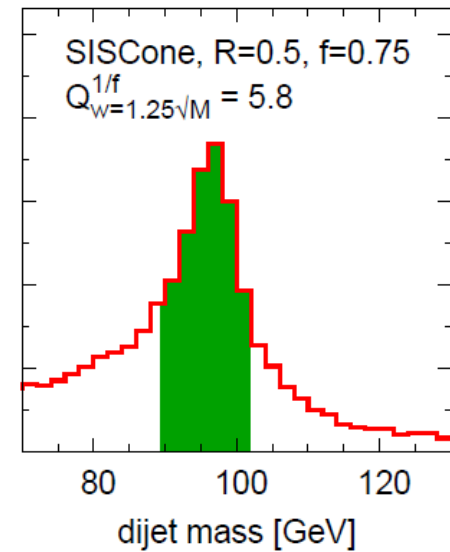
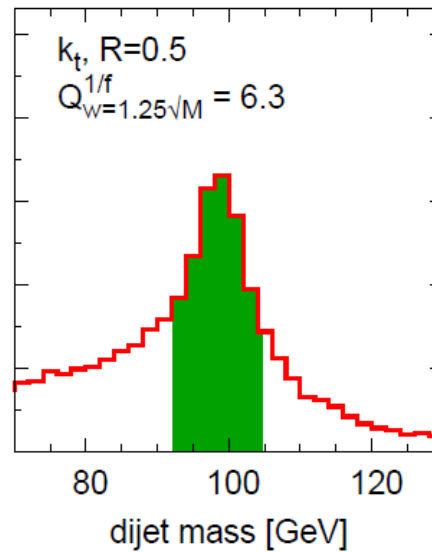
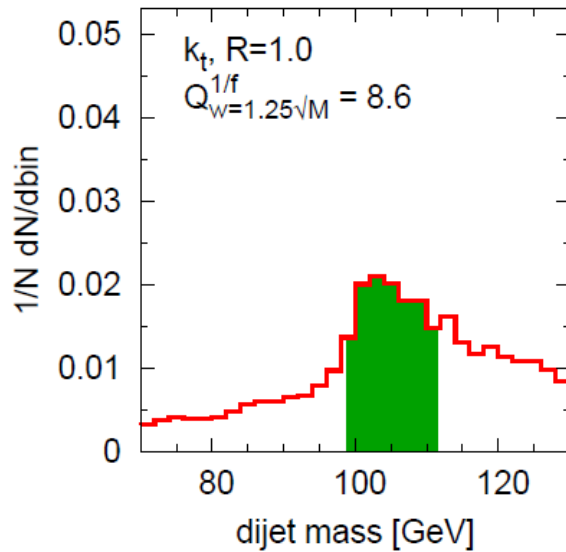
Right plot – various jet finders with best configuration



$$Q_{w=x\sqrt{M}}^{1/f} \equiv \frac{\text{Max \# reco. massive objects in window of width } w = x\sqrt{M}}{\text{Total \# generated massive objects}}^{-1}$$



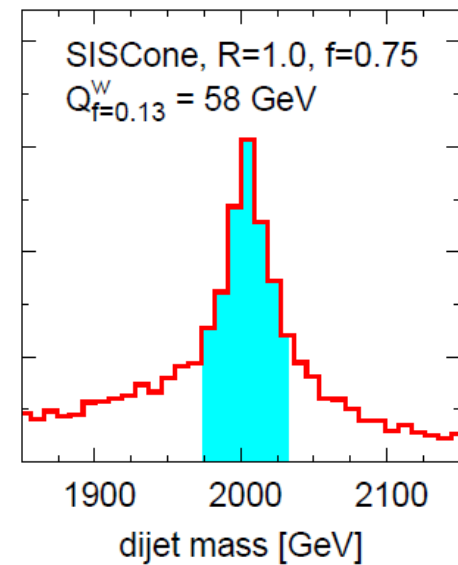
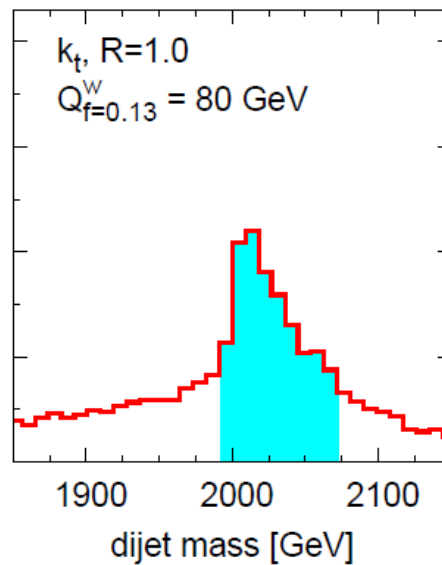
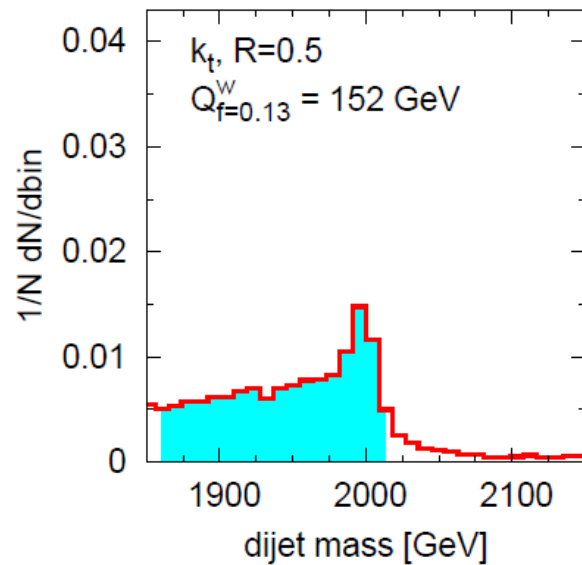
qq 100 GeV



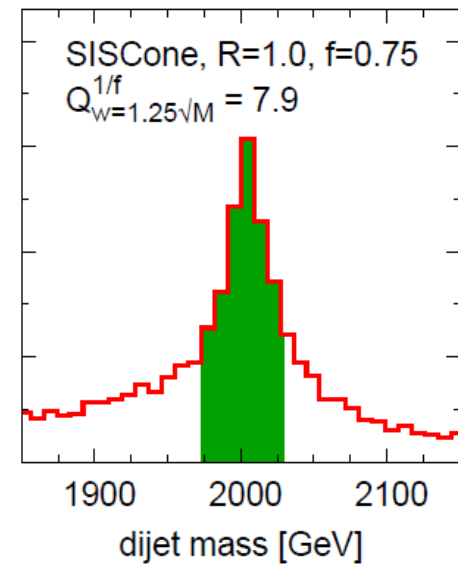
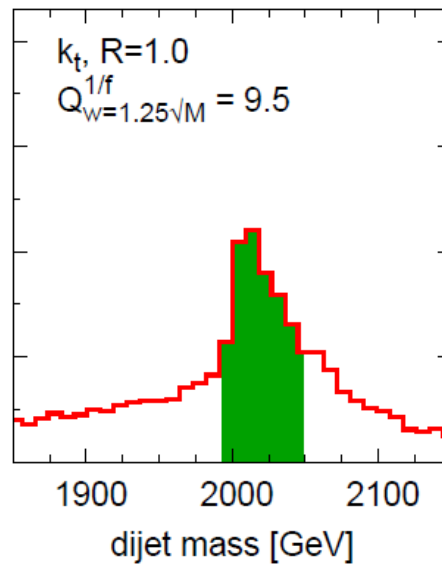
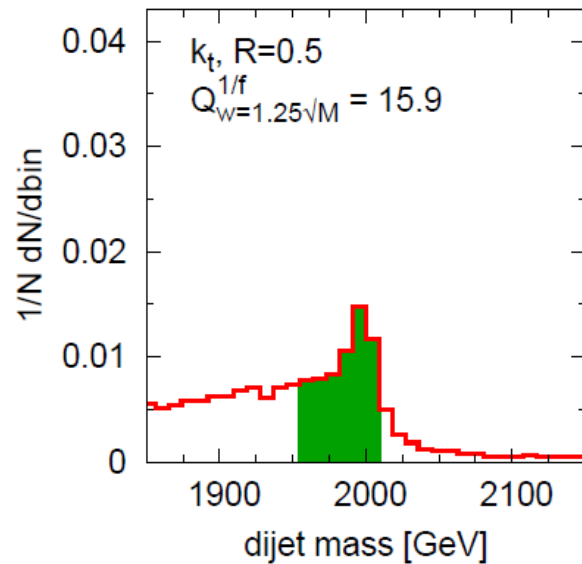
qq 100 GeV

 (from Cacciari, Rojo, Salam, Soyez, **JHEP 0812:032,2008**)


$$Q_{w=x\sqrt{M}}^{1/f} \equiv \left(\frac{\text{Max \# reco. massive objects in window of width } w = x\sqrt{M}}{\text{Total \# generated massive objects}} \right)^{-1}$$

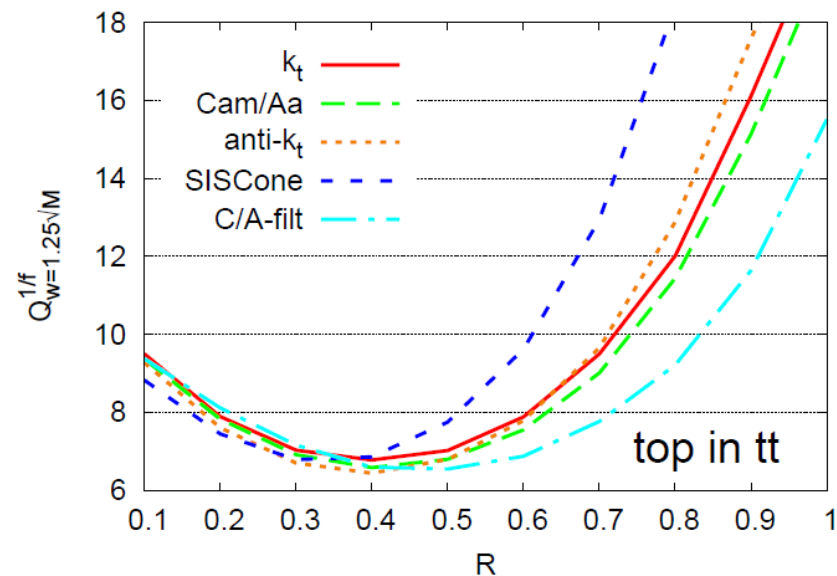
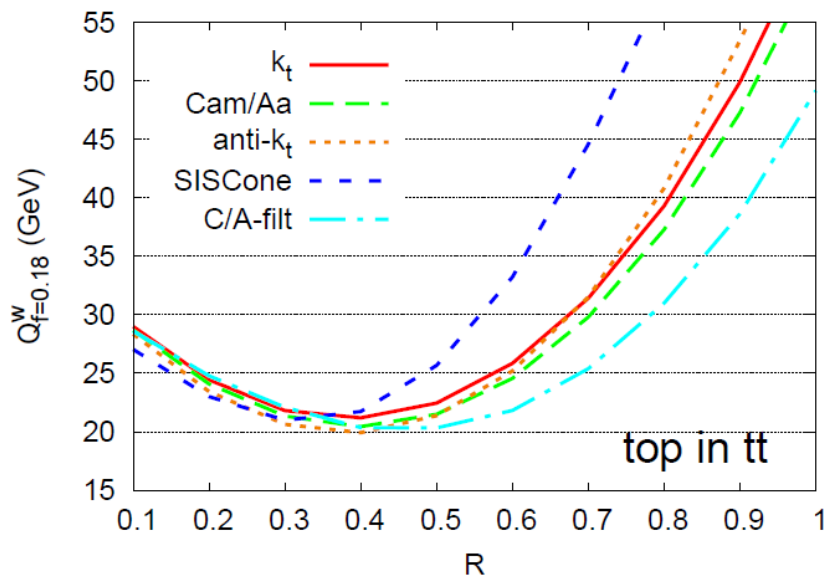
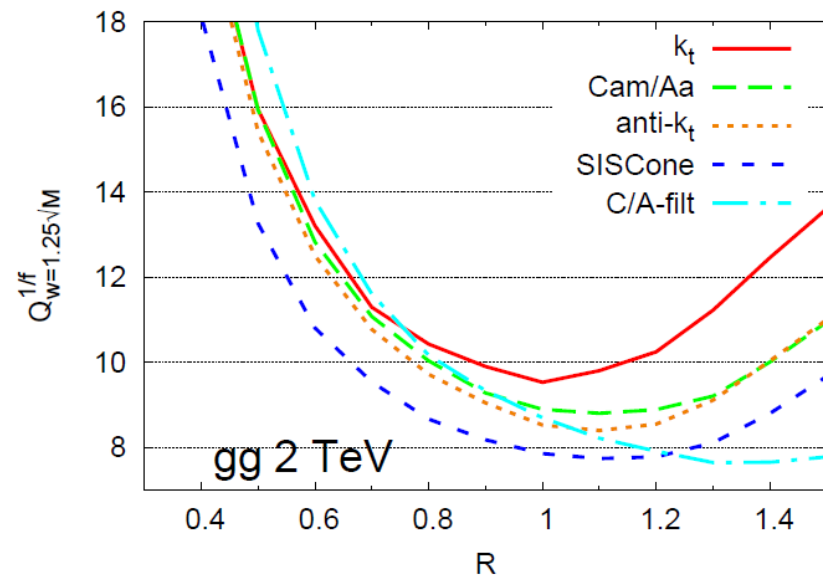
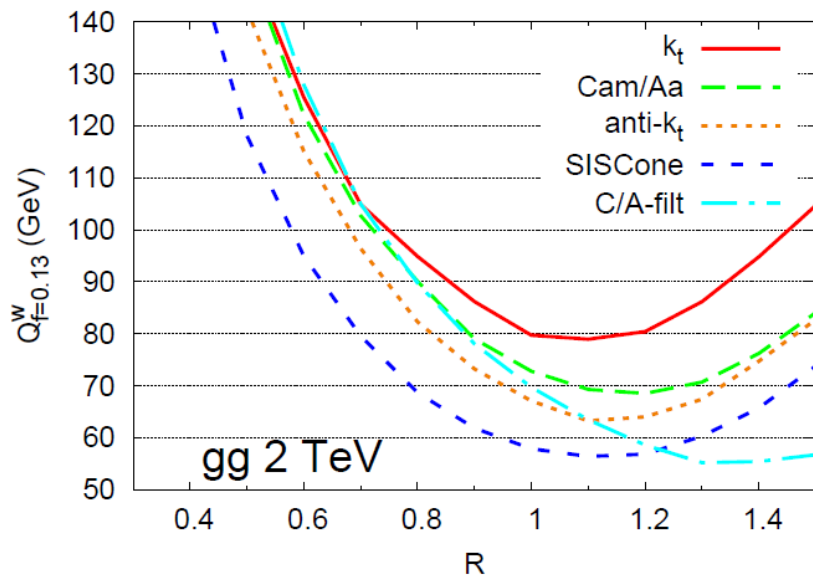


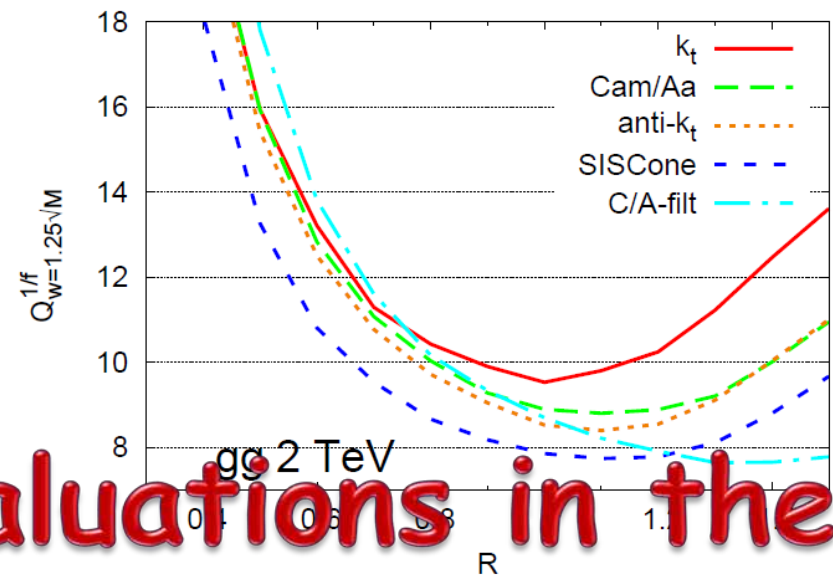
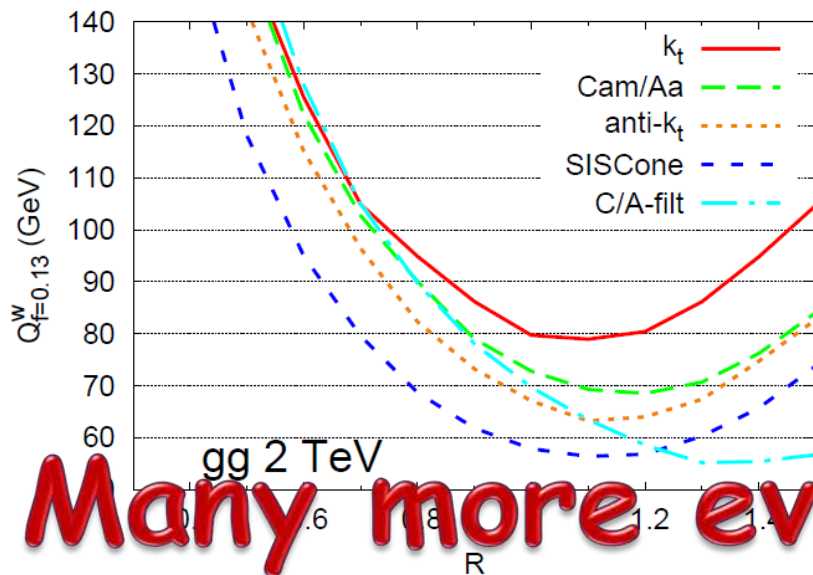
gg 2 TeV



gg 2 TeV

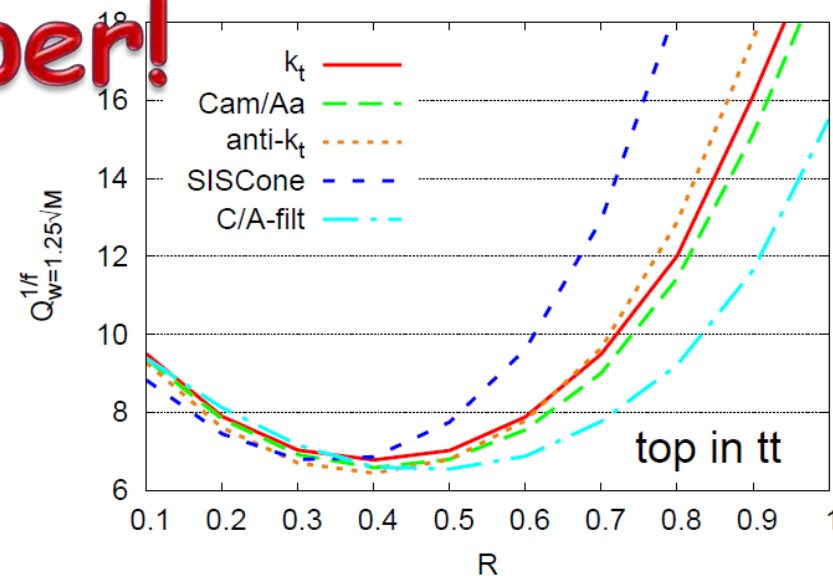
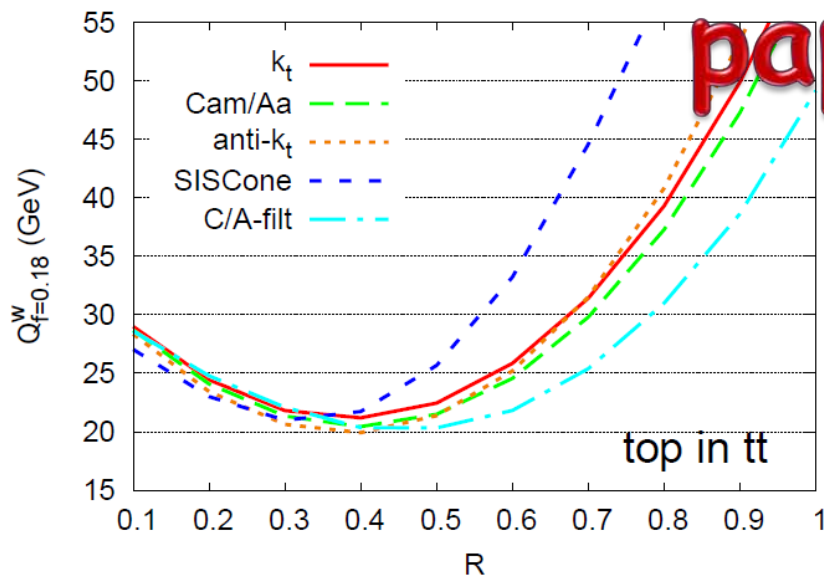
(from Cacciari, Rojo, Salam, Soyez, *JHEP* 0812:032,2008)


 (from Cacciari, Rojo, Salam, Soyez, *JHEP* 0812:032,2008)

Many more evaluations in the

paper!



(from Cacciari, Rojo, Salam, Soyez, [JHEP 0812:032,2008](#))



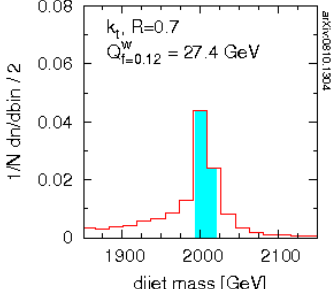
Web-based jet performance evaluation available

<http://www.lpthe.jussieu.fr/~salam/jet-quality>

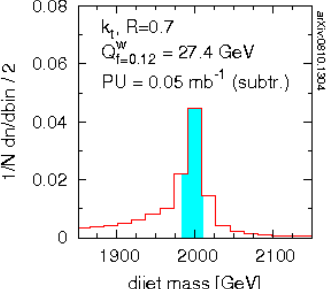
Testing jet definitions: qq & gg cases

by M. Cacciari, J. Rojo, G.P. Salam and G. Soyez, arXiv:0810.1304

qq, M = 2000 GeV



qq, M = 2000 GeV



k_t
 C/A
 anti- k_t
 SIScone
 C/A-filt

$Q_{F=Z}^W$
 $Q_{F=X\sqrt{M}}^{1/f}$
 x 2

qq
 gg

pileup: none
 0.05
 0.25 mb⁻¹/ev

subtraction:

k_t
 C/A
 anti- k_t
 SIScone
 C/A-filt

$Q_{F=Z}^W$
 $Q_{F=X\sqrt{M}}^{1/f}$
 x 2

qq
 gg

pileup: none
 0.05
 0.25 mb⁻¹/ev

subtraction:

This page is intended to help visualize how the choice of jet definition impacts a dijet invariant mass reconstruction at LHC.

The controls fall into 4 groups:

- the jet definition
- the binning and quality measures
- the jet-type (quark, gluon) and mass scale
- pileup and subtraction

The events were simulated with Pythia 6.4 (DWT tune) and reconstructed with FastJet 2.3.

For more information, view and listen to the **flash demo**, or click on individual terms.

This page has been tested with Firefox v2 and v3, IE7, Safari v3, Opera v9.5, Chrome 0.2.

Find: Highlight all Match case

Done



Introduction to Hadronic Final State Reconstruction in Collider Experiments (Part IX)

Peter Loch
University of Arizona
Tucson, Arizona
USA

CERN press release March 30, 2010

Rolf Heuer (Director General, CERN):

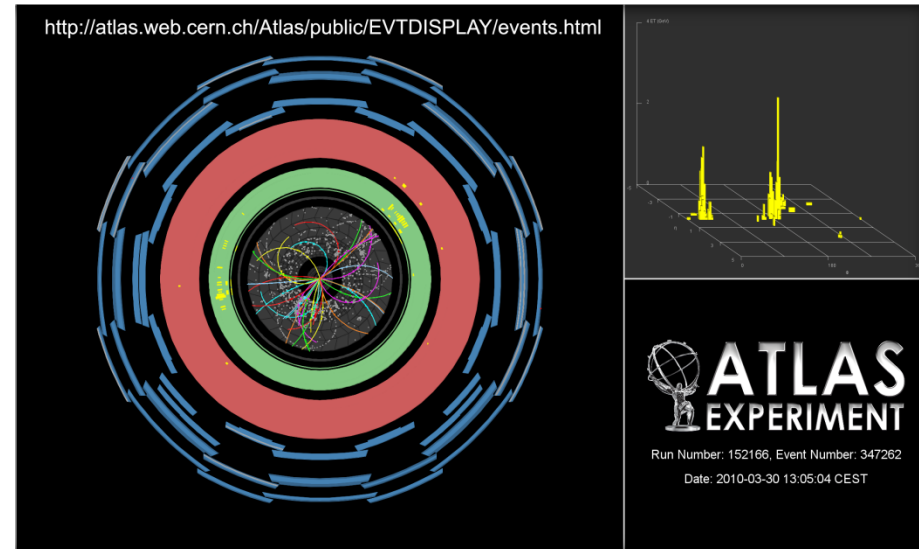
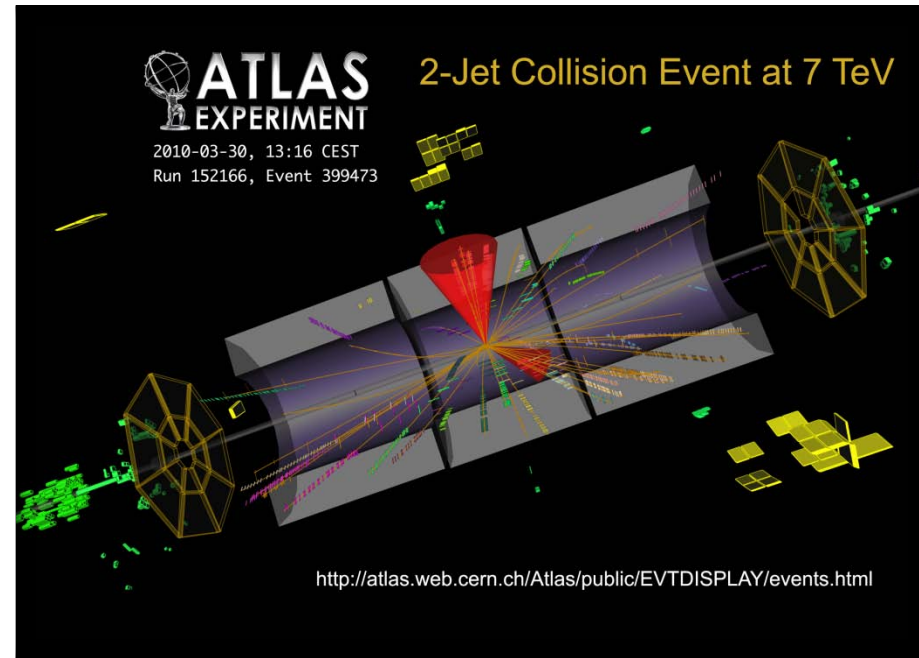
“Beams collided at 7 TeV in the LHC at 13:06 CEST today, marking the start of the LHC research program. Particle physicists around the world are looking forward to a potentially rich harvest of new physics as the LHC begins its first long run at an energy three and a half times higher than previously achieved at a particle accelerator. ...”

That was at 4:06am (Arizona) this morning...

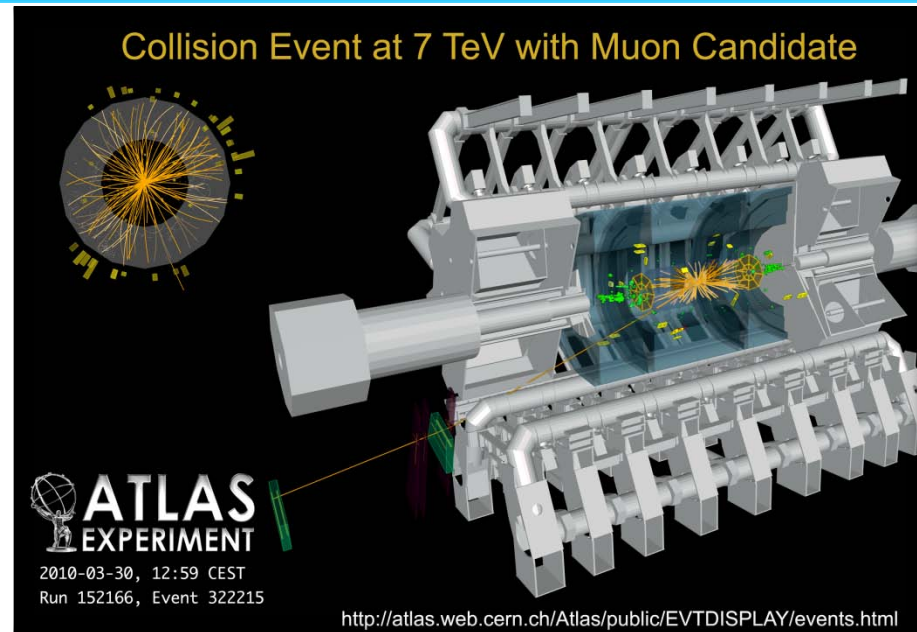
We were probably not awake but are as excited!

... and we already see two-jet events!

See event displays on the right!
Two different events!

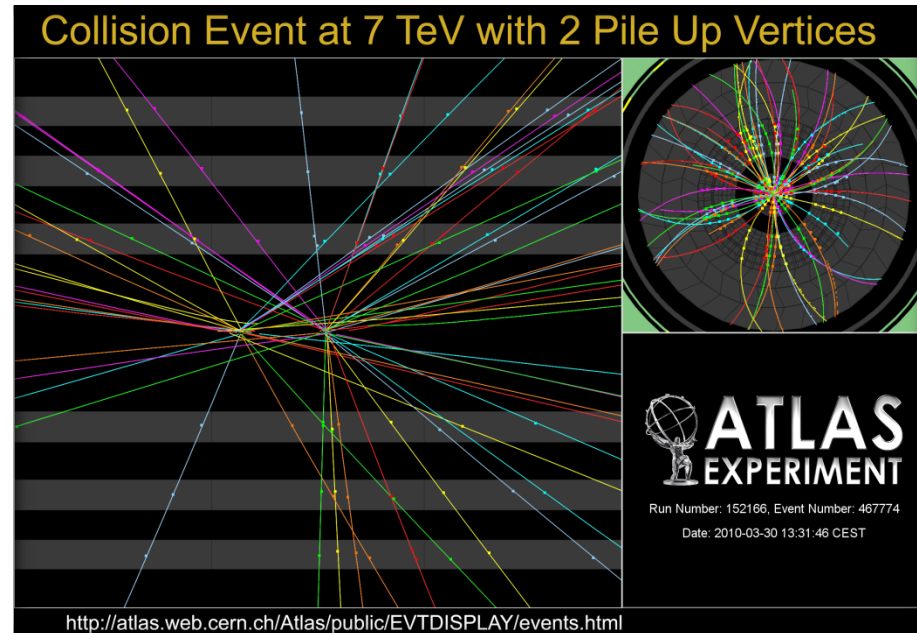


Top: Muon candidate



Two collisions at the same time

Pile-up!



Recall: the experimentalists' view on jets

A bunch of particles generated by hadronization of a common source

Quark, gluon fragmentation

As a consequence, the particles in this bunch have correlated kinematic properties

Reflecting the source by sum rules and Conservation laws

The **interacting** particles in this bunch generated an observable signal in a detector

Protons, neutrons, pions, photons, electrons, muons, other particles with laboratory lifetimes $> \sim 10\text{ps}$, and the corresponding anti-particles

The **non-interacting** particles do not generate a directly observable signal

Neutrinos, mostly

What is jet reconstruction, then?

Model/simulation: particle jet

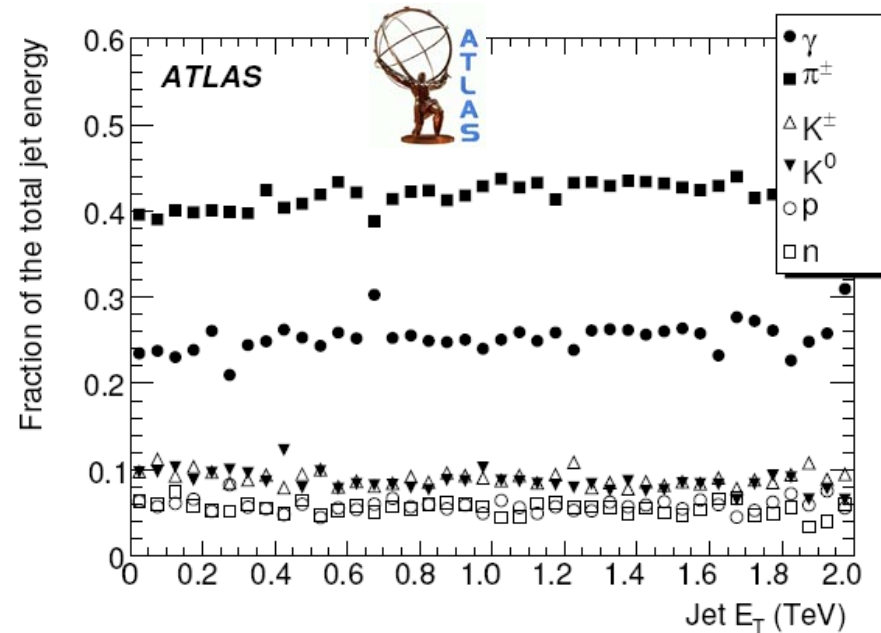
Attempt to collect the final state particles described above into objects (jets) representing the original parton kinematic

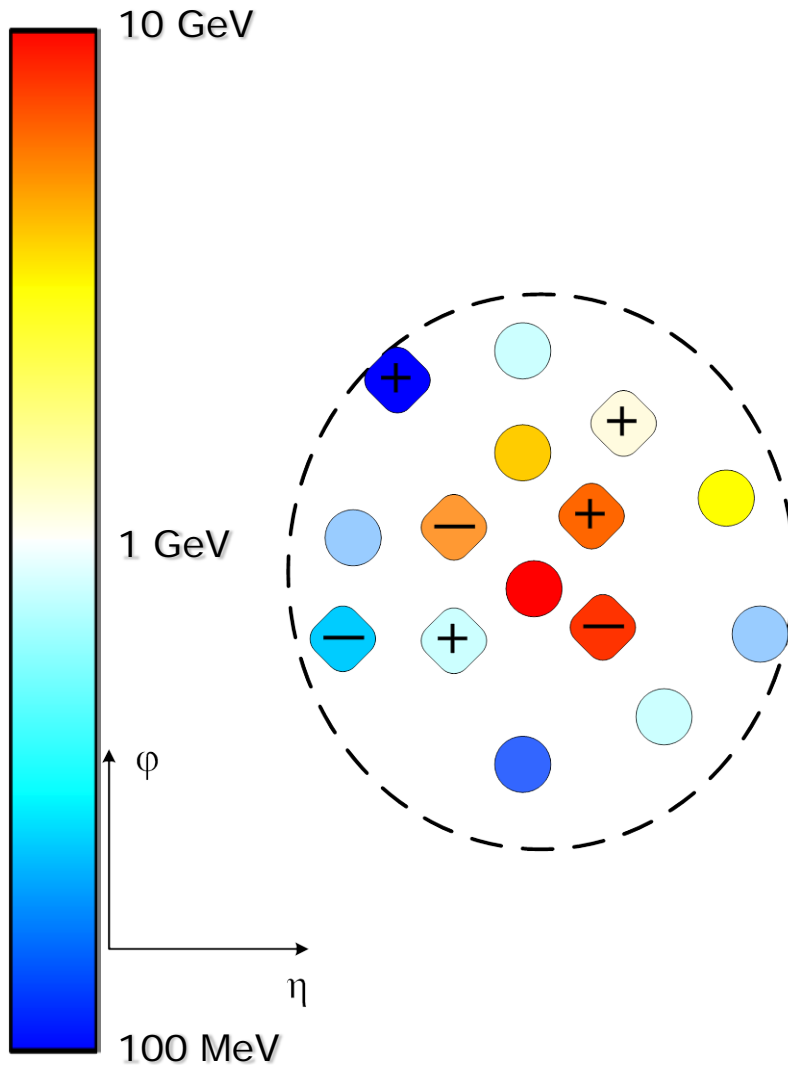
Re-establishing the correlations

Experiment: detector jet

Attempt to collect the detector signals from these particles to measure their original kinematics

Usually not the parton!





Change of composition

Radiation and decay inside detector volume
 "Randomization" of original particle content

Defocusing changes shape in lab frame

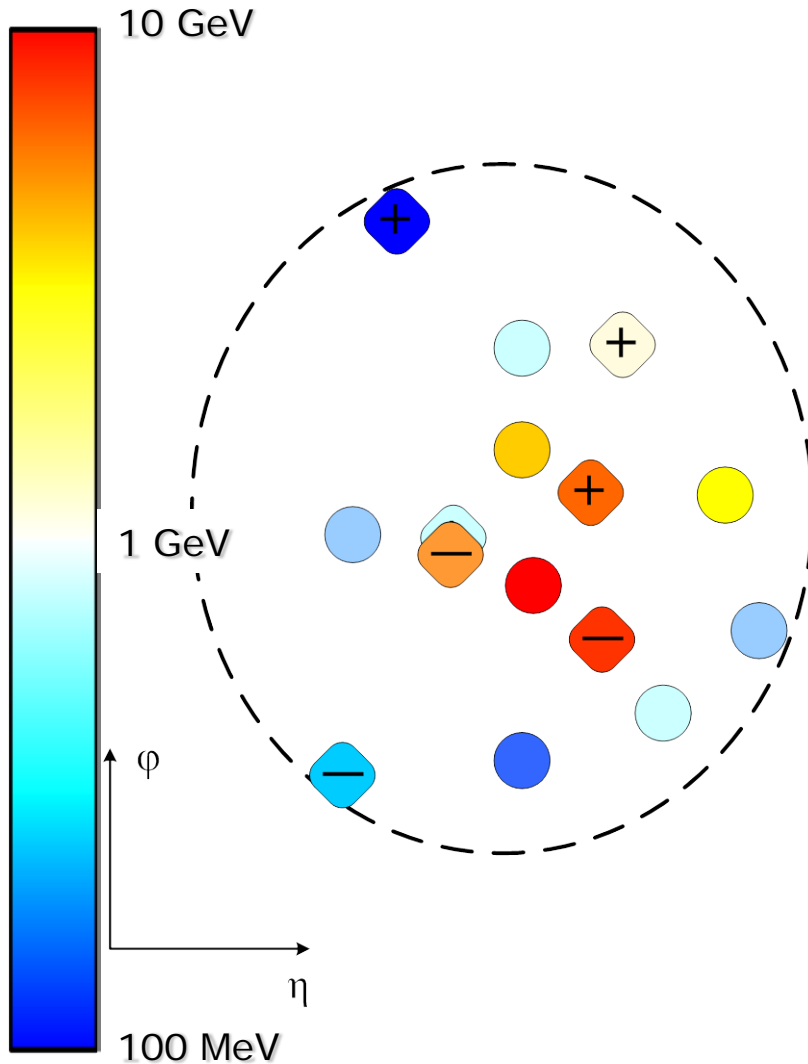
Charged particles bend in solenoid field

Attenuation changes energy

Total loss of soft charged particles in magnetic field
 Partial and total energy loss of charged and neutral particles in inactive upstream material

Hadronic and electromagnetic cascades in calorimeters

Distribute energy spatially
 Lateral particle shower overlap



Change of composition

Radiation and decay inside detector volume

"Randomization" of original particle content

Defocusing changes shape in lab frame

Charged particles bend in solenoid field

Attenuation changes energy

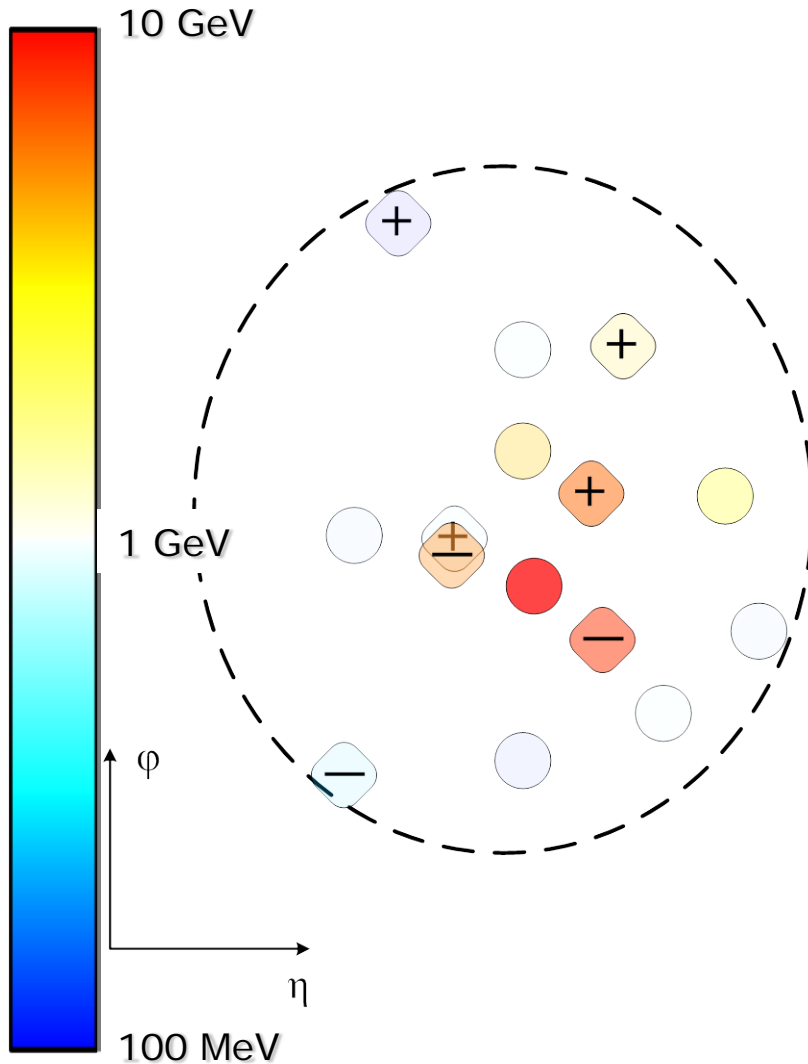
Total loss of soft charged particles in magnetic field

Partial and total energy loss of charged and neutral particles in inactive upstream material

Hadronic and electromagnetic cascades in calorimeters

Distribute energy spatially

Lateral particle shower overlap



Change of composition

Radiation and decay inside detector volume

"Randomization" of original particle content

Defocusing changes shape in lab frame

Charged particles bend in solenoid field

Attenuation changes energy

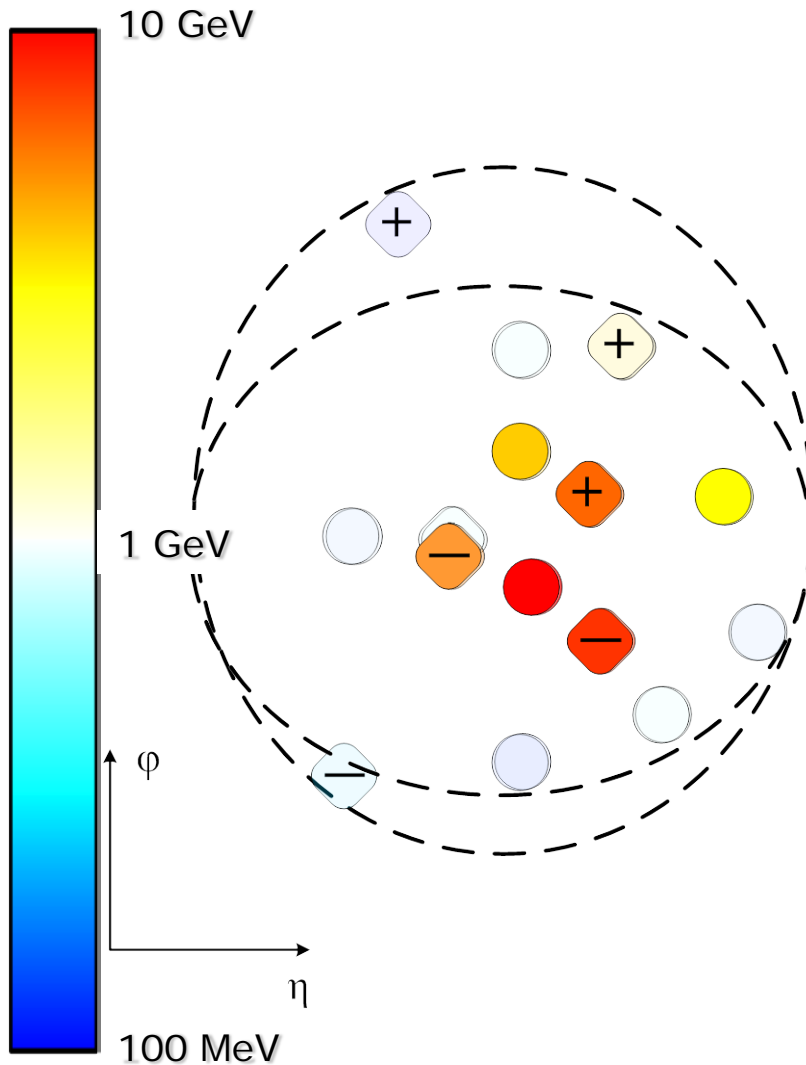
Total loss of soft charged particles in magnetic field

Partial and total energy loss of charged and neutral particles in inactive upstream material

Hadronic and electromagnetic cascades in calorimeters

Distribute energy spatially

Lateral particle shower overlap



Change of composition

Radiation and decay inside detector volume

"Randomization" of original particle content

Defocusing changes shape in lab frame

Charged particles bend in solenoid field

Attenuation changes energy

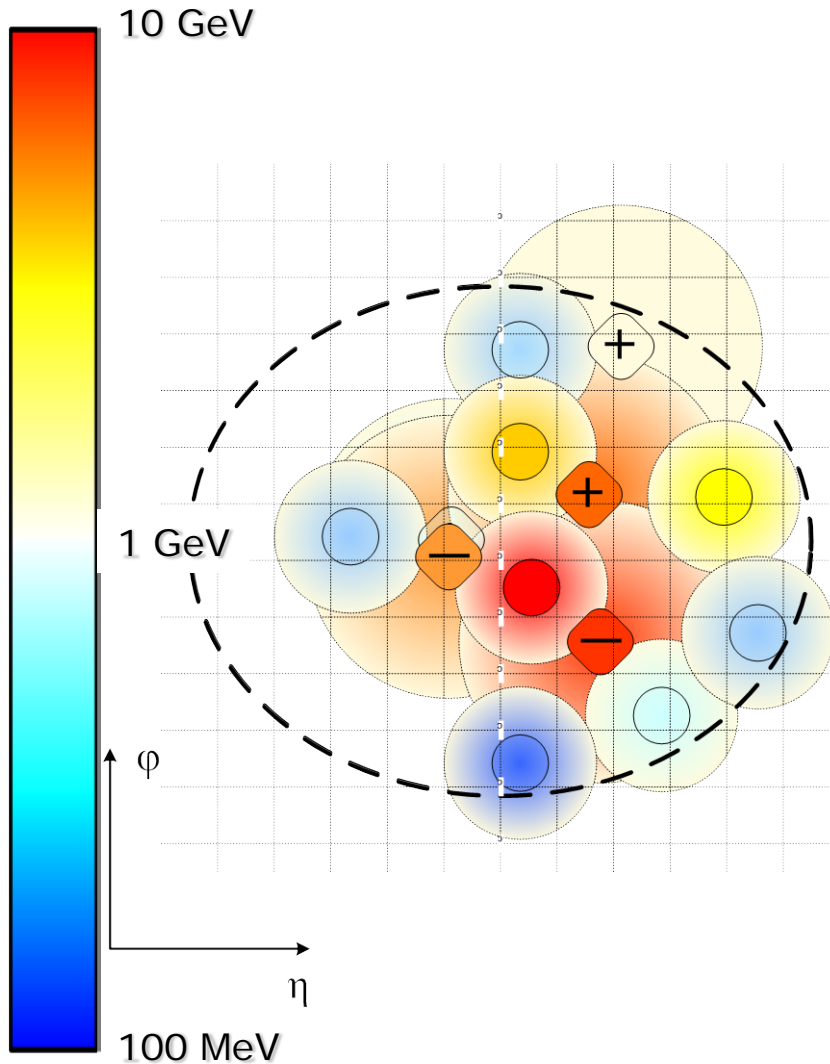
Total loss of soft charged particles in magnetic field

Partial and total energy loss of charged and neutral particles in inactive upstream material

Hadronic and electromagnetic cascades in calorimeters

Distribute energy spatially

Lateral particle shower overlap



Change of composition

Radiation and decay inside detector volume
 "Randomization" of original particle content

Defocusing changes shape in lab frame

Charged particles bend in solenoid field

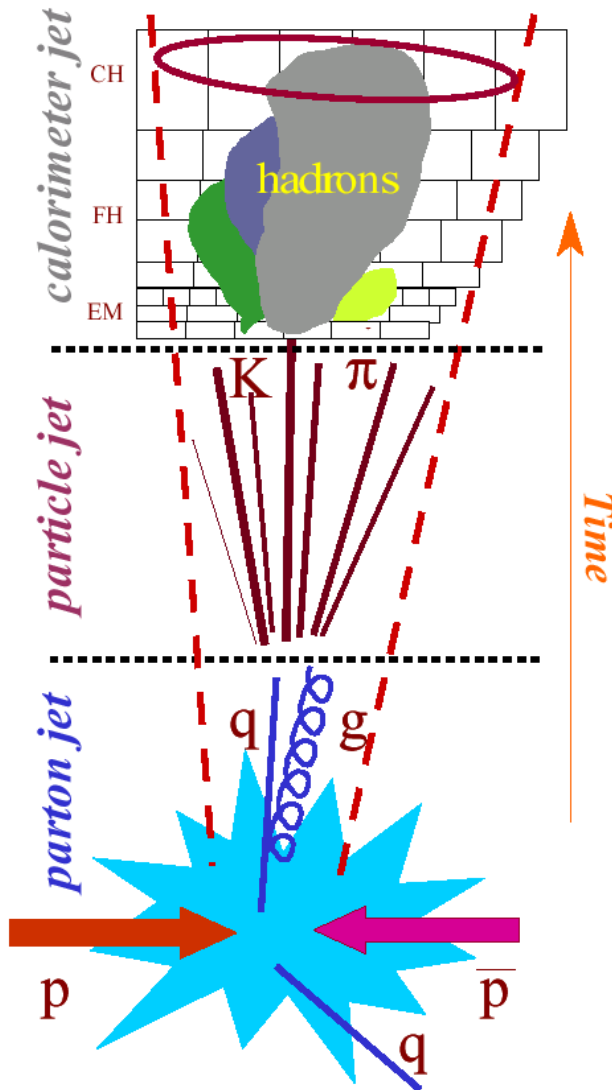
Attenuation changes energy

Total loss of soft charged particles in magnetic field
 Partial and total energy loss of charged and neutral particles in inactive upstream material

Hadronic and electromagnetic cascades in calorimeters

Distribute energy spatially
 Lateral particle shower overlap

Experiment ("Nature")



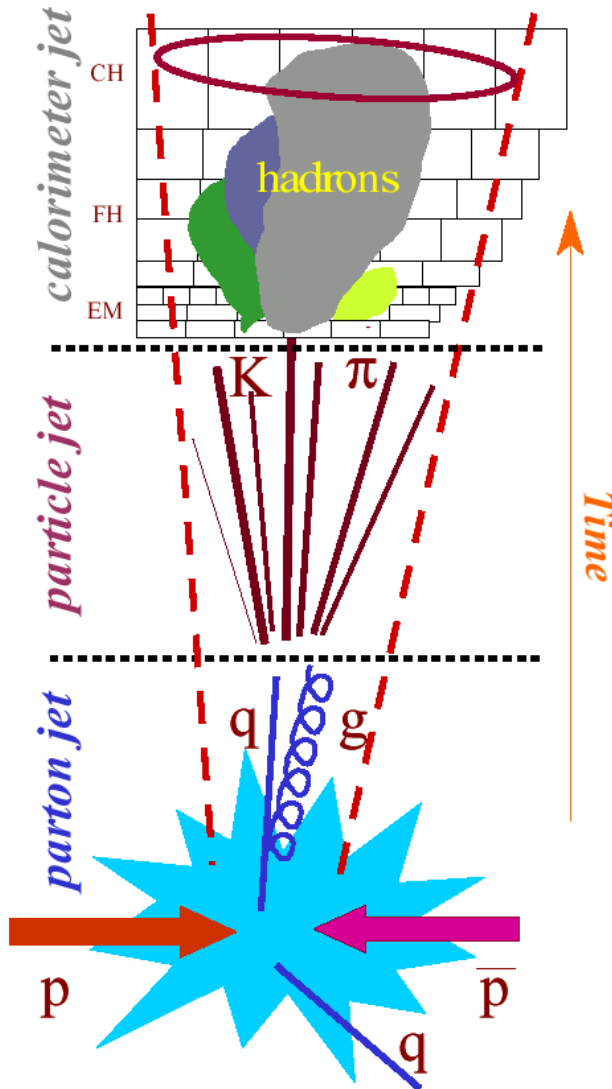
Jet Reconstruction Challenges

- longitudinal energy leakage
- detector signal inefficiencies (dead channels, HV...)
- pile-up noise from (off- and in-time) bunch crossings
- electronic noise
- calo signal definition (clustering, noise suppression...)
- dead material losses (front, cracks, transitions...)
- detector response characteristics ($e/h \neq 1$)
- jet reconstruction algorithm efficiency
- lost soft tracks due to magnetic field

- added tracks from underlying event
- added tracks from in-time (same trigger) pile-up event
- jet reconstruction algorithm efficiency

physics reaction of interest (interaction or parton level)

Experiment ("Nature")



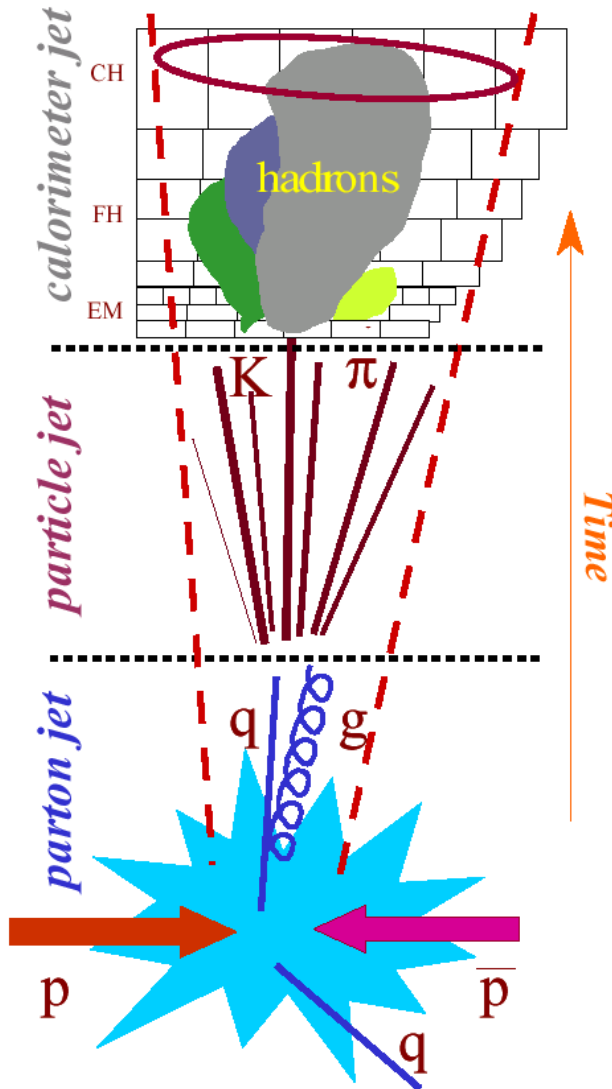
Jet Reconstruction Challenges

jet calibration task is to unfold all this to reconstruct the particle level jet driving the signals...

added tracks from underlying event
 added tracks from in-time (same trigger) pile-up event
 jet reconstruction algorithm efficiency

physics reaction of interest (interaction or parton level)

Experiment ("Nature")



Jet Reconstruction Challenges

jet calibration task is to unfold all this to reconstruct the particle level jet driving the signals...

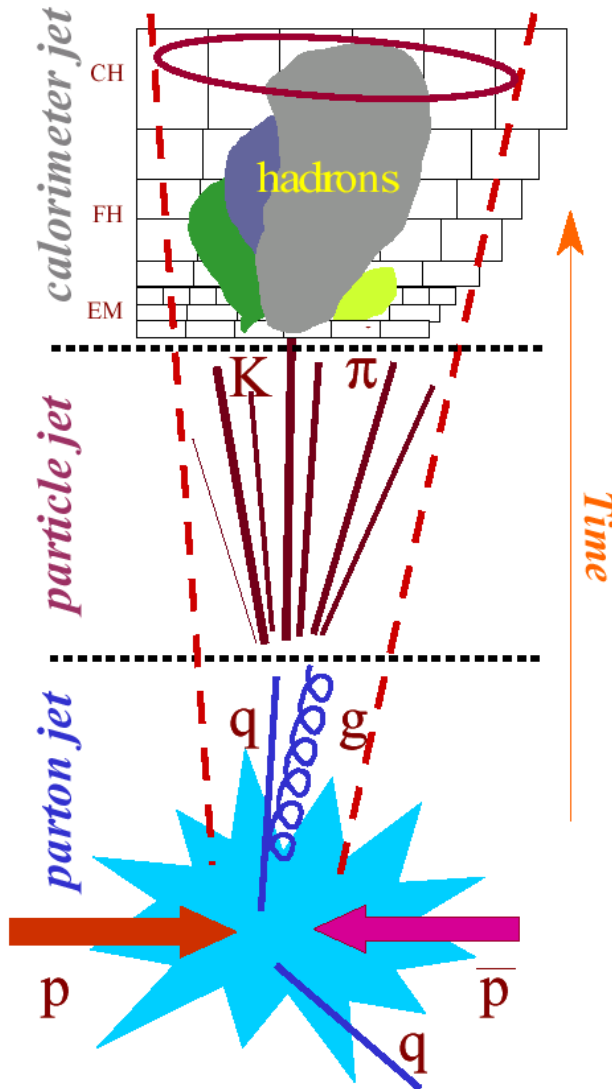
longitudinal energy leakage
detector signal efficiency (charge, photon, HV...)
pile-up noise from (on- and in-time) bunch crossings
careful signal definition (clustering, noise suppression...)
load motor pulses (from clocks, transitions...)
jet cone, crystal algorithm efficiency
lost soft tracks due to magnetic field

...modeling and calculations establish the link between particle and interaction level...

added tracks from in-time (same trigger) pile-up event
reconstruction efficiency

physics reaction of interest (interaction or parton level)

Experiment ("Nature")



Jet Reconstruction Challenges

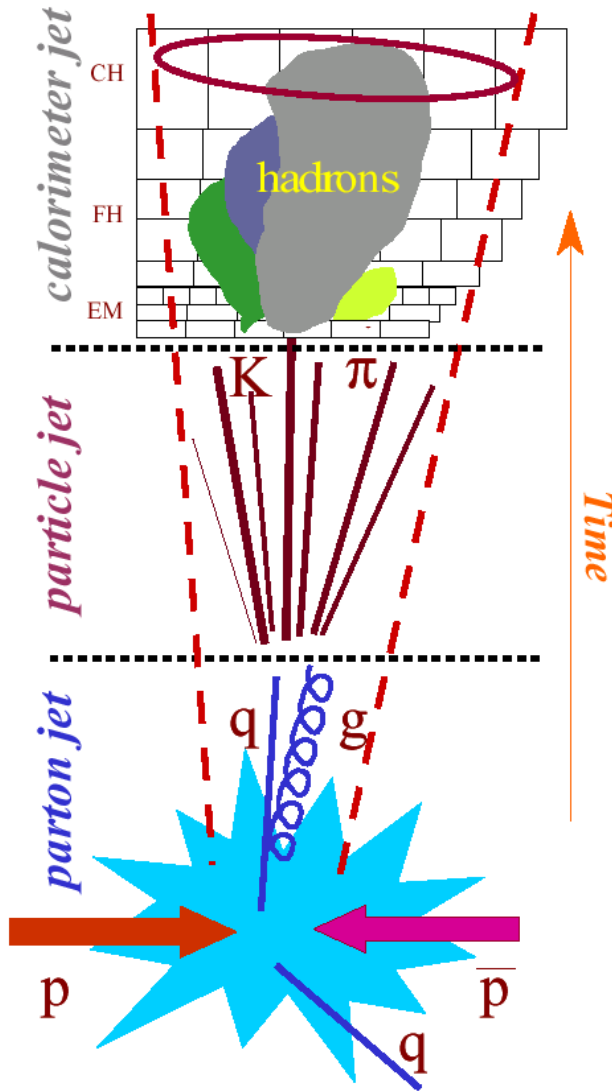
jet calibration task is to unfold all this to reconstruct the particle level jet driving the signals...

...modeling and calculations establish the link between particle and interaction level...

...but how is this really done?

physics reaction of interest (interaction or parton level)

Experiment ("Nature")



The experiment starts with the actual collision or the generator...

Triggered collision with signal parton collision, fragmentation & underlying event (**experiment**), or:
 Interaction level calculation with fragmentation and underlying event modeling (**simulations**)

... go to the particles in the simulation ...

Here particle level event represent the underlying interaction and the full complexity of the physics of the collision in the experiment

... collect the detector signals ...

From the readout (**experiment**), or:

Take the stable (observable) particles and simulate the signals in the detector (e.g., the calorimeter and tracking detector)(**simulations**)

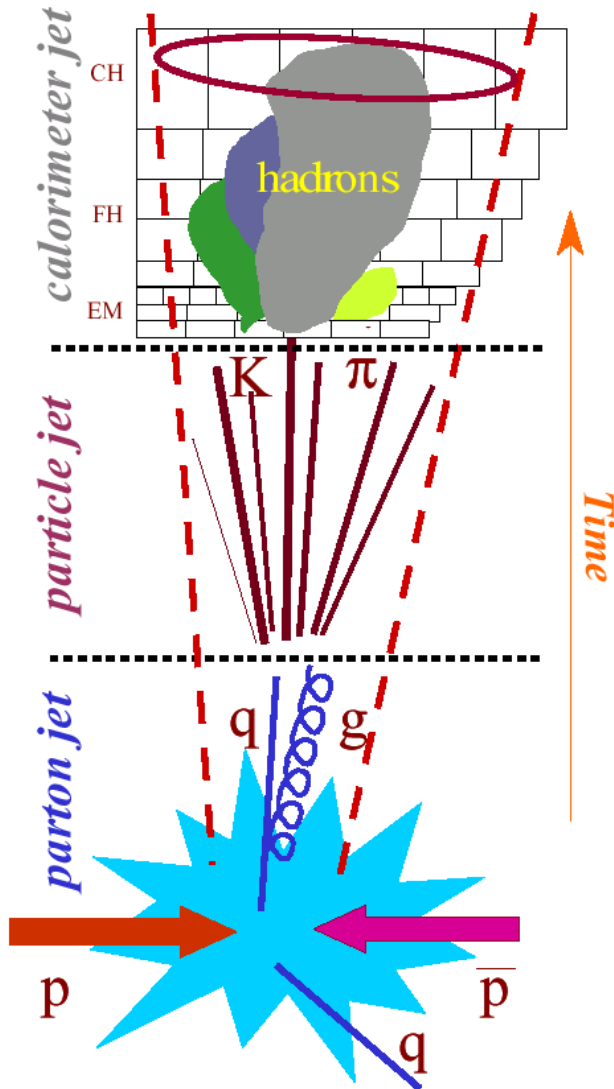
... and compare them!

Complex – need to include all experimental biases like event selection (trigger bias), topology and detector inefficiencies

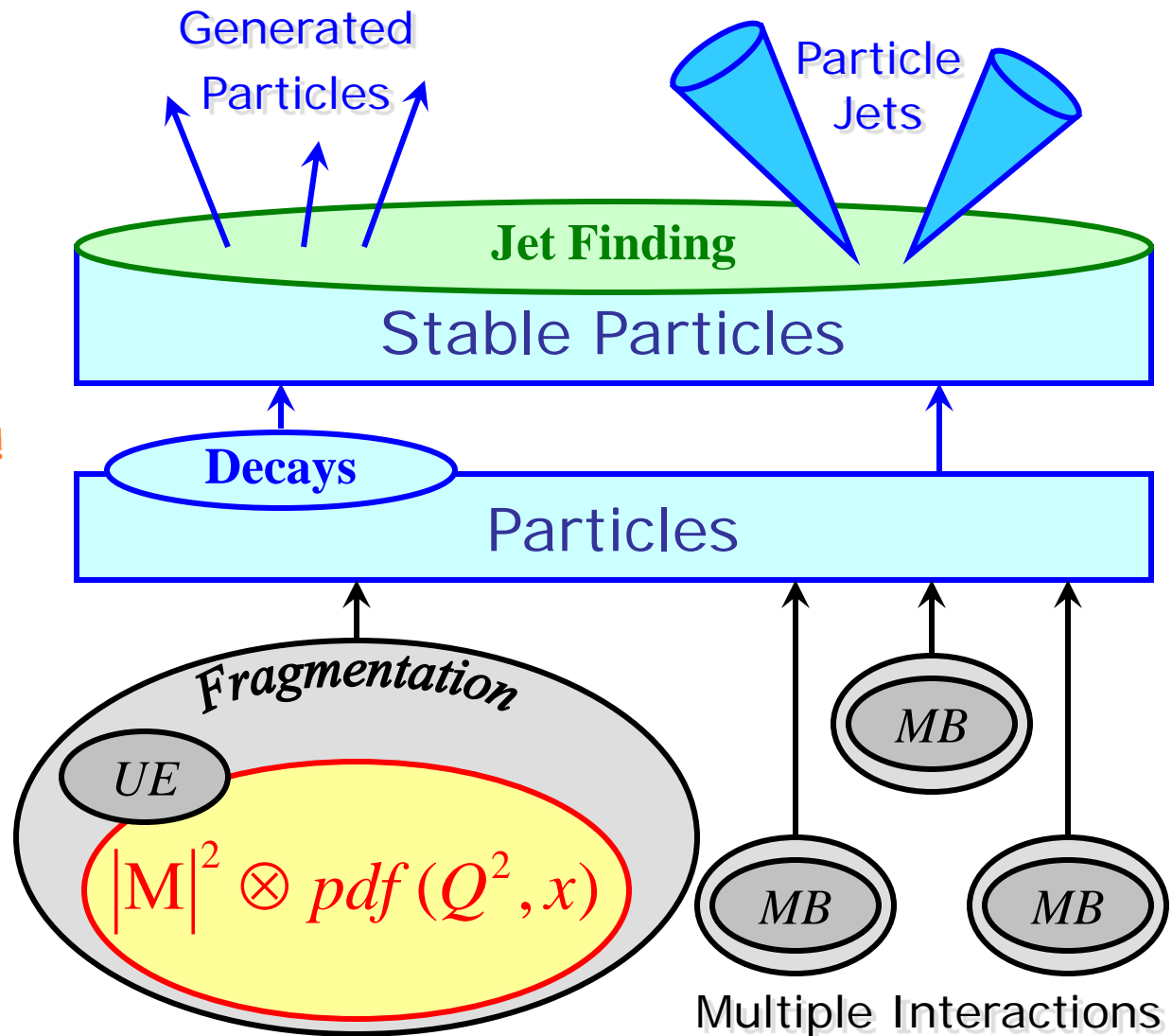
This establishes particle jet references for the detector jets!

Of course only in a statistical sense, i.e. at the level of distributions!

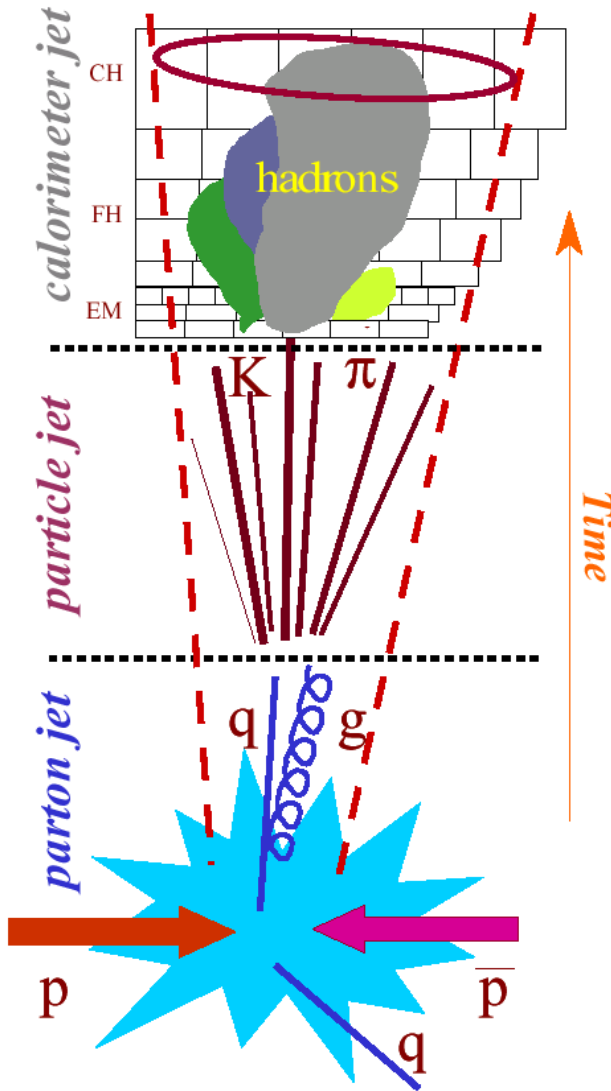
Experiment ("Nature")



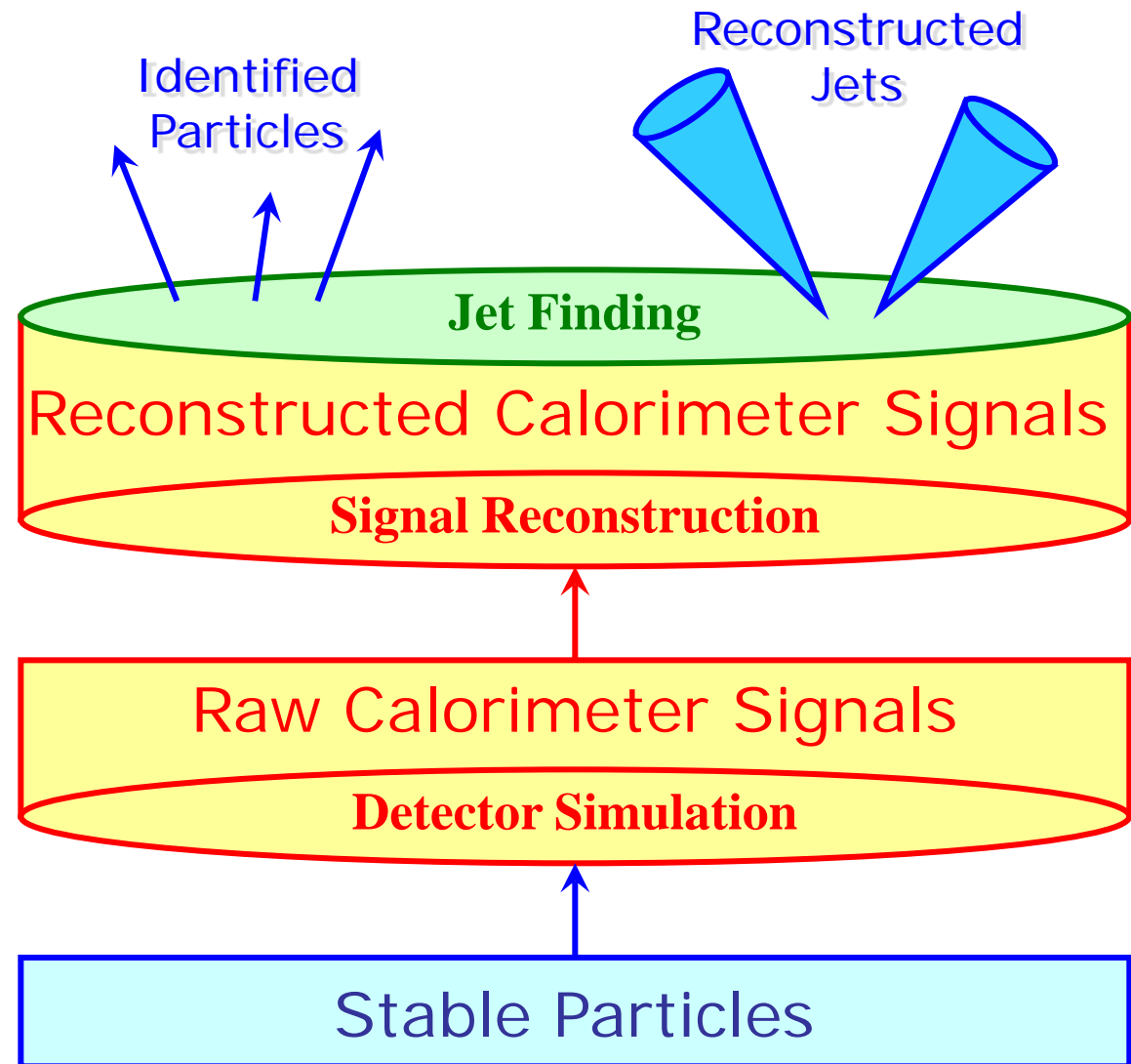
Modeling Particle Jets



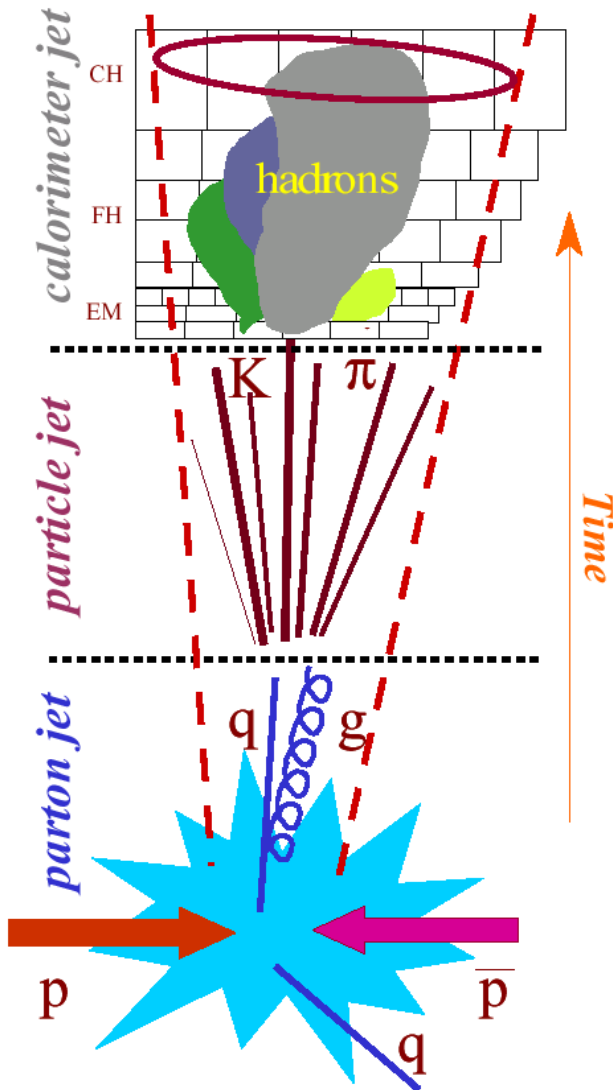
Experiment ("Nature")



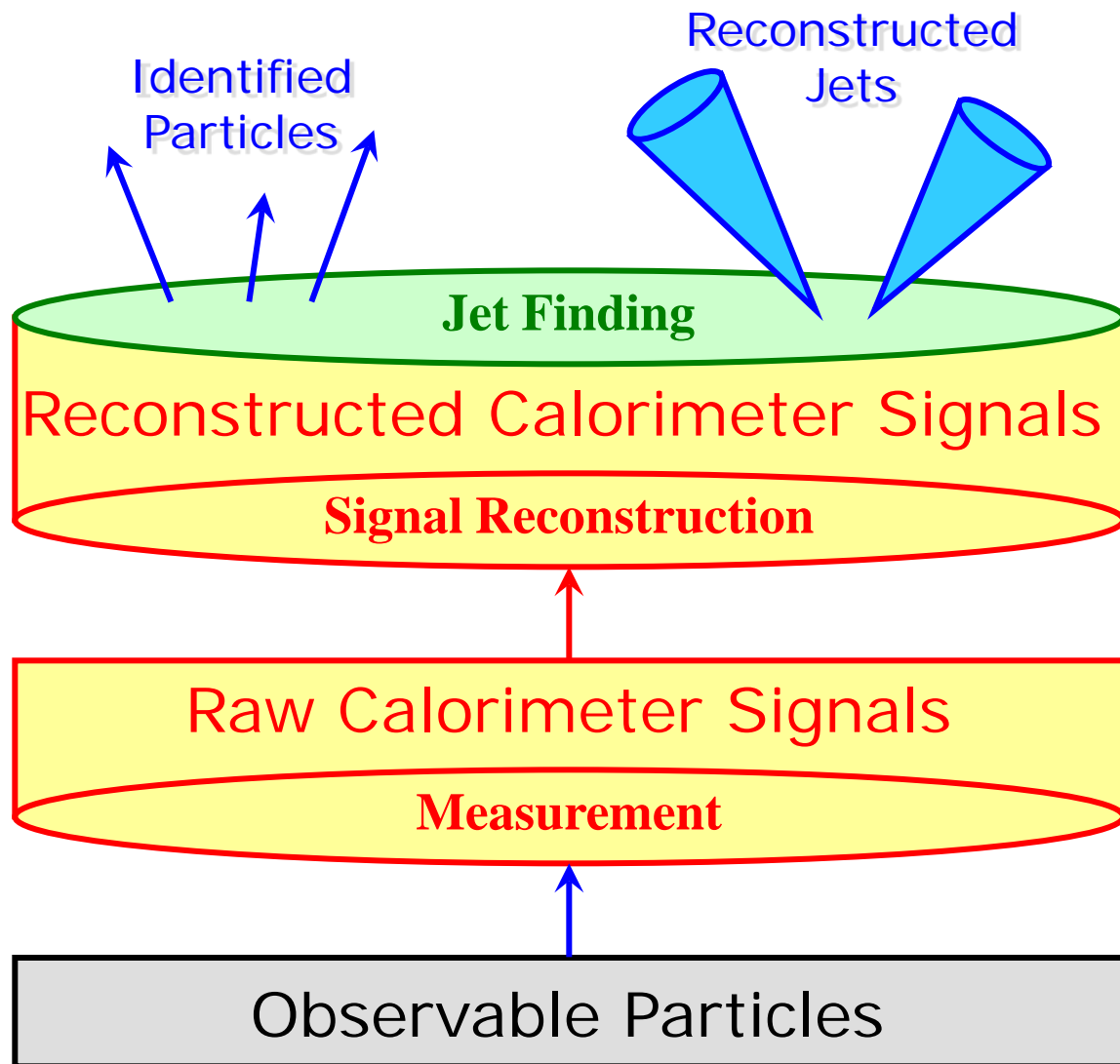
Modeling Calorimeter Jets



Experiment ("Nature")



Measuring Calorimeter Jets



What is jet calibration?

Straight forward: attempt to reconstruct a measured jet such that its final four-momentum is close to the true jet kinematics generating the signal

Why is it needed?

Could compare simulated and measured calorimeter signals at any scale and deduct the true kinematics from the corresponding particle jet in simulation

Remember energy scales in calorimeters?

But need to reconstruct **any** jet in the experiment

Even (or especially) the ones in events we have not simulated – which probably means new physics?

To understand these events the best measurement of the true jet independent of the availability of simulations for this specific event – no simulation bias allowed in general!

Can we calibrated without simulations at all?

Complex physics and detector environment – hard to avoid simulations for precision reconstruction!

But there are **in-situ** jet calibrations (more at another time from a special guest speaker!)

So jet reconstruction needs to include a calibration

Use a simulated calibration sample representing simple final state

Chose a somewhat understood Standard Model topology like QCD di-jets

Calibrate using measurable jet features

Establish functions using jet observables as parameters to calibrate calorimeter jets from a basic scale to the final jet energy scale

If done right, simulation biases can be reduced, especially concerning the correct simulation of the event topology

Understand the limitations (systematic error) in the context of the analysis

All this is the global subject of the remaining lectures!



Any jet calibration needs to be validated

First step is the initial **closure test** – apply the calibration to the same samples which were used to extract it

Residual (average) deviations from the expected or true jet energy should be small – can be considered a first input to the systematic error!

Then apply calibration to jets in other topologies/physics channels and measure deviation from expected kinematics – this is the **validation**

Often done with simulated physics as they have an intrinsic truth reference (particle jets)

Samples with widely different topology than calibration sample preferred, possibly even several topologies

Understanding biases introduced in any given procedure is part of the validation

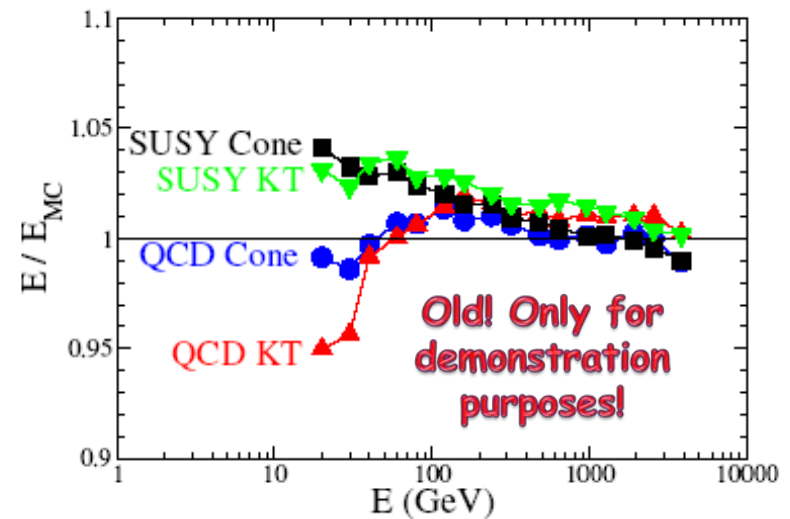
Need to develop calibrations with least biases

Biases can be introduced by the use of simulations – physics model limitations, inappropriate calorimeter shower simulations and signal extraction modeling, ...

Also experimental biases due to trigger and event selections changing shapes of distributions etc. – more later!

Need to understand if small or hidden biases in calibration sample and chosen calibration model do not increase for other topologies

Calorimeter signal definition can introduce biases due to different sensitivities to noise, jet shape reconstruction, ...



Some obvious procedural requirements

Need the same signal treatment in data and simulation

Including the same jet finder and jet finder configuration

Need to understand the detector data very well

Need to unfold all signal extraction inefficiencies and any detector problem

Can be done by including those into the simulated signal reconstruction (e.g. noise) or by developing corrections for the experimental data

Need to understand the detector simulation very well

Signal defining electromagnetic and hadronic shower features need to be reproduced to highest possible precision

Jet reconstruction validation

Compare basic performance measures for data and simulation

Signal linearity, relative energy resolution, jet shapes...

Level of comparison is good estimate for systematic error of a given reconstruction and calibration

Assumes that simulation reflects state-of-art understanding of physics and detector

Lack of understanding (data is the “truth”) then reflects measurement error

Ok, but...

Still have not told you **how** simulation based jet calibration is really done!

Like to lay down the ground rules first!



Need to have another look at the calorimeter

Basically all calorimeters at collider experiments show some level of non-compensation

For sure the ones in ATLAS and CMS are!

Needs to be corrected for jet calibration

And all other hadronic final state contributions like isolated hadrons, tau-leptons, and low p_T hadronic signals

Can this be done for highest spatial calorimeter granularity (cells)?

Not easy to see – individual cell signal without any other context hard to calibrate in non-compensating calorimeters

Better to establish a larger context first to find out which calibration the calorimeter cell signal needs

Reconstructed jet itself – in ATLAS this is called **Global Calibration**

Topological cell clusters without jet context – in ATLAS this is called **Local Calibration**

Cannot recommend to use cells directly to find jets:

High multiplicity on input for jet finders

Negative signal treatment required for four-momentum recombination

Noise can create $E < 0$ in cells

Jets should consist of significant (relevant) signal objects

Cell signal not a good image of the particle flow in jets

Larger calorimeter signal objects clearly preferred

Towers of cells – add cell signal up in projective calorimeter towers

Topological **clusters** of cells – add cell signals following signal correlations in showers



Impose a regular grid view on event

$$\Delta\eta \times \Delta\phi = 0.1 \times 0.1 \text{ grid}$$

Motivated by particle E_t flow in hadron-hadron collisions

Well suited for trigger purposes

Collect cells into tower grid

Cells signals can be summed with geometrical weights

Depend on cell area containment ratio

Weight = 1 for projective cells of equal or smaller than tower size

Summing can be selective

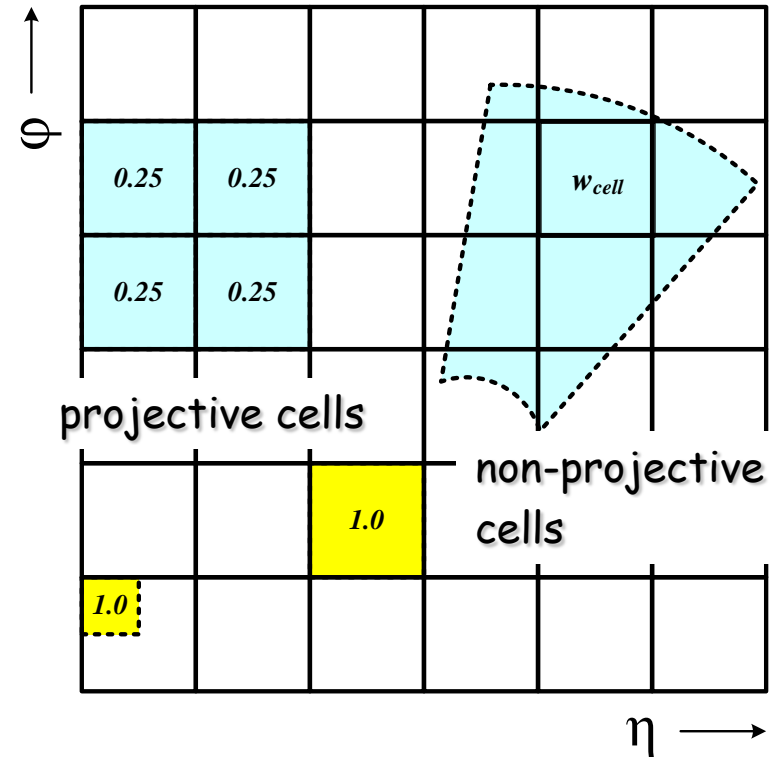
Noise filter can be applied!

Towers have massless four-momentum representation

Fixed direction given by geometrical grid center

$$(E_{\eta\phi}, \eta, \phi) \mapsto (E = p, p_x, p_y, p_z)$$

$$p = \sqrt{p_x^2 + p_y^2 + p_z^2}$$



$$E_{\eta\phi} = \sum_{(A_{\text{cell}}^{\eta\phi} \cap A_{\eta\phi}) \neq 0} w_{\text{cell}} E_{\text{cell}}$$

$$w_{\text{cell}} = \begin{cases} 1 & \text{if } A_{\text{cell}}^{\eta\phi} \leq \Delta\eta \times \Delta\phi \\ < 1 & \text{if } A_{\text{cell}}^{\eta\phi} > \Delta\eta \times \Delta\phi \end{cases}$$



Introduction to Hadronic Final State Reconstruction in Collider Experiments (Part X)

Peter Loch
University of Arizona
Tucson, Arizona
USA



Need to have another look at the calorimeter

Basically all calorimeters at collider experiments show some level of non-compensation

For sure the ones in ATLAS and CMS are!

Needs to be corrected for jet calibration

And all other hadronic final state contributions like isolated hadrons, tau-leptons, and low p_T hadronic signals

Can this be done for highest spatial calorimeter granularity (cells)?

Not easy to see – individual cell signal without any other context hard to calibrate in non-compensating calorimeters

Better to establish a larger context first to find out which calibration the calorimeter cell signal needs

Reconstructed jet itself – in ATLAS this is called **Global Calibration**

Topological cell clusters without jet context – in ATLAS this is called **Local Calibration**

Cannot recommend to use cells directly to find jets:

High multiplicity on input for jet finders

Negative signal treatment required for four-momentum recombination

Noise can create $E < 0$ in cells

Jets should consist of significant (relevant) signal objects

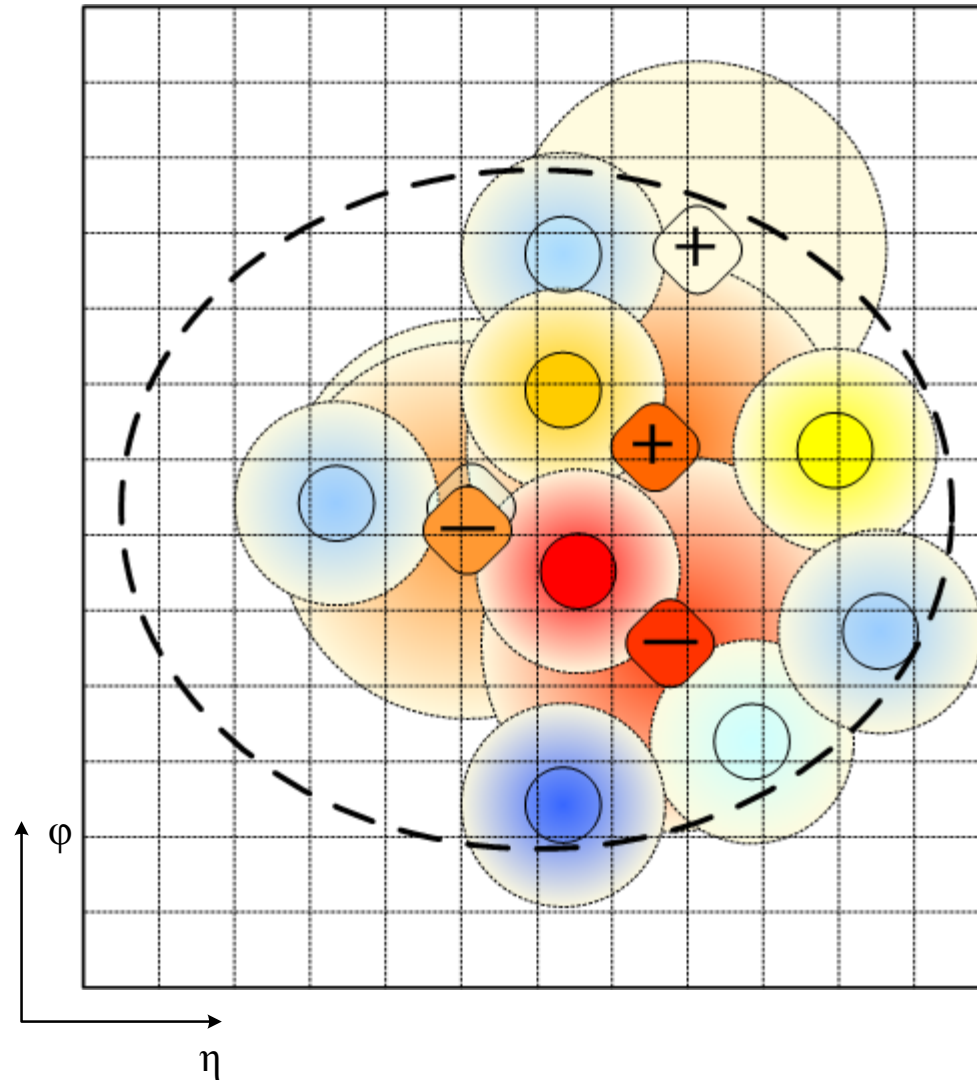
Cell signal not a good image of the particle flow in jets

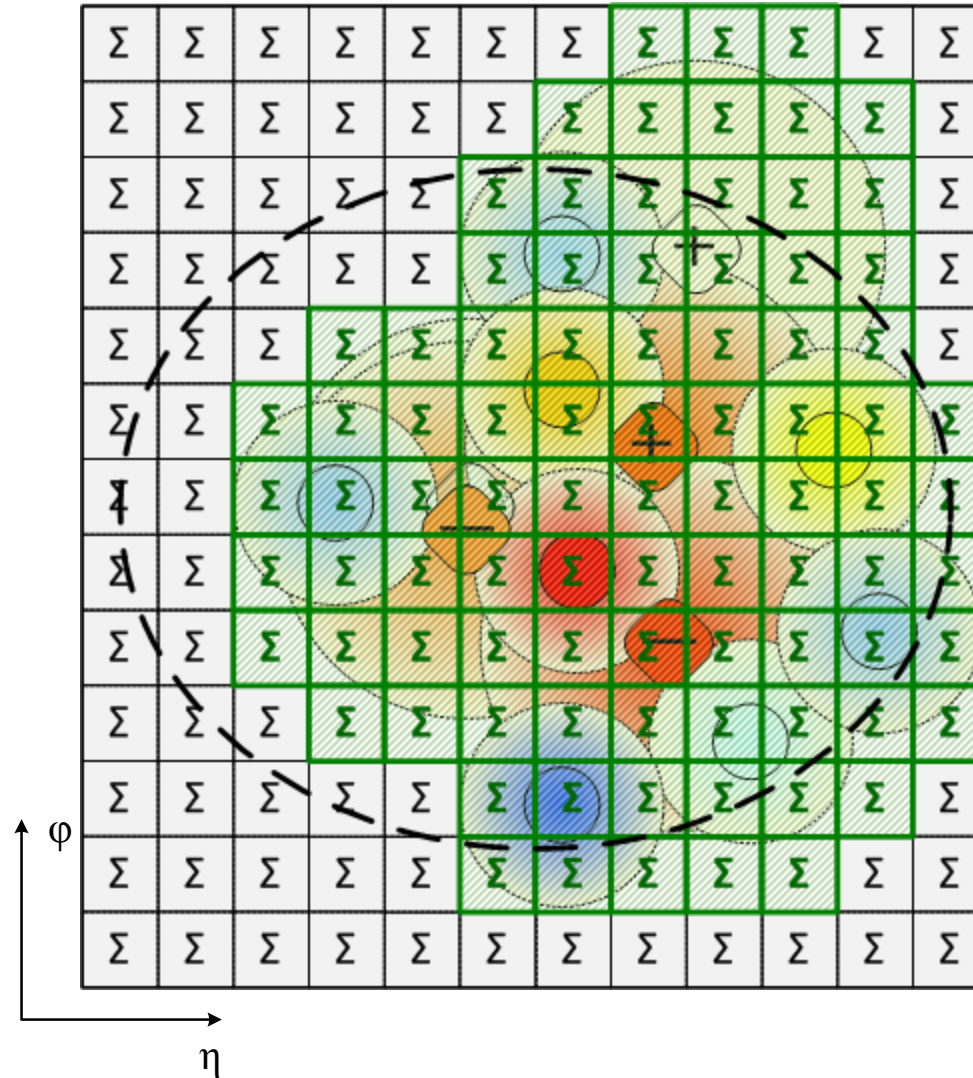
Larger calorimeter signal objects clearly preferred

Towers of cells – add cell signal up in projective calorimeter towers

Topological **clusters** of cells – add cell signals following signal correlations in showers







Impose a regular grid view on event

$$\Delta\eta \times \Delta\phi = 0.1 \times 0.1 \text{ grid}$$

Motivated by particle E_t flow in hadron-hadron collisions

Well suited for trigger purposes

Collect cells into tower grid

Cells signals can be summed with geometrical weights

Depend on cell area containment ratio

Weight = 1 for projective cells of equal or smaller than tower size

Summing can be selective

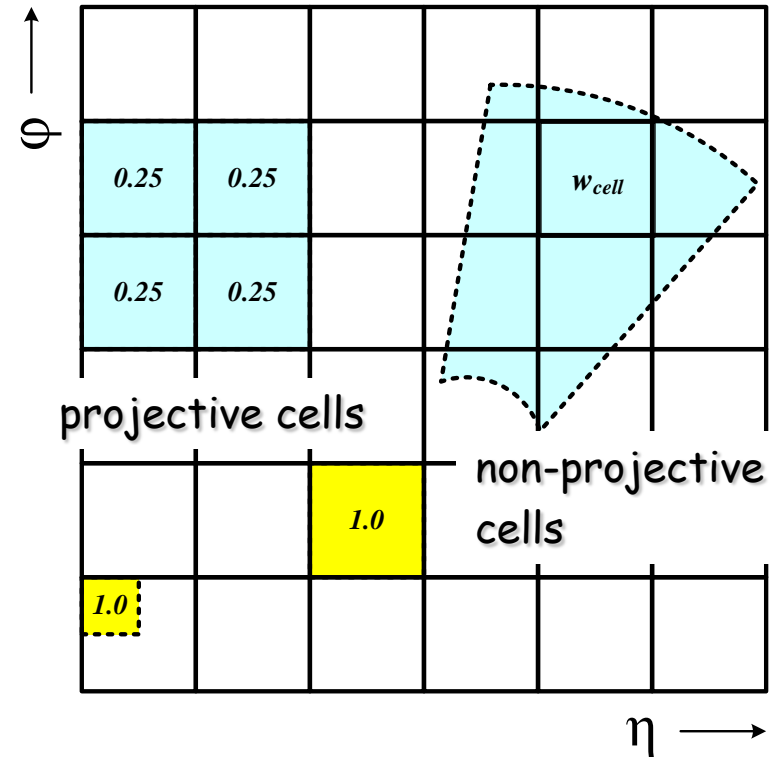
Noise filter can be applied to cell signals!

Towers have massless four-momentum representation

Fixed direction given by geometrical grid center

$$(E_{\eta\phi}, \eta, \phi) \mapsto (E = p, p_x, p_y, p_z)$$

$$p = \sqrt{p_x^2 + p_y^2 + p_z^2}$$



$$E_{\eta\phi} = \sum_{(A_{\text{cell}}^{\eta\phi} \cap A_{\eta\phi}) \neq 0} w_{\text{cell}} E_{\text{cell}}$$

$$w_{\text{cell}} = \begin{cases} 1 & \text{if } A_{\text{cell}}^{\eta\phi} \leq \Delta\eta \times \Delta\phi \\ < 1 & \text{if } A_{\text{cell}}^{\eta\phi} > \Delta\eta \times \Delta\phi \end{cases}$$



Signal integration

Towers represent longitudinally summed cell signals

2-dimensional signal objects

Can include partial and complete signals from several particles

Towers can preserve more detailed signal features

Associated information to be collected at tower formation

E.g., energy sharing in electromagnetic and hadronic calorimeters

Longitudinal signal center of gravity

Signal splitting

Towers can split signal from single particles

Hadronic shower width can be larger than tower bin, especially at higher pseudo-rapidity

Can cause problems with infrared safety

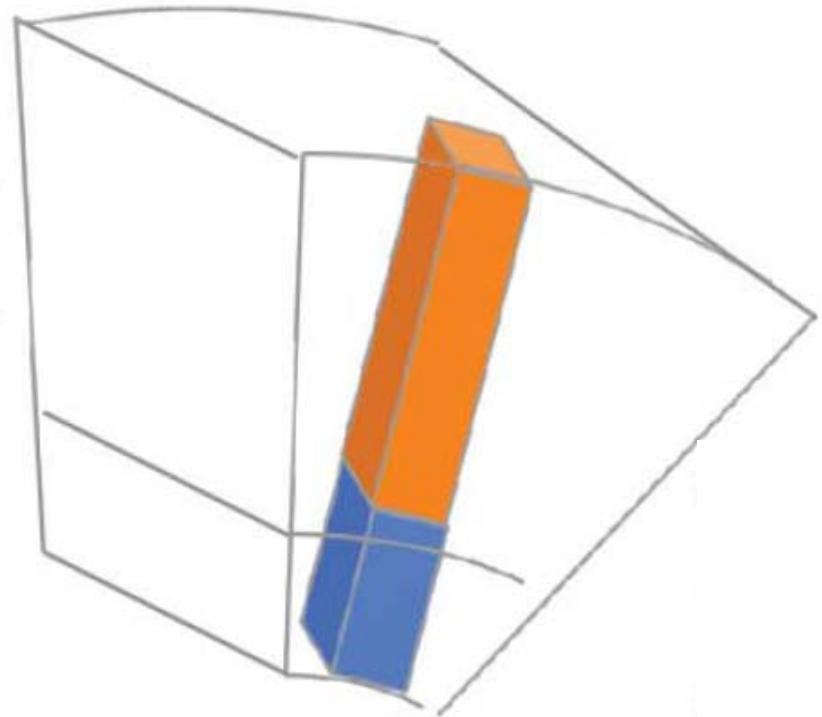
Can cause problems for seeded jet finders

Collateral instability

Can lead to lost signals cone-like jets

Energy in tower bins outside of jet can belong to particle signal in jet

(drawing by K. Perez, Columbia University)



Unbiased calorimeter tower is a "slab" of energy in a regular pseudorapidity-azimuth grid (each tower covers the same area in these coordinates)



Collect cell into energy “blobs”

Idea is to collect all cell signals belonging to a given particle into one cluster of cells

Basically reconstruct the shower for each particle entering the calorimeter

Needs algorithm to form energy blobs at the location of the shower signal in the calorimeter

Follow the shower-induced cell signal correlations

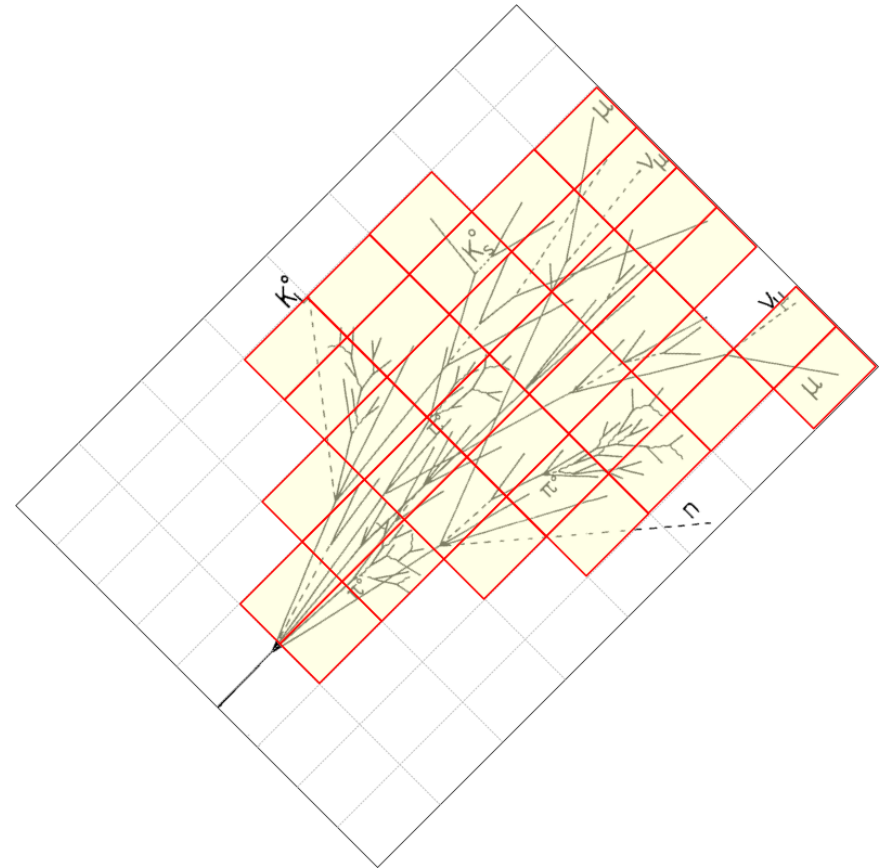
Extract most significant signal from all calorimeter cells

Cluster formation uses signal significance as guidance

Not the total signal – noise changes from calorimeter region to calorimeter region

Implicit noise suppression in cluster formation

Cluster signals should include least amount of noise



Collect cell into energy “blobs”

Idea is to collect all cell signals belonging to a given particle into one cluster of cells

Basically reconstruct the shower for each particle entering the calorimeter

Needs algorithm to form energy blobs at the location of the shower signal in the calorimeter

Follow the shower-induced cell signal correlations

Extract most significant signal from all calorimeter cells

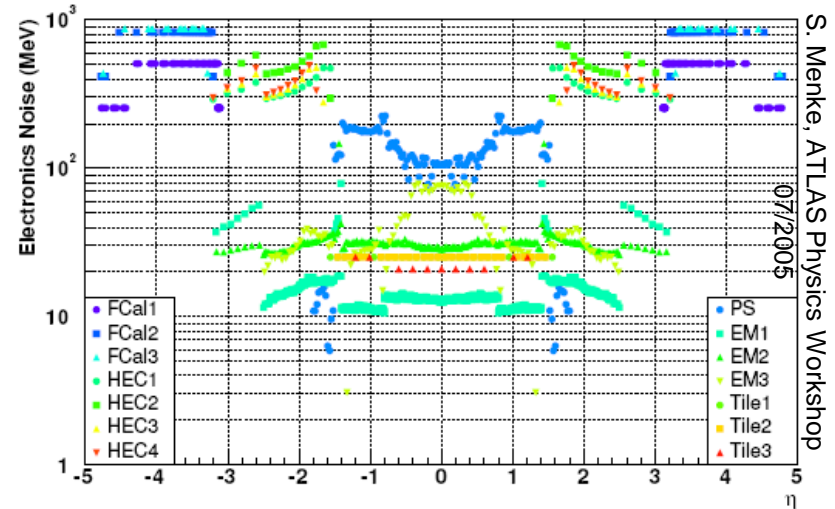
Cluster formation uses signal significance as guidance

Not the total signal – noise changes from calorimeter region to calorimeter region

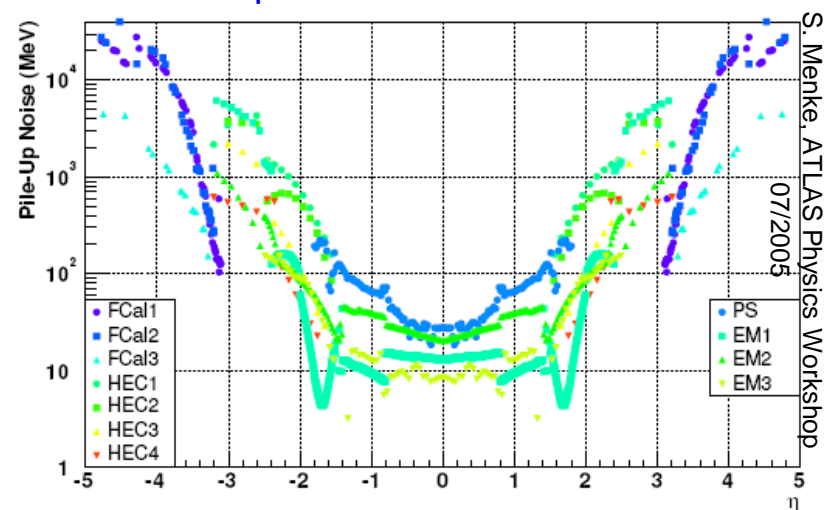
Implicit noise suppression in cluster formation

Cluster signals should include least amount of noise

Electronic Noise in Calorimeter Cells



Pile-Up Noise in Calorimeter Cells



Cluster seeding

Defined by signal significance above primary threshold

Cells above this threshold can seed cluster

Cluster growth

Defined by signal significance above secondary threshold

Cells neighbouring seeds with significance above this threshold drive cluster growths

Cluster signal

Defined by cells with significance above basic threshold

Cells to be considered in cluster energy sums

Use of negative signal cells

Thresholds are considered for the absolute (unsigned) signal magnitude

Large negative signals can seed and grow clusters

Parameters for each stage optimized with testbeam data

Experimental single pion shower shapes guide cluster algorithm development
Clean tuning reference!

Primary threshold

$$\left| \frac{E_{\text{cell}}}{\sigma_{\text{cell}}} \right| > S, \text{ default } S = 4$$

Secondary threshold

$$\left| \frac{E_{\text{cell}}}{\sigma_{\text{cell}}} \right| > N, \text{ default } N = 2$$

Collecting

$$\left| \frac{E_{\text{cell}}}{\sigma_{\text{cell}}} \right| > P, \text{ default}$$

$$P = 2$$

(note $S \geq N \geq P$)

Famous "4/2/0" clustering in ATLAS



Cluster seeding

Defined by signal significance above primary threshold

Cells above this threshold can seed cluster

Cluster growth control

Defined by signal significance above secondary threshold

Cells neighbouring seeds with significance above this threshold drive cluster growths

Cluster signal

Defined by cells with significance above basic threshold

Cells to be considered in cluster energy sums

Use of negative signal cells

Thresholds are considered for the absolute (unsigned) signal magnitude

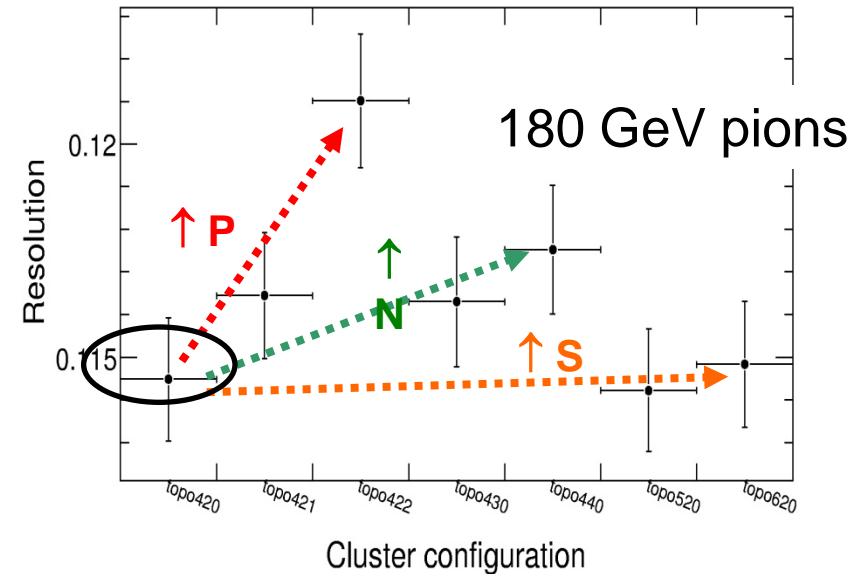
Large negative signals can seed and grow clusters

Parameters for each stage optimized with testbeam data

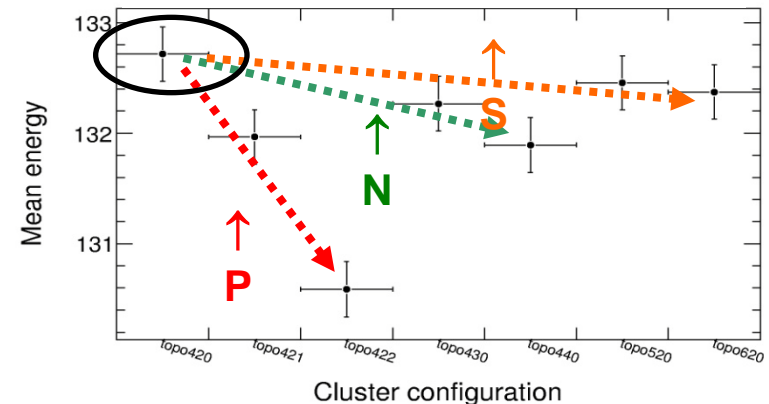
Experimental single pion shower shapes guide cluster algorithm development

Clean tuning reference!

Resolution of Sum E_{clus}

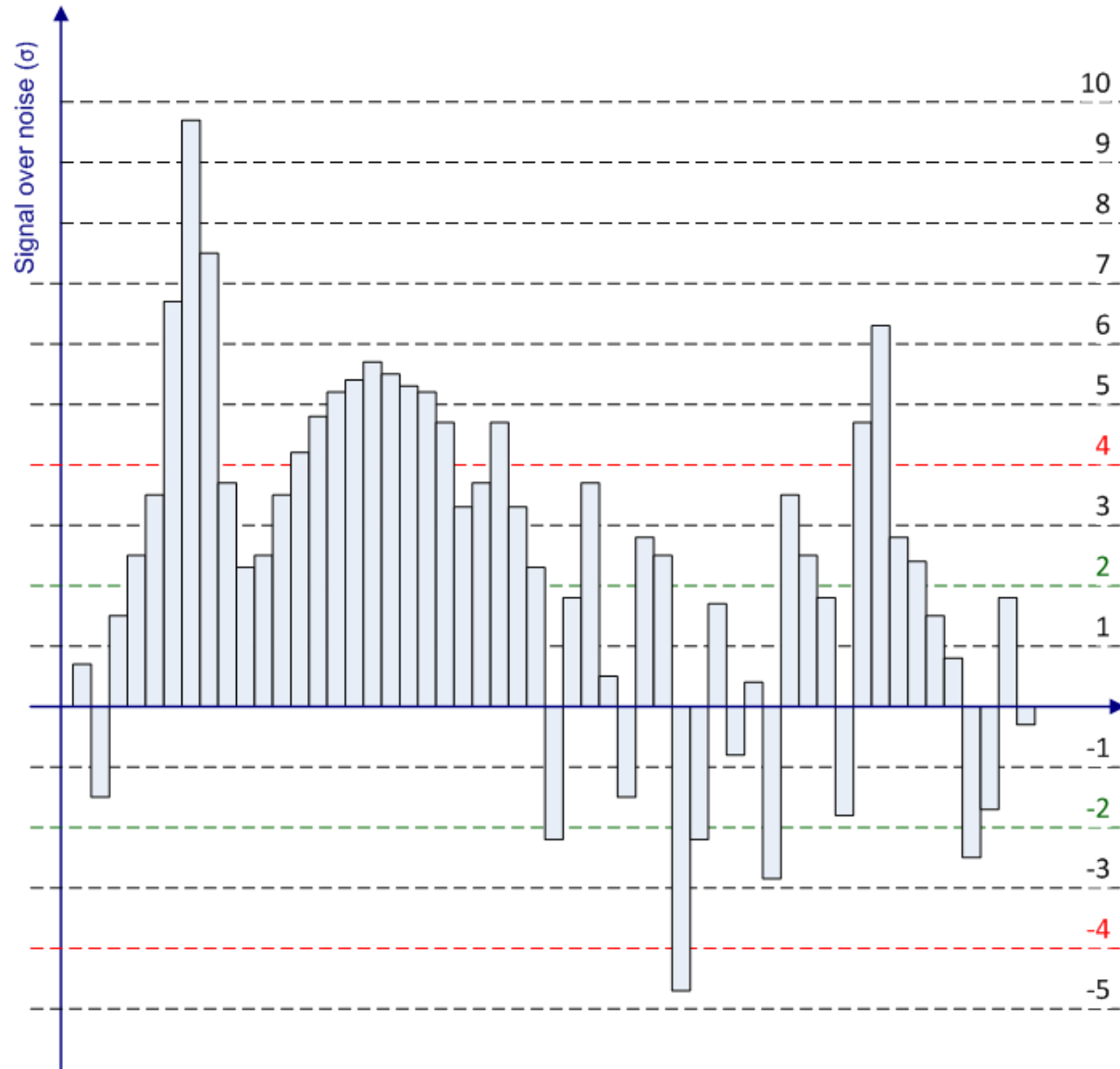


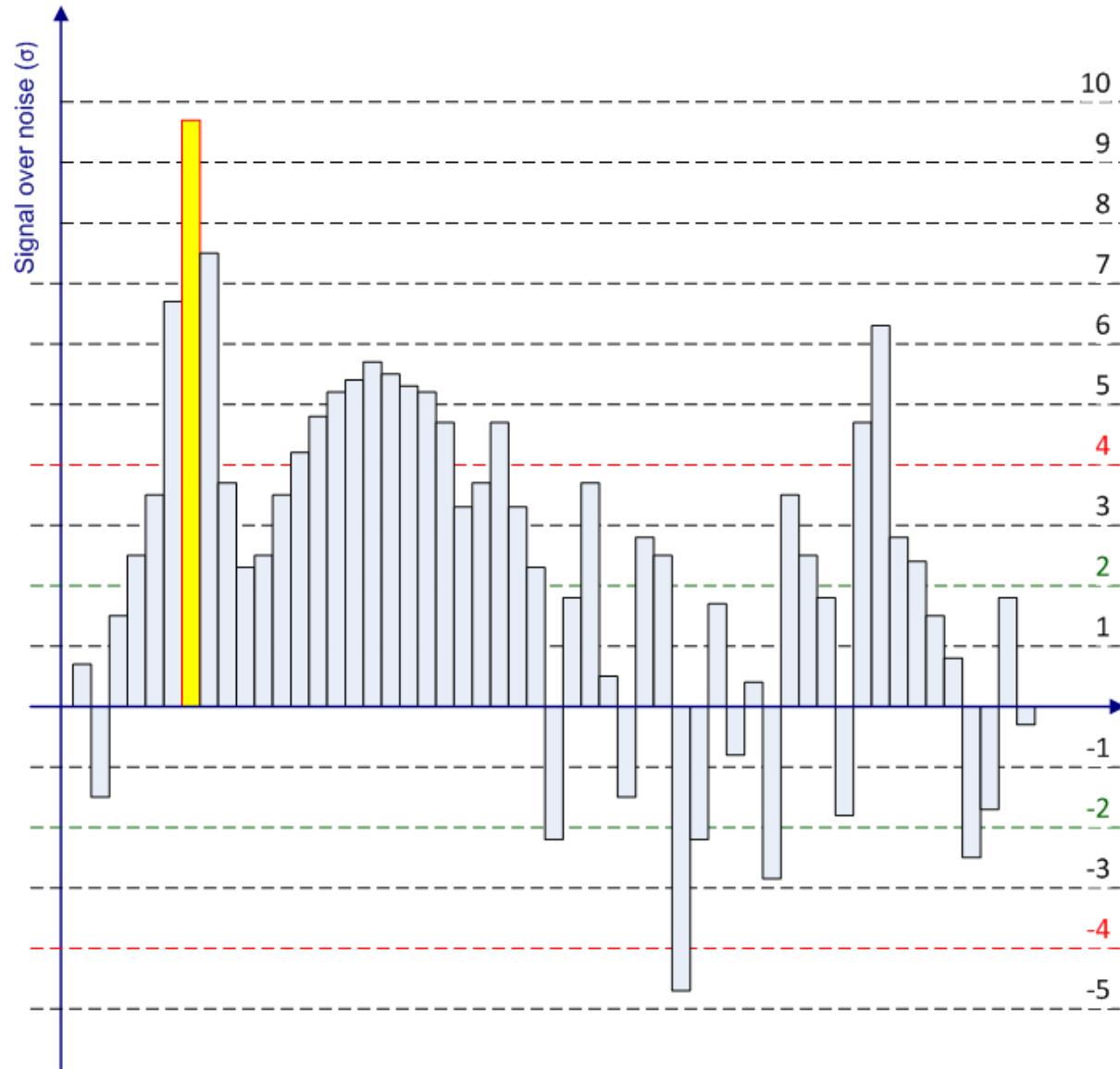
Mean of Sum E_{clus}

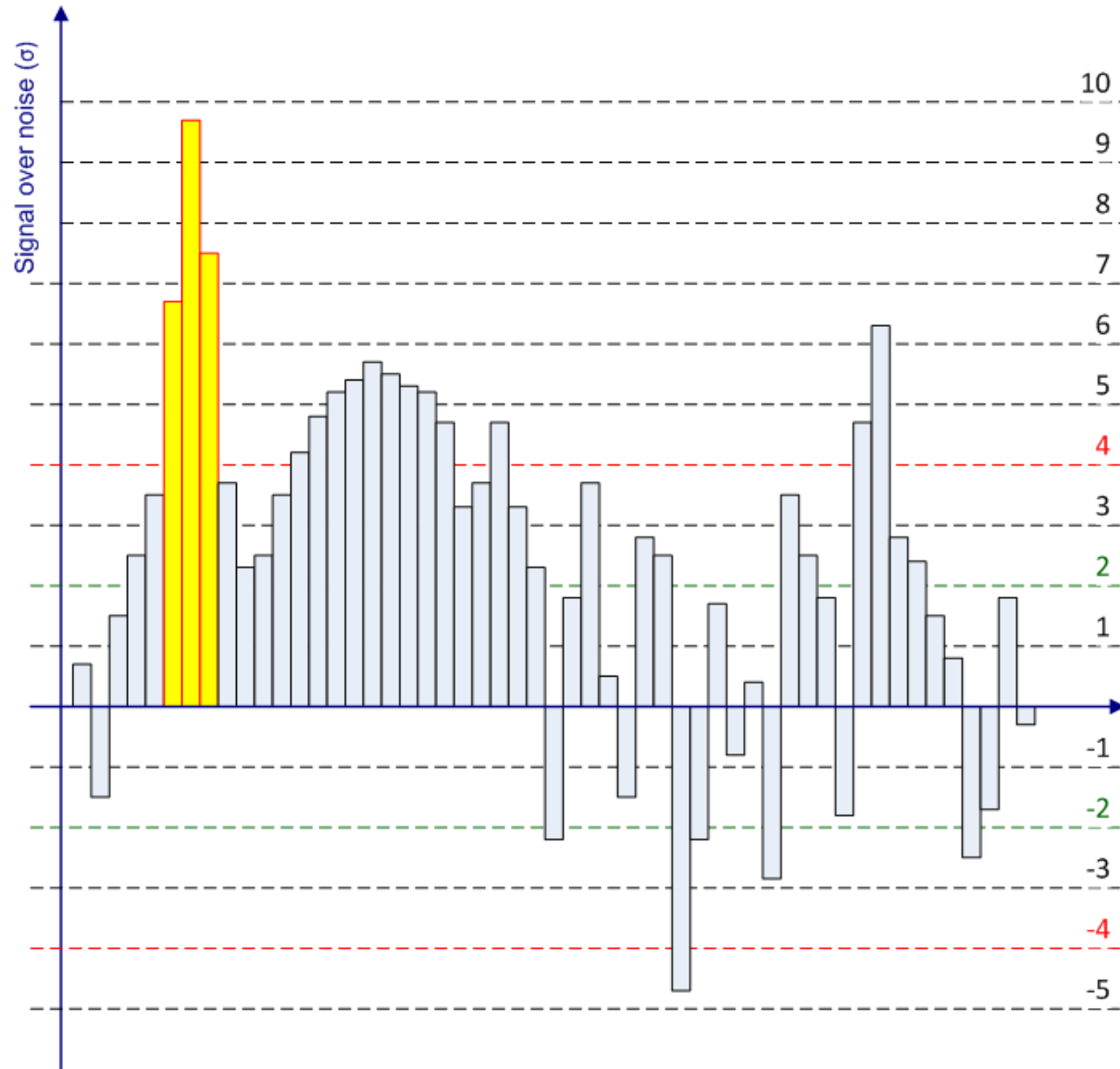


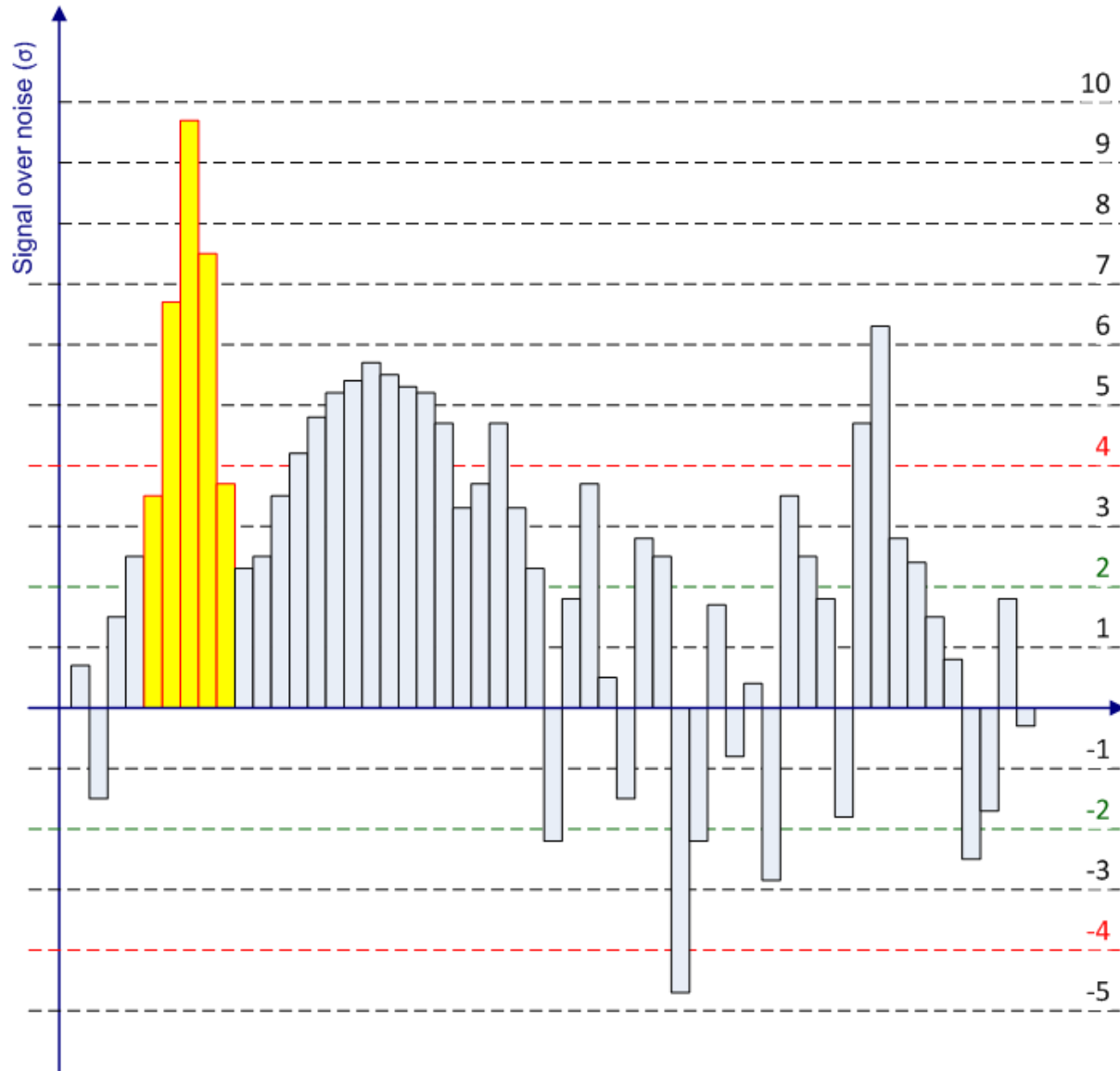
1. Find cell with most significant seed over primary threshold S
2. Collect all cells with significance above basic threshold P
 - Consider neighbours in three dimensions
 - Defined by (partly) shared area, (partly) shared edge, or shared corner point
 - E.g., 26 neighbours for perfectly cubed volumes of equal size
 - Neighbours can be in other calorimeter regions or even other calorimeter sub-systems
 - Granularity change to be considered in neighbouring definition
3. For all cells neighbouring seeds with signal significance above secondary threshold N , collect neighbours of neighbours if their signal significance is above P
 - Same rules as for collection around primary seed
4. Continue until cluster does not grow anymore
 - Automatically generate “guard ring” of small signal cells at cluster margin
 - In three dimensions, of course
5. Take next not yet used seed cell and collect next cluster

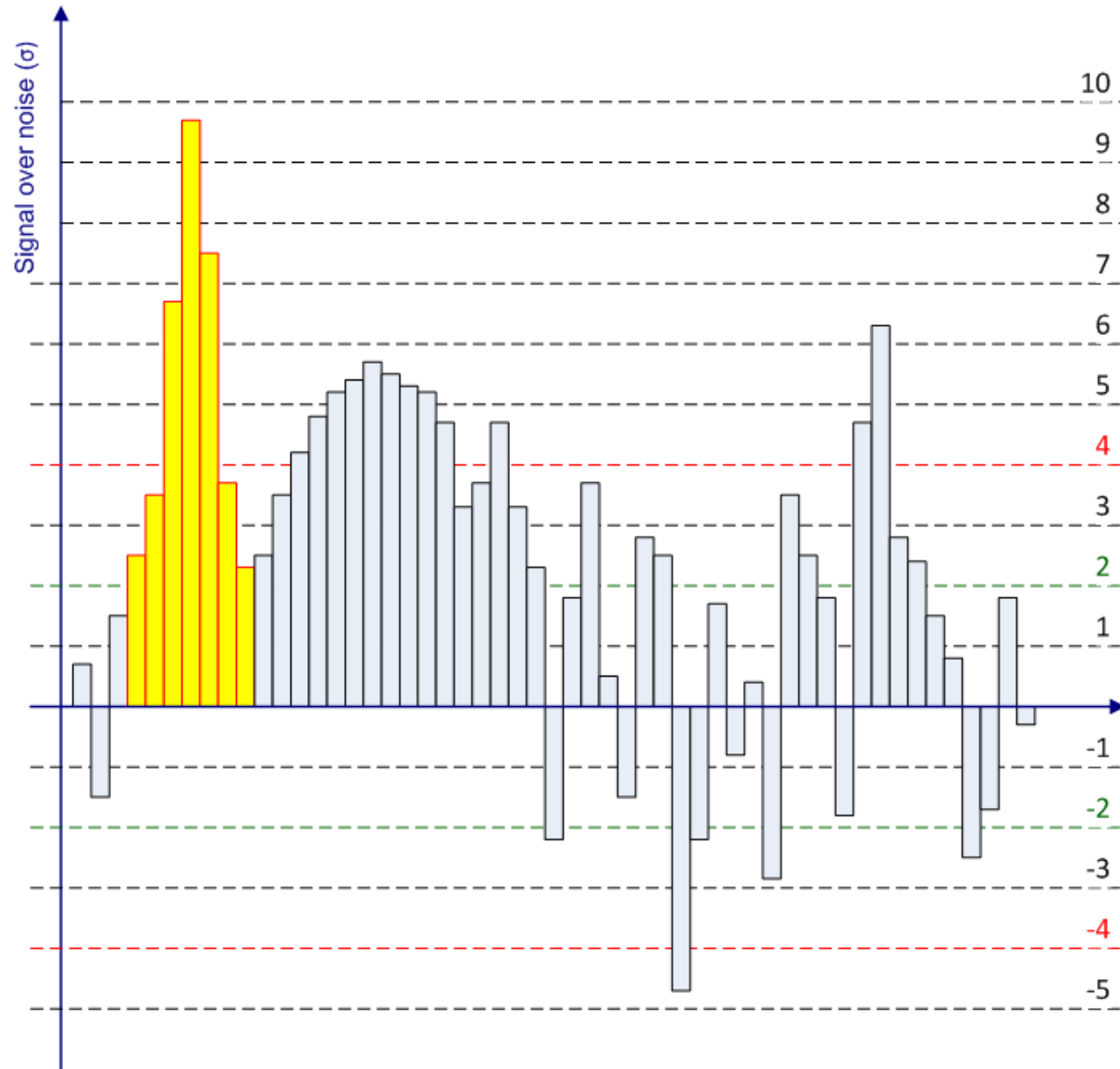


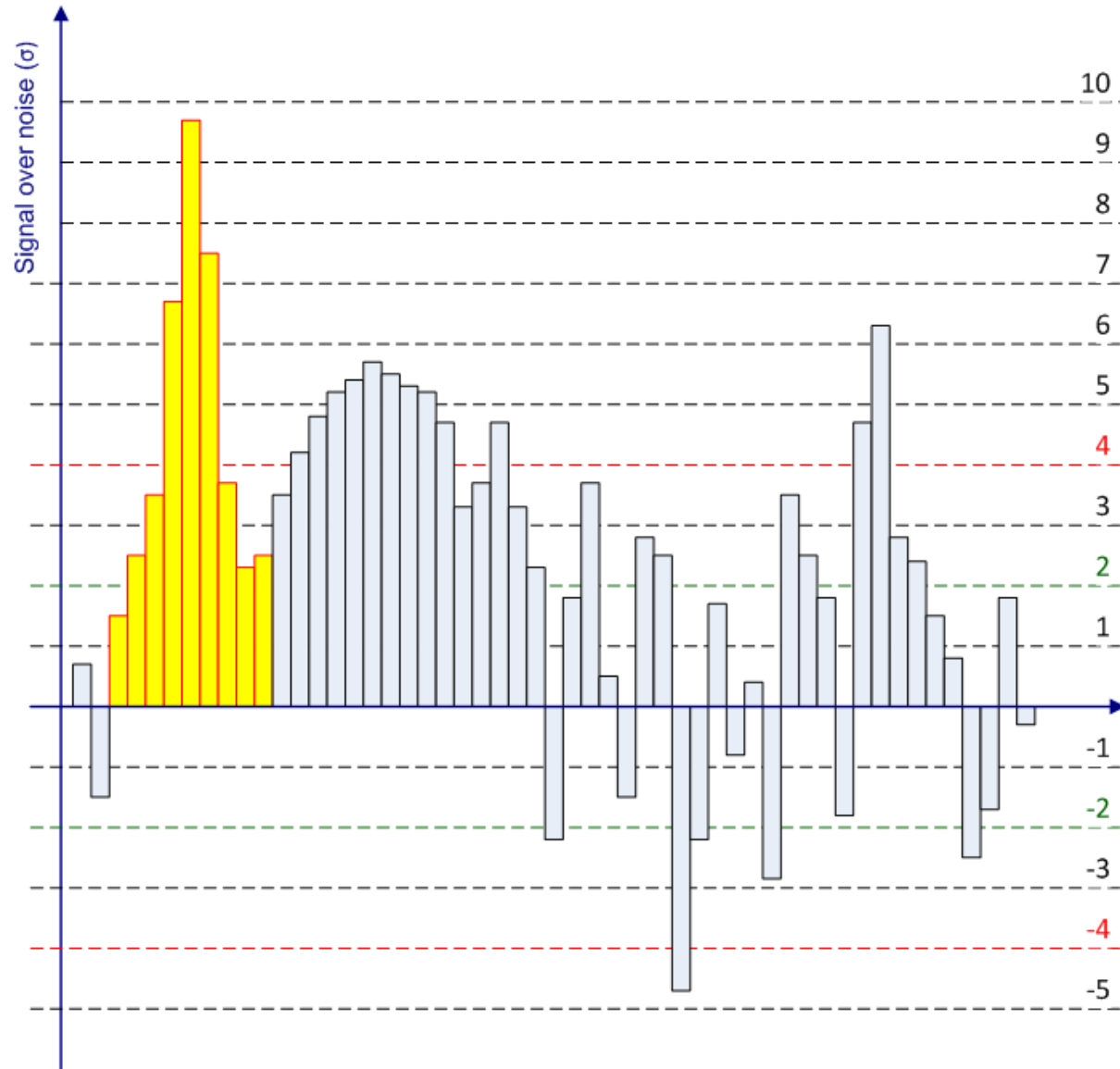


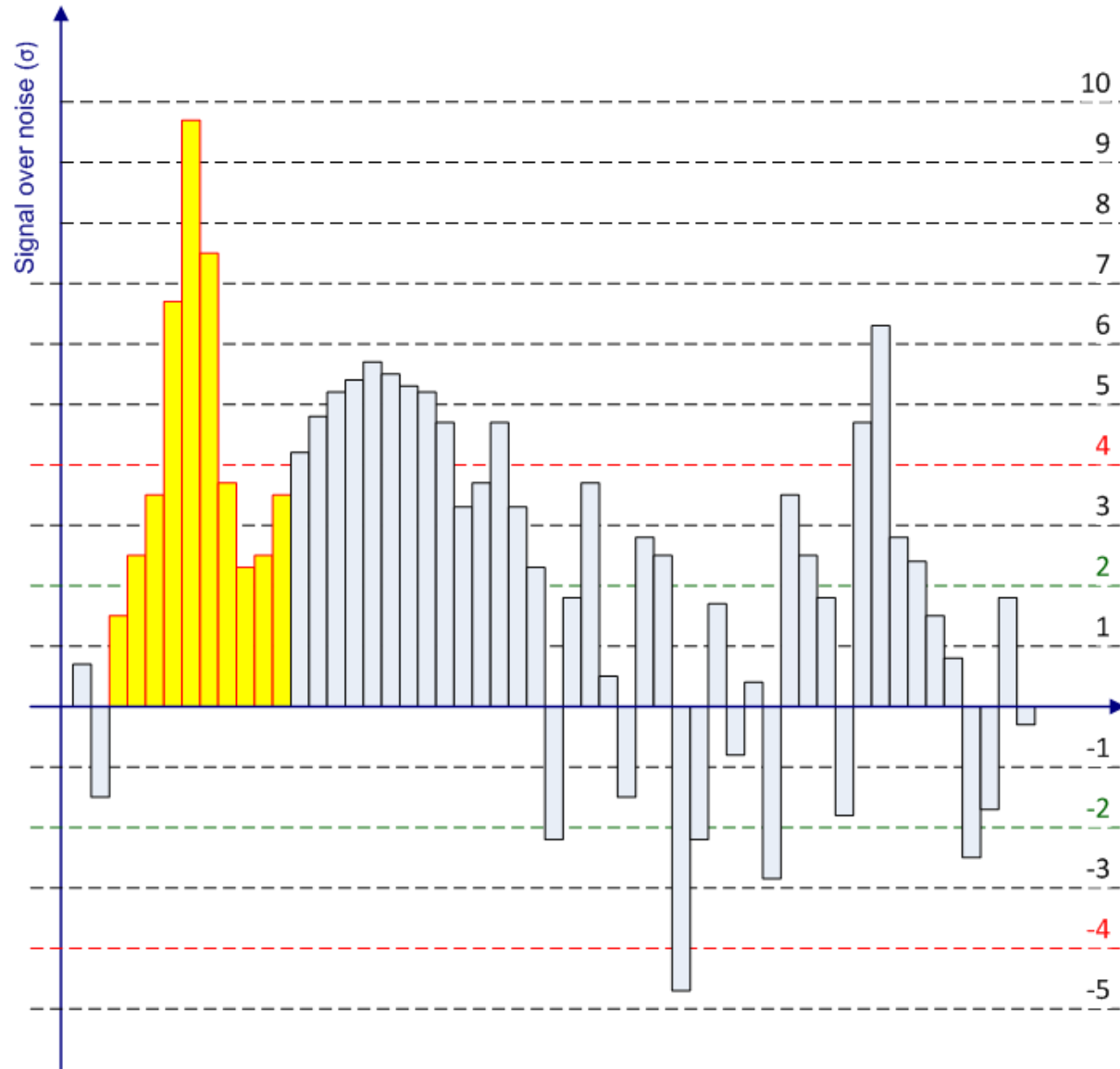


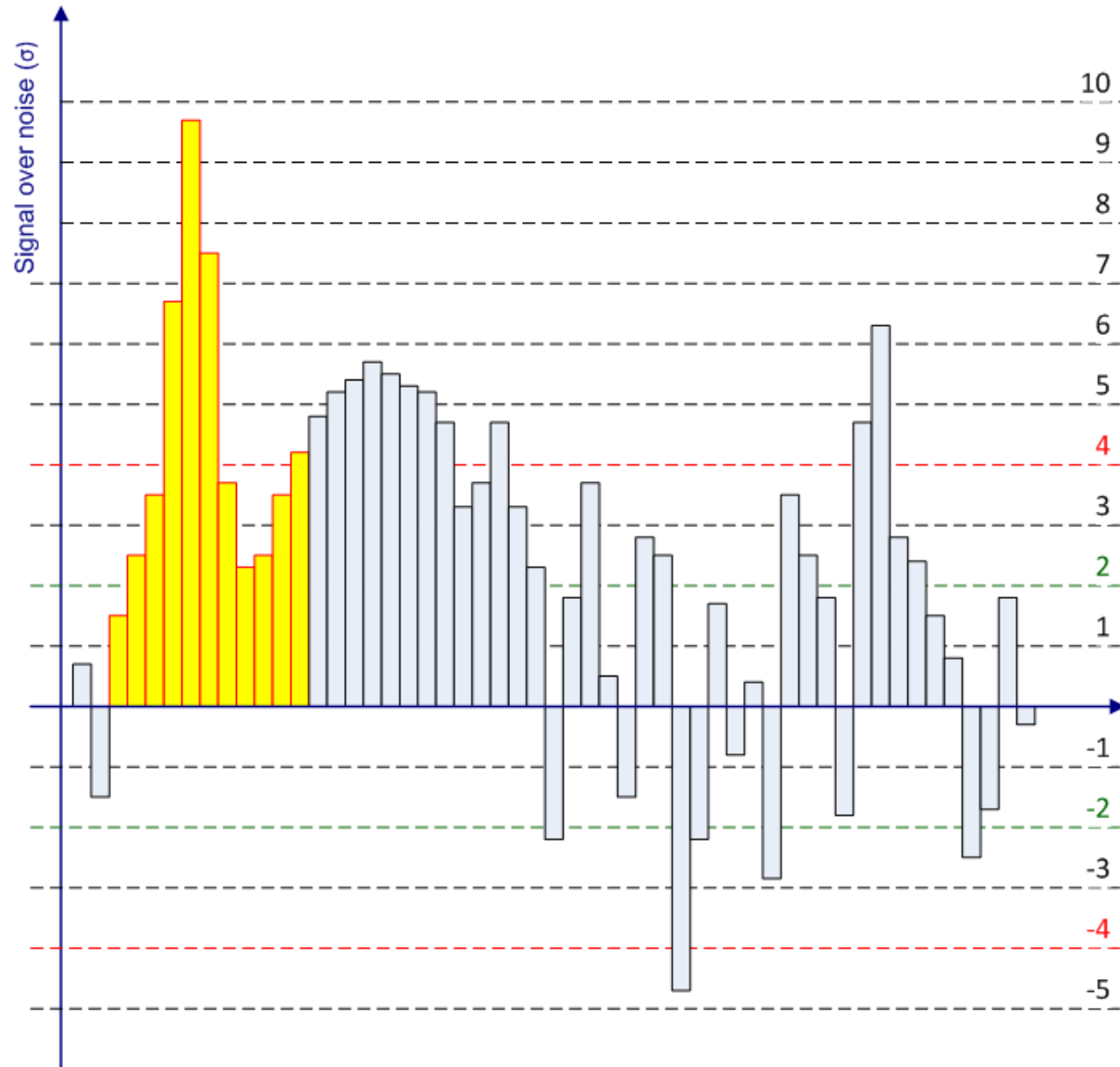


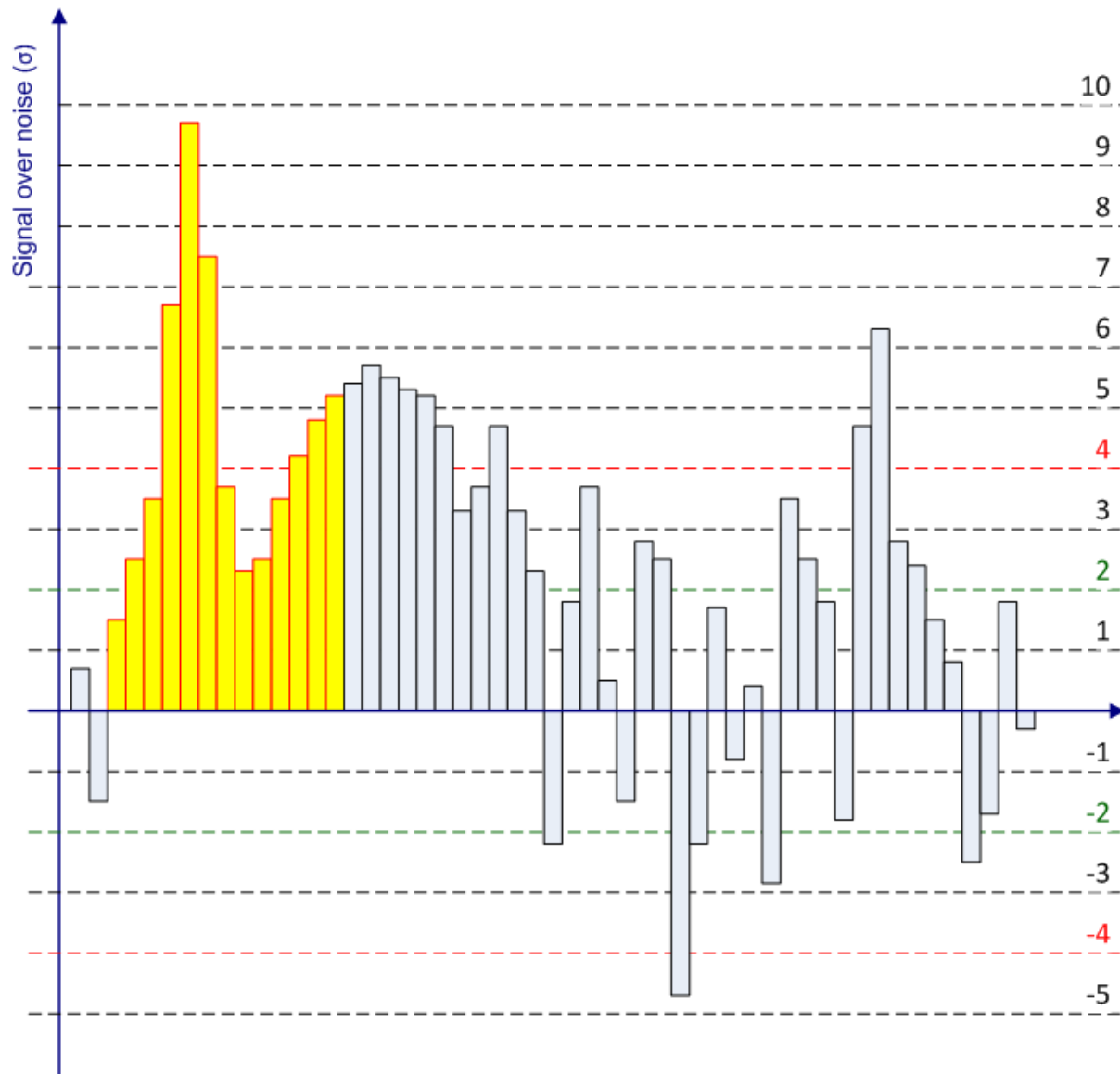


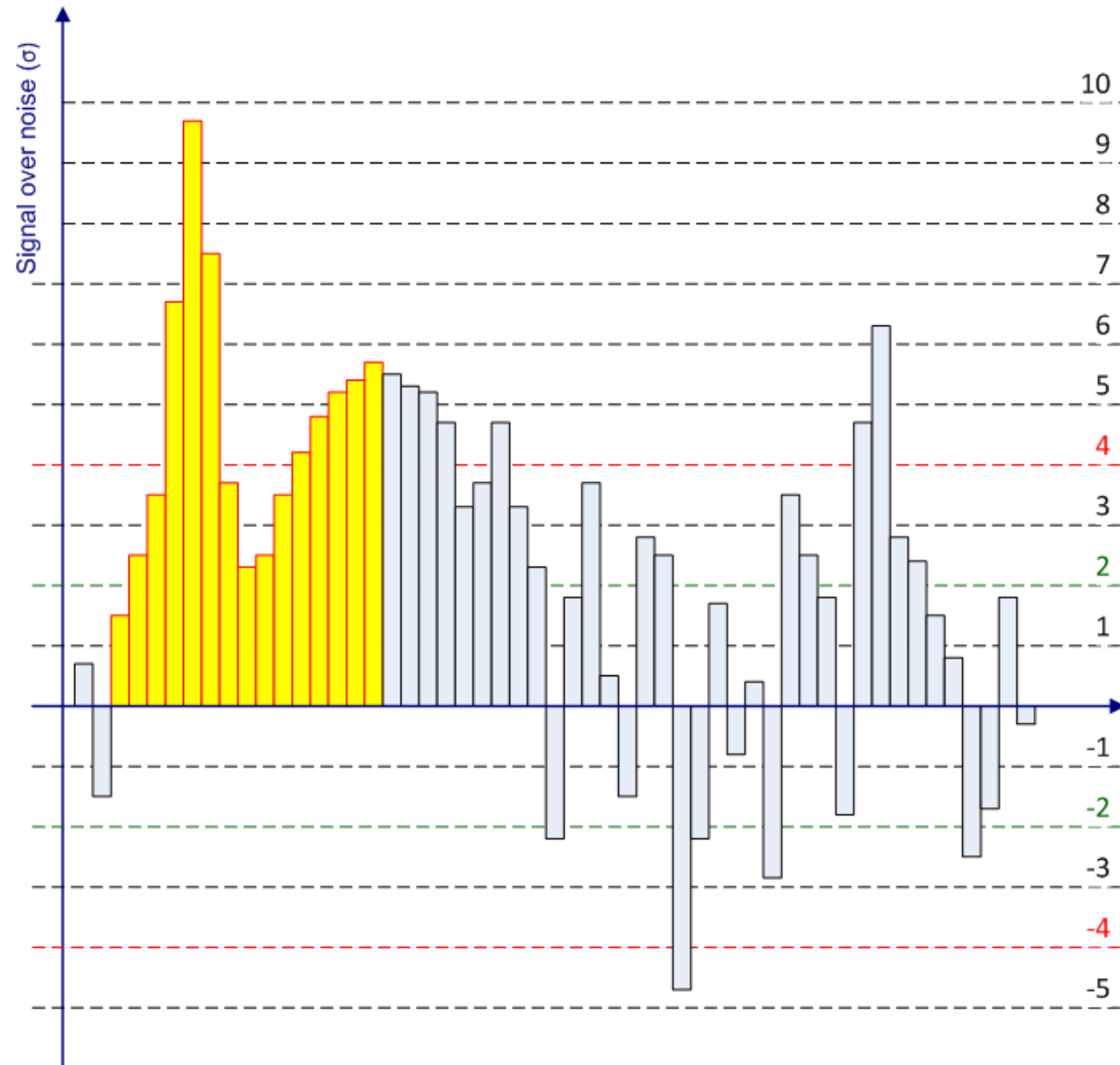


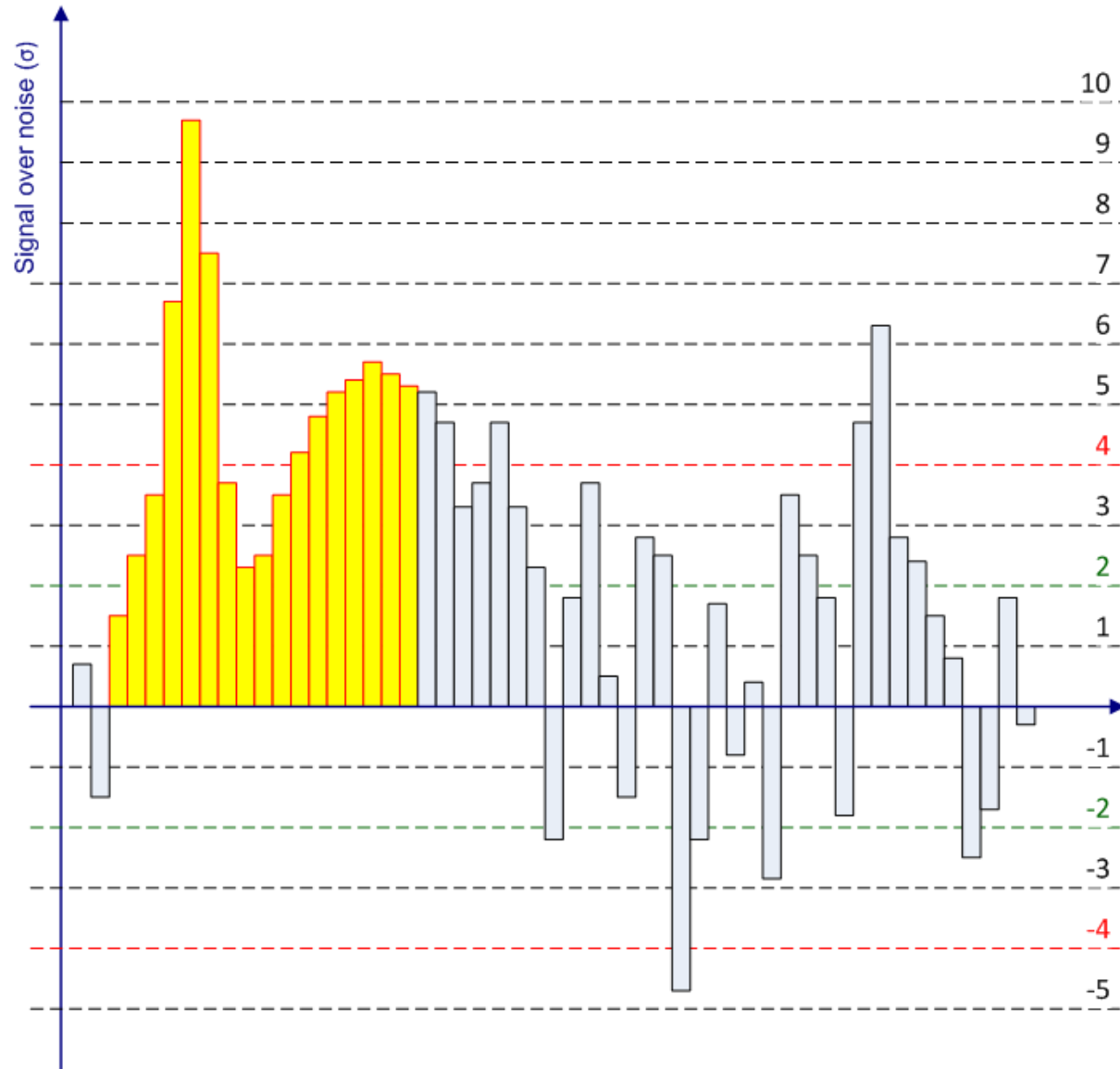


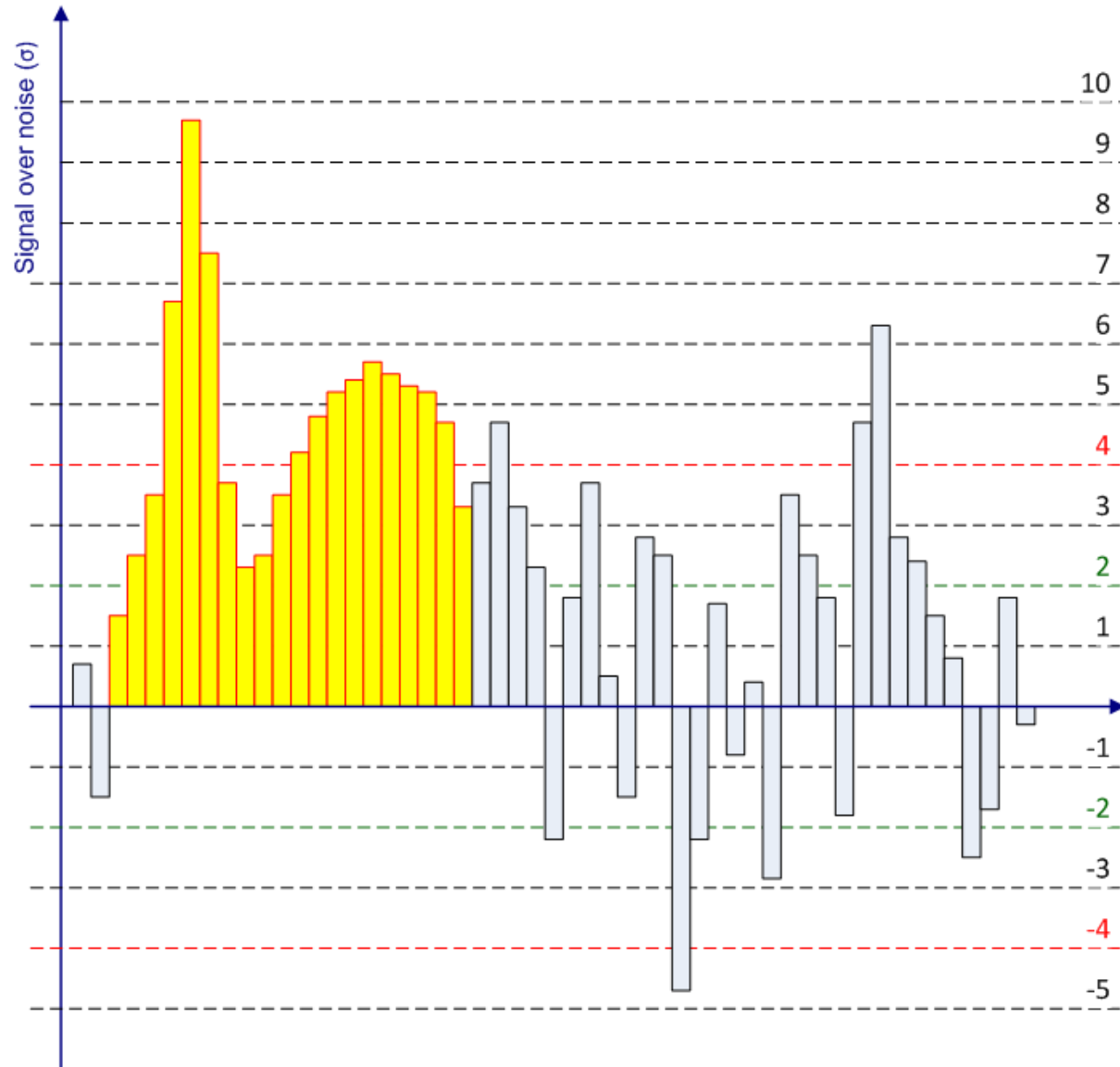


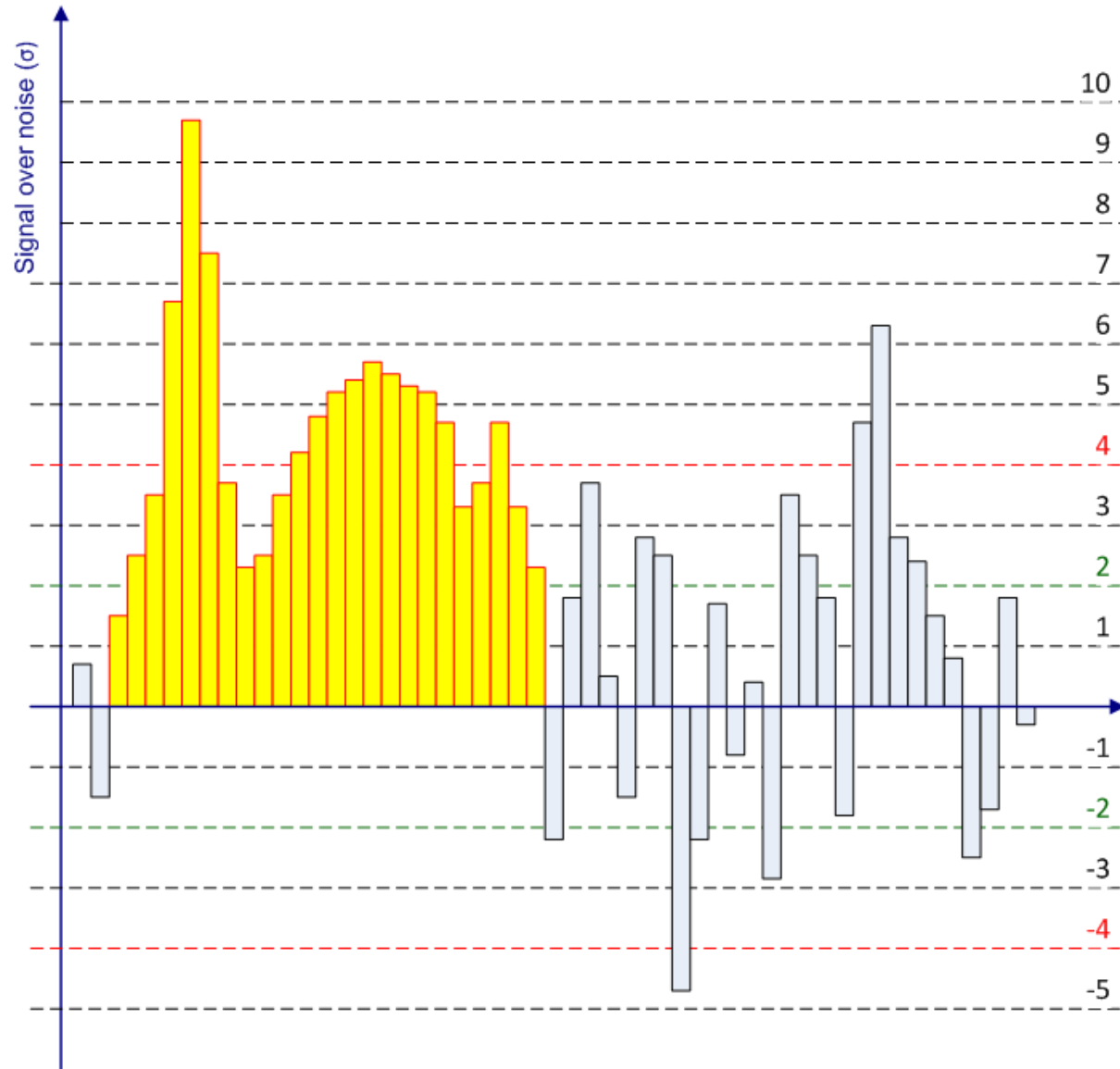


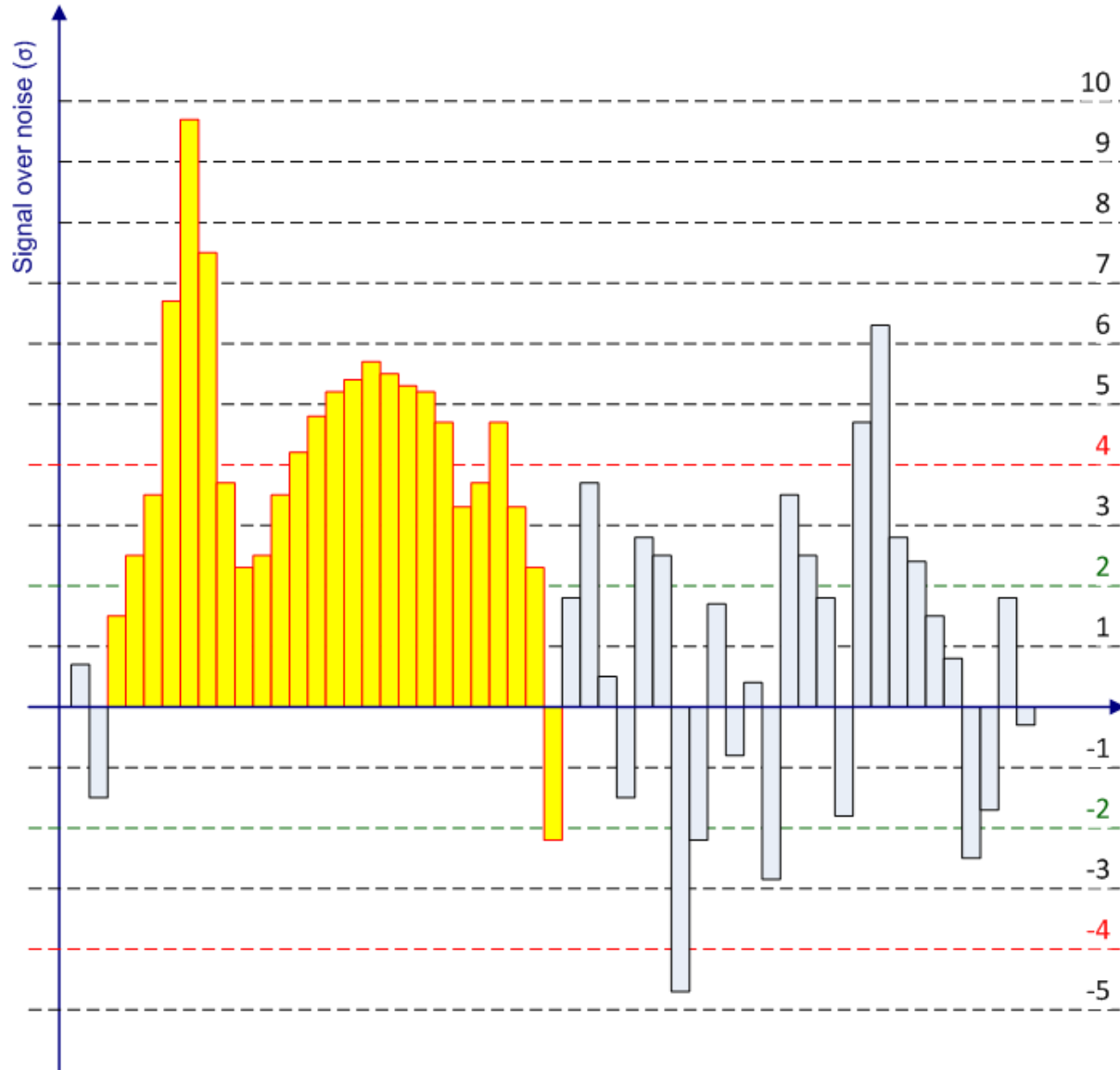


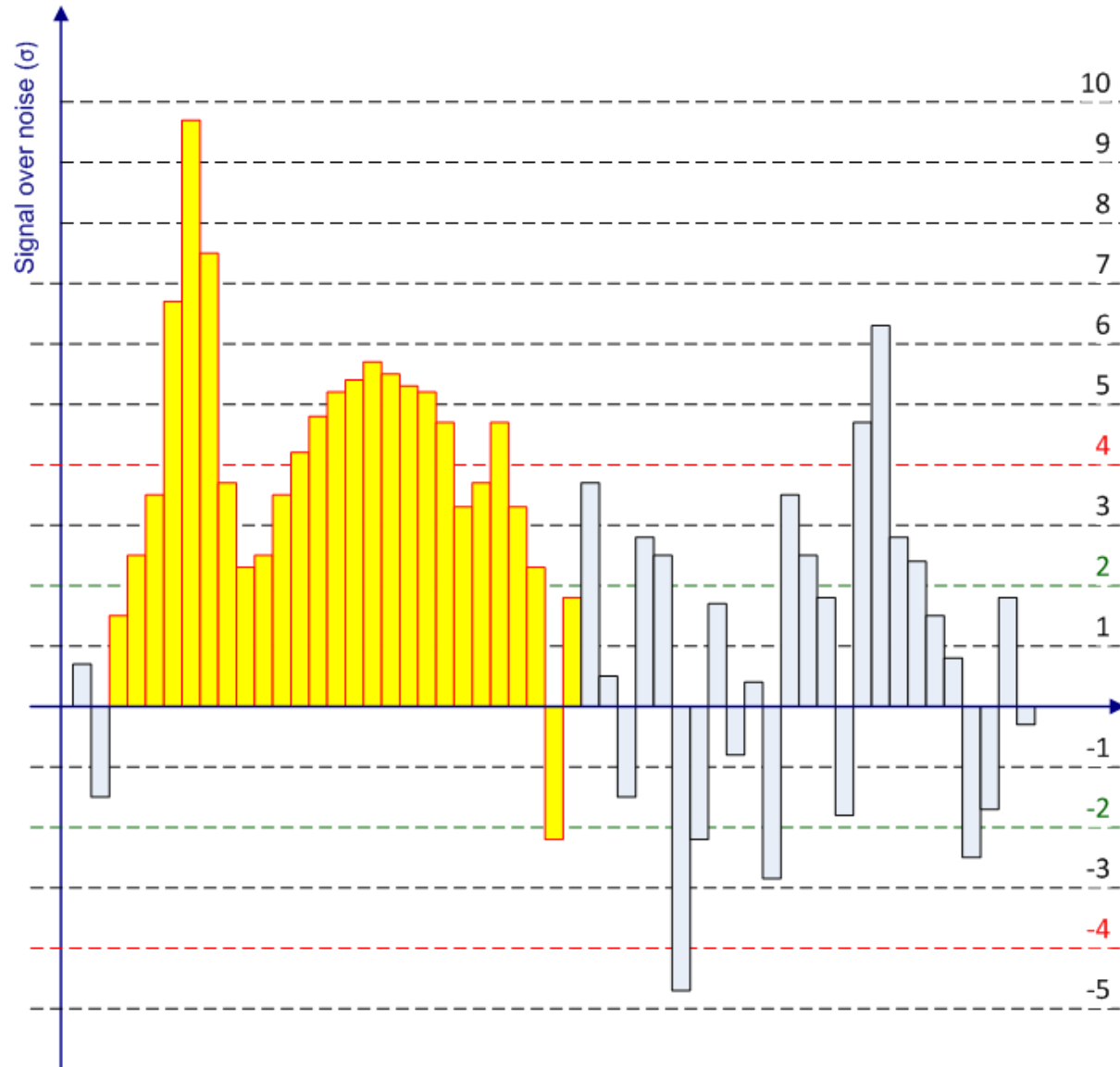


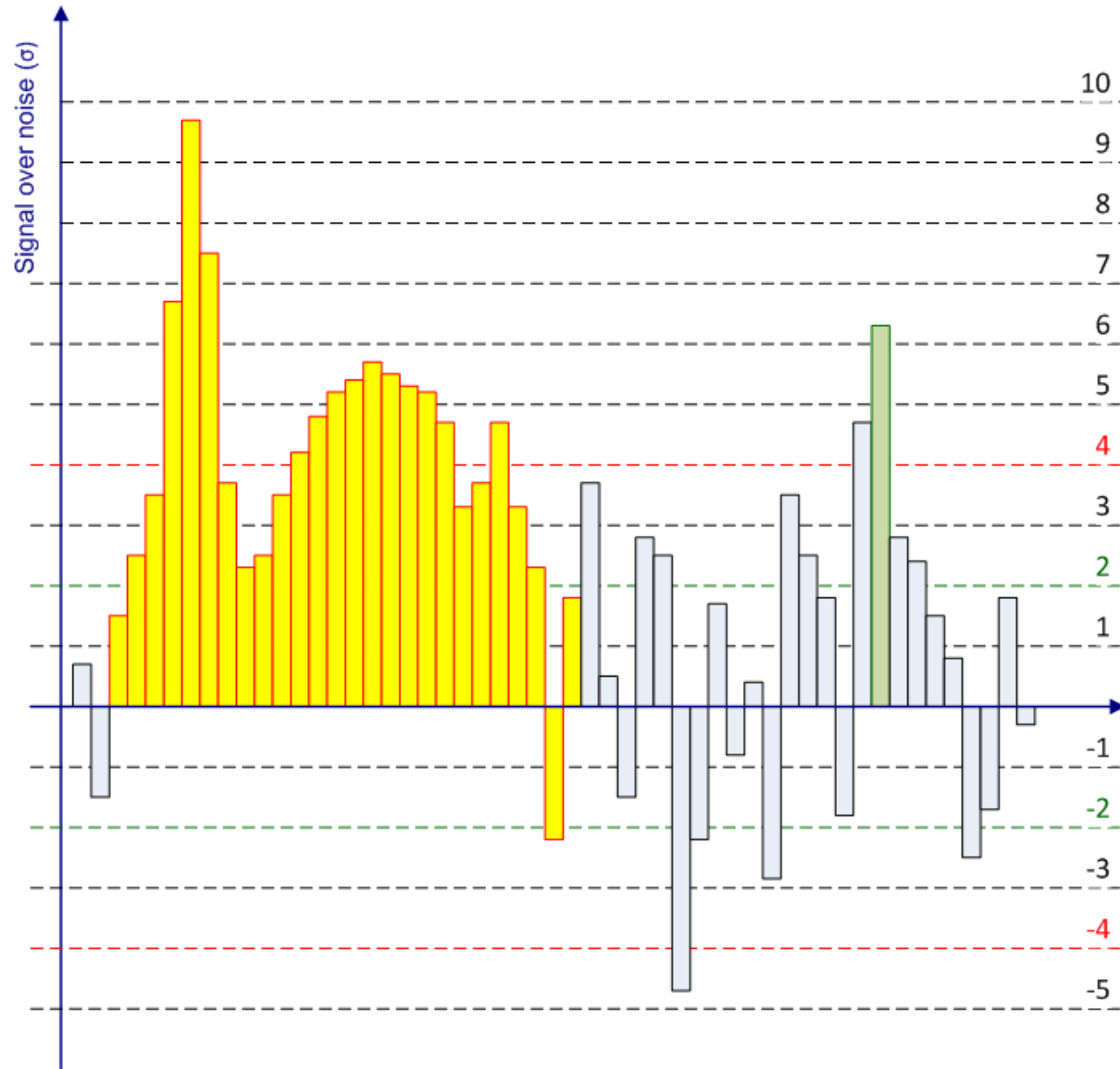


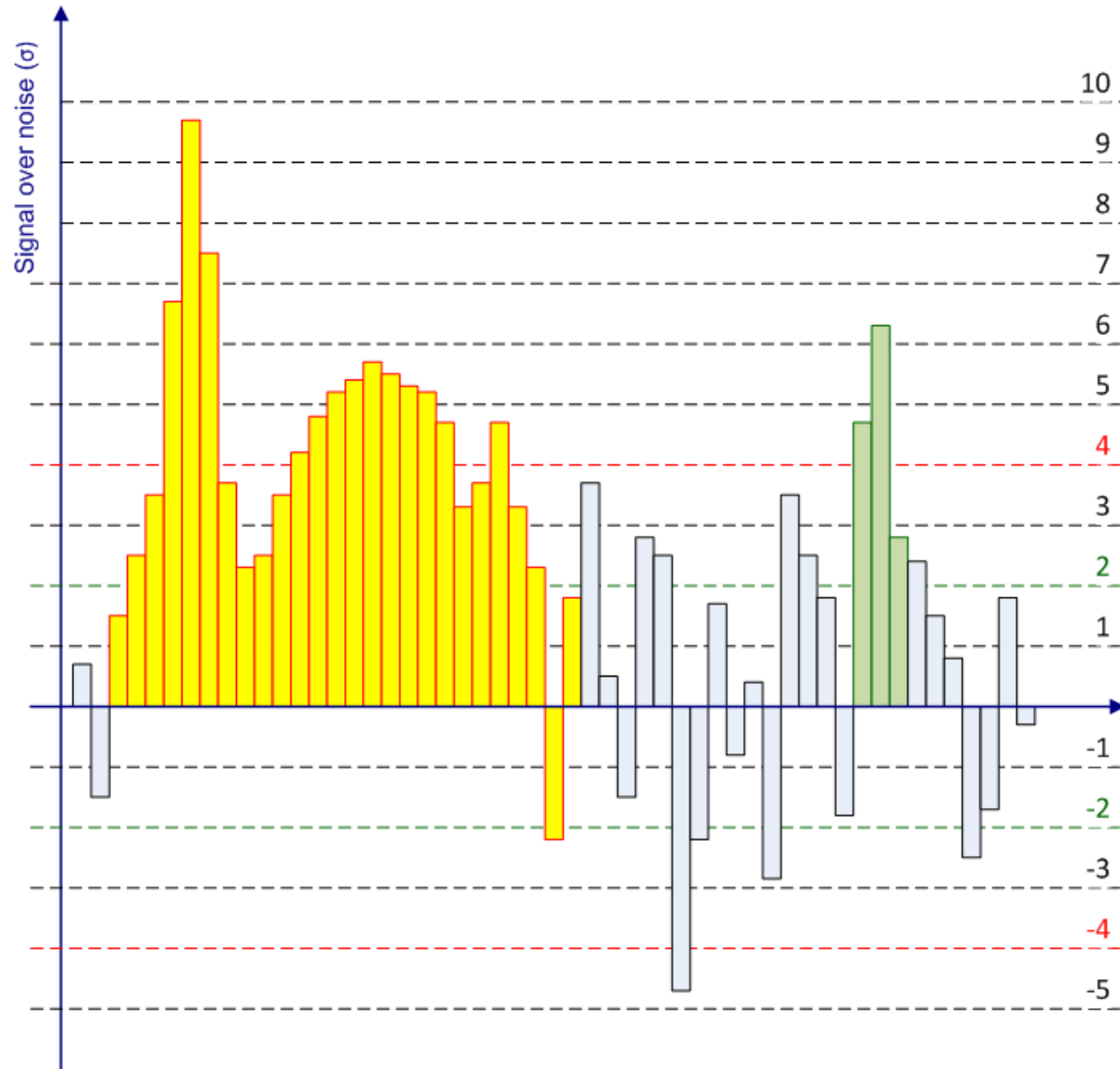


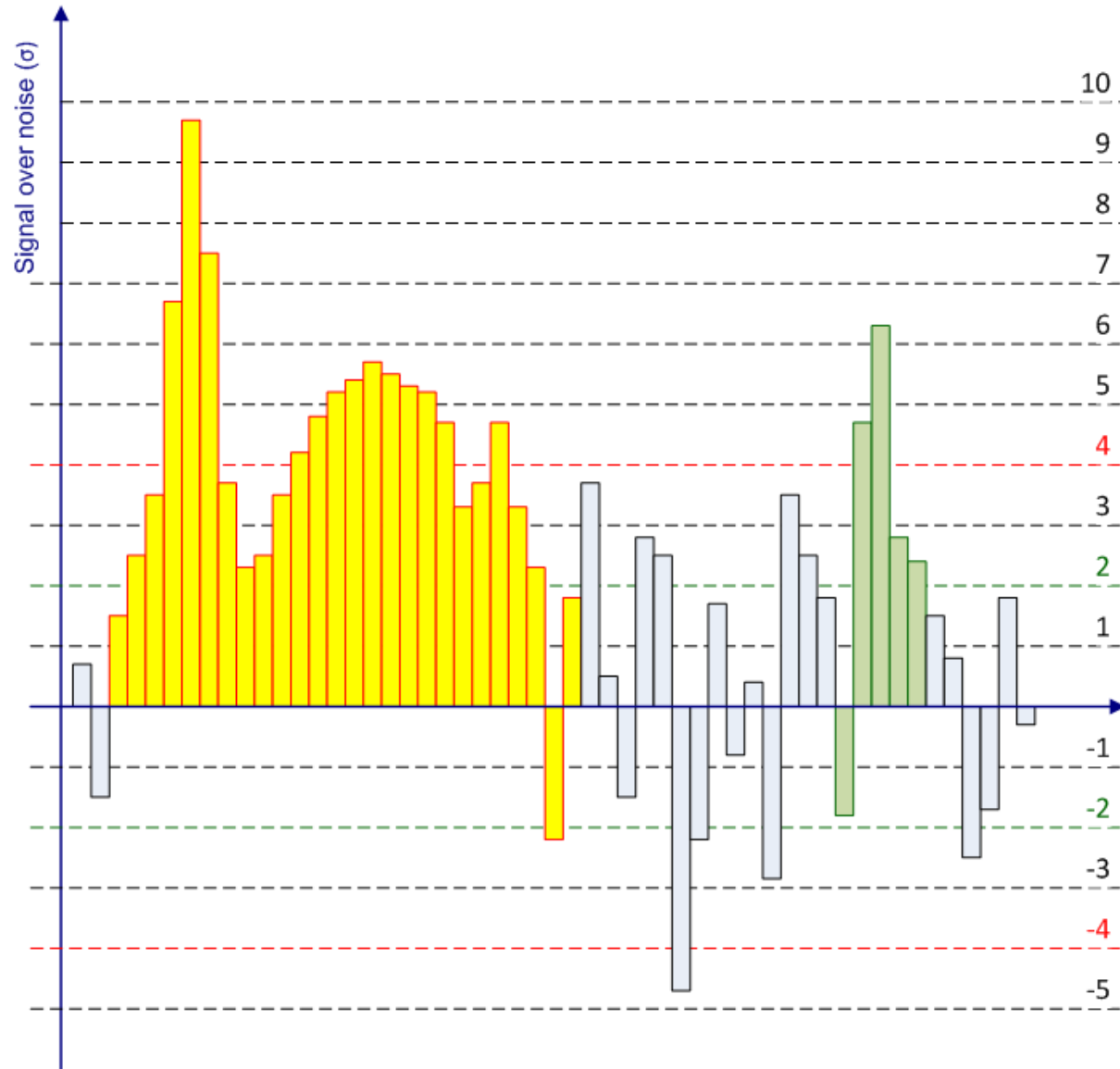


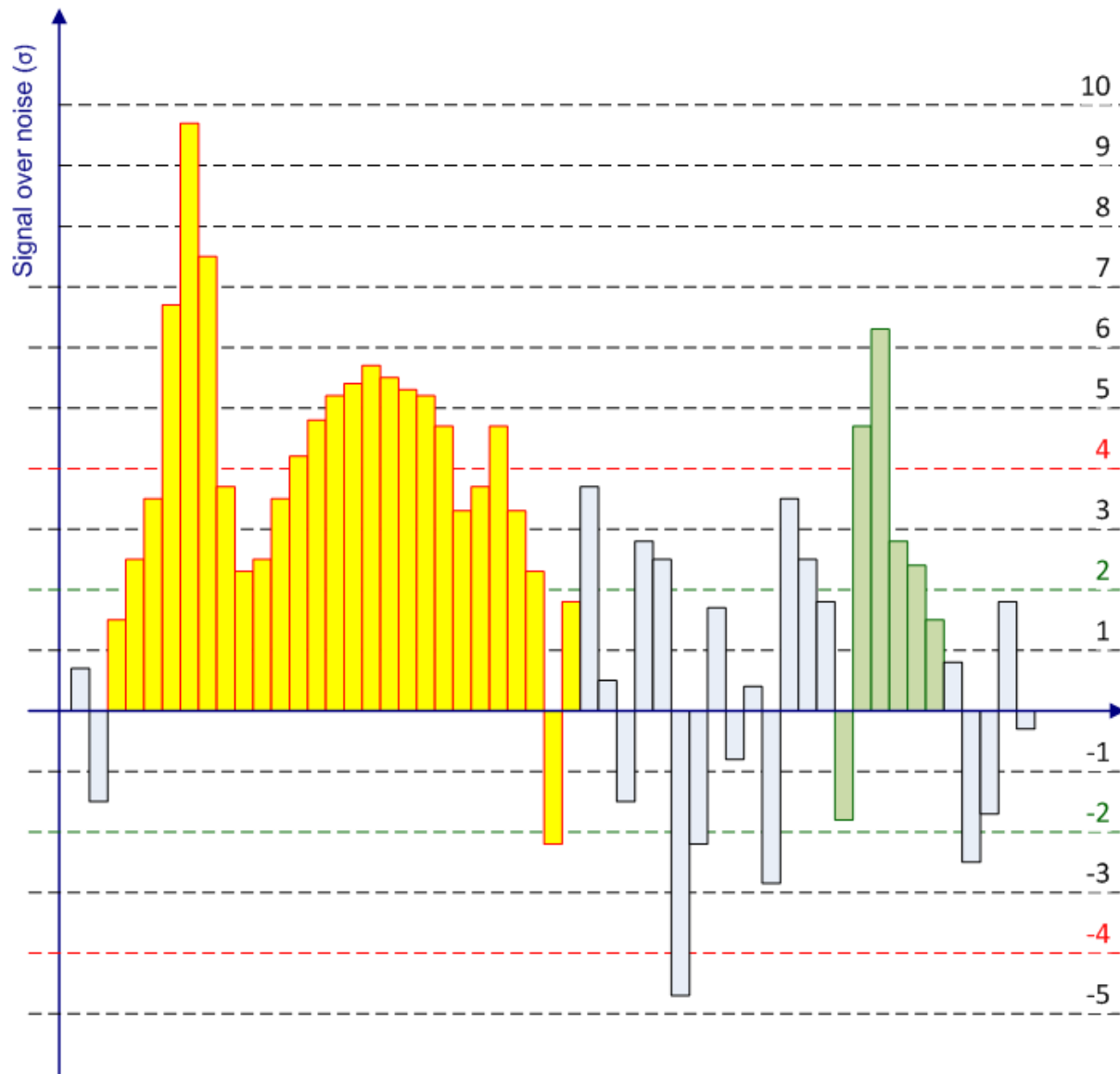


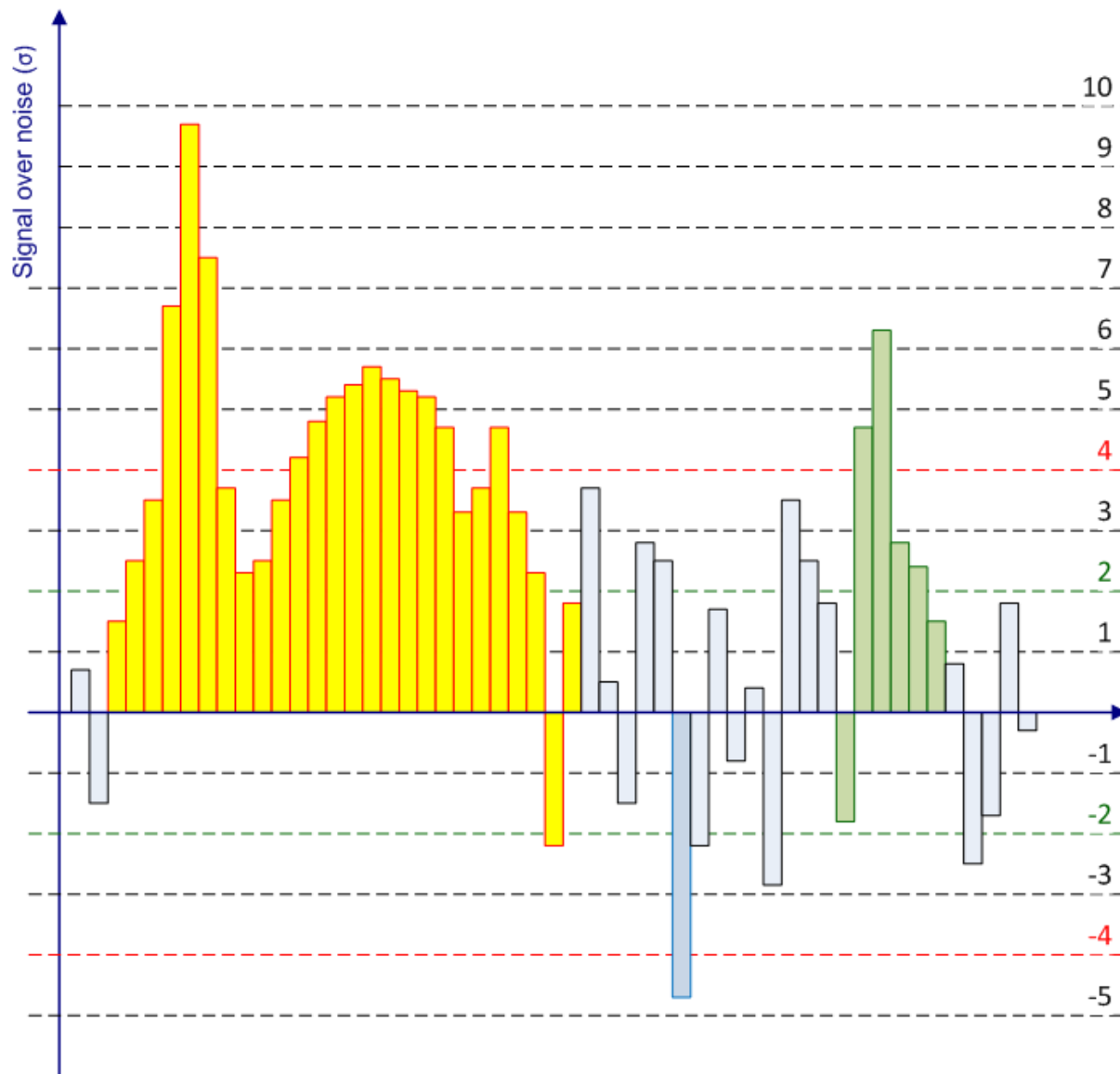


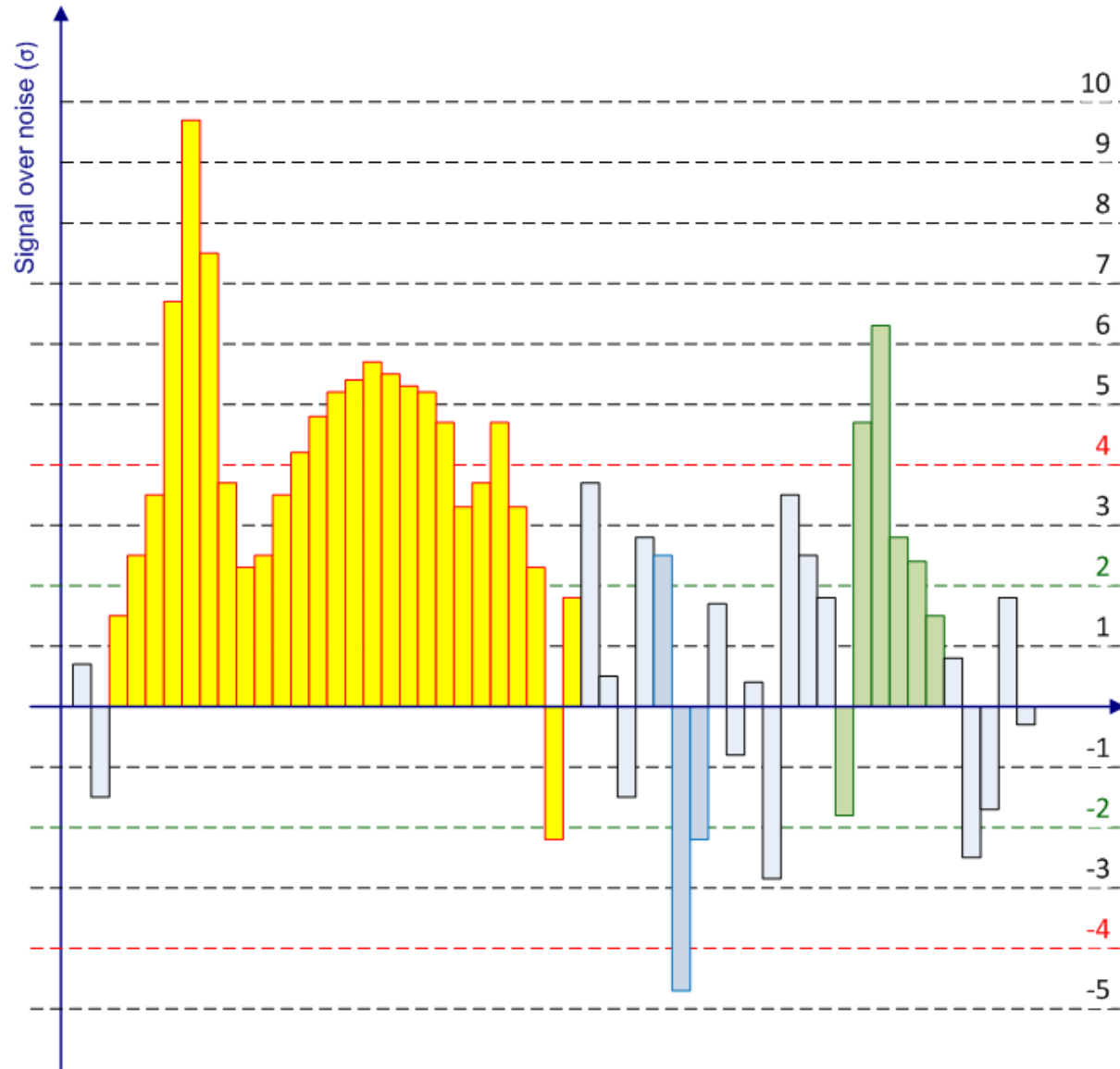


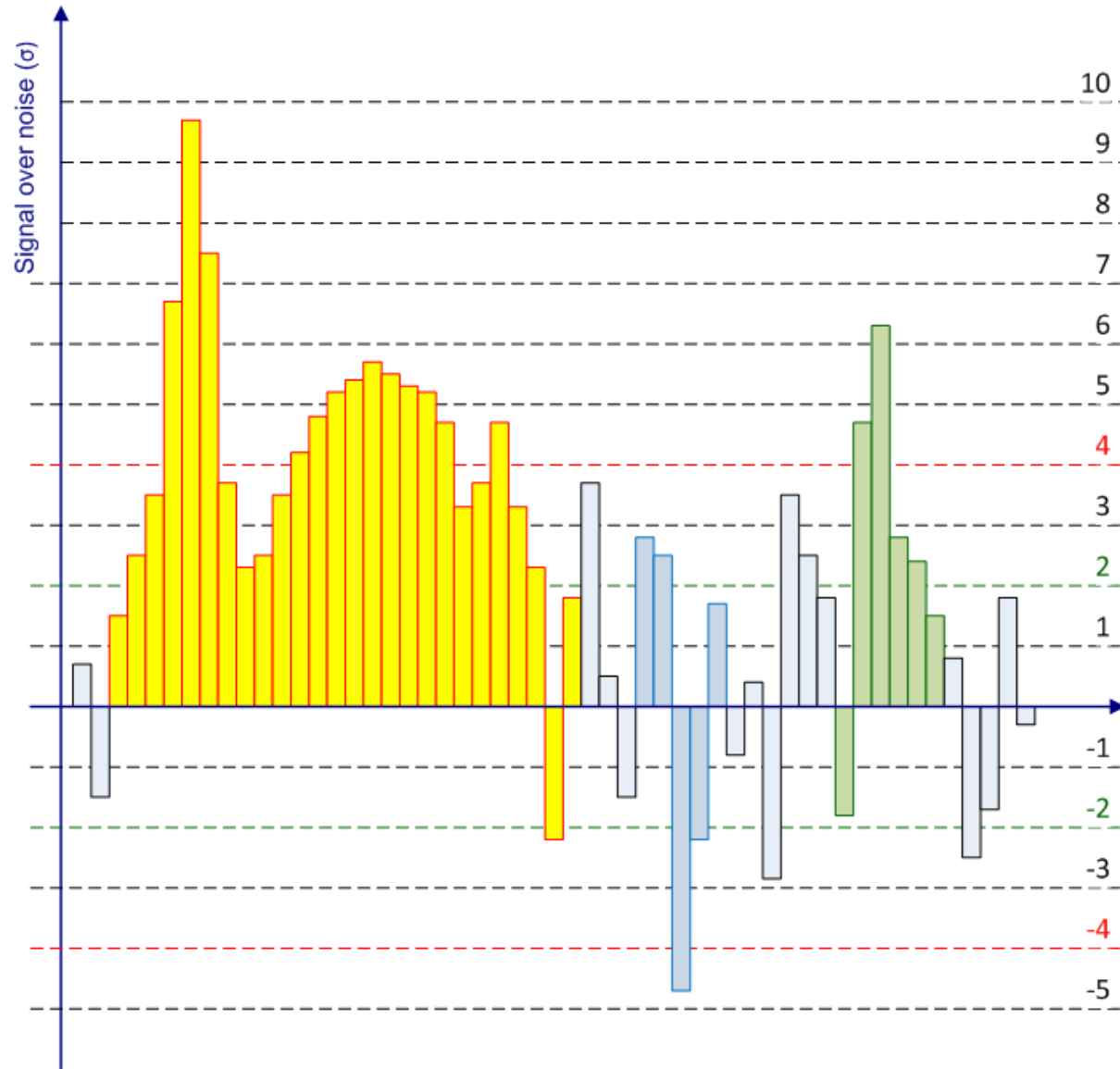


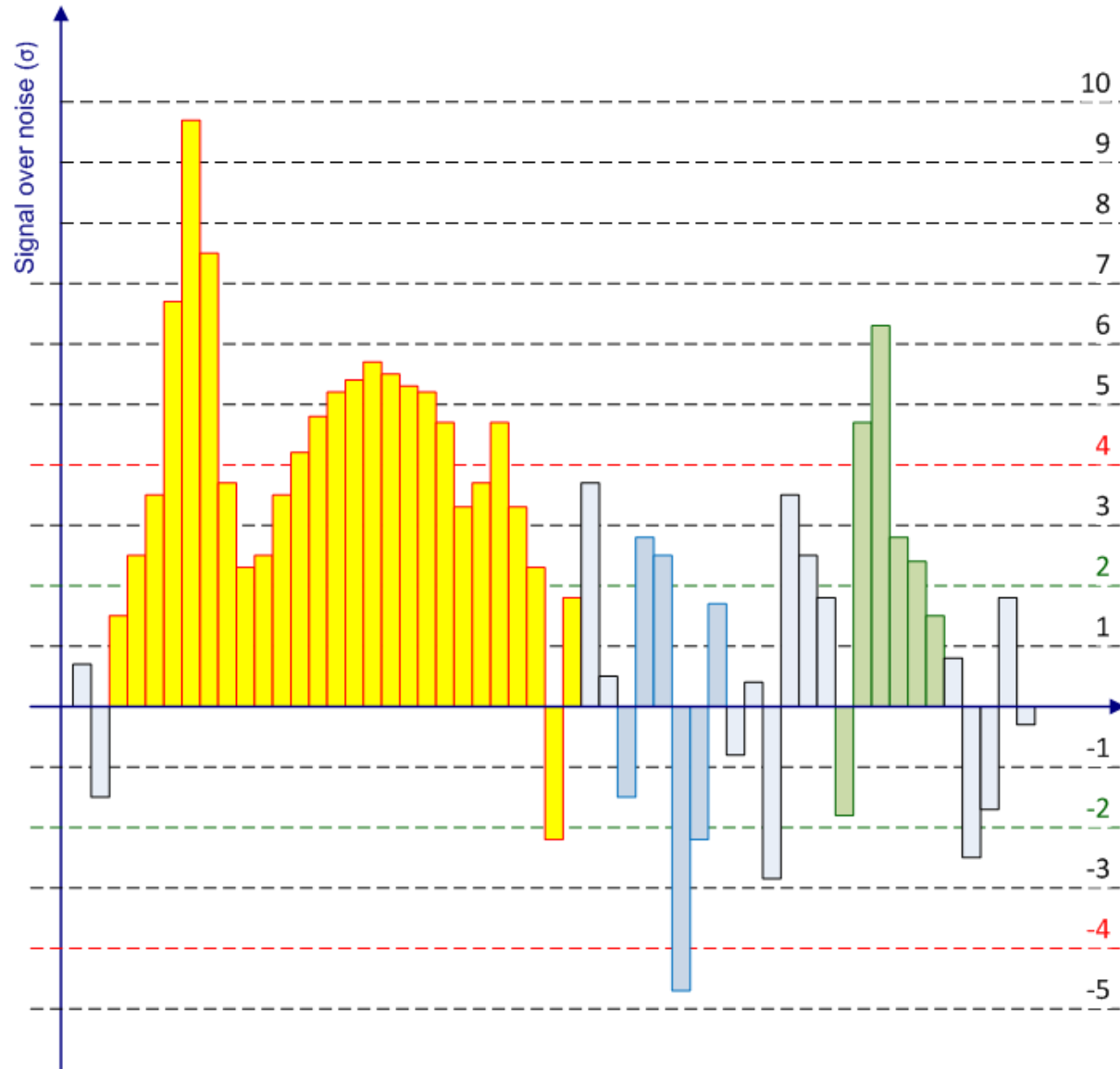


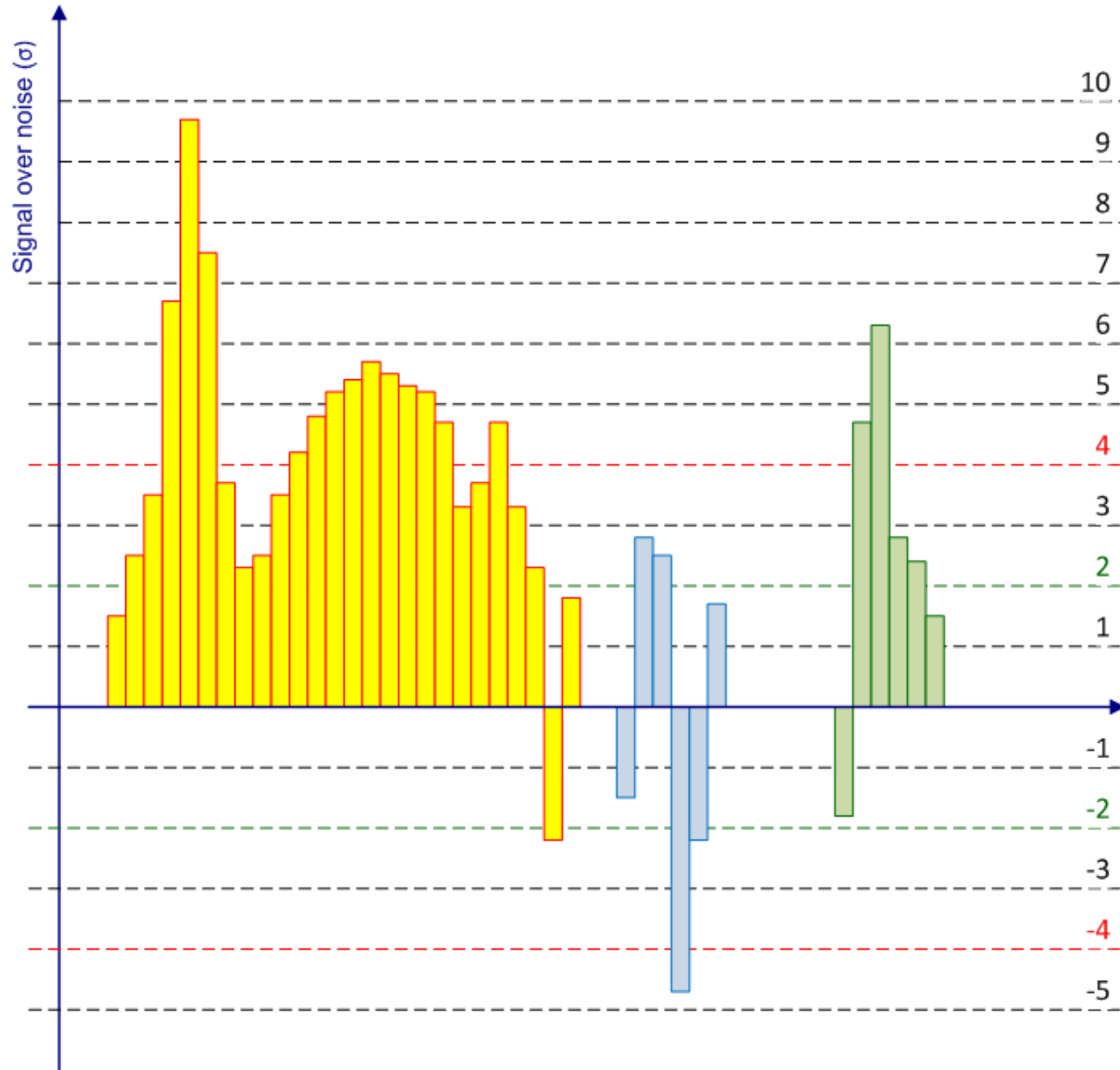












Large topologically connected regions in calorimeter can lead to large cell clusters

Lost particle flow structure can introduce problems for jets

Infrared safety, in particular

Need to refine the clustering algorithm

Try to match single particle shower shapes better

Splitting the clusters

Examine spatial cluster signal structure – find local signal maxima

“hill and valley” structural analysis in three dimensions

Split cluster between two maxima

In three dimensions, of course!

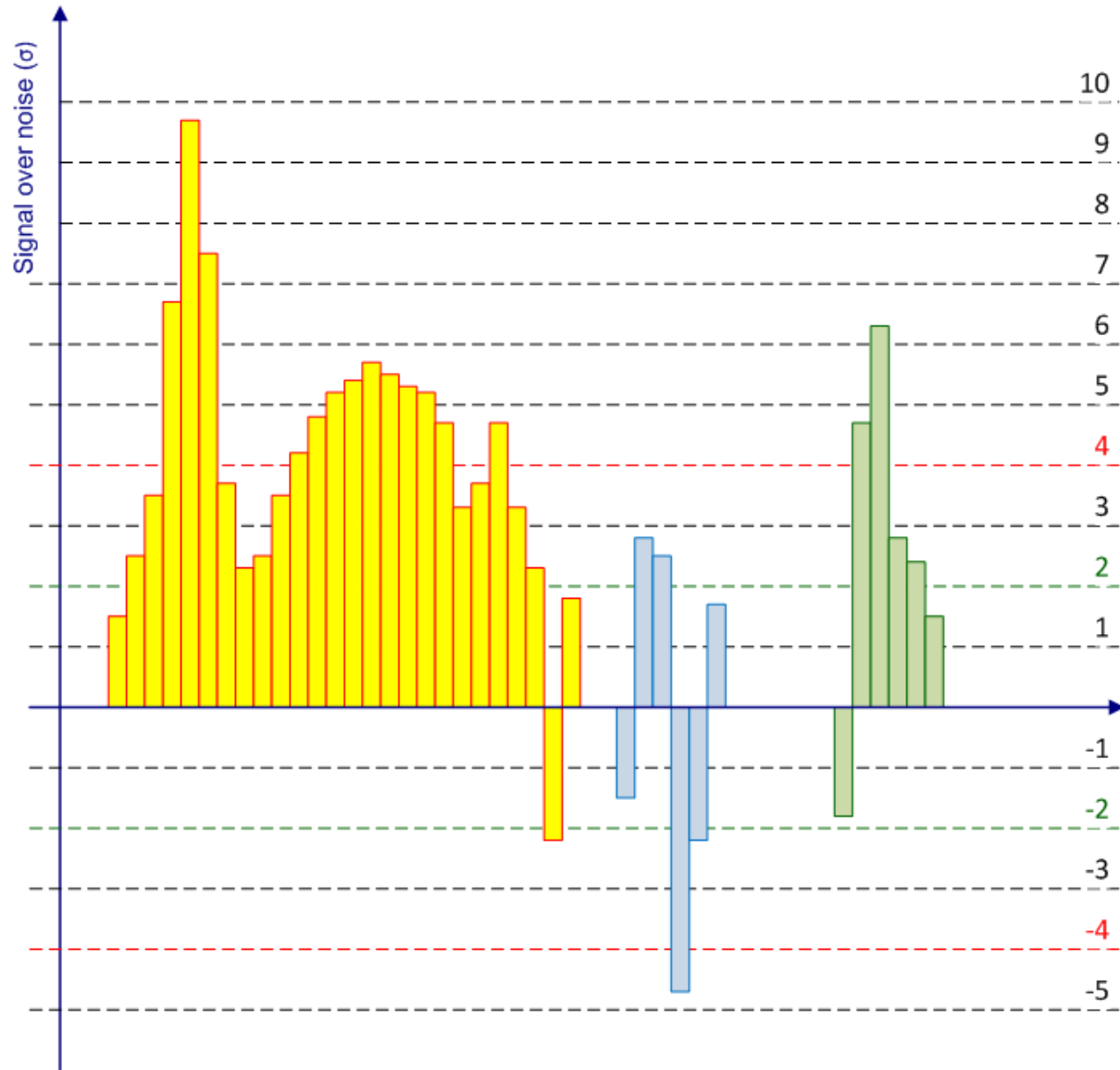
Share energy of cells in signal valleys

Needs sharing rules – introduces “geometrically” weighted cell energy contribution to cluster signal

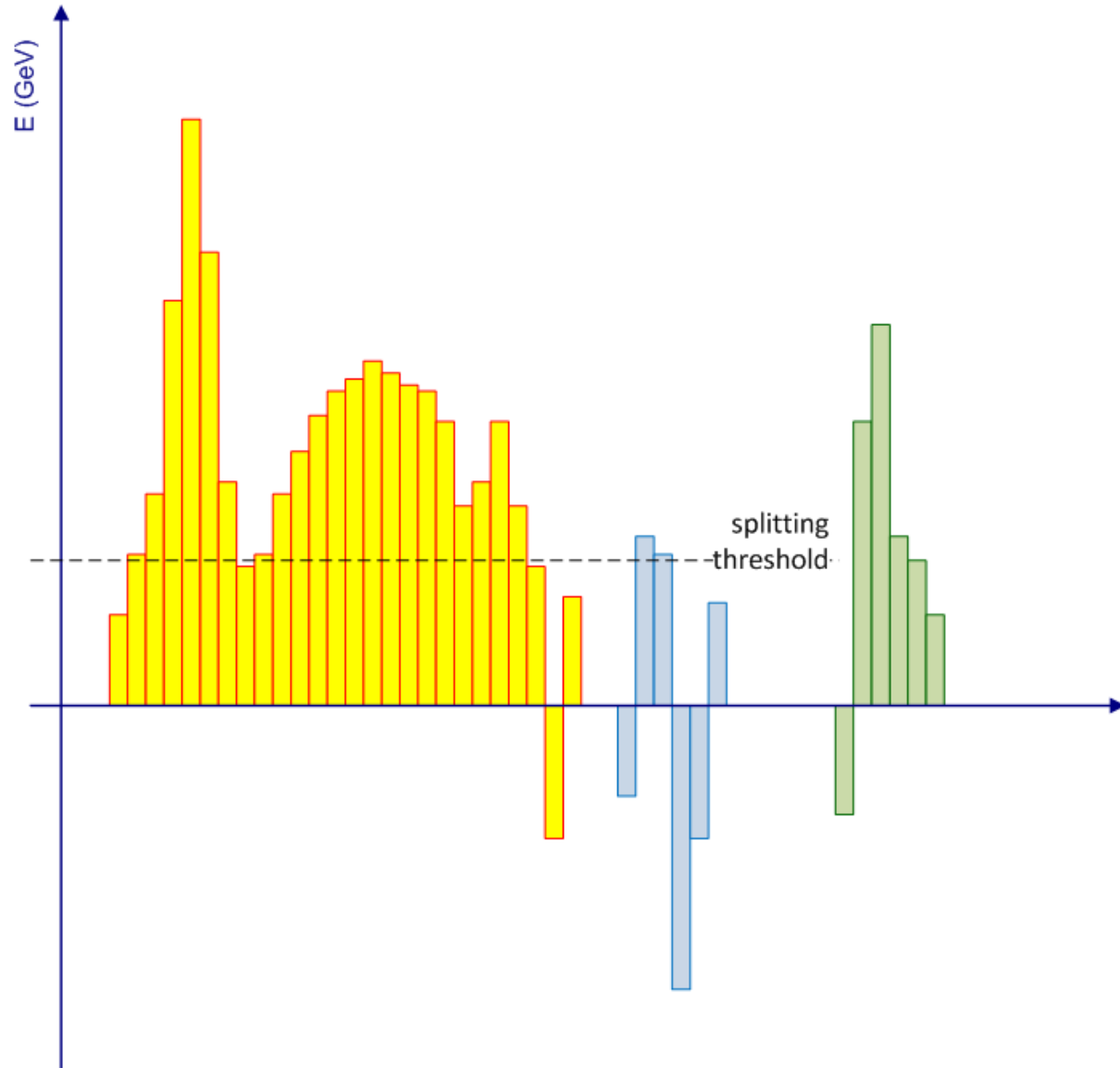
Introduces new tunable parameter

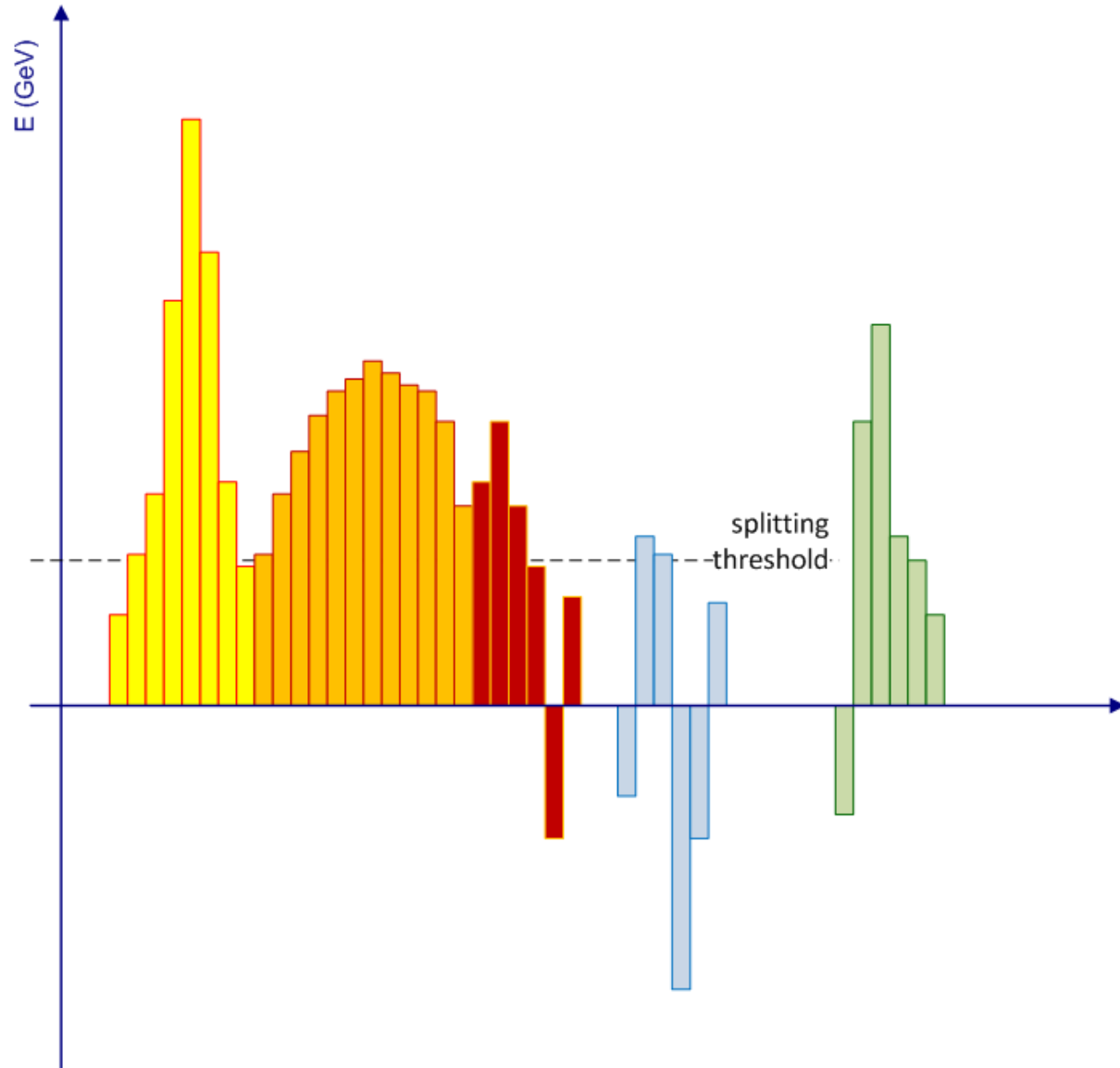
Local signal maximum threshold is defined in units of energy, not significance!





Cluster Splitting





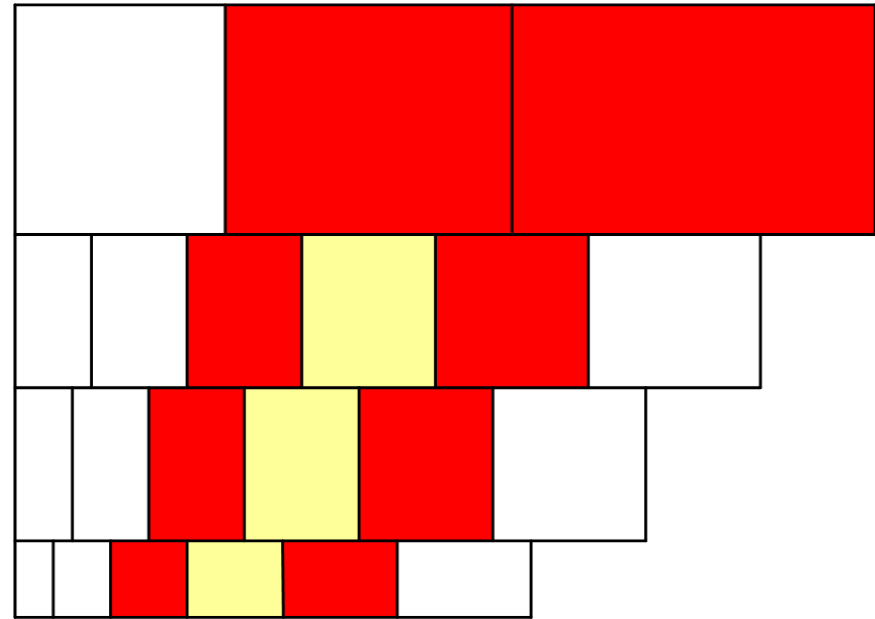
Splitting technique

Guided by finest calorimeter
granularity

Typically in electromagnetic
calorimeter

Allows to split larger cell signals
without signal valley

Typically in hadronic calorimeters



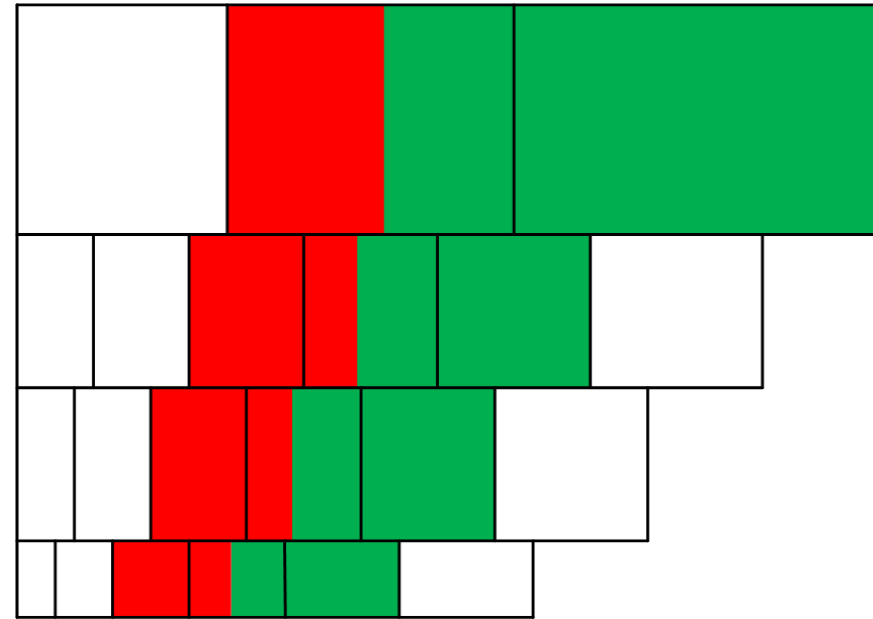
Splitting technique

Guided by finest calorimeter
granularity

Typically in electromagnetic
calorimeter

Allows to split larger cell signals
without signal valley

Typically in hadronic calorimeters



Rule for energy sharing (ATLAS example):

$$w_1 = \frac{E_1}{E_1 + rE_2}$$

$$w_2 = 1 - w_1$$

$$r = e^{d_1 - d_2}$$

(d_i is the distance of the cell from the centroid of cluster i)

Each cell can only appear in up to two clusters



Clusters have shapes

Geometrical moments and sizes

Lateral and longitudinal

Tilt of principal axis

With respect to direction
extrapolation from primary
vertex (magnetic field!)

Density and compactness
measures

Cluster energy distribution in
cells

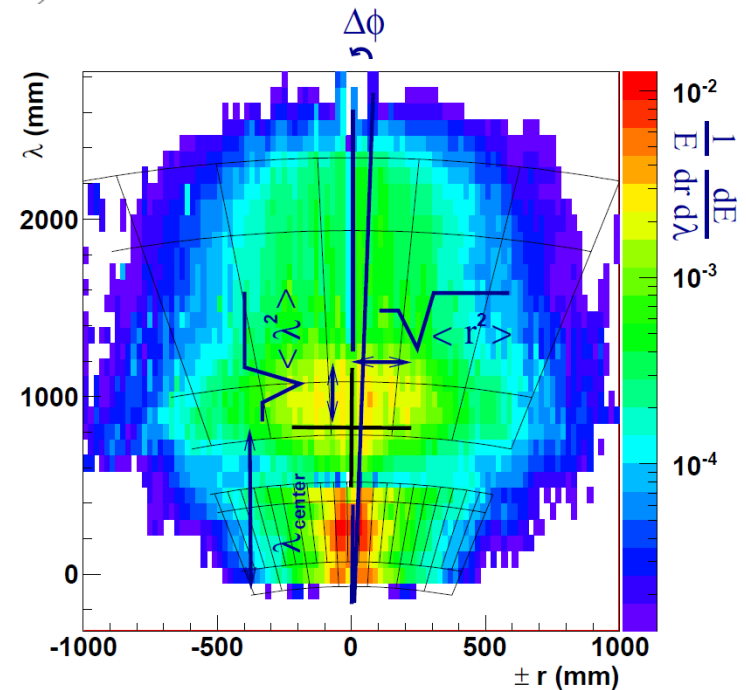
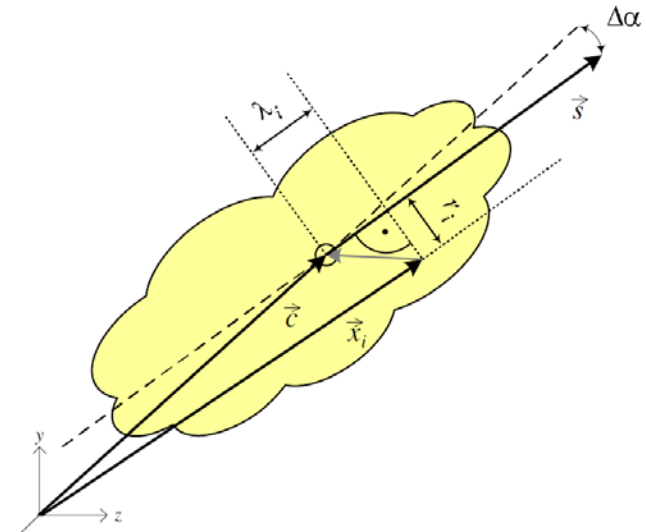
Energy sharing between
calorimeter segments and
modules

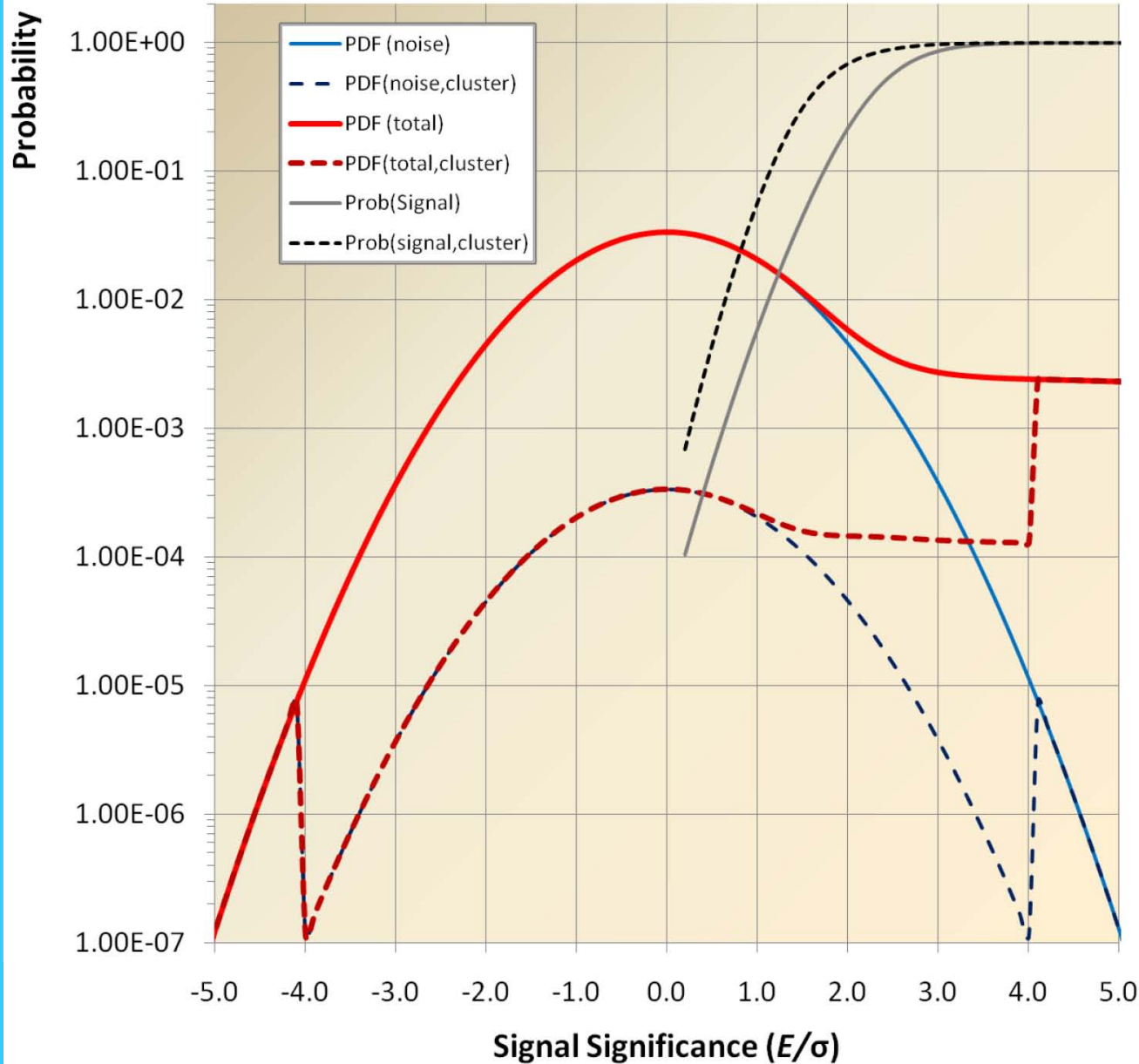
Shower structures

Useful for cluster calibration

Exploit shape sensitivity to
shower character

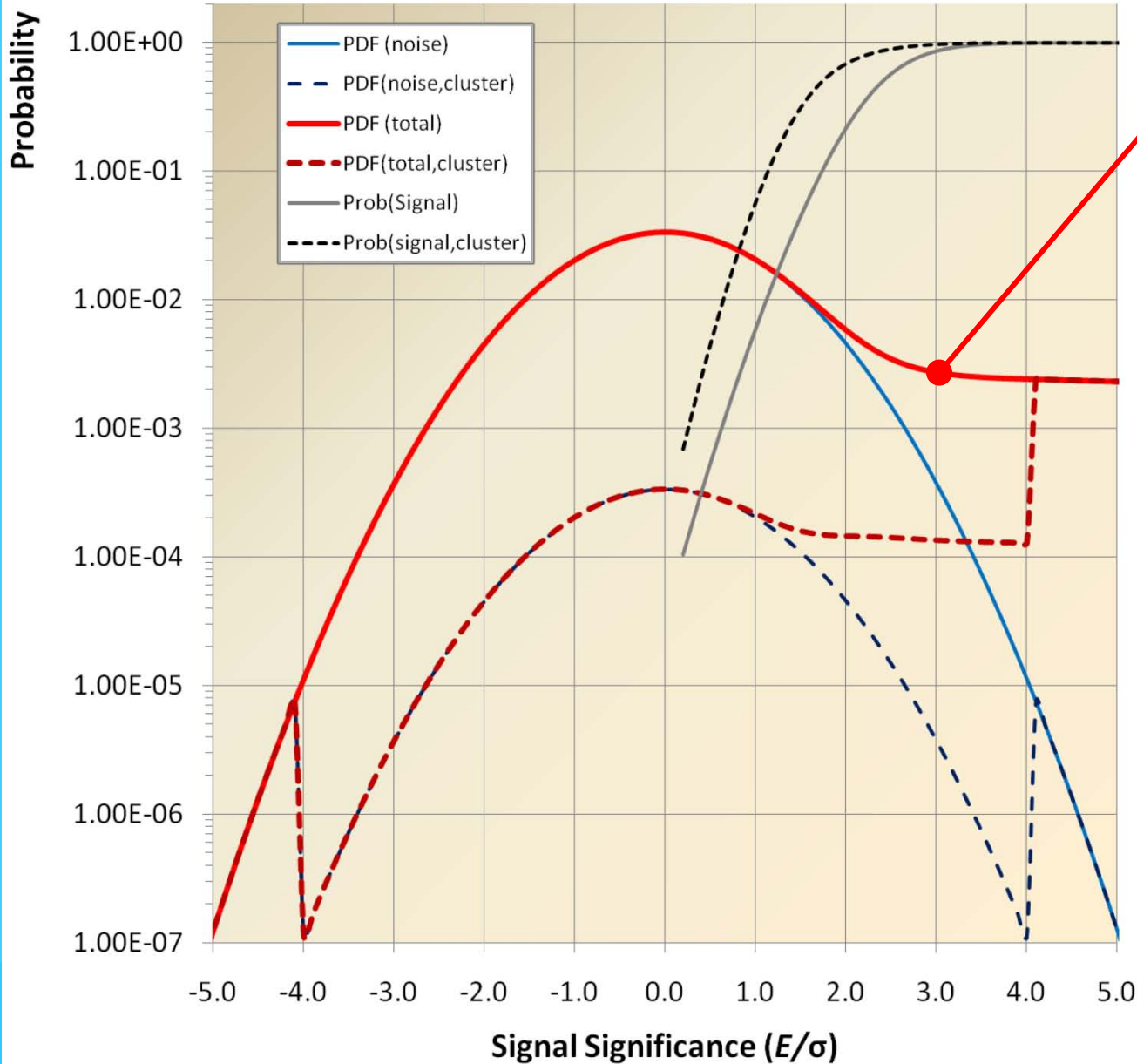
Hadronic versus electromagnetic

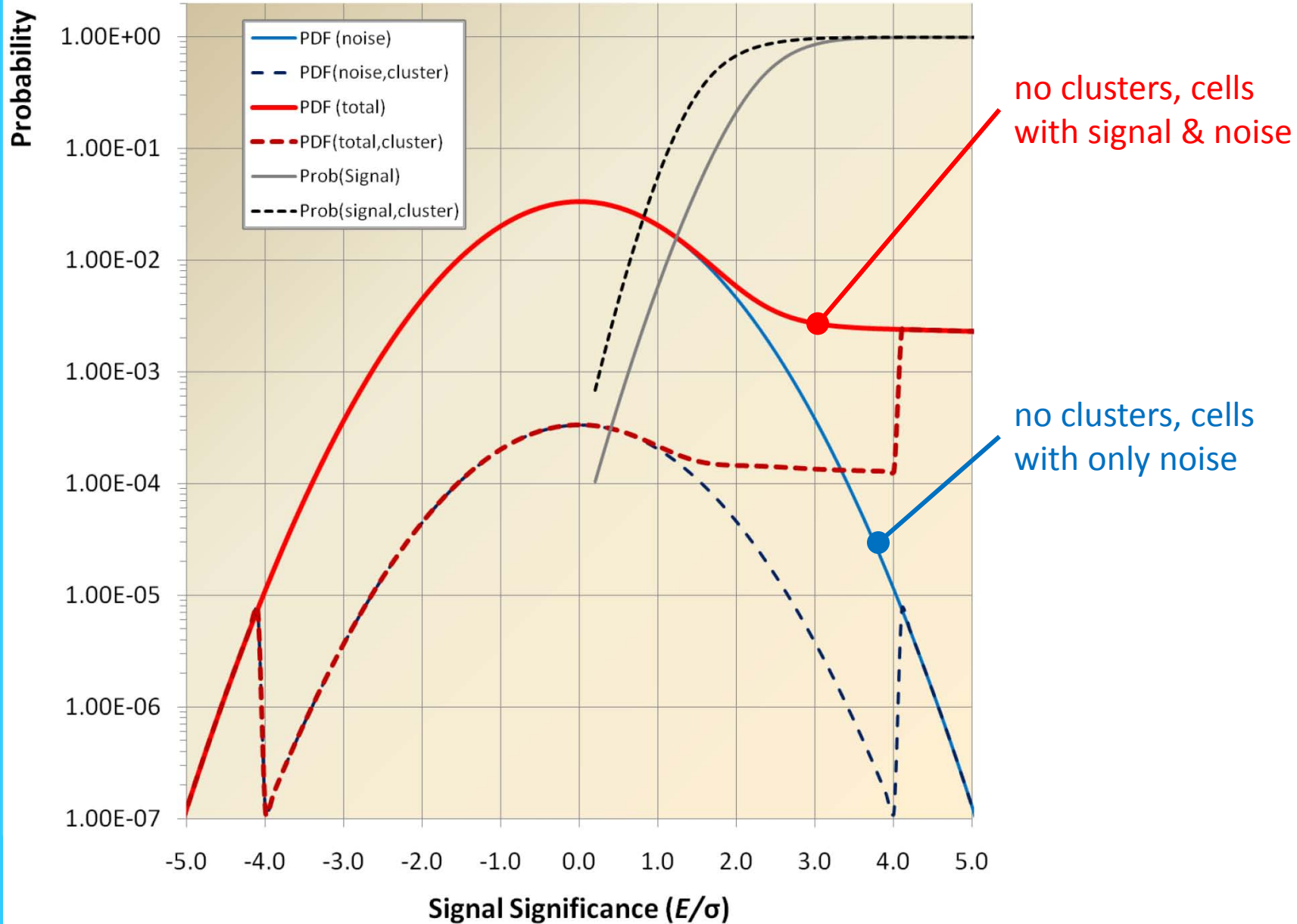


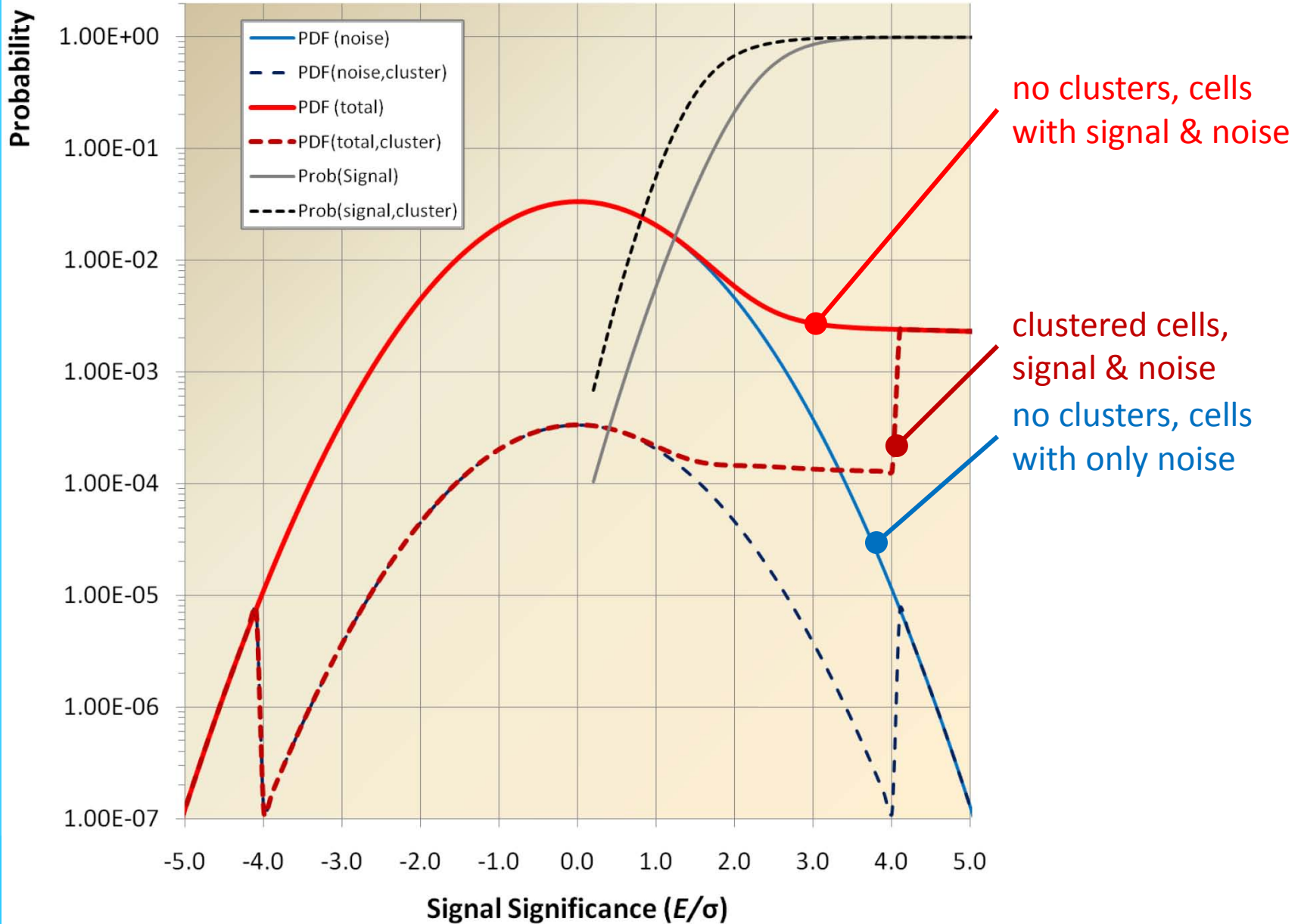


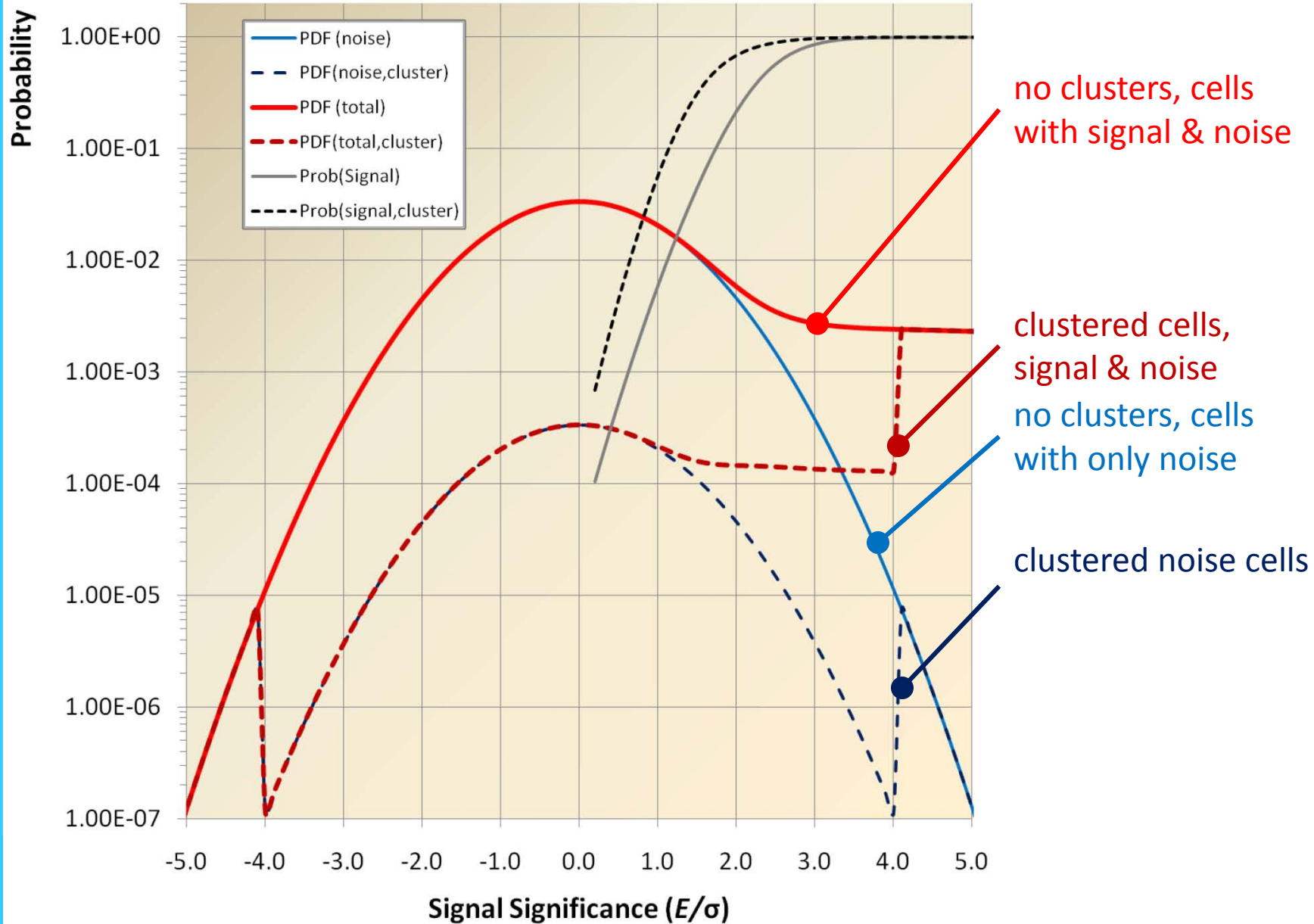
Modeled effect of topological clustering on the cell signal significance spectrum, for purposes of illustration here with only the primary (seed) threshold, no secondary (growth) threshold.

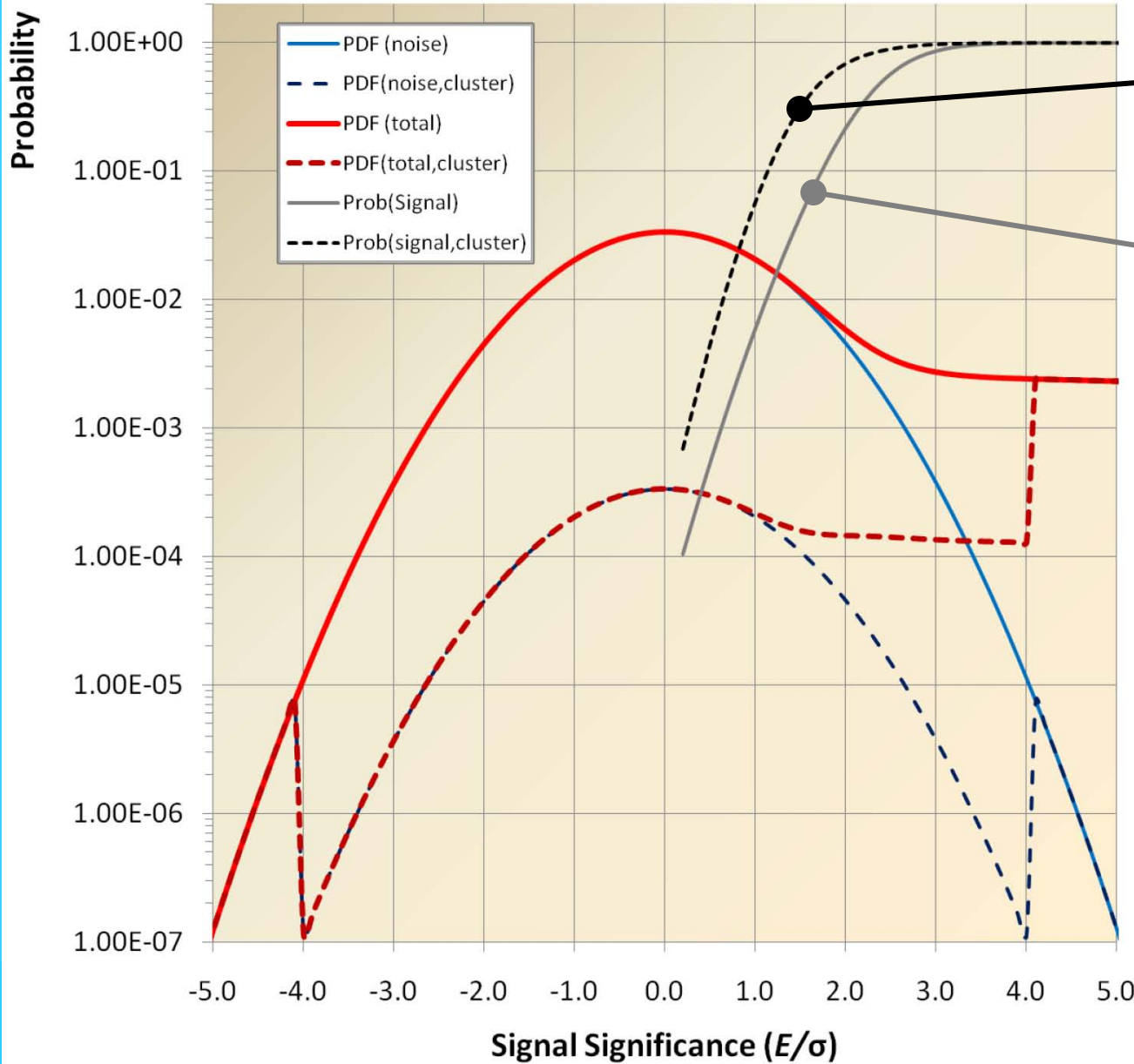








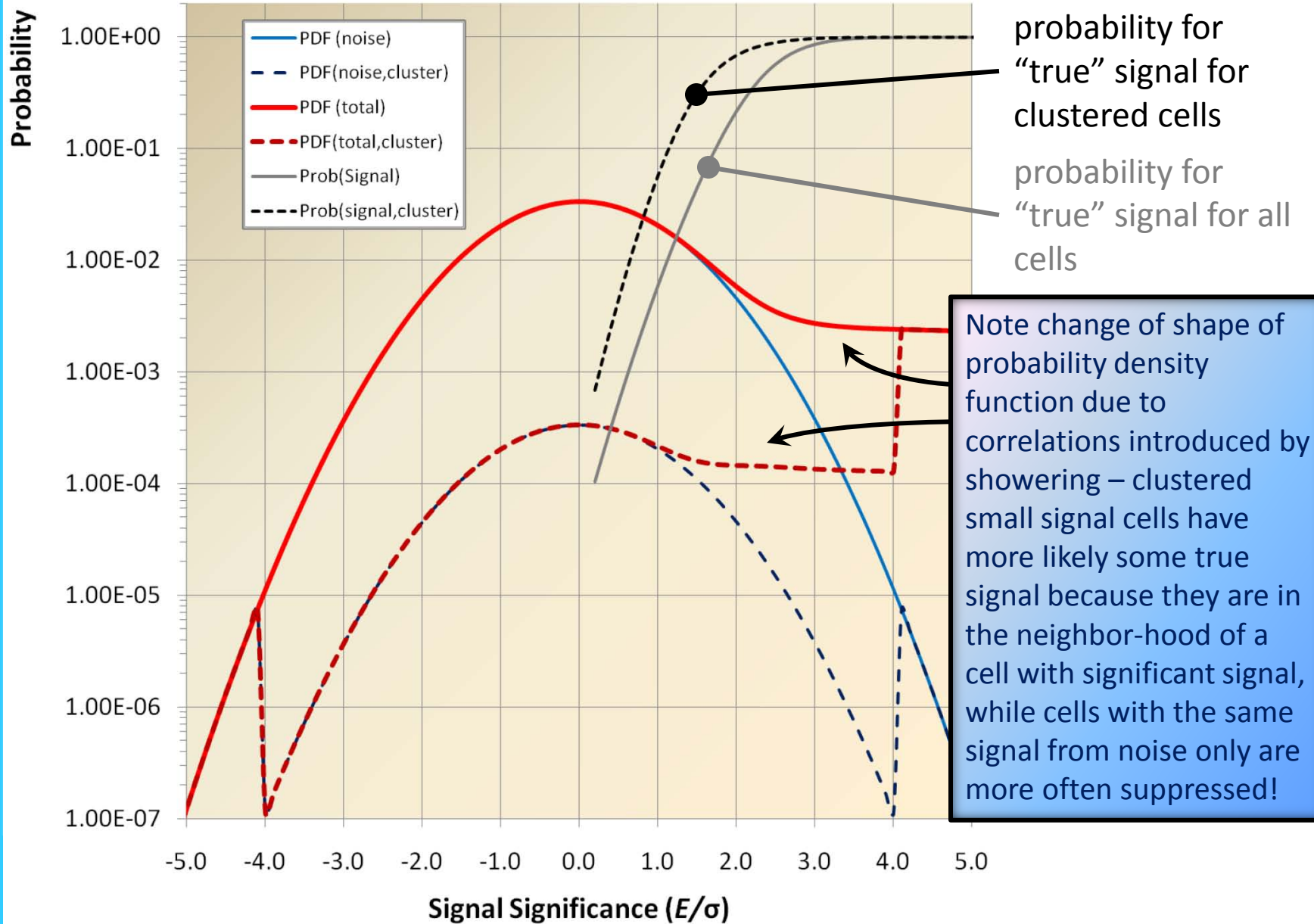


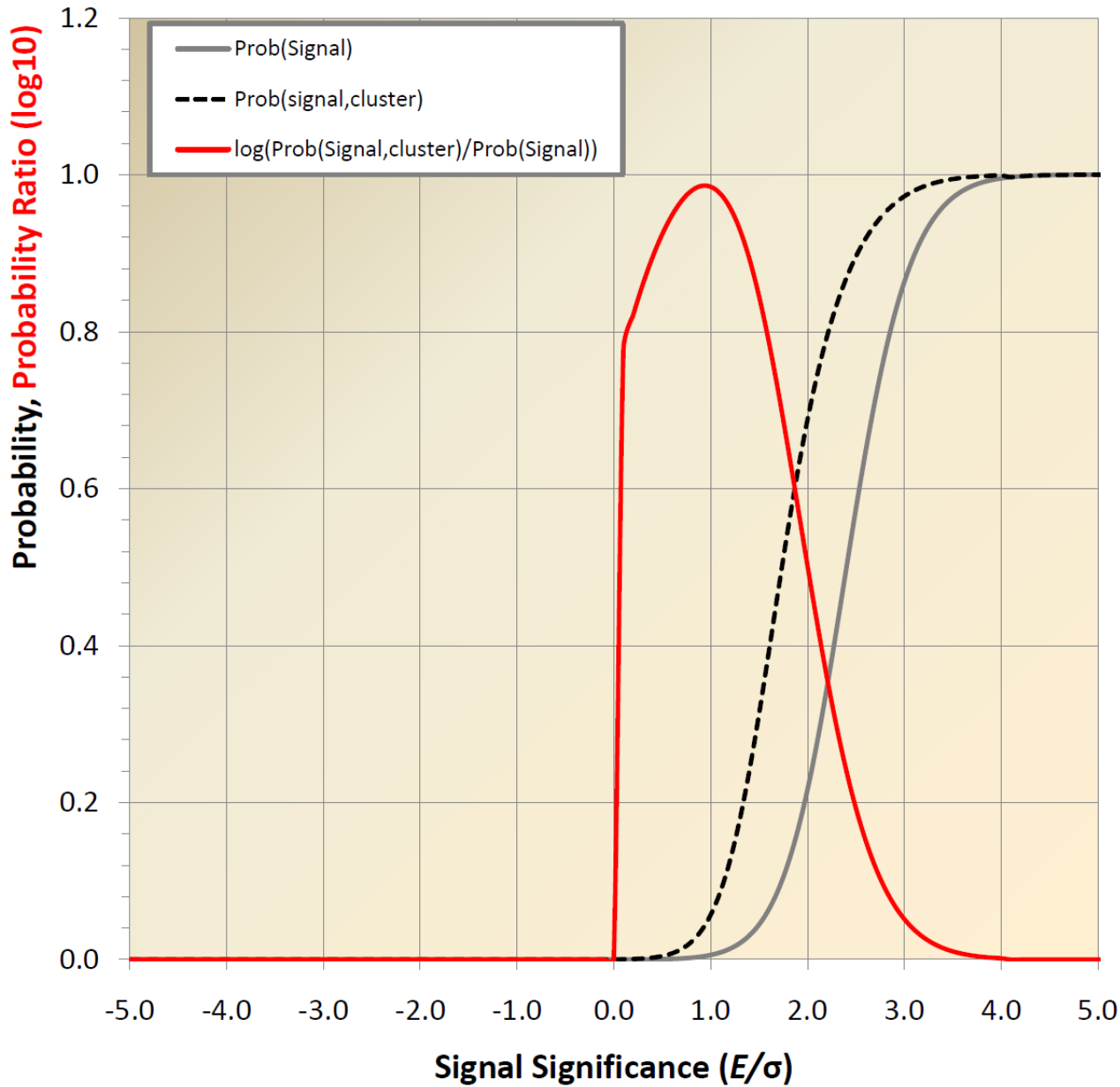


probability for "true" signal for clustered cells

probability for "true" signal for all cells







Significant boost of likelihood that small signals are generated by particles (rather than noise) in clustered cells!



Cluster signal

Sum of clustered cell energies

Possibly with geometrical weight introduced by cluster splitting

Cluster direction & location

Barycenter in (η, ϕ) from energy weighted cell directions

Negative signal cells contribute with absolute of their signal

Small effect on direction of final cluster from particles – negative signals are noise, i.e. small!

Consistent approach for direction calculation

Leaves true signal and noise clusters at the right direction

Same approach for geometrical signal center

“center of gravity”

Cluster four-momentum

Massless pseudo-particle approach similar to tower

Consistent with cluster idea of reconstructing showers rather than particles

Total cluster signal:

(electromagnetic energy scale)

$$E_{0, \text{cluster}} = \sum_{\text{clustered cells}} w_{\text{cell, cluster}} E_{0, \text{cell}}$$

(with $w_{\text{cell, cluster}} \neq 1$ only for cells shared between clusters)

Direction and location:

$$\eta_{\text{cluster}} = \frac{\sum_{\text{clustered cells}} w_{\text{cell, cluster}} |E_{0, \text{cell}}| \eta_{\text{cell}}}{\sum_{\text{clustered cells}} w_{\text{cell, cluster}} |E_{0, \text{cell}}|}$$

$$\phi_{\text{cluster}} = \frac{\sum_{\text{clustered cells}} w_{\text{cell, cluster}} |E_{0, \text{cell}}| \phi_{\text{cell}}}{\sum_{\text{clustered cells}} w_{\text{cell, cluster}} |E_{0, \text{cell}}|}$$

$(x_{\text{cluster}}, y_{\text{cluster}}, z_{\text{cluster}})$

$$= \frac{\sum_{\text{clustered cells}} w_{\text{cell, cluster}} |E_{0, \text{cell}}| (x_{\text{cell}}, y_{\text{cell}}, z_{\text{cell}})}{\sum_{\text{clustered cells}} w_{\text{cell, cluster}} |E_{0, \text{cell}}|}$$



Cluster signal

Sum of clustered cell energies

Possibly with geometrical weight introduced by cluster splitting

Cluster direction & location

Barycenter in (η, φ) from energy weighted cell directions

Negative signal cells contribute with absolute of their signal

Small effect on direction of final cluster from particles – negative signals are noise, i.e. small!

Consistent approach for direction calculation

Leaves true signal and noise clusters at the right direction

Same approach for geometrical signal center

“center of gravity”

Cluster four-momentum

Massless pseudo-particle approach similar to tower

Consistent with cluster idea of reconstructing showers rather than particles

Cluster four-momentum

(electromagnetic energy scale)

$$(E_{\text{cluster}}, \vec{p}_{\text{cluster}}) = E_{0,\text{cluster}} \begin{pmatrix} 1 \\ \cos \varphi_{\text{cluster}} / \sinh \eta_{\text{cluster}} \\ \sin \varphi_{\text{cluster}} / \sinh \eta_{\text{cluster}} \\ \tanh \eta_{\text{cluster}} \end{pmatrix}$$

with:

$$E_{\text{cluster}} = |\vec{p}_{\text{cluster}}| = p_{\text{cluster}}$$



Signal integration

Clusters sum cell signals without grid

3-dimensional signal objects

Can include partial and complete signals from several particles

Clusters preserve some detailed signal features

Associated information to be collected at cluster formation

E.g., energy sharing in electromagnetic and hadronic calorimeters

Longitudinal signal center of gravity

Shapes

Signal splitting

Topological clusters need splitting algorithm

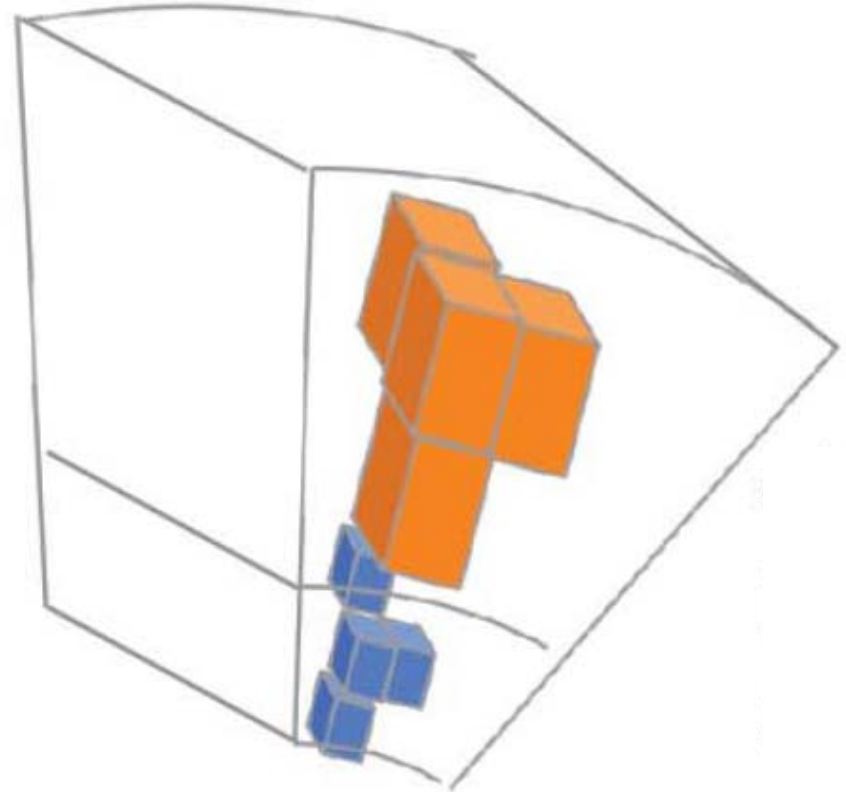
Cannot follow individual showers perfectly in jet environments

Can cause problems with infrared safety

Few problems with seed and energy leakage

Can include energy from cells even outside of jet cone

(drawing by K. Perez, Columbia University)



Topological cell cluster is a "blob" of energy dynamically located inside the calorimeter (even crossing sub-detector boundaries)

Signal formation

Fill towers with cells from topological clusters

These survived noise suppression

Same energy collection as unbiased towers

Signal integration

Sum cell signals on tower grid

2-dimensional signal objects

Can include partial and complete signals from several particles

Same additional signal features as unbiased towers

Associated information to be collected at tower formation

E.g., energy sharing in electromagnetic and hadronic calorimeters

Longitudinal signal center of gravity

Signal splitting

Can split showers, have problems with seeds, and cell energy “leakage”

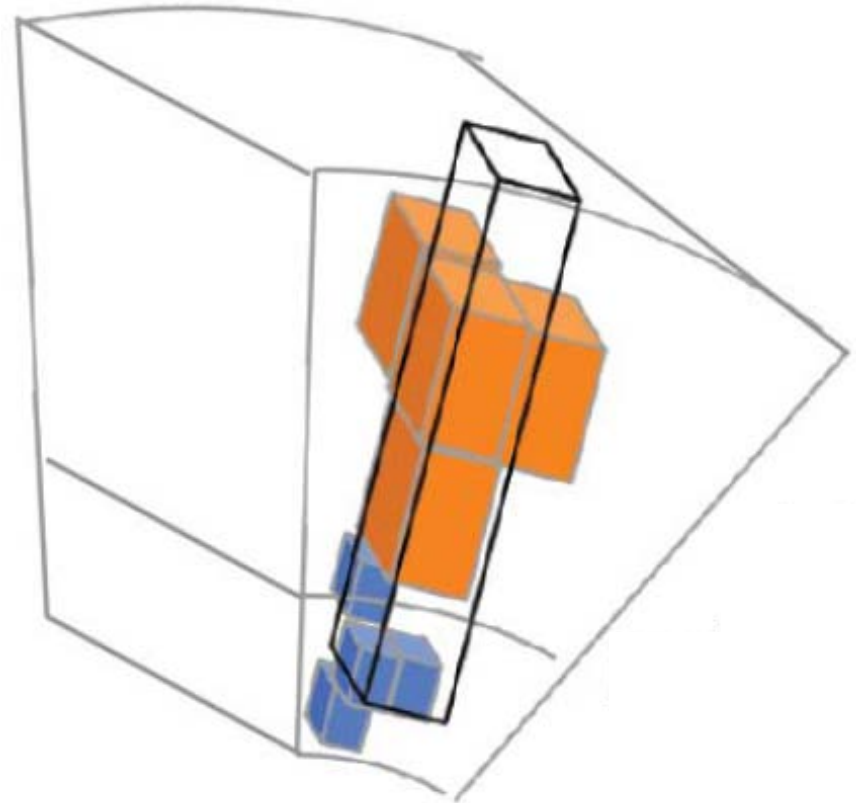
Same problems as unbiased tower

Applies regular geometrical splitting

Transverse energy flow motivated energy distribution

Avoid splitting threshold parameter

(drawing by K. Perez, Columbia University)



Noise suppressed towers are sparsely populated slabs of energy in a regular pseudorapidity-azimuth grid (each tower covers the same area in these coordinates)



Introduction to Hadronic Final State Reconstruction in Collider Experiments (Part XI)

Peter Loch
University of Arizona
Tucson, Arizona
USA



General cluster features

Motivated by shower reconstruction

No bias in signal definition towards reconstruction of a certain, possibly very specific, physics signal object like a jet

Clusters have shapes and location information

Spatial cell energy distributions and their correlations drive longitudinal and lateral extensions

Density and energy sharing measures

Signal center of gravity and (directional) barycenter

Shapes are sensitive to shower nature

At least for a reasonable clustering algorithm

Local (cluster) calibration strategy

First reconstruct truly deposited energy at cluster location...

e/h, mostly

...then correct for other energy losses in the vicinity of signal cluster

Dead material energy losses and signal losses due to noise suppression

Calibration input

Reconstructed cluster shapes represent shower shapes

E.g., dense and compact clusters indicate electromagnetic shower activity anywhere in the calorimeter

Can be intrinsic to a hadronic shower!

Calibration functions can exploit the cluster shapes to apply the corrections for $e/h \neq 1$ dynamically

Location of cluster together with shape

E.g., dense and compact clusters located in electromagnetic calorimeter indicate electron or photon as particle originating the signal

Cluster not (part of) hadronic shower signal!

Clusters can be classified before calibration

Electron/photon clusters need different calibration than dense clusters from hadronic showers!

Cluster calibration extensions

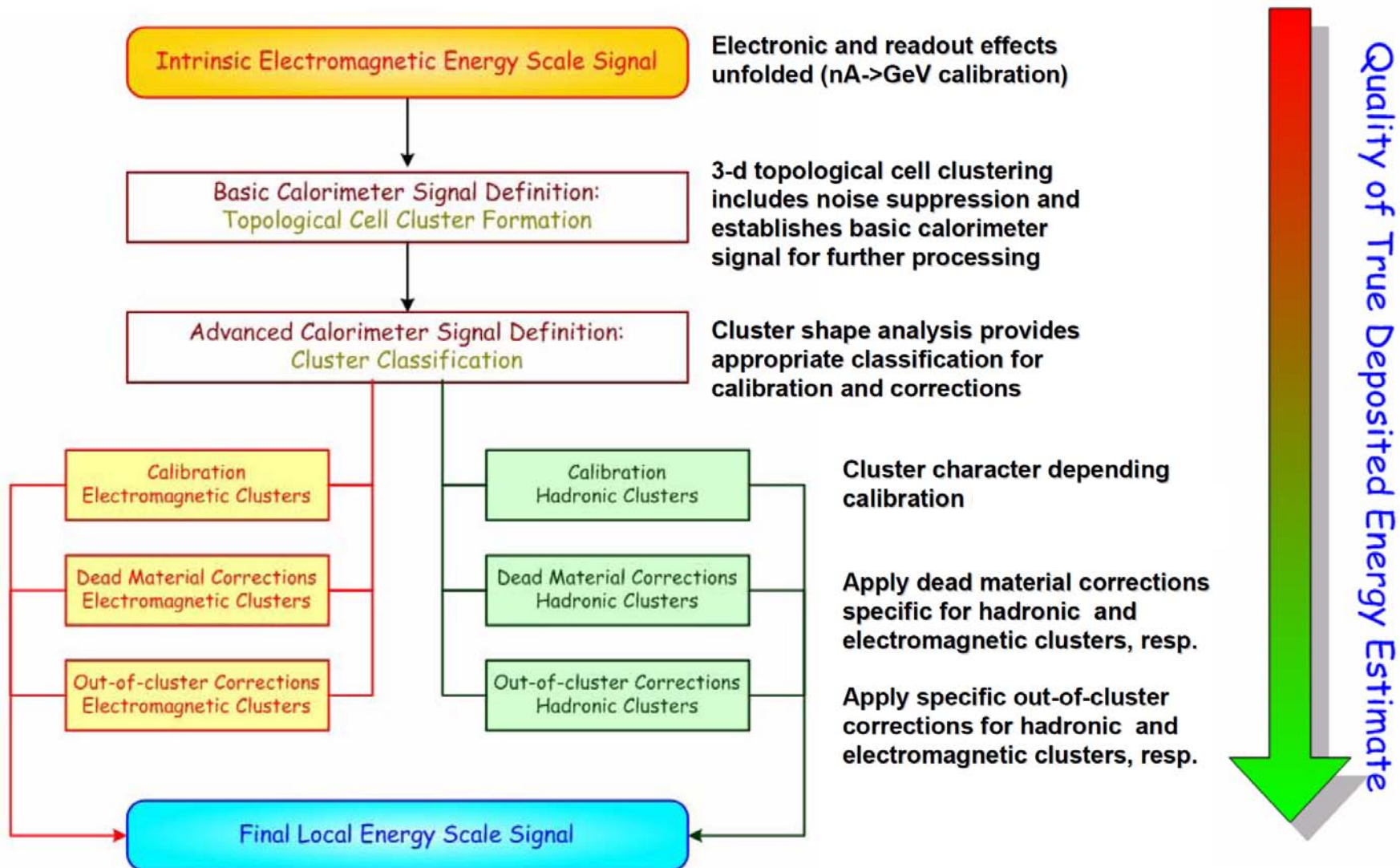
Shapes, location and size also indicate possible energy losses around the cluster

Some correlations between energy losses in inactive material in front or inside of clusters

Cluster size and signal neighbourhood sensitive to lost true signal in noise suppression algorithm

Out-of-cluster corrections





Phase-space pion counting method

Classify clusters using the correlation of

Shower shape variables in single π^\pm MC events

λ_{cluster} = cluster center of gravity depth in calorimeter

$$\bar{\rho}_{\text{cluster}} = \frac{1}{E_{0,\text{cluster}}} \sum_{\text{cells in cluster}} E_{0,\text{cell}} \cdot \rho_{\text{cell}}$$

Electromagnetic fraction estimator in bin of shower shape variables:

$$F \equiv \frac{\varepsilon(\pi^0)}{\varepsilon(\pi^0) + 2\varepsilon(\pi^-)}$$

$$\varepsilon(X) = \frac{N(X) \text{ producing a cluster in a given } (\eta, E_{0,\text{cluster}}, \lambda_{\text{cluster}}, \bar{\rho}_{\text{cluster}})}{N(X) \text{ total}}$$

Implementation

keep F in bins of η , E , λ , ρ of clusters for a given cluster

If $E < 0$, then classify as unknown

Lookup F from the observables $|\eta|$, E , λ , ρ

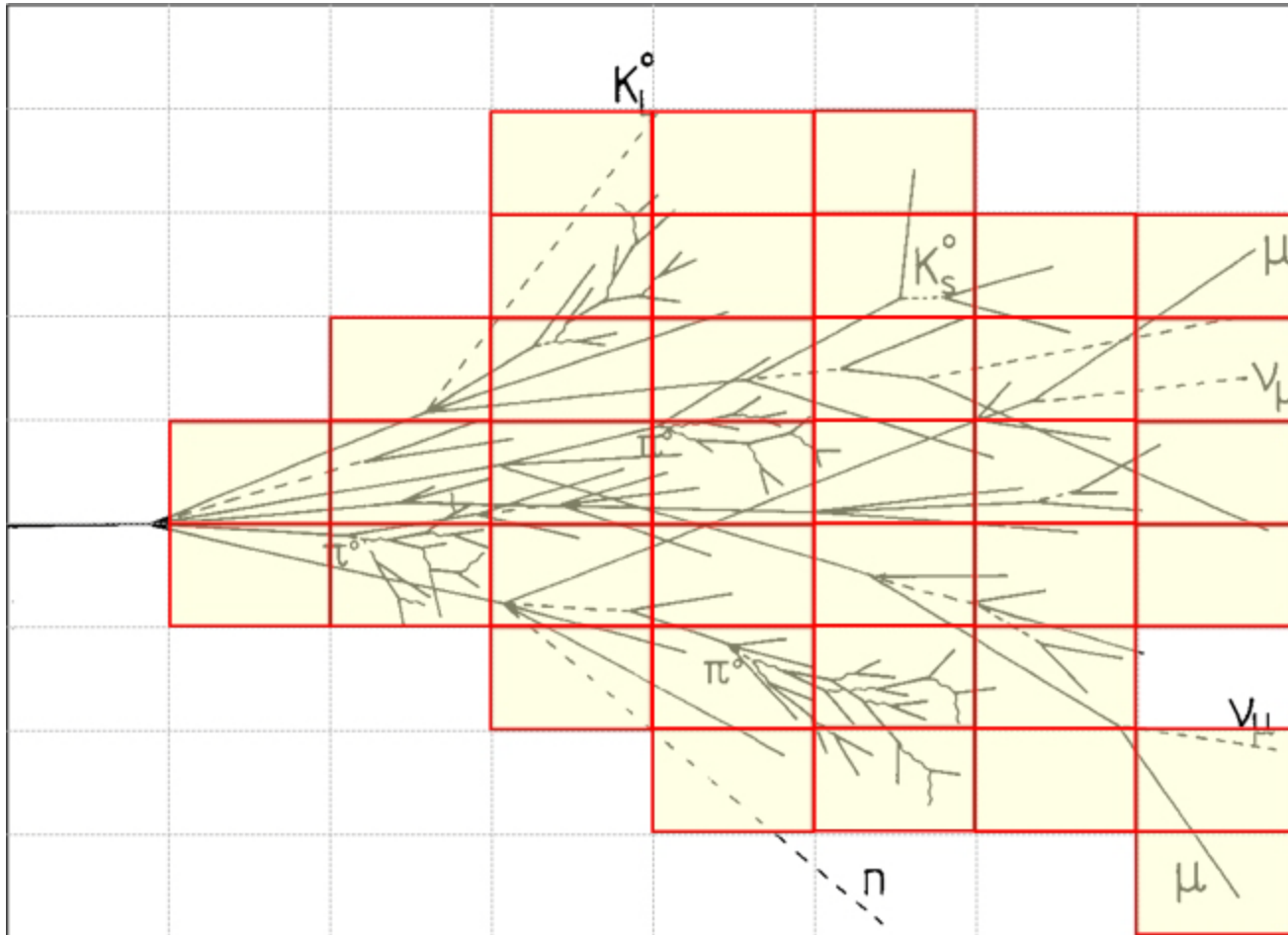
Cluster is EM if $F > 50\%$, hadronic otherwise



Calibration with cell signal weights

Idea is to compensate for lack of pion response in each cell

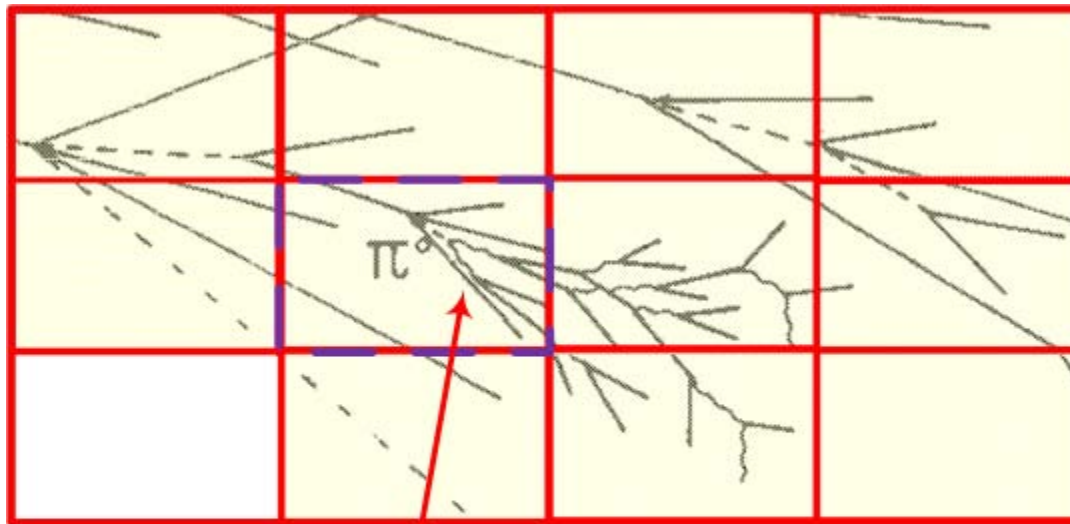
Pioneered in CDHS and applied in H1



Calibration with cell signal weights

Idea is to compensate for lack of pion response in each cell

Pioneered in CDHS and applied in H1



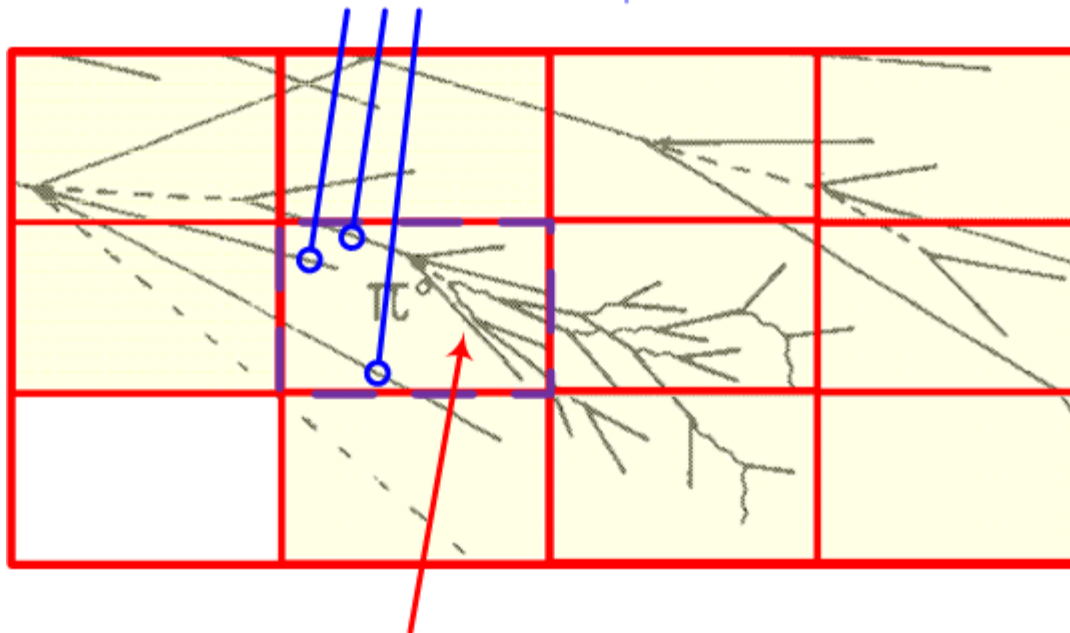
$$E_{\text{cell}}^{\text{em}} = [E_{\text{cell}}^{\text{em}}]_{\text{active}} + [E_{\text{cell}}^{\text{em}}]_{\text{passive}}$$

Calibration with cell signal weights

Idea is to compensate for lack of pion response in each cell

Pioneered in CDHS and applied in H1

$$E_{\text{cell}}^{\text{ion}} = \left[E_{\text{cell}}^{\text{ion}} \right]_{\text{active}} + \left[E_{\text{cell}}^{\text{ion}} \right]_{\text{passive}}$$

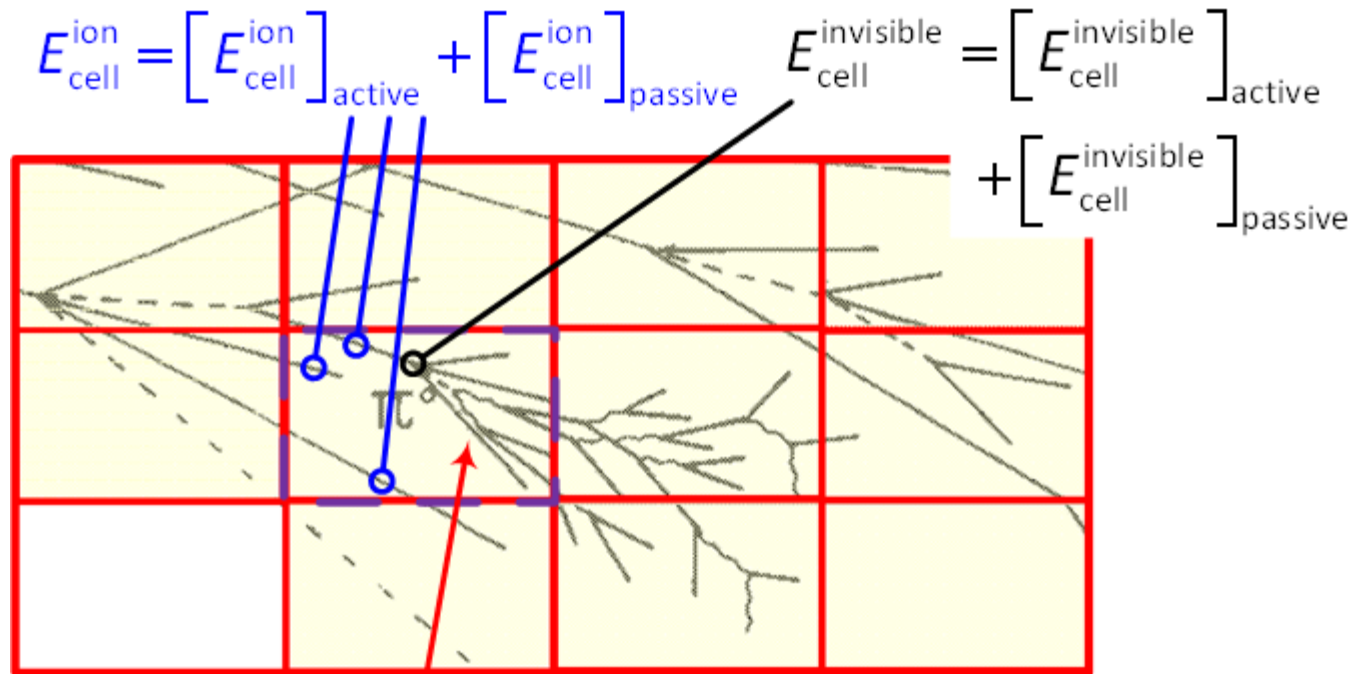


$$E_{\text{cell}}^{\text{em}} = \left[E_{\text{cell}}^{\text{em}} \right]_{\text{active}} + \left[E_{\text{cell}}^{\text{em}} \right]_{\text{passive}}$$

Calibration with cell signal weights

Idea is to compensate for lack of pion response in each cell

Pioneered in CDHS and applied in H1



$$E_{\text{cell}}^{\text{em}} = \left[E_{\text{cell}}^{\text{em}} \right]_{\text{active}} + \left[E_{\text{cell}}^{\text{em}} \right]_{\text{passive}}$$

Calibration with cell signal weights

Idea is to compensate for lack of pion response in each cell

Pioneered in CDHS and applied in H1

Uses deposited energies in cells

Deposit can be in active or passive medium of calorimeter!

$$w_{\text{cell,cluster}}^{\text{calib}} = \left\langle \frac{E_{\text{deposited,cell}} = E_{\text{cell}}^{\text{em}} + E_{\text{cell}}^{\text{ion}} + E_{\text{cell}}^{\text{invisible}} + E_{\text{cell}}^{\text{escaped}}}{\text{"deposited" energy anywhere within cell boundaries}} \cdot \frac{E_{0,\text{cell}} = c_{\text{em}} \cdot A \left(\left[E_{\text{cell}}^{\text{em}} \oplus E_{\text{cell}}^{\text{ion}} \right]_{\text{active}}, t, \vec{X}, \dots \right)}{\text{reconstructed em scale signal}} \right\rangle$$

($E_{\text{cell}}^{\text{escaped}}$ is the energy escaping the calorimeter, i.e. carried by neutrinos - it is often assigned to the cell in which the neutrino vertex is located)



Calibration with cell signal weights

Idea is to compensate for lack of pion response in each cell

Pioneered in CDHS and applied in H1

Uses deposited energies in cells

Deposit can be in active or passive medium of calorimeter!

$$w_{\text{cell,cluster}}^{\text{calib}} = \left\langle \frac{E_{\text{deposited,cell}} = E_{\text{cell}}^{\text{em}} + E_{\text{cell}}^{\text{ion}} + E_{\text{cell}}^{\text{invisible}} + E_{\text{cell}}^{\text{escaped}}}{\text{"deposited" energy anywhere within cell boundaries}} \right\rangle$$

$$E_{0,\text{cell}} = c_{\text{em}} \cdot A \left(\left[E_{\text{cell}}^{\text{em}} \oplus E_{\text{cell}}^{\text{ion}} \right]_{\text{active}}, t, \vec{X}, \dots \right)$$

reconstructed em scale signal

Only signal contribution from energy deposited by electromagnetic sub-showers and through ionization by charged particles!



Calibration with cell signal weights

Idea is to compensate for lack of pion response in each cell

Pioneered in CDHS and applied in H1

Uses deposited energies in cells

Deposit can be in active or passive medium of calorimeter!

Energy deposited in cell not available in experiment

Use of detector simulations

Deposited energy and signal available

Use “unit cell” volume concept to collect invisible energies

Shower model dependent!

Use single pion testbeam data

Develop model for weights in cells

Fit parameters of model using cells testbeam

Minimize resolution with beam energy constraint

Statistical – does not necessarily produce the correct weights!



Basic idea

Use a dynamically self-adjusting calibration weight

High cell signal density →
electromagnetic deposit

Low cell signal density → hadronic
deposit

Principal weighting function characteristics

Depends on cell energy density

Depends on cell location

Accidental application to electron signals
should yield correct energy as well

Extraction of weighting functions

Minimize resolution in (pion) testbeam data

Fitting function model

May not produce the correct weights –
may even be unphysical!

Use simulation

Deterministic approach relates signal to
deposited energy within cell volume – no
fitting!

May depend on details of (hadronic)
shower modeling

$$E_{\text{rec,cell}} = w_{\text{cell}}(\dots) \cdot E_{0,\text{cell}} = E_{\text{deposited,cell}}$$



Basic idea

Use a dynamically self-adjusting calibration weight

High cell signal density \rightarrow
electromagnetic deposit

Low cell signal density \rightarrow hadronic
deposit

Principal weighting function characteristics

Depends on cell energy density

Depends on cell location

Accidental application to electron signals
should yield correct energy as well

$$E_{\text{rec,cell}} = w_{\text{cell}}(\dots) \cdot E_{0,\text{cell}} = E_{\text{deposited,cell}}$$

$$w_{\text{cell}}(\dots) = w(\rho_{\text{cell}} = E_{0,\text{cell}}/V_{\text{cell}}, \vec{X}, \dots)$$

Extraction of weighting functions

Minimize resolution in (pion) testbeam data

Fitting function model

May not produce the correct weights –
may even be unphysical!

Use simulation

Deterministic approach relates signal to
deposited energy within cell volume – no
fitting!

May depend on details of (hadronic)
shower modeling



Basic idea

Use a dynamically self-adjusting calibration weight

High cell signal density \rightarrow
electromagnetic deposit

Low cell signal density \rightarrow hadronic
deposit

Principal weighting function characteristics

Depends on cell energy density

Depends on cell location

Accidental application to electron signals
should yield correct energy as well

Extraction of weighting functions

Minimize resolution in (pion) testbeam data

Fitting function model

May not produce the correct weights –
may even be unphysical!

Use simulation

Deterministic approach relates signal to
deposited energy within cell volume – no
fitting!

May depend on details of (hadronic)
shower modeling

$$E_{\text{rec,cell}} = w_{\text{cell}}(\dots) \cdot E_{0,\text{cell}} = E_{\text{deposited,cell}}$$

$$w_{\text{cell}}(\dots) = w(\rho_{\text{cell}} = E_{0,\text{cell}}/V_{\text{cell}}, \vec{x}, \dots)$$

e.g. in H1:

$$E_{\text{rec,cell}} = \underbrace{\left(1 + \alpha(\vec{x}, \dots) \cdot e^{-\beta(\vec{x}, \dots) \cdot \rho_{\text{cell}}}\right)}_{=w(\rho_{\text{cell}}, \vec{x}, \dots)} \cdot E_{0,\text{cell}},$$

with $\lim_{\rho_{\text{cell}} \rightarrow \infty} E_{\text{rec,cell}} = E_{0,\text{cell}}$



Basic idea

Use a dynamically self-adjusting calibration weight

High cell signal density →
electromagnetic deposit

Low cell signal density → hadronic
deposit

Principal weighting function characteristics

Depends on cell energy density

Depends on cell location

Accidental application to electron signals
should yield correct energy as well

Extraction of weighting functions

Minimize resolution in (pion) testbeam data

Fitting function model

May not produce the correct weights –
may even be unphysical!

Use simulation

Deterministic approach relates signal to
deposited energy within cell volume – no
fitting!

May depend on details of (hadronic)
shower modeling

Fit $\alpha(\vec{x}, \dots), \beta(\vec{x}, \dots)$ with

$$\chi^2 = \sum_{\text{events}} \frac{(E_{\text{rec, cell}} - E_{\text{beam}})^2}{\sigma^2} = \min$$

i.e.:

$$\frac{\partial \chi^2}{\partial \alpha} = 0 \quad \text{and} \quad \frac{\partial \chi^2}{\partial \beta} = 0$$



Basic idea

Use a dynamically self-adjusting calibration weight

High cell signal density \rightarrow
electromagnetic deposit

Low cell signal density \rightarrow hadronic
deposit

Principal weighting function characteristics

Depends on cell energy density

Depends on cell location

Accidental application to electron signals
should yield correct energy as well

Extraction of weighting functions

Minimize resolution in (pion) testbeam data

Fitting function model

May not produce the correct weights –
may even be unphysical!

Use simulation

Deterministic approach relates signal to
deposited energy within cell volume – no
fitting!

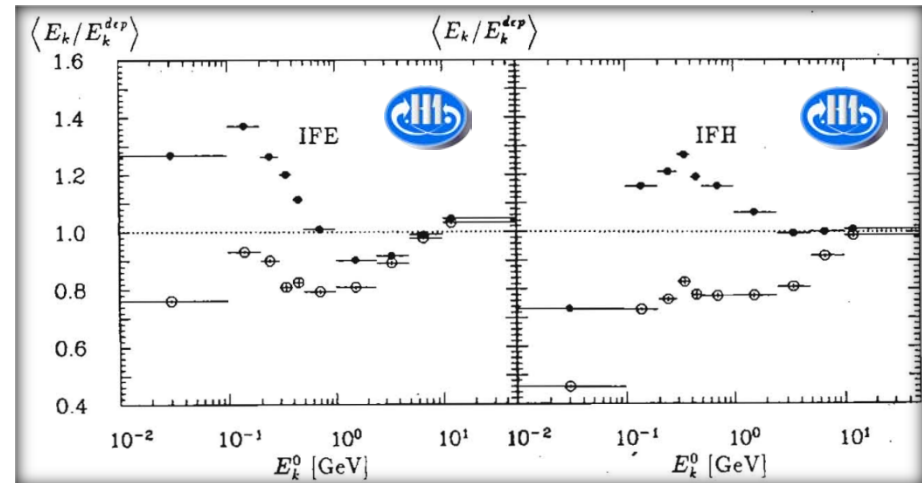
May depend on details of (hadronic)
shower modeling

Fit $\alpha(\vec{x}, \dots), \beta(\vec{x}, \dots)$ with

$$\chi^2 = \sum_{\text{events}} \frac{(E_{\text{rec,cell}} - E_{\text{beam}})^2}{\sigma^2} = \min$$

i.e.:

$$\frac{\partial \chi^2}{\partial \alpha} = 0 \quad \text{and} \quad \frac{\partial \chi^2}{\partial \beta} = 0$$



$$\circ \quad \frac{E_{\text{rec,cell}}}{E_{0,\text{cell}}} \quad \bullet \quad \frac{E_{\text{deposited,cell}}}{E_{0,\text{cell}}}$$



Basic idea

Use a dynamically self-adjusting calibration weight

High cell signal density \rightarrow
electromagnetic deposit

Low cell signal density \rightarrow hadronic
deposit

Principal weighting function characteristics

Depends on cell energy density

Depends on cell location

Accidental application to electron signals
should yield correct energy as well

Extraction of weighting functions

Minimize resolution in (pion) testbeam data

Fitting function model

May not produce the correct weights –
may even be unphysical!

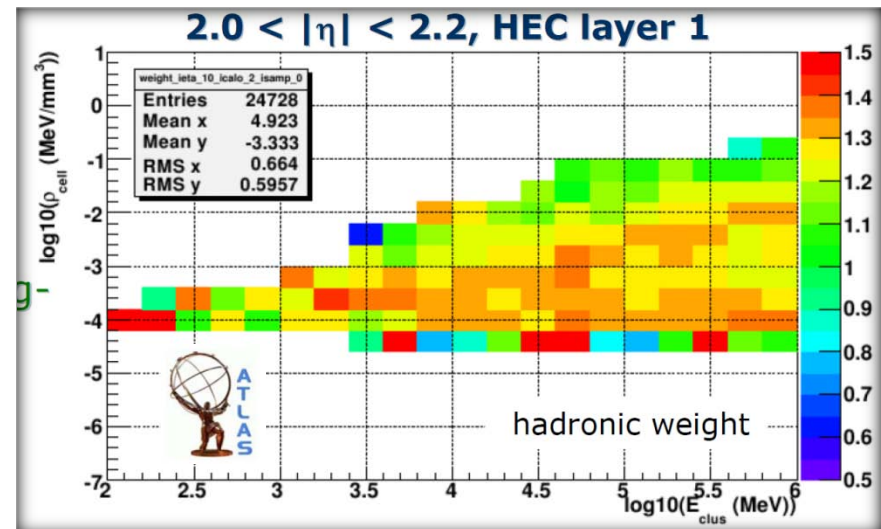
Use simulation

Deterministic approach relates signal to
deposited energy within cell volume – no
fitting!

May depend on details of (hadronic)
shower modeling

ATLAS cluster-based approach:

1. Use only cells in hadronic clusters
2. Cluster sets global energy scale as a reference for densities
3. Calculate $E_{\text{deposited,cell}}/E_{0,\text{cell}}$ from **single pion simulations** in bins of cluster energy, cell energy density, cluster direction, and calorimeter sampling layer
4. Store $[E_{\text{deposited,cell}}/E_{0,\text{cell}}]^{-1}$ in look-up tables



Basic idea

Use a dynamically self-adjusting calibration weight

High cell signal density →
electromagnetic deposit

Low cell signal density → hadronic
deposit

Principal weighting function characteristics

Depends on cell energy density

Depends on cell location

Accidental application to electron signals
should yield correct energy as well

Extraction of weighting functions

Minimize resolution in (pion) testbeam data

Fitting function model

May not produce the correct weights –
may even be unphysical!

Use simulation

Deterministic approach relates signal to
deposited energy within cell volume – no
fitting!

May depend on details of (hadronic)
shower modeling

ATLAS cluster-based approach:

1. Use only cells in hadronic clusters
2. Cluster sets global energy scale as a reference for densities
3. Calculate $E_{\text{deposited,cell}}/E_{0,\text{cell}}$ from **single pion simulations** in bins of cluster energy, cell energy density, cluster direction, and calorimeter sampling layer
4. Store $[E_{\text{deposited,cell}}/E_{0,\text{cell}}]^{-1}$ in look-up tables
5. Retrieve weights for any cell in any cluster from look-up table to reconstruct cell and cluster energies

$$E_{\text{rec,cluster}}^{\text{calib}} = \sum_{\text{cells in cluster}} E_{\text{rec,cell}} = \sum_{\text{cells in cluster}} w_{\text{cell,cluster}}^{\text{calib}} (E_{0,\text{cluster}}, \eta_{\text{cluster}}, S_{\text{cell}}, \rho_{\text{cell}}) \cdot E_{0,\text{cell}}$$



Dead material

Energy losses not directly measurable

Signal distribution in vicinity can help

Introduces need for signal corrections up to O(10%)

Exclusive use of signal features

Corrections depend on electromagnetic or hadronic energy deposit

Major contributions

Upstream materials

Material between LArG and Tile (central)

Cracks

dominant sources for signal losses

$|\eta| \approx 1.4-1.5$

$|\eta| \approx 3.2$

Clearly affects detection efficiency for particles and jets

Already in trigger!

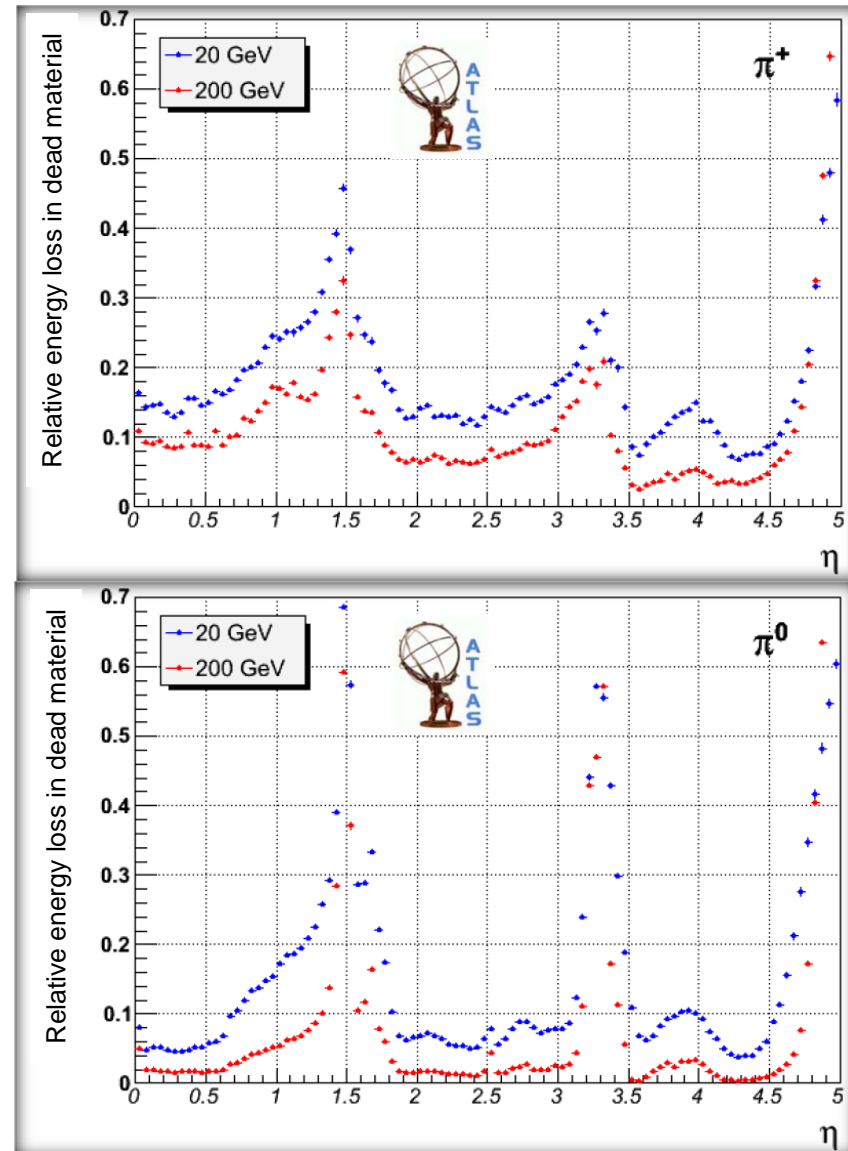
Hard to recover jet reconstruction inefficiencies

Generate fake missing E_t contribution

Topology dependence of missing E_t reconstruction quality

Additive correction:

$$E_{\text{rec,cluster}}^{\text{calib+DM}} = E_{\text{rec,cluster}}^{\text{calib}} + E_{\text{rec,cluster}}^{\text{DM}}(\vec{x}_{\text{cluster}}, \dots)$$



Compensate loss of true signal

Limited efficiency of noise suppression scheme

Discard cells with small true energy not close to a primary or secondary seed

Accidental acceptance of a pure noise cell

Can be significant for isolated pions

10% at low energy

Correction derived from single pions

Compensates the isolated particle loss

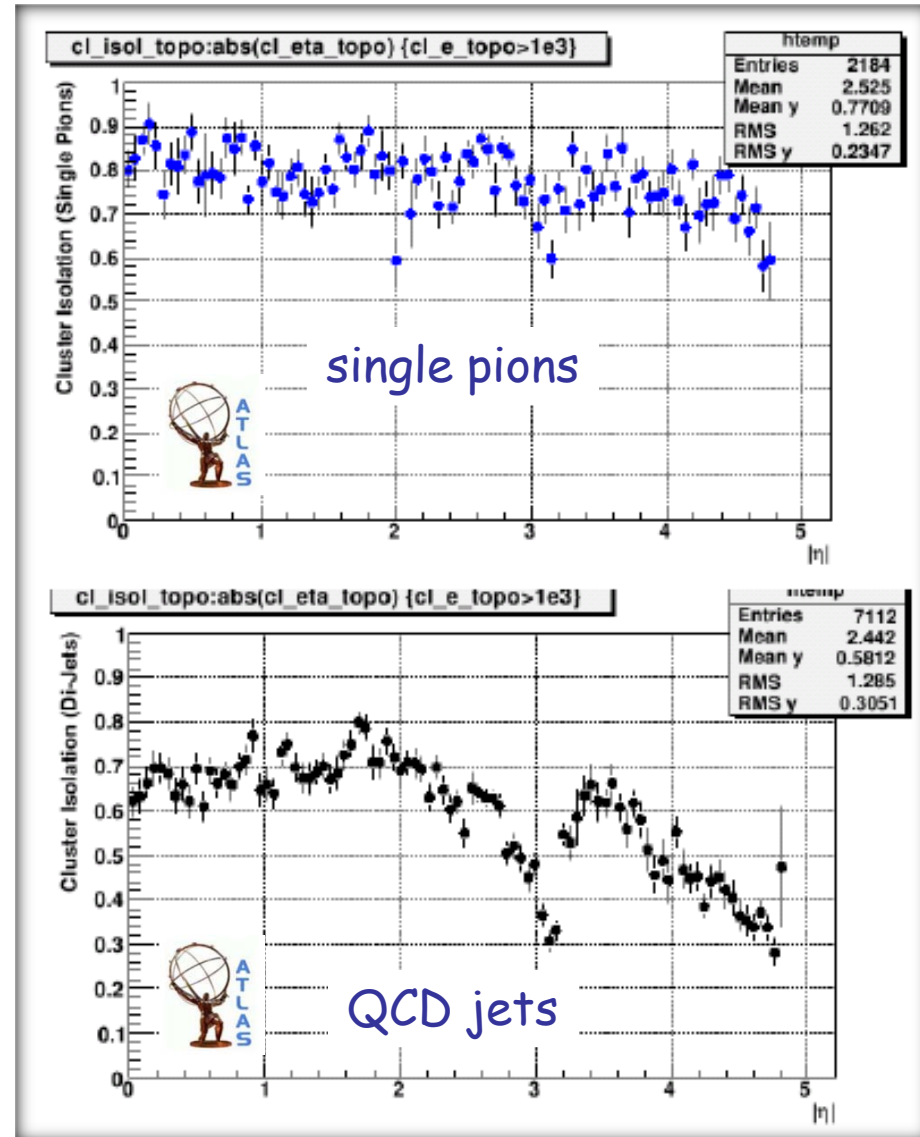
But in jets neighboring clusters can pick up lost energy

Use isolation moment to measure effective “free surface” of each cluster

Scale single pion correction with this moment (0...1)

Additive correction:

$$\begin{aligned}
 E_{\text{rec,cluster}}^{\text{calib+DM+OOC}} &= E_{\text{rec,cluster}} \\
 &= E_{\text{rec,cluster}}^{\text{calib+DM}} + E_{\text{rec,cluster}}^{\text{OOC}}(\vec{x}_{\text{cluster}}, m_{\text{isol}}, E_{0,\text{cluster}}, \dots)
 \end{aligned}$$



Attempt to calibrate hadronic calorimeter signals in smallest possible signal context

Topological clustering implements noise suppression with least bias signal feature extraction

Residual concerns about infrared safety!

No bias towards a certain physics analysis

Calibration driven by calorimeter signal features without further assumption

Good common signal base for all hadronic final state objects

Jets, missing E_t , taus

Factorization of cluster calibration

Cluster classification largely avoids application of hadronic calibration to Electromagnetic signal objects

Low energy regime challenging

Signal weights for hadronic calibration are functions of cluster and cell parameters and variables

Cluster energy and direction

Cell signal density and location (sampling layer)

Dead material and out of cluster corrections are independently applicable

Factorized calibration scheme

Local calibration does not reproduce jet energy

Energy losses not correlated with cluster signals can not be corrected

Magnetic field losses

Dead material losses

Needs additional jet energy scale corrections

Use specific jet context to derive those

Only applicable to cluster jets!

$$E_{true}^{jet} = E_{dep}^{calo} + E_{mag}^{loss} + E_{low}^{loss} + E_{leak}^{loss} + E_{out}^{loss} - E_{UE\otimes PU}^{gain} - E_{env}^{gain}$$

E_{dep}^{calo} energy deposited in the calorimeter within signal definition

E_{mag}^{loss} charged particle energy lost in solenoid field

E_{low}^{loss} particle energy lost in dead material

E_{leak}^{loss} energy lost due to longitudinal leakage

E_{out}^{loss} energy lost due to jet algorithm/calorimeter signal definition

$E_{UE\otimes PU}^{gain}$ energy added by underlying event and/or pile-up

E_{env}^{gain} energy added by response from other nearby particles/jets

only source of signal!



Use jet context for cell calibration

Determine cell weights using jet energy constraints

Same principle idea as for local cell weighting, but different global energy scale

Needs jet truth reference

Jet context relevant

Supports assumption of hadronic signal activity

Has enhanced electromagnetic component contributing to the weighting function
 parameterizations of all cells – larger (volume/area) context than topological clustering

May be biased with respect to calorimeter signal definition and jet algorithms

Jet energy references for calorimeter jets

Simulation

Matching particle level jet (same jet definition) energy

Experiment

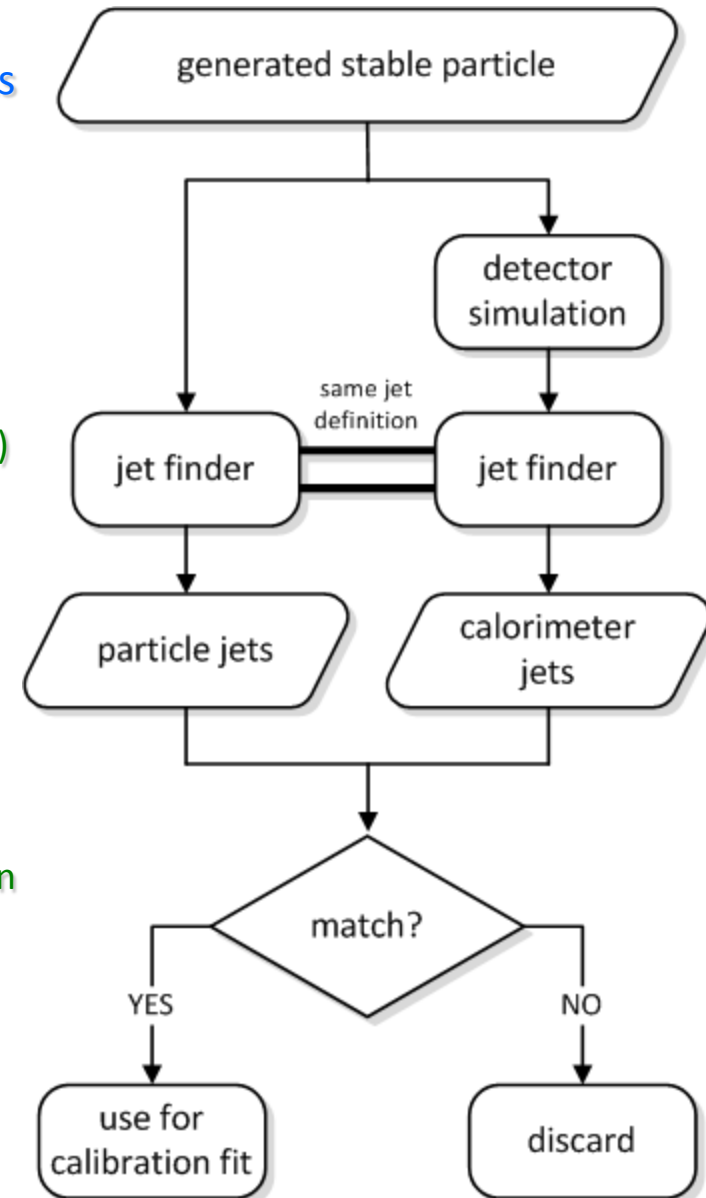
pT balance with electromagnetic system like photon or Z-boson

W mass spectroscopy

Sampling energy based jet calibration

Coarser than cell signals but less numerical complexity

Fewer function parameters



Simulated particle jets

Establish “true” energy reference to constrain calibration function fits for calorimeter jets

Attempt to reconstruct true jet energy

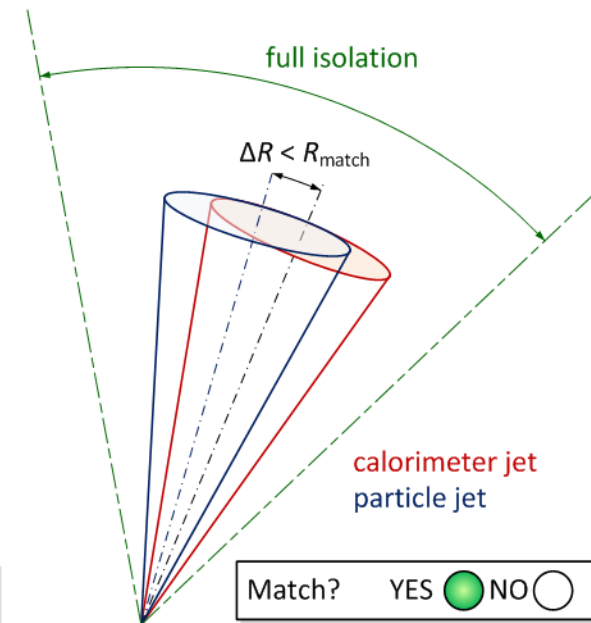
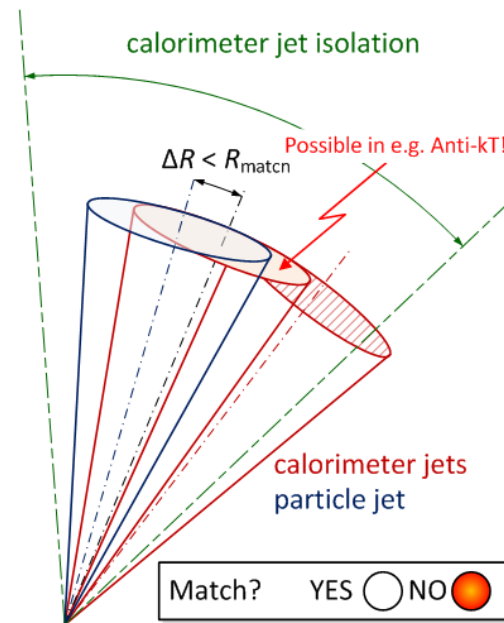
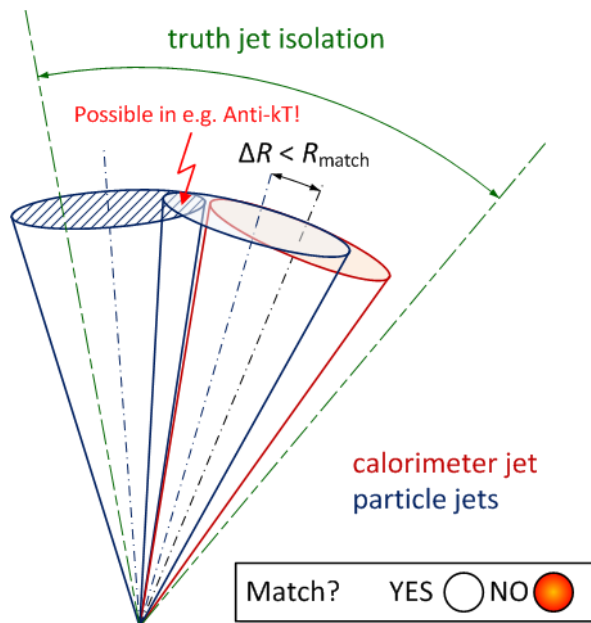
Need matching definition

Geometrical distance

Isolation and unique 1-to-1 jet matching

$$\Delta R =$$

$$\sqrt{(\eta_{\text{particle,jet}} - \eta_{\text{rec,jet}})^2 + (\phi_{\text{particle,jet}} - \phi_{\text{rec,jet}})^2}$$



Select matched jet pair

Typically small matching radius

$$R_{\text{match}} = 0.2 - 0.3$$

Restrict jet directions to regions with good calorimeter response

No excessive dead material

Away from cracks and complex transition geometries

Calibration functions

Cell signal weighting

Large weights for low density signals

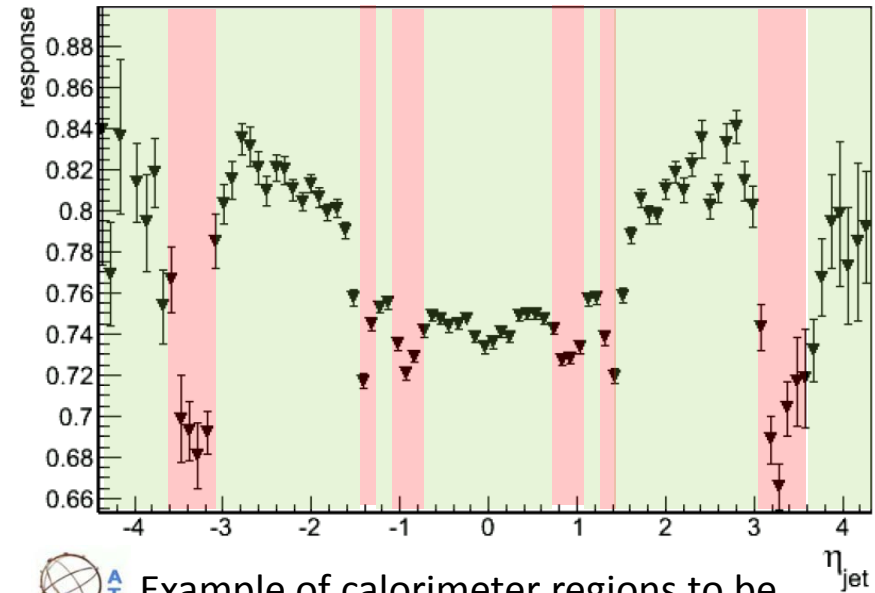
Small weights for high density signals

Sampling layer signal weighting

Weights determined by longitudinal energy sharing in calorimeter jet

Functions can be complex

Often highly non-linear systems



Example of calorimeter regions to be considered for jet calibration fits in ATLAS (tinted green). The red tinted regions indicate calorimeter cracks and transitions. The points show the simulated jet response on electromagnetic energy scale, as function of the jet pseudorapidity. (figure for illustration purposes only!)



Select matched jet pair

Typically small matching radius

$$R_{\text{match}} = 0.2 - 0.3$$

Restrict jet directions to regions with good calorimeter response

No excessive dead material

Away from cracks and complex transition geometries

Calibration functions

Cell signal weighting

Large weights for low density signals

Small weights for high density signals

Sampling layer signal weighting

Weights determined by longitudinal energy sharing in calorimeter jet

Functions can be complex

Often highly non-linear systems

$$E_{\text{rec,cell}} = w_{\text{cell}}(\rho_{\text{cell}}, \dots) \cdot E_{0,\text{cell}}$$

$$w_{\text{cell}}(\rho_{\text{cell}}, \dots) \begin{cases} \nearrow \text{for } \rho_{\text{cell}} \uparrow \\ \searrow \text{for } \rho_{\text{cell}} \downarrow \end{cases}$$

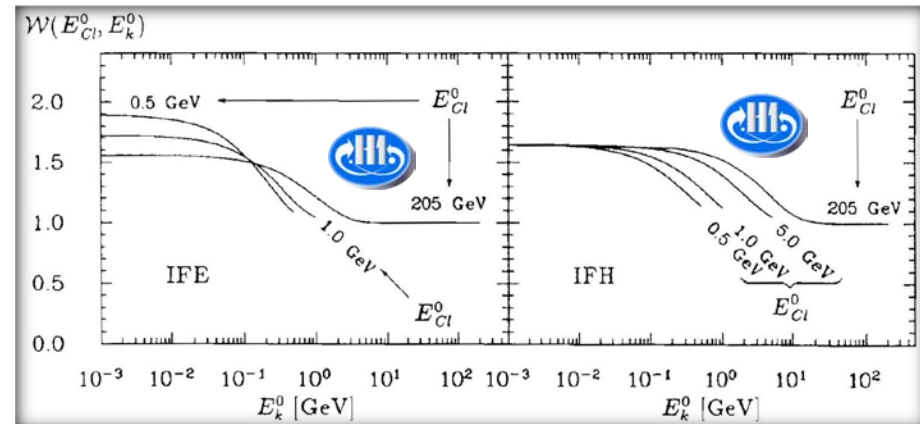
Typical boundary conditions:

$$\max(w_{\text{cell}}(\rho_{\text{cell}}, \dots)) \approx 1.5 - 3.0$$

(avoid boosting noise!)

$$\min(w_{\text{cell}}(\rho_{\text{cell}}, \dots)) = 1.0$$

(avoid suppressing em response!)



Example: cell signal weights \mathcal{W} , parameterized as function of the cell energy E_k^0 and the cluster energy E_{cl}^0



Select matched jet pair

Typically small matching radius

$$R_{\text{match}} = 0.2 - 0.3$$

Restrict jet directions to regions with good calorimeter response

No excessive dead material

Away from cracks and complex transition geometries

Calibration functions

Cell signal weighting

Large weights for low density signals

Small weights for high density signals

Sampling layer signal weighting

Weights determined by longitudinal energy sharing in calorimeter jet

Functions can be complex

Often highly non-linear systems

$$E_{\text{rec,cell}} = w_{\text{cell}}(\rho_{\text{cell}}, \dots) \cdot E_{0,\text{cell}}$$

$$w_{\text{cell}}(\rho_{\text{cell}}, \dots) \begin{cases} \nearrow \text{for } \rho_{\text{cell}} \uparrow \\ \searrow \text{for } \rho_{\text{cell}} \downarrow \end{cases}$$

Typical boundary conditions:

$$\max(w_{\text{cell}}(\rho_{\text{cell}}, \dots)) \approx 1.5 - 3.0$$

(avoid boosting noise!)

$$\min(w_{\text{cell}}(\rho_{\text{cell}}, \dots)) = 1.0$$

(avoid suppressing em response!)

Example for non-algebraic functional form:

(similar in ATLAS)

$$w_{\text{cell}}(\rho_{\text{cell}}, \mathfrak{R}_{\text{cell}}) = \omega_{ij} \text{ for } \begin{cases} \log(\rho)_i \leq \log(\rho_{\text{cell}}) < \log(\rho)_{i+1} \\ \mathfrak{R}_{\text{cell}} \in \mathfrak{R}_j \end{cases}$$

$\mathfrak{R}_{\text{cell}}$ is a region descriptor for a given cell,

$$\text{like } \mathfrak{R}_{\text{cell}} = \underbrace{\{M_{\text{cell}}, S_{\text{cell}}\}}_{\substack{\text{calorimeter module id,} \\ \text{sampling id}}}$$



Select matched jet pair

Typically small matching radius

$$R_{\text{match}} = 0.2 - 0.3$$

Restrict jet directions to regions with good calorimeter response

No excessive dead material

Away from cracks and complex transition geometries

Calibration functions

Cell signal weighting

Large weights for low density signals

Small weights for high density signals

Sampling layer signal weighting

Weights determined by longitudinal energy sharing in calorimeter jet

Functions can be complex

Often highly non-linear systems

$$E_{\text{rec},S} = w_S E_{0,S} = w_S \cdot \sum_{\text{cells in sampling } S} E_{0,\text{cell}}$$

Possible parameterizations:

$$w_S = w_S(f_{\text{EMC}}), \text{ with } f_{\text{EMC}} = \frac{\sum_{\text{jet cells in EMC}} E_{0,\text{cell}}}{\sum_{\text{all jet cells}} E_{0,\text{cell}}}$$

Example for non-algebraic functional form:

$$w_S(f_{\text{EMC}}) = \omega_{S,i} \text{ for } F_{\text{EMC},i} \leq f_{\text{EMC}} < F_{\text{EMC},i+1}$$



Fitting

Possible constraints

Resolution optimization

Signal linearity

Combination of both

Regularization of calibration functions

Try to linearize function ansatz

Use polynomials

Can reduce fits to solving system of linear equations

Non-linear function fitting

Use numerical approaches to find (local) minimum for multi-dimensional test functions (e.g., software like MINUIT etc.)

Reconstructed jet energy with cell calibration:

$$E_{\text{rec,jet}} = \sum_{\text{cells in jet}} w_{\text{cell}}(\rho_{\text{cell}}, \mathcal{R}_{\text{cell}}) \cdot E_{0,\text{cell}}$$

Fit $\{\omega_{ij}\}$ such that...

$$\chi^2 = \sum_{\text{matching jet pairs}} \frac{(E_{\text{rec,jet}} - E_{\text{particle,jet}})^2}{\sigma_{\text{rec,jet}}^2 + \sigma_{\text{particle,jet}}^2} = \min$$

Reconstructed jet energy with sampling calibration:

$$E_{\text{rec,jet}} = \sum_{S \text{ in jet}} w_S(f_{\text{EMC}}) \cdot E_{0,S}$$

Fit $\{\omega_{i,S}\}$ using the same χ^2 test function!

Note that $\sigma_{\text{rec,jet}}^2 \sim E_{\text{rec,jet}}^{-1}$!



Attempted de-convolution of signal contributions

Normalization choice convolutes various jet response features

E.g., cell weights correct for dead material and magnetic field induced energy losses, etc.

Limited de-convolution

Fit corrections for energy losses in material between calorimeter modules with different functional form
 Separation in terms, but still a correlated parameter fit

Reconstructed jet energy with cell calibration:

$$E_{\text{rec,jet}} = \sum_{\text{cells in jet}} w_{\text{cell}}(\rho_{\text{cell}}, \mathcal{R}_{\text{cell}}) \cdot E_{0,\text{cell}} + E_{\text{DM,jet}}$$

Use χ^2 test function such that...

$$\begin{aligned} \chi^2 &= \sum_{\text{matching jet pairs}} \frac{(E_{\text{rec,jet}} - E_{\text{particle,jet}})^2}{\sigma_{\text{rec,jet}}^2 + \sigma_{\text{particle,jet}}^2} \\ &= \sum_{\text{matching jet pairs}} \frac{\left(\left[\sum_{\text{cells in jet}} w_{\text{cell}}(\rho_{\text{cell}}, \mathcal{R}_{\text{cell}}) \cdot E_{0,\text{cell}} + \alpha \cdot \sqrt{E_{0,S=\text{before}}} \cdot E_{0,S=\text{behind}} \right] - E_{\text{particle,jet}} \right)^2}{\sigma_{\text{rec,jet}}^2 + \sigma_{\text{particle,jet}}^2} \\ &= \min \end{aligned}$$



with empirically motivated ansatz for $E_{\text{DM,jet}}$ for dead material between sampling layers $S = \text{before}$ and $S = \text{behind}$, in a combined fit of $(\{w_{\text{cell}}\}, \alpha)$



Attempted de-convolution of signal contributions

Normalization choice convolutes various jet response features

E.g., cell weights correct for dead material and magnetic field induced energy losses, etc.

Limited de-convolution

Fit corrections for energy losses in material between calorimeter modules with different functional form
Separation in terms, but still a correlated parameter fit

Reconstructed jet energy with cell calibration:

$$E_{\text{rec,jet}} = \sum_{\text{cells in jet}} w_{\text{cell}}(\rho_{\text{cell}}, \mathcal{R}_{\text{cell}}) \cdot E_{0,\text{cell}} + E_{\text{DM,jet}}$$

Use χ^2 test function such that...

$$\chi^2 = \sum_{\text{matching jet pairs}} \frac{(E_{\text{rec,jet}} - E_{\text{particle,jet}})^2}{\sigma_{\text{rec,jet}}^2 + \sigma_{\text{particle,jet}}^2}$$

$$= \sum_{\text{matching jet pairs}} \frac{\left(\left[\sum_{\text{cells in jet}} w_{\text{cell}}(\rho_{\text{cell}}, \mathcal{R}_{\text{cell}}) \cdot E_{0,\text{cell}} + \alpha \cdot \sqrt{E_{0,S=\text{before}} \cdot E_{0,S=\text{behind}}} \right] - E_{\text{particle,jet}} \right)^2}{\sigma_{\text{rec,jet}}^2 + \sigma_{\text{particle,jet}}^2}$$

= min

with empirically motivated ansatz for $E_{\text{DM,jet}}$ for dead material between sampling layers $S = \text{before}$ and $S = \text{behind}$, in a combined fit of $(\{w_{\text{cell}}\}, \alpha)$

Relatively low level of factorization in this particular approach with correlated (by combined fit) parameters!



Introduction to Hadronic Final State Reconstruction in Collider Experiments (Part XII)

Peter Loch
University of Arizona
Tucson, Arizona
USA



Plots for this session

Most if not all plots shown in this session are meant as examples and for illustration purposes

Educational showcases to highlight certain features of energy scales and calorimeter response

They do not represent the up-to-date estimates for ATLAS jet reconstruction performance

In general much better than the (old) results shown here!

Not many new plots can be shown in public yet!

The performance plots shown are published

Reflection of state-of-art at a given moment in time

No experimental collision data available at that time!



Experiment and simulation

Calorimeter towers

2-dim signal objects from all cells or only cells surviving noise suppression (topological towers in ATLAS)

Calorimeter clusters

3-dim signal objects with implied noise suppression (topological clusters in ATLAS)

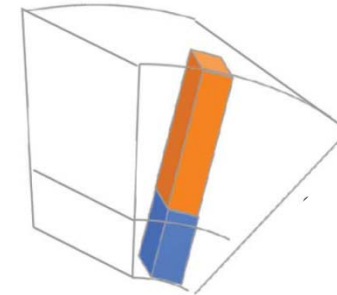
Tracks

Reconstructed inner detector tracks – only charged particles with $p_T > p_{T_{\text{threshold}}} = 500$ MeV – 1 GeV (typically)

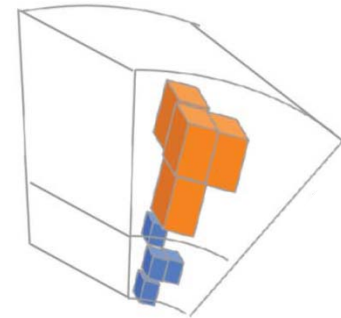
Simulation only

Generated stable particles

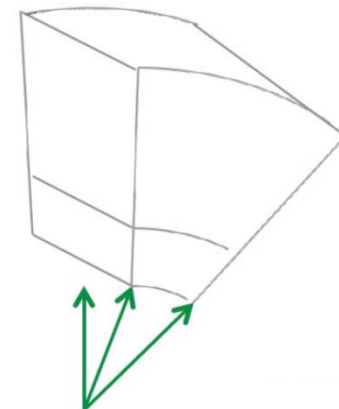
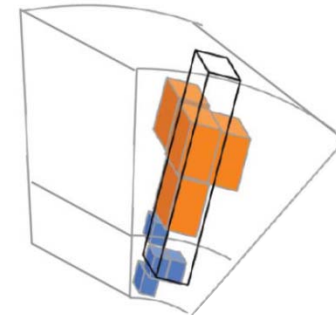
Typically $\tau_{\text{lab}} > 10$ ps to be a signal source



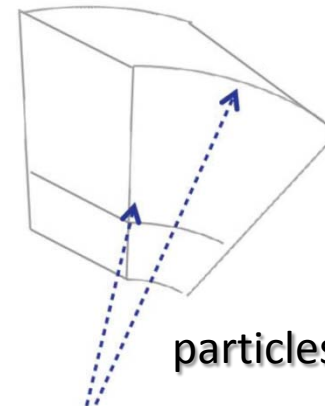
towers



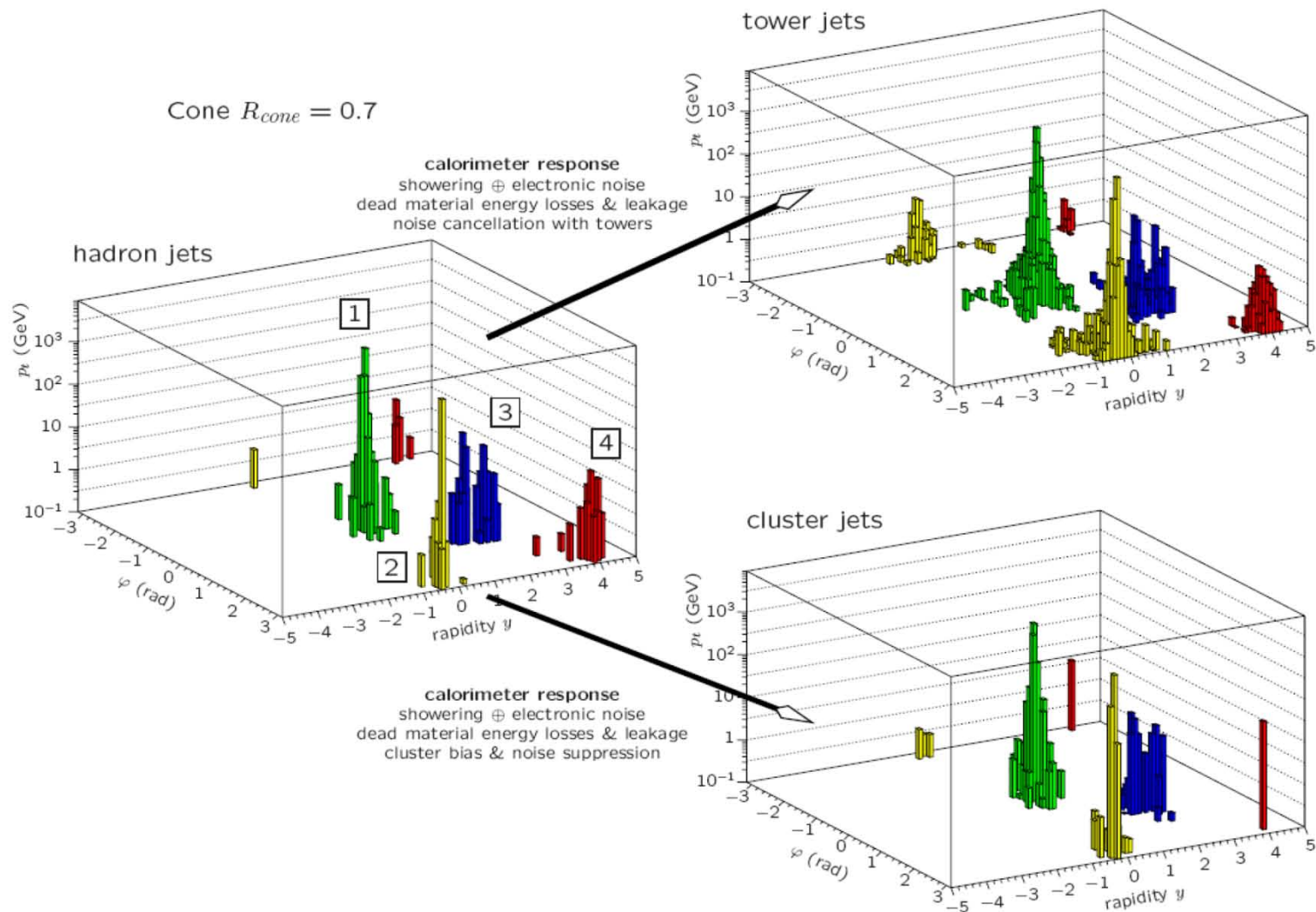
clusters



tracks



particles



Calorimeter jet response

Electromagnetic energy scale

Available for all signal definitions

No attempt to compensate or correct signal for limited calorimeter acceptance

Global hadronic energy scale

All signal definitions, but specific calibrations for each definition

Calibrations normalized to reconstruct full true jet energy in "golden regions" of calorimeter

Local hadronic energy scale

Topological clusters only
 No jet context – calibration insufficient to recover calorimeter acceptance limitations – no corrections for total loss in dead material and magnetic field charged particles losses)

Unbiased and noise-suppressed towers:

$$\underbrace{\begin{pmatrix} E_{0,\text{jet}} \\ \vec{p}_{0,\text{jet}} \end{pmatrix}}_{\text{reconstructed calorimeter jet}} = \underbrace{\begin{pmatrix} \sum_{\text{towers in jet}} E_{0,\text{tower}} \\ \sum_{\text{towers in jet}} \vec{p}_{0,\text{tower}} \end{pmatrix}}_{\text{reconstructed calorimeter jet}} < \underbrace{\begin{pmatrix} \sum_{\text{particles in jet}} E_{\text{particle}} \\ \sum_{\text{particles in jet}} \vec{p}_{\text{particle}} \end{pmatrix}}_{\text{matched particle jet (truth reference)}}$$

Topological cell clusters:

$$\underbrace{\begin{pmatrix} E_{0,\text{jet}} \\ \vec{p}_{0,\text{jet}} \end{pmatrix}}_{\text{reconstructed calorimeter jet}} = \underbrace{\begin{pmatrix} \sum_{\text{clusters in jet}} E_{0,\text{cluster}} \\ \sum_{\text{clusters in jet}} \vec{p}_{0,\text{cluster}} \end{pmatrix}}_{\text{reconstructed calorimeter jet}} < \underbrace{\begin{pmatrix} \sum_{\text{particles in jet}} E_{\text{particle}} \\ \sum_{\text{particles in jet}} \vec{p}_{\text{particle}} \end{pmatrix}}_{\text{matched particle jet (truth reference)}}$$

Note at any scale:

$$m_{\text{jet}} = \sqrt{E_{\text{jet}}^2 - \vec{p}_{\text{jet}}^2} > 0 \text{ for } N_{\text{towers}}, N_{\text{clusters}} > 1$$



Calorimeter jet response

Electromagnetic energy scale

Available for all signal definitions

No attempt to compensate or correct signal for limited calorimeter acceptance

Global hadronic energy scale

All signal definitions, but specific calibrations for each definition

Calibrations normalized to reconstruct full true jet energy in "golden regions" of calorimeter

Local hadronic energy scale

Topological clusters only
No jet context – calibration insufficient to recover calorimeter acceptance limitations – no corrections for total loss in dead material and magnetic field charged particles losses)

Cell based calibration for all calorimeter signals and jets in "golden spot":

$$\begin{aligned}
 & \overbrace{\left(\begin{array}{l} E_{\text{rec,jet}} \\ \vec{p}_{\text{rec,jet}} \end{array} \right)}^{\text{reconstructed calorimeter jet}} = \left(\begin{array}{l} \sum_{\text{cells in jet}} w(\rho_{\text{cell}}, \mathcal{R}_{\text{cell}}) \cdot E_{0,\text{cell}} + E_{\text{DM}} \\ \sum_{\text{cells in jet}} w(\rho_{\text{cell}}, \mathcal{R}_{\text{cell}}) \cdot \vec{p}_{0,\text{cell}} + E_{\text{DM}} \frac{\vec{p}_{0,\text{jet}}}{|\vec{p}_{0,\text{jet}}|} \end{array} \right) \\
 & = \left(\begin{array}{l} \sum_{\text{particles in jet}} E_{\text{particle}} \\ \sum_{\text{particles in jet}} \vec{p}_{\text{particle}} \end{array} \right) \\
 & \underbrace{\hspace{10em}}_{\text{matched particle jet (truth reference)}}
 \end{aligned}$$

(cells are extracted from unbiased or noise suppressed towers or topological clusters forming the jet)



Calorimeter jet response

Electromagnetic energy scale

Available for all signal definitions

No attempt to compensate or correct signal for limited calorimeter acceptance

Global hadronic energy scale

All signal definitions, but specific calibrations for each definition

Calibrations normalized to reconstruct full true jet energy in “golden regions” of calorimeter

Local hadronic energy scale

Topological clusters only

No jet context – calibration insufficient to recover calorimeter acceptance limitations – no corrections for total loss in dead material and magnetic field charged particles losses)

Locally calibrated clusters only:

$$\underbrace{\begin{pmatrix} E_{\text{rec,jet}} \\ \vec{p}_{\text{rec,jet}} \end{pmatrix}}_{\text{reconstructed calorimeter jet}} = \underbrace{\begin{pmatrix} \sum_{\text{clusters in jet}} E_{\text{rec,cluster}} \\ \sum_{\text{towers in jet}} \vec{p}_{\text{rec,cluster}} \end{pmatrix}}_{\text{reconstructed calorimeter jet}} \leq \underbrace{\begin{pmatrix} \sum_{\text{particles in jet}} E_{\text{particle}} \\ \sum_{\text{particles in jet}} \vec{p}_{\text{particle}} \end{pmatrix}}_{\text{matched particle jet (truth reference)}}$$



Final Jet Energy Scale (JES)

Final jet calibration

All corrections applied

Best estimate of true (particle) jet energy

Flat response as function of p_T

Uniform response across whole calorimeter

Relative energy resolution

Depends on the calorimeter jet response – calibration applies compensation corrections

Resolution improvements by including jet signal features

Requires corrections sensitive to measurable jet variables

Can use signals from other detectors

Determination with simulations

Measure residual deviations of the calorimeter jet response from truth jet energy

Derive corrections from the calorimeter response at a given scale as function of p_T (linearity) and pseudorapidity (uniformity) for all particle jets

Use numerical inversion to parameterize corrections

Conversion from truth variable dependence of response to reconstructed variable response



From simulations

Compare calorimeter response with particle jet energy as function of the particle jet energy

All jets, all regions, full kinematic coverage

Residual deviation from linearity

Depend on calorimeter energy scale – large for electromagnetic energy scale and local calibration due to missing jet level corrections

Small for global calibration due to jet energy normalization

Corrections can be extracted from residuals

A bit tricky – need to use numerical inversion (see later)

From experiment

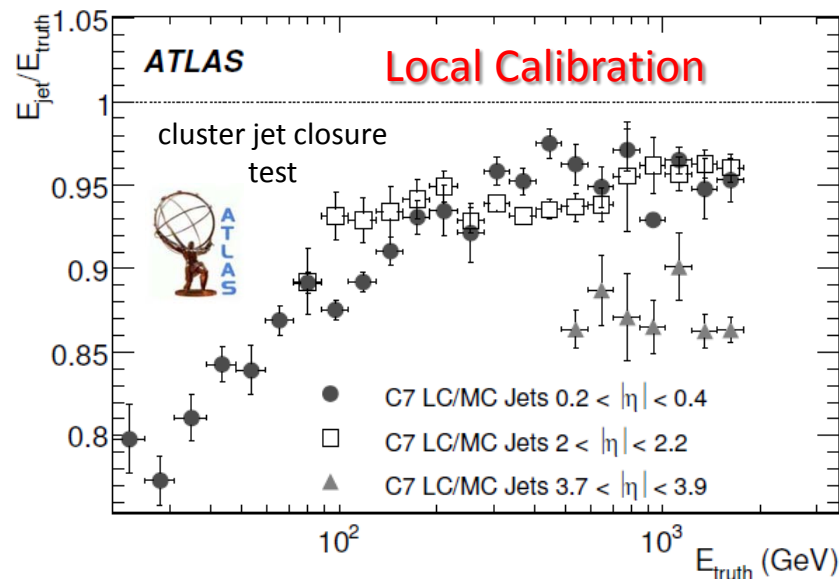
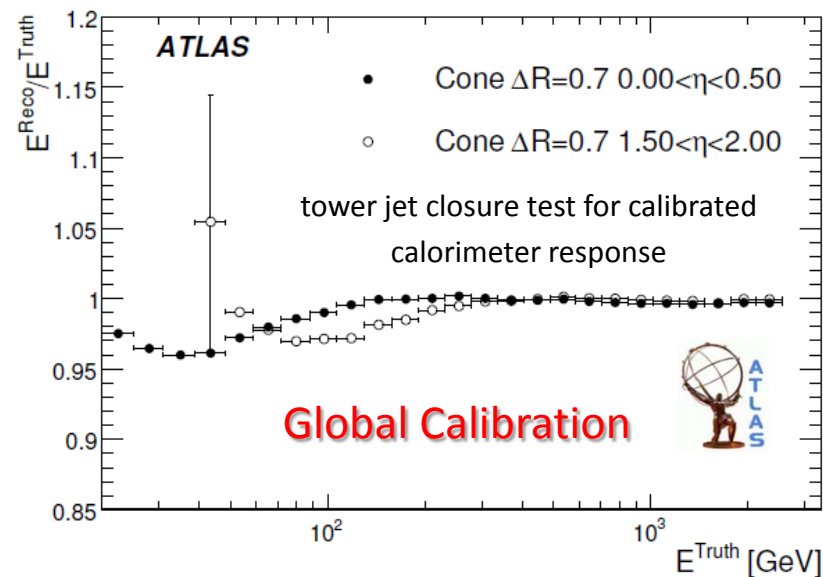
Validate and extract calibrations from collision data

W boson mass in hadronic decay is jet energy scale reference

pT balance of electromagnetic signal (Z boson, photon) and jet

Note change of reference scale

In-situ channels provide interaction (parton) level truth reference!



Simulations

Compare calorimeter response with particle jet energy as function of the jet direction

All jets in full kinematic range

Residual non-uniformities expected in cracks

Only jets in “golden regions” used for calibration

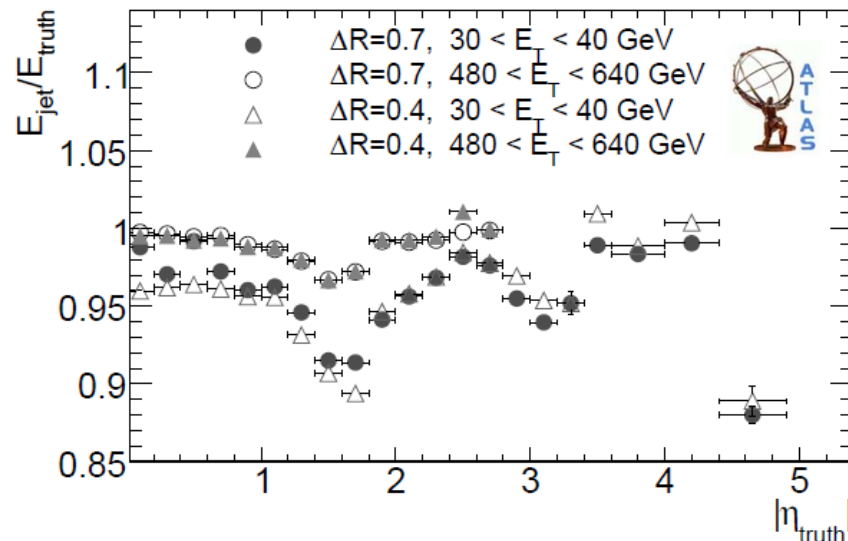
From experiment

Di-jet pT balance

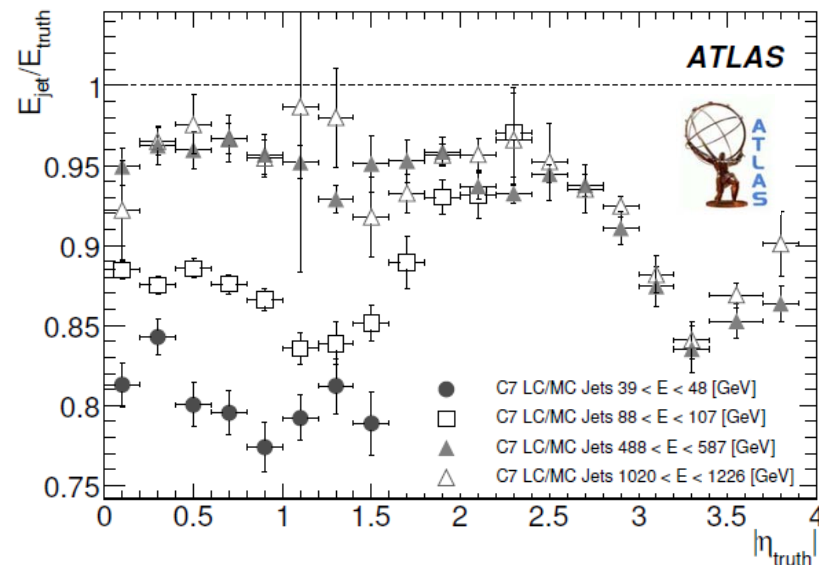
Balance pT of well calibrated jet in “golden region” with jet in other calorimeter regions

Can also use photon pT balance with jets outside of “golden region”

Global Calibration



Local Calibration



Simulations

Measure fluctuations of calorimeter jet energy as function of truth jet energy

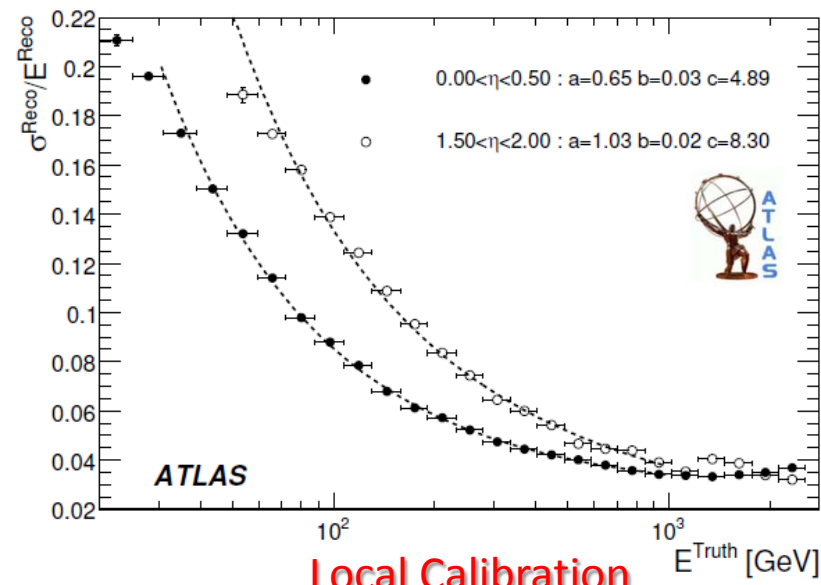
All jets in full kinematic range and in various regions of pseudo-rapidity

From experiment

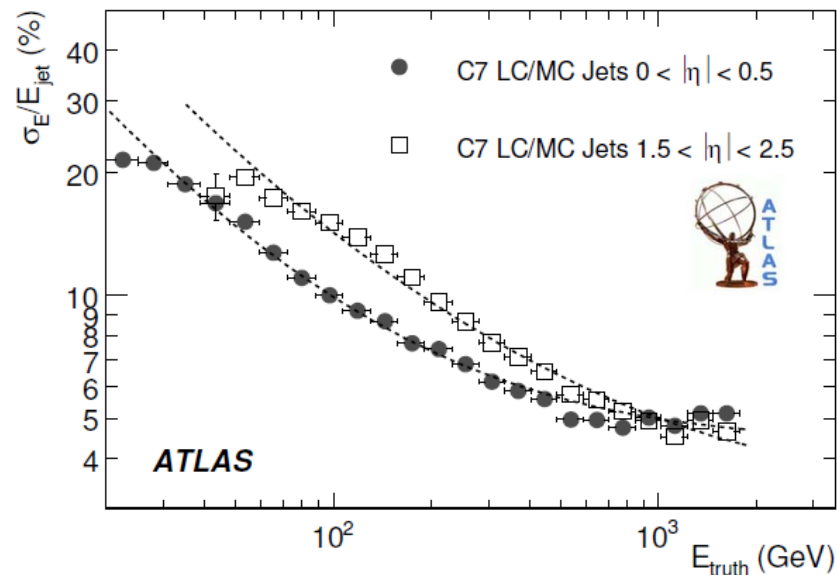
Di-jet final states

Measure relative fluctuations of jet energies in back-to-back (pT) balanced di-jets

Global Calibration



Local Calibration



Golden rule of calorimetric energy measurement

The fully calibrated calorimeter signal is most probably the true jet (or particle) energy

Interpretation holds only for symmetrically distributed fluctuations – mean value is identical to average value

The resolution of the measurement is given by the characteristics of the signal fluctuations

Can only be strictly and correctly understood in case of Gaussian response distributions

We need a normally distributed response!

Problem for all calibration techniques

Residual deviations from expected jet reconstruction performance must be measured as function of true quantities

Only then is the fluctuation of the response $R = E_{\text{reco}}/E_{\text{true}}$ really Gaussian after calibration

But need to apply corrections to measured jets

Need parameterization as function of reconstructed quantities

Simple re-binning does not maintain the Gaussian characteristics of the fluctuations – hard to control error!

Use numerical inversion to transfer the calibrations from true to measured parameters

Maintains Gaussian character



Toy model

Generate flat jet energy spectrum

Uniform energy distribution for E_{jet} in $[E_{\text{min}}, E_{\text{max}}]$

Smear true jet energy with Gaussian

Assume perfect average calibration

Width of distribution follows calorimetric energy resolution function

Calculate the response

In bins of E_{true} and in bins of $E_{\text{smear}} = E_{\text{reco}}$

Repeat exercise with steeply falling energy spectrum

Calibrated response:

$$\langle E_{\text{smear}} \rangle = \langle E_{\text{reco}} \rangle = \langle E_{\text{true}} \rangle$$

Calorimeter resolution function (no noise):

$$\frac{\sigma_E}{E} = \sqrt{\frac{a^2}{E_{\text{true}}} + c^2}$$

Smear energy:

$$E_{\text{smear}} = E_{\text{true}} + r \cdot \sigma_E$$

r is a random number following the Gaussian PDF:

$$g(r) = \frac{1}{\sqrt{2\pi}} \exp\left[-\frac{1}{2}r^2\right]$$

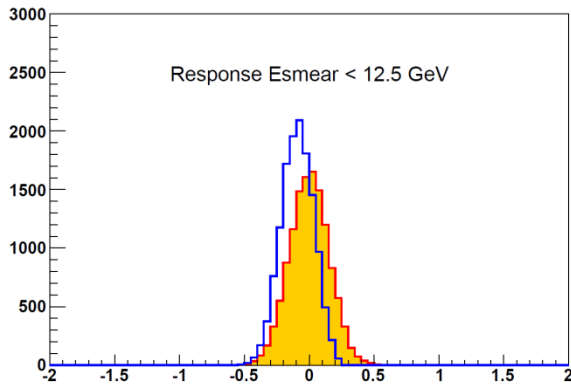
i.e. distributed around 0 with a width of 1

Response fluctuations:

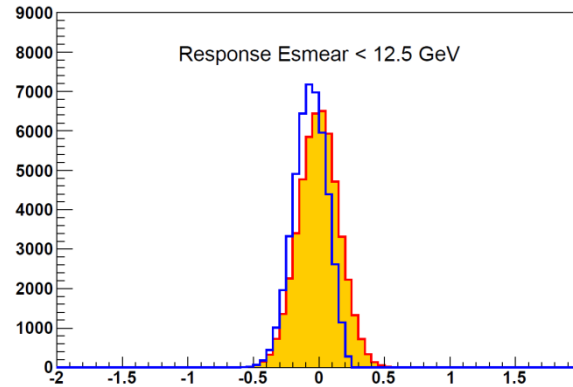
$$R = \frac{E_{\text{smear}} - E_{\text{true}}}{E_{\text{true}}} \text{ with } \langle R \rangle = 0$$



$$p(E_{\text{true}}) = \text{const}$$



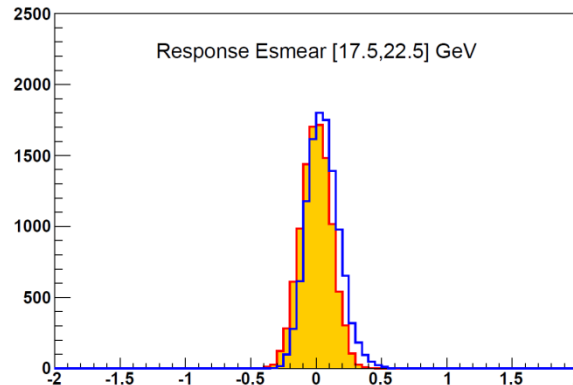
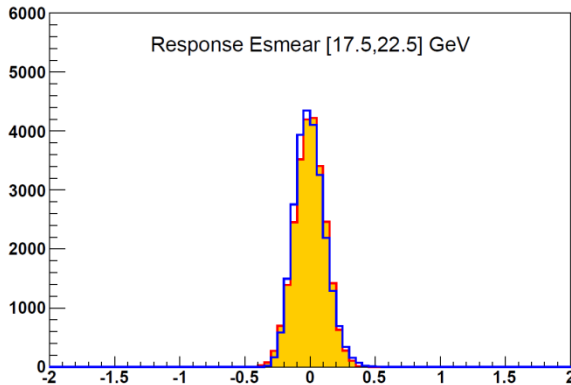
$$p(E_{\text{true}}) \propto E_{\text{true}}^{-4}$$



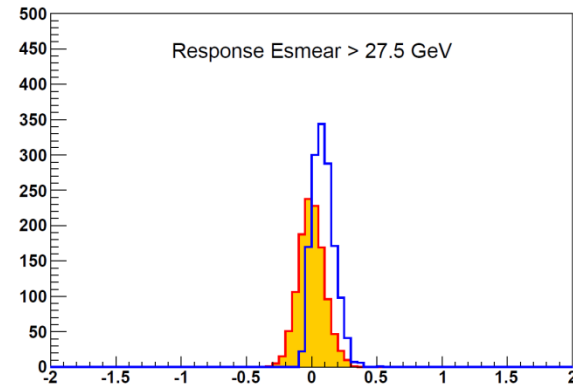
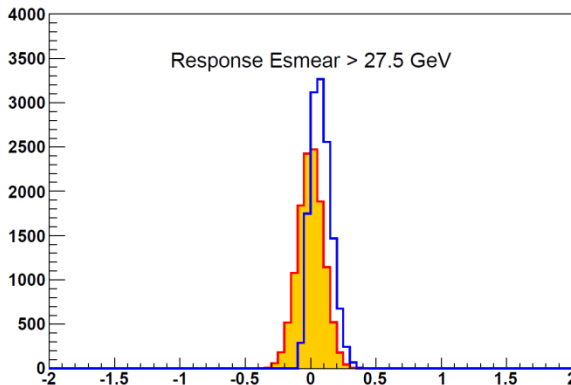
 binned in E_{true}

 binned in E_{smear}

Lower edge of E spectrum



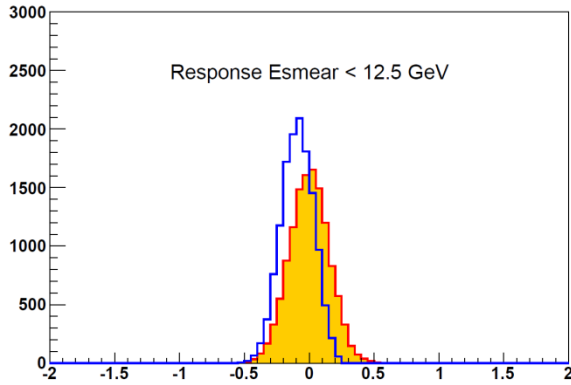
Center of E spectrum



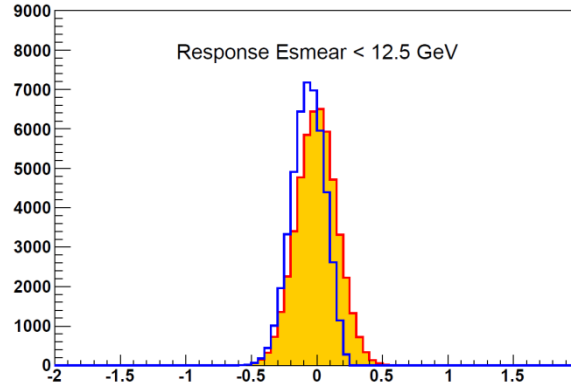
High end of E spectrum



$$p(E_{\text{true}}) = \text{const}$$



$$p(E_{\text{true}}) \propto E_{\text{true}}^{-4}$$

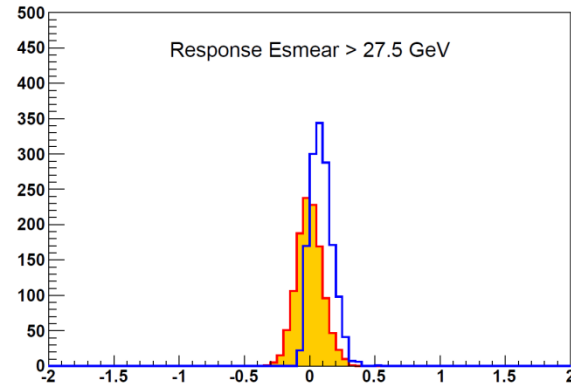
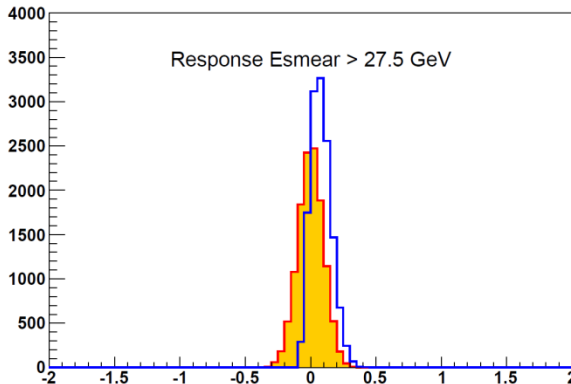
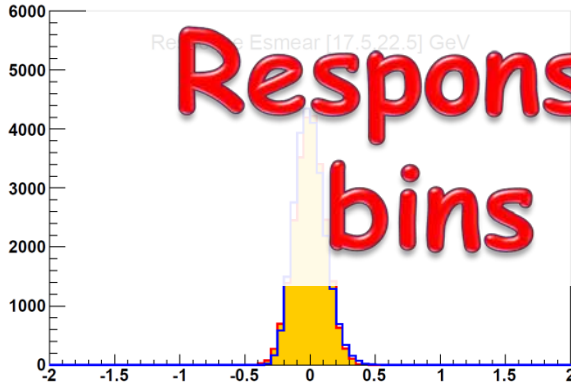


- binned in E_{true}
- binned in E_{smear}

Lower edge of E spectrum

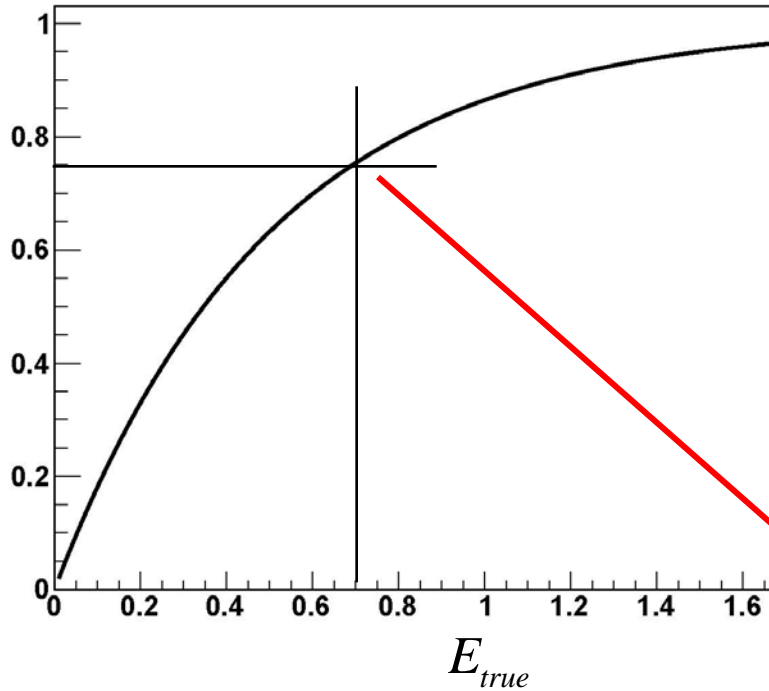
Response only Gaussian in bins of true energy!

Center of E spectrum

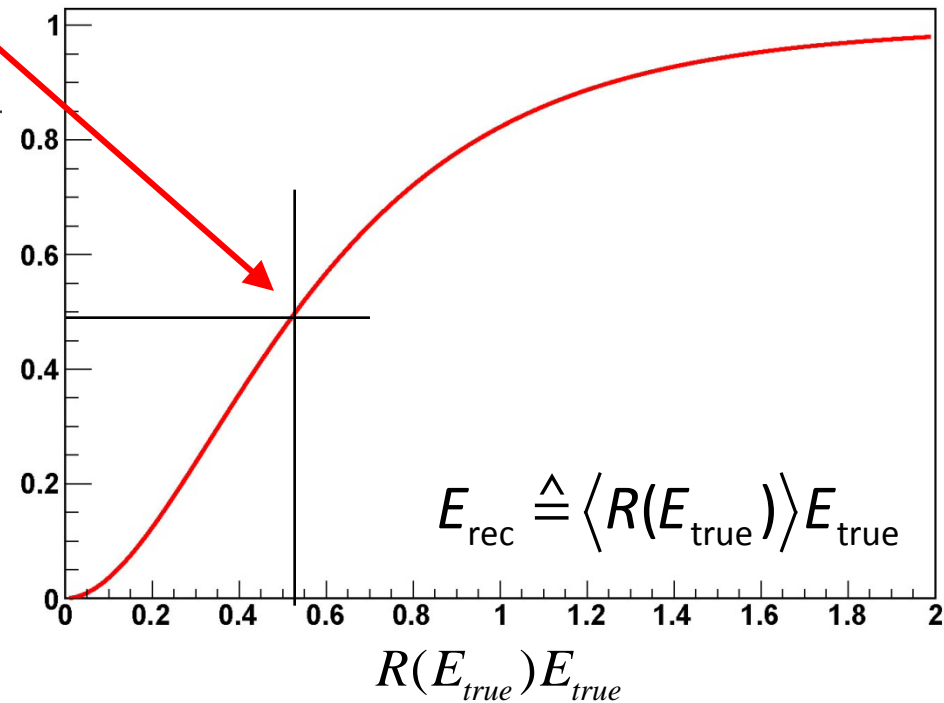


High end of E spectrum



$R(E_{true})$


Transfer of response function
from dependence on true
variable to dependence on
measured variable

 $R(E_{rec})$


$$R(E_{rec}) = R(\langle R(E_{true}) \rangle \cdot E_{true})$$

$$E_{rec} \hat{=} \langle R(E_{true}) \rangle E_{true}$$



Often simple functions

Address residual energy (pT) and direction dependence of calorimeter jet response

Determine response functions R in bins of true jet pT and reconstructed pseudo-rapidity $\eta_{\text{rec,jet}}$

Apply numerical inversion to determine calibration functions in reconstructed variable space ($p_{\text{T,rec,jet}}, \eta_{\text{rec,jet}}$)

Use calibration functions to get jet energy scale

Technique can be applied to locally or globally calibrated jet response, with likely different calibration functions

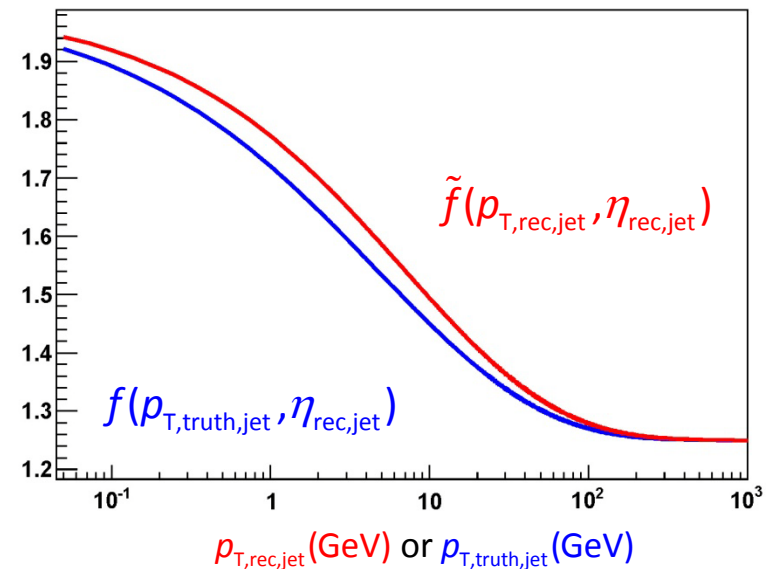
$$f(p_{\text{T,true,jet}}, \eta_{\text{reco,jet}}) = R^{-1}(p_{\text{T,true,jet}}, \eta_{\text{reco,jet}})$$

with $\eta_{\text{reco,jet}} \approx \eta_{\text{true,jet}}$ and

$$R^{-1}(p_{\text{T,true,jet}}, \eta_{\text{reco,jet}}) = \left\langle \frac{E_{\text{true,jet}}}{E_{\text{rec,jet}}} \right\rangle (p_{\text{T,true,jet}}, \eta_{\text{reco,jet}})$$

then apply numerical inversion

$$f(p_{\text{T,true,jet}}, \eta_{\text{reco,jet}}) \xrightarrow{\text{numerical inversion}} \tilde{f}(p_{\text{T,rec,jet}}, \eta_{\text{reco,jet}})$$



Often simple functions

Address residual energy (pT) and direction dependence of calorimeter jet response

Determine response functions R in bins of true jet pT and reconstructed pseudo-rapidity $\eta_{\text{rec,jet}}$

Apply numerical inversion to determine calibration functions in reconstructed variable space $(p_{\text{T,rec,jet}}, \eta_{\text{rec,jet}})$

Use calibration functions to get jet energy scale

Technique can be applied to locally or globally calibrated jet response, with likely different calibration functions

global calibration:

$$\begin{pmatrix} E_{\text{calib,jet}} \\ \vec{p}_{\text{calib,jet}} \end{pmatrix} =$$

$$\tilde{f}(p_{\text{T,rec,jet}}, \eta_{\text{rec,jet}}) \cdot \left(\begin{array}{c} \overbrace{\sum_{\text{cells in jet}} w(\rho_{\text{cell}}, \mathcal{R}_{\text{cell}}) \cdot E_{0,\text{cell}} + E_{\text{DM}}}^{E_{\text{reco,jet}}} \\ \underbrace{\sum_{\text{cells in jet}} w(\rho_{\text{cell}}, \mathcal{R}_{\text{cell}}) \cdot \vec{p}_{0,\text{cell}} + E_{\text{DM}} \frac{\vec{p}_{0,\text{jet}}}{|\vec{p}_{0,\text{jet}}|}}_{\vec{p}_{\text{reco,jet}}, \text{ with } p_{\text{T,rec,jet}} = |\vec{p}_{\text{reco,jet}}| \sqrt{1 - \tanh^2 \eta_{\text{reco,jet}}}} \end{array} \right)$$

local calibration:

$$\begin{pmatrix} E_{\text{calib,jet}} \\ \vec{p}_{\text{calib,jet}} \end{pmatrix} = \tilde{f}'(p_{\text{T,rec,jet}}, \eta_{\text{rec,jet}}) \cdot \left(\begin{array}{c} \sum_{\text{clusters in jet}} E_{\text{rec,cluster}} \\ \sum_{\text{towers in jet}} \vec{p}_{\text{rec,cluster}} \end{array} \right)$$



Why not use direct relation between reconstructed and true energy?

Same simulation data input

Has been used in some experiments

Dependence on truth energy spectrum

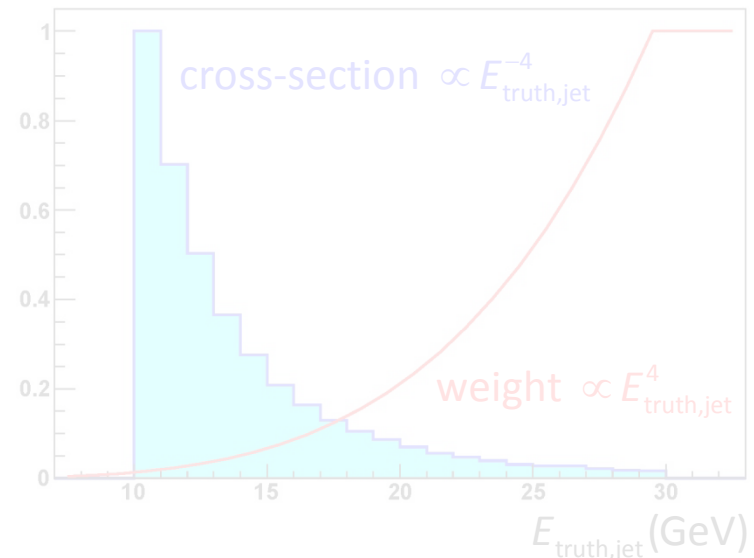
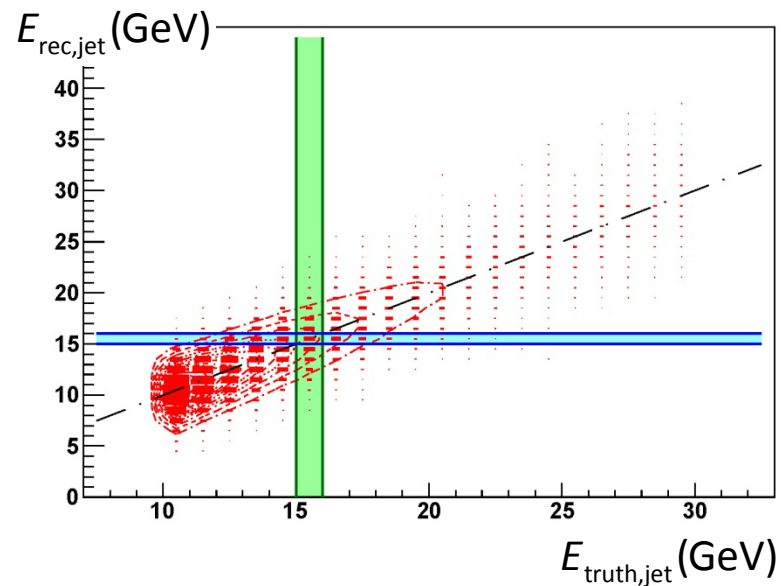
Need to make sure calibration sample is uniform in truth energy

Alternatively, unfold driving truth energy spectrum

Residual non-gaussian behaviour of truth energy distribution

Error on reconstructed energy hard to understand

Could still use response distribution \rightarrow same issues as discussed on previous slide!



Why not use direct relation between reconstructed and true energy?

Same simulation data input

Has been used in some experiments

Dependence on truth energy spectrum

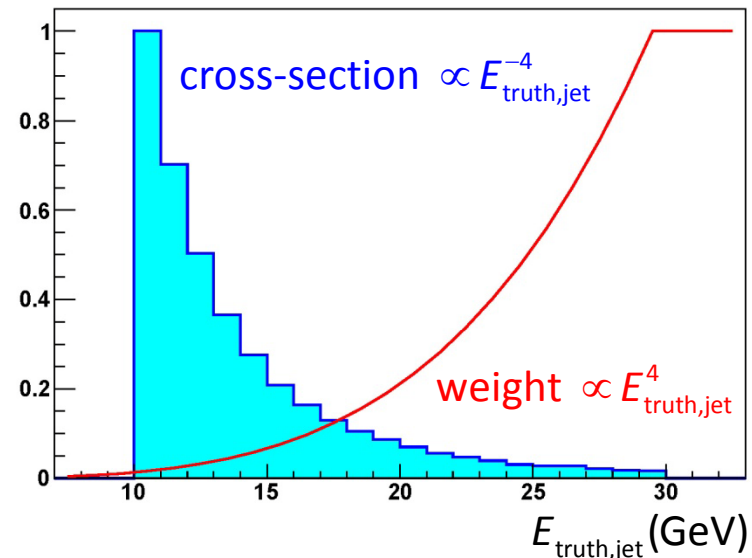
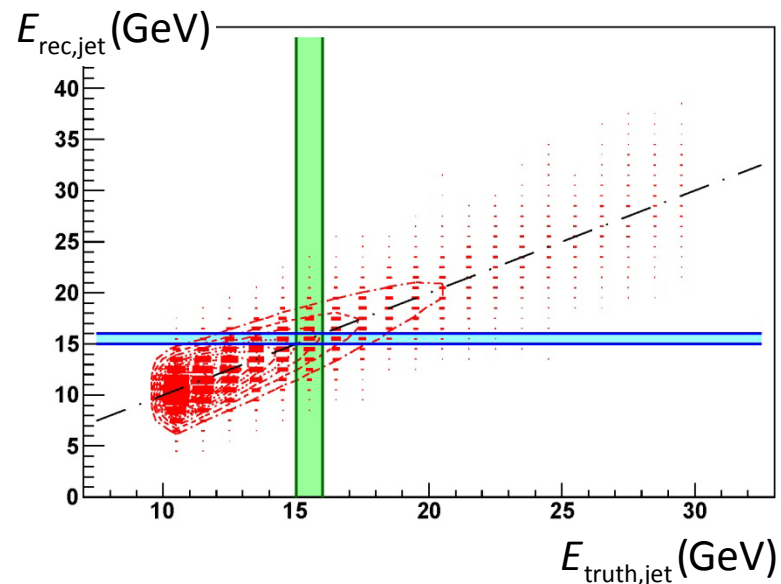
Need to make sure calibration sample is uniform in truth energy

Alternatively, unfold driving truth energy spectrum

Residual non-gaussian behaviour of truth energy distribution

Error on reconstructed energy hard to understand

Could still use response distribution \rightarrow same issues as discussed on previous slide!



Why not use direct relation between reconstructed and true energy?

Same simulation data input

Has been used in some experiments

Dependence on truth energy spectrum

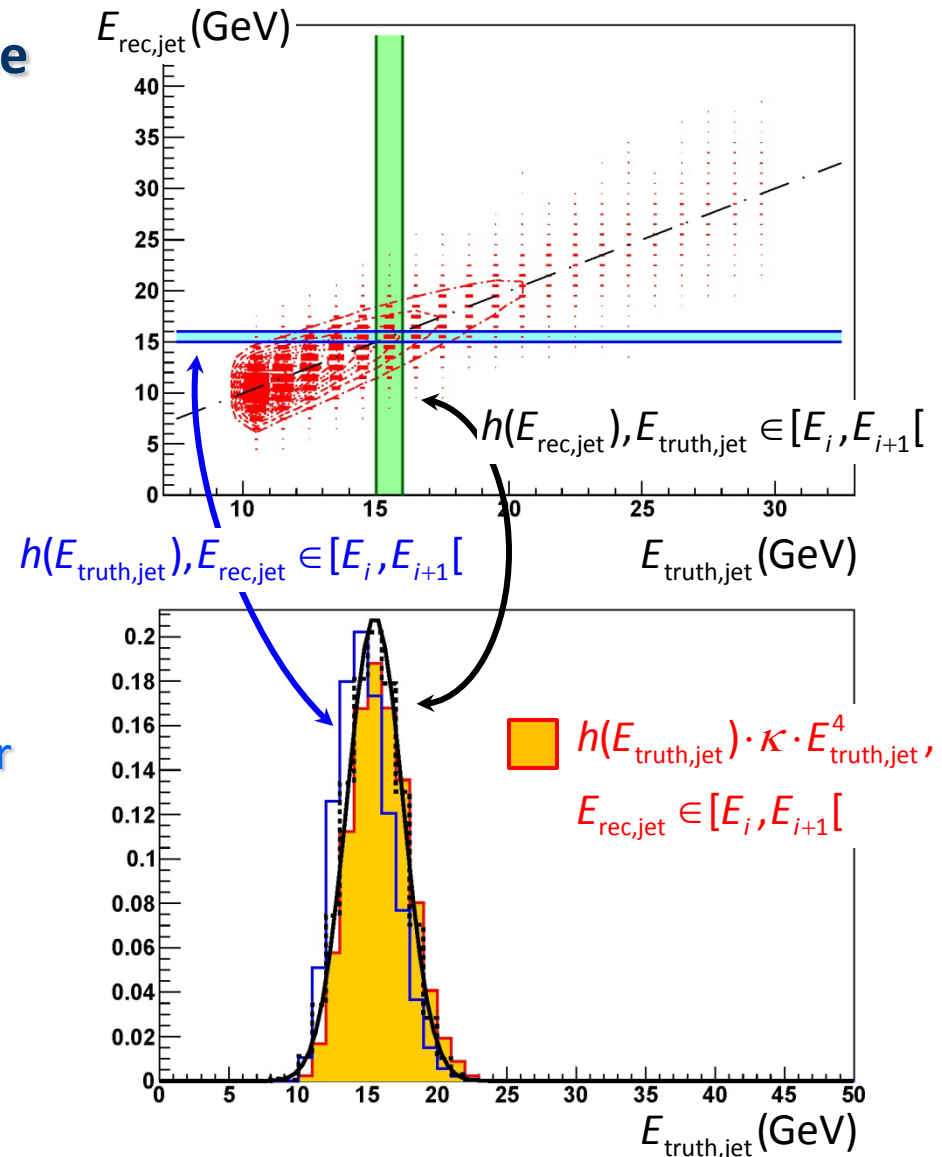
Need to make sure calibration sample is uniform in truth energy

Alternatively, unfold driving truth energy spectrum

Residual non-gaussian behaviour of truth energy distribution

Error on reconstructed energy hard to understand

Could still use response distribution \rightarrow same issues as discussed on previous slide!



Strategy from simulations

Determine all calibrations with fixed conditions

- Ideal detector model – everything is aligned
- Fixed (best) GEANT4 shower model – from testbeam evaluations
- Fixed calorimeter signal definition – e.g., towers
- Fixed jet definition – like seeded cone with size 0.7
- Fixed final state – QCD di-jets preferred

Study change in performance for changing conditions with ideal calibration applied

- Detector misalignment and changes in material budgets
- Different shower GEANT4 model
- Different calorimeter signal definitions – e.g., clusters
- Different jet definitions – e.g., kT, AntikT, different cone or cone sizes...
- Different physics final state – preferably more busy ones like SUSY, ttbar,...

Use observed differences as systematic error estimates

Use of collision data

Compare triggered final states with simulations

- Level of comparison represents understanding of measurement – systematic error (at least for standard final states)

Use in-situ final states to validate calibration

- Careful about biases and reference levels (see session 9)



Calibration functions determined with “perfect” detector description and one reference jet definition

Validate performance in perfect detector

Signal linearity & resolution

Quality of calibration for a real detector

A priori unknown real detector

Absolute and relative alignments, inactive material distributions

Estimate effect of distorted (real) detector

Implement realistic assumptions for misalignment in simulations

Small variations of inactive material thicknesses and locations

But use “perfect” calibration for reconstruction

Change jet signals

Tower or clusters

E.g, change from reference calorimeter signal

Different jet finder

E.g., use kT instead of cone

Different configuration

E.g., use narrow jets (cone size 0.4) instead of wide jets (0.7)



Response

Linear within +/-1% after calibration applied for $p_T > 100$ GeV

Clear improvement compared to basic signal scale

Problems with low p_T regime

ATLAS limit $p_T > 20-40$ GeV, depending on luminosity

May be resolution bias – under study

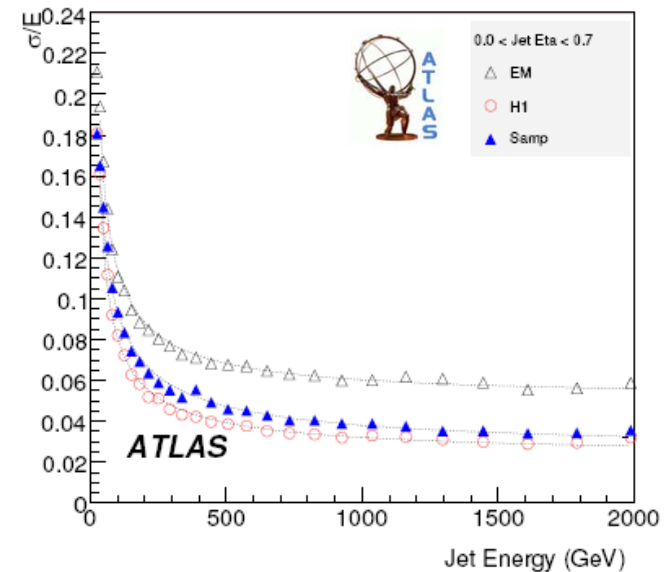
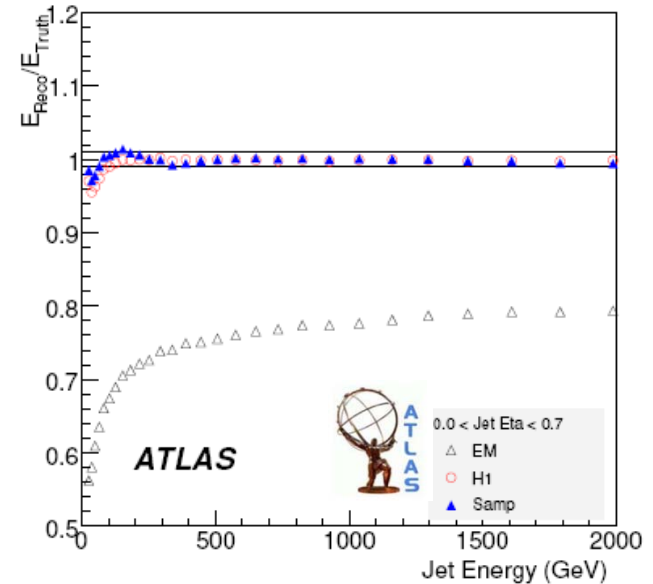
Resolution

Jet energy resolution clearly improved by calibration as well

Slight dependence on calibration strategy

Close to required performance

$$\frac{\sigma}{E} \approx \frac{65\%}{\sqrt{E}} \oplus 3\%$$

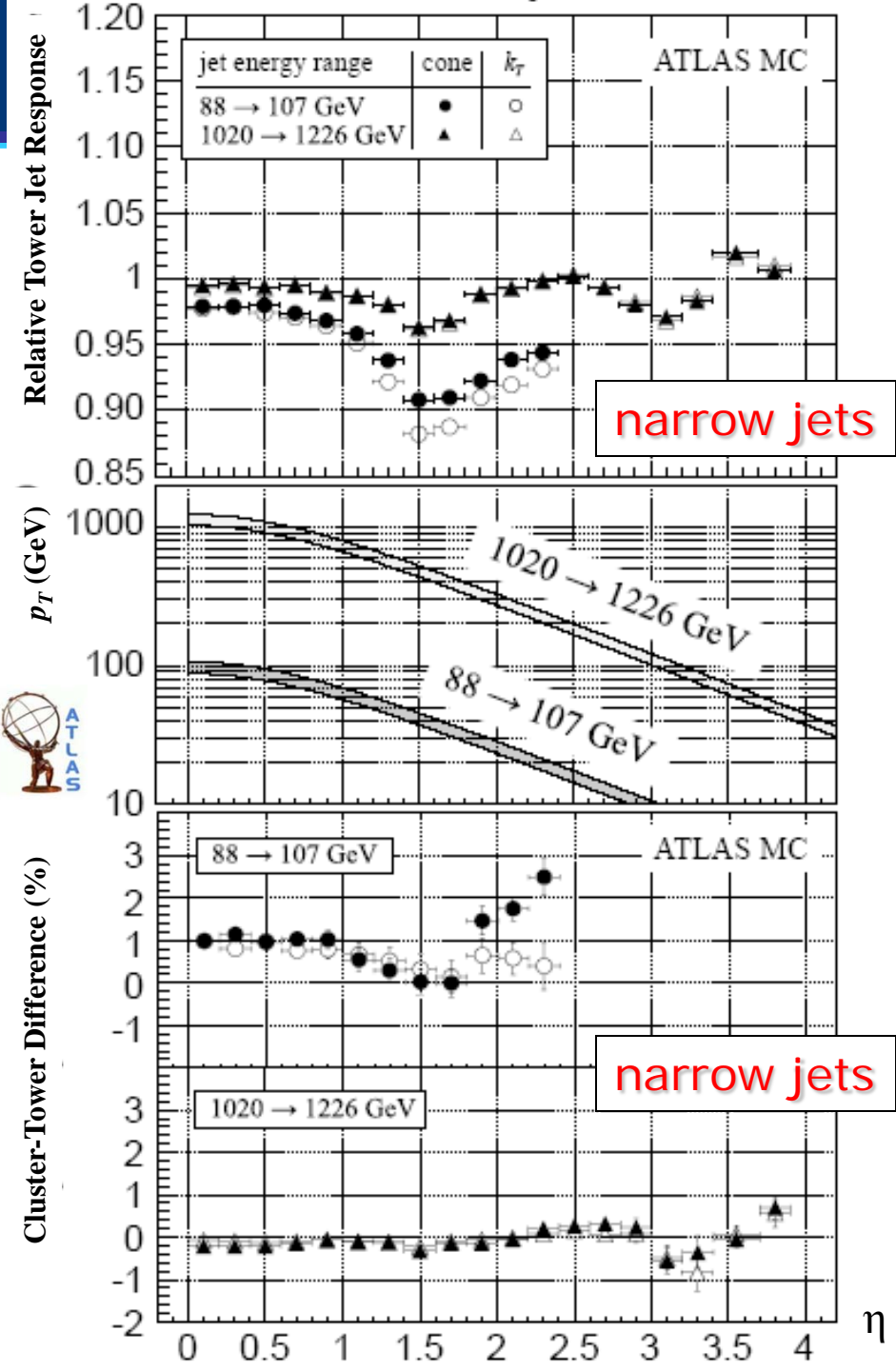


Characterizes “real” detector jet response

- Variation of response with direction
- Changing inactive material distribution
- Cracks between calorimeter modules

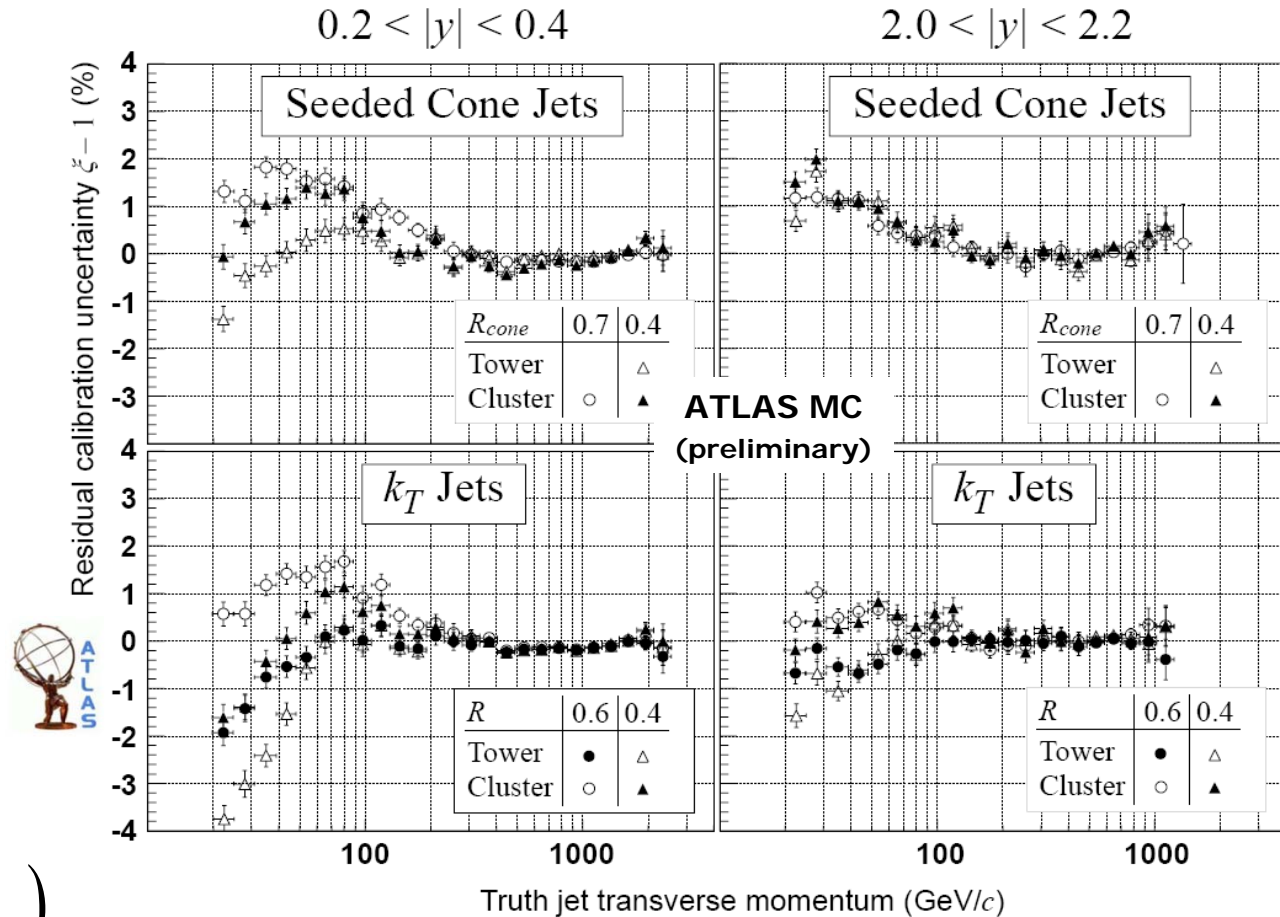
Variations

- No strong dependence on calorimeter signal definition
 - Towers/clusters
- ATLAS cone jet performs better in crack region at low p_T



Estimated effect of a distorted detector

Effect of detector distortion depends on jet size, calo signal choice, and kinematic domain



$$\xi = \frac{\left(E_{\text{rec,jet}} / E_{\text{truth,jet}} \right)_{\text{distorted}}}{\left(E_{\text{rec,jet}} / E_{\text{truth,jet}} \right)_{\text{ideal}}}$$



Larger fluctuations for k_T jets at low p_T

Vacuum effect for tower jets?

Less pronounced for cluster jets

Noise suppression important in this domain

Very similar resolutions at high p_T

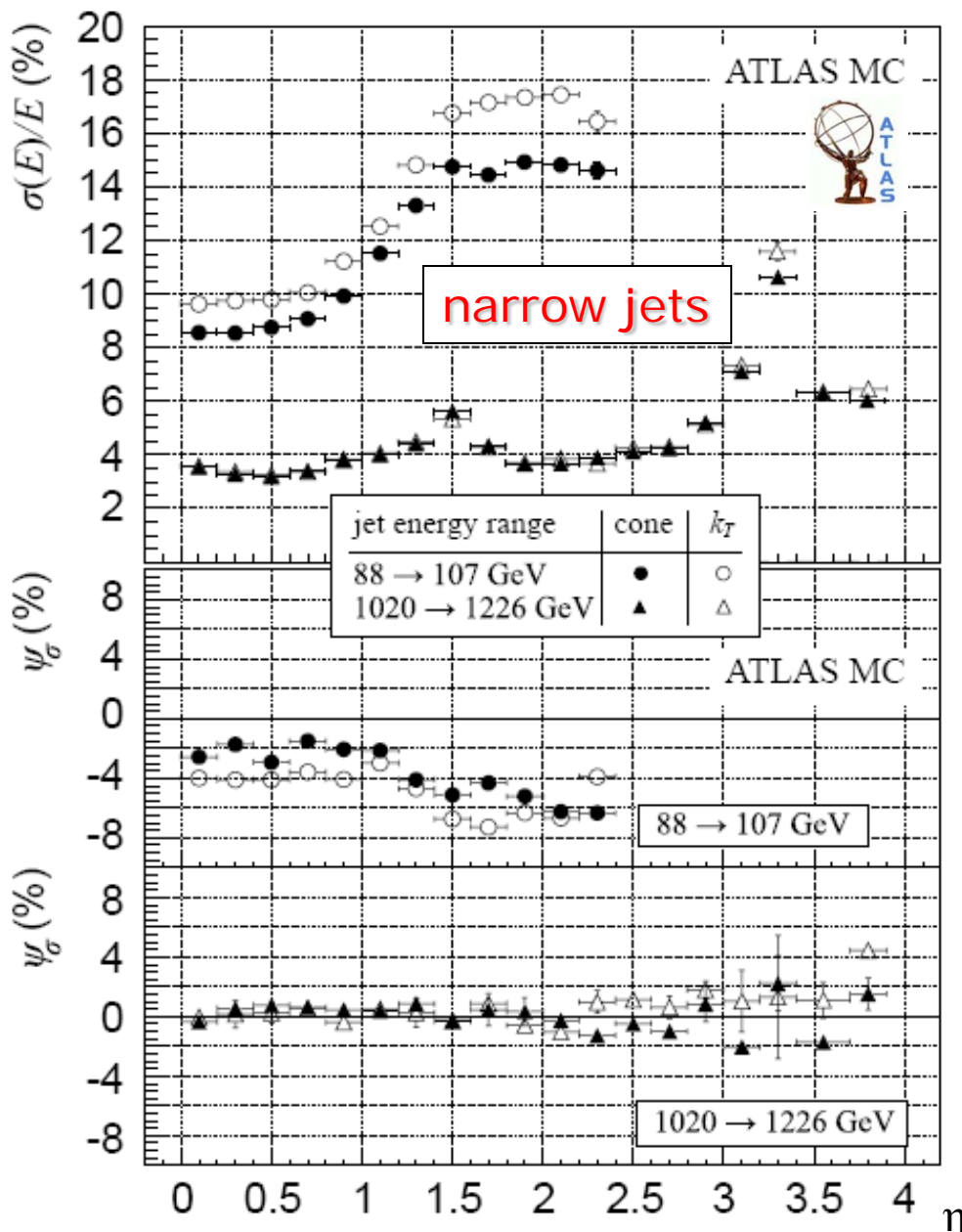
No strong dependence on jet definition

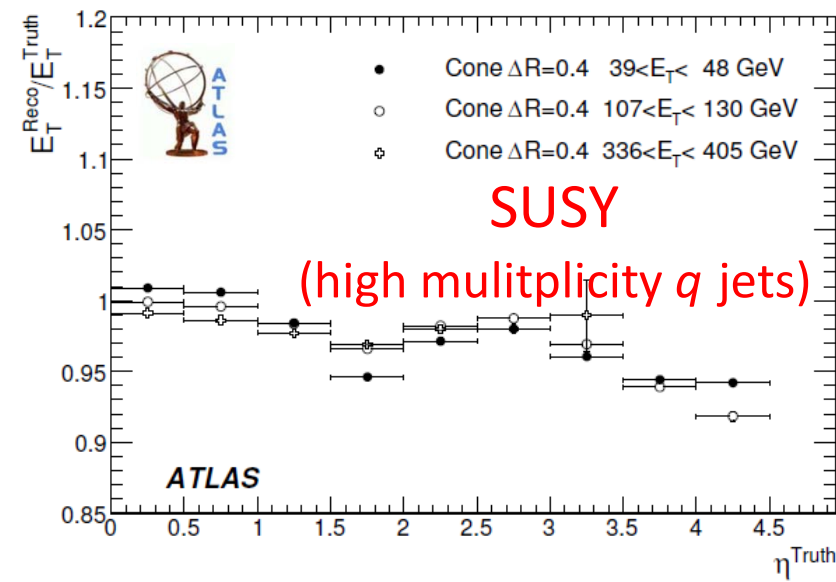
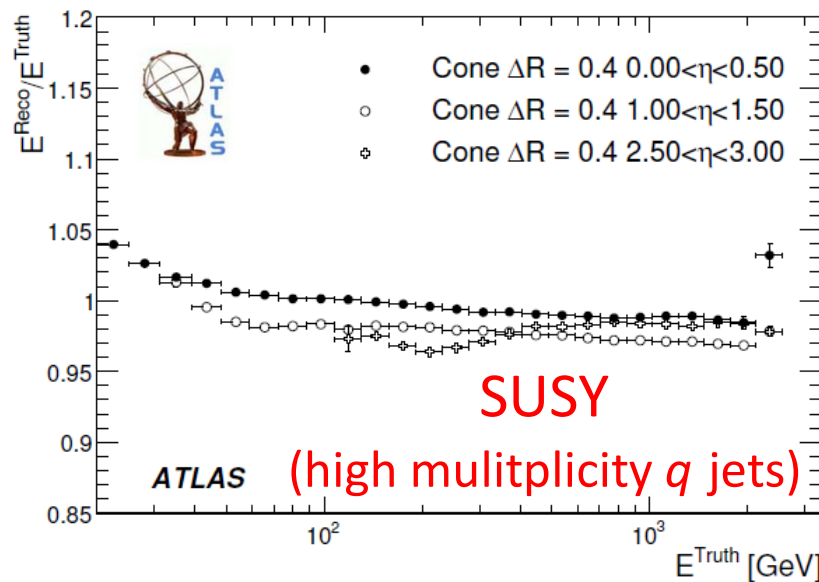
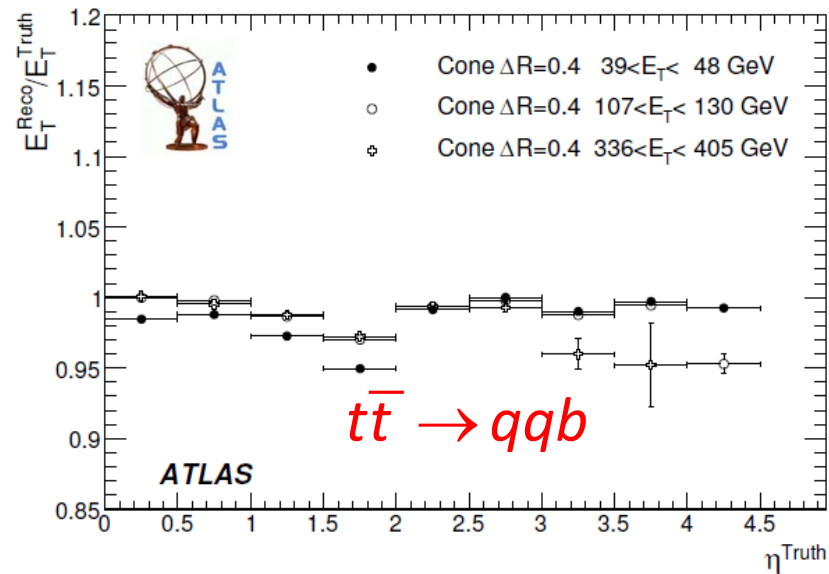
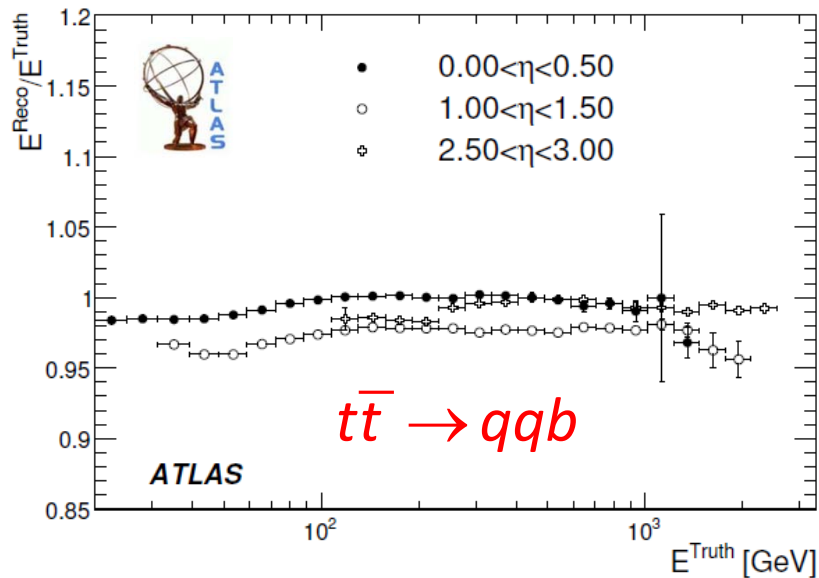
No strong dependence on calorimeter signal definition

No significant noise contribution anymore

$$\Delta_\sigma = \left(\frac{\sigma}{E}\right)_{\text{cluster}}^2 - \left(\frac{\sigma}{E}\right)_{\text{tower}}^2$$

$$\psi_\sigma = \begin{cases} \sqrt{\Delta_\sigma} & \text{for } \Delta_\sigma > 0 \\ -\sqrt{-\Delta_\sigma} & \text{for } \Delta_\sigma < 0 \end{cases}$$





Introduction to Hadronic Final State Reconstruction in Collider Experiments (Part XIII)

Peter Loch
University of Arizona
Tucson, Arizona
USA



Factorized calibration allows use of collision data

CMS sequence applies factorized scheme with required and optional corrections

Required corrections can initially be extracted from collision data

Average signal offset from pile-up and UE can be extracted from minimum bias triggers

Relative direction dependence of response can be corrected from di-jet p_T balance

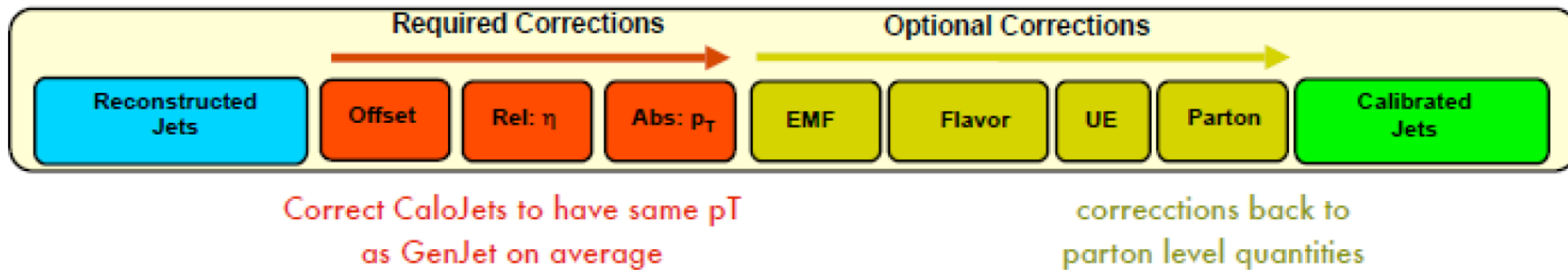
The absolute p_T scale correction can be derived from prompt photon production

Optional corrections refine jet calibration

Use jet by jet calorimeter or track observables to reduce fluctuations

Includes energy fractions in EMC, track p_T fractions, underlying event corrections using jet areas, flavor dependencies and others...

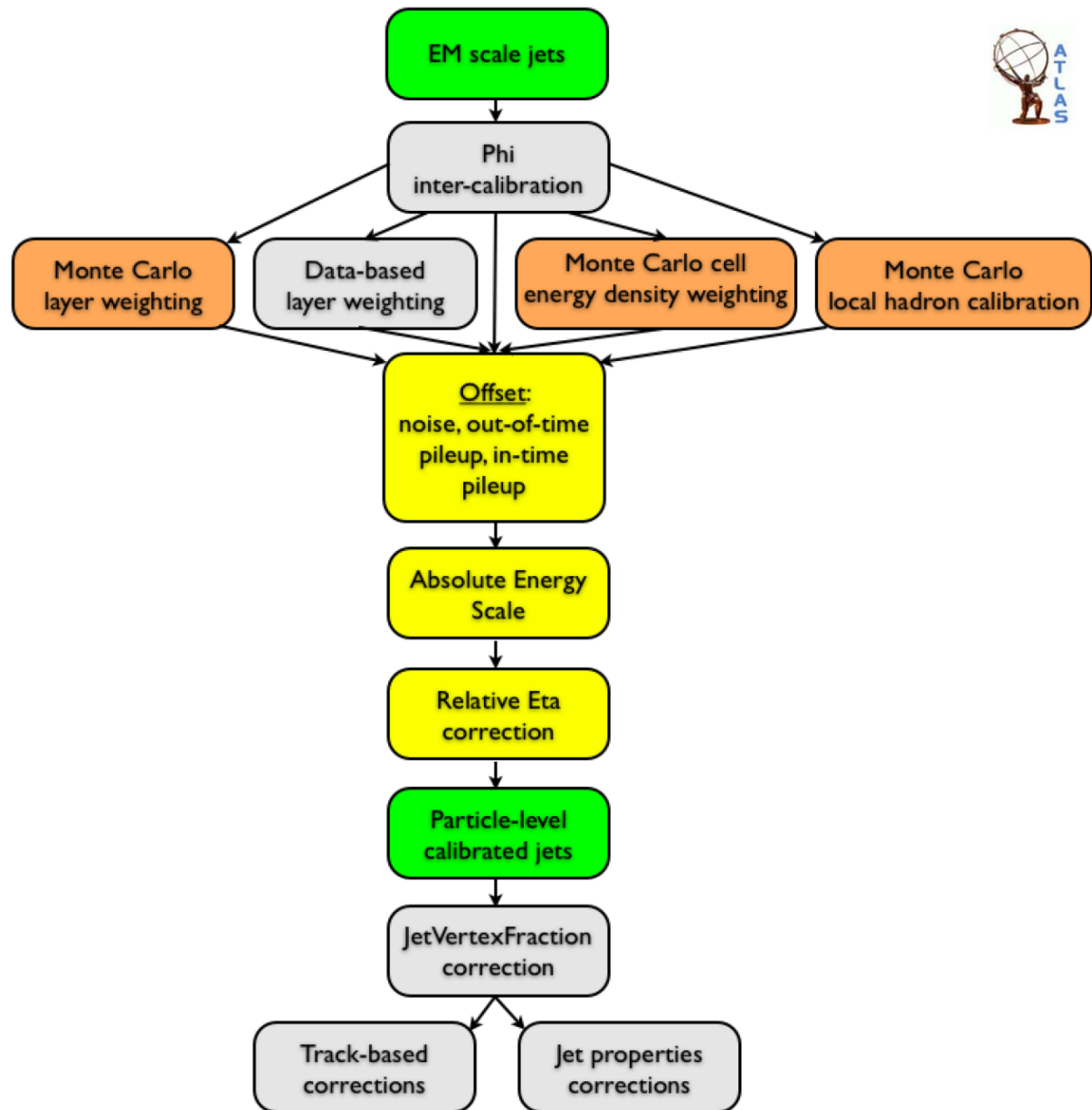
May need very good simulations!



optional

data driven

MC



PileUp subtraction

Goal:

Correct in-time and residual out-of-time pile-up contribution to a jet on average

Tools:

Zero bias (random) events, minimum bias events

Measurement:

Et density in $\Delta\eta \times \Delta\phi$ bins as function of # vertices

TopoCluster feature (size, average energy as function of depth) changes as function of # vertices

Remarks:

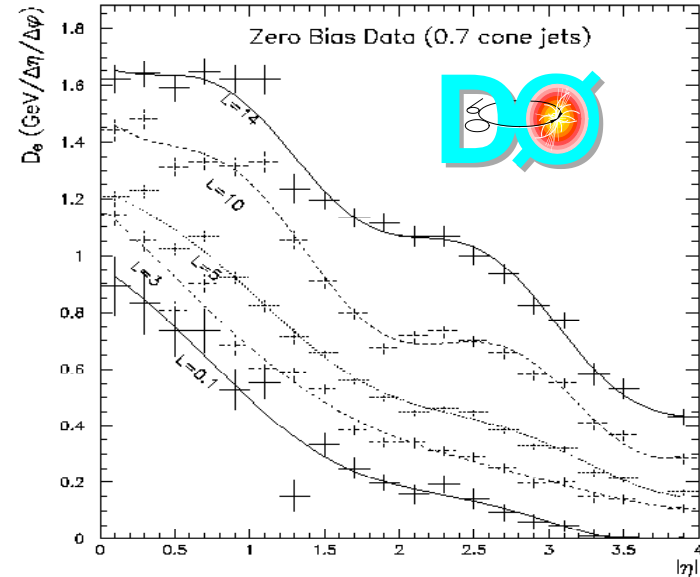
Uses expectations from the average Et flow for a given instantaneous luminosity

Instantaneous luminosity is measured by the # vertices in the event

Requires measure of jet size (AntiKt advantage)

Concerns:

Stable and safe determination of average



Determination of the Absolute Jet Energy Scale in the D0 Calorimeters. NIM A424, 352 (1999)

$$\rho_{\text{PU}}(\eta, \mathcal{L}) = \rho_{\text{PU}}(\eta, N_{\text{vtx}}) = \frac{\langle E_{\text{T}}^{\text{PU}} \rangle(\eta, N_{\text{vtx}})}{\Delta\eta \times \Delta\phi}$$

$$E_{\text{offset, jet}}^{\text{PU}} = \underbrace{\rho_{\text{PU}}(\eta, N_{\text{vtx}})}_{E_{\text{T, jet}}^{\text{PU}}} \cdot \overbrace{A_{\text{jet}}^{\text{jet area}}}$$

Note that magnitude of correction depends on calorimeter signal processing & definition – application easier to see for tower based jets!



Balancing jet pT with electromagnetic system

Truth from collision

Based on idea that electromagnetic particles are well measured
Limits accuracy to precision of photon or electron signal reconstruction

Provides interaction (parton) level reference

Note that simulation based approaches use particle level reference

Can use direct photon production

Kinematic reach for jet pT $\sim 200\text{-}400$ GeV for 1% precision – depends on center of mass energy
Relatively large cross-section
Background from QCD di-jets – one jet fluctuates into π^0 faking photon

Can also use Z+jet(s)

Cross-section suppressed, but less background – two electron final state cleaner

Can also use two muon final state

Note specific physics environment

Underlying event different from other final states

Less radiation in photon/Z hemisphere

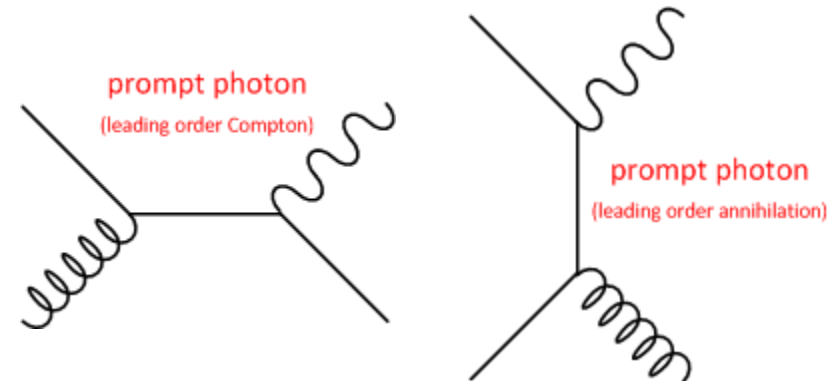
Often only good reference for quark jets

Narrow jets in lower radiation environment

prompt (direct) photon production:

$gq \rightarrow \gamma q$ QCD Compton scattering
($\sim 95\%$ of $\sigma_\gamma^{\text{tot}}$)

$q\bar{q} \rightarrow \gamma g$ annihilation



balance photon with (mostly) quark jet pT to validate or constrain

$p_{T,\text{reco},\text{jet}}$

Balancing jet p_T with electromagnetic system

Truth from collision

- Based on idea that electromagnetic particles are well measured
- Limits accuracy to precision of photon or electron signal reconstruction

Provides interaction (parton) level reference

- Note that simulation based approaches use particle level reference

Can use direct photon production

- Kinematic reach for jet $p_T \sim 200\text{-}400$ GeV for 1% precision – depends on center of mass energy
- Relatively large cross-section
- Background from QCD di-jets – one jet fluctuates into π^0 faking photon

Can also use Z+jet(s)

- Cross-section suppressed, but less background – two electron final state cleaner
- Can also use two muon final state

Note specific physics environment

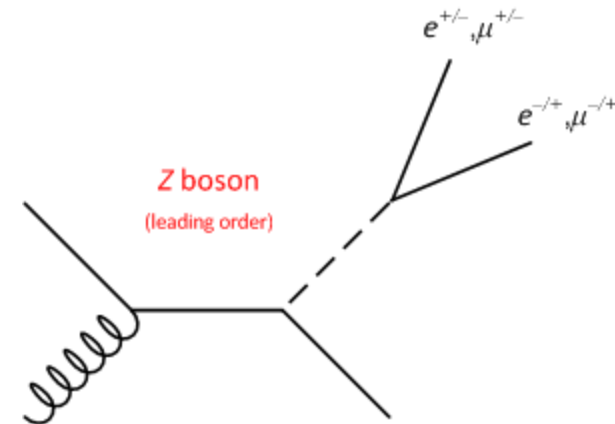
Underlying event different from other final states

- Less radiation in photon/Z hemisphere

Often only good reference for quark jets

- Narrow jets in lower radiation environment

Z-boson + jet production:



balance Z p_T reconstructed from decay leptons with quark jet p_T to validate or constrain $p_{T,\text{reco},\text{jet}}$

Absolute response

Goal:

Correct for energy (pT)
dependent jet response

Tools:

Direct photons, Z+jet(s),...

Measurement:

pT balance of well calibrated
system (photon, Z) against jet in
central region

Remarks:

Usually uses central reference
and central jets (region of flat
response)

Concerns:

Limit in precision and estimates
for systematics w/o well
understood simulations not clear
Needs corrections to undo out-
of-cone etc. to compare to
particle level calibrations

ratio test variable ($\kappa = \gamma, Z$):

$$f_{\text{absolute}}(\zeta_{\text{probe}}) = \left[1 + \frac{\rho_{T,\text{reco,jet}} - \rho_{T,\kappa}}{\rho_{T,\kappa}} \right]^{-1}$$

variation of jet response
with photon/Z ρ_T

with

$$\zeta_{T,\text{probe}} = \begin{cases} \rho_{T,\kappa} & \text{reference pT} \\ \frac{\rho_{T,\kappa} + \rho_{T,\text{reco,jet}}}{2} & \text{average pT} \\ E' = \rho_{T,\kappa} \cosh \eta_{\text{reco,jet}} & \text{expected jet energy} \end{cases}$$

(relate to reconstructed jet variables with numerical inversion)

relative projection along reference pT:

$$\frac{\mathcal{P}_{\parallel}}{\rho_{T,\kappa}} = \frac{\rho_{T,\text{reco,jet}} \cos \angle(\vec{\rho}_{T,\text{reco,jet}}, \vec{\rho}_{T,\kappa})}{\rho_{T,\kappa}} = \frac{\vec{\rho}_{T,\text{reco,jet}} \cdot \vec{\rho}_{T,\kappa}}{\rho_{T,\kappa}^2}$$

correction from $\frac{\mathcal{P}_{\parallel}}{\rho_{T,\kappa}} + 1 \equiv 0$ for well calibrated jets:

$$f_{\text{absolute}}(\zeta_{\text{probe}}) = \left| \frac{\rho_{T,\kappa}}{\mathcal{P}_{\parallel}} \right|$$



Missing Transverse Energy Projection Fraction method (MPF)

Uses pT balance in photon+jet events to determine jet response

Technically on any jet response scale, but most useful if jet signal is corrected for e/h and other (local) detector effects

Based on projection of event missing transverse energy (MET) on photon pT direction

MET mostly generated by jet response

Least sensitive to underlying event and pile-up due to randomization in azimuth

Allows to validate the jet energy response

Reference can be energy instead of pT

Basis of absolute jet energy scale in DZero

Also under study for LHC

Considerations

Perfect balance at parton level perturbed at particle level

Parton showering and hadronization, including initial and final state radiation (ISR & FSR)

Can be suppressed by selecting back-to-back photon-jet topologies

Imperfect calorimeter response generates missing transverse energy

Handle for calibration

p_T balance in prompt photon production:

$$\underbrace{\vec{p}_{T,\gamma}}_{\text{parton level}} + \underbrace{\vec{p}_{T,\text{jet}}}_{\text{parton level}} = \underbrace{\vec{E}_{T,\gamma} + \vec{p}_{T,\text{jet}}}_{\text{particle level}} = 0 \Rightarrow \vec{E}_{T,\gamma} + \vec{E}_{T,\text{jet}} \approx 0$$

with calorimeter response and projection on $\vec{E}_{T,\gamma}$:

$$e\vec{E}_{T,\gamma} + j(E_{\text{jet}})\vec{E}_{T,\text{jet}} = -\vec{E}_T^{\text{miss}} \\ \Rightarrow E_{T,\gamma} + j(E_{\text{jet}})\vec{E}_{T,\text{jet}} \cdot \hat{n}_\gamma = -\hat{n}_\gamma \cdot \vec{E}_T^{\text{miss}}$$

calculate \vec{E}_T^{miss} from all calorimeter signals excluding the photon signal:

$$\vec{E}_T^{\text{miss}} = -\vec{E}_{T,\gamma} - \sum_{\substack{\text{all calo signals} \\ \text{not from } \gamma}} \vec{E}_{T,\text{calo}} \\ \Rightarrow j(E_{\text{jet}}) = \frac{\sum_{\substack{\text{all calo signals} \\ \text{not from } \gamma}} \vec{E}_{T,\text{calo}} \cdot \hat{n}_\gamma}{\vec{E}_{T,\text{jet}} \cdot \hat{n}_\gamma} = \frac{\sum_{\substack{\text{all calo signals} \\ \text{not from } \gamma}} \vec{E}_{T,\text{calo}} \cdot \hat{n}_\gamma}{E_{T,\gamma}}$$

suppress biases by measuring response as function of

$E' = E_{T,\gamma} \cosh \eta_{\text{jet}}$ yielding empirically:

$$j(E') = b_0 + b_1 \ln \frac{E'}{E_{\text{scale}}} + b_2 \ln^2 \frac{E'}{E_{\text{scale}}}$$

use numerical inversion for $E_{\text{rec,jet}} \mapsto E'!$



Missing Transverse Energy Projection Fraction method (MPF)

Uses p_T balance in photon+jet events to determine jet response

Technically on any jet response scale, but most useful if jet signal is corrected for e/h and other (local) detector effects

Based on projection of event missing transverse energy (MET) on photon p_T direction

MET mostly generated by jet response
 Least sensitive to underlying event and pile-up due to randomization in azimuth

Allows to validate the jet energy response

Reference can be energy instead of p_T

Basis of absolute jet energy scale in DZero

Also under study for LHC

Considerations

Perfect balance at parton level perturbed at particle level

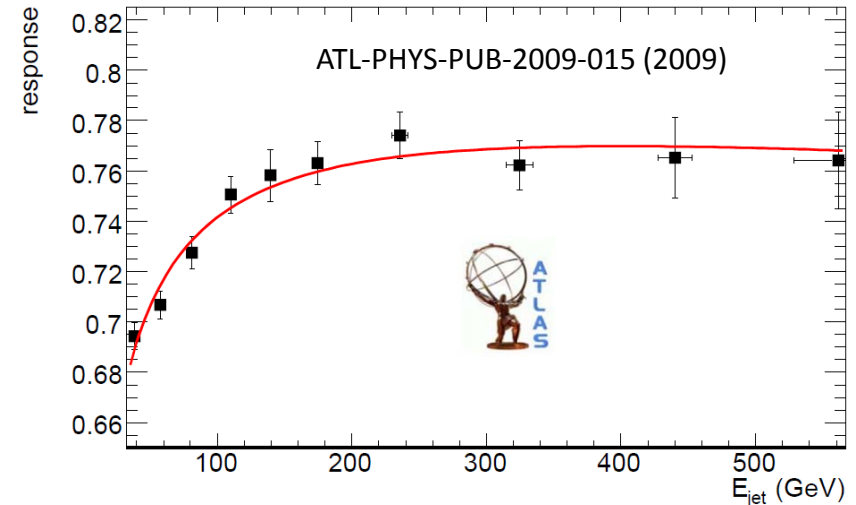
Parton showering and hadronization, including initial and final state radiation (ISR & FSR)

Can be suppressed by selecting back-to-back photon-jet topologies

Imperfect calorimeter response generates missing transverse energy

Handle for calibration

ATLAS Simulations



$$j(E') = b_0 + b_1 \ln \frac{E'}{E_{scale}} + b_2 \ln^2 \frac{E'}{E_{scale}}$$



Photon+jet(s)

Well measured electromagnetic system
balances jet response

Central value theoretical uncertainty $\sim 2\%$
limits precision

Due to photon isolation requirements

But very good final state for evaluating
calibrations

Can test different correction levels in
factorized calibrations

E.g., local hadronic calibration in ATLAS

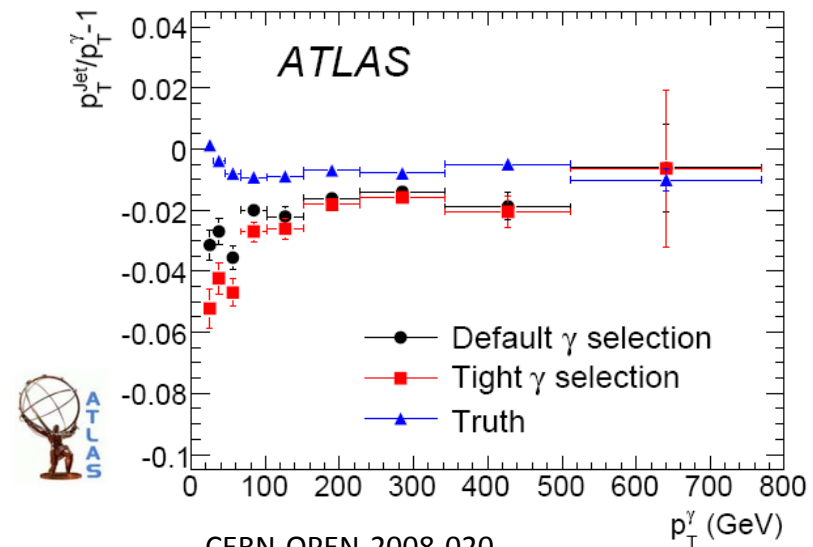
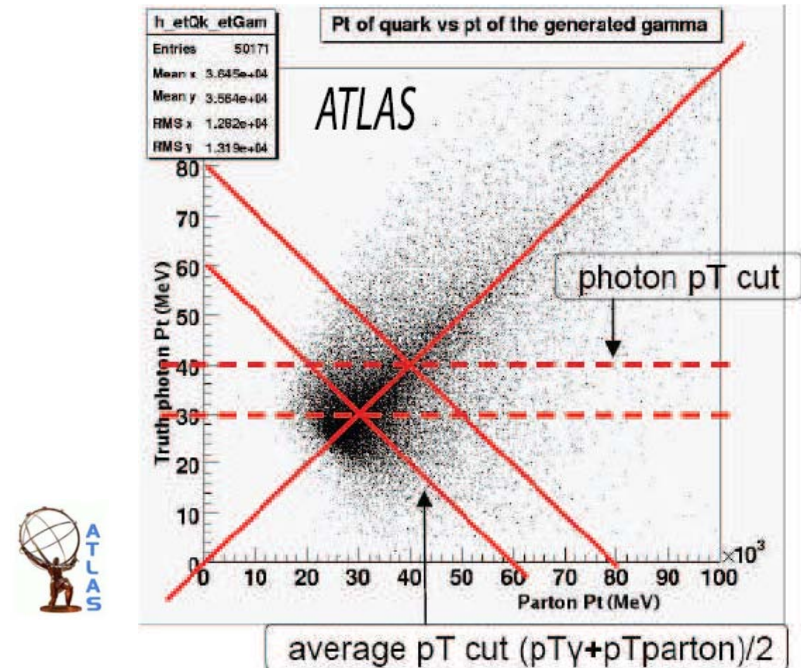
Limited p_T reach for 1-2% precision

25 \rightarrow 300 GeV within 100 pb^{-1}

Z+jet(s)

Similar idea, but less initial statistics

Smaller reach but less background



Photon+jet(s)

Well measured electromagnetic system
balances jet response

Central value theoretical uncertainty $\sim 2\%$
limits precision

Due to photon isolation requirements

But very good final state for evaluating
calibrations

Can test different correction levels in
factorized calibrations

E.g., local hadronic calibration in ATLAS

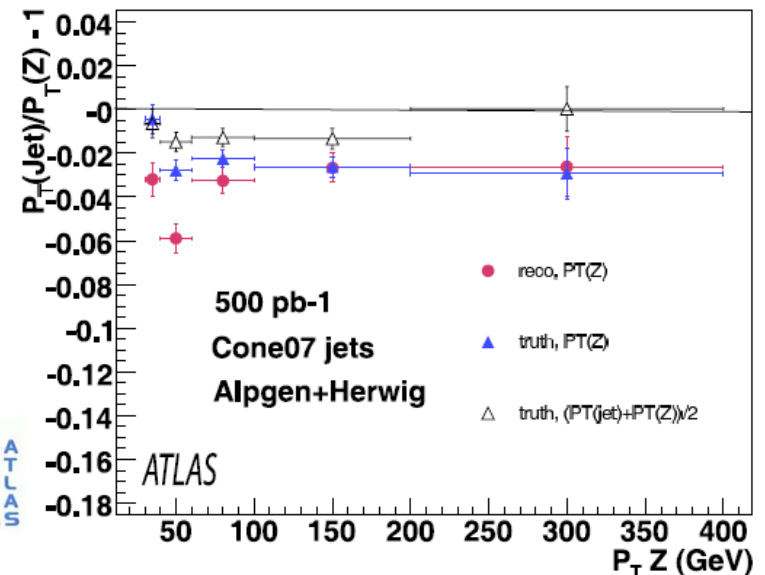
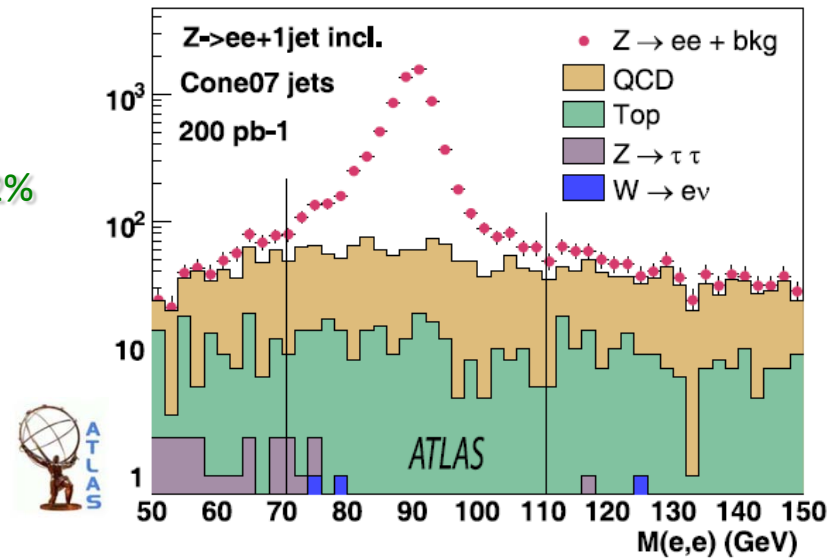
Limited p_T reach for 1-2% precision

25- \rightarrow 300 GeV within 100 pb-1

Z+jet(s)

Similar idea, but less initial statistics

Smaller reach but less background



In-situ calibration validation handle

Precise reference in $t\bar{t}$ events

Hadronically decaying W-bosons

Jet calibrations should reproduce W-mass

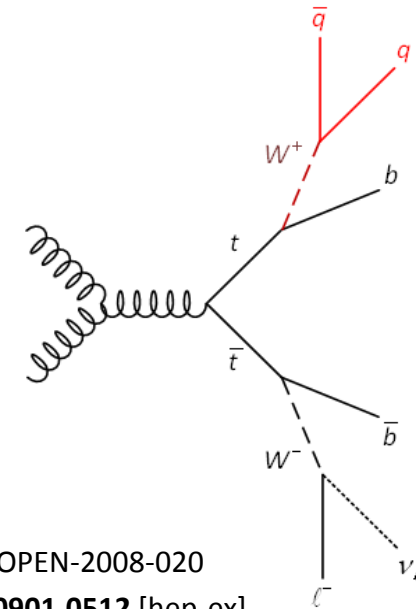
Note color singlet source

No color connection to rest of collision – different underlying event as QCD

Also only light quark jet reference

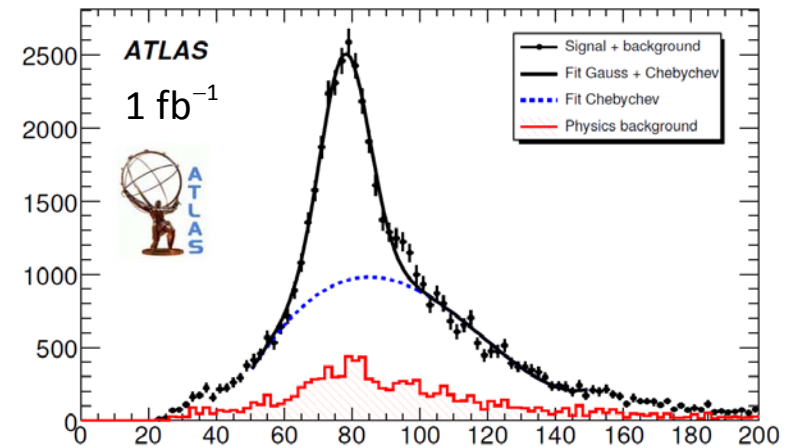
Expected to be sensitive to jet algorithms

Narrow jets perform better – as expected



CERN-OPEN-2008-020

arXiv:0901.0512 [hep-ex]



Simulated di-jet invariant mass ($M_{W, reco}$)

spectrum for kT jets with $R = 0.4$ (narrow jets)

in $t\bar{t}$ final states at $\sqrt{s} = 14$ TeV



W boson mass from two jets

Clean event sample can be accumulated quickly

Original studies for center of mass energy of 14 TeV and luminosity of $10^{33} \text{ cm}^{-2}\text{s}^{-1}$
~130 clean events/day in $t\bar{t}b\bar{a}r$

Angular and energy scale component in reconstruction

Energy scale dominant

invariant mass from decay jets:

$$M_{W,\text{reco}} = \sqrt{2E_{\text{jet},1}E_{\text{jet},2}(1 - \cos\theta_{\text{jet},1,\text{jet},2})}$$

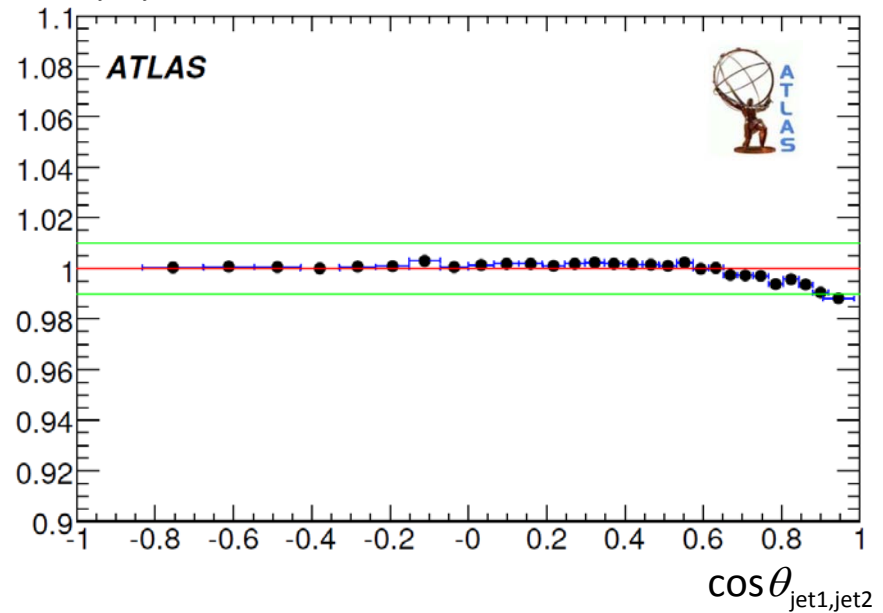
bias from angular mismeasurement:

$$\mathcal{K}(\cos\theta_{\text{jet},1,\text{jet},2}) = \frac{1 - \cos\theta_{\text{parton},1,\text{parton},2}}{1 - \cos\theta_{\text{jet},1,\text{jet},2}} \approx 1$$

is small

$$\mathcal{K}(\cos\theta_{\text{jet},1,\text{jet},2})$$

arXiv:0901.0512 [hep-ex]



W boson mass from two jets

Clean event sample can be accumulated quickly

Original studies for center of mass energy of 14 TeV and luminosity of $10^{33} \text{ cm}^{-2}\text{s}^{-1}$
~130 clean events/day in $t\bar{t}$

Angular and energy scale component in reconstruction

Energy scale dominant

invariant mass from decay jets:

$$M_{W,\text{reco}} = \sqrt{2E_{\text{jet},1}E_{\text{jet},2}(1 - \cos\theta_{\text{jet},1,\text{jet},2})}$$

bias from angular mismeasurement:

$$\mathcal{K}(\cos\theta_{\text{jet},1,\text{jet},2}) = \frac{1 - \cos\theta_{\text{parton},1,\text{parton},2}}{1 - \cos\theta_{\text{jet},1,\text{jet},2}} \approx 1$$

is small \rightarrow major contribution from energy scale:

$$M_{W,\text{PDG}}$$

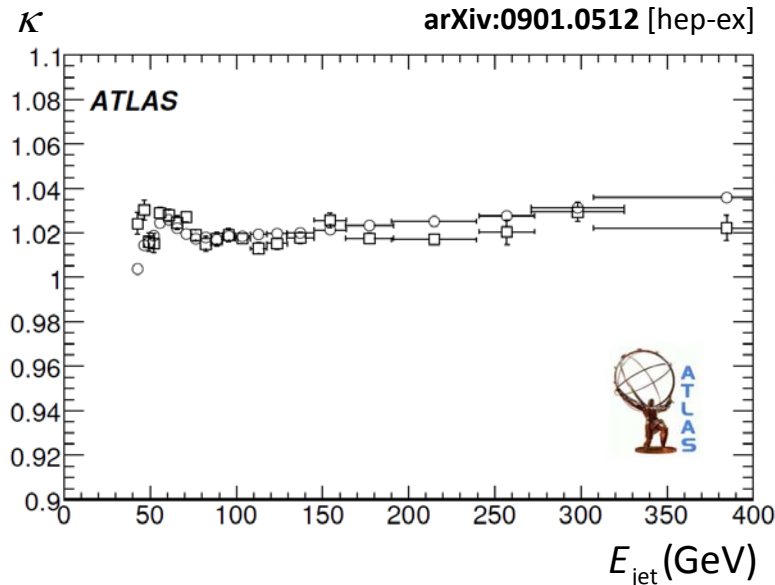
$$= \sqrt{2\kappa(E_{\text{jet},1})E_{\text{jet},1}\kappa(E_{\text{jet},2})E_{\text{jet},2}\mathcal{K}(\cos\theta_{\text{jet},1,\text{jet},2})(1 - \cos\theta_{\text{jet},1,\text{jet},2})}$$

$$\approx \sqrt{2\kappa(E_{\text{jet},1})E_{\text{jet},1}\kappa(E_{\text{jet},2})E_{\text{jet},2}(1 - \cos\theta_{\text{jet},1,\text{jet},2})}$$

$$= \sqrt{\kappa(E_{\text{jet},1})\kappa(E_{\text{jet},2})} \cdot M_{W,\text{reco}}$$

simple rescaling method assuming energy independent

scale shift $\rightarrow \kappa(E_{\text{jet},1}) = \kappa(E_{\text{jet},2}) = \kappa$ works reasonably well



W mass from templates

Produce W mass distribution templates

Use parton or particle level simulations

Smear with JES and resolution variations

Store W mass distributions as function of smearing parameters

Find response and resolution smearing parameters

Find best fit template

JES scale α relative to perfect jet response;

resolution parameter β relative to nominal jet energy resolution;

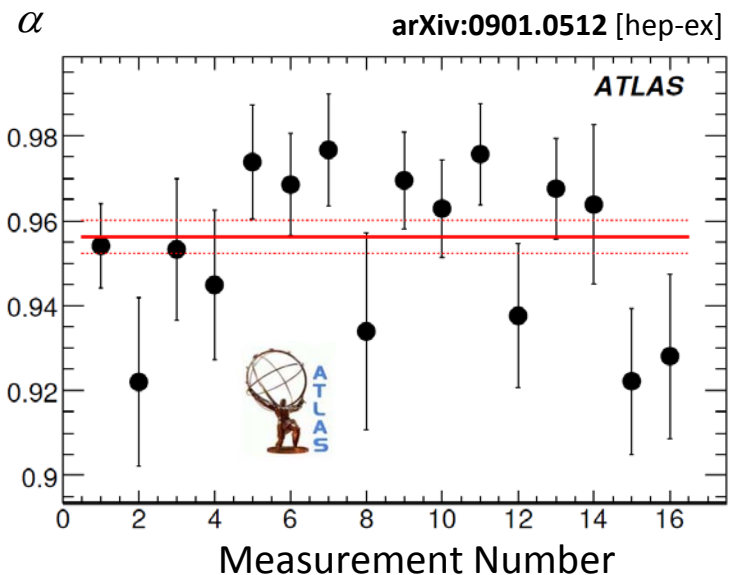
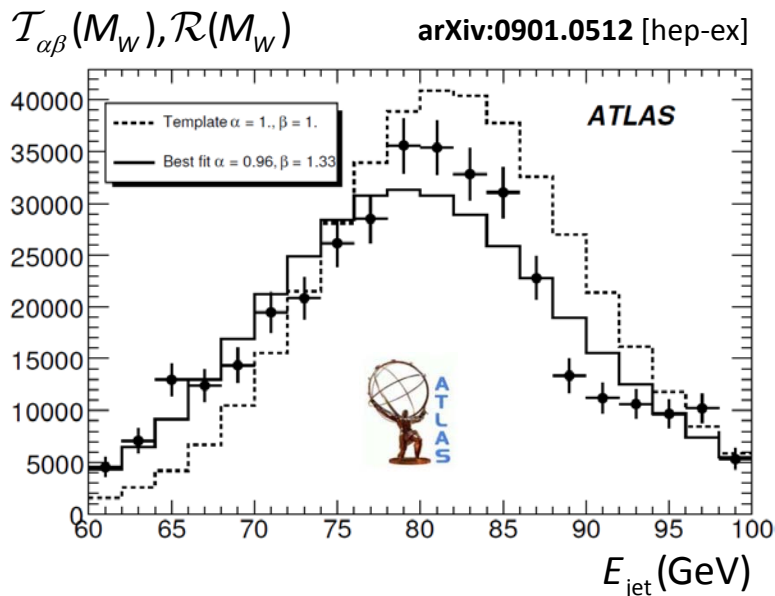
find best matching template distribution $\mathcal{T}_{\alpha\beta}(M_W)$

for reconstructed distribution $\mathcal{R}(M_W)$:

$$\chi^2 = \int (\mathcal{T}_{\alpha\beta}(M_W) - \mathcal{R}(M_W))^2 / (\sigma_{\mathcal{T}_{\alpha\beta}(M_W)}^2 + \sigma_{\mathcal{R}(M_W)}^2) dM_W = \min$$

stability of fit tested by subdividing total sample into 16

"measurements" ($770 \text{ pb}^{-1} \rightarrow 16 \times 48 \text{ pb}^{-1}$):



Boosted W

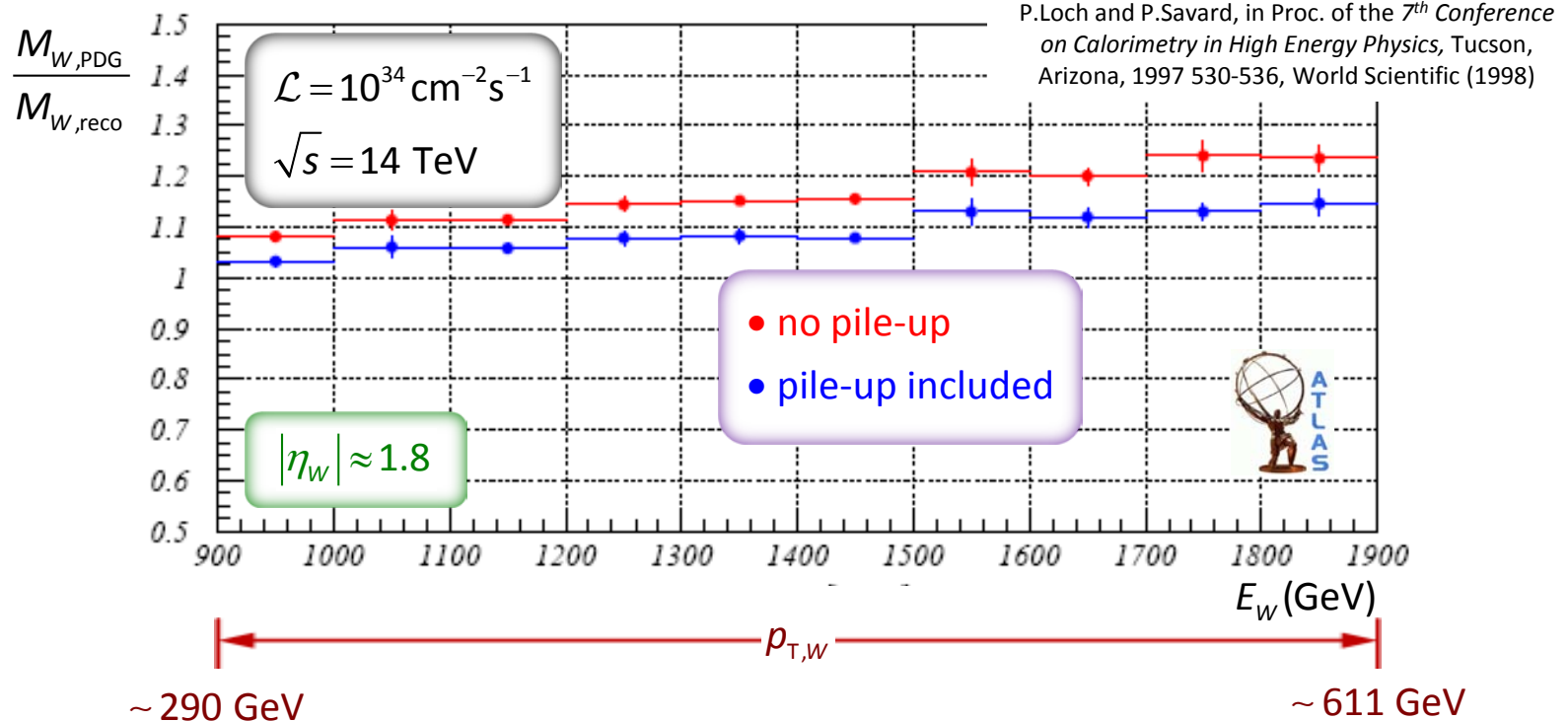
p_T boost reduces angle between decay jets

Reconstructed mass underestimates true W mass

See example below for W boosted into the ATLAS end-cap calorimeter region

Pile-up can add energy to the system

Not an improvement of the measurement – accidental and thus uncorrelated jet energy shifts lead to shift in reconstructed mass



Di-jet balance

Calibrate jet in “golden” reference region

Use e.g. photon pT balance

Use this jet as “truth” reference

Balance pT with jet in more complex calorimeter region

Note: relative energy resolution of reference jet can be worse than probe jet – more forward jet has more energy at same pT

Resolution bias needs to be controlled

Apply corrections to all jets at given direction

Need to understand topology – additional soft jet contribution

Can also be used to measure jet energy resolution

Need to consider phase space sharing with possible additional soft jets

Multi-jet balance

Validation of very high pT jets

In-situ calibrations with photons etc. only reaches 200-300 GeV (pT)

But need to validate very high pT jet scale as well

Bootstrap approach

Find multi-jet events with one hard jet in non-validated phase-space

Balance hard jet with several well calibrated lower pT jets (e.g., from photons)

Look for more harder jets and use scale corrections from lower pT jets (bootstrap corrections)

Note that errors evolve from low to high pT

Hard to achieve $O(1\%)$ precision

Likely need simulation based approach



Correct direction-dependent jet response

Establish absolute scale in “golden region” of the detector

Balancing p_T of a central (lower energy) jet with a more forward (higher energy jet)

Avoid biases by compensating reference jet response first

Determine direction dependent correction factors

Use p_T asymmetry measure for back-to-back jet
 Careful – resolution bias due to different jet energy ranges can still be present!

Jet energy resolution from di-jet p_T balance

Select event topology

Di-jets back-to-back in azimuth

Same rapidity region

Similar p_T

Use asymmetry measure to calculate jet energy resolution

Width of the distribution of A

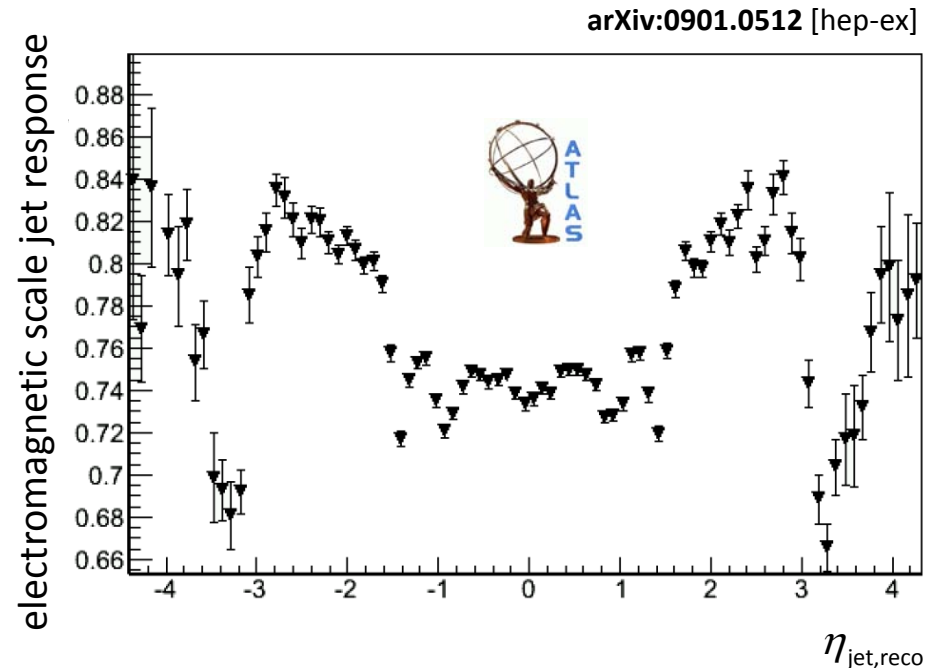
Understand soft radiation contribution

p_T balance approach ($D\phi$)

Use di-jet energy resolution dependence on third jet p_T as scale to unfold radiation contribution

kT balance approach (UA2, CDF)

Determination of radiation contribution using bisector decomposition



asymmetry measure:

$$A = \frac{p_{T, \text{reco}}^{\text{probe}} - p_{T, \text{reco}}^{\text{reference}}}{(p_{T, \text{reco}}^{\text{probe}} + p_{T, \text{reco}}^{\text{reference}})/2} = \frac{p_{T, \text{reco}}^{\text{probe}} - p_{T, \text{reco}}^{\text{reference}}}{p_{T, \text{reco}}^{\text{average}}}$$

correction factors (use numerical inversion):

$$c(p_{T, \text{reco}}^{\text{average}}, \eta_{\text{probe}}) = \frac{2 - A(p_{T, \text{reco}}^{\text{average}}, \eta_{\text{probe}})}{2 + A(p_{T, \text{reco}}^{\text{average}}, \eta_{\text{probe}})} \mapsto c(p_{T, \text{reco}}^{\text{probe}}, \eta_{\text{probe}})$$



Correct direction-dependent jet response

Establish absolute scale in “golden region” of the detector

Balancing p_T of a central (lower energy) jet with a more forward (higher energy jet)

Avoid biases by compensating reference jet response first

Determine direction dependent correction factors

Use p_T asymmetry measure for back-to-back jet
 Careful – resolution bias due to different jet energy ranges can still be present!

Jet energy resolution from di-jet p_T balance

Select event topology

Di-jets back-to-back in azimuth

Same rapidity region

Similar p_T

Use asymmetry measure to calculate jet energy resolution

Width of the distribution of A

Understand soft radiation contribution

p_T balance approach ($D\phi$)

Use di-jet energy resolution dependence on third jet p_T as scale to unfold radiation contribution

kT balance approach (UA2, CDF)

Determination of radiation contribution using bisector decomposition

asymmetry measure (slightly modified):

$$A = \frac{p_{T,\text{reco}}^{\text{jet1}} - p_{T,\text{reco}}^{\text{jet2}}}{p_{T,\text{reco}}^{\text{jet1}} + p_{T,\text{reco}}^{\text{jet2}}} = \frac{p_{T,\text{reco}}^{\text{jet1}} - p_{T,\text{reco}}^{\text{jet2}}}{2p_{T,\text{reco}}^{\text{average}}}$$

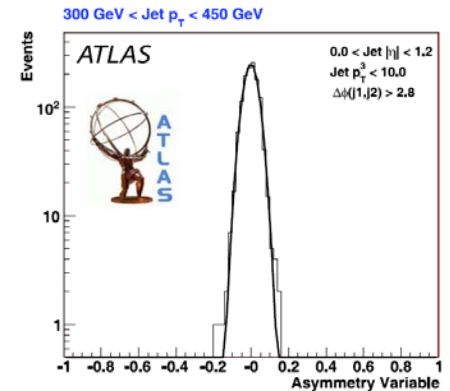
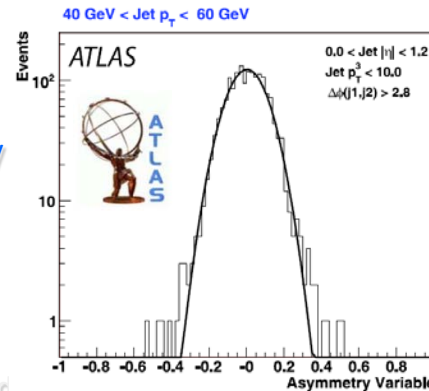
p_T resolution for jets in same η region with similar p_T :

$$\frac{\sigma_{p_T}}{p_{T,\text{reco}}^{\text{average}}} = \sqrt{2}\sigma_A \approx \frac{\sigma_E}{E}$$

resolution is symmetrized by randomly computing

$$p_{T,\text{reco}}^{\text{jet1}} - p_{T,\text{reco}}^{\text{jet2}} \text{ or } p_{T,\text{reco}}^{\text{jet2}} - p_{T,\text{reco}}^{\text{jet1}}$$

for each event



Correct direction-dependent jet response

Establish absolute scale in “golden region” of the detector

Balancing p_T of a central (lower energy) jet with a more forward (higher energy jet)

Avoid biases by compensating reference jet response first

Determine direction dependent correction factors

Use p_T asymmetry measure for back-to-back jet
 Careful – resolution bias due to different jet energy ranges can still be present!

Jet energy resolution from di-jet p_T balance

Select event topology

Di-jets back-to-back in azimuth

Same rapidity region

Similar p_T

Use asymmetry measure to calculate jet energy resolution

Width of the distribution of A

Understand soft radiation contribution

p_T balance approach ($D\phi$)

Use di-jet energy resolution dependence on third jet p_T as scale to unfold radiation contribution

kT balance approach (UA2, CDF)

Determination of radiation contribution using bisector decomposition

determine clean di-jet resolution by linear extrapolation of

$$\frac{\sigma_{p_T}}{p_T}(p_{T,\text{reco},\text{jet3}} < p_{T,\text{threshold}}, p_{T,\text{reco}}^{\text{average}}),$$

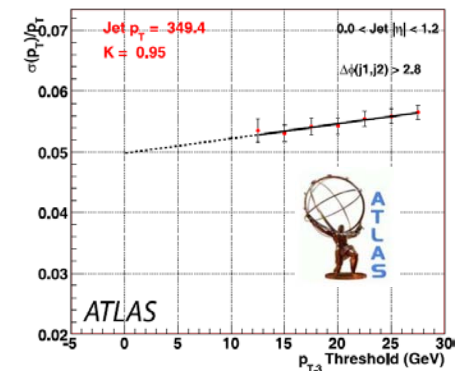
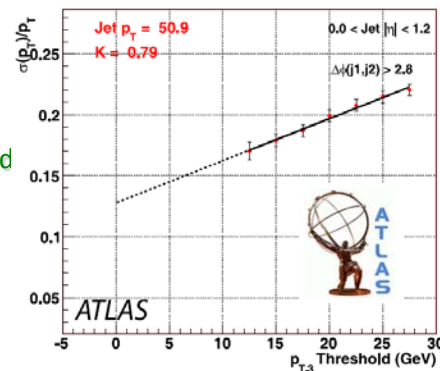
typically with $p_{T,\text{threshold}} \geq p_{T,\text{min}} = (7 - 10) \text{ GeV}$,

implied by calorimeter jet reconstruction, to

$$p_{T,\text{reco},\text{jet3}} = 0:$$

$$\lim_{p_{T,\text{reco},\text{jet3}} \rightarrow 0} \frac{\sigma_{p_T}}{p_T}(p_{T,\text{reco}}^{\text{average}})$$

fit has some bias problems due to phase space limitations at low $p_{T,\text{reco}}^{\text{average}}$ together in the presence of $p_{T,\text{min}}$



Correct direction-dependent jet response

Establish absolute scale in “golden region” of the detector

Balancing pT of a central (lower energy) jet with a more forward (higher energy jet)

Avoid biases by compensating reference jet response first

Determine direction dependent correction factors

Use pT asymmetry measure for back-to-back jet
 Careful – resolution bias due to different jet energy ranges can still be present!

Jet energy resolution from di-jet pT balance

Select event topology

Di-jets back-to-back in azimuth
 Same rapidity region
 Similar pT

Use asymmetry measure to calculate jet energy resolution

Width of the distribution of A

Understand soft radiation contribution

pT balance approach (DØ)

Use di-jet energy resolution dependence on third jet pT as scale to unfold radiation contribution

kT balance approach (UA2, CDF)

Determination of radiation contribution using bisector decomposition

resolution correction factor from

$$\mathcal{K}(p_{T,\text{reco}}^{\text{average}}) = \mathcal{K}(p_{T,\text{reco}})$$

$$= \frac{\lim_{p_{T,\text{reco},\text{jet3}} \rightarrow \infty} (\sigma_{p_T} / p_{T,\text{reco}})(p_{T,\text{reco}})}{\sigma_{p_T} / p_{T,\text{reco}} (p_{T,\text{reco},\text{jet3}} < 10 \text{ GeV}, p_{T,\text{reco}})}$$

such that

$$\left(\frac{\sigma_{p_T}}{p_{T,\text{reco}}} \right)_{\text{corrected}} = \mathcal{K}(p_{T,\text{reco}}) \frac{\sigma_{p_T}}{p_{T,\text{reco}}} (p_{T,\text{reco},\text{jet3}} < 10 \text{ GeV}, p_{T,\text{reco}})$$

with a parameterization of the p_T dependence of the correction by

$$\mathcal{K}(p_{T,\text{reco}}) = a + b \cdot \log p_{T,\text{reco}}$$

The detailed documentation of this approach, including a full systematic evaluation and discussion of the low pT bias using ATLAS simulations, is available to ATLAS members only in:

E. Hughes, D. Lopez, A. Schwartzman,
[ATL-COM-PHYS-2009-408 \(2009\)](#)



Correct direction-dependent jet response

Establish absolute scale in “golden region” of the detector

Balancing pT of a central (lower energy) jet with a more forward (higher energy jet)

Avoid biases by compensating reference jet response first

Determine direction dependent correction factors

Use pT asymmetry measure for back-to-back jet
 Careful – resolution bias due to different jet energy ranges can still be present!

Jet energy resolution from di-jet pT balance

Select event topology

Di-jets back-to-back in azimuth
 Same rapidity region
 Similar pT

Use asymmetry measure to calculate jet energy resolution

Width of the distribution of A

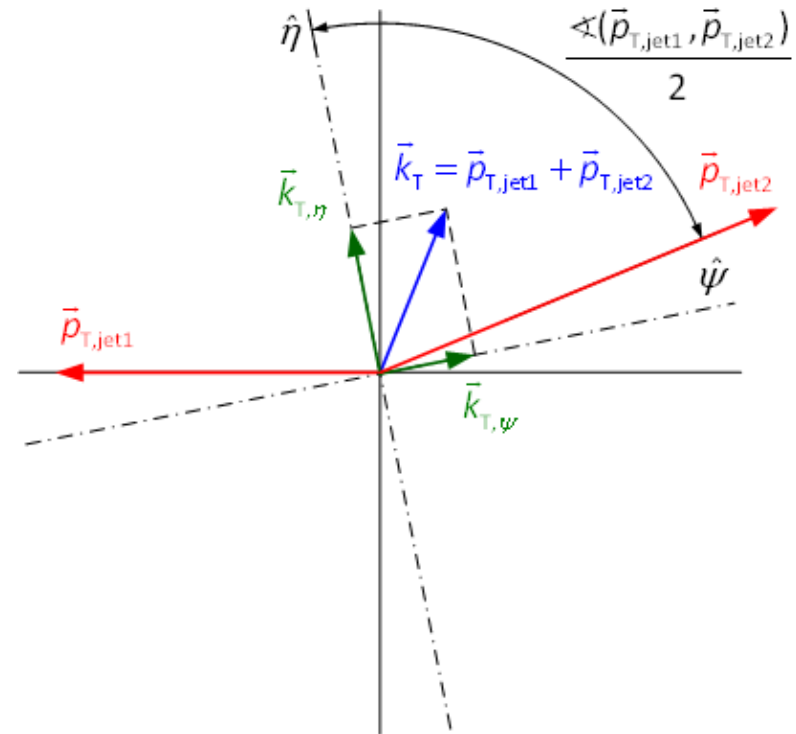
Understand soft radiation contribution

pT balance approach ($D\phi$)

Use di-jet energy resolution dependence on third jet pT as scale to unfold radiation contribution

kT balance approach (UA2, CDF)

Determination of radiation contribution using bisector decomposition



$\vec{k}_{T,\psi}$ most sensitive to calorimeter resolution effects:

$$\sigma_{\psi}^2 = \sigma_{E,\text{calo}}^2 + \sigma_{\text{radiation},\parallel}^2, \text{ with } \sigma_{E,\text{calo}} \gg \sigma_{\text{radiation},\parallel}$$

$\vec{k}_{T,\eta}$ most sensitive to (gluon) radiation effects:

$$\sigma_{\eta}^2 = \sigma_{\text{radiation},\perp}^2$$

(ignoring effects from angular resolution, underlying event, out of cone losses)

assume radiation is random wrt jet directions:

$$\sigma_{\text{radiation},\perp}^2 = \sigma_{\text{radiation},\parallel}^2 \Rightarrow \sigma_{E,\text{calo}}^2 = \sqrt{\sigma_{\psi}^2 - \sigma_{\eta}^2}$$



Correct direction-dependent jet response

Establish absolute scale in “golden region” of the detector

Balancing pT of a central (lower energy) jet with a more forward (higher energy jet)

Avoid biases by compensating reference jet response first

Determine direction dependent correction factors

Use pT asymmetry measure for back-to-back jet
 Careful – resolution bias due to different jet energy ranges can still be present!

Jet energy resolution from di-jet pT balance

Select event topology

Di-jets back-to-back in azimuth
 Same rapidity region
 Similar pT

Use asymmetry measure to calculate jet energy resolution

Width of the distribution of A

Understand soft radiation contribution

pT balance approach ($D\phi$)

Use di-jet energy resolution dependence on third jet pT as scale to unfold radiation contribution

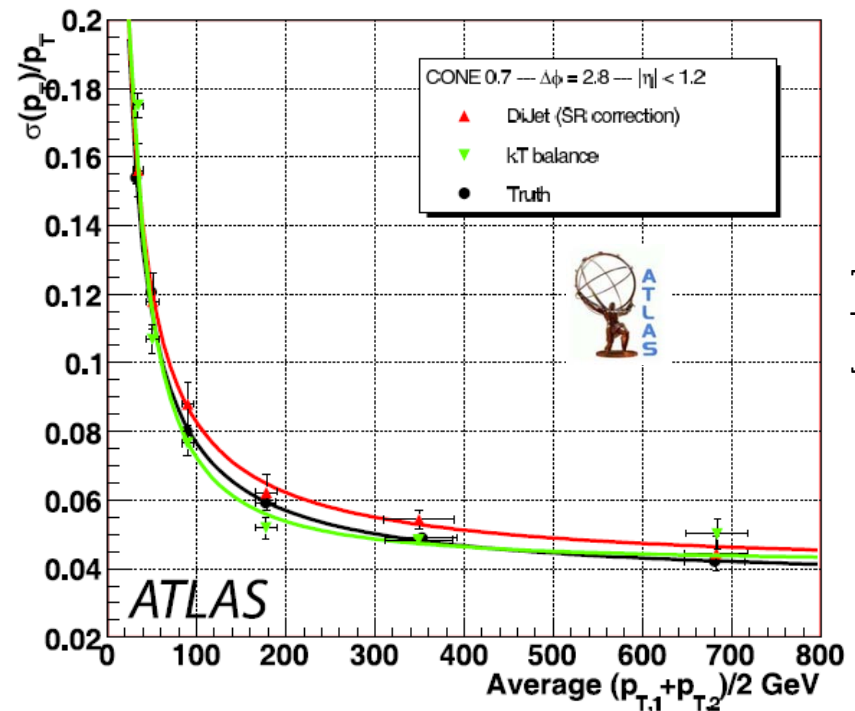
kT balance approach (UA2, CDF)

Determination of radiation contribution using bisector decomposition

note $\sigma_\psi(p_{T,\text{reco}}^{\text{average}}) \propto \sqrt{p_{T,\text{reco}}^{\text{average}}}$, and

$\sigma_\eta \approx \text{const} < \sigma_\psi(p_{T,\text{reco}}^{\text{average}} > p_{T,\text{min}})$

as expected!



Dangerous background for W+n jets cross-sections etc.

Lowest pT jet of final state can be faked or misinterpreted as coming from underlying event or multiple interactions

Extra jets from UE are hard to handle

No real experimental indication of jet source

Some correlation with hard scattering?

Jet area?

No separate vertex

Jet-by-jet handle for multiple proton interactions

Match tracks with vertices to calorimeter jet

Calculate track pT fraction from given vertex

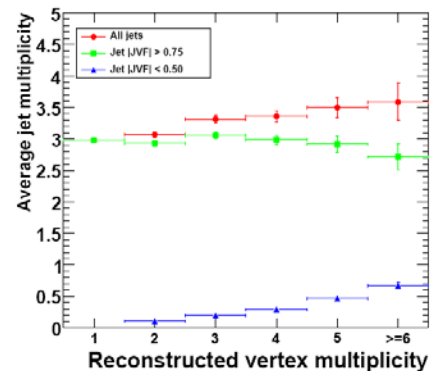
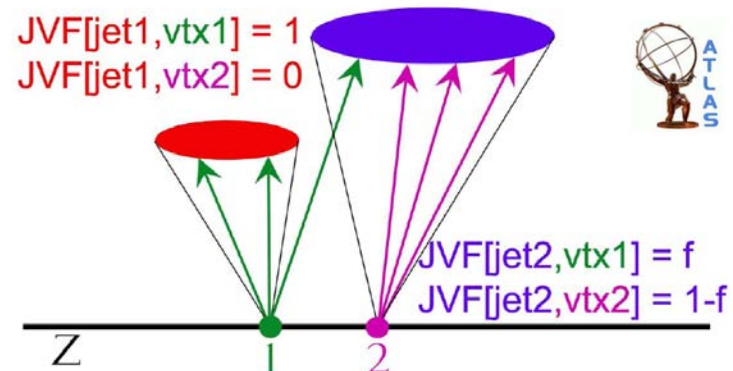
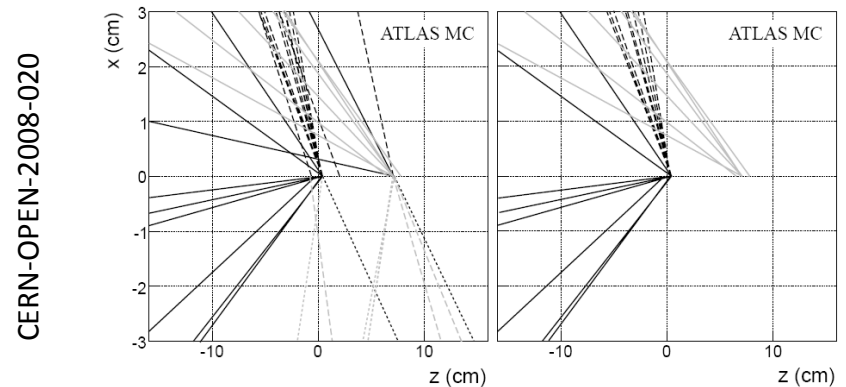
Classic indicator for multiple interactions is number of reconstructed vertices in event

Tevatron with $\text{RMS}(z_{\text{vertex}}) \sim 30$ cm

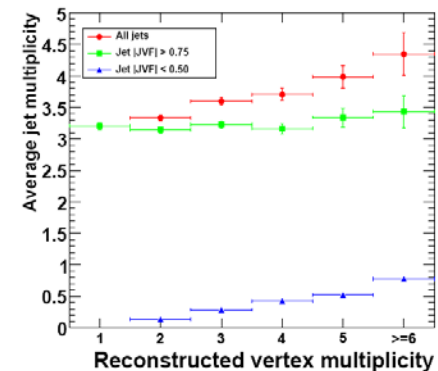
LHC $\text{RMS}(z_{\text{vertex}}) \sim 8$ cm

If we can attach vertices to reconstructed jets, we can in principle identify jets not from hard scattering

Limited to pseudorapidities within 2.5!



(c) Di-jet (J6)



(d) $t\bar{t}, W \rightarrow$ jets



Track jets

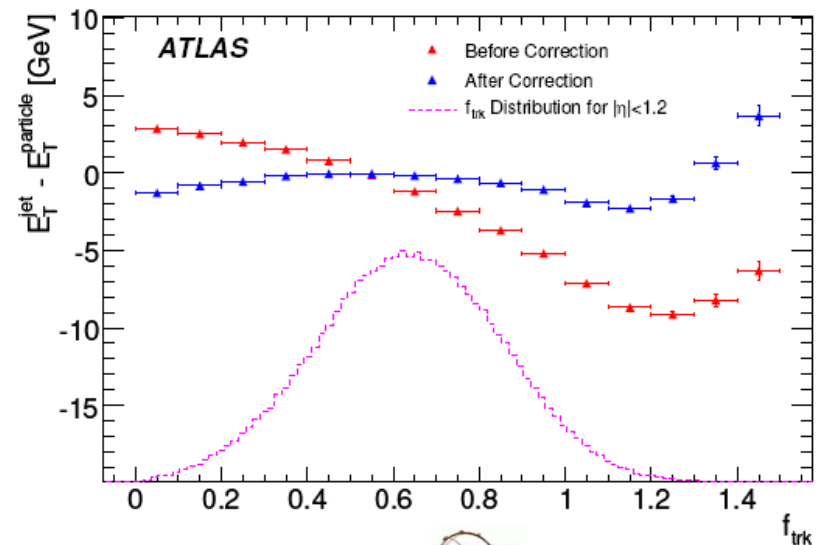
Find jets in reconstructed tracks
~60% of jet p_T , with RMS ~0.3 –
not a good kinematic estimator

Dedicated 3-dim jet algorithm

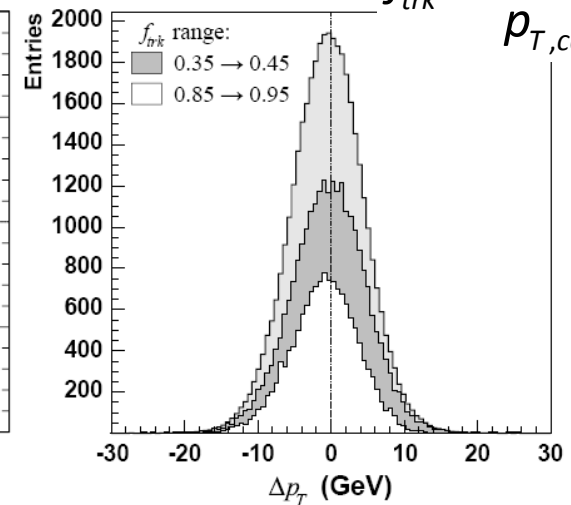
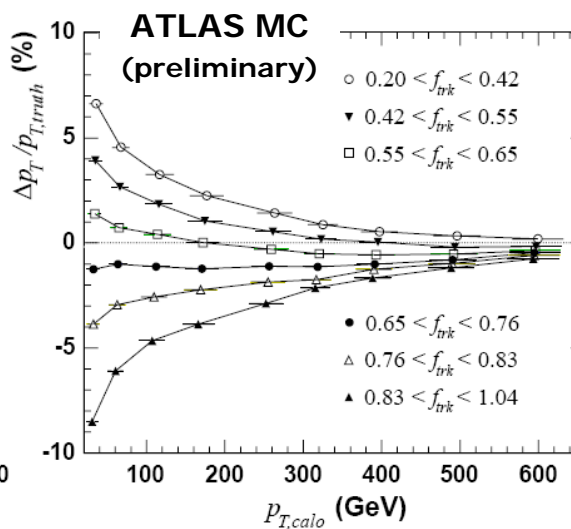
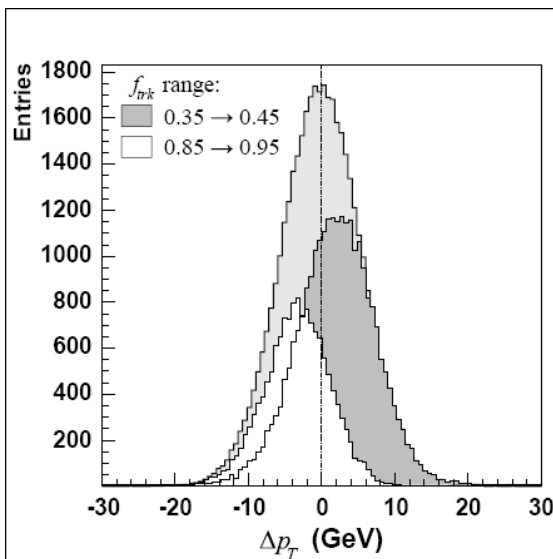
Cluster track jets in pseudo-
rapidity, azimuth, and
 $\Delta(Z_{\text{Vertex}})$

Match track and calorimeter jet

Helps response!



$$f_{\text{trk}} = \frac{p_{T,\text{track}}}{p_{T,\text{calo}}}$$



Longitudinal jet energy leakage

Dangerous – can change jet p_T
cross-section shape at high p_T

Fake compositeness signal

Correlated with muon spectrometer hits

Not strong correlation expected

Insufficient for precise JES

Will likely not produce reconstructed tracks, only

Helps to tag suspicious jets

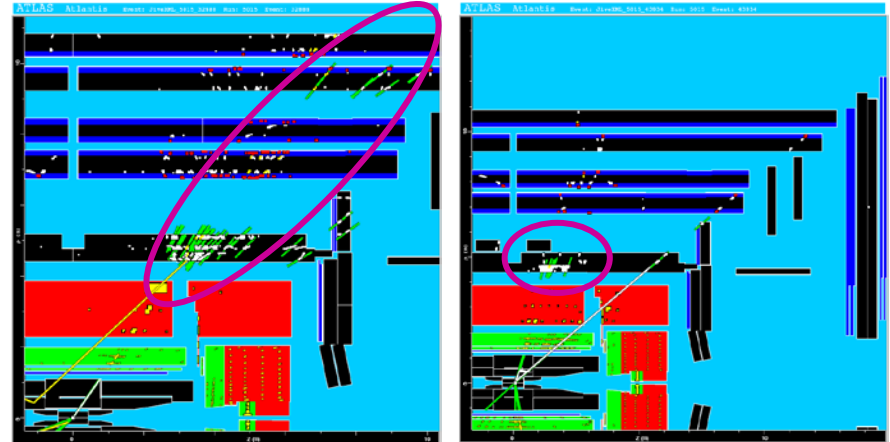
Suppress suspicious events/jets

Careful – real muon may be inside jet

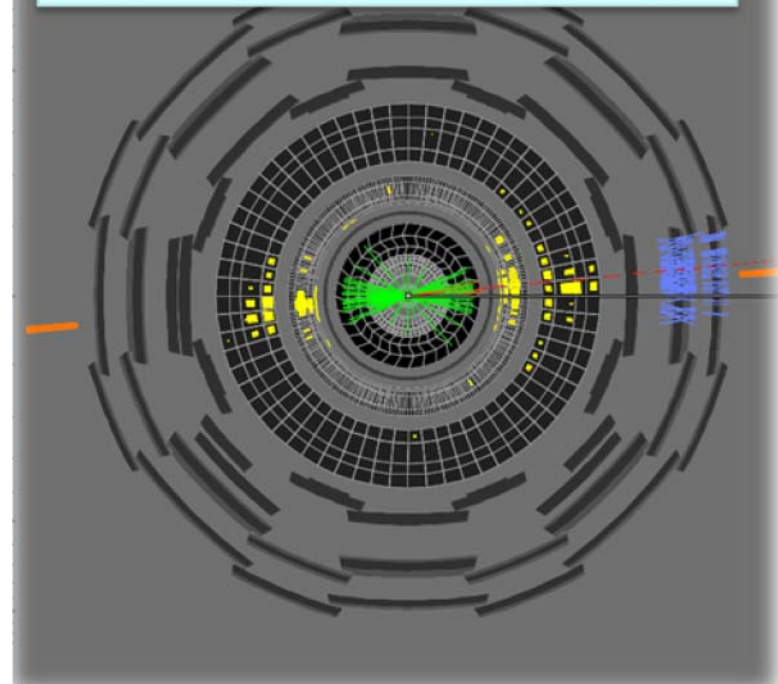
b decay

Should produce track – cleaner signal inside jet

Also background for missing transverse energy!

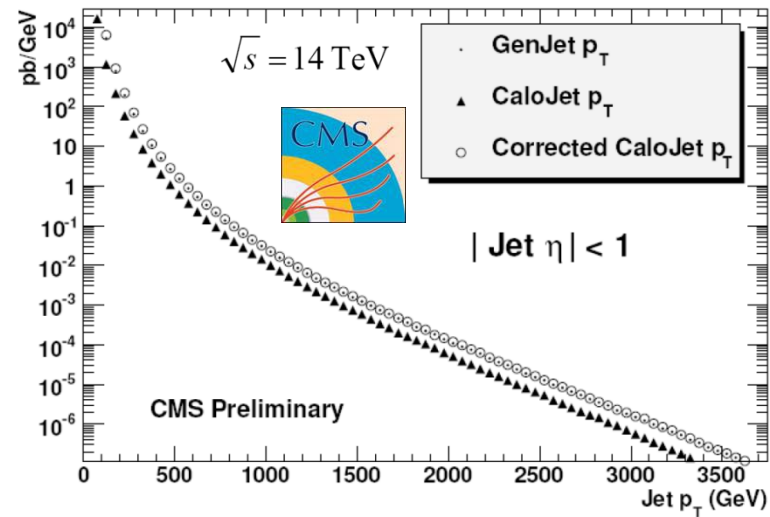
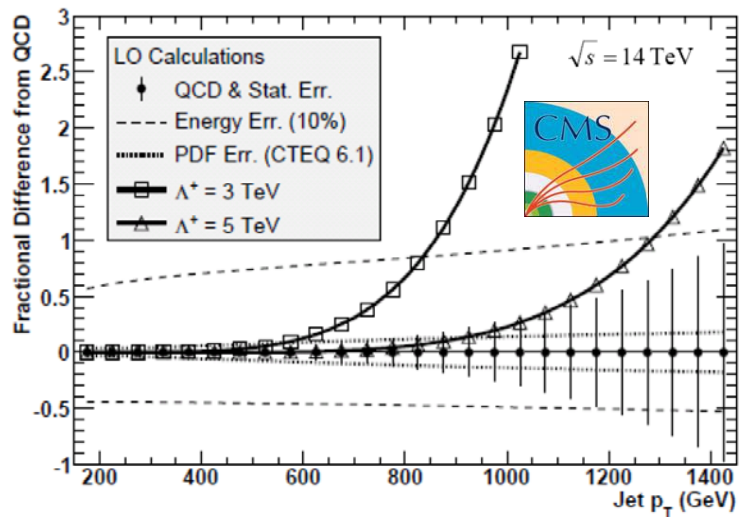


A typical jet with shower leakage



Effect of calibration on inclusive jet cross-section

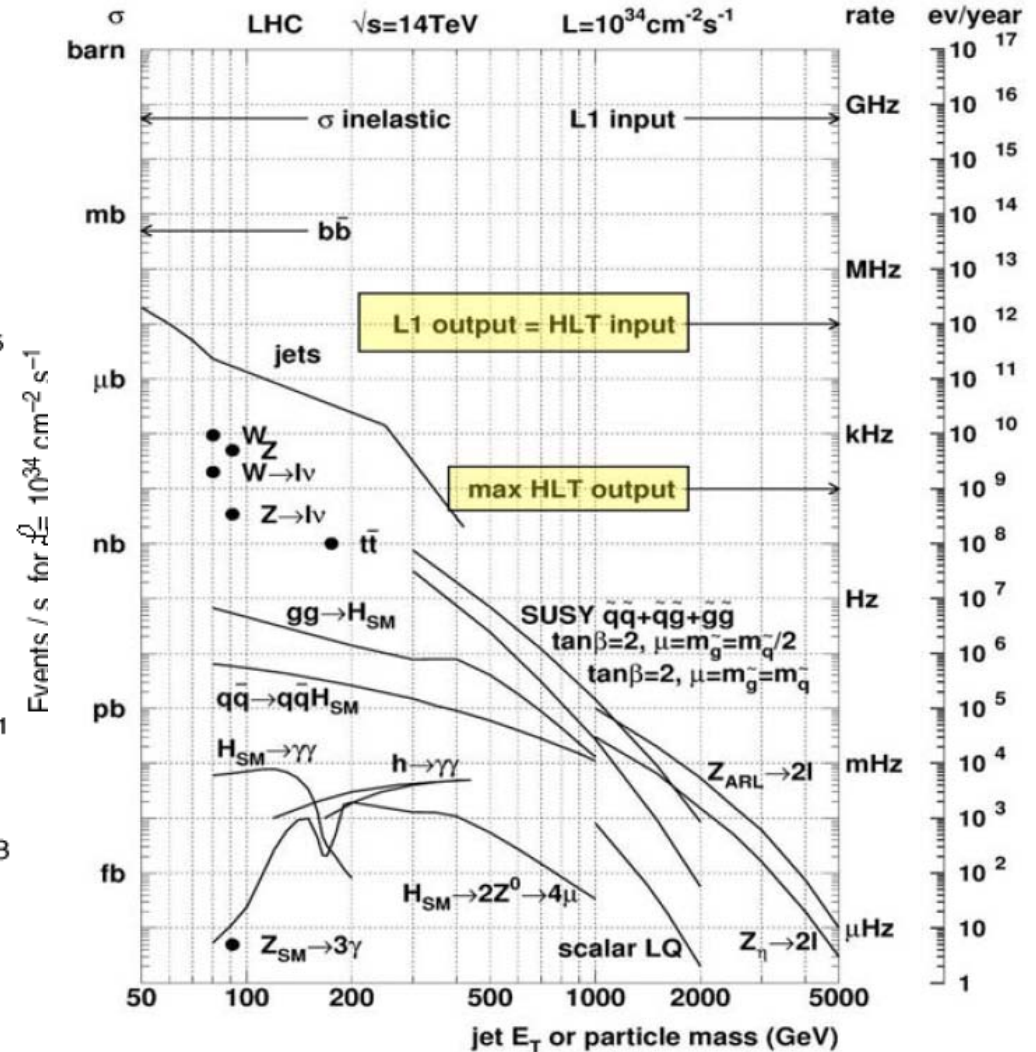
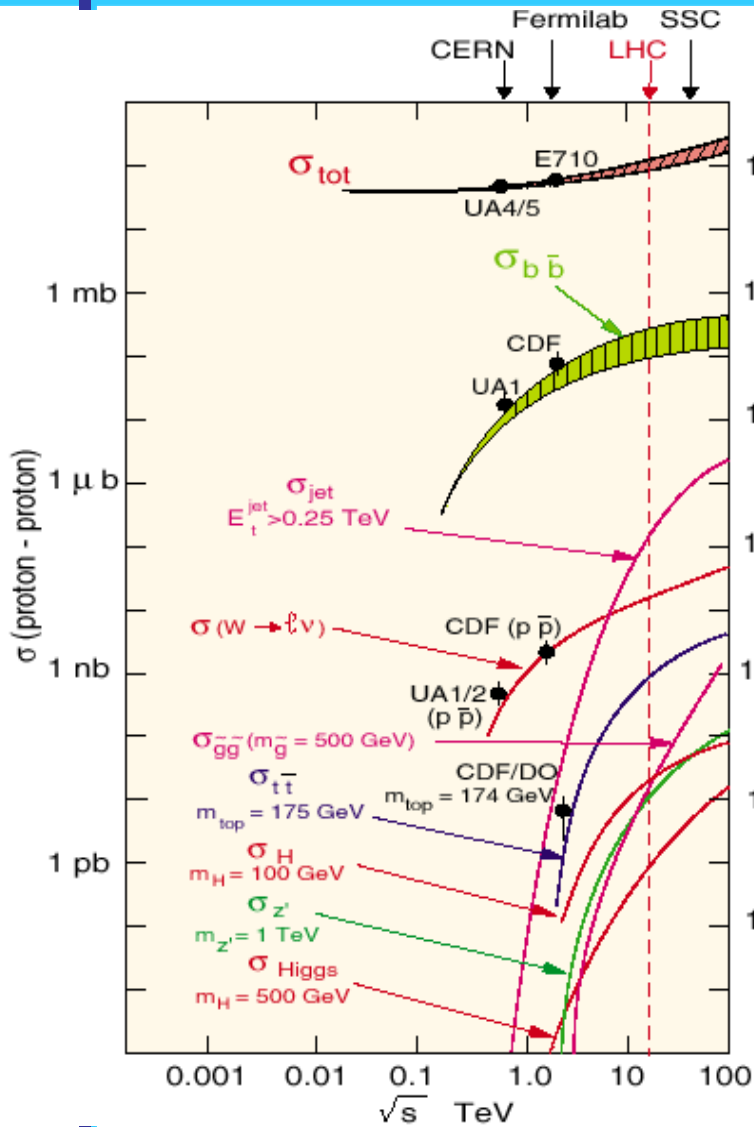
One the first physics results expected from ATLAS & CMS



CMS PAS SBM-07-001







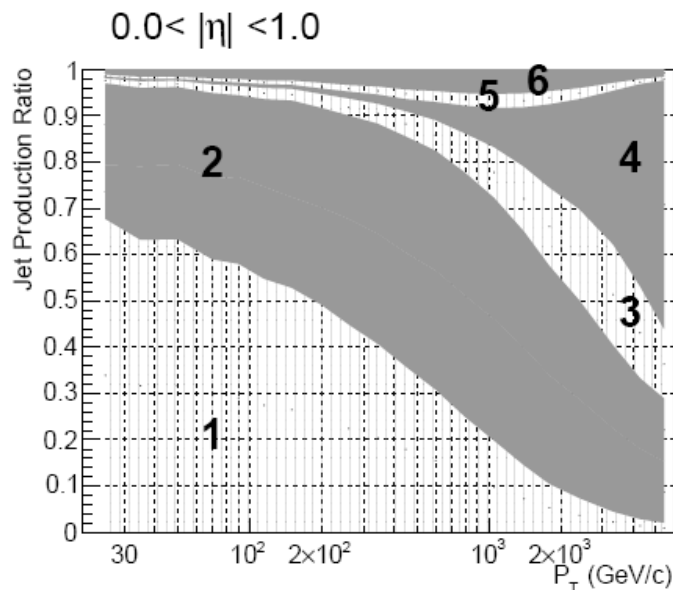
Jet physics

High transverse momentum jets
quickly accessible!

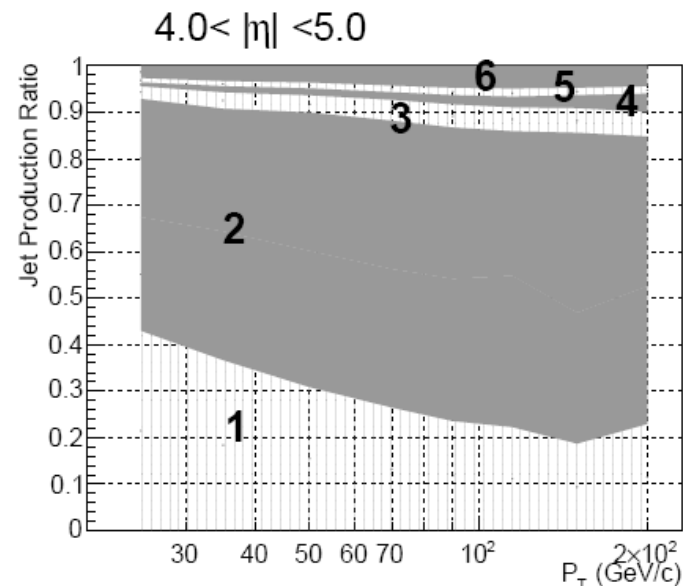
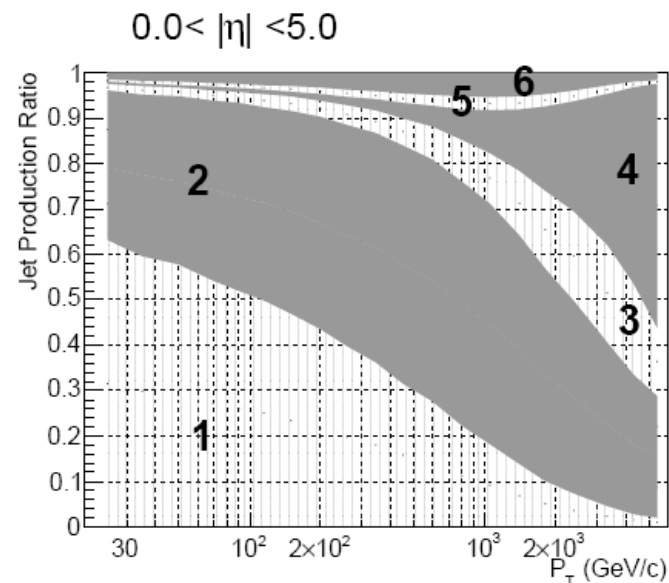
100,000 jets with $p_T > 1$ TeV at 1
fb⁻¹

Early attempt at inclusive cross-section

Most likely jet origin changes
with p_T and direction



- 1 gg
- 2 gq
- 3 qq
- 4 qq'
- 5 $q\bar{q}$
- 6 $q\bar{q}'$



Neglecting orders in ME calculations

K-factor NLO-LO can be significant

Much smaller effect of scale variations in NLO

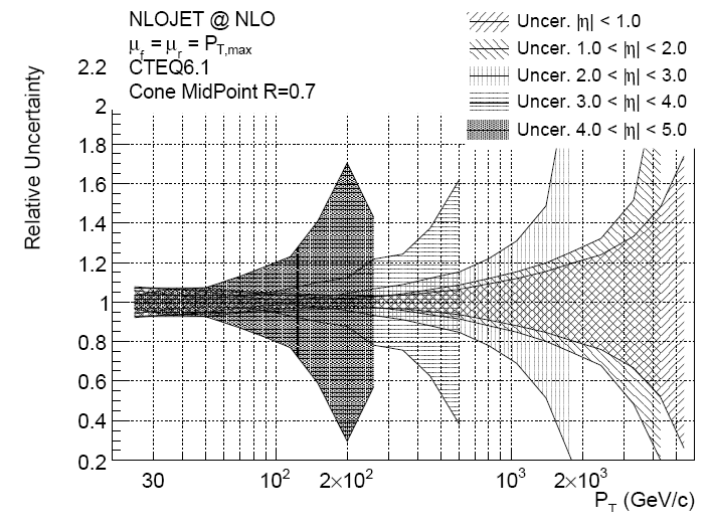
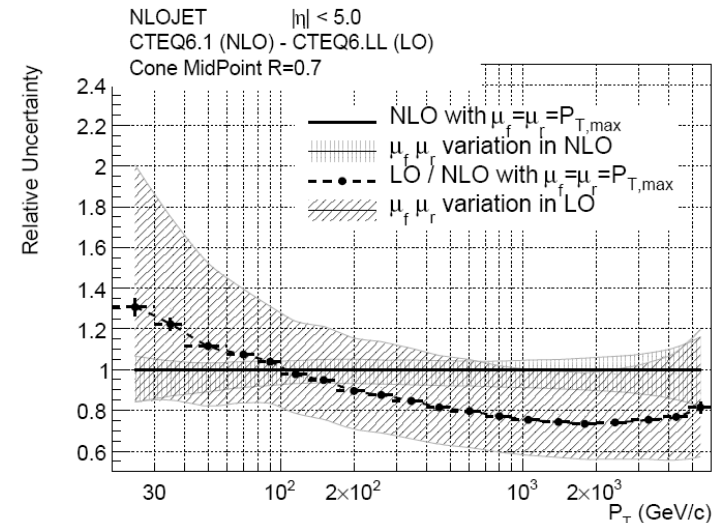
PDF uncertainties

Driven by gluon structure function uncertainties

Especially at higher p_T

Plot shows error PDFs in various regions

CTEQ 6.1 family



QCD swamps trigger and acquisition band width

Highly prescaled low p_T triggers

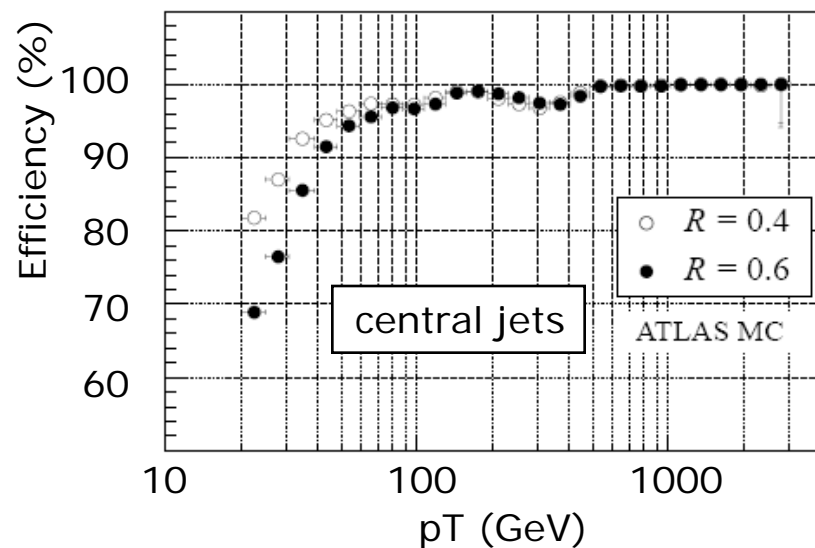
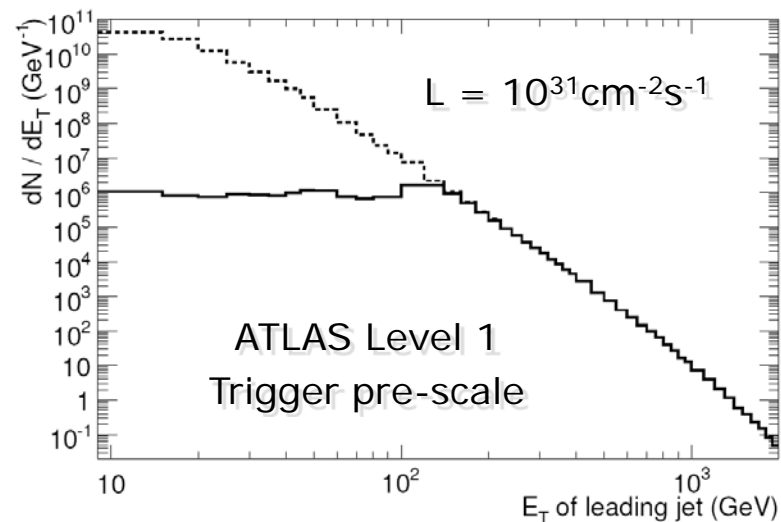
Trigger rates follow cross-section for $p_T > \sim 300$ GeV

Depending on luminosity

Need to understand trigger bias effect on cross-section measurement

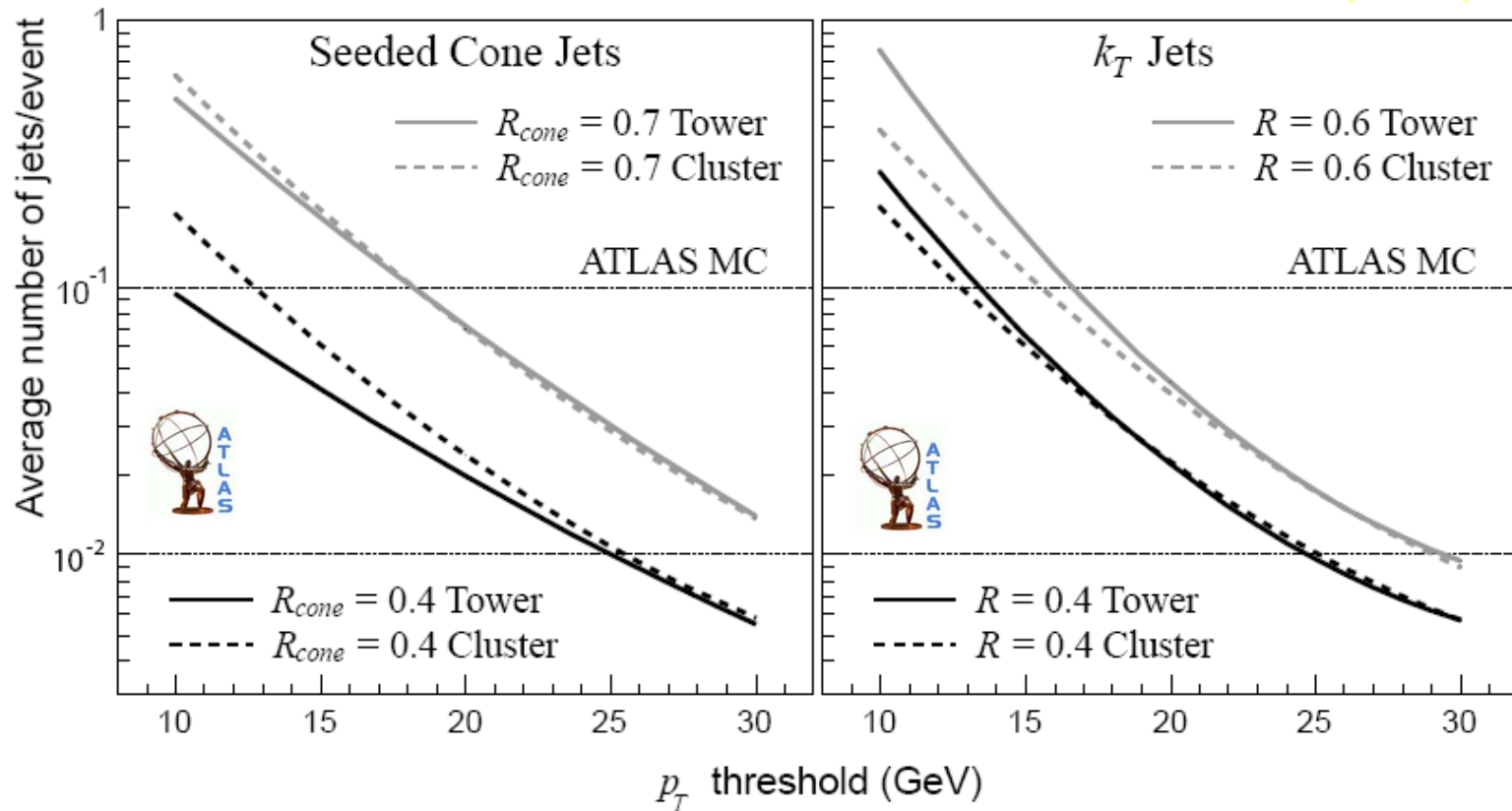
Low p_T problematic due to efficiency and purity issues anyway!

Safe $p_T > \sim 60-80$ GeV



Average number of jets in minimum bias events estimates fake jet reconstruction rate as function of p_T threshold

no pileup!

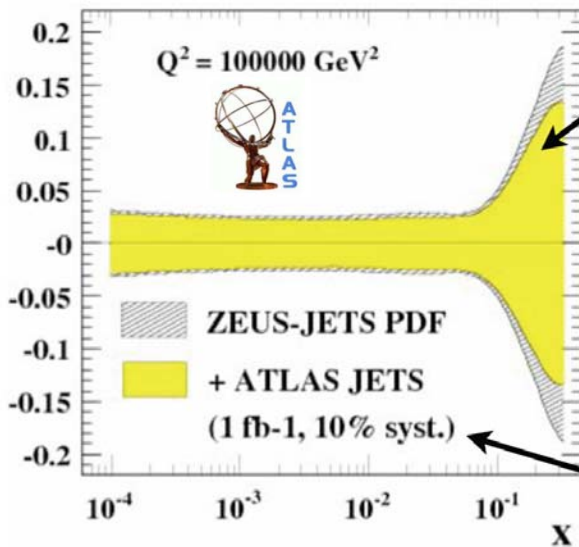


From inclusive jet cross-sections

Measure cross-section in regions of pseudo-rapidity

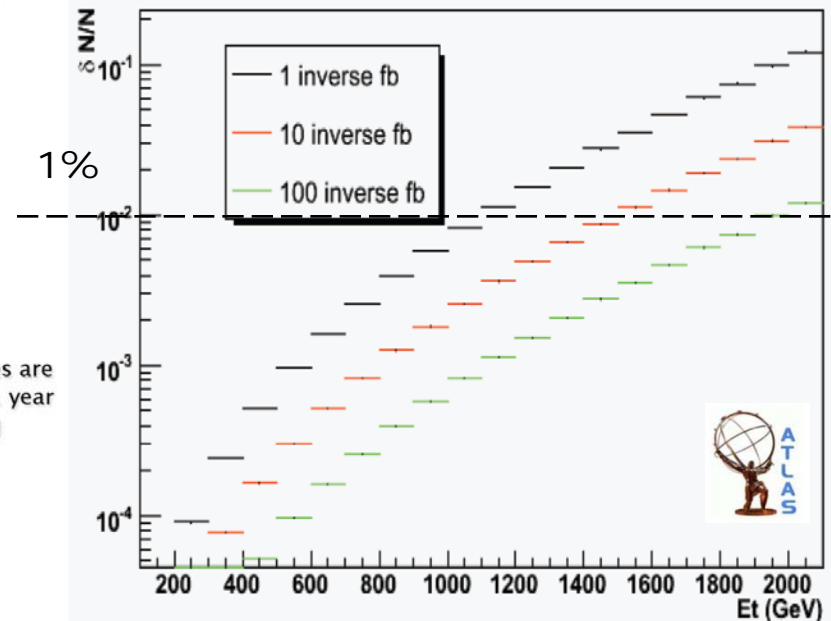
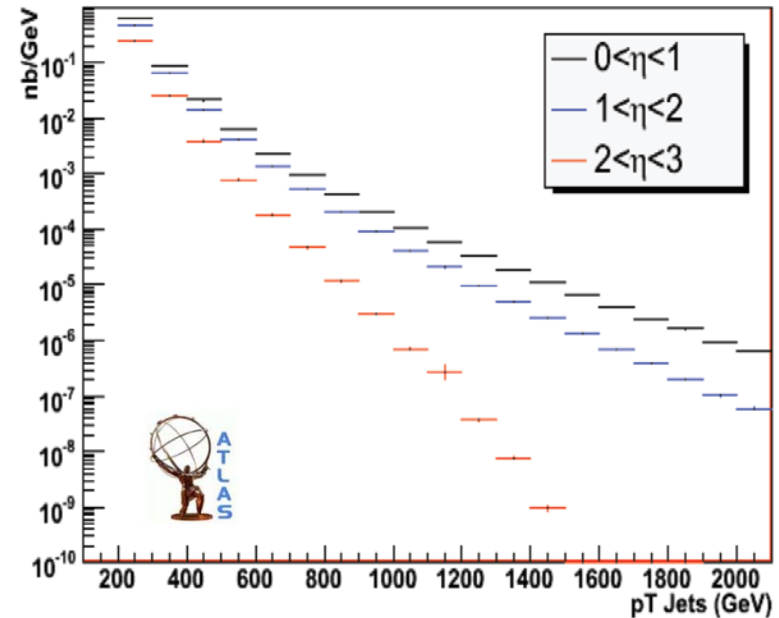
Statistical error quickly reduced

Trigger, JES more important



Preliminary indications suggest that ATLAS data can constrain the high x-gluon.

Systematic uncertainties are uncorrelated, 10fb⁻¹=1 year of nominal data-taking



Introduction to Hadronic Final State Reconstruction in Collider Experiments (Part XIV)

Peter Loch
University of Arizona
Tucson, Arizona
USA



Particle flow inside a jet hints to source

Jet can be a discovery tool by itself

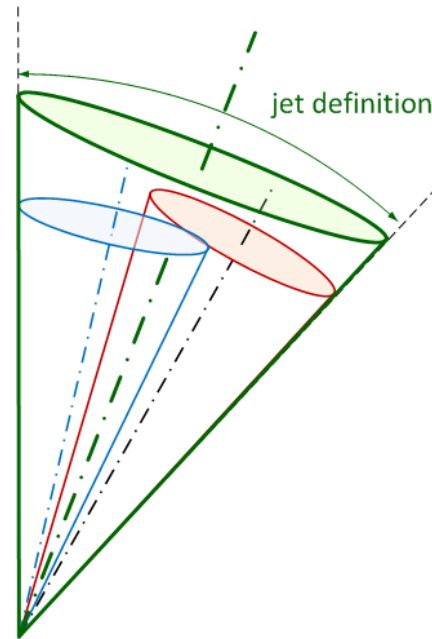
In particular most interesting for boosted (new) heavy particle like Kaluza-Klein excitations

But also interesting for Standard Model particles like boosted top quarks

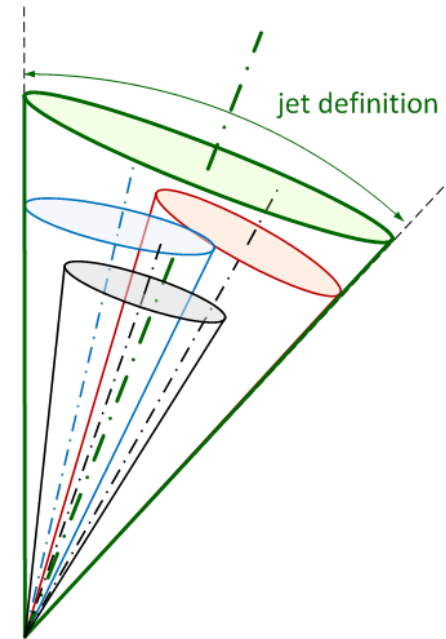
Usefulness depends on the ability to resolve decay structure

E.g., 2-prong (like W) or 3-prong (top) decays

Resolution scale given by mass of particle (or by particle hypothesis) – to be reflected with detector capabilities



2 – prong decay inside reconstructed jet, e.g. from $W \rightarrow q\bar{q}$ (SM) or heavy new object like $\phi \rightarrow gg$ or $Z' \rightarrow q\bar{q}$ (BSM)



3 – prong decay inside reconstructed jet, e.g. from $t \rightarrow q\bar{q}b$ (SM) or heavy new object like $\phi_{KK} \rightarrow Q\bar{Q}b + X$ or $t' \rightarrow q\bar{q}b$ (BSM)



Observables and tools

Single jet mass

Mass generated by four-momentum recombination should reflect heavy source

Scales proportional to p_T for light quark or gluon jet

Subject to severe detector effects

Lateral energy spread by individual particle cascades reduces single jet mass resolution

Calorimeter signal definition choices on top of shower spread can enhance or reduce sensitivity to in-jet particle flow and thus improve or worsen single jet mass resolution

$$\begin{pmatrix} E_{\text{jet}} \\ \vec{p}_{\text{jet}} \end{pmatrix} = \begin{pmatrix} \sum_{\text{constituents}} E_{\text{constituent}} \\ \sum_{\text{constituents}} \vec{p}_{\text{constituent}} \end{pmatrix} \Rightarrow m_{\text{jet}} = \sqrt{E_{\text{jet}}^2 - |\vec{p}_{\text{jet}}|^2}$$

mass of gluon/light quark jets:

LO 1-parton jets have vanishing mass

NLO 2-parton configurations at given p_{jet} generate average invariant jet mass:

$$\langle m_{\text{jet}}^2 \rangle_{\text{NLO}} \approx \bar{c} \left(p_{\text{jet}} / \sqrt{s} \right) \alpha_s \left(p_{\text{jet}} / 2 \right) p_{\text{jet}}^2 R_{\text{cone}}^2$$

with:

$\bar{c} \left(p_{\text{jet}} / \sqrt{s} \right)$ pre-function of magnitude $\mathcal{O}(1)$ (absorbes color charges and pdf, slowly decreases with rising p_{jet})

$\alpha_s \left(p_{\text{jet}} / 2 \right)$ strong coupling at scale $\mu = p_{\text{jet}} / 2$

\Rightarrow expect linear mass in NLO to scale with p_{jet} :

$$\sqrt{\langle m_{\text{jet}}^2 \rangle_{\text{NLO}}} \approx \sqrt{\bar{c} \alpha_s} p_{\text{jet}} R_{\text{cone}}$$

rule of thumb at $\sqrt{s} = 14$ TeV:

$$\sqrt{\langle m_{\text{jet}}^2 \rangle_{\text{NLO}}} \approx 0.2 \cdot p_{\text{jet}} R_{\text{cone}}$$



Observables and tools

Single jet mass

Mass generated by four-momentum recombination should reflect heavy source

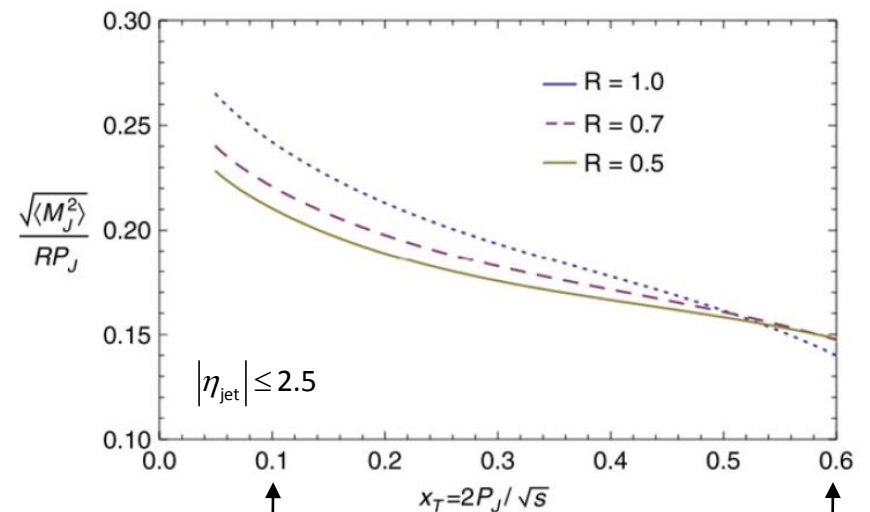
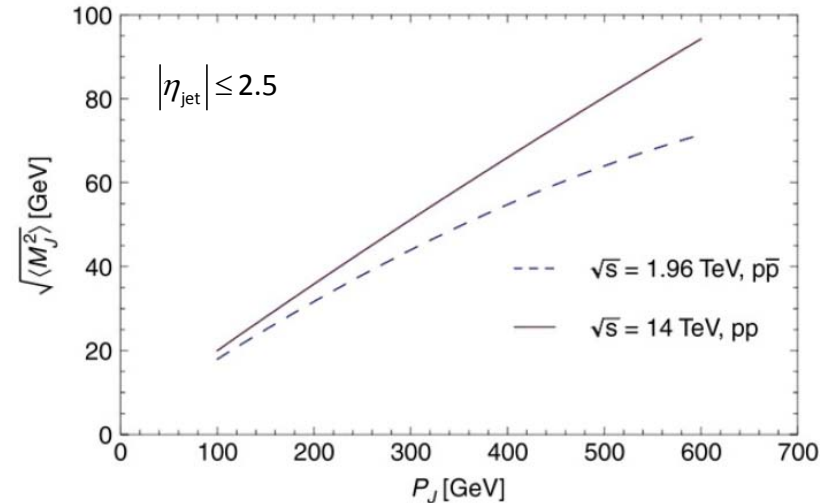
Scales proportional to p_T for light quark or gluon jet

Subject to severe detector effects

Lateral energy spread by individual particle cascades reduces single jet mass resolution

Calorimeter signal definition choices on top of shower spread can enhance or reduce sensitivity to in-jet particle flow and thus improve or worsen single jet mass resolution

NLO Jet Mass Calculations



$$p_{T,\text{jet}}^{\text{min}} \approx 115 \text{ GeV} \longrightarrow p_{T,\text{jet}}^{\text{min}} \approx 685 \text{ GeV}$$

$$p_{\text{jet}} = 700 \text{ GeV} \longrightarrow p_{\text{jet}} = 4.2 \text{ TeV}$$



Observables and tools

Single jet mass

Mass generated by four-momentum recombination should reflect heavy source

Scales proportional to pT for light quark or gluon jet

Subject to severe detector effects

Lateral energy spread by individual particle cascades reduces single jet mass resolution

Calorimeter signal definition choices on top of shower spread can enhance or reduce sensitivity to in-jet particle flow and thus improve or worsen single jet mass resolution

$$\begin{pmatrix} E_{\text{jet}} \\ \vec{p}_{\text{jet}} \end{pmatrix} = \begin{pmatrix} \sum_{\text{constituents}} E_{\text{constituent}} \\ \sum_{\text{constituents}} \vec{p}_{\text{constituent}} \end{pmatrix} \Rightarrow m_{\text{jet}} = \sqrt{E_{\text{jet}}^2 - |\vec{p}_{\text{jet}}|^2}$$

- requires good reconstruction of particle flow in jet by detector signal → depends on chosen calorimeter signal definition, e.g. test

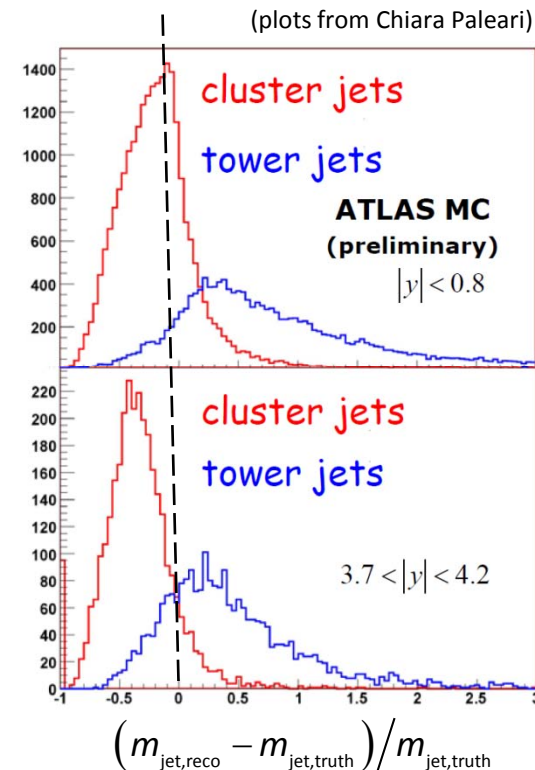
$$\frac{m_{\text{jet, reco}} - m_{\text{jet, truth}}}{m_{\text{jet, truth}}}$$

for matching truth and

calorimeter jets

- plot on the right shows the spectrum of this relative mass difference for simulated QCD di-jets (kT, R = 0.6) in ATLAS

(old plot, educational purpose only!)



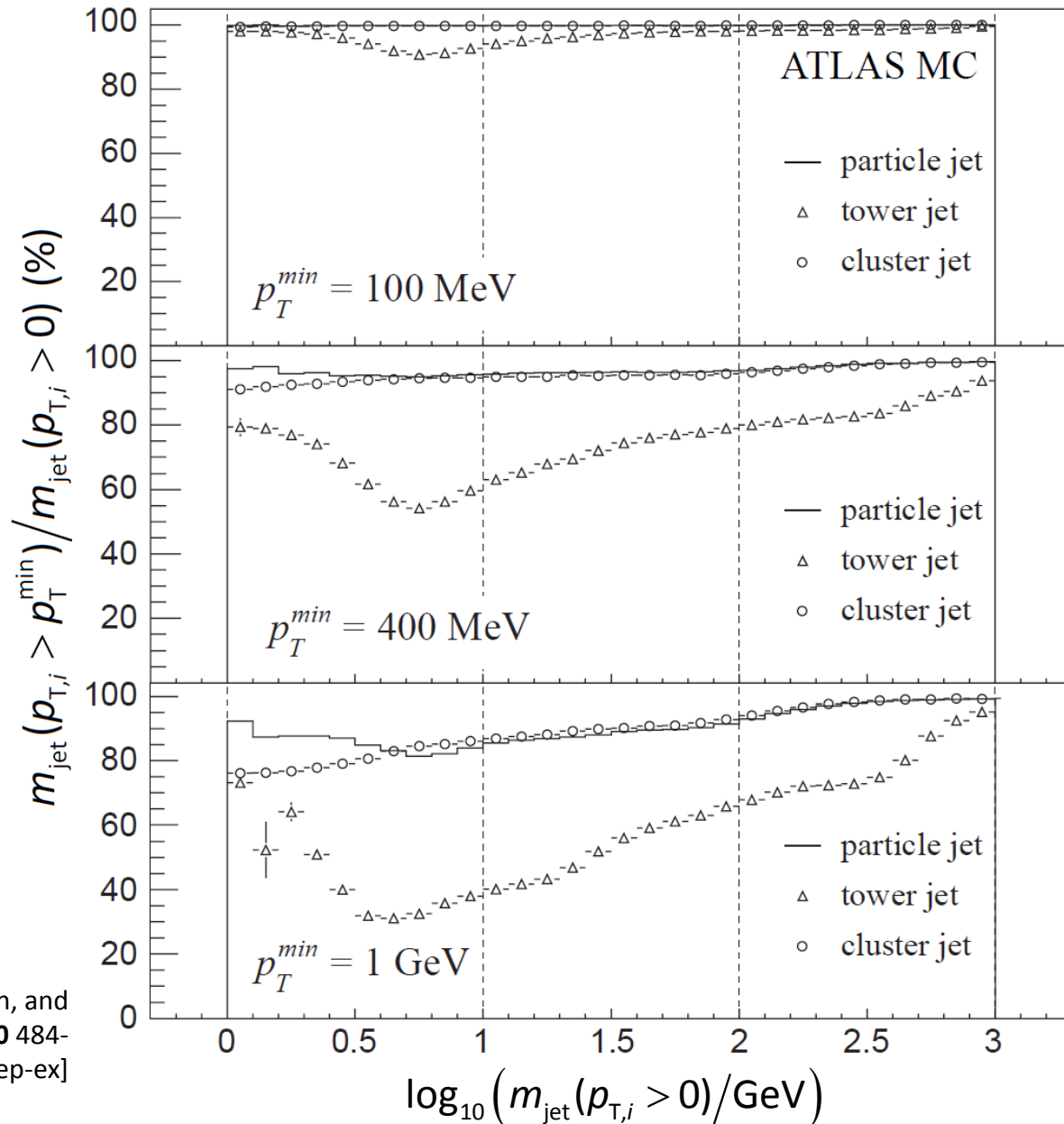
Relative mass change

Truncate jet mass

Calculate mass using only constituents above p_T thresholds

Compare ratio to unbiased mass

Particle (hadron), cluster, tower jets



S.D.Ellis, J.Huston, K.Hatakeyama, P.Loch, and M.Tönnesmann, *Prog.Part.Nucl.Phys.***60** 484-551 (2008); also in [arXiv:0901.0512](https://arxiv.org/abs/0901.0512) [hep-ex]



Observables and tools

Recombination scales and order in kT like algorithms

Jet decomposition tracing back the (recursive) recombination

Can be considered resolving fragmentation to a given scale

Scale of last clustering step relates to mass of source in two-prong decay

Scale of next-to-last clustering step relates to mass of source in three-prong decay

Can be expected to correlate with jet mass in heavy particle decays

But different resolution – likely less sensitive to detector effects!

y – scale in kT algorithms provides a p_T scale at which a given recombination can be undone
recall variables:

$$d_i = p_{T,i}^2 \text{ and } d_{ij} = \min(d_i, d_j) \frac{\Delta R_{ij}}{R}$$

principal kT clustering rules:

- (1) build list of d_i and d_{ij} from all protojets
- (2) if common minimum is a d_i , call i from list and call it a jet
- (3) else combine i and j to a jet and add to list, and remove the previous protojets i and j
- (4) repeat from (1) until no protojets are left

define y – scale

$$y_{\text{scale}}^2 = y_n \times p_{T,\text{jet}}^2, \text{ with } n \text{ being a resolution parameter}$$

example: $n = 2$ refers to the last recombination in the clustering sequence, i.e. $d_{12} < d_1, d_2$:

$$y_{\text{scale}}^{1 \rightarrow 2} = \sqrt{y_2} \times p_{T,\text{jet}} = \sqrt{\min(d_1, d_2)}$$

relates to mass in two-prong decays



Observables and tools

Recombination scales and order
in kT like algorithms

Jet decomposition tracing back
the (recursive) recombination

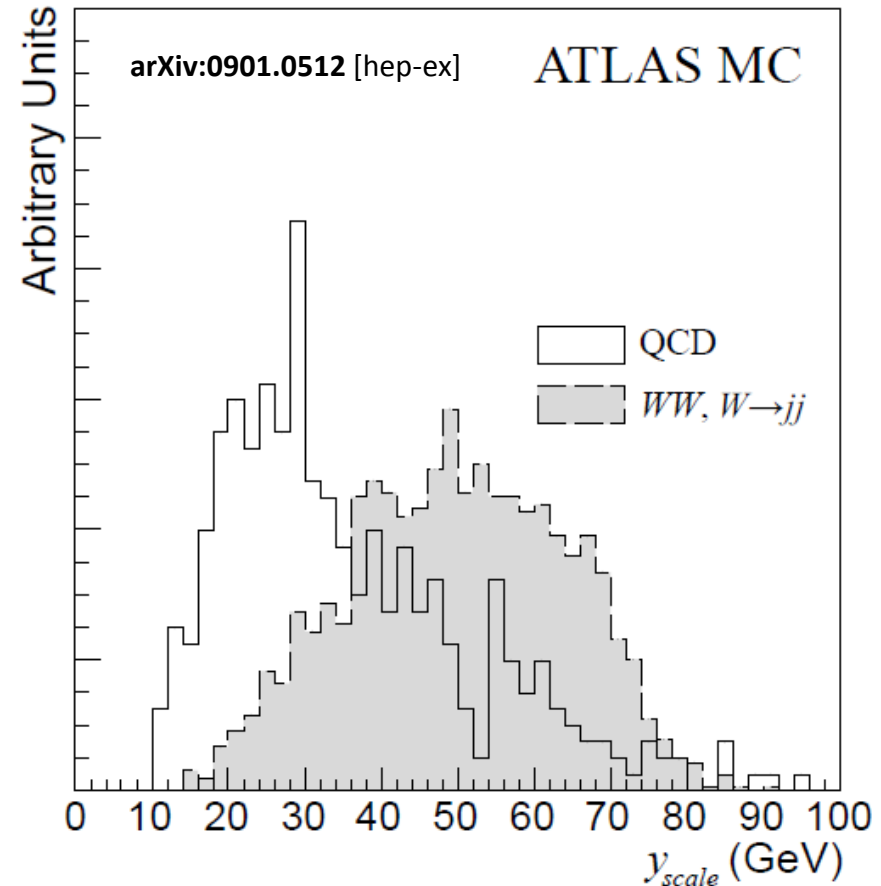
Can be considered resolving
fragmentation to a given scale

Scale of last clustering step
relates to mass of source in two-
prong decay

Scale of next-to-last clustering
step relates to mass of source in
three-prong decay

Can be expected to correlate with
jet mass in heavy particle decays

But different resolution – likely
less sensitive to detector effects!



$y_{scale}^{1 \rightarrow 2}$ for jets with $m_{jet} > 40$ GeV, for QCD and hadronically
decaying boosted W .

Note that for QCD $y_{scale}^{1 \rightarrow 2}$ is logarithmically below $p_{T,jet}$ due
to the strong ordering (in k_T) in QCD evolution, while

$\langle y_{scale}^{1 \rightarrow 2} \rangle \approx m_W$ reflects the 2-prong decay of the W boson



Observables and tools

Recombination scales and order
in kT like algorithms

Jet decomposition tracing back
the (recursive) recombination

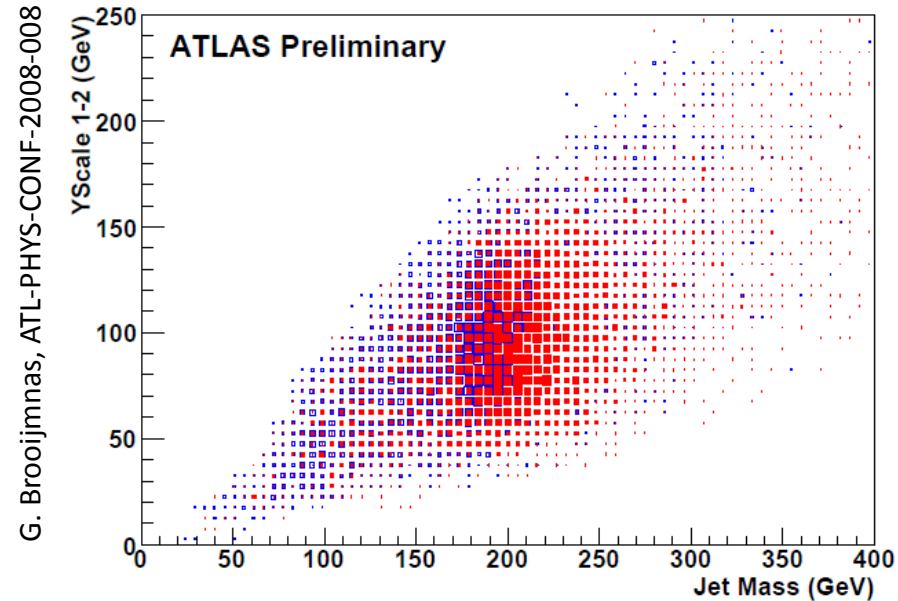
Can be considered resolving
fragmentation to a given scale

Scale of last clustering step
relates to mass of source in two-
prong decay

Scale of next-to-last clustering
step relates to mass of source in
three-prong decay

Can be expected to correlate with
jet mass in heavy particle decays

But different resolution – likely
less sensitive to detector effects!



ATLAS simulation:

$Z' \rightarrow t\bar{t}$, $m_{Z'} = 2(3)$ TeV

$p_T(t) > 300$ GeV

- $y_{\text{scale}}^{1 \rightarrow 2}$ probes **top decay**,

peaks at ≈ 100 GeV $\approx \frac{m_{\text{top}}}{2}$

- $y_{\text{scale}}^{2 \rightarrow 3}$ probes **W decay**,

peaks at ≈ 40 GeV $\approx \frac{m_W}{2}$



Observables and tools

Recombination scales and order
in kT like algorithms

Jet decomposition tracing back
the (recursive) recombination

Can be considered resolving
fragmentation to a given scale

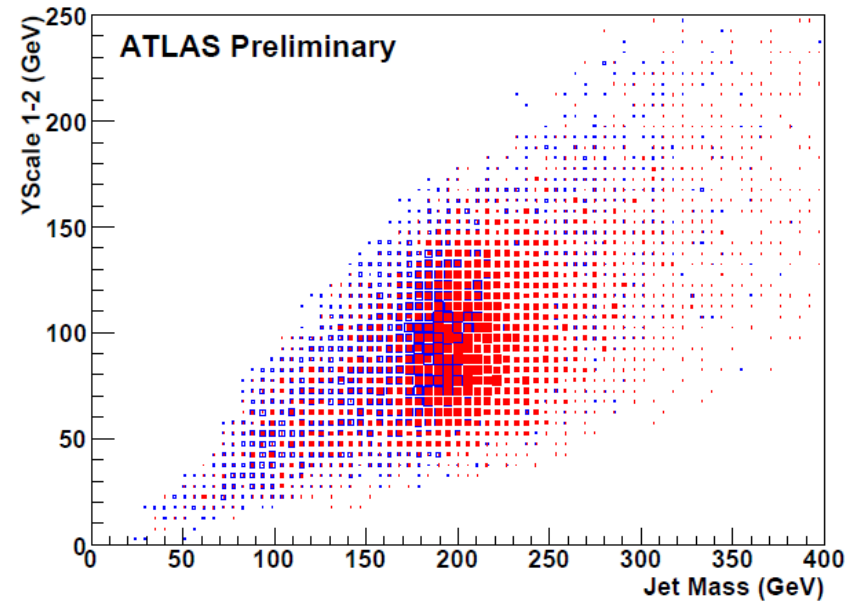
Scale of last clustering step
relates to mass of source in two-
prong decay

Scale of next-to-last clustering
step relates to mass of source in
three-prong decay

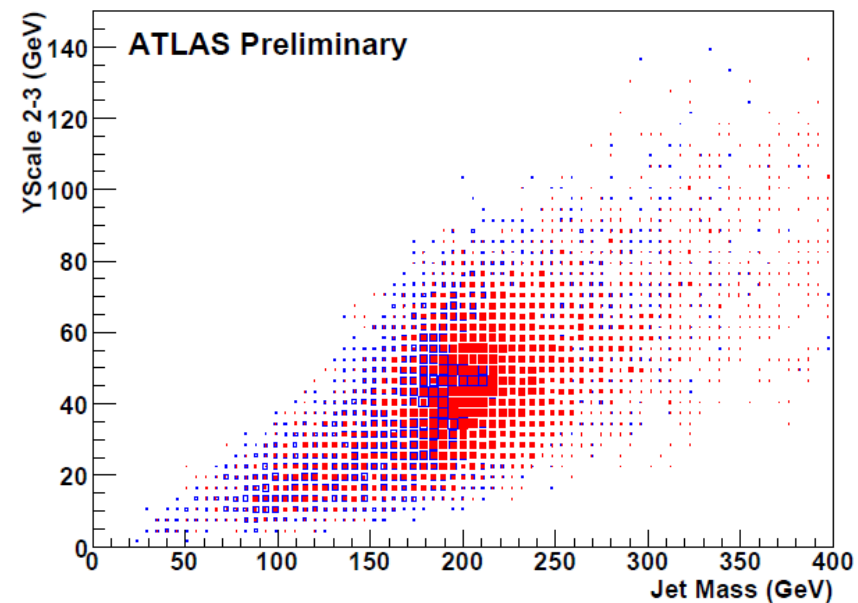
Can be expected to correlate with
jet mass in heavy particle decays

But different resolution – likely
less sensitive to detector effects!

G. Brooijmnas, ATLAS-PHYS-CONF-2008-008



G. Brooijmnas, ATLAS-PHYS-CONF-2008-008



Observables and tools

Recombination scales and order
in kT like algorithms

Jet decomposition tracing back
the (recursive) recombination

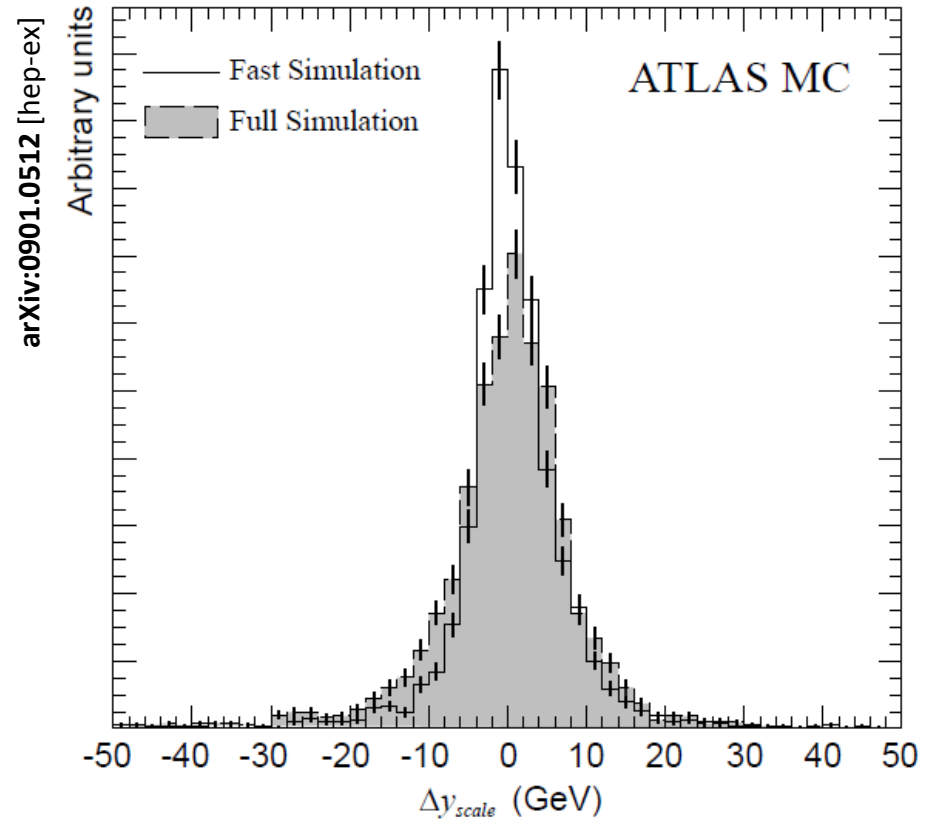
Can be considered resolving
fragmentation to a given scale

Scale of last clustering step
relates to mass of source in two-
prong decay

Scale of next-to-last clustering
step relates to mass of source in
three-prong decay

Can be expected to correlate with
jet mass in heavy particle decays

But different resolution – likely
less sensitive to detector effects!



$$\Delta y_{scale} = y_{scale}^{1 \rightarrow 2} \Big|_{particle} - y_{scale}^{1 \rightarrow 2} \Big|_{calo} \quad \text{for jets with}$$

$m_{jet} > 40$ GeV from hadronically decaying boosted W .

$y_{scale}^{1 \rightarrow 2} \Big|_{calo}$ is calculated for parameterized, response smearing simulation (fast, no lateral shower spread) and from detailed full simulation → indications that

$y_{scale}^{1 \rightarrow 2}$ is little sensitive to details of showering.



Observables and tools

Direct attempt to reconstruct sub-jets within jet

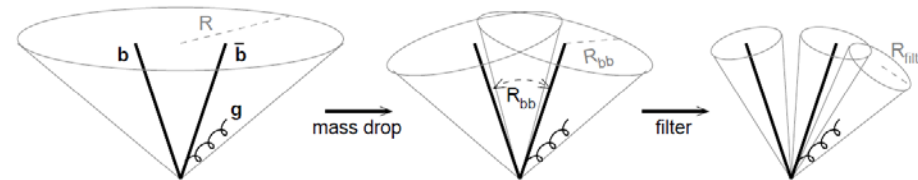
Narrow jet reconstruction in bigger jet motivated by mass drop

Includes signal enhancement strategy

Requires additional (3rd) jet from gluon radiation in the decay system

J.M. Butterworth, A.R. Davison, M.Rubin, G.P.Salam,
Phys.Rev.Lett.100:242001,2008

Look for $H \rightarrow b\bar{b}g$ with $p_{T,H} > 200$ GeV in WH / ZH production - about 5% of total cross-section:



$$R_{bb} \approx \frac{1}{\sqrt{z(1-z)}} \frac{m_H}{p_T}, \quad p_T \gg m_H$$

use Cambridge/Aachen kT flavour jet finder to find large jet ($R = 1.2$), $p_T > 200$ GeV for sub-jet analysis

- (1) break jet j into two subjects j_1, j_2 , with $m_{j_1} > m_{j_2}$, by undoing last recombination
- (2) if there is a significant mass drop such that $m_{j_1} < \mu m_j$, and the splitting $j \rightarrow (j_1, j_2)$ is not too asymmetric, i.e.

$$\min(p_{j_1}^2, p_{j_2}^2) / m_j^2 \Delta R_{j_1, j_2}^2 > y_{cut},$$

then the jet j is assumed to be the heavy particle neighbourhood and the analysis stops

- (3) else, set $j = j_1$ and go back to step (1)

apply filter to all heavy particle neighbourhoods, with a finer angular scale $R_{filter} < R_{bb}$, e.g., $R_{filter} = \min(0.3, R_{bb}/2)$ seems to be good for LHC, and take the 3 hardest objects that appear $\rightarrow H \rightarrow b\bar{b}g$, including the hardest ($\mathcal{O}(\alpha_s)$) radiation. Tag the b jets and calculate the invariant mass.



Observables and tools

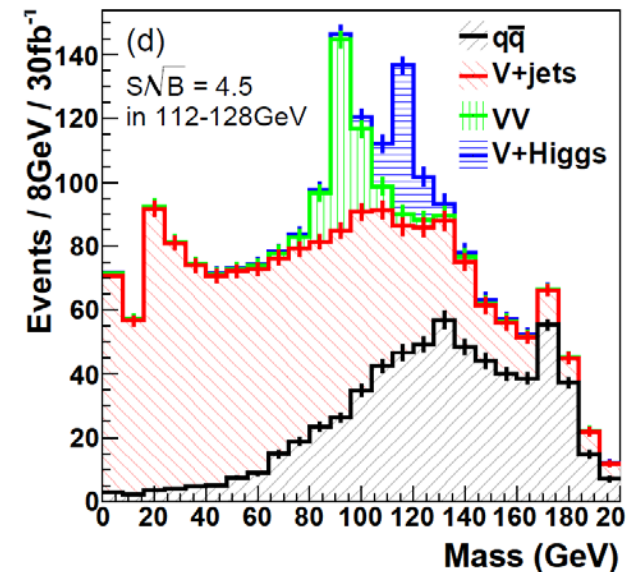
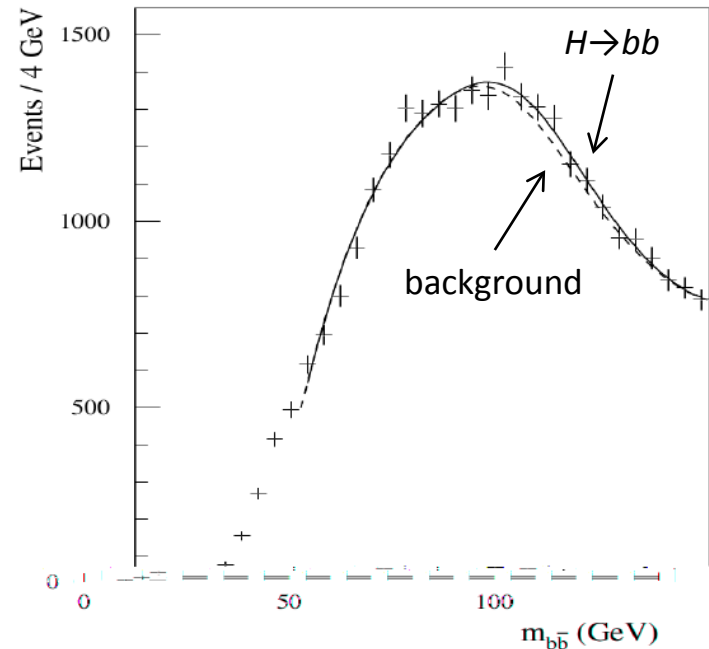
Direct attempt to reconstruct
sub-jets within jet

Narrow jet reconstruction in
bigger jet motivated by mass
drop

Includes signal enhancement
strategy

Requires additional (3rd) jet from
gluon radiation in the decay
system

J.M. Butterworth, A.R. Davison, M.Rubin, G.P.Salam,
Phys.Rev.Lett.100:242001,2008



Observables and tools

Jet pruning

Enhancement of jet components
to increase substructure resolution

Applied in kT-style jet clustering
procedure

Jet trimming

Applies a filter by removing soft
sub-jets in a jet

Soft pT cut-off evaluated
dynamically jet by jet

Jet Pruning

- attempt to suppress underlying event and pile-up contributions to jets
- cleans jets by vetoing spurious recombinations during clustering → kT and C/A jets only!
- sensitive variables are angular distance $\phi = \Delta R_{12}$ and relative p_T hierarchy $z \equiv \min(p_{T,1}, p_{T,2})/p_{T,p}$, in recombination $1,2 \rightarrow p$
- suppress large distances and large hierarchies at each clustering iteration

$$\phi > R_{\text{cut}}$$

$$z < z_{\text{cut}}$$

works better for heavy particle decays than for QCD:

- not clear what R_{cut} is for QCD – $R_{\text{cut}} \approx m/p_T$ for heavy particle decays
- also not clear what z_{cut} should be – contamination looks hard early in clustering, especially for kT; for heavy particles, $z_{\text{cut}} = 0.1(0.15)$ works well for kT(C/A) jets from boosted top



Observables and tools

Jet pruning

Enhancement of jet components
to increase substructure resolution

Applied in kT-style jet clustering
procedure

Jet trimming

Applies a filter by removing soft
sub-jets in a jet

Soft pT cut-off evaluated
dynamically jet by jet

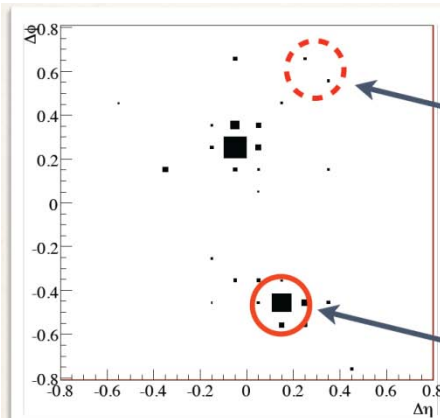
Jet Pruning

- attempt to suppress underlying event and pile-up contributions to jets
- cleans jets by vetoing spurious recombinations during clustering → kT and C/A jets only!
- sensitive variables are angular distance $\phi = \Delta R_{12}$ and relative p_T hierarchy $z \equiv \min(p_{T,1}, p_{T,2})/p_{T,p}$, in recombination $1,2 \rightarrow p$
- suppress large distances and large hierarchies at each clustering iteration

$$\phi > R_{\text{cut}}$$

$$z < z_{\text{cut}}$$

works better for heavy particle decays than for QCD:



Pruning would throw this away because it's wide angle and much softer than the core of the jet.

It would keep this because although it's at a wide angle, it's not soft.

Boosted Higgs Jet

D.Krohn, *Jet Trimming*, talk given at the *Theoretical-experimental workshop on jet & jet substructure at LHC*, University of Washington, January 10-15, 2010 (based on D.Krohn, J.Thaler, L.T. Wang, [arXiv:0912.1342](https://arxiv.org/abs/0912.1342))



Observables and tools

Jet pruning

Enhancement of jet components
to increase substructure resolution

Applied in kT-style jet clustering
procedure

Jet trimming

Applies a filter by removing soft
sub-jets in a jet

Soft pT cut-off evaluated
dynamically jet by jet

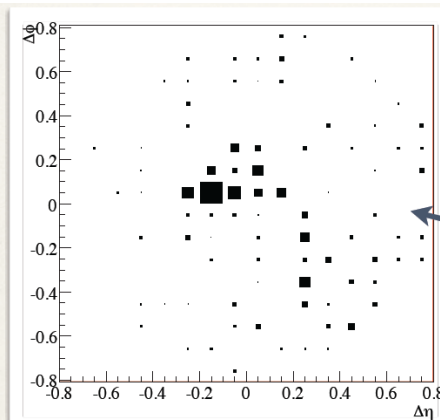
Jet Pruning

- attempt to suppress underlying event and pile-up contributions to jets
- cleans jets by vetoing spurious recombinations during clustering → kT and C/A jets only!
- sensitive variables are angular distance $\phi = \Delta R_{12}$ and relative p_T hierarchy $z \equiv \min(p_{T,1}, p_{T,2})/p_{T,p}$, in recombination $1,2 \rightarrow p$
- suppress large distances and large hierarchies at each clustering iteration

$$\phi > R_{\text{cut}}$$

$$z < z_{\text{cut}}$$

works better for heavy particle decays than for QCD:



It's harder to get Pruning to work here.

What is the appropriate R_{cut} ?

What is the appropriate z_{cut} ?

D.Krohn, *Jet Trimming*, talk given at the *Theoretical-experimental workshop on jet & jet substructure at LHC*, University of Washington, January 10-15, 2010 (based on D.Krohn, J.Thaler, L.T. Wang, [arXiv:0912.1342](https://arxiv.org/abs/0912.1342))



Observables and tools

Jet pruning

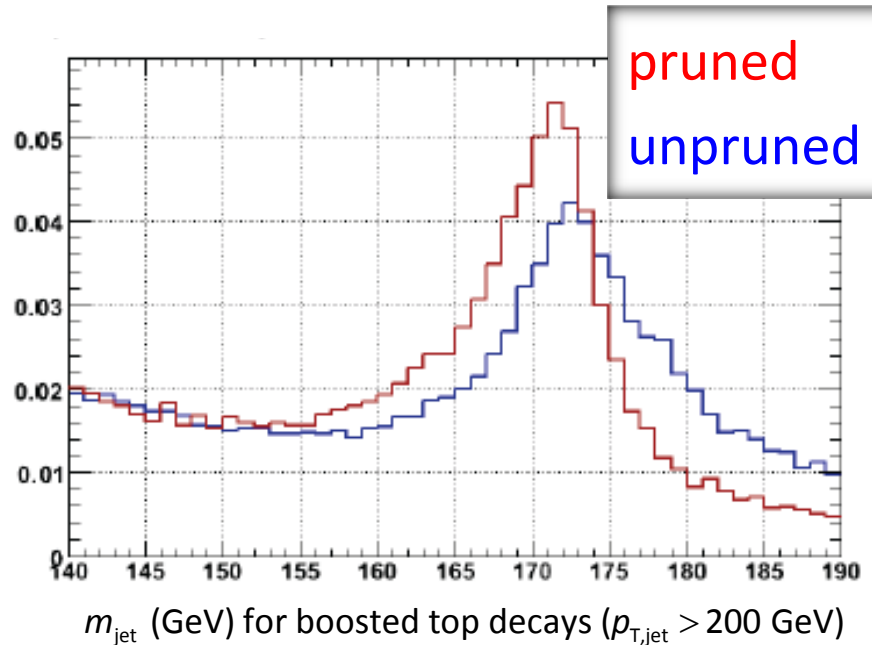
Enhancement of jet components
to increase substructure resolution
Applied in kT-style jet clustering
procedure

Jet trimming

Applies a filter by removing soft
sub-jets in a jet
Soft p_T cut-off evaluated
dynamically jet by jet

Jet Pruning

- improves jet mass measurement for boosted top etc.



J. Walsh, *Understanding Jet Substructure*, talk given at the *Theoretical-experimental TeraScale workshop on event shapes*, University of Oregon, February 23-27, 2009



Observables and tools

Jet pruning

Enhancement of jet components
to increase substructure resolution

Applied in kT-style jet clustering
procedure

Jet trimming

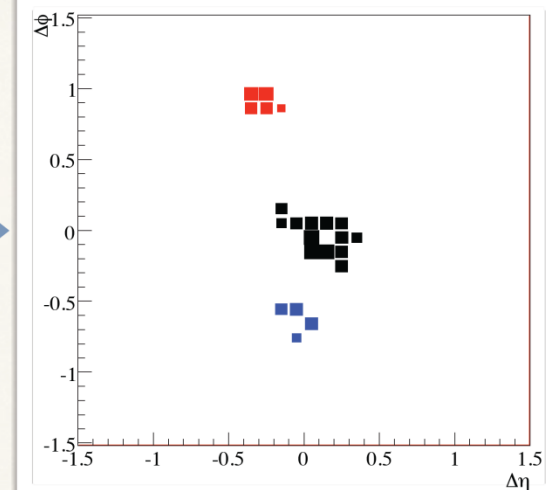
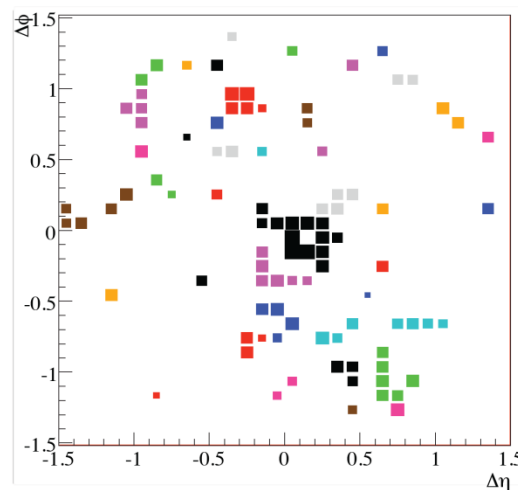
Applies a filter by removing soft
sub-jets in a jet

Soft pT cut-off evaluated
dynamically jet by jet

Jet Trimming

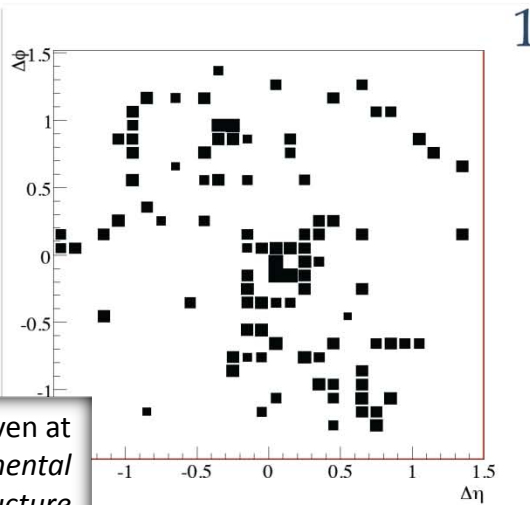
- main motivation is removing contaminations from e.g. pile-up and underlying event, from a fully reconstructed jet
- measures softness/hardness of contamination relative to whole jet – no judgements at the clustering stage
- approach:
 - (1) fully reconstruct jet from calorimeter signals
 - (2) cluster narrow sub-jets, typically with $R_{\text{sub}} = 0.2$
 - (3) discard sub-jets i with $p_{T,i} < f_{\text{cut}} \Lambda_{\text{hard}}$
 - (4) rebuild jet from surviving sub-jets
- typical choice for Λ_{hard} is $\Lambda_{\text{hard}} = p_{T,\text{jet}}$

D.Krohn, *Jet Trimming*, talk given at the *Theoretical-experimental workshop on jet & jet substructure at LHC*, University of Washington, January 10-15, 2010 (based on D.Krohn, J.Thaler, L.T. Wang, [arXiv:0912.1342](https://arxiv.org/abs/0912.1342))

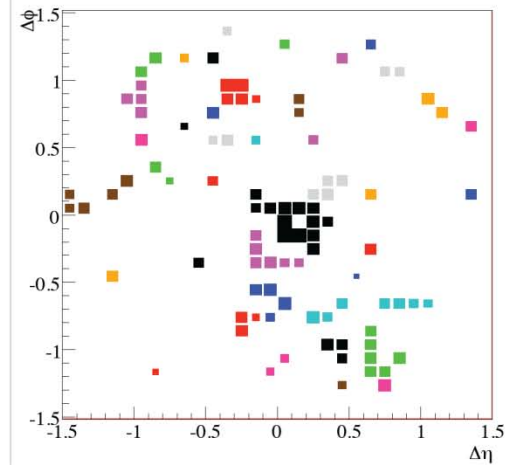


Start

D.Krohn, *Jet Trimming*, talk given at the *Theoretical-experimental workshop on jet & jet substructure at LHC*, University of Washington, January 10-15, 2010 (based on D.Krohn, J.Thaler, L.T. Wang, [arXiv:0912.1342](https://arxiv.org/abs/0912.1342))



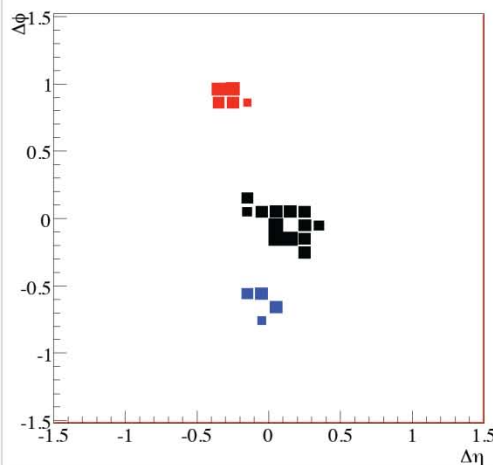
1



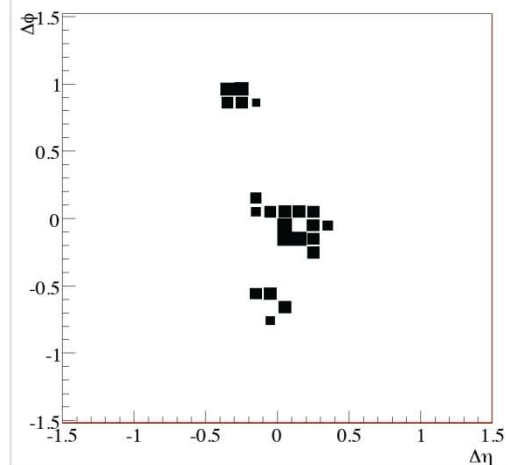
2

Cluster into subjects

Discard soft subjects



3

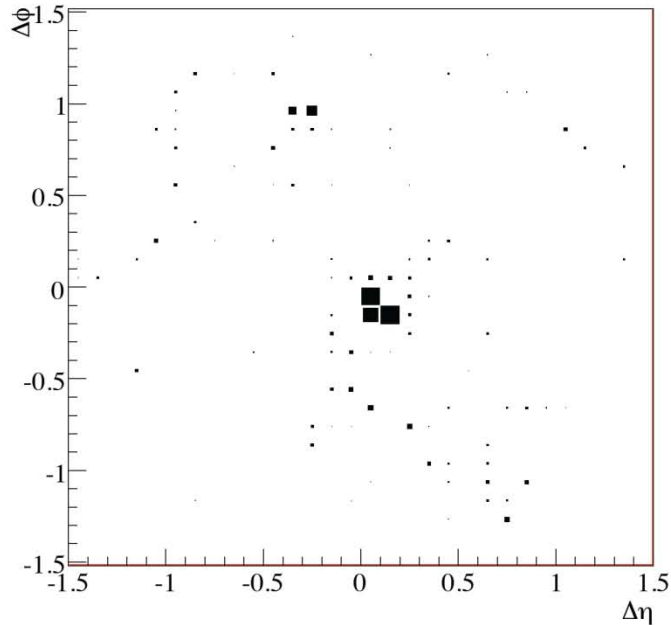


4

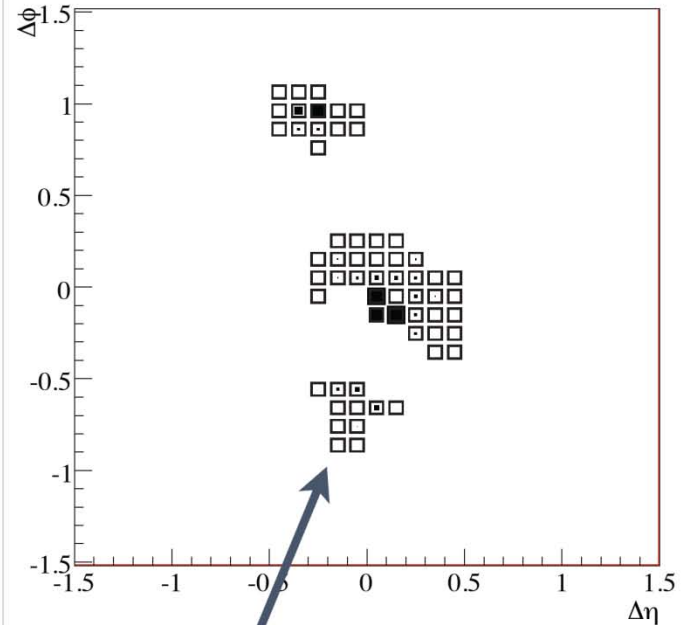
Reassemble



Before Trimming



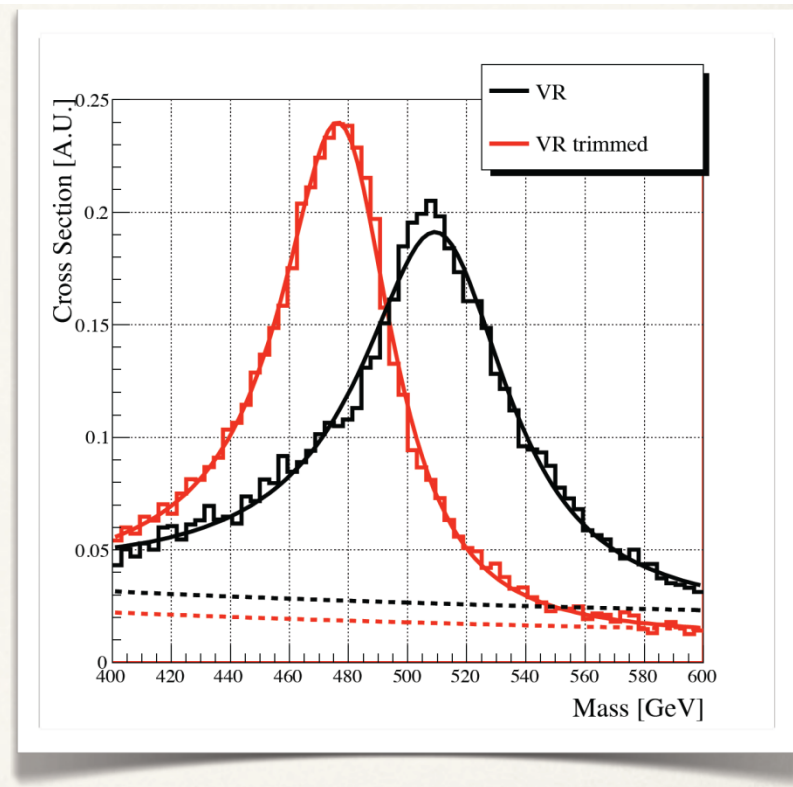
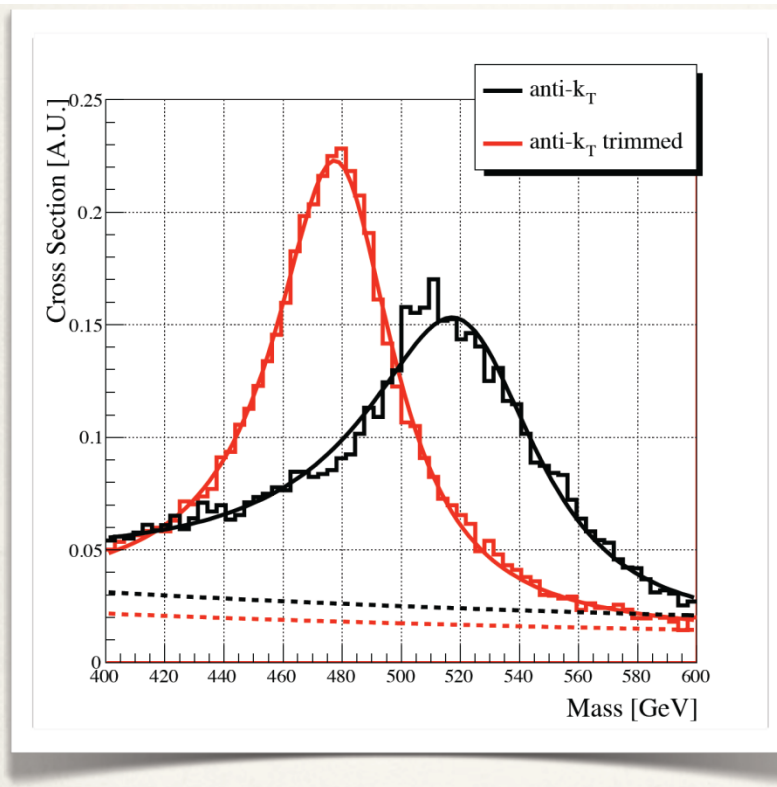
After Trimming



Empty squares
denote extent
of jet area

D.Krohn, *Jet Trimming*, talk given at the *Theoretical-experimental workshop on jet & jet substructure at LHC*, University of Washington, January 10-15, 2010 (based on D.Krohn, J.Thaler, L.T. Wang, [arXiv:0912.1342](https://arxiv.org/abs/0912.1342))





D.Krohn, *Jet Trimming*, talk given at
 the *Theoretical-experimental
 workshop on jet & jet substructure
 at LHC*, University of Washington,
 January 10-15, 2010 (based on
 D.Krohn, J.Thaler, L.T. Wang,
arXiv:0912.1342)

Trimmed and variable radius (VR) jets from
 $\phi \rightarrow qq, gg$
 (for VR, see D. Krohn, J. Thaler, and L.-T. Wang,
Jets with Variable R , JHEP 06 (2009) 059)

